Physicochemical Problems of Mineral Processing

Index No. 32213X

ISSN 1643-1049

47

2011

Physicochemical
Problems
of Mineral Processing
47 (2011)

Instructions for preparation of manuscripts
It is recommended that the following guidelines be followed by the authors of the manuscripts

- Original papers dealing with the principles of mineral processing and papers on technological aspects of mineral processing will be published in the journal which appears twice a year
- The manuscript can be sent to the Editors for reviewing any time of year
- The manuscript should be written in English. For publishing in other languages an approval of the editor is necessary
- Contributors whose first language is not the language of the manuscript are urged to have their manuscript competently edited prior to submission
- The manuscript should not exceed 12 pages
- There is a 100 EUR fee for printing the paper. No fee is required for the authors participating in the Annual Symposium on Physicochemical Problems on Mineral Processing
- Manuscripts and all correspondence regarding the symposium and journal should be sent to the editor.

Submission of papers is tantamount to a transfer of copyrights by the author(s) to Oficyna Wydawnicza PWr Publisher covering publication in printed as well as electronic media (CD-ROM or Internet) of the articles and any modifications of it.

Address of the Editorial Office
Wroclaw University of Technology
Wybrzeze Wyspianskiego 27, 50-370 Wroclaw, Poland
Institute of Mining Engineering
Laboratory of Mineral Processing

Location of the Editiorial Office:
pl. Teatralny 2, 50-051 Wroclaw, Poland
phone: (+48 71) 320 68 79, (+48 71) 320 68 78
fax: (+48 71) 344 81 23
jan.drzymala@pwr.wroc.pl
zygmunt.sadowski@pwr.wroc.pl
andrzej.luszczkiewicz@pwr.wroc.pl
pawel nowak <ncnowak@cyf-kr.edu.pl>
www.minproc.pwr.wroc.pl/journal

Physicochemical Problems of Mineral Processing 47 (2011)

www.minproc.pwr.wroc.pl/journal

WROCŁAW 2011

Editors
Jan Drzymała editor-in-chief
Zygmunt Sadowski
Andrzej Łuszczkiewicz
Paweł Nowak

Editiorial Board
Ashraf Amer, Wiesław Blaschke, Marian Brożek, Stanisław Chibowski, Tomasz Chmielewski, Beata Cwalina, Janusz Girczys, Andrzej Heim, Jan Hupka, Teofil Jesionowski, Andrzej Konieczny, Janusz Laskowski, Kazimierz Małysa, Andrzej Pomianowski (honorary chairman), Stanisława Sanak-Rydlewska, Jerzy Sablik, Kazimierz Sztaba (chairman), Barbara Tora, Tadeusz Tumidajski

Technical assistance
Przemysław B. Kowalczuk

The papers published in the Physicochemical Problems of Mineral Processing journal are abstracted in Chemical Abstracts, Thomson Reuters (Science Citation Index Expanded, Materials Science Citation Index, Journal Citation Reports), Coal Abstracts, Google Scholar and other sources

This publication was supported in different forms by
Komitet Górnictwa PAN
(Sekcja Wykorzystania Surowców Mineralnych)
Akademia Górniczo-Hutnicza w Krakowie
Politechnika Śląska w Gliwicach
Politechnika Wrocławska

ISSN 1643-1049

OFICYNA WYDAWNICZA POLITECHNIKI WROCŁAWSKIEJ
WYBRZEŻE WYSPIAŃSKIEGO 27, 50-370 WROCŁAW, POLAND

CONTENTS

Physicochem. Probl. Miner. Process. 47(2011) 5-16
www.minproc.pwr.wroc.pl/journal/

Physicochemical Problems of Mineral Processing
ISSN 1643-1049

Received March 30, 2011; reviewed; accepted April 10, 2011

The use of ultra-flocculation in optimization of the experimental flocculation procedures

Nickolaj N. RULYOV *, Janusz S. LASKOWSKI **, Fernando CONCHA ***

* Institute of Biocolloid Chemistry, National Academy of Sciences of Ukraine, Kiev, Ukraine
** NB Keevil Institute of Mining Engineering, The University of British Columbia, Vancouver, Canada, jsl@mining.ubc.ca
*** Department of Metallurgical Engineering, University of Concepcion, Chile

Abstract. The use of sea water in the flotation of Cu-Mo sulfide ores requires better understanding of the effect of electrolyte concentration on performance of flocculants used in the solid/liquid separation unit operations. This paper deals with optimisation of the experimental procedure that will be used in studying the effect of sea water on flocculation.

In the tests reported in this paper the tailings from one of Chile major flotation plants were subjected to the flocculation tests with Orifloc-2010 polyacrylamide in a Couette type reactor. It was shown that the flocculation efficiency can be dramatically improved by optimising the shear rate in the reactor, and that the procedure based on the ultra-flocculation can be used as a standardized experimental procedure in testing flocculants.

keywords: solid/liquid separation, flocculation, flocculants, flocculant testing, sedimentation

1. Introduction

The flocculants used by mineral processing industry are high molecular weight polymers that are soluble in water. Since a polymer can be soluble in water only if it is very hydrophilic these macromolecules must strongly interact with water and the properties/conformation of such macromolecules in water must depend on the polymers-solvent interactions. This is referred to as "goodness of solvent".

The main function of polymeric flocculants is to produce large and strong flocs. It is generally accepted that polymers used as flocculants aggregate suspensions of fine particles by a bridging mechanism. The bridging is considered to be a consequence of the adsorption of the segments of the flocculant macromolecules onto the surfaces of more than one particle. As pointed out by Kitchener (1972), the merit of modern polymeric flocculants is their ability to produce larger, stronger flocs than those obtained by coagulation. Theoretically, the flocculants may be applied either after destabilizing of the suspension via coagulation, or without prior destabilization:

- stable suspension → coagulation → flocculant addition→ flocculation
- stable suspension → flocculant addition→ flocculation.

It is known that flocculants are not very effective for treating stable suspensions and so the first option, which involves prior destabilization by coagulation, is always better.

Hogg et al. (1993) showed that the appropriate choice of flocculants is determined primarily by chemical factors (mineral composition, solution chemistry, etc.), but the performance of the flocculant depends more on physical variables, such as agitation intensity and the rate of flocculant addition.

Several techniques have been proposed to determine the settling velocity in laboratory experiments, the "jar tests" being the most common (Coe and Clevenger 1916; Richardson and Zaki 1954; Michael and Bolgers 1962). Jar tests involves homogenizing suspensions in settling cylinders, introducing the flocculant and mixing by moving a plunger up and down in the cylinders, or by inverting the cylinders several times. This procedure is claimed not to be satisfactory because of the local over-dosing that can occur when the relatively concentrated flocculant solution meets the slurry (Kitchener 1978); but more important is that the agitation in this method does not produce the optimum flocculation. Farrow and Swift (1996) demonstrated that the jar test has several problems. It is important to realize that adsorption and flocculation are not separate sequential processes, but occur simultaneously (Hogg, 1999). The commonly used improved experimental procedure includes addition of the flocculant to a vigorously agitated suspension which is immediately stopped after addition of the reagent (Keys and Hogg, 1979). Different mixing/polymer addition conditions may result in very different floc sizes and settling rates. Owen et al. (2009) showed that mixing of the slurry with a dilute flocculant solution within the feedwell determines the performance of commercial thickeners. It was also shown that under certain conditions intense agitation for short times may even change the nature of flocculation, from total flocculation to a selective flocculation of only some mineral constituents (Ding and Laskowski 2007).

The vast majority of commercial flocculants are based on partially hydrolyzed polyacrylamide. As a result of hydrolysis even "nonionic" polyacrylamides contain some anionic groups. This is expressed as "degree of anionicity" (the degree of anionicity of completely hydrolyzed polyacrylamide is 100%, so it is a polyacrylic acid).

The effectiveness of polymers as flocculants depends on their molecular weight, the sign of their charge (e.g. anionic or cationic) and the relative charge density (for polyacrylamides this is expressed by degree of anionicity). Recent data (Xu and Cymerman 1999) indicate that the best flocculants for the Syncrude tailings (mostly clays) were moderately anionic high molecular weight polyacrylamides (optimum around 20-30% anionicity). This agrees very well with Ferrera et al.´s (2008) results. Henderson and Wheatley (1987) demonstrated a very strong effect of intrinsic viscosity (that is indirectly molecular weight) on sedimentation rate of flocculated tailings for polyarylamides with varying anionicities.

Another important group of flocculants is polyethylene oxide, $(-CH_2CH_2O-)_n$. Scheiner et al. (1985) showed that PEO can be successfully applied in dewatering coal-clay waste from coal preparation plants. The process requires the use of calcium (lime) or magnesium salts, and PEO. Their results strongly indicate the need for prior coagulation before efficient bridging by flocculant can occur. In this process lime is added up to pH 9 or higher and the PEO dosage required to get optimum results varied from 50 to150 g/Mg. Our results confirmed that different flocculants require different hydrodynamic conditions for best flocculation (Sworska et al., 2000).

In many countries water has become a scare commodity. The lack of fresh water in the area of Atacama Desert (Northern Chile) is forcing the copper industry to utilize seawater. Salinity of seawater is approximately 3.5%, and NaCl concentration is around 0.5 M, with important secondary ions such as: sulfate ions (2.7 g/kg); magnesium ions (1.29 g/kg); calcium ions (0.41 g/kg); bicarbonate ions (0.145 g/kg); etc. Traditionally seawater has been considered of low metallurgical quality for the flotation of Cu-Mo sulfide ores, and a desalination stage was believed to be necessary. This is true when the same flotation technology which is used with fresh water is applied with seawater. Consequently, the main challenge in the flotation of Cu-Mo-Au ores is the successful use of seawater without desalination in copper mineral processing mills. This will also require better understanding the effect of electrolytes on flocculation.

It can be expected that increased concentration of electrolyte may affect many flocculation sub-processes:

- it destabilizes suspension by coagulation improving the overall effect of the flocculant;
- it affects the conformation of the flocculant macromolecules in the solution;
- it affects adsorption of polymer macromolecules onto solid particles, and it affects flocculant overall ability to flocculate that is to bridge suspended particles;
- because of the presence of Ca^{2+} and Mg^{2+} ions in sea water other flocculants than PAM may be better in this environment (for instance PEO).

Some of such effects have been studied, mostly for the systems encountered in potash ores flotation, the process in which sylvite (KCl) is separated from halite (NaCl) by flotation in KCl-NaCl saturated brine (6-7 mole/dm^3 solution). The effect of carboxymethyl cellulose ($M = 2.5 \cdot 10^5$ Da) on stability of mineral suspensions under such conditions was studied by Pawlik et al. (2003), and the effect of guar gum ($M = 1.39 \cdot 10^6$ Da) by Pawlik and Laskowski (2006) which was followed by Ma and Pawlik (2007). Preliminary results for polyacrylamide flocculants were reported by Ferrera et al. (2009).

In order to study such effects on flocculation we found it necessary to first optimize experimental procedures utilized in studying efficiency of flocculation. The use of a shear vessel (similar to rotational Couette viscometers) in assessing flocculation efficiency has the advantage of quantifying the mixing intensity through

the shear rate. The shear vessel in the past was used to study coagulation and was also used in the flocculation studies (Farrow and Swift 1996). Rulyov (1999, 2004) and Rulyov et al. (2005a, 2005b, 2009) has shown that the contacting diluted flocculant solution with the suspension in the shear vessel can: (1) vastly improve flocculant efficiency, and (2) allow studying the effect of hydrodynamic conditions on flocculation.

Farrow and Swift (1996) constructed their shear vessel with concentric cylinders of 200 and 210 mm in diameter and 120 mm in length. At the bottom of the vessel a glass tube 14 mm in diameter and 220 mm in length is used to measure the settling velocity. The experiments were made at a constant rotational velocity of 200 rpm. The outflow of the shear vessel was introduced immediately in the settling column. The authors concluded that the combination of shear vessel and settling column overcame most of the problems associate with jar test, in particular the strong dependence of batch settling test on mixing rate and cylinder diameter.

Using shear vessel Rulyov (1999) and Rulyov et al. (2000) have shown that the mixing time in flocculation can be reduced down from minutes to 5-6 seconds by the appropriate hydrodynamic treatment of the suspension at a given shear rate. This treatment, termed "ultra-flocculation" (Rulyov 2004; Rulyov et al 2005), ensures that not only flocculant molecules distribute fast and evenly within the suspension and adsorb on the surface of the particles, but also provides the formation of large and dense flocs. Depending on the size, size distribution and density of the particles in the dispersion, as well as on their volume concentration, the optimum values of the mean shear rate γ may vary in a wide range $300 < \dot{\gamma} < 5000\ s^{-1}$. The significant advantage of ultra-flocculation is that it ensures a good mix of small and large particles in flocs before they get into the settling tube, thus providing for fast sedimentation and high degree supernatant clarification (Rulyov et al. 2009).

2. Experimental

In this work an instrument known as *UltraflocTester*, that combines a shear vessel with variable shear rate and an optoelectronic device (similar to the one developed by Gregory and Nelson (1984)) that measures the mean-root-square fluctuation of intensity of light beam passing normally through transparent tube while the formed flocs pass through tube are used to analyze the relationship of flocculation efficiency (or mean flocs size) with solid concentration, flocculant dosage and shear rate.

2.1. Material, experimental set-up and method

Flotation tailings from one of the major copper flotation plants in Chile, were used in all experiments. Solid volume fraction varied over the range from 1.8 to 15 %; material density was 2700 kg/m^3. An average particle size x_{50}=20 μm with size distribution characterized by x_{80}=40 μm and x_{20}=20 μm was determined using a

Sympatec Helos-Rhodos laser dispersion instrument. Orifloc-2020 polyacrylamide was applied as a flocculant. The set-up used to perform ultra-flocculation tests is shown in Figs. 1 and 2.

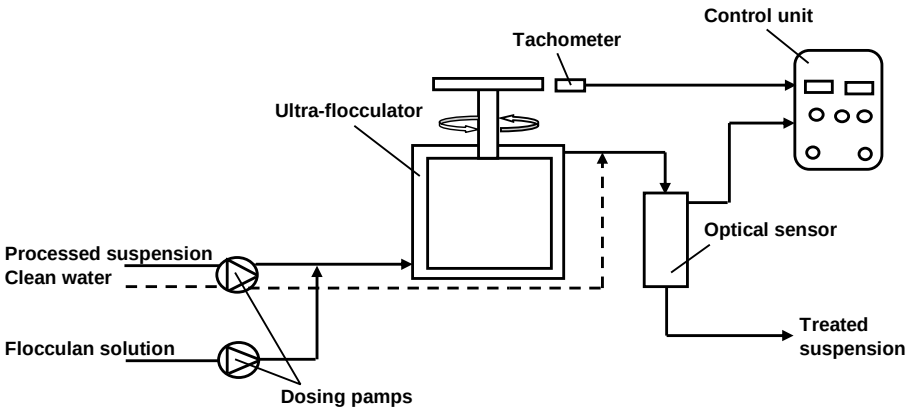

Fig. 1. Schematic illustration of the UltraflocTester, UFT-TFS-029

Fig. 2. Photograph of the UltraflocTester: UFT-TFS-029, Turboflotservice Company

It consists of a small shear vessel, referred to as ultra-flocculator in Fig.1. This Couette reactor, with a rotating cylinder of 28 mm and a gape of 1.5 mm was fed continuously with the suspension of tailings by a positive displacement pump. Before entering the Couette reactor the pulp receives continuously a dilute flocculant solution, at a flow-rate to give a pre-determined dosage. After 6 seconds conditioning at a pre-

determined shear rate, the flocculated suspension is discharged from the instrument through a 3 mm inner diameter transparent tube equipped with an opto-electronic sensor which registers the fluctuation of intensity of light beam passing normally through mentioned transparent tube (in accordance with techniques proposed by Gregory and Nelson 1984). The electronic signal is processed and displayed in a three digital format thus showing in relative units the values of flocculation efficiency (or mean flocs size) and the mean shear rate $\dot{\gamma}$.

The different operational conditions were obtained by changing the flocculant feed rate and the shear rate while maintaining a constant feed rate of suspension to the instrument. When the feed suspension concentration exceeded the threshold for its optical analysis capacity, (φ_0=6%), it was diluted by introducing clean water between the shear reactor and the optoelectronic sensor (shown by a dash line in Fig. 1). In the tests designed to measure settling rate of the treated suspension, dilution was not used. In this case the suspension from the outlet of the tester was continuously fed to a small settling cylinder 14 cm^3 in volume and, as soon as the suspension filled the cylinder, it was allowed to settle and the initial settling velocity was recorded.

3. Results and discussion

The operational conditions of the experiments and the output of the instrument are given in Table 1.

Table 1. General data

Solid concentration [g/dm^3]	Solid concentration % by volume φ_0	Settling Velocity V_{opt}/V_{100} [mm/s]	Shear rate $\dot{\gamma}$ [s^{-1}]	Flocculant dosage [g/Mg]	$C_s \cdot V_{opt}$ $10^{-4}\cdot$[g/cm$^2\cdot$s]	F_{opt}/F_{100} $10^{-4}\cdot$[m/s]
50	1.8	20/14	600	10	1000	3.72/2.60
100	3.7	13.6/9.0	500	8	1360	5.03/3.51
200	7.4	2.26/1.50	350	16	452	1.67/1.11
300	11.1	0.50/0.24	300	10	150	0.51/0.27
405	15.0	0.15/0.07	600	20	60	0.22/0.10

In Table 1 V_{opt} and V_{100} stand for the initial settling velocity after treatment at optimal shear rate $\dot{\gamma}_{opt}$ and at shear rate equal $\dot{\gamma}$=100 s^{-1}, F_{OPT} and F_{100} are the corresponding solid-flux densities.

3.1. Effect of flocculant dosage on the efficiency of flocculation

The flocculation was carried out over 6 seconds at optimal values of the mean shear rate $\dot{\gamma}$, for the respective suspension concentrations (see Table 1).

Figure 3 demonstrates that the flocculation efficiency (relative floc size) increases monotonically with flocculant dosage, reaching 90 relative units with a dosage of 10 g/Mg for the low range of particle concentration and 20 g/Mg for the higher range. The observed increase in the flocculant dosage with the increase of the

suspension concentration can most likely be attributed to the slowdown of the process of the flocculant macromolecules distribution within the volume of the suspension with increased solid concentration.

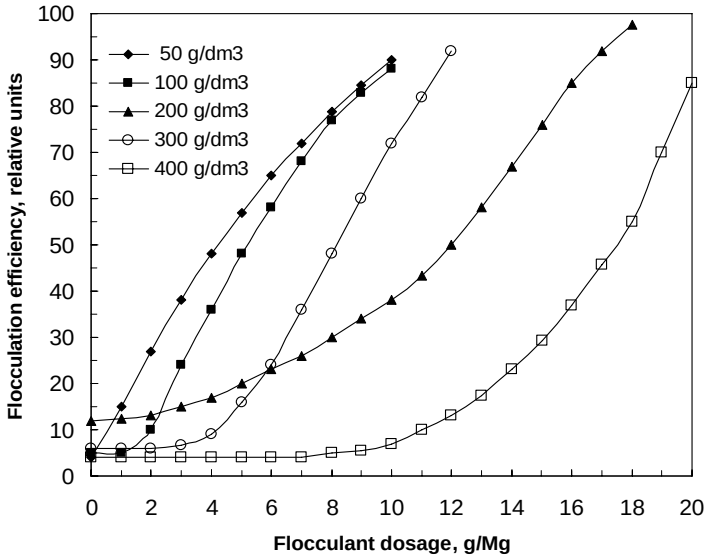

Fig. 3. Flocculation efficiency (relative mean floc size) versus flocculant dosage with the solid volume concentration as parameter

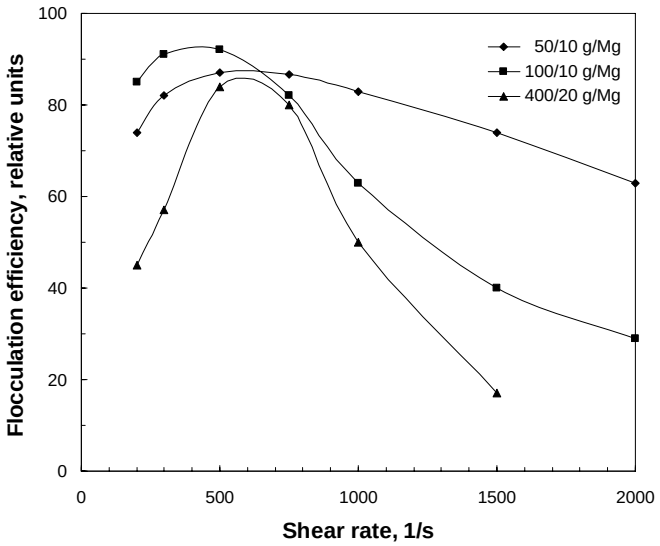

Fig. 4. Effect of average shear rate on flocculation efficiency (mean flocs size) for a different solids volume concentration (%) / flocculant dosage (g/Mg)

Figure 4 shows the effect of shear rate, $\dot{\gamma}$, on the flocculation efficiency, These results clearly demonstrate that maximum exists between 400 to 600 s^{-1}, depending on the solid concentration, with increasing values for higher concentrations.

The shift of the maximum of flocculation efficiency to higher shear values for higher flocculant dosages may be due to increased strength of the bridges bonding particles within flocs. As it was shown by Rulyov et al (2005), it allows for the formation of larger and stronger flocs.

3.2. Effect of the shear rate on the settling velocity

Since the shear rate influences the flocculation efficiency in the way expressed in the previous section, one would expect similar influence on the settling velocity. This was confirmed as shown in Figures 5.

The results given in Figure 5 indicate that the optimum shear rate corresponding to the maximum flocculation efficiency also corresponds to the maximum initial settling rate of the flocculated suspension. This confirms that the ultra-flocculation test is an effective method for identification of the optimal flocculation conditions.

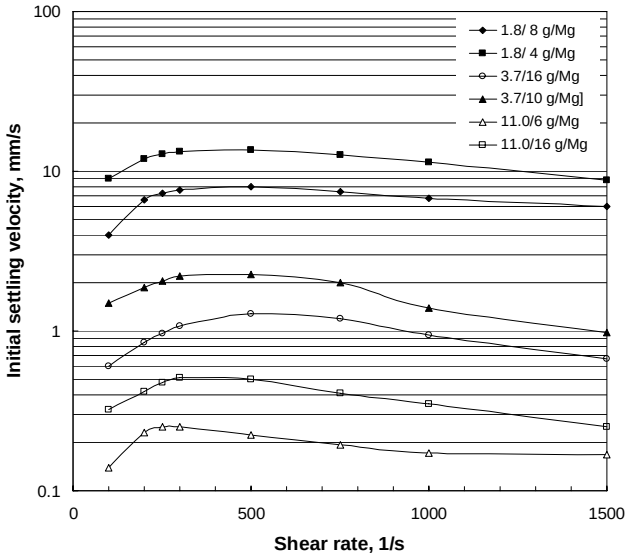

Fig. 5. Initial settling velocity versus average shear rate for a different solids volume concentration (%)/flocculant dosage (g/Mg)

3.3. Effect of the solid volume concentration on the optimal shear rate

It is important to establish the optimum solid concentration for flocculation in a commercial thickener. In the majority of industrial thickeners flocculation takes place in the feedwell where the feed is diluted with circulating water. Knowing the

solid concentration that gives the best flocculation should permit calculation of the water dilution flow rate.

Figure 6 shows the effect of suspension volume concentration on the optimum shear rate for a given flocculation. Since the shear rate required for a good flocculation initially decreases with solid content, but increases again if the solid volume content is further increased, the minimum appears on the relationship between shear rate and solids content. Therefore, for the most efficient flocculation each solid concentration in the pulp requires selection of the optimum shear rate.

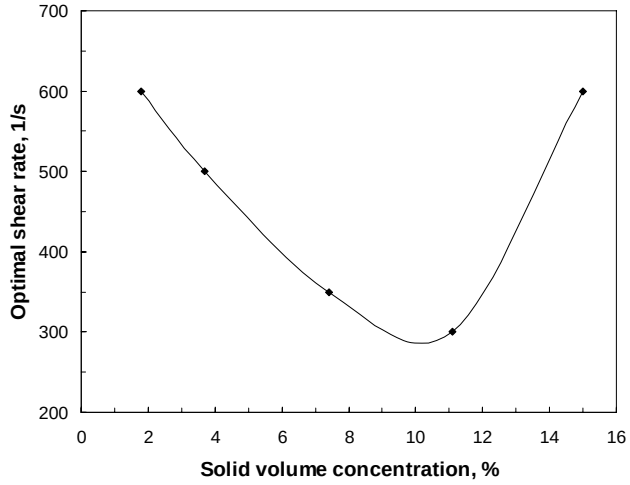

Fig. 6. Optimal average shear rate versus suspension solid volume concentration.

This relationship between shear rate and solids concentration can be explained using Smoluchowski theory, because at a given suspension concentration the floc size increases to maximum within a short time interval. On the other hand, with the increase in suspension concentration the distribution of flocculant macromolecules within the volume of suspension slows down. In particular, this is confirmed by increased consumption of the flocculant with the increased suspension concentration at a constant time interval. However, due to convective diffusion, with increasing shear rate the rate of flocculant molecules dissemination in the suspension significantly increases, leading to the growth of the dependence of the optimum shear rate on concentration in the region of large concentration values. This may also lead to some decrease in the required flocculant dosage as shown by Rulyov et al (2005).

4. Summary

In this project the results were obtained in the tests carried out with the flotation tailings from one of major Chilean copper flotation plants using a commercial polyacrylamide flocculant utilized by this industry. The results indicate that with the

use of ultraflocculation the efficiency of the radial thickener can be increased by more than 1.5 times.

The results reported in this paper are part of the larger project aimed at utilization of sea water in flotation of Cu-Mo sulfide ores and must also answer the question on the effect of sea water on solid/liquid separation. Since polymer adsorption and flocculation are not separate sequential processes but occur simultaneously the performance of the flocculant very strongly depends on physical variables (agitation intensity, rate of flocculant addition, solids content, concentration of polymer stock solution, etc.). It is therefore of primary importance to use the proper experimental procedure in the studies on the effect of "goodness of solvent" on flocculation. The tests confirmed that the ultra-flocculation procedure, and UltraflocTester UFT-TFS-029, can conveniently be utilized to find optimum hydrodynamic conditions under which the effect of the goodness of solvent on the flocculation in processing flotation tailings from Chilean copper industry in sea water can be studied.

Acknowledgements

This work was conducted via INOVA Project 08MC01-18 and AMIRA P 968. This financial support is gratefully acknowledged.

References

Coe, K.S., Clevenger, G.H., 1916. *Method of determining the capacity of slime settling tanks*, Trans. AIME 55, 203-210.

Ding, K.J., Laskowski, J.S., 2007. *Effect of conditioning on selective flocculation with polyacrylamide in the coal reverse flotation*, Trans. IMM 116, 108-114.

Farrow, J.B., Swift, J.D., 1996. *A new procedure for assessing the performance of flocculants*, Int. J. Mineral Process. 46, 263-275.

Ferrera, V., Arinaitwe, E., Pawlik, M., 2009. *A role of flocculant conformation in the flocculation process*, Advances in Mineral Processing Science and Technology - Proc. 7th UBC-McGill-UA Symposium (C.O. Gomez, J.E. Nesset and S.R. Rao, eds.), Metallurgical Society of CIM, 397-408.

Gregory, J., Nelson, D.W., 1984. *A new method for flocculation monitoring.* Solid-Liquid Sparation (J. Gregory, Ed.) Ellis Horwood, Chichester, 172-182.

Henderson, J.M., Wheatley, A.D., 1987. *Factors affecting the efficient flocculation of tailings by polyacrylamides*, Coal Preparation 4, 1-41.

Hogg, R., Brunnaul, P., Suharyono, H., 1993. *Chemical and physical variables in polymer-induced flocculation*, Mineral and Metallurg. Processing 10, 81-85.

Hogg, R., 1999. *Polymer adsorption and flocculation*, Polymers in Mineral Processing –Proc. 3rd UBC-McGill Int. Symp. (J.S. Laskowski, ed.), Metalurgical Society of CIM, Quebec City, 1999, 3-17.

Keys, R.O. and Hogg, R., 1979. *Mixing problems in polymer flocculation*, AIChE Symp. Series 75(190), 63-72.

Kitchener, J.A., 1978. *Flocculation in mineral suspensions*, The Scientific Basis of Flocculation (K.J. Ives, ed.), Sijthoff & Noordhoff, 283-328.

Michael A.S., Bolger, J.C., 1962. *Settling rates and sediment volumes of flocculated kaolin suspentsions*, Ind. Eng. Chem. Fundam 1, 24-33.

Owen, A.T., Nguyen, T.V. Fawell, P.D., 2009. *The effect of flocculant solution transport and addition conditions on feedwell performance in gravity thickeners,* Int. J. Mineral Processing 93, 115-127.

Pawlik, M., Laskowski, J.S. Ansari, A., 2003. *Effect of carboxymethyl cellulose and ionic strength on stability of mineral suspensions in potash ore flotation systems*, J. Coll. Interf. Sci. 260, 251-258.

Pawlik, M., Laskowski, J.S., 2006. *Stabilization of mineral suspensions by guar gum in potash ores flotation systems*, Canadian J. Chem. Eng. 84, 532-538.

Ma, X. Pawlik, M., 2007. *Adsorption of guar gum on potash slimes*, Canadian Metall. Quarterly 46, 321-328.

Ma, X., Pawlik, M., 2007. *Intrinsic viscosities and Huggins constants of guar gum in alkali metal chloride solutions*, Carbohydrate Polymers 70, 15-24.

Richardson, J.F., Zaki, W.N., 1954. *Sedimentation and fluidization: Part I.* Trans. Inst. Chem. Eng. 32, 35-53.

Rulyov, N.N., Maes, A., Korolyov, V. J., 2000. *Optimization of hydrodynamic treatment regime in the processes of sorption-flocculation water purification from organic contaminants*, Colloids & Surfaces A: 175, 371-381.

Rulyov, N.N., 1999. *Application of ultra-flocculation and turbulent micro-flotation to the removal of fine contaminants from water*, Colloids & Surfaces A: 151, 283-291.

Rulyov, N.N., 2004. *Utra-flocculation: Theory, experiment and applications*. Particle Size Enlargement in Mineral Processing - Proc.5th UBC McGill Int. Symp. Fundamentals of Mineral Processing (J.S. Laskowski, ed.), CIM Metall. Soc., Hamilton, 197-214.

Rulyov, N.N., Dontsova, T.A., Korolyov, V.Ja., 2005a. *Ultra-flocculation of diluted fine dispersed suspensions*, Miner. Process. Extr. Metall. Rev. 26, 203 – 217.

Rulyov, N.N., Dontsova, T.A., Nebesnova, T.V., 2005b. *The pair binding energy of particles and flocs size formed in turbulent flow*, Khimya i Tekhnologia Vody, 27(1), 1-17.

Rulyov, N.N., Korolyov, B.Y., Kovalchuk, N.M., 2009. *Ultra-flocculation of quartz suspension: effects of shear rate, dispersion and solids concentration*, Trans. IMM 118, 175-181.

Scheiner, B.J., Smelley, A.G., Stanley, D.A., 1985. *Dewatering of Mineral Waste Using the Flocculant Polyethylene Oxide*, U.S. Bureau of Mines Bulletin 681.

Sworska, A., Laskowski, J.S., Cymerman, G., 2000. *Flocclation of the Syncrude Fine Tailings, Part I: Effect of pH, Polymer Dosage and Mg^{2+} and Ca^{2+} Cations*, Int. J.

Miner. Process. 60, 143-152; *Flocculation of the Syncrude Fine Tailings, Part II: Effect of Hydrodynamic Conditions*, Int. J. Miner. Process. 60, 153-161.

Xu, Y., Cymerman, G., 1999. *Flocculation of fine oil sand tails*, Polymers in Mineral Processing –Proc. 3rd UBC-McGill Int. Symp. (J.S. Laskowski, ed.), Metalurgical Society of CIM, Quebec City, 591-604.

Physicochem. Probl. Miner. Process. 47(2011) 17-26
www.minproc.pwr.wroc.pl/journal/

Physicochemical Problems of Mineral Processing
ISSN 1643-1049

Received March 1, 2011; reviewed; accepted April 8, 2011

Differentiation of organic carbon, copper and other metals contents by segregating flotation of final Polish industrial copper concentrates in the presence of dextrin

Dariusz FOSZCZ *, Jan DRZYMALA **

* AGH University of Science and Technology, Al. Mickiewicza 30, 30-059 Krakow, Poland
foszcz@agh.edu.pl
** Wroclaw University of Technology, Wybrzeze Wyspianskiego 27, 50-370 Wroclaw, Poland
jan.drzymala@pwr.wroc.pl

Abstract. Existing and new data on production of two copper concentrates differing in copper, organic carbon and other metals contents by reflotation of the final industrial flotation copper concentrates from KGHM Polska Miedz S.A. in the presence of dextrin as a depressing reagent of the mineral particles containing organic carbon are presented in the paper

keywords: flotation, reflotation, segregation flotation, organic carbon, copper, sulfides, dextrin, maltodextrin, industrial concentrates

1. Introduction

The final industrial flotation copper concentrate produced by KGHM Polska Miedz S.A. is a collective product containing several valuable elements such as Cu, Ag, S, Pb, Zn, Ni, Co, V, Mo, Re, Au etc., and unwanted elements including As, Hg, organic carbon (C_{org}) etc. Further processing of the concentrates by smelting is complex and increasing requirements imposed both by technology and environment call for improvements and new methods of copper ore and produced concentrate beneficiation. One of the problems encountered by KGHM at the beginning of this century was the excessive amount of Pb in the final industrial copper concentrates. In response to this demand a new technology was developed, proposed and patented (Drzymala et al., 2000/2001, 2007), which was based on reflotation of the final concentrate in the presence of dextrin (Drzymala et al., 2002) to produce two different copper concentrates. The first copper concentrate, being the froth product of reflotation, was enriched mostly in copper minerals including chalcocite and silver minerals. The second copper concentrate, being the reflotation tailing, also called the cell product, was enriched in C_{org} and, in the case of ZWR Lubin, also in the Pb minerals. Principles of the separation were described in details in a report of investigations commissioned in 2000 by the Polish Ministry of Higher Education, then

called the Committee on Scientific Research (KBN), entitled *Modified polysaccharides as selective depressing reagents in flotation of copper material containing lead minerals* (Drzymala et al., 2002). The results of the investigation can be summarized by two figures extracted taken from this report which are shown in Fig. 1. These figures clearly show that reflotation of the final industrial Polish concentrates leads to two concentrates having different compositions, especially of organic carbon and copper.

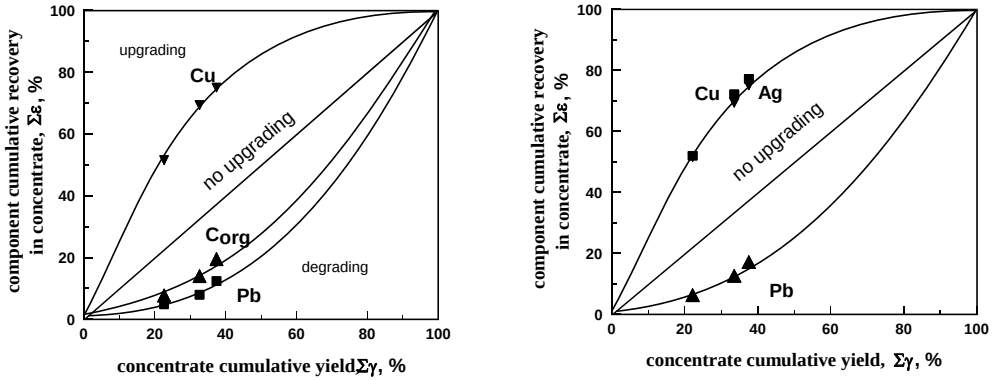

Fig. 1. a) Flotation results (Mayer upgrading curve) of the final industrial copper concentrates from ZWR Lubin in the presence of 50 g/Mg xanthate, 50 g/Mg α-terpineol and 2.5 kg/Mg dextrin prepared from potato starch by roasting at 256°C for 1 hour. Feed: 0.092% Ag, 18.5% Cu and 5.52% Pb (Drzymala et al., 2002), b) in the presence of 5 kg/Mg dextrin of molecular mass about 4 kg/mol and 50 g/Mg of xanthate along with 50 g/Mg of α-terpineol (without pH regulation). Ag minerals float together with Cu compounds. Feed: 7.08% C_{org}, 18.5% Cu and 5.45% Pb) (Drzymala et al., 2002). In this segregation flotation selectivity of dextrin as depressant is utilized

The approach of using dextrin was based on the known, for many years, fact that regulation of hydrophobic particles flotation, including graphite, coal and other naturally hydrophobic materials, can be accomplished by application of dextrin (Miller et al., 1984; Nyamekye and Laskowski, 1991). It is also suitable for the Polish copper concentrates.

Even though the new process of reflotation in the presence of dextrin was promising, it has never been implemented by KGHM due to improvements in the smelting technology, especially regarding lead. However, increasingly strict requirements imposed by the Huty Miedzi Głogow smelter on organic carbon content in the copper concentrates, which are the feed for the flash furnace, had been forcing the managers of the Mineral Processing Division (Oddział Zakłady Wzbogacania Rud or shortly O/ZWR) of KGHM to look for new and possibly simple technologies of copper concentrates production which would differ in C_{org} content. Investigations on the content of Cu and C_{org} in different size fractions of the final industrial copper concentrates lead to a simple solution based on size classification in HC ϕ350

hydrocyclones (ZWR Rudna, 2002-5). This approach appeared to be successful and was providing elevated contents of C_{org} and reduced content of Cu in the overflow while opposite situation was observed in the underflow stream. However, this technology was also a source of the problems with dewatering of the C_{org}-rich overflow product. The complication originated from the presence of fines which created dewatering difficulties even though flocculants were employed (O/ZWR, 2005). This forced the O/ZWR managers to search again for new solutions.

New investigation presented in the report on *An investigation into the evaluation of an alternative flowsheet and reagent scheme for beneficiation of the Polkowice carbonaceous copper or*e (O/ZWR, 2007) was commissioned by O/ZWR in 2007 at KGHM CUPRUM LTD, which pointed to a possible solution based on production of concentrates with different contents of Cu and C_{org} in the products by reflotation of the final industrial copper concentrates using time as a parameter. It was confirmed by investigation described in the report entitled *Determination of influence of upgradeability of the processed ores on the quality of copper concentrates for the needs of optimization of mining-smelting process of copper production process. Stage III* (O/ZWR, 2009) and performed by AGH in 2009 for O/ZWR. The ability of production of two concentrates having different C_{org} and Cu contents by simple and fast reflotation of the final industrial concentrates was confirmed in an industrial installation at the Rudna Processing Plant (O/ZWR Rudna) put into operation on June 8, 2010. The flotation method of production of copper concentrates differing in Cu and C_{org} content was based on different kinetics of flotation of copper minerals and carbonaceous matter present in the concentrate. It was established that well liberated copper minerals float efficiently and fast. Extending the flotation time leads to flotation of poorly liberated copper minerals forming intergrowths. This reduces copper concentrates quality in terms of Cu content. On the other hand particles containing C_{org} require more time to be transported with bubble to the concentrate. The relation between organic carbon and copper content in the re-floated, in a laboratory flotation machine, final industrial copper concentrate from side A and side B of ZWR Rudna (O/ZWR, 2009), being a result of different kinetics of flotation of C_{org} and Cu is shown in Fig.2.

The industrial reflotation, also referred to as segregation flotation, has been monitored and tested in 2010 within a new project *Elaboration of technology of concentrate production with different caloric values by segregation flotation* (O/ZWR, 2010). It was established that the time needed for separation, based on kinetics of flotation, was very short. Additional laboratory tests revealed that the optimum flotation time was 1 minute while in 2009 it was 6 minutes (O/ZWR, 2010). This complicated the separation process and called for further changes in the operation and construction of the whole reflotation installation. Therefore, adaptation works have been performed to change the processing flowsheet. In the following tests principal parameters, including pulp level in the flotation machine, air flow rate to the flotation machine, flotation time, flotation machine cell volume, feed flow rate, spraying the

concentrate froth with water, reagents addition etc. were investigated. The results of one of the series of the industrial segregation flotation trails are presented in Fig. 3.

Figure 3 shows that there is some separation between C_{org} and Cu (Fig. 3a) and no separation between Cu and Pb when the final copper concentrate is subjected to the segregation flotation.

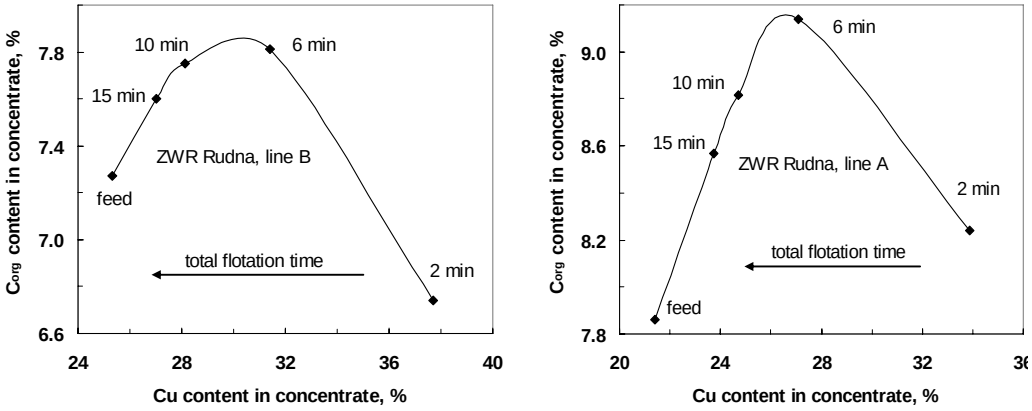

Fig. 2. Relation between organic carbon and copper content in the refloated in a laboratory flotation machine final industrial copper concentrate from side A and side B of ZWR Rudna (O/ZWR, 2009)

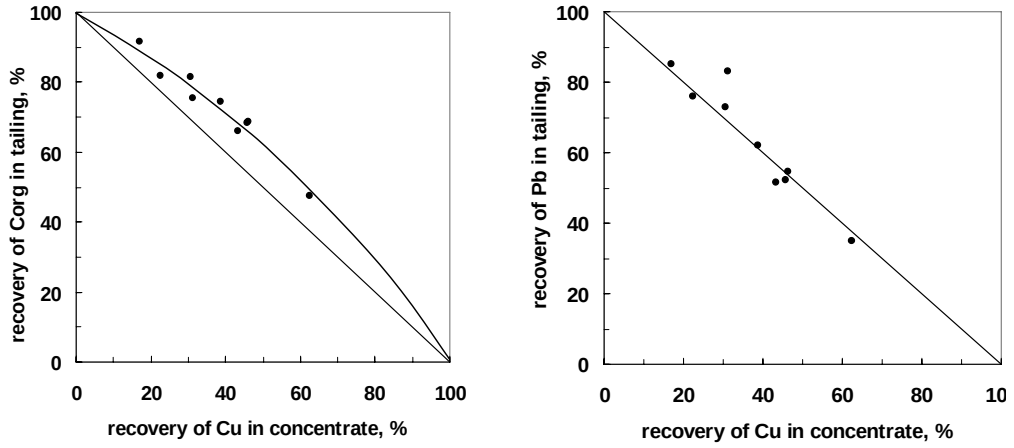

Fig. 3. Results of reagent free reflotation of the final industrial flotation copper concentrates leading to different Cu and Corg recoveries in the two products of the process at ZWR Rudna (O/ZWR, 2010, series I). Reflotation performed with industrial flotation machines MF011 and MF013. Different data points were obtained by varying flotation conditions. Separation results from different kinetics of Cu and Corg flotation (Fig. a). No separation between Cu and Pb is observed (Fig. b)

Since the results of segregation flotation were still unsatisfactory, a new effort was undertaken (O/ZWR, 2010) to use different depressants, including dextrin, which

confirmed previous findings (Drzymala et al., 2002) that dextrin can be an efficient reagent leading to reduction of the C_{org} content in the froth product obtained by reflotation of the final industrial flotation copper concentrate from KGHM.

The results of laboratory and industrial tests involving segregation flotation of the final industrial flotation copper concentrates from ZWR Rudna in the presence of dextrin to get two copper concentrates differing in Cu and C_{org} contents are presented in this paper.

2. Experimental

2.1. Laboratory experiments

In the reflotation experiments involving polysaccharides, a relatively high molecular weight dextrin, having the so-called dextrose equivalent (DE) equal to 6-8 and labeled as maltodextrin was used. I can be noticed that on the DE scale starch has 0 value while glucose/dextrose has the value of 100. Both selection and dose of the dextrin were based on the results described in the patent (Drzymala et al, 2007), other published data (Drzymala and Kozlowski, 2004) and availability of this dextrin on the market.

The feed (15 dm^3 of slurry) for the laboratory experiments was the same as the feed for the industrial segregation flotation performed in the two MF011 and MF033 flotation machines. The laboratory test were performed in a Mechanobr type flotation machine working at 2450 rpm and air flow rate equal to 120 dm^3/h. It was equipped with a 1 dm^3 cell in volume.

2.2. Industrial trials

The industrial scale reflotation tests were carried out in the presence of dextrin. The conditions of the tests with dextrin, to determine its influence on separation of C_{org} and Cu, was based on laboratory investigation tests and patent PL 195693 (Drzymala et al., 2000/1; 2007). The industrial trial was carried out at predetermined dose of maltodextrin DE 6-8 as the dextrin equal to about 2 kg per one megagram of dry mass (2 kg/Mg) of the final industrial copper concentrate. Since the production was about 7000 Mg per shift and reflotation concentrate yield was about 7%, an addition of 120 kg of dextrin per hour was necessary. A dose of 60 kg of dextrin, having a low DE6-8 dextrose equivalent, was used as 10% aqueous solution. The results obtained in the absence of the reagent on October 12, 2010 between 5:30 am to 12:30 pm were compared with those obtained in the presence of dextrin conducted between 12:30 and 13:00 pm. The reagent was added to the concentrate trough of the MF09 flotation machine. Taking into account the capacity of side A of ZWR Rudna for the industrial final copper concentrate and flotation kinetics, the samples of reflotation products were collected with a 6 minutes delay. Frequency of sampling in the course of regent addition was 3 minutes due to a short time of the industrial test.

3. Results and discussion

3.1. Reflotation of the final industrial flotation copper concentrates in the presence and absence of dextrin

The results of separation of Cu from C_{org} by reflotation are presented in Tables 1-2. Table 1 shows contents of Cu and C_{org} in the feed and in the products of separation while Table 2 gives calculated upgrading parameters such as yield and recovery as well as separation factor *a*. The separation factor, reflecting upgrading of Cu in relation to C_{org} is defined as (Drzymala and Ahmed, 2005)

$$\varepsilon_{Cu} = a\frac{100-\varepsilon_{C_{org}}}{a-\varepsilon_{C_{org}}} \tag{1}$$

where

ε_{Cu} – recovery of copper in the froth product

ε_{Corg} – recovery of organic carbon in the cell product

a – separation (selectivity) factor (100 for ideal separation and ~1000 for no separation). The value of *a* can be based on individual data points or the whole upgrading curve plotted as the Fuerstenau upgrading curve.

Table 1. Cu and C_{org} contents in the feed and products of reflotation (segregation flotation) in industrial flotation machines MF011 and MF033 in the presence of maltodextrin (DE 6-8)

Date/shift, time		Dextrin	Feed		Froth product		Cell product	
			Cu	C_{org}	Cu	C_{org}	Cu	C_{org}
12.10.10 shift I	5:30 am to 12:30 pm	absent	26.02	8.59	26.40	8.74	32.99	9.49
	12:30 pm to 13:30 pm	present	24.39	9.14	21.48	9.68	38.57	6.68

In addition to Tables 1 and 2 Figure 4 presents the results of Cu and C_{org} separation by reflotation in the presence and absence of dextrin.

A significant obstacle in analysis of the reflotation results was erroneous determination of Cu and C_{org} in the feed and the cell product in the absence of dextrin. Despite this shortcoming, it was possible to established that dextrin applied in the reflotation of the final industrial copper concentrate leads to new copper concentrate having reduced amount of C_{org} (6.68% in the presence of dextrin and 9.49% in the absence) and elevated content of Cu (38.57% in the presence of dextrin and 32.99% in the absence). It proves that applied dextrin and reflotation procedure provide two copper concentrates differing in organic carbon content.

Table 2. Upgrading results parameters and separation factor *a* of separation Cu from C_{org} in the presence of maltodextrin (DE 6-8)

Data/shift, time		Cu		Corg		C_{org} recovery for balance based on Cu	separation factor (Cu from Corg) (*a*)
		froth product yield	froth product recovery	froth product yield	cell product recovery		
12.10.10 shift I	from 5:30 am to 12:30 pm	30.0*	38.0	-20.0	122.1	71.2	292.6
	from 12:30 pm to 13:30 pm	17.0	26.9	18.0	86.8	87.9	159.9

* - froth product yield was assumed as for shift III on 11.10.2010 due to imbalance of Cu in the flotation products

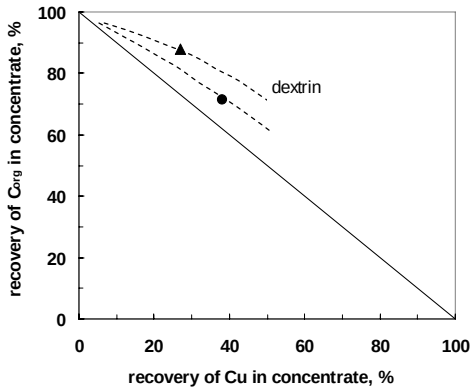

Fig. 4. The Fuerstenau upgrading curve showing relation between recovery of C_{org} in the cell product and Cu recovery in the froth product for industrial trial of reflotation in the absence and presence of maltodextrin DE 6-8 at the dose of 1.93 kg/Mg. The throughput was 7640 Mg per shift, concentrate yield 6,84%

3.2. Laboratory reflotation tests

The laboratory flotation tests were carried out to supplement the industrial trail results obtained in the presence of maltodextrin DE 6-8. The sample for tests was the final industrial copper concentrate collected on October 12, 2010 during shift I between 5:30 am and 12:30 pm. It was the so-called balanced sample prepared by the Center for Quality Investigations (CBJ) after removing the so-called balance determination sample. The following samples were investigated: 1) flotation for the collected sample at the original solids density (flotation F0) in the absence of dextrin, and 2) flotation of the sample collected in the presence of maltodextrin (flotation F1). Figure 5 shows the change of the Cu content in the reflotation froth products. It results from the data on the Cu content in the froth products, collected after indicated in the figure flotation times, that as expected, the dextrin addition does not depress flotation

of copper minerals while it depresses C_{org} flotation. This leads to a beneficial differentiation of the flotation products in respect to the Cu and C_{org} assay.

The content of C_{org} in the froth products collected after different time intervals (Fig. 5) indicates that dextrin significantly reduces the kinetics of C_{org} flotation leading to a reduction of C_{org} grade in the froth concentrate and increased C_{org} content in the cell product.

Figure 6 shows separation of C_{org} from Cu in terms of separation factor *a* calculated separately for each product of segregation flotation and flotation time. It confirms very efficient (low *a* values) and persisting depression of C_{org} and its separation from Cu in the presence of dextrin and poor separation (high *a* values) of C_{org} from Cu in the absence of dextrin.

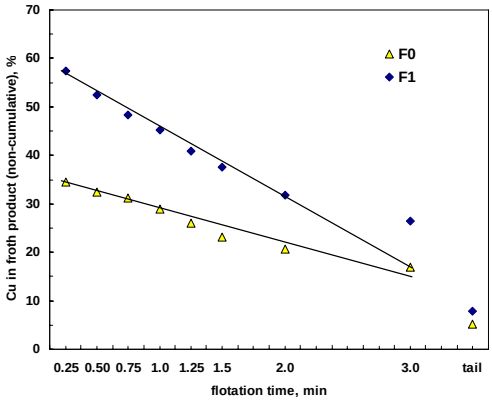

Fig. 5. Results of laboratory batch tests on reflotation of final industrial copper concentrates performed in the absence (F0) and presence (F1) of dextrin, shown as Cu content in the froth product as a function of flotation time

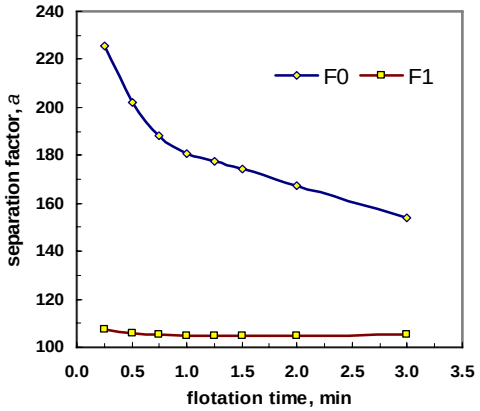

Fig. 6. Relation between separation factor *a*, reflecting separation of Cu and C_{org} during fractionated batch laboratory flotation, and flotation time. Results in the presence (F1) and in the absence (F0) of dextrin

The same results plotted as the Fuerstenau upgrading curve (Fig. 7) prove again a good efficiency of separation of Cu from C_{org} in the presence of dextrin. According to Fig. 7. it is possible, for instance, to obtain froth product with Cu recovery equal to 50-60% with only 10% recovery of C_{org} in that product, that is 90% recovery of C_{org} in the cell product. Thus, it is feasible to separate the final industrial copper concentrate into two copper concentrates: the froth product enriched in Cu and the cell product enriched in C_{org}.

The laboratory experiments conducted to enriched the industrial tests show that segregation flotation (reflotation) of the final industrial flotation copper concentrates in the absence and presence of dextrin is very efficient.

An important element in a further creation of technology for production of two concentrates having different caloric values by segregation flotation in the presence of

dextrin will be the determination of the dose and other parameters influencing the process.

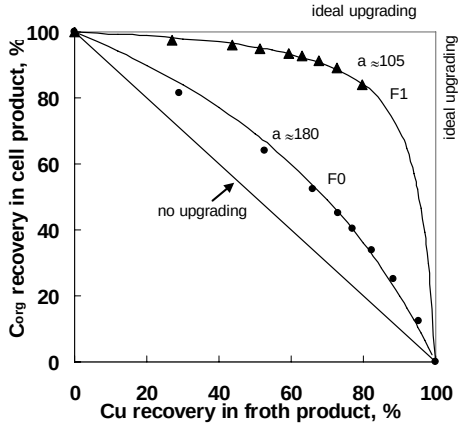

Fig. 7. Separation curve for laboratory batch tests on reflotation of final industrial copper concentrates performed in the absence (F0) and presence (F1) of dextrin in the form of the Fuerstenau upgrading curve

4. Conclusions

Both industrial and laboratory flotation results presented and discussed in this paper confirmed previous data that dextrin is an effective C_{org} depressant for splitting, by reflotation also called segregation flotation, the final industrial flotation copper concentrate into two copper concentrates differing in Cu and C_{org} contents. The reflotation provides the froth product enriched in Cu and depleted in C_{org} while the cell product with elevated amount of C_{org} and reduced assay of Cu. A final decision on application of dextrin for production of the two industrial copper concentrates should be based on optimization of reagent dose in combination with economical analysis.

It becomes now necessary to evaluate the possible benefits of smelting of the new concentrates from the Cu and C_{org} content points of view. It would allow to determine the optimal dose of the dextrin in the process.

Acknowledgements

Authors wish to thank KGHM Polska Miedz S.A. for permission to publish this paper. Financial support by the Polish Statutory Research Grant (343-165) is greatly acknowledged.

References

Drzymala J., Kapusniak J., Koziol J., Kozlowski A., Luszczkiewicz A., Tomasik P., 2002. *Modyfikowane polisacharydy jako selektywne depresory we flotacji surowcow miedziowych zawierajacych mineraly olowiu*. Raport Instytutu Gornictwa 2002, I-11/S-68/2002.

Drzymala J., Kapusniak J., Tomasik P.: 2000/2001, *Sposob wytwarzania koncentratow miedziowych bogatych w chalkozyn*. Data zgloszenia 19.01.2000, zgloszenie ogloszono 30.07. 2001, nr zgloszenia P 337953.

Drzymala J., Kapusniak J., Tomasik P.: 2007. *Sposob wytwarzania koncentratow bogatych w chalkozyn*, Patent PL 195693 B.

Drzymala J., Kozlowski A., 2004. *Wplyw masy molowej polisacharydow zawierajacych mery D-glukozowe z wiazaniami glikozydowymi na selektywnosc odolowiania koncentratu miedzi.* Prace Naukowe Instytutu Gornictwa Politechniki Wroclawskiej 106, Studia i materialy 30, 31-43.

Drzymala Jan, Kapusniak Janusz, Tomasik Piotr, 2003. *Removal of lead minerals from copper industrial flotation concentrates by xanthate flotation In the presence of dextrin*, Int. J. Miner. Process, 70, 147-155.

O/ZWR, 2009, Report 1048, *Okreslenie wpływu wzbogacalnosci przerabianych rud na jakość koncentratów miedziowych dla potrzeb optymalizacji gorniczo-hutniczego procesu wytwarzania miedzi*. Etap III. Foszcz D., Luszczkiewicz A., Drzymala J., Tumidajski T., Trybalski K., Muszer A., Niedoba T., Henc T., AGH Krakow, 69.

O/ZWR, 2005, Report 1008, *Przemysłowe badanie metod przyspieszania sedymentacji koncentratów w O/ZWR*., Grotowski A., Mizera A., Butra J., CUPRUM Wrocław.

O/ZWR, 2007, Report 1025.4, *An investigation into the evaluation of an alternative flowsheet and reagent scheme for beneficiation of the Polkowice carbonaceous copper ore*, Jessup T., McKenzie S., SGS Lakefield Canada for KGHM CUPRUM LTD.

O/ZWR, 2010, Report 1060, *Opracowanie technologii produkcji koncentratów o zroznicowanej kalorycznosci na etapie flotacji segregujacej*, Trybalski K. (head), Foszcz D., Gawenda T., Krawczykowski D, Marciniak-Kowalska J. (Chapter 3.1, App. 1), Nowak A. (Chapter 6, App.), Ranosz R. (Chapter 6),AGH University of Science and Technology, Krakow, Poland.

Miller J.D., Chang S.S., Lin, C.L.: *Coadsorption phenomena in the flotation of pyrite from coal reverse flotation*. Coal Preparation 1984, 1, 21-32.

Nyamekye G.A, Laskowski J.S., 1991. *The differential flotation of INCO matte with the use of polysaccharides*, in: Dobby G.S., Argyropoulos, S.A., Rao, S.R., (Eds). Proc. Copper '91 Int. Symp, 1991, 2, 231-243.

ZWR Rudna, 2002-5, KGHM Polska Miedz S.A., unpublished.

Foszcz, D., Drzymala, J., *Różnicowanie zawartości miedzi i węgla organicznego poprzez flotację segregującą końcowych przemysłowych koncentratów miedziowych w obecności dekstryn*, Physicochem. Probl. Miner. Process., 47 (2011) 17-26, (w jęz. ang.)

W pracy przedstawiono znane oraz nowe dane dotyczące produkcji dwóch koncentratów miedziowych o zróżnicowanych zawartościach miedzi i węgla organicznego na drodze ponownej flotacji przemysłowgo końcowego koncentratu miedziowego z KGHM Polska Miedź S.A. przy użyciu dekstryny jako odczynnika depresującego ziarna mineralne zawierające węgiel organiczny.

słowa kluczowe: flotacja, reflotacja, flotacja segregująca, węgiel organiczny, miedź, siarczki miedzi, dextryna, maltodextryna, koncentraty przemysłowe

Physicochem. Probl. Miner. Process. 47(2011) 27-40
www.minproc.pwr.wroc.pl/journal/

Physicochemical Problems of Mineral Processing
ISSN 1643-1049

Received March 20, 2011; reviewed; accepted April 6, 2011

Enhanced solvent extraction of cadmium and iron from phosphoric acid in chloride media

Mohamed H.H. MAHMOUD *,, Qahtani MOHSEN ****

* Taif University, College of Science, Chemistry Department, Taif, KSA, mheshamm@gmail.com
** Central Metallurgical R & D Institute, P.O.Box 87, Helwan, Cairo, Egypt

Abstract. Cadmium and iron are common impurities in wet process phosphoric acid (WPA). These impurities should be minimized to the acceptable levels before the commercialization of the WPA. Organic extractant such as trioctylammine (TOA) will be protonated in acidic media and can act as a liquid anion exchanger for separation of anionic chloro-species of Cd^{2+} and Fe^{3+} from WPA. Synthetic solutions containing phosphoric acid, 40 ppm Cd^{2+} and 3% Fe^{3+} (calculated as Fe_2O_3) were prepared and the different parameters affecting the extraction of these metal ions with TOA were investigated. The extraction of the two metal ions was found to be neglected in absence of chloride ions and it sharply increased by increasing HCl concentration. More than 98% of Cd^{2+} was extracted with 20% TOA in kerosene from 30% H_3PO_4 in presence of 1-3% HCl. Almost complete extraction of Fe^{3+} was achieved in presence of 10% HCl at similar experimental conditions. The TOA concentration of about 10% and 30% could completely extract Cd^{2+} and Fe^{3+} at 10% HCl for 10 min, respectively. A third phase formation was observed when TOA in kerosene was contacted with acidic aqueous solutions and this was eliminated by modification of TOA with 10% n-octanol but the extraction efficiency was slightly declined. The extraction process was quite fast, where 3 minutes was found to be sufficient for equilibrium extraction of both metal ions. Increasing the H_3PO_4 concentration enhanced the extraction of Fe^{3+} but little affected that of Cd^{2+}. Most of the two metal ions can be easily stripped by contacting the loaded TOA with water but emulsion formation was observed and the phase separation was difficult. Acidic solutions such as 0.5 M HClO4 can solve the problem and strip about 90% of both metal ions. Small amount of H_3PO_4 (about 1% of the started acid) was co-extracted and stripped together with Cd^{2+} and Fe^{3+} under same conditions.

keywords: phosphoric acid, solvent extraction, trioctylammine, iron, cadmium, chlorospecies

1. Introduction

Phosphoric acid is the second most produced acid after sulfuric acid. It was used as a raw material for the production of fertilizers, detergents, food products, toothpastes and alimentary supplies for cattle. Commercial H_3PO_4 is mostly manufactured using thermal and wet processes. In thermal process, H_3PO_4 is firstly produced by reduction of phosphate rock, followed by oxidation and hydration (Slack, 1968). Phosphate rocks, depending on their origin, can contain radioactive elements like uranium, thorium and radon or heavy metals. The wet process mostly involves the reaction of phosphate rock with H_2SO_4 followed by filtration and acid concentration. The wet process phosphoric acid (WPA) is usually accompanied by a number of undesirable ionic impurities, like fluoride, iron, cadmium, copper, chromium, zinc, uranium, radioactive elements those originally present in the phosphate rocks which interfere in the technological process of phosphoric acid and/or fertilizer. These impurities also can be partially precipitated as phosphates while the acid is concentrated or stored. The removal of heavy metals from the WPA is environmentally important referring mainly to their toxicity (Schrödter et al., 1998). It is for this reason that historically, the WPA has not been used in the food, detergent and in other industries where high purity acid is necessary, only the thermal route phosphoric acid with higher purity was used. Indeed, about 95% of the WPA is directly used as a fertilizer and excluded from the use in non-fertilizer applications. Because of the large quantities of energy required to manufacture the thermal acid, its cost has risen considerably, the separation techniques have therefore been developed to purify WPA so that it can replace the thermal acid (Ennaassia et al., 2001). Although most of the precipitated sludge in the WPA can be removed in the clarification stage, a considerable amounts of impurities remained in a soluble form in the acid. Purification of WPA is the goal in the production of some industrial phosphate salts and miscellaneous applications for food, beverage, toothpaste and cleaning markets also require high purity (Kijkowska et al., 2002).

Several methods for purification of WPA were evaluated including precipitation, ion-exchange, liquid–liquid extraction (Chehid Elleuch et al., 2006, Wang et al., 2010, Kumar et al., 2009, Joshi et al., 2009 and Radhikaa et al., 2010) adsorption on activated carbon (Monser et al., 1999) and membrane technologies such as electrodialysis (ED), reverse osmosis and nanofiltration (Gonzalez et al., 2002). Cleaning the WPA from heavy metals was made by precipitation as sulfides (Qafas et al., 2001). Further purification by precipitation of cationic impurities, especially, Fe, Al, Mg, and Ca, is possible. One simple way of removing these cations is to increase the pH of the WPA until the precipitation. David, 1974, tried to remove Mg and small percent of iron and aluminum by mixing the crude H_3PO_4 with hexafluorosilicic acid. However, all precipitation techniques

usually suffer from high P_2O_5 losses accompanied with the solid precipitate making the process economically infeasible.

Iron and cadmium are common impurities in WPA that is produced from phosphate rocks from some origins. Separation of these ions from WPA is difficult and need sophisticated techniques. Most of the iron content in the phosphate rock is dissolved in the WPA. Fertilizer's grade phosphoric acid of 50% P_2O_5 should contain <1.5% Fe_2O_3. Otherwise, the filtration rate of the acid will be low and the water-soluble P_2O_5 content of the prepared fertilizers will be also low. Processing of the high iron Egyptian phosphate concentrates by the dihydrate process produces 50% P_2O_5 acid with about 4 % Fe_2O_3. In our previous works, we could reduce this high iron content to the industrially acceptable limit by precipitation with K_2SO_4 (Abdel-Aal et al.,1999) and controlled the acid filtration rate using surfactants (Abdel-Aal et al., 2007). Cadmium is an extremely toxic element and cause harmful effect on plants, animals and humans. Igneous phosphate rocks contains very little cadmium (<1mg Cd/kg phosphorus) while sedimentary sources contain much higher levels of cadmium (43 to 380 mg Cd/kg phosphorus) (Gowariker 2009). Cadmium transfers from the phosphate rock to the WPA during the acid production. Cadmium as a contaminating element affects a wide variety of living organisms and is accumulated in the human body. Human exposure to Cd can affect pulmonary, kidney, gut and liver functions. Cadmium exposure can also cause common diseases, such as prostate cancer, gastro-intestinal poisoning and bone damage. Since WPA is used in phosphate fertilizers, and intended for use in the food and detergent industries, cadmium can enter the environmental cycle as well. So removal of cadmium from WPA is essential. There are various remedial processes, such as precipitation, ion exchange, solvent extraction and membrane processes which have been used to remove cadmium from WPA. Of these processes, solvent extraction has shown high efficiency (Nazari et al., 2005, Tomaszewska et al., 2007, Alguacil and Alonso 2004). A continuous micro-pilot scale mixer-settler was successfully tested for both extraction and stripping of cadmium from phosphoric acid media using D2EHDTPA in dodecane as extractant (Touati et al., 2009). Mellah and Benachour, 2006, proposed bis-(2-ethylhexyl)-phosphoric acid (D2EHPA) for the recovery of cadmium (II) and zinc(II) from phosphoric acid solution. Cadmium(II) was extracted at a higher pH than zinc(II), which suggested that the separation of zinc(II) and cadmium(II) could be attained by extraction with D2EHPA controlling aqueous pH.

In this paper, separation of Cd^{2+} and Fe^{3+} from phosphoric acid was studied with solvent extraction using trioctylamine (a tertiary amine). The latter is known to work as anion exchanger when be protonated in acidic media. Cadmium (II) and iron (III) have a common properties of formation of anionic chloro species at a specific chloride ion concentration. The main idea behind this work is the enhancement of these metals extraction through promotion of their anionic chloro species in phosphoric acid by

controlling the chloride ion concentration. The different parameters affecting the extraction and stripping processes will be investigated in order to enhance the separation of these two metal ions from phosphoric acid with trioctylamine.

2. Experimental

2.1. Materials

Analytical grade phosphoric acid, H_3PO_4 (85%) and cadmium sulfate, CdSO4 (99%) were provided by Prolabo. Hydrochloric acid, HCl (35%), ferric chloride, $FeCl_3$, and potassium chloride KCl all of AR grade were provided by Merck. Trioctylamine, TOA (Henkel) was used as an active organic extractant. Pure Kerosene (El-Naser Chemical Company, Egypt) was mostly used to dilute the organic extractant. Toluene, xylene, and carbon tetrachloride were supplied by Merck and also used as solvents for the extractant. Normal octanol (Henkel) was used as a modifier. Other chemicals used in this study were of analaytical grade.

2.2. Procedures

Synthetic solutions of phosphoric acid containing heavy metals, 3% iron (estimated as Fe_2O_3) and 40 ppm cadmium, were prepared by dissolving the required weights of $FeCl_3$ and $CdSO_4$ in specific amounts of distilled water as required to dilute the concentrated phosphoric acid to concentrations ranging between 10 to 40% P_2O_5. The concentrations of chloride ion in phosphoric acid were adjusted by dissolving known amounts of concentrated HCl or KCl. The precipitated solids in phosphoric acid after one week aging were separated by filtration, washed with ethanol, dried at 40 ºC in a vacuum drier for 48 hours and then analyzed by Scanning Electron Microscope (SEM) and X-ray Diffraction analysis (XRD). The TOA solutions of different concentrations were prepared by dissolving the measured volumes of TOA in either kerosene, toluene, xylene or carbon tetrachloride.

In solvent extraction experiments, the required volume of the diluted organic extractant was placed in a 250 cm^3 cylindrical glass vessel and a specific volume of an aqueous phase of a solution containing phosphoric acid, iron and cadmium ions was added and the mixture was shacked in a water bath thermostat shaker (GFL Model 1083) for the period of time required. The temperature was set at 27 ºC. After phase separation by centrifugation, a sample from aqueous phase was withdrawn, diluted by distilled water, and used for chemical analysis of Fe, Cd ions and P_2O_5. In stripping experiments, an exact volume of the loaded organic solution was mixed with the required volume of a suitable aqueous solution and shacked in the water bath thermostat shaker. The speciation diagrams of Cd^{2+} and Fe^{3+} in acidic chloride solutions was constructed using *Stabcal*

software developed by Dr. Hsin H. Huang, Department of Metallurgical and Materials Engineering, Montana Tech of the University of Montana, Butte, Montana, USA.

2.3. Measurements

Concentrations of cadmium and iron were measured after dilution with distilled water by an Atomic Absorption Spectrometer, model Perkin Elmer 3100. The crystalline phases present in the dried sample of the precipitated solids separated from phosphoric acid were identified by X-ray diffraction (XRD) on a Bruker axis D8 diffractometer using Cu-K_α radiation. The average crystallite size of the powders was estimated automatically from corresponding XRD data (using X-ray line-broadening technique employing the classical Scherrer formula). P_2O_5 content was determined spectrophotometrically between 460 and 480 nm by the known yellow method (Jeffery et al., 1989).

3. Results and discussion

3.1. Speciation of Cd^{2+} and Fe^{3+} in chloride solutions

It was important to define the forms of Fe^{3+} and Cd^{2+} ions those exist at chloride solutions. This will contribute in controlling extraction of these metals in solvent extraction experiments. Cadmium(II) forms cationic, neutral and anionic chloro-complexes depending on the choride ion concentration. The species present in equilibrium are: Cd^{2+}, $CdCl^{+}$, $CdCl_2$, $CdCl_3^{-}$ and $CdCl_4^{2-}$. The distribution of cadmium ions in chloride solutions was estimated using *Stabcal* software according to their stability constants, and the results are plotted in Fig. 1a. The cationic species Cd^{++} and $CdCl^{+}$ are predominant at very dilute HCl concentrations, where the fractions of neutral, $CdCl_2$, and anionic species $CdCl_3^{-}$ and $CdCl_4^{2-}$ are progressing with increasing the HCl concentrations. At HCl concentrations more than about 1.5 M, only the anionic species are predominant.

The speciation diagram of Fe^{3+} in acidic chloride solutions were constructed using *Stabcal* software and results are presented in Fig. 1b. It can be seen that cationic iron species such as Fe^{3+}, $FeCl^{2+}$, $FeCl_2^{+}$ are predominant at low HCl concentrations and the neutral species $FeCl_3$ is the main one at moderate to high HCl concentrations. Moreover, the species $FeCl_4^{-}$ is the only anionic form of all and formed at moderate HCl concentrations and became the main one at concentrated HCl solutions. It can be generally noticed that, the formation of anionic iron chlorocomplex, $FeCl_4^{-}$, exists at much concentrated HCl solutions compared with those of cadmium,$CdCl_3^{-}$ and $CdCl_4^{2-}$.

The variation of the form of Fe^{3+} and Cd^{2+} with concentration of HCl can suggest the corresponding variation of the extracted species with trioctylamine (TOA) in this study. The form of the predominant species at a specific Cl^{-} concentration can thus predict the extraction mechanism and the form of the extracted metal ions.

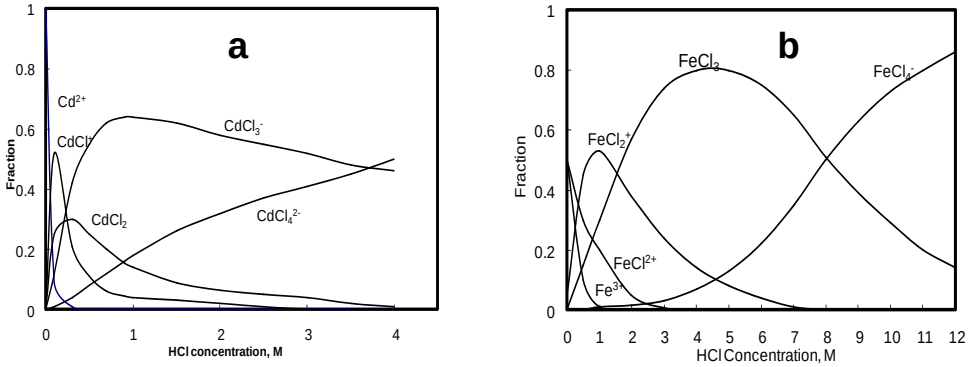

Fig. 1. Speciation diagram of Fe^{3+} and Cd^{2+} at different HCl concentrations

3.2. Effect of chloride ion concentration on extraction of Cd^{2+} and Fe^{3+} with TOA

The extraction of iron and cadmium from 30% phosphoric acid with 20% TOA in kerosene was investigated at different HCl concentrations for 10 minutes and the results are shown in Fig. 2. It is obvious from these results that the extraction of iron is very sensitive to chloride ion concentration and was continuously increasing with increasing the acid concentration. Iron forms the anionic chlorospecies, $FeCl_4^-$, that is extractable to the organic phase with the protonated TOA ($R_3NH^+Cl^-$) through anion exchange mechanism as shown as follows:

$$R_3N + HCl \rightarrow R_3NH^+Cl^-$$

$$R_3NH^+Cl^- + FeCl_4^- \rightarrow R_3NH^+FeCl_4^- + Cl^-.$$

Increasing the HCl concentration favors the formation of the extractable anionic chlorocomplex, $FeCl_4^-$, over the other existing chlorospecies those are noncharged or cationic. This can explain the continuous increase in the extraction of iron by increasing the HCl concentration. At 10% HCl, about 91% of iron was extracted while 14% HCl gave almost complete extraction.

The added amount of HCl to the contaminated phosphoric acid can be optimized to reach the acceptable limit of 1.5% Fe in phosphoric acid. For instance, about 5% HCl can reduce the Fe content to half of its initial amount, i. e., 1.5%. It is worthy to mention that presence of definite amounts of HCl is acceptable in phosphoric acid production industry. The phosphoric acid with the remaining HCl will be neutralized with NH_4OH in the next stages if it is used for production of fertilizers. This will produce mono-ammonium phosphate (MAP) and di-ammonium phosphate (DAP). Neutralization of the contained

HCl content produces NH_4Cl which can be consider as an additional source of nitrogen to the plants.

Another series of experiments was performed at similar conditions but with using KCl, as a source of chloride ions instead of HCl, and the results are also shown in Fig. 2. KCl was selected as it contains K ion which is known as a valuable plant's nutrient and its existence in phosphoric acid is an added value. In this case, the extraction was very slowly increasing with increasing Cl^- concentration (lower than 6%) and then was gradually increasing at higher Cl^- concentrations. The drop in Fe extraction with KCl, compared with that of HCl at lower range of Cl^- concentrations, may be due to the lower acid concentration where the stability of the extractable form of iron $FeCl_4^-$ is lower.

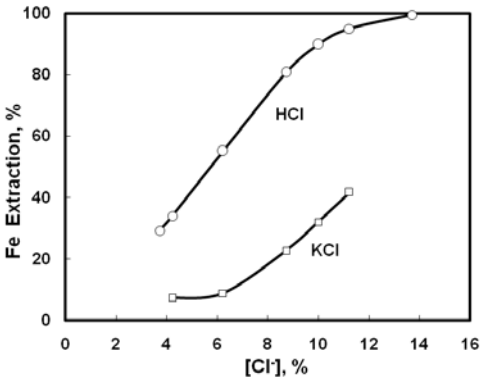

Fig. 2. Effect of HCl and KCl concentrations on extraction of Fe^{3+} from phosphoric acid

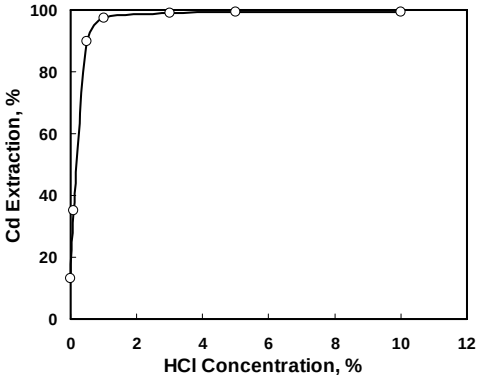

Fig. 3. Effect of HCl concentrations of extraction of Cd^{2+} from phosphoric acid

The effect of increasing HCl concentration on Cd^{2+} extraction showed a sharper increase compared with that of iron at similar experimental conditions (Fig. 3). About 98% of cadmium was extracted using 1% HCl. Only 3% HCl gave almost complete extraction of Cd^{2+}. The easier extraction of Cd^{2+} compared with that of Fe^{3+} can be explained as the anionic chlorospecies of cadmium, $CdCl_3^-$, exist at much lower chloride ion concentration compared with that of iron (see Fig. 1a and ab). That is, at very diluted HCl concentration, such as 0.1%, $CdCl_3^-$ is formed and at more concentrated HCl the form $CdCl_4^{2-}$ is more predominant. However, the only anionic species of iron, $FeCl_4^-$, is formed at much higher HCl concentrations compared to those of Cd^{2+}. The extraction of Cd^{2+} is expected to take place via the following reactions :

$$R_3NH^+Cl^- + CdCl_3^- \rightarrow R_3NH^+CdCl_3^- + Cl^-$$

$$2R_3NH^+Cl^- + CdCl_4^{2-} \rightarrow (R_3NH^+)_2\ CdCl_4^{2-} + 2Cl^-.$$

3.2.1. Identification of the precipitated solids in phosphoric acid

A brownish-black precipitated solids were found in those phosphoric acid samples containing KCl as additive after aging overnight. There was no precipitate at the start but it was growing slowly by time and its amount was found almost unchanged after about 6 days. A sample of these precipitated solids was separated after aging for one week at room temperature of around 25-30 ºC, washed, dried and analyzed by TEM and XRD. The TEM micrograph of the precipitated solids (plate 1) shows well formed hexagonal crystals. The XRD (Fig. 4) shows that the solids are a single crystalline phase of potassium iron phosphate hydrate with the formula $KFe_3P_6O_{20}\cdot 10H_2O$.

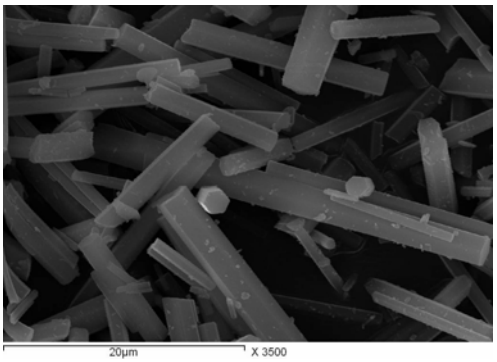

Plate 1: Scanning Electron Microscope micrograph of the precipitated crystalline solids in phosphoric acid after addition of KCl

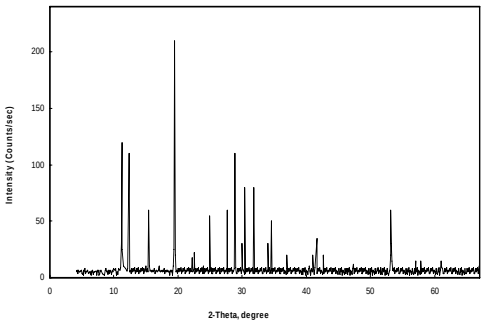

Fig. 4. X-ray diffraction analysis of the precipitated solids in phosphoric acid after addition of KCl

Table 1. EDX weight % of the precipitated solids in phosphoric acid after addition of KCl

Element	Weight, %	Weight, % as calculated from the formula $KFe_3P_6O_{20}\cdot 10H_2O$
O	58.10	53.75
P	21.57	20.82
K	3.23	4.36
Fe	17.10	18.81
H	-----	2.24

The analysis results of the precipitated particles by Energy Dispersive X-ray Spectroscopy (EDX) are given in Table 1. The EDX analysis indicated that the main constituents are phosphorus, oxygen, iron and potassium. The EDX weight percentage of the constituted elements was found close to that calculated from the structure of $KFe_3P_6O_{20}\cdot 10H_2O$. It is obvious that this precipitate, containing important elements such

as P and K, is considered valuable and its discard is not applicable. Apart from the cleaning of iron from the acid, a considerable amount of P_2O_5 and K will be lost in such a precipitate. On the other hand, if the precipitate is left in the acid, it will complicate the following stages of acid concentration and subsequent neutralization for fertilizers production. In the following experiments 10% HCl will be used as a more suitable concentration from the practical point of view.

3.3. Effect of the type of solvent on extraction of Cd^{2+} and Fe^{3+} from phosphoric acid by TOA.

Several types of solvents, namely kerosene, toluene, xylene, carbon tetrachloride those belong to different organic families were tested for dilution of TOA and used for extraction of Cd^{2+} and Fe^{3+} from 30 % P_2O_5 phosphoric acid contained 10 % Cl^- added as HCl. The shaking time was 10 min with organic to aqueous phase ratio of 2: 1. The TOA was completely soluble in all tested solvents. Using different solvents had little effect on the extraction percent of Cd^{2+} and Fe^{3+}. The extraction of Cd^{2+} was ranging from 96% to about 100%, where that of Fe^{3+} is ranging from 87% to 91% for all tested solvents. Carbon tetrachloride gave the lowest extraction, 96% and 87%, where the other three solvents gave extraction ranging around 98-100% and 89-91% for Cd^{2+} and Fe^{3+}, respectively. Kerosene was selected as the suitable solvent as it gives good extraction, has high boiling point, high solubility, low toxicity and it is commercially available with low price.

3.4. Effect of TOA concentration on extraction of Fe^{3+} and Cd^{2+}

The effect of TOA concentration (from 0.1 to 30%) on extraction of Fe^{3+} and Cd^{2+} from 30% P_2O_5 phosphoric containing 10 % Cl^- added as HCl acid is shown in Fig. 5. The shaking time was 10 min with organic : aqueous phase ratio of 2: 1.

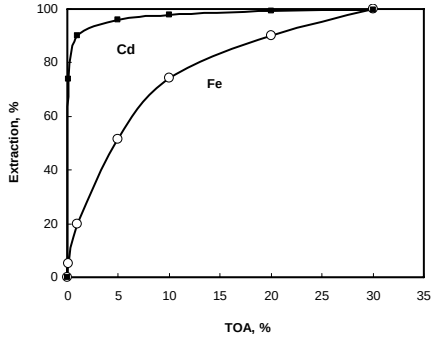

Fig. 5. Effect of TOA concentration on extraction of Cd^{2+} and Fe^{3+} from phosphoric acid

It can be noticed that increasing the TOA concentration increased the extraction percentages of both metal ions. Cadmium(II) was sharply extracted with increasing the TOA concentration at lower range (less than 1% TOA) and then gradually increased, whereas that of Fe^{3+} was gradually extracted along with the TOA concentration. At only 0.1% TOA, the Cd^{2+} extraction reached about 75% but that of Fe^{3+} did not exceed 5%. At 10% TOA the extraction percentages reached 99% and 75% for Cd^{2+} and Fe^{3+}, respectively. Almost complete extraction of Cd^{2+} and Fe^{3+} could be obtained with 30% TOA.

3.5. Effect of mixing time on extraction of Cd^{2+} and Fe^{3+} with TOA

The effect of mixing time on extraction of Cd^{2+} and Fe^{3+} with 20% TOA in kerosene from 30% P_2O_5 acid and 10% HCl is shown in Fig. 6. The extraction of both metal ions is too fast that is about 86% of $Cd^{2+}$and 77% of Fe^{3+} were extracted after only one minute of mixing time. These values increased to 99% and 89%, respectively, after 3 min and very little increased at longer mixing time. These fast kinetics support the metals extraction through the above suggested anion exchange mechanisms. In the following experiments, 10 min was chosen to ensure the maximum values of metals extraction (about 100% and 90% for Cd^{2+} and Fe^{3+}, respectively.

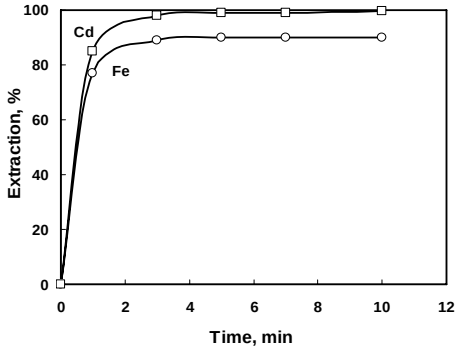

Fig. 6. Effect of mixing time on extraction of Cd^{2+} and Fe^{3+} from phosphoric acid

3.6. Effect of n-octanol concentration on extraction of Fe^{3+} and Cd^{2+}

A third phase formation was observed during the solvent extraction experiments with TOA in kerosene from acidic solutions. This may be due to the limited dissolution of the TOA after protonation when contacted with the acid in aqueous phase. In such case, a modifier can be used to enhance the solubility through a charge interaction with the protonated amine. A long chain alcohol is suitable reagent for this purpose. Preliminary investigation revealed that the third phase can be removed after addition of more than 5%

n-octanol. However, this addition can affect the extraction of Cd^{2+} and Fe^{3+} from phosphoric acid solution. Therefore, we have studied the effect of n-octanol concentration on extraction behavior of Cd^{2+} and Fe^{3+} and results are shown in Fig. 7. The experimental conditions were: 30% P_2O_5 acid, 10% HCl, 20% TOA in kerosene and 10 min mixing time. It is obvious from these results that increasing concentration of n-octanol adversely affect the extraction of both metal ions, especially at n-octanol concentrations more than 5%. This may be attributed to the interaction of n-octanol with the active sites of the TOA extractant. In presence of 10% n-octanol, the extraction reached 98% and 88% for Cd^{2+} and Fe^{3+}, respectively.

3.7. Effect of phosphoric acid concentration on extraction of Cd^{2+} and Fe^{3+} with TOA

A series of experiments was performed to study the effect of phosphoric acid concentration (from 5 to 38%) on extraction of Cd^{2+} and Fe^{3+} with 20% TOA in kerosene and 10% n-octanol for 10 min. The results given in Fig. 8 indicate that increasing phosphoric acid concentrations had little effect on metals extraction. Cadmium(II) extraction was almost unchanged, and that of Fe^{3+} slightly increased. This may be due to the higher stability of the anionic chlorospecies of Fe^{3+} at concentrated acidic solutions.

The dihydrate process firstly produces phosphoric acid of about 28% P_2O_5 (called filter acid) which is further concentrated to about 48-50% P_2O_5 (called conc. acid or commercial acid). In the hemihydrate process, filter acid of around 40% P_2O_5 is directly produced and that will be concentrated if needed. It is worthy to mention that the 50% P_2O_5 acid is viscous and needs filtration to remove the precipitated solids (sludge) before solvent extraction. Viscous liquids are not favored in solvent extraction mainly due to phase separation problems. These encouraged us to suppose that the separation of impurities could be simpler from acids with about 40% P_2O_5 as maximum concentration to avoid inconveniences. The purified acid can then be concentrated to the desired P_2O_5 concentration.

3.8. Stripping of Cd^{2+} and Fe^{3+} from Loaded TOA

It is clear from the above investigation that the key factor for the uptake of the two metal ions to the organic phase is the extent of formation and stability of their anionic chlorocomplexes in the aqueous phase. Higher concentration of acidic chloride solutions enhanced the metal ions extraction. Thus, contacting the loaded organic phase with aqueous solutions free of chloride ions may favor the release of the metal ions from the organic phase to the aqueous phase. Most of the two metal ions can be easily stripped by contacting the loaded TOA with water but emulsion formation was observed and the phase separation was difficult. In slightly acidic solutions, no emulsion phase was

observed during stripping. The stripping of the two metals from 20% TOA in kerosene and 10% n-octanol was examined using stripping solutions with different nature and acidities.

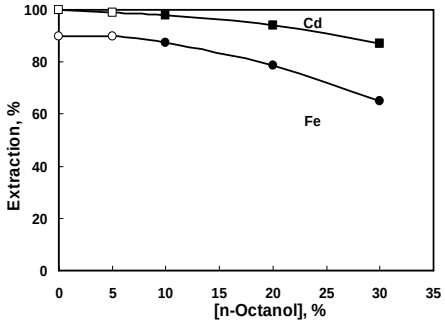

Fig. 7. Effect of n-octanol concentration on on extraction of Cd^{2+} and Fe^{3+} with TOA in kerosene from phosphoric acid. Open: third phase and closed: no third phase

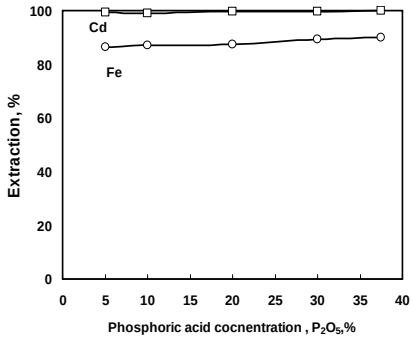

Fig. 8. Effect of phosphoric acid concentration extraction of Cd^{2+} and Fe^{3+} with TOA

Table 2. Stripping of Cd^{2+} and Fe^{3+} from TOA with different solutions and acidities

Nature of stripping solutions	Equilibrium pH	Stripping, %	
		Cd	Fe
Hydrochloric acid	0.5	1.5	7.6
Hydrochloric acid	1.0	3.0	18.7
Hydrochloric acid	1.5	2.0	28.5
Perchloric acid	0.00	93.5	85.2
Perchloric acid	0.30	90.1	90.3
Phosphoric acid	0.50	74.3	94.2
Phosphoric acid	1.21	63.9	95.6
Water	2.39	54.5	96.2

Hydrochloric, perchloric, phosphoric, acetic acids and water were examined and results are given in Table 2. The mixing time was 10 min and the organic to aqueous phase ratio was 1: 2. Dilute hydrochloric acid solutions did not strip any significant amount of Cd^{2+}, where, the maximum stripped amount of Fe^{3+} was about 28%. In contrast, dilute perchloric acid could strip more than 90% of the two metal ions. In dilute phosphoric acid the maximum stripping were 74% and 94% for Cd^{2+} and Fe^{3+}, respectively. In distilled water, only about 55% of Cd^{2+} could be stripped and that of Fe^{3+} was 96% where the

equilibrium pH reached 2.4. The P_2O_5 concentrations were analyzed in the stripping solutions after the experiments. A small amount of about 1% at maximum of phosphoric acid was found lost in the strip solutions.

4. Conclusion

Cadmium and iron are common impurities in wet process phosphoric acid (WPA). These metal ions considered undesirable in the WPA due to technological and hazardous effects and their minimization to the acceptable levels is essential. Solvent extraction is one of the very promising techniques for this purpose. Iron and cadmium can form anionic chlorocomplexes in chloride solutions. When these anions are contacted with organic anion exchanger such as protonated trioctylamine, they could be separated to the organic phase. This phenomena was investigated in this work. It was found that the extraction of both metal ions is very sensitive to the content of HCl in phosphoric acid. Increasing the HCl promoted the formation of chlorospecies of iron and cadmium and hence enhanced their extraction. The extraction parameters were optimized to achieve highest possible uptake of the two metal ions. The extraction was quite fast, that is almost complete extraction of Cd^{2+} and about 90% of Fe^{3+} was achieved within only 3 minutes.

Acknowledgement

The author wish to thank Taif University, Deanship of Scientific Research, for support of this work under Project no. 1/1431/874.

References

Abdel-Aal E. A., Ibrahim I. A., Mahmoud M. H. H., El-barbary T. A., Ismail A. K., Iron Removal from Wet-Process Phosphoric Acid by Sludge Precipitation, Minerals and Metallurgical Processing, 16 (1999) p. 44,.

Abdel-Aal E.A., Mahmoud M.H.H., El-Shall H., Ismail A.K., Increasing the filtration rate of phospho-gypsum using surfactant, Hydrometallurgy 85 (2007) p. 53.

Alguacil F.J., Alonso M., Transport of cadmium from a mixture of HCl and H_3PO_4 using phosphine oxides (Cyanex 921 and Cyanex 923) as carriers: the influence of the membrane diluents (Exxsol D100 and Solvesso 100), Hydrometallurgy 74 (2004) p. 195–202.

Chehid Elleuch M.B., Amor M.B., Pourcelly G., Phosphoric acid purification by a membrane process: electrodeionization on ion-exchange textiles, Sep. Purif. Technol. 51 (2006) 285–290.

David G., US Patent 3,819,810 (June 25, 1974).

Ennaassia E., Qafas Z., El Kacemi K., Edelahi M.K., Simultaneous removal of Cd2+ and As(III) from phosphoric acid solutions by coprecipitation of CdS and As_2S_3 with Na_2S, Sci. Lett. 3 (3) (2001) 1–14.

Gonzalez M.P., Navarro R., Saucedo I., Avila M., Revilla J., Bouchard C., Purification of phosphoric acid solutions by reverse osmosis and nanofiltration, Desalination 147 (2002) p. 315–320.

Gowariker V., The Fertilizer Encyclopedia, John Wiley & Sons, 2009, p.95.

Jeffery G. H., Bassett J., Mendham J., Denney R. C., Vgel's Text Book of Quantitative Chemical Analysis, fifth edition, Longman Scientific & Technical, UK, 1989 p. 702.

Joshi J.M., Pathak P.N., Pandey A.K., Manchanda V.K., Study on synergistic carriers facilitated transport of uranium(VI) and europium(III) across supported liquid membrane from phosphoric acid media, Hydrometallurgy 96, 2009,p. 117–122

Kijkowska R., Pawlowska-Kozinska D., Kowalski Z., Jodko M., Wzorek Z., Wet process phosphoric acid obtained from kola apatite. Purification from sulphates, fluorine and metals, Sep. Purif. Technol. 28 (2002) 197–205.

Kumar Singh S., Dhami P.S., Tripathi S.C., Dakshinamoorthy A., Studies on the recovery of uranium from phosphoric acid medium using synergistic mixture of (2-Ethyl hexyl) Phosphonic acid, mono (2-ethyl hexyl) ester (PC88A) and Tri-n-butyl phosphate (TBP), Hydrometallurgy 95, 2009, p. 170–174

Mellah A., Benachour D., The solvent extraction of zinc and cadmium from phosphoric acid solution by di-2-ethyl hexyl phosphoric acid in kerosene diluents, Chemical Engineering and Processing 45 (2006) p. 684–690.

Monser L., Ben Amor M., Ksibi M., Purification of wet phosphoric acid using modified activated carbon, Chem. Eng. Process. 38 (1999) 267– 271.

Nazari K., Ghadiri A., Babaie H., Elimination of cadmium from wet process phosphoric acid with Alamine 336, Minerals Engineering 18 (2005) p.1233–1238.

Qafas E.E.Z., El-Kacemi K., Edelahi M.C., Simultaneous removal of Cd^{2+} and As(III) from phosphoric acid solutions by co-precipitation of CdS and As_2S_3 with Na_2S, Sci. Lett. 3 (2001) 3.

Radhikaa S., Nagaphani Kumara B., Lakshmi Kantama M., Ramachandra Reddy B. , Liquid–liquid extraction and separation possibilities of heavy and light rare-earths from phosphoric acid solutions with acidic organophosphorus reagents Separation and Purification Technology 75 (2010) p. 295–302.

Schrödter K., Bettermann, G. Staffel T., Klein T., Hofmann T., Phosphoric Acid and Phosphates. Ullmann's Encyclopedia of Industrial Chemistry, sixth ed., Wiley-Vch, D-69451 Weinheim, Germany, 1998.

Slack V, Phosphoric Acid, 1, Marcel Dekker, New York, 1968.

Tomaszewska M., Borowiak-Resterna A., Olszanowski A., Cadmium extraction from chloride solutions with model N-alkyl- and N,N-dialkyl-pyridine carboxamides, Hydrometallurgy 85 (2007) p. 116–126.

Touati M., Benna-Zayani M., Kbir-Ariguib N., Trabelsi-Ayadi M., Buch A., Grossiord J.L., Pareau D., Stambouli M., Extraction of cadmium (II) from phosphoric acid media using the di(2-ethylhexyl) dithiophosphoric acid (D2EHDTPA): Feasibility of a continuous extraction-stripping process, Hydrometallurgy 95 (2009) p.135–140.

Treitler T.L., Bunin D.S., Phosphoric acid purification, US Patent 3,379,501 (April, 1968).

Wang L., Long Z., Huang X., Yu Y., Cui D., Zhang G., Recovery of rare earths from wet-process phosphoric acid, Hydrometallurgy 101 (2010) p. 41–47.

Physicochem. Probl. Miner. Process. 47(2011) 41-50
www.minproc.pwr.wroc.pl/journal/

Physicochemical Problems of Mineral Processing
ISSN 1643-1049

Received March 3, 2011; reviewed; accepted April 11, 2011

Beneficiation of quartz waste by flotation and by ultrasonic treatment

Ferihan GOKTEPE *, Halil IPEK ** , Mustafa GOKTEPE ***

* Balıkesir University, Balıkesir Technical College, Mining Department, Balıkesir, Turkey, ferihangoktepe@gmail.com, Tel : +90 266 2496900, Fax: +90 266 6121164
** Osmangazi University, Engineering Faculty, Mining Engineering Department, Eskisehir, Turkey
*** Balıkesir University, Science and Literature Faculty, Physics Department, Balıkesir, Turkey

Abstract. Quartz is one of the most important industrial minerals used in glass and ceramic industries and high quality quartz are preferred. Impurities from quartz are usually removed by magnetic separation or flotation. This study is concerned to beneficiate the quartz from the quartz plant waste from Aydın-Çine region in Turkey by flotation and by ultrasonic bath treatment. The material with 94.8% Si is removed as a waste in the plant, after washing, grinding and classifying were applied. Flotation experiments showed that SiO_2 content increased to 98.3% with 80% recovery after removing the -53 micrometer size fraction by desliming. When ultrasonic bath treatment is applied the SiO_2 content increased from 94.8% to 99.2% after - 106 micrometer (30%) was removed as a slime. Results showed that better results were obtained with ultrasounic treatment. The aim of this study is to recover the quartz from waste and to add an economic value and therefore to reduce the waste stock for the environmental concern.

keywords: quartz, waste, beneficiation, ultrasonic bath treatment, flotation, impurities

1. Introduction

Industrial minerals, such as silica sand, kaolin and feldspars are often contaminated with deleterious impurities particularly in the form of iron, titanium and aluminium oxides. These industrial minerals are mainly used as raw materials for the production optical fibres, glass, ceramics and refractory materials. High quality quartz containing minor amount of iron and aluminium oxides are preferred. The specifications for different uses of silica sand are summarised in Table 1 (Chammas et al. 2001).

Iron minerals are generally separated from quartz by combination of magnetic separation and flotation process that feldspar is removed from quartz sands by a conventional froth flotation process by using amines as a collector and hydrofluoric acid as an activator which is harmful for the environment (Ozkan et al. 2001). In the literature, flotation of sand sample was subjected to sulfonate flotation to obtain sand concentrate having 0.11% Fe_2O_3 with 68% sand recovery (Önal et al. 2002). The other

study was also showed that using sulfonate type of reagents at pH 3 resulted a 99.5 % SiO_2 with 86% recovery and Fe_2O_3 content was decreased to 0.056 % by flotation after removing below 0.106 mm as a slime (Bayat et al. 2001). Vieira et al. (2007) has showed that particle size, even in a very narrow range, is very important for flotation results of quartz.

Table 1. Specifications of silica sand for different uses (Chammas et al. 2001)

Uses	Particle size (μm)	Chemical Composition
Glass-grade	100-600	SiO_2 98.5-99%, Al_2O_3 0.2-1.6%, Fe_2O_3 (<0.18% glass container) and Fe_2O_3 <0.04% (flat glass)
Fist Glass grade		SiO_2 99.8 %, < Al_2O_3 0.1 %, Fe_2O_3 <0.02 %
Optical Glass		Fe_2O_3<10 ppm
Optical Fibers		Fe_2O_3<1 ppm
Ceramic Grade	<75	SiO_2 97.5 %, Al_2O_3 < 0.55 %, Fe_2O_3 <0.2 %
Higher Premium ceramics	<45	Fe_2O_3 <100 ppm
Refractories		SiO_2 >97 %, Al_2O_3 < 0.1%, Fe_2O_3<0.2 %, alkalies <0.3%
Foundry Grade		SiO_2 98.6.-99.6 %, Al_2O_3 0.08-0.5 %, Fe_2O_3 <0.0.3 %

On the other hand, the use of high power ultrasonic in industrial processes has increased last decade and the use of ultrasonic cleaning baths ranging from the small laboratory to large industrial cleaning tanks of several kilowatts is well known. Ultrasonic vibrations activate or accelerate many processes in liquid systems. The frequency range of 20-100 kHz is the most commonly used. Ultrasonic energy is form of mechanical vibration energy, propagates as waves through all material media including solids, liquids and gasses at characteristic velocity. Ultrasonic power can be applied externally as in a cleaning bath or by the insertation of an ultrasonic horn (solid probe) into slurry itself. Ultrasonic waves require only a liquid phase to transmit its energy to another system without the necessity of a special attribute that is the main benefit of ultrasound. Sound travels through a fluid as a three-dimensional pressure wave consisting of alternating cycles of compression and rarefaction. The rarefaction cycle is in the form of a negative pressure and the following compression cycle is a sudden burst of large and localised energy. The alternating behaviour of these cycles are known as the cavitation process, imposes significant effect on any solid phase within the liquid (Farmer et al. 2000; Önal et al. 2003; Altun et al. 2009). Numerous researchers evaluated ultrasound in chemical processes for cleaning of metal surfaces, acceleration of sedimentation and dewatering processes, waste water treatment and metal precipitation. One substantial benefit of ultrasonics in mineral processing can be the removal of surface coatings of clay and iron oxides from mineral surfaces. This is mainly achieved through the large, but very localised, forces produced by cavitation. Cavitation occurred by ultrasonic energy is a phenomenon of microbubble formation due to the degassing and change of phase to vapours. The

microbubbles are formed on the surface of the solids and assist in the separation of the solid and liquid due to the formation of gas liquid surfaces much lower surface energy compared to solid liquid surface (Farmer et al. 2000; Önal et al. 2003). The effect of energy released by cavitation is to help clean the surfaces of minerals suspended in slurry. Ultrasound can be used as a single process or as a pretreatment process or a combination with one of mineral processing techniques, such as to improve efficiency and/or selectivity of the flotation process (Cilek et al. 2009). Ozkan (2002) has found that applying ultrasound as a pre-treatment process or simultaneous treatment during magnesite flotation had positive effect. Also Ozkan and Kuyumcu (2006) and Altun et al. (2009) showed that ultrasonic coal and oil shales flotation yields more combustible recovery and lower ash values in concentrates than conventional flotation. Qi and Aldrich (2002) demonstrated that ultrasonic treatment is expediting precipitation, enhancing reagent adsorption and promoting the mechanical removal of the zinc hydroxide from the surface of the gypsum particles. The application of sonication to the reduction of iron oxide in a silica sand from 0.025% to less than 0.012% Fe_2O_3 is presented and the ultimate reduction in iron oxide contamination is reported to be dependent on the sonication power (Farmer et al. 2000). Önal et al. (2003) have showed that when ultrasonic treatment was applied during the sedimentation, it positively affected the sedimentation of clay and increased the settling rates by lowering the settling time. Ipek et al. (2001) and Sonmez et al. (2004) demonstrated that marketable product with high grade boron was obtained by ultrasonic sound waves as a process or as a pre-treatment before the magnetic separation. It has also been noted that ultrasonic treatment can be easily used at non-laboratory conditions with ultrasonic inducers and horns working at low power consumption. Although the investment expenses might be high for ultrasonic beneficiation but energy and operating costs are reported to be very low (Sonmez et al. 2004).

In this study, quartz tailing was experimented by using two different methods to compare them for removal of impurities. Reasonably high SiO_2 content was obtained from this sample with both methods and obtained material is suitable for a wide range of applications such as glass making.

2. Material and methods

2.1. Material

The material is a waste material of plant from Aydın–Çine region in Turkey. After crushing, grinding, classifying and washing were applied, about 1000 ton/year material is removed as a waste. The sampe was analysed with X-ray Floresans Spectrometry by Cam-Ser A.Ş. The chemical analyses of material are shown in Table 2 that sample contains 94.8 % SiO_2 and main impurities are Al_2O_3 with about 3% and other alkalies. All impurities % increased as size fraction decreased. Table 2 also

shows the sieve analyses of the sample that 80% of the sample is below 425 micrometer and 8% is below 38 micrometer.

Table 2. Sieve and XRF analyses of sample

Size (micrometer)	Weight (%)	SiO_2 (%)	Al_2O_3 (%)	Fe_2O_3 (%)	TiO_2 (%)	CaO (%)	MgO (%)	Na_2O (%)	K_2O (%)	LOI (%)
+850	6.00	98.81	0.55	0.045	0.008	0.05	0.04	0.07	0.12	0.31
-850+600	4.26	98.60	0.57	0.102	0.011	0.07	0.11	0.07	0.17	0.30
-600+425	7.68	98.66	0.60	0.078	0.011	0.06	0.17	0.07	0.17	0.18
-425+300	11.15	98.63	0.65	0.054	0.010	0.05	0.09	0.09	0.24	0.19
-300+212	14.47	98.16	0.93	0.054	0.016	0.05	0.04	0.15	0.36	0.24
-212+150	13.99	97.07	1.61	0.067	0.018	0.06	0.05	0.39	0.48	0.26
-150+106	13.47	94.79	2.97	0.381	0.025	0.08	0.06	0.97	0.62	0.10
-106+75	9.57	91.73	4.86	0.141	0.032	0.12	0.10	1.77	0.85	0.40
-75+53	6.52	88.75	6.45	0.226	0.047	0.21	0.23	2.18	1.12	0.77
-53+38	4.89	87.58	6.98	0.284	0.071	0.26	0.38	2.26	1.27	0.92
-38	8.00	83.83	9.72	0.091	0.162	0.12	0.42	1.45	1.81	2.04
Head	100.00	94.81	2.94	0.137	0.035	0.09	0.06	0.77	0.62	0.54

2.2. Flotation

Before the flotation tests, the sample was stirred, washed and then sieved on a 53 micrometer sieve and about 15% of slime was removed by this process. The analysis of the washed sample is shown in Table 3. This shows that SiO_2 content increased from 94.8% to the 97%, so that all impurities decreased. Therefore, flotation tests were applied to the washed sample. The particle size was below 425 micrometer in flotation experiments. Experiments were carried out in bench scale of 1 dm^3 Denver type flotation cell. At the begining of flotation, pulp is stirred at 900 rpm and 3 minutes of conditioning time was given for the reagents. Na Oleat was used as a collector for impurities and clay minerals at 2000 g/t dossages and 50 g/t pine oil was added as a frother. Flotation was performed for 10 minutes at 1200 rpm stirring rate. Flotation was performed at natural pH and no adjustment has been done.

Table 3. The analysis of washed sample

SiO_2, %	Al_2O_3, %	Fe_2O_3, %	TiO_2, %	CaO, %	MgO, %	Na_2O, %	K_2O, %	LOI, %
97.07	1.64	0.058	0.019	0.07	0.03	0.50	0.41	0.20

2.3. Ultrasound

Ultrasound was used as an alternative method to remove the surface coating of slime and clay type minerals from the quartz surface and beneficiate the quartz.

Ultrasonic bath experiments were performed in a stainless steel tank with 12 transducers in 400x300x450 mm dimensions and power supply with 500 W. Basically, in the ultrasonic bath an electrical current produced with high frequency a voltage by applying to crystals with piezoelectric properties that is obtained by high frequency vibrations. In the experiments, the tank was filled up to the determined level and it was run for 10 minutes to reduce the amount of solvent air and sample was added. Experiments were performed with 25% pulp density and 15, 30, 45, 60 minutes ultrasonic treatment time were chosen to see the effect of residence time to obtain optimum time. Then, pulp was screened through a series of sieves and sieve fractions dried, weighed and analysed.

Economical implication of the both processes in terms of practicality were not considered and the way of application of ultrasonic at industrial scale are not discussed in this paper, only laboratory test results are presented here.

3. Results and discussion

3.1. Flotation

Flotation tests were performed to float impurities from quartz. Flotation results are shown at Table 4 where first results are belong to 30% pulp density and second results are belong to 18% pulp density. Table 4 shows that 22% of sample was collected as a froth product with 4.84 % Al_2O_3 and 0.16 %Fe_2O_3 and 1.71 % Na_2O at 30 % pulp density. Therefore the non-float product was obtained with 80% recovery with 98.4% SiO_2 content and substantial amount of Al_2O_3 and Fe_2O_3 and Na_2O removal was achived. But if 15% slime removal was also taken into account, overall recovery is 65%, which is low.

Özkan et al. (2001) obtained 99.4% SiO_2 with 83% recovery with NaOleat but it was a two stage flotation experiments where dodesil amin asetat (DAA) was also used as a second collector. When pulp density was reduced to 18%, lower grade and lower recovery was obtained and therefore this not improved the results.

Table 4. Flotation results

Products	Grade, %								SiO_2 Distribution, %
	Wt. %	SiO_2	Al_2O_3	Fe_2O_3	TiO_2	CaO	Na_2O	K_2O	
1.Float	21.8	92.34	4.84	0.162	0.048	0.14	1.71	0.76	20.77
1.Non-float	78.2	98.39	0.74	0.029	0.011	0.050	0.16	0.31	79.23
Feed	100	97.07	1.64	0.058	0.019	0.07	0.50	0.41	100.0
2.Float	25.4	95.47	2.63	0.126	0.026	0.09	0.77	0.53	24.95
2.Non-float	74.6	97.61	1.30	0.035	0.016	0.063	0.41	0.37	75.05
Feed	100	97.07	1.64	0.058	0.019	0.07	0.50	0.41	100.0

3.2. Ultrasound

Table 5 shows the SiO_2 grade of fractions and their distribution for the 0, 15, 30, 45 and 60 minutes of ultrasonic treatment. With or without any treatment SiO_2 content decreased as size fractions decreased. Without ultrasound application maximum SiO_2 content was 98.8% with maximum size fractions, +850 micrometer. When 15 minutes ultrasonic treatment was applied 99.4% SiO_2 was obtained with the fraction of -600+425 micrometer. When 60 minutes ultrasonic treatment was applied, 99.52% SiO_2 was obtained with the same fraction. When all treatment time was considered SiO_2 content decreased at -75 micrometer while +75 micrometer SiO_2 content increased. The mechanism of ultrasounic cavitation show that fine clay particles and iron oxides were removed from the quartz particle surface by the pull a part effect of ultrasonic sound waves.

Table 6 presents the Al_2O_3 content and distribution for all sieve fractions for 0, 15, 30, 45 and 60 minutes of ultrasound application. As size fraction decreased, Al_2O_3 content increased and, depending on the application time, about 35-45% of Al_2O_3 accumulated in below 38 micrometer size fraction. These results demonstrate that ultrasonic waves provide the dispersion in the pulp and contributed to removal of fines and clays out of quartz particles.

Table 7 demonstrates the Fe_2O_3 contents and distributions of all size fractions for 0, 15, 30, 45 and 60 minutes residence time. It shows that without ultrasound application Fe_2O_3 distribution was 38% in the -150+106 micrometer size fraction, but with application of ultrasound it decreased to 6%. It could be seen that 50-65% of Fe_2O_3 was concentrated on the -38 micrometer fraction which was 5% without ultrasound application. These results show that applying ultrasonic treatment enhanced the removal of iron oxides, from the quartz surface, especially from -150+106 micrometer fraction.

It can be seen from Tables 5, 6 and 7 that below 106 micrometer the Fe_2O_3 and Al_2O_3 contents are higher and as expected SiO_2 content is lower. Therefore if below 106 micrometer is separated, which is about 30% of the sample, than 70% of the sample with 99.2 % SiO_2 product could be obtained as a concentrate and below 106 micrometer fraction can be evaluated as tailings.

Figures 1, 2 and 3 are drawn to show the SiO_2, Al_2O_3, Fe_2O_3 content versus ultrasonic treatment time with +106 micrometer fraction which is evaluated as concentrate. Figure 1 shows the SiO_2 content for different ultrasonic treatment time. This shows that fines and clay particles were removed from quartz surfaces by using ultrasound waves and then by seiving efficient separation of quartz from the impurities was obtained.

It is also clear that as pulp's residence time in the ultrasound tank was increased SiO_2 content increased as well. But increasing the residence time to 60 minutes did not improve the results and similar results were obtained as 45 minutes. Fig. 2 demonstrates that Al_2O_3 content for different ultrasonic treatment time. Al_2O_3 content is reduced by application of ultrasound, but increasing the treatment time did not

improve the results and almost similar results were obtained for all residence time, only with 60 minutes residence time it increased slightly. Fig. 3 shows the Fe_2O_3 content of sample with treatment time. It could be seen that as treatment time increased a cleaner product have been obtained, but increasing it from 45 minutes to 60 minutes did not improve the results on the contrary Fe_2O_3 content is slightly increased.

These figures showed that ultrasound application time is certainly an important factor removal of impurities from the quartz particles and could be said that optimum time is 45 minutes for this particular waste material.

Table 5. SiO_2 content of sample with ultrasonic treatment

Size	SiO_2 Grade (%)					SiO_2 Distribution (%)				
Fraction	Ultrasound treatment time (minutes)					Ultrasound treatment time (minutes)				
(μm)	0	15	30	45	60	0	15	30	45	60
+850	98.81	99.24	99.33	99.34	99.33	6.25	6.55	6.84	6.05	6.21
-850+600	98.60	99.23	99.23	99.29	99.30	4.43	4.28	3.92	4.15	3.61
-600+425	98.66	99.39	99.44	99.48	99.52	7.99	8.27	7.81	7.96	7.18
-425+300	98.63	99.25	99.22	99.37	99.37	11.60	10.79	10.65	11.24	10.45
-300+212	98.16	98.95	99.09	99.06	99.03	14.98	13.74	13.60	14.22	15.26
-212+150	97.07	98.40	98.53	98.49	98.63	14.33	14.13	15.52	14.65	15.42
-150+106	94.79	97.54	97.57	97.34	97.36	13.46	13.44	13.39	13.88	17.05
-106+75	91.73	93.51	94.72	94.64	94.69	9.26	9.53	9.26	8.21	7.97
-75+53	88.75	86.61	87.32	87.00	87.33	6.11	4.86	5.41	5.79	4.77
-53+38	87.58	85.49	85.36	86.59	85.81	4.52	5.91	3.83	3.76	3.95
-38	83.83	81.35	80.70	80.85	80.44	7.07	8.63	9.99	10.27	8.69
Head	94.81	94.81	94.81	94.81	94.81	100.0	100.00	100.00	100.00	100.0

Table 6. Al_2O_3 content of sample with ultrasonic treatment

Size	Al_2O_3 Grade (%)					Al_2O_3 Distribution (%)				
Fraction	Ultrasound treatment time (minutes)					Ultrasound treatment time (minutes)				
(μm)	0	15	30	45	60	0	15	30	45	60
850	0.55	0.22	0.18	0.18	0.21	1.12	0.47	0.40	0.35	0.42
-850+600	0.57	0.22	0.18	0.21	0.17	0.83	0.31	0.23	0.28	0.20
-600+425	0.60	0.20	0.18	0.17	0.16	1.57	0.54	0.46	0.44	0.37
-425+300	0.65	0.29	0.24	0.22	0.23	2.46	1.02	0.83	0.80	0.78
-300+212	0.93	0.41	0.34	0.35	0.35	4.58	1.84	1.50	1.62	1.74
-212+150	1.61	0.71	0.66	0.67	0.61	7.66	3.29	3.35	3.21	3.08
-150+106	2.97	1.37	1.37	1.37	1.47	13.60	6.09	6.06	6.29	8.30
-106+75	4.86	2.33	2.32	2.36	2.33	15.83	7.66	7.31	6.60	6.32
-75+53	6.45	3.28	2.86	3.14	2.94	14.31	5.94	5.71	6.75	5.17
-53+38	6.98	3.36	3.42	3.25	3.96	11.61	7.49	4.95	4.55	5.88
-38	9.72	10.40	10.60	10.60	10.70	26.44	35.58	42.35	43.43	37.28
Total	2.94	2.94	2.94	2.94	2.94	100.00	100.00	100.00	100.00	100.00

Table 7. Fe_2O_3 content of sample with ultrasonic treatment

Size	Fe_2O_3 Grade (%)					Fe_2O_3 Distribution (%)				
Fraction	Ultrasound treatment time (minutes)					Ultrasound treatment time (minutes)				
(μm)	0	15	30	45	60	0	15	30	45	60
850	0.045	0.030	0.016	0.022	0.016	1.971	1.371	0.763	0.928	0.693
-850+600	0.102	0.039	0.028	0.032	0.079	3.172	1.164	0.766	0.927	1.989
-600+425	0.078	0.020	0.024	0.018	0.017	4.373	1.152	1.303	0.997	0.850
-425+300	0.054	0.036	0.023	0.018	0.019	4.395	2.709	1.709	1.408	1.383
-300+212	0.054	0.034	0.024	0.019	0.027	5.704	3.268	2.279	1.888	2.879
-212+150	0.067	0.044	0.032	0.025	0.025	6.842	4.371	3.490	2.573	2.704
-150+106	0.381	0.060	0.045	0.045	0.058	37.460	5.724	4.273	4.441	7.028
-106+75	0.141	0.091	0.076	0.072	0.073	9.849	6.416	5.142	4.325	4.252
-75+53	0.226	0.125	0.119	0.121	0.106	10.756	4.863	5.099	5.582	4.008
-53+38	0.284	0.161	0.146	0.135	0.132	10.137	7.709	4.529	4.050	4.211
-38	0.091	0.69	0.71	0.73	0.72	5.314	50.667	60.894	64.208	53.816
Total	0.137	0.137	0.137	0.137	0.137	100.00	100.00	100.00	100.00	100.00

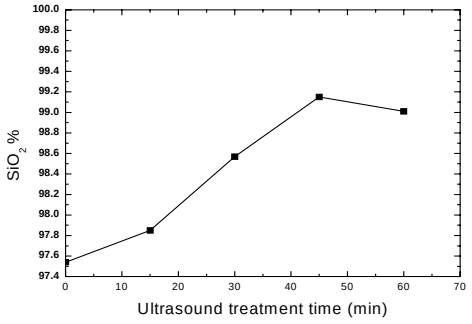

Fig. 1. SiO_2 content versus ultrasonic treatment time with +106 micrometer size fraction

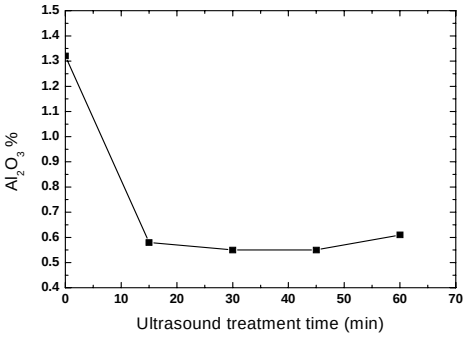

Fig. 2. Al_2O_3 content versus ultrasonic treatment time with +106 micrometer size fraction.

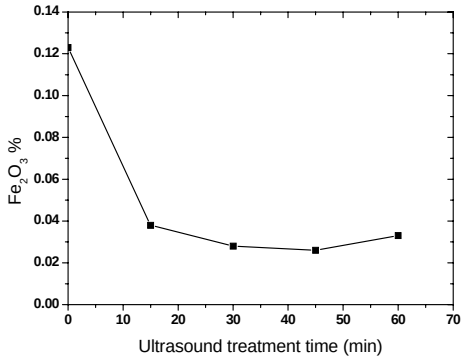

Fig. 3. Fe_2O_3 content versus ultrasonic treatment time with +106 micrometer size fraction

As laboratory study showed that classifying very narrow size fractions did not changed the results but below 106 micrometer SiO_2 content dropped dramatically. Therefore if below 106 micrometer is removed as tailings, totally +106 micrometer can be referred as concentrate with 99.2% SiO_2. If industrial application is considered, -106 micrometer can be removed by hydrocyclones after 45 minutes ultrasound application. Although economical evaluation has not been done it can be easily said that it would be easier and more economical with ultrasound than flotation process.

4. Conclusion

In this study quartz plant waste was used as a sample and by stirring, washing and removing slime has already increased the SiO_2 grade from 95% to 97%. But it is still not suitable for specifications due to high Al_2O_3, Fe_2O_3, TiO_2, Na_2O and K_2O and low SiO_2 content.

To increase the SiO_2 content and decrease the impurities, flotation was performed to the washed sample where 15% of the sample was removed as a slime. Na-Oleat was used as a collector in flotation at natural pH. 80% recovery with 98.3% SiO_2 content was obtained but when 15% slime was added, recovery can be calculated 65%. Although, recovery and grade is relatively low, obtained result is suitable for some certain specification.

When ultrasound was applied to remove the impurities from quartz; Fe_2O_3 content decreased from 0.123% to less than 0.026%, Al_2O_3 reduced from 1.32% to 0.546% and SiO_2 content was increased from 97.54% to 99.20%. If -106 micrometer is separated, 70% of sample with 99.2% SiO_2 can be obtained. The ultimate reduction of a contamination is dependent on ultrasound time and cleaner concentrates were obtained as the residence time was increased. Optimum results were obtained with 45 minutes ultrasonic treatment. The effect of ultrasonic waves on the dispersion of clay particles increased with increasing particle size fraction and ultrasonic waves penetrated better between coarser particles that leading to cleaner concentrates. Therefore, to use the process effectively and make the process beneficial, optimisation of ultrasonic treatment time and particle size are certainly critical factors.

When two methods were compared better grade and better recovery was obtained with ultrasounic treatment than flotation.

As a result, high grade quartz with reasonable recovery has been obtained and impurities-clay particles were removed from the surfaces of particles by using ultrasound waves. Obtained material is glass and foundry grade and suitable for manufacturing of these product.

Acknowledgments

The authors gratefully acknowledges the Cam-Ser A.Ş. for kindly doing the analyses.

References

ALTUN N. E., HWANG J.Y., HİCYİLMAZ C., 2009, Enhancement of flotation performance of oil shale cleaning by ultrasonic treatment, International Journal of Mineral Processing, 91, 1-13.

BAYAT O., VAPUR H., KILIÇ Ö., ASLAN V., AKARSU H. F., 2001, Adana kuvars kumtaşı flotasyonunda Öğütmenin etkisi. 4.Endüstriyel Hammaddeler Sempozyum Kitabı, Editors: H. Köse, V. Arslan, M.Tanrıverdi.

CHAMMAS E., PANİAS D., TAXİARCHOU M., ANASTASSAKİS G.N., PASPALİARİS I., 2001, Removal of iron and other major impurities from silica sand for the production of high added value materials, Proceedings of the 9th Balkan Mineral Processing Congress, İstanbul.

CİLEK E.C. AND OZGEN S., 2009, Effect of ultrasound on separation selectivity and efficiency of flotation, Minerals Engineering, 22, 14, 1209-1217.

FARMER A.D., COLLİNGS A.F., JAMESON G.J., 2000, Effect of ultrasound on surface cleaning of silica particles, International Journal of Mineral Processing, 60, 101-113.

IPEK H., GURSOY H., 2001, Possible use of -3 mm ulexite tailings as marketable product, VI Southernhemisphere meeting on mineral technology, Rio de Janeiro.

ÖNAL G., ÖZER M., ARSLAN F., 2003, Sedimentation of clay in ultrasonic medium, Minerals Engineering, 16, 129-134.

ÖNAL.G., KAYTAZ Y., DOĞAN Z. 2002, Iron removal of Yalıköy Sand Dunes. IX th International Mineral Processing Symposium, Extended Abstracts, Cappadocia/Turkey.

ÖZKAN S.G., 2002, Beneficiation of magnesite slimes with ultrasonic treatment, Minerals Engineering, 15, 99-101.

ÖZKAN Ş., KURŞUN İ., İPEKOĞLU B., 2001. Trakya Bölgesi kuvars kumlarından feldspat uzaklaştırılması için yeni bir flotasyon yaklaşımı. 4.Endüstriyel Hammaddeler Sempozyum Kitabı, Editors:H. Köse, V. Arslan, M.Tanrıverdi, TMMOB.

ÖZKAN S. G., KUYUMCU H.Z., 2006, Investigation of mechanism of ultrasound on coal flotation, International Journal of Mineral Processing, 81, 201-203.

Qİ B.C., ALDRİCH C., 2002, Effect of ultrasonic treatment on zinc removal from hydroxide precipitates by dissolved air flotation, Minerals Engineering, 15, 105-1111.

SONMEZ E., KOCA S., OZDAG H., IPEK H., 2004, Beneficiation of colemanite concentrates from fine wastes by using ultrasound waves, Minerals Engineering, 17, 359-361.

VİEİRA A. M., PERES E.C.A., 2007, The effect of amine type, pH and size range in the flotation of quartz., Minerals Engineering,

Physicochem. Probl. Miner. Process. 47(2011) 51-60
www.minproc.pwr.wroc.pl/journal/

Physicochemical Problems of Mineral Processing
ISSN 1643-1049

Received February 23, 2011; reviewed; accepted April 11, 2011

Partitioning of major and trace elements of a Turkish lignite with size and density

Gulhan OZBAYOGLU

Atilim University, Faculty of Engineering, İncek/Gölbaşi, Ankara, Turkey, gulhan@atilim.edu.tr

Abstract. This research was devoted to determine the concentration and distribution of major and trace elements in a Turkish lignite and to investigate the partitioning behaviour of them in various size and density fractions to estimate the possibility of removal of trace elements by conventional coal cleaning. Three size fractions which were used in industrial coal cleaning processes were chosen. Each size fraction was separated into various density fractions by float and sink tests, which were evaluated for major and trace elements. These tests showed that by applying the same size and density fractions of industrial coal cleaning processes, more than 70% of Mo, Nb, Nd, W, Hg and Zr could be removed, which were approximately equal to the result achieved for ash removal.

keywords: physical coal cleaning, lignite, trace elements, partitioning of trace elements

1. Introduction

Coal is the world's most abundant fossil fuel which is mainly used to generate electricity. Coal contributes about 40% of world's electricity generation. Turkey has 11.6 Pg (petagrams, billion tons) of lignite reserves. The production is around 84 Tg (teragrams, million tons of which 40% of the country's lignite production is washed. Lignite accounts for 20% of country's electricity generation. The quality and properties of the coal used in power plants determines its environmental effect. During combustion, coal-fired plants emissions may cause serious environmental and health risks. Trace elements in coal are important as they are potentially hazardous to human health and ecosystems. Around 25 trace elements are considered to be of environmental interest (Swaine, 2000, Spears et al. 1999). Elements As, B, Cd, Hg, Mo, Pb, Se and S are in the group of major concern in the classification of trace elements by level of concern introduced by the US National Research Council (Clarke and Sloss, 1992). Elements of moderate concern include Cr, Cu, Ni, V, Zn, and fluorine while Ba, Co, Mn, Sb, Sr, Li, Na, Ge, and Br are in the group of minor concern. Every trace element may be associated, to some extent, with the inorganic or organic matters of coal (Liu et al., 2004). The major elements which constitute the mineral matter of coal are shown by their oxides in the chemical analysis. They

consist of SiO_2, Al_2O_3, Fe_2O_3 and CaO and little amounts of P_2O_5, Na_2O, K_2O and TiO_2 at which many valuable and/or hazardous trace elements are concentrated.

Most of the trace elements in coal are associated with three major minerals: pyrite, kaolinite and illite. The inorganic matters in coal, including trace elements, are not uniformly distributed, either in particle size or density fractions. Besides, they behave differently in physical separation and in combustion. Each trace element is different in its modes of occurrence and concentration (Song et al. 2007; Spears et al.1999; Solari et al. 1989; Gluskoter et al. 1977). If these inorganic matters can be removed from the coal, their associated trace elements should follow. The beneficial aspect of conventional coal cleaning is that, in addition to bulk ash removal, much of the trace element content, notably those associated with sulfide and other minerals, can be removed. Although, there is a general relationship between overall ash and trace elements removal, for individual trace element, the removal percentage is specific to the coal and to the cleaning process used (CAER, 1996; DeVito et al., 1994; Akers, 1995; Swaine, 1998; Conaway, 2001). The partitioning of trace elements has been investigated under the conditions of different coal ranks and coal preparation types (heavy medium, jigging and froth flotation). It was reported that the partitioning behaviour of trace elements are mainly controlled by their modes of occurrence, the distribution forms of its carrier minerals and the cleaning technique types. Tang et al. (2009) supposed that the migration and distribution of the 15 toxic trace elements during coal washing might be controlled by clay minerals and pyrite. The trace elements associated with fine minerals (Pb, U, and Be) and organic constituents (Br) could not be reduced by physical coal cleaning nor can they be enriched in the cleaned coal (Wenfeng et al. 2006).

The objective of this study was i) to determine the concentration and distribution of trace and major elements in a Turkish lignite, ii) to determine the partitioning behaviour of trace elements in coal by size and density used in existing coal preparation plant.

2. Materials and method

The Tertiary age Soma lignite (R_{max} 0.435), which is located in the western part of Turkey, was used in this study. The representative sample was analyzed to determine its ash, moisture, volatile matter, fixed carbon and total sulfur contents as well as its major and trace element contents. XRF and ICP-OES techniques were used in the analyses of major and trace elements. Size and density effects on the partition of major and trace elements were examined by conducting screen analysis on the representative run of mine sample and float-sink tests on three size fractions, namely +50 mm, (-50+18) mm, -18 mm which were chosen in accordance with the sizes normally used in industrial coal preparation plants. Each size fraction was separated in a laboratory vessel to generate sp. gr. levels between 1.3 to 1.9 by the use of $ZnCl_2$. The sink of each size fraction was evaluated for major and trace elements.

3. Results and discussions

3.1. Chemical composition of the sample

Representative sample of Soma lignite consisted of 40.65% ash, 39.97% volatile matter, 0.63% total sulfur and 12.97 MJ/kg heating value on dry basis. Major and trace element contents of the sample are shown in Table 1. Analytical errors were estimated at ≤ 5% for both proximate analysis and major/trace elements. As seen in Table 1, CaO, SiO_2, Al_2O_3 and Fe_2O_3 are the dominant major compounds which are followed by Na_2O, K_2O and MgO. Among the trace elements examined in raw coal, Co, Nb, Ag, Sb and Ce levels are above US coals and Ni, Se, Br, Zr, Mo, Cd, and La levels are below US coals levels (Xu et al., 2004). Trace elements in ten Turkish coal fired power plants showed that the concentration of As, Co Cu, Ga, Mn, Li, Sc, Sn, Ta, Tl and some rare earth elements in coals exceed the currently available ranges for most world coals (Karayigit et al., 2000).

Table 1. Major and trace element contents of representative sample of Soma lignite

Major Elements	%	Trace Elements	ppm	Trace Elements	ppm
Na_2O	1.05	Co	4.19	La	2.00
MgO	0.83	Ni	14.21	Ce	2.00
Al_2O_3	8.25	Se	1.02	Nd	33.61
SiO_2	10.33	Zr	35.50	W	0.74
P_2O_5	0.19	Nb	2.63	Hg	0.79
SO_3	1.61	Mo	0.59	Bi	0.87
K_2O	0.91	Ag	1.68		
CaO	16.03	Cd	2.00		
TiO_2	0.12	Sn	12.93		
MnO	0.02	Sb	4.64		
Fe_2O_3	3.24	Cs	4.00		

3.2. Mineralogical composition

The XRD investigation of the representative sample showed that the minerals in the coal are quartz, carbonate minerals, gypsum, smectite, clay minerals and feldspar. The clay minerals were represented mainly by kaolinite and to a lesser extends illite. As is known, clay minerals and feldspar are transformed into aluminosilicate during combustion. Carbonate minerals were calcite, dolomite and siderite. This agrees with the findings of Karayiğit et al. (2000), who reported a considerable amount of siderite occurrences in Soma coals. During combustion, carbonate minerals are converted into oxides and formed Ca-Mg silicates.

Al_2O_3 was mainly due to the occurrences of kaolinite and feldspar. SiO_2 mostly originated from quartz, as well as feldspar and clay minerals. Dolomite was the main source of MgO, while CaO was derived from calcite, dolomite and siderite.

Screen analysis evaluated for major and trace element contents and distributions are shown in Table 2 and 3.

Table 2. Major elements contents and distributions in screen fractions

Major Elements	Screen Fractions					
	(+50 mm) Weight %:21.59		(-50+18)mm Weight %:26.71		(-18 mm) Weight %:51.70	
	%	%Distrib	%	%Distrib	%	%Distrib
Na_2O	1.14	23.53	1.02	26.05	1.02	50.42
MgO	0.74	19.28	0.84	27.08	0.86	53.64
Al_2O_3	3.15	8.24	7.70	24.94	10.66	66.82
SiO_2	4.22	8.82	10.12	26.15	13.00	65.03
P_2O_5	0.16	18.27	0.21	29.71	0.19	52.01
K_2O	0.29	6.89	0.94	27.65	1.15	65.46
CaO	19.46	26.21	18.74	31.22	13.20	42.57
TiO_2	0.06	10.51	0.16	34.77	0.13	54.72
MnO	0.03	29.41	0.02	23.98	0.02	46.61
Fe_2O_3	3.62	24.09	2.91	23.96	3.26	51.95
SO_3	1.64	21.97	1.38	22.87	1.72	55.16

As indicated in Table 2, major elements in screen fractions showed that the contents of Na_2O, CaO, MnO, and Fe_2O_3 decreased with the decrease in particle size while Al_2O_3, SiO_2 and K_2O contents increased 3-fold in the finest size of screen fractions when contrasted with the coarse size.

When trace elements are concerned, their partition was observed in screen fractions as shown in Table 3. As is seen, most of the trace elements contents and distributions increased with the fineness of the size fractions. Especially, the increase in contents of Nb and Zr are 5- and 3-fold, respectively in the finest fraction than in coarse fraction. It can be observed that more than 60% of Co, Ni, Se, Zr, Nb, Ag and Nd distribution are found in the finest fraction. On the other hand, distributions of Sb and W are more or less uniform in three size fractions. As stated before, the size fractions are the same with the existing coal preparation plant. If the top size of coal

were decreased to liberate inorganic materials, more removal of trace elements in the sinks would be achieved.

In order to determine the density effect on the partition of major and trace elements, float-sink tests were carried out on each screen fraction. The sink products obtained at 1.90 specific gravity of float and sink test of each screen fraction were evaluated in terms of removal of major and trace elements. The results are shown in Table 4 and 5.

When major elements' contents of screen fractions and their +1.90 sp. gr. sink products were compared, it was found that Na_2O, Al_2O_3, P_2O_5, K_2O, SO_3 and Fe_2O_3 contents decreased in the sink products while CaO, SiO_2, MgO, TiO_2 and MnO contents increased. Most of the calcite and dolomite were concentrated in the sink.

Table 3. Trace elements contents and distributions in screen fractions

Trace Elements	Screen Fractions					
	(+50 mm) Weight %:21.59		(-50+18) mm Weight %:26.71		(-18 mm) Weight %:51.70	
	ppm	%Distr	ppm	%Distr	ppm	%Distr
Co	3.0	15.46	3.0	19.13	5.3	65.41
Ni	7.6	11.55	12.6	23.69	17.8	64.77
Se	0.9	18.89	0.8	20.78	1.2	60.33
Zr	14.3	8.70	33.3	25.05	45.5	66.25
Nb	0.7	5.74	2.7	27.42	3.4	66.83
Mo	1.0	36.82	1.0	45.55	0.2	17.63
Ag	0.5	6.44	2.0	31.87	2.0	61.69
Cd	2.0	21.59	2.0	26.71	2.0	51.70
Sn	11.7	19.54	16.1	33.27	11.8	47.19
Sb	6.2	28.77	6.6	37.89	3.0	33.34
Cs	4.0	21.59	4.0	26.71	4.0	51.70
La	2.0	21.59	2.0	26.71	2.0	51.70
Ce	2.0	21.59	2.0	26.71	2.0	51.70
Nd	21.2	13.62	30.9	24.55	40.2	61.83
W	1.0	29.12	1.0	35.54	0.5	34.86
Hg	1.0	27.22	1.0	33.67	0.6	39.11
Bi	1.0	24.92	0.5	15.41	1.0	59.67

Table 4. Major elements distributions in (+1.90) sink products of float–sink tests of screen fractions.

Major Elements	+1.90 sp. gr. sink products of screen fractions					
	(+50mm) Weight % 13.73*		(-50+18) mm Weight % 13.60*		(-18 mm) Weight % 18.00*	
	%	% Distrib.	%	% Distrib.	%	% Distrib.
Na_2O	0.65	8.54	0.83	10.79	0.74	12.74
MgO	1.16	19.22	1.14	18.70	1.00	21.72
Al_2O_3	5.36	8.92	4.98	8.21	5.86	12.79
SiO_2	13.88	18.44	13.81	18.17	15.38	26.79
P_2O_5	0.14	12.77	0.14	12.64	0.14	16.77
K_2O	0.66	9.98	0.62	9.28	0.71	14.07
CaO	33.06	28.31	31.69	26.88	18.88	32.43
TiO_2	0.23	25.73	0.22	24.35	0.22	32.25
MnO	0.05	31.22	0.04	24.43	0.04	32.58
Fe_2O_3	2.63	11.13	2.32	9.72	2.45	13.59
SO_3	0.48	4.09	0.43	4.05	0.53	5.92

*) These weights are given according to the original feed

As seen in the table above, Ni, Se, Zr, Nb, and Nd concentrations (grades) are more in sink products of float and sink tests of different size fractions than original trace elements contents of screen sizes. These trace elements showed the affinity to the inorganic matter. On the other hand, Sb, Co and Bi grades decreased in the sink products, especially in the fine sizes. From the literature survey, no direct evidence was found to support any particular mode of occurrence of antimony in coal. Swaine (1990) asserted that antimony is apparently organically bound in coal which is in good aggrement with our findings. However, Finkelman (1994) indicated that antimony may be found in solid solution in pyrite.

Ogala et al. (2009), Conaway (2001) and Swaine (1990) assert that antimony and beryllium are organically bound in the coal. In most of U.S. coals, arsenic and antimony are mainly associated with mineral matter, especially with pyrite and sphalerite, respectively (Finkelman, 1994). In Chines coal, elements of Br and Ba show a strong affinity to the organic matter, while Cs, Cd, Pb, Zn and Hg are partly associated with organic matter and the other trace elements are mainly associated with

the mineral matter (Wang, 2004). Australian coals contain substantially lower key environmental elements selenium, arsenic and mercury than those most of the international coals (Acarp, 1996). The majority of cobalt and nickel are organically bound, but some associations with mineral matter cannot be excluded (Swaine, 1990; Gluskoter et al., 1977).

When sink is removed at 1.80 sp. gr., the major and trace elements rejections from the sink products of float and sink tests of different size fractions are compared with the sink of 1.90 sp. gr in Table 6 and 7, respectively.

Table 5. Trace elements distributions of +1.90 sp. gr. sink products of float and sink tests of screen fractions

Trace Elements	Screen Fractions					
	+1.90 of (+50 mm) Weight % 13.73		+1.90 of (-50+18)mm Weight % 13.60		+1.90 of (-18 mm) Weight % 18.00	
	ppm	%Distr	ppm	%Distr	ppm	%Distr
Co	3.1	10.06	3.1	9.97	3.11	13.19
Ni	16.5	15.94	16.1	15.42	13.4	17.03
Se	1.3	17.36	1.1	14.55	1.1	19.25
Zr	52.9	20.44	47.5	18.17	49.7	25.22
Nb	3.4	17.85	3.4	17.32	4.3	29.15
Mo	1.0	23.41	0.4	9.28	1.0	30.70
Ag	2.0	13.73	2.0	13.60	2.0	18.00
Cd	2.0	13.73	2.0	13.60	2.0	18.00
Sn	14.1	14.98	15.8	16.65	12.1	16.89
Sb	3.0	8.88	4.7	13.65	3.0	11.64
Cs	4.0	13.73	4.0	13.60	4.0	18.00
La	2.0	13.73	2.0	13.60	2.0	18.00
Ce	2.0	13.73	2.0	13.60	2.0	18.00
Nd	50.3	20.55	42.7	17.28	46.9	25.11
W	1.0	19.07	1.0	18.89	1.0	25.00
Hg	1.0	17.31	1.0	17.15	1.0	22.69
Bi	0.3	4.75	1.0	15.70	1.0	20.78

Trace element removals at 1.90 sp. gr. varied from the lowest percentage of 33.22 for Co to the highest of 64.32% for Nb. For 1.80 sp. gr. the lowest and highest trace element removals were 37.42% for Co and 75.52% for Nd. Trace element rejections above 50% at 1.90 sp. gr. were for Se, Zr, Nb, Mo, Nd, W and Hg. However, at 1.80 sp. gr. most of the trace elements, excluding Bi, Sb and Co, could be removed at a level of above 50%. Wang(2004) found that by physical coal cleaning processes, more than 60% of As and Hg were, and more than 30% of Sb, S, Pb and Cd were removed.

Table 6. Summary of total removal of major elements at +1.90 and +1.80 sp gr. fractions of float and sink tests

Major Elements	Removal in +1.90 sink fraction,%	Removal in +1.80 sink fraction,%
Na_2O	32.07	40.62
MgO	59.64	64.70
Al_2O_3	29.92	35.97
SiO_2	63.40	74.75
P_2O_5	42.18	36.91
K_2O	33.33	39.19
CaO	87.62	93.09
TiO_2	82.33	97.06
MnO	88.23	96.38
Fe_2O_3	34.44	38.92
SO_3	14.06	16.94

Table 7. Summary of total removal of trace elements at +1.90 and +1.80 sp. gr. fractions of float and sink tests

Trace Elements	Removal in +1.90 sink fraction,%	Removal in +1.80 sink fraction,%
Co	33.22	37.42
Ni	48.39	55.18
Se	51.16	56.57
Zr	63.83	73.60
Nb	64.32	75.35
Mo	63.39	72.74
Ag	45.33	51.06
Cd	45.33	51.06
Sn	48.52	54.12
Sb	34.17	37.84
Cs	45.33	63.97
La	45.33	52.26
Ce	45.33	51.06
Nd	62.94	75.52
W	62.96	70.72
Hg	57.15	70.36
Bi	41.23	46.84

4. CONCLUSIONS

The degree of removal of trace elements depends on the mode of occurrence, and on the degree of liberation of the trace element bearing mineral and the specific gravity (density) of the medium. Based on float and sink tests, it was found that more

than 70% of Mo, Nb, Nd, W, Hg and Zr could be removed at 1.80 sp. gr. which were approximately equal to the result achieved for ash (77.78%), showing a high degree of removal due to their association with inorganic matter. From 37 to 50% of Co, Sb and Bi could be rejected, showing a relatively low degree of removal as they show strong association with organic matter. Hence, it will be more difficult for them to be removed by physical coal cleaning method. From 50 to 70% of Se, Ag, Cd, Sn, La, Ce and Ni were removed due to their partial association with the organic matter. As higher trace element rejections can be achieved by removing the maximum possible amount of ash, the trace element removals at + 1.8 sp.gr. are higher than +1.9 sp.gr as the ash removals from the sink fractions were 77.78% against 69.57% at 1.90 sp.gr. The ash contents of cleaned coals were reduced to 18.42% at 1.8 sp.gr and 22.58% at +1.9 sp.gr.

Acknowledgements

The author would like to acknowledge to Dr. Selahaddin Anaç for his permission to perform chemical analyses at the TKI-Soma laboratories.

References

ACARP REPORT, (1996) Trace elements in Coal, Issue No.3, http://www.acarp. com.au/Newsletters/tracelelements.html

AKERS, D.J.(1995) *The redistribution of trace elements during beneficiation of coal, in D.J.Swaine, F.Goodarzi (eds), Environmental Aspects of Trace Elements in Coal, Kluwer Academic Publishing, Netherlands, 93–110*

CLARKE, L.B. and SLOSS, L.L. (1992) *Trace elements-Emissions during coal combustion and gasification, IEA Report IEACR/49,IEA Coal Research, London*

CONAWAY, S.M.(2001), *Characterizing trace element association in the Pittsburgh No.8, Illinois No.6 and Coalburg coal seams, M.Sc Thesis, Virginia Polytechnic Institute and State University, U.S.A.*

DEVITO M.S. ROSENDALE, L.W. and CONRAD, V.B.(1994) *Comparison of trace element contents of raw and clean commercial coals, Fuel Processing Technology, 39, 87–106*

FINKELMAN, R.B.(1994), *Modes of occurrence of potentially hazardous elements in coal: levels of confidence, Fuel Processing Technology, vol.39, Issues 1–3, 21–34*

GLUSKOTER, H.J. RUCH, R.R. MILLER, W.G. CAHILL, R.A. DREHER, G.B. and KUHN, J.K.(1977), *Illinois State Geological Survey, Circular 499*

KARAYİĞİT, A.I. GAYER, R.A. QUEROL, X. and ONACAK, T.(2000), *Contents of major and trace elements in feed coals from Turkish coal-fired power plants. International Journal of Coal Geology 44: 169–184*

LIU,G., VASSILEV, S.V., GAO, L., ZHENG, L., PENG, Z., (2004), *Mineral and chemical composition and trace element contents in coals and coal ashes from*

Huaibei coal field, Energy Conversion and Management, Vol.46, Issue 13-14, 2001-2009

SOLARI, J.A.FIEDLER, H. SCHNEIDER, C.L.(1989) *Modelling of the distribution of trace elements in coal, Fuel 68, 536–539*

SONG, D.YONG, Q. ZHANG, J. WANG, W.and ZHENG,C., (2007), *Concentration and distribution of trace metals in some coals from Northern China, International Journal of Coal Geology, 69, 179-191*

SPEARS, D.A. MANZARANES-PAPYANOPOULOS, L.I. and BOOTH, C.A.(1999), *The distribution and origin of trace elements in a UK coal; the importance of pyrite, Fuel 78, 1671–1677*

SWAINE, D.J.(1990), *Trace elements in coal, Butterworth, London, 278*

SWAINE, D. (2000), *Why trace elements are important, Fuel Processing Technology, 65–66, 21–33*

SWAINE, D.J.(1998) *Trace elements during the mining, and beneficiation of coal, Coal Preparation 19, 3–6, 177–193*

TANG, Y. CHANG, C. ZHANG, Y. LI, W.(2009), *Migration and distribution of fifteen toxic elements during the coal washing of the Kailuan Coalfield, Hebei Province, China, Energy, Exploration and Exploitation, Vol.27, No: 2, 143–152*

WANG, W.F.(2004), *Modes of occurrence and cleaning potential of trace elements in coals from the northern Ordos Basin and Shanxi Province, China, Acta Geologica Sinica-English edition 78, 960–969*

WENFENG, W.YONG, Q. CHONGTAO, W. ZHUANGFU, L. YINHAI, G. YANMING, Z. (2006), *Partitioning of elements and macerals during preparation of Antaibao coal, International Journal of Coal Geology, 68, 223–232*

XU, M.YAN, R. ZHENG, C. QIAO, Y. HAN, J. SHENG, C.(2004), *Status of trace element emission in a coal combustion process: a review, Fuel Processing Technology, vol.85, Issue 2–3, 215–237*

Physicochem. Probl. Miner. Process. 47(2011) 61-78
www.minproc.pwr.wroc.pl/journal/

Physicochemical Problems of Mineral Processing
ISSN 1643-1049

Received February 8, 2011; reviewed; accepted April 11, 2011

Gas entrainment rate and flow characterization in downcomer of a Jameson cell

Tuba TASDEMIR, Adem TASDEMIR, Bahri OTEYAKA

Eskişehir Osmangazi University, Dept. of Mining Engineering, Division of Mineral Processing, 26480, Eskişehir, Turkey, atasdem@ogu.edu.tr, Tel: +90 222 239 37 50 Ext: 3438

Abstract. The Jameson cell which is a new type of gas-liquid contacting device and can be considered as a type of plunging jet column, has been in use worldwide for the separation of fine minerals, coal particles and wastewater treatment etc. Flow characteristics in the downcomer of a Jameson cell are very important since the hydrodynamics of the cell is largely depends on the flow conditions. The hydrodynamics influences flow regimes in the downcomer and hence the gas holdup and bubble diameter are strongly affected by flow conditions. Depending on the air entrainment rate entered to the system, different flow regimes are observed in the downcomer. Bubbly flow which is observed at less air quantities is desired instead of churn-turbulent flow where the gas entrainment rate increase. In this research, the effect of operating conditions including nozzle diameter, downcomer diameter, jet velocity and jet length on gas entrainment rate, Qg , was evaluated experimentally for an air-water system for the bubbly and churn-turbulent flow. Between these factors, downcomer diameter was found to have very little effect on gas entrainment rate while increasing values of other factors had an increasing effect on it. The results were evaluated by forward stepwise linear regression (MLR) and a piecewise regression with Quasi-Newton estimation of breakpoint (PLR) to estimate the flow conditions and gas entrainment rates. The model by PLR was useful to understand the boundary of the flow characteristics since the two equations were valid in a certain air entrainment ranges, i.e. different flow conditions. The model developed was successful to determine the transition region from bubbly flow to churn-turbulent flow. Experimental data were in good agreement with theoretically predicted value.

keywords: gas entrainment rate, Jameson cell, two phase flow, linear regression

1. Introduction

The solution of the flotation problems is increasingly dependent on more precise understanding of the phenomena involved. The separation selectivity and efficiency of the flotation process depends not only on the differences in the

physicochemical surface properties of various minerals but also on the hydrodynamics of flotation. While there is a substantial and rapidly growing literature on flotation surface chemistry, the deep concern of the hydrodynamics of flotation machines has been neglected to a great extent. As a whole, the flotation process depends on the first hand on surface chemistry controls to provide the potential conditions for particle-bubble attachment and then on the hydrodynamic conditions within the flotation machines which actually develop the attachment between particles and bubbles. In the flotation machines, the hydrodynamic conditions are strongly affected by the air quantity entered to the system. Flotation is an interfacial phenomenon which instead of whose performance depends on the availability of bubble surface area. Thus, airflow rate is an important operational parameter in flotation as it determines the bubble surface area flux.

Bubble columns have been applied successfully as high performance gas-liquid contacting devices in industries such as chemical, biochemical, petrochemical, wastewater treatment and mineral processing. A type of confined plunging liquid jet (CPLJ) bubble column – Jameson cell is used as one of such high performance contactors and is type of a downflow bubble column with gas entrainment by a liquid jet. Jameson Cells are now gaining widespread acceptance for multiphase processes, including mineral and coal flotation and wastewater treatment systems because of its self-sucking characteristics of gas phase and efficient dispersion of the gas phase into liquid phase (Evans et al., 1995, 1996; Jameson and Manlapig, 1991; Mohanty and Honaker, 1999; Jameson, 1999; Yan and Jameson, 2004, Şahbaz et al., 2008).

Since the probability and attachment take place in the downcomer zone of Jameson cell, understanding the hydrodynamic properties of the cell is very important. The hydrodynamic conditions are greatly influenced by the amount of air entering to the downcomer. As the air quantity increases within the downcomer, the turbulent conditions get dominant in the system. This causes particle-bubble detachment for especially coarse particles (Taşdemir et al., 2007a; Çınar et al., 2007). The detachment is a result of action of external forces upon the flotation aggregates which are generated by turbulent motions in the flotation machine and concerns especially large and heavy particles with relatively low hydrophobic properties. The probability of occurrence of this event, apart from the above mentioned factors, depends upon the intensity of turbulence of the medium (Brozek and Mlynarczykowska, 2010).

Many authors studied hydrodynamic properties (gas holdup, gas-liquid interfacial area, mass transfer coefficients etc.) of these contactors (Ohkawa et al., 1985, 1986, 1987; Yamagiwa et al., 1990; Evans, 1990; Evans et al, 2001; Liu and Evans, 1998; Atkinson et al, 2003; Mandal et al, 2003, 2005; Bin, 1993; Evans and Jameson, 1995, Taşdemir et al., 2007b). However, a small number of publications are available regarding gas entrainment rate and flow behavior of CPLJ bubble columns which their hydrodynamics are strongly characterized by different flow patterns depending on the gas flow rate (Okhawa et al., 1985, 1986, 1987; Yamagiwa et al., 1990; Evans, 1990; Evans and Jameson, 1995). In these studies, the gas entrainment

rate was correlated to a number of variables including nozzle diameter, jet velocity, jet length, column diameter and the flow characteristics in the column were investigated. Okhawa et al. (1985) studied the flow characteristics of downflow bubble columns with gas entrainment by a liquid jet. They observed that there were four types of flow regimes in the column: bubble stagnant flow, non-uniform bubbling flow, uniform bubbling flow and churn-turbulent flow. Yamagiwa et al. (1990) reported that for downflow bubble column, with increasing liquid velocity in the column, flow behavior changed from non-uniform bubbling flow to uniform bubbling flow and then to churn-turbulent flow. But with further increase of liquid velocity, a uniform bubbly flow was again obtained. They also proposed experimental equations for estimating gas holdup and gas entrainment rate. Evans (1990) comprehensively described the performance of confined plunging liquid jet bubble column. From visual observation of flow states in the column, he was found that there were four flow regimes (bubbly flow, slug flow, churn-turbulent flow and annular flow). Evans and Jameson (1995) examined the hydrodynamics of the both bubbly and churn-turbulent flow in the column. Only a few parameters like gas and liquid flow rates, geometry and construction of the nozzle can be controlled by design and operation of these columns. The decisive parameters like gas holdup, gas-liquid interfacial area and mass transfer coefficients are not directly adjustable. Consequently, design and scale-up of CPLJ bubble columns are a difficult task, as the influence of operating conditions, column geometry and physicochemical properties of the phase on the hydrodynamics is not yet fully understood.

In the Jameson Cells, a homogeneous bubbly flow is highly desirable as it offers the maximum gas liquid contacting area with a stable operation. However, in the churn-turbulent regime, the interfacial surface area concentration is considerable lower than in bubbly flow. The transition from bubbly flow to churn-turbulent flow leads to the deterioration of the column performance. Thus, determination the limit of the transition in the downcomer bubble columns is very important. The hydrodynamics of the Jameson cell are strongly characterized by different flow regimes depending on the gas and liquid flow rate. Flow regimes in the column are closely related to gas entrainment characteristics such as gas entrainment rate and gas holdup. However, in the present system of plunging liquid jet where the gas is sucked by high velocity liquid jet, flow regimes and gas entrainment rate primarily depend on properties of free jet such as jet velocity, jet length and nozzle (jet) diameter.

In this research, gas entrainment rate was experimentally measured in a Jameson cell which is a type of plunging liquid jet bubble column by using ranges of nozzle diameters, column diameters, jet velocities and jet lengths. The flow regimes were reported during the experiments and an empirical model predicting gas entrainment was proposed to determine the transition between bubbly flow and churn-turbulent flow in the downcomer for an air-water system by simple measurable variables.

2. Jameson cell and flow regimes in the downcomer

A schematic diagram of a Jameson Cell is shown in Fig. 1. It is comprised of a vertical column (downcomer), which is enclosed at the top and open at the base. The base of the column is below the liquid level in the riser, thus creating an airtight chamber. The liquid feed is in the form of a high velocity jet, which passes through the headspace at the top of the column and entrains gas as it plunges into the liquid inside the column. The plunging jet exchanges momentum with the surrounding fluid which results in a region of high shear, recirculation and energy dissipation, referred to as the mixing zone. The mixing zone forms a turbulent region. In this zone, the entrained gas is broken into fine bubbles. Below the mixing zone is a uniform downward bubbly flow region referred to as the pipe- low zone. In the pipe flow zone, the turbulence level is significantly lower and the flowing liquid steadily transports bubbles downward. The bubbles then pass into the riser section where they disengage from the liquid (Evans, 1990; Evans et al., 1995).

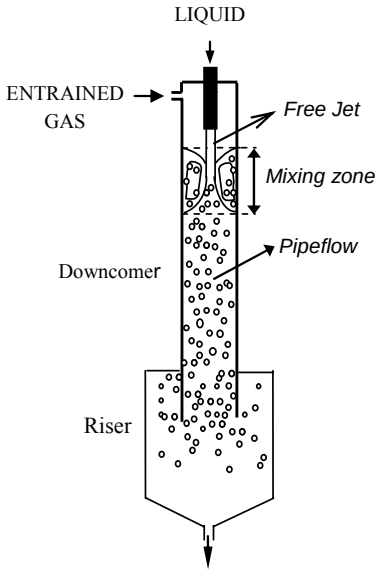

Figure 1. Schematic diagram of a Jameson Cell (Evans et al., 1995)

The flow conditions of bubble column reactors have a significant effect on the operation and performance of bubble column and hence it is desirable to maintain a constant flow regime throughout the column. Depending on the flow conditions there are mainly four types of flow regimes observed in bubble column. They are homogeneous bubbly flow, heterogeneous churn flow, slug flow and annular flow (Mandal et al, 2005; Wild et al, 2003; Evans, 1990; Sanchez-Pino and Moys 1991; Vial et al. 2001; Kantarcı et al, 2005). These are depicted in Fig. 2, where from left to right, superficial gas rate (j_g) in the column is gradually increased. The formation and

stability of these regimes and their limits primarily depend upon parameters like superficial gas velocity, liquid viscosity and velocity.

Bubbly flow occurs at low to moderate liquid and gas flow rate and low void fractions. The gas bubbles have approximately the same size and are homogeneously distributed in the column cross-section. Slug flow occurs with a further increase in gas flow rate. The flow consists of larger, longer, cap-shaped bubbles so called Taylor bubbles. For higher gas flow rate the length and velocity of the slugs increases until the shearing forces present make them unstable. A breakdown of the bubble occurs and the flow is highly turbulent. This type of flow is called churn-turbulent flow. Annular flow occurs at very high gas rate. Annular flow is characterized by liquid flowing as a film around the column wall, surrounding a high velocity gas core.

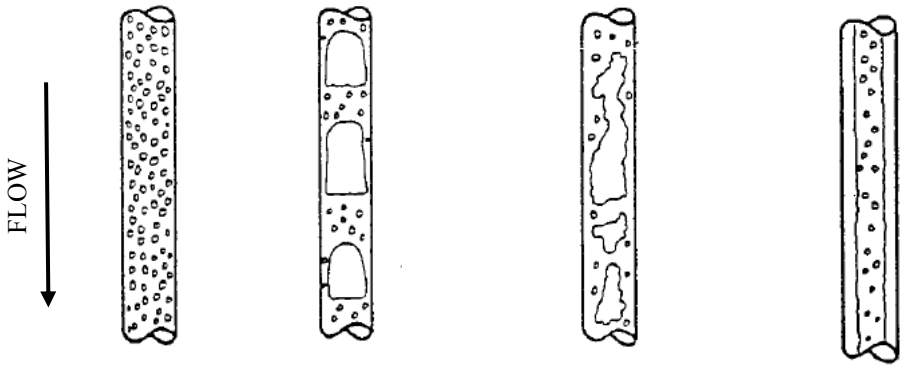

Figure 2. Flow regimes observed in a plunging jet bubble column (Evans, 1990)

For most applications of a Jameson Flotation Cell, the flow regime desired in the pipe-flow zone is bubbly flow. Bubbly flow has advantageous characteristics, most notably its stability and its large interfacial area. As the gas flow rate increases, the flow regimes changes to churn-turbulent flow. Churn-turbulent flow has detriments that include a relatively small interfacial area as well as large bubbles that may coalesce and rise within the column, preventing additional gas flow. From the view point of plunging jet bubble columns, it is therefore pertinent to study the hydrodynamic mechanisms and the flow conditions that transform the flow from bubbly to churn-turbulent (Evans and Jameson, 1995).

3. Materials and method

3.1. Experimental

A schematic diagram of the experimental set-up is shown in Fig. 3. It consists of a feed tank, pump, cell (riser), downcomers in different diameters and nozzles in different diameters which can be mounted simply. The cell which was made of

plexiglass, was 1000 mm high with 195 mm inside diameter. Five downcomer inside diameters were used (16, 21, 26, 36, 46 mm). Each downcomer, made of plexiglass, was 1800 mm length and immersed 400 mm below the liquid surface in the cell. The top of the downcomer housed at different nozzles of 3, 4, 5, 6, 7, 10 mm inside diameter. A centrifugal pump was used to deliver the feed liquid to the nozzle. The liquid flow rate was controlled with a throttling valve in the feed line and a flowmeter was used to measure liquid volumetric flow rate. The manometer was also used to measure the pressure. The air feed into the downcomer was regulated by a valve and volumetric air flow rate was measured using a rotameter. Liquid jet length, distance from the nozzle exit to the liquid surface, were measured by a scale fitted to the downcomer wall.

In the experiments, downcomer diameter (D_C), nozzle diameter (D_N), jet length (L_J) and jet velocity (V_J) were varied within the ranges shown in Table 1. Immersion depth of downcomer and frother quantity were held constant. All experiments were carried out with air-water system at a frother (aerofroth 65, mixture of polyglycols produced by CYTEC Industries) dosage of 20 ppm.. The Jameson cell was operated at several nozzle diameters, downcomer diameters, free jet lengths and jet velocities. To start, these parameters were set to required value. The underflow and overflow from the cell were collected in a feed tank and re-circulated to the downcomer. When the system was at steady state, at each operating parameter, gas entrainment rates were recorded and the flow regimes were determined by visual inspection.

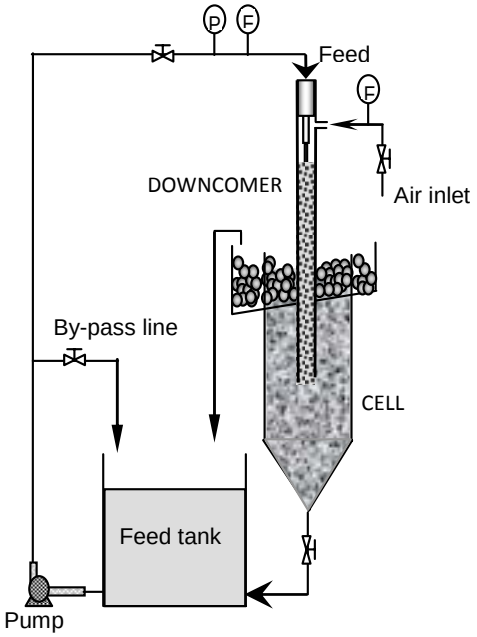

Figure 3. Schematic diagram of experimental apparatus (P: pressure indicator, F: flowmeter)

Table 1. Range of variables in experimental conditions

Downcomer diameter (mm)	: 16, 21, 26, 36, 46
Nozzle diameter (mm)	: 3, 4, 5, 6, 7,10
Jet length (cm)	: 3, 8, 13, 23, 33, 43
Jet velocity (m/s)	: 6 – 16

3.2. Statistical analyses

After measuring the independent parameters affecting air entrainment rates in Jameson cell, the dependent variable, air entrainment rate, was modeled as a function of independent parameters. Multiple linear regression (MLR) and piecewise linear regression (PLR) were used to obtain quantitative models. These statistical analyses were carried out with STATISTICA 8.0 software package (StatSoft Inc., 1984-2007).

3.2.1. Multiple Linear Regression (MLR)

MLR method provides equation that relates the independent parameters to the air entrainment rate. MLR models usually take the form:

$$Q_g = a_0 + a_1x_1 + \ldots + a_nx_n$$

where the intercept (a_0) and the regression coefficients of the predictors (a_i) are determined using least-squares method. The predictors (x_i) included in the equation are used to describe molecular structure of the analysis and *n* is the number of predictors.

In this study, relationships between the Q_g and the predictors were established by using the forward-stepwise MLR technique.

3.2.2. Piecewise Linear Regression (PLR)

Empirical equation is based on piecewise linear regression method with breakpoint (PLR). Quasi-Newton methods have been used for multi-variant optimization. It is non-linear method that has been used to minimize least square loss function through iterative convergence of predefined empirical equation. The iterative method works for multi-independent variables and dependent variable air entrainment rate both above and below the breakpoint. A non-linear optimization approach achieves acceptable lower residual values with predicted values very close to observed values.

The Quasi-Newton method utilizes the loss function $(observed - predicted)^2$ to arrive at a solution closest possible to observed data. At each iteration loss function is computed to minimize square of difference between the observed and predicted Q_g using pre-defined empirical equation. The method is an optimization process, which runs as long as initial values, stepping values, number of iterations and convergence

criteria are favorable. It terminates if any of these bounding conditions are fulfilled. Therefore, loss function can approach theoretically up to R^2 100%.

In PLR, two separate linear regression equations are produced before and after critical a breakpoint as follows:

$$y = (b_{01} + b_{11}x_1 + \ldots + b_{m1}x_m)\ (y \leq b_n) + (b_{02} + b_{12}x_1 + \ldots + b_{m2}x_m)\ (y > b_n) \quad (1)$$

where b_n is the breakpoint of y values. Each term in parenthesis represents a logical operation. This model estimates two separate linear equations; one for the y values that are less than or equal to the breakpoint (b_n) and one for the y values that are greater than the breakpoint. That model allows the user to specify or estimate breakpoints for the range of the dependent or y values.

4. Results and discussion

4. 1. Parameters affecting air entrainment rate in downcomer of Jameson cell

One of the interesting aspects of this type of bubble column is the air entrainment by a liquid jet. Many operating parameters such as jet velocity, jet length, nozzle and downcomer diameters may affect the air entrainment rate. Air entrainment basically occurs due to characteristics of plunging jet and rate of entrainment is mostly controlled by the jet velocity and jet length. The results obtained are presented at various jet velocities in the following plots. Thus, the plots given in here show also the effect of jet velocity on air entrainment rates.

4.1.1. The effect of downcomer diameter

Figure 4 shows the effect of downcomer diameter on the measured air entrainment rate as a function of jet velocity at costant nozzle diameter (3 mm) and jet length (3 cm). The air entrainment rate increases with jet velocity increasing and slightly decreases with downcomer diameter increasing but for D_C up to 36 mm, for higher D_C and jet velocities (10.6 and 12 m/s) air entrainment rate increases what finally gives that influence of D_C can be neglected.

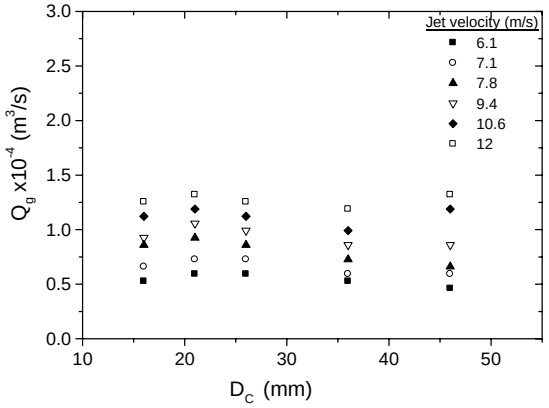

Figure 4. Air entrainment rate versus downcomer diameter for different jet velocities (D_N: 3 mm and L_J: 3 cm)

A generalized plot was given in Figure 5. This figure shows air entrainment rates obtained by different nozzle and downcomer combinations at 3 cm jet length. The plot summarizes air entrainment rate values when different nozzle and downcomer diameters are used. It can be seen that air quantity increases with increasing nozzle diameter at constant downcomer diameter, but almost constant with increasing downcomer diameter. This result is consistent with literature (Yamagiva, et. al., 1990) which was indicating that gas entrainment rate was almost independent of column diameter. Therefore, the diameter of downcomer was held constant and the 36 mm diameter was used in rest of experiments in this study.

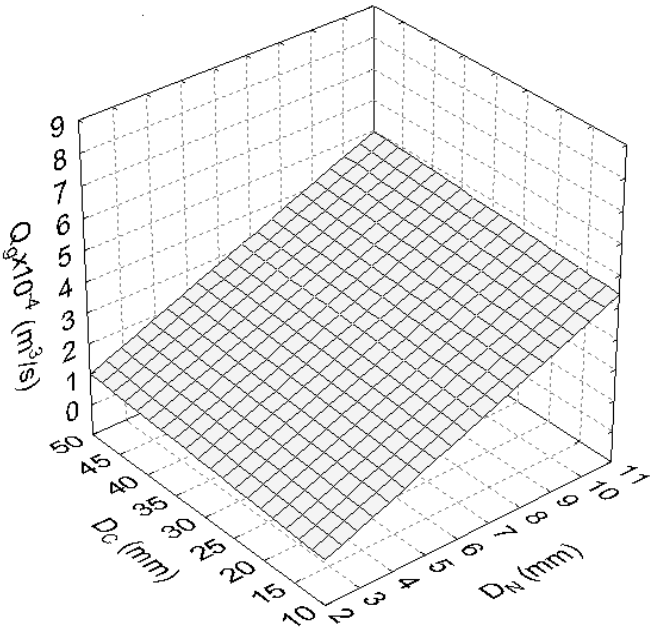

Figure 5. Air entrainment rates obtained with different downcomer and nozzle diameter combinations (L_J: 3 cm)

4.1.2. Effect of nozzle diameter

The effect of nozzle diameter on air entrainment rate is given in Fig. 6. The results obtained at constant downcomer diameter (36 mm) and jet length (3 cm) are shown and plotted as a function of nozzle diameter for each jet velocity tested. It can be seen that for all cases air entrainment rate increased linearly with increasing nozzle diameter at constant jet velocity. It can also be noticed that air entrainment rate increased with increasing jet velocity at constant nozzle diameter. The similar conclusion was reported by Yamagiwa et al., (1990) that air entrainment rate is a function of jet diameter and velocity since energy input into the system increases with their increase.

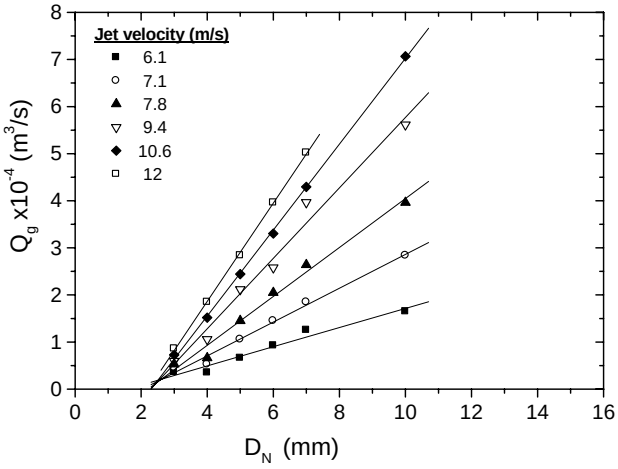

Fig. 6. Air entrainment rate versus nozzle diameter for different jet velocities (D_C: 36 mm and L_J: 3 cm)

4.1.3. Effect of jet length

The relation between the gas entrainment and liquid jet length for various jet velocities measured at constant nozzle and downcomer diameter is presented in Fig. 7. Increasing jet length increases the air quantity entered at constant jet velocities. At constant jet lengths, amount of air entered increases as the jet velocities increases. Jet length is a function of air quantity since increasing amount of air increases the jet lengths.

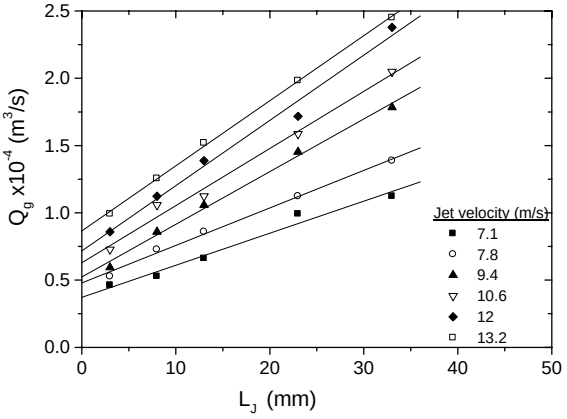

Fig. 7. Air entrainment rate vs jet length for different jet velocities (D_N 3 mm and D_C 36 mm)

In summary, the results indicate that gas entrainment rate was mainly affected by nozzle diameter, jet velocity and jet length parameters. It was also found that the effect of downcomer diameter on it was little compared to other factors and could be negligible. These results are agree with previous studies (Evans, 1990; Evans et al., 1995; Ohkawa et al., 1985, 1987; Yamagiwa et al., 1990; Kusabiraki et al., 1990; Funatsu et al., 1988; Liu and Evans, 1998). The increase in air entrainment rate with increasing with nozzle diameter, jet length and jet velocity was due to the increase in kinetic energy of the jet, surface roughness of the jet and contacting perimeter between the jet and receiving liquid surface. (Evans, 1990; Yamagiwa et al., 1990).

4.2. The flow behavior of gas and liquid in a downcomer of Jameson cell

The flow conditions were reported visually and transition regions from bubbly flow to churn-turbulent flow conditions were determined in each test. The results are given as a function of jet velocity at different jet lengths tested.

In Figure 8, gas entrainment rates have been plotted as a function of jet velocity for each jet length. It can be seen that for all cases the gas entrainment rate increased with increasing jet velocity and jet length. Also from visual observation of flow states in the column, the lines of transition from the bubbly to churn-turbulent flow have been drawn in Fig. 8. These lines define approximate boundaries of these flow regimes. It was observed that flow behavior of the gas-liquid mixture changed from homogenous bubbly flow to churn-turbulent flow with increasing jet velocity and jet length. The similar tendency was also observed in other experimental conditions as the nozzle diameters were varied. At low volumetric gas values (approximately $Q_g < 3x10^{-4}$ m^3/s), bubbly flow exists in the pipe flow zone of downcomer. However as Q_g is increased over a certain limit value, the gas bubbles coalesce to form large bubbles and heterogeneous churn-turbulent flow results.

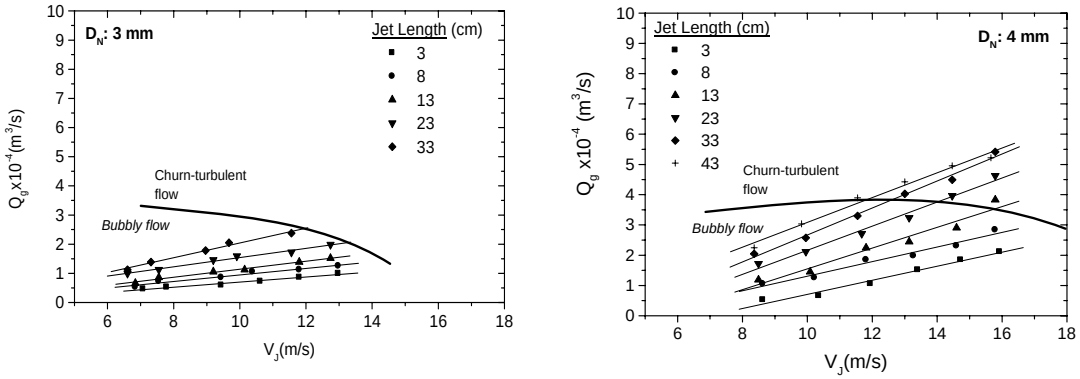

Figure 8. Observed flow regimes and measured air entrainment rates versus jet velocity for different jet lengths (D_C: 36 mm and D_N: 3, 4, 5, 6, 7 mm)

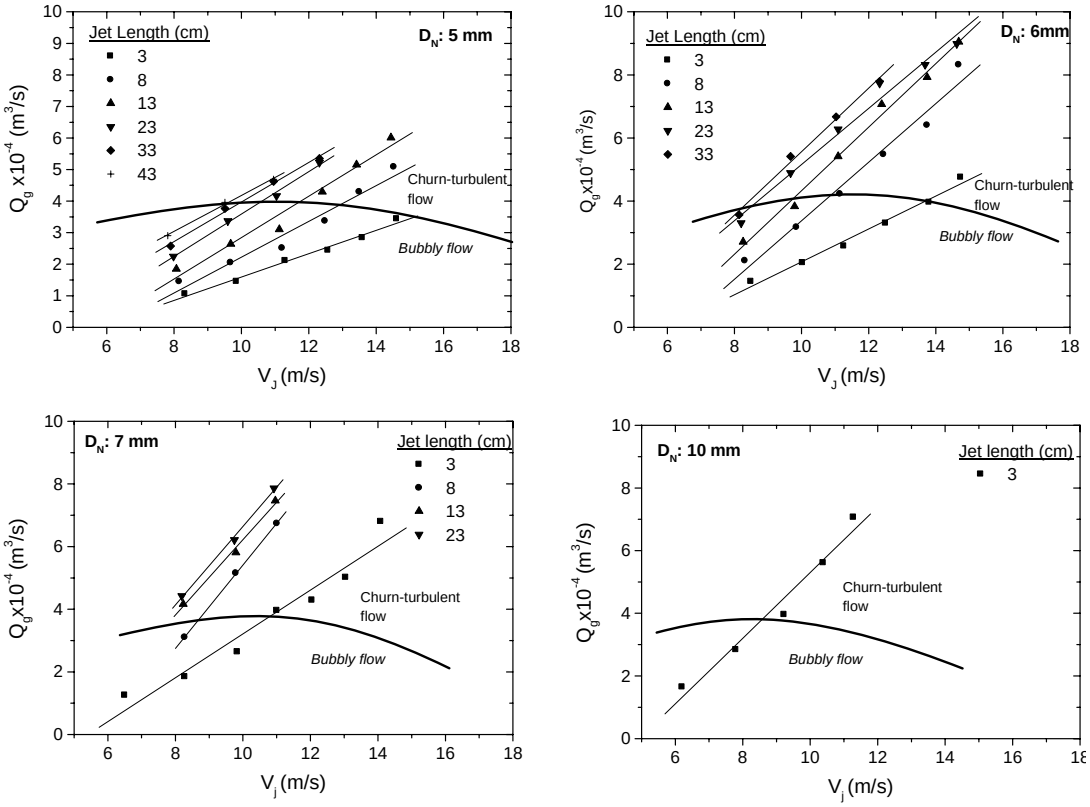

Continuation of Fig. 8.

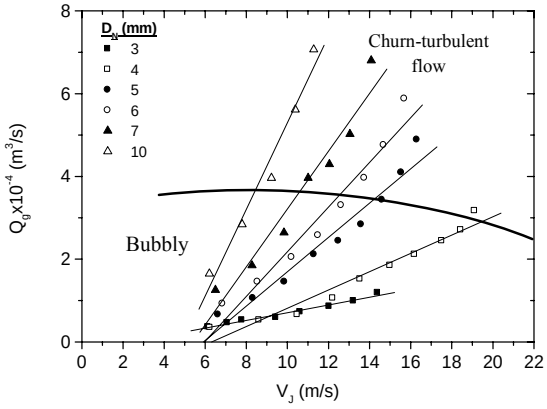

Figure 9. Observed flow regimes and measured air entrainment rates versus jet velocity for different nozzle diameters (D_C: 36 mm and L_J: 3 cm)

The observed flow regimes and effect of nozzle diameter on gas entrainment rate are given in Fig. 9 as a function of jet velocity for a constant downcomer diameter and jet length. It can be seen that the air entrainment rate increased with increasing nozzle diameter at constant jet velocity. The transition from bubbly to churn-turbulent flow is also highlighted in Fig.9. Similar to results presented in Fig. 8, bubbly flows were observed when Q_g <3x10^{-4} m^3/s. When the air entrainment rate exceeds this value, churn-turbulent flow regimes were dominant in the system.

4.3. Statistical analyses for air entrainment rate

Air entrainment rate is considered as dependent variable that varies proportionally with independent variables like nozzle diameter (D_N), jet velocity (V_J) and jet length (L_J).

The results were first evaluated by applying a forward stepwise MLR to identify the most effective variable or variables on the air entrainment rate. In the first step, each of the independent variables are evaluated individually and the variable that has the largest *F* value greater than or equal to the *F to enter* value is entered into regression equation. Table 2 summarizes the obtained results. The nozzle diameter, D_N, met the *F to enter* criteria first and was added to the model firstly, indicating that it is the most effective variable on air entrainment rate compared to other variables. The other important variables in sequences are jet velocity and jet length. All these parameters are statistically significant according to the *p* values.

Table 2. Estimation of the relationship between Q_g and independent variables by multiple regression stepwise method

	Intercept	Coefficent D_N	Coefficent V_J	Coefficent L_J	R^2	*F* to enter	*p*
Step 1	-0.343	0.738			0.31	66.45	0.0000
Step 2	-0.785	0.795	0.371		0.55	88.74	0.0000
Step 3	-6.828	0.918	0.400	0.076	0.73	130.49	0.0000

Table 3. Estimation of the relationship between Q_g and independent variables by PLR method

$Intercept_1$	Coef. D_N	Coef. V_J	Coef. L_J	$Intercept_2$	Coef. D_N	Coef. V_J	Coef. L_J	Breakpoint	R^2
-2.753	0.425	0.204	0.048	-8.705	1.091	0.523	0.068	3.3x10^{-4}	0.85

However, according to the determination coefficient of the forward stepwise MLR (R^2) it is difficult to model such a dynamic relation using conventional linear methods. Variations of D_N, V_J and L_J do not follow any distinct linear combination and with respect to Q_g. Therefore, a non-linear estimation approach is used to compute the relation between a set of independent variables and a dependent variable. A PLR empirical equation is devised and solved using non-linear Quasi-Newton method. Q_g

estimation equation with coefficients is derived by minimizing loss function for Q_g separately. The analysis results are given in Table 3.

PLR model represents a significant improvement compared to the MLR model. PLR model explains 12% more of the variance (R^2=0.73) in the air entrainment rate than MLR model. The PLR model explains more than 85% of the variance of Q_g in the downcomer prediction set versus only 73% explained by the MLR. These improvements can be better seen in Fig. 10 (a) and (b), where observed versus predicted air entrainment rates are plotted for both MLR and PLR approaches respectively. It can be seen that the great dispersion of data points obtained by MLR, especially for prediction set, and the significant improvement reached for the same data sets when the PLR method is employed. Fig. 10 (a) reveals curvature in the plots which an indication that nonlinear relationships exist between Q_g and the predictors in the MLR model.

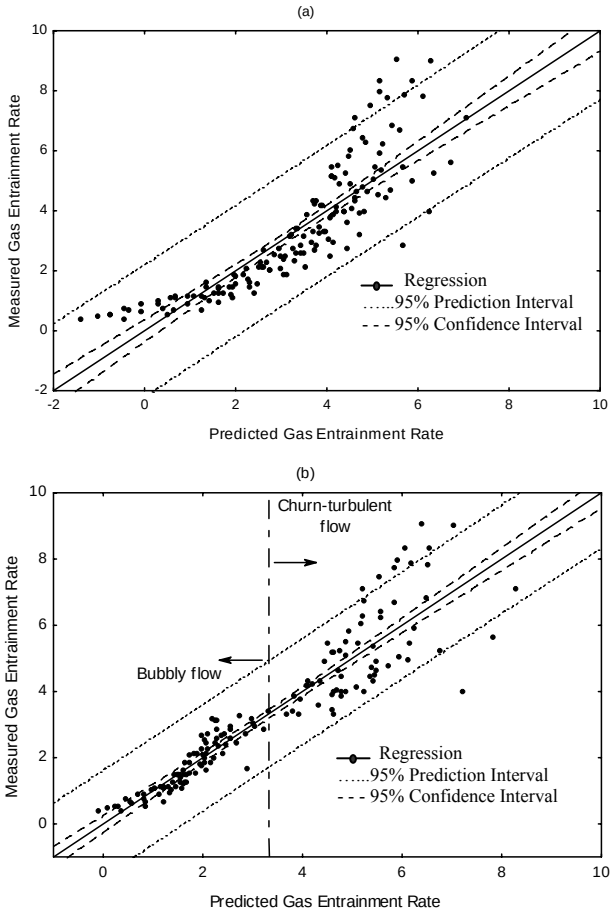

Figure 10. Graphical comparison of predicted versus observed results obtained by MLR model (a) and PLR model (b)

Given that the regression coefficient obtained using PLR model was higher than in MLR model, it seems that there is a discontinuity in the relationship between the dependent and the independent variable, Q_g. In the present case, the breakpoint was $3.3x10^{-4}$ m^3/s, which is predicted by the software. This breakpoint determined by the model was coherent with the visual observations during the experimental studies. Thus, model suggests that bubbly flow conditions exists in the system if the gas entrainment rate is equal to or smaller than $3.3\ x10^{-4}$ m^3/s. Otherwise, the churn-turbulent flow occurs when $Q_g > 3.3\ x10^{-4}$ m^3/s. The PLR model showed adequate fits as indicated by its high correlation coefficient (R = 0.92) showing a discontinuous relationship between variables.

The agreement between predicted and observed air entrainment rates is clearly better before breakpoint since the predicted values are closer to the regression line as compared to predicted values after breakpoint. The performance of the piecewise linear regression after breakpoint of $3.3\ x10^{-4}$ m^3/s during the fitting procedure clearly reveals a significant scattering of the computed data points with respect to the ideal trend. This might be due to the fact that the coefficients of D_N, V_J and L_J variables were almost two times higher after breakpoint, (Table 3). This could mean that increasing of these parameters causes the dominant churn-turbulent flow conditions, resulting in undesired flowing in the downcomer.

5. Conclusions

In the present work, gas entrainment rate and flow characteristics of a Jameson cell were experimentally investigated. The effect of nozzle diameter, downcomer diameter, jet velocity and jet length on gas entrainment rate for the bubbly and churn-turbulent flow are determined in two phase gas-liquid system. It was found that the rate of gas entrainment is strongly dependent on these parameters, except downcomer diameter. Gas entrainment rate increased with increasing nozzle diameter, jet velocity, and jet length and was almost independent of downcomer diameter.

It was found that flow regimes in the column were closely related to gas entrainment rate and gas entrainment rate primarily depended on properties of free jet such as jet velocity, jet length and nozzle (jet) diameter. The importance of variables on Q_g was arranged as nozzle diameter, jet velocity and jet length respectively by forward stepwise MLR. From visual observation of flow states in the column, transition boundaries from bubbly flow to churn-turbulent flow conditions were determined. It was shown that flow behavior of the gas-liquid mixture changed from homogenous bubbly flow to churn-turbulent flow with increasing jet velocity, jet length and nozzle diameter due to increased gas entrainment. At low gas volumetric values (approximately $Q_g < 3x10^{-4}$ m^3/s), bubbly flow exists in the pipe flow zone of downcomer. However as Q_g exceeds this value, the gas bubbles coalesce to form large bubbles and heterogeneous churn-turbulent flow results.

An empirical model was developed by using piecewise regression with Quasi-Newton estimation of breakpoint to estimate the flow conditions and gas entrainment

rates. The model estimated the breakpoint as $3.3x10^{-4}$ m^3/s which was consistent with the visual observation of flow states in the column during the experiments. The model determined is useful to understand the boundary of the flow characteristics since the two equations was valid in a certain air entrainment ranges, i.e. different flow conditions. The model developed was successful to determine the transition region from bubbly flow to churn-turbulent flow within the ranges of experimental parameters tested in this study.

Acknowledgement

The authors would like to thank Prof. G. J. Jameson for his support and suggestions during design stage of Jameson cell device used in this research.

References

ATKINSON, B.W., JAMESON, G.J., NGUYEN, A.V. and EVANS, G.M., 2003, Increasing Gas-Liquid Contacting Using a Confined Plunging Liquid Jet, Journal of Chemical Technology and Biotechnology, 78: 269-275.

BIN, A.K., 1993, Gas Entrainment by Plunging Liquid Jets. Chemical Engineering Science. 48(21): 3585-3630.

BROZEK, M. and MLYNARCZYKOWSKA, A., 2010, Probability of Detachment of Particle Determined According to the Stochastic Model of Flotation Kinetics, Physicochemical Problems of Mineral Processing, 44: 23-34.

ÇINAR, M., ŞAHBAZ, O., ÇINAR, F., KELEBEK, Ş. and ÖTEYAKA, B., 2007, Effect of Jameson Cell Operating Variables and Design Characteristics on Quartz Dodecylamine Flotation System, 20: 1391-1396.

EVANS, G.M., 1990, A Study of a Plunging Jet Bubble Column, Ph. D. Thesis, Newcastle University, Australia.

EVANS, G.M. and JAMESON G.J., 1995, Hydrodynamics of a Plunging Liquid Jet Bubble Column, Chemical Engineering Research & Design, 73: 679-684.

EVANS, G.M., ATKINSON, B.W. and JAMESON, G.J., 1995, The Jameson Cell, Flotation Science and Engineering, Edited by K.A. Matis, 331-363.

EVANS, G.M., ATKINSON, B.W. and JAMESON, G.J., 1996, Recent Advances in Jameson Cell Technology, Column'96, 39-49.

EVANS, G.M., BIN, A. K., and MACHNIEWSKI, 2001, Performance of Confined Plunging Liquid Jet bubble Column as a Gas-liquid Reactor, Chemical Engineering Science, 56: 1151-1157.

FUNATSU, K., HSU, Y. and KAMOGAWA, T., 1988, Gas Holdup and Gas Entrainment of a Plunging Water Jet with a Constant Entrainment Guide, Can. J. Chem. Eng., 66: 19-28.

JAMESON, G.J. and MANLAPIG, E.V., 1991, Applications of the Jameson Cell, Column'91, Proceedings of an International Conference on Column Flotation, Sudbury, Ontario, 673-687.

JAMESON, G.J., 1999, Hydrophobicity and Floc Density in Induced-Air Flotation for Water Treatment, Colloids Surfaces A: Physicochem. Eng. Asp, 151: 269-281.

KANTARCI, N., BORAK, F. and ULGEN, K.O., 2005, Bubble Column Reactors, Process Biochemistry, 40: 2263-2283.

KUSABIRAKI, D., NIKI, H., YAMAGIWA, K. and OHKAWA, A., 1990, Gas Entrainment Rate and Flow Pattern of Vertical Plunging Jets, Can. J. Chem. Eng., 68: 893-901.

LIU, G. and EVANS, G.M.,1998, Gas Entrainment and Gas Holdup in a Confined plunging Liquid Jet Reactor, Proceedings of the 26th Australasian Chemical Engineering Conference, (Chemeca 98), Port Douglas, Australia.

MANDAL, A., KUNDU, G. and MUKHERJEE, D., 2003, Gas Holdup and Entrainment Characteristics in a Modified Downflow Bubble Column with Newtonian and Non-Newtonian Liquid, Chemical Engineering and Processing, 42: 777-787.

MANDAL, A., KUNDU, G. and MUKHERJEE, D., 2005, Comparative Study of Two-Phase Gas-Liquid Flow in the Ejector Induced Upflow and Downflow Bubble Column, International Journal of Chemical Reactor Engineering, 3: 1-13.

MOHANTY, M.K. and HONAKER, R.Q., 1999, Performance Optimization of Jameson Flotation Technology for Fine Coal Cleaning, Minerals Engineering, 12(4): 367-381.

OHKAWA, A., SHIOKAWA, Y., SAKAI, N. and IMAI, H., 1985, Flow Characteristics of Downflow Bubble Columns with Gas Entrainment by a Liquid Jet, j. Chem. Eng. Japan, 18: 466-469.

OHKAWA, A., KUSABIRAKI, D., KAWAI, Y. and SAKAI, N.,1986, Some Flow Characteristics of a Vertical Liquid Jet System Having Downcomers, Chem. Eng. Sci., 41: 2347-2361.

OHKAWA, A., KUSABIRAKI, D., KAWAI, Y. and SAKAI, N., 1987, Flow Characteristics of an Air-entrainment Type Aerator Having a Long Downcomer, Chem. Eng. Sci., 42: 2788-2790.

SANCHEZ-PINO, S.E. and MOYS, M.H., 1991, Characterization of Co-Current Downwards Flotation Columns, Column'91, 1: 341-355.

ŞAHBAZ, O., ÖTEYAKA, B., KELEBEK, Ş., UÇAR, A. and DEMİR, U., 2008, Separation of Unburned Carbonaceous Matter in Bottom Ash Using Jameson Cell, Separation and Purification Technology, 62: 103-109.

TAŞDEMIR, A., TAŞDEMIR, T., and ÖTEYAKA, B., 2007a, The Effect of Particle Size and Some Operating Parameters in the Separation Tank and the Downcomer on the Jameson Cell Recovery, Minerals Engineering, 20: 1331-1336.

TAŞDEMIR, T., ÖTEYAKA, B. and TAŞDEMIR, A., 2007b, Air Entrainment Rate and Holdup in the Jameson Cell, Minerals Engineering, 20/8: 761-765.

STATISTICA 8.0, StatSoft Inc., 1984-2007.

VIAL C., PONCIN, S., WILD, G. and MIDOUX, N., 2001, A Simple Method for Regime Identification and Flow Characterization in Bubble Columns and Airlift Reactors, Chemical Engineering and Processing, 40: 135-151.

WILD, G., PONCIN, S., LI, H. and OLMOS, E., 2003, Some Aspects of the Hydrodynamics of Bubble columns, International Journal of Chemical Reactor Engineering, 1: 1-36.

YAMAGIWA, K., KUSABIRAKI, D. and OHKAWA, A., 1990, Gas Holdup and Gas Entrainment Rate in Downflow Bubble Column with Gas Entrainment by a Liquid Jet Operating at High Liquid Throughput, J. Chem. Eng. Japan, 23: 343-348.

YAN, Y.D. and JAMESON, G.J., 2004, Application of the Jameson Cell Techonology for Algae and Phosphorus Removal from Maturation Ponds, Int. J. Miner. Process., 73: pp 23-28.

Physicochem. Probl. Miner. Process. 46(2011) 79-90
www.minproc.pwr.wroc.pl/journal/

Physicochemical Problems of Mineral Processing
ISSN 1643-1049

Received April 7, 2011; reviewed; accepted April 15, 2011

The effect of modifiers and precipitation conditions on physicochemical properties of $MgCO_3$ and its calcinates

Agnieszka PILARSKA, Dominik PAUKSZTA, Karolina SZWARC Teofil JESIONOWSKI

Poznan University of Technology, Institute of Chemical Technology and Engineering, M. Skłodowskiej - Curie 2, PL-60965 Poznan, Poland, teofil.jesionowski@put.poznan.pl, phone: +48(61)6653720, fax: +48(61)6653649

Abstract. The effects of modifiers and process conditions on synthesis of magnesium oxide by the carbonatization method and properties of the product are studied. Magnesium carbonate obtained from magnesium hydroxide and carbon dioxide was subjected to thermal decomposition at 800ºC. The reaction of precipitation was performed checking the influence of temperature, rate and mode of reagents introduction, type and concentration of the modifier. The modifiers were the non-ionic compounds from the group of poly(ethylene glycols). The magnesium oxides produced were characterised by determination of their dispersive-morphological properties, wettability profiles, specific surface area, total volume and mean size of pores. The products were also subjected to identification by the X-ray diffraction method and TG/DTA analysis. The results revealed a significant impact of the concentration and type of modifiers on the physicochemical properties of MgO samples obtained and permitted selection of the best products for particular applications.

keywords: MgO, carbonatization, modification, thermal decomposition, particle size distribution, surface morphology

1. Introduction

One of the most important magnesium compounds is magnesium carbonate occurring in nature in the form of magnesite (anhydrous carbonate $MgCO_3$). As a result of thermal decomposition, $MgCO_3$ gives magnesium oxide and carbon dioxide (Bandi, 1976). Magnesium carbonate is described as light, white, amorphous and odourless powder capable of odour absorption. The temperature of its decomposition is in the range 230–680ºC. It is practically insoluble in water and alcohols but easily dissolves in acids (Gennaro, 1985).

There are two pharmaceutical varieties of magnesium carbonate: light and heavy. The bulk density of the light one is 2–2.5 smaller than that of the heavy variety,

and each variety is obtained by different methods. In general the light variety is obtained by mixing magnesium sulphate or chloride with sodium carbonate (Gennaro 1985, Botha 2001). Precipitation in a cold solution gives a very bulky powder called *magnesia alba levis* or a light species of magnesium carbonate of the formula $3MgCO_3 \cdot Mg(OH)_2 \cdot 3H_2O$. Precipitation in an elevated temperature gives species known as *magnesia alba ponderosa* or heavy powder of the formula $3MgCO_3 \cdot Mg(OH)_2 \cdot 4H_2O$. The light variety can also be obtained from dolomite ($MgCO_3 \cdot CaCO_3$) subjected to calcination, suspension in water and then saturation with carbon dioxide under pressure. The filtrate is heated to a temperature at which magnesium bicarbonate is converted into magnesium carbonate. Yildrim (2010) reported a method of obtaining magnesium carbonate and then magnesium oxide by the leach-precipitation-pyrohydrolysis process.

In our work magnesium carbonate was synthesised by the carbonatization method with an addition of a modifier. The magnesium carbonate was subjected to calcination to get magnesium oxide. Thermal analysis was made to identify the thermal effects accompanying the sample decomposition and to estimate mass loss at certain temperatures. Similar studies have been performed earlier (Khan 2001, Morozow 2001, Vagvölgyi 2008). Morozow characterised the relation between the degree of the sample decomposition and changes in the specific surface area. Khan has studied thermal analysis of magnesium carbonate in the atmosphere of nitrogen, carbon dioxide and air versus the rate of heating, he tried to explain the origin of the exothermic peak.

Methods of magnesium carbonate synthesis have not been much discussed in literature. Much more attention has been devoted to the methods of synthesis of hydromagnesite (Hollingbery 2010; Hongchang 2011). In the method proposed by us an element of novelty is the use of PEG compounds as modifiers. The modifiers were introduced to help obtain the powdered products of the possibly smallest size particles and possibly hydrophobic character (Wang 2007, Dongmin 2009, Pang 2009, Meshkani 2010).

2. Experimental

Magnesium carbonate was obtained in the reaction between the suspension of magnesium hydroxide ($Mg(OH)_2$, POCh SA) and CO_2, with addition of a non-ionic compound from the group of poly(ethylene glycols) purchased from Sigma-Aldrich of different molecular masses as a modifier. Solutions of modifiers in different concentrations were prepared by dilution in ethanol. Precipitation was performed in a reactor of 500 cm^3 in capacity, equipped with a high-speed stirrer (1800 rpm) Eurostar digital made by IKA-Werke GmbH. The substrates were introduced in two modes. In one mode carbon dioxide was introduced to the suspension with the modifier at the rate of either 1 or 7 dm^3/min, for 3 h, to get pH of 8, while in the second mode carbon dioxide was introduced in parallel with the suspension of magnesium hydroxide into a water system containing PEG. The suspension of a concentration of 5 or 10% was

supplied by a peristaltic pump ISM833A, Ismatec. The process was performed at 40°C. The magnesium carbonate precipitate was dried at 105ºC, for about 8 h and calcined in a programmable furnace Controller P320 MB1, made by Nabertherm GmbH, at 300°C, 600°C or 800°C for 1.5 h to get the final product of magnesium oxide.

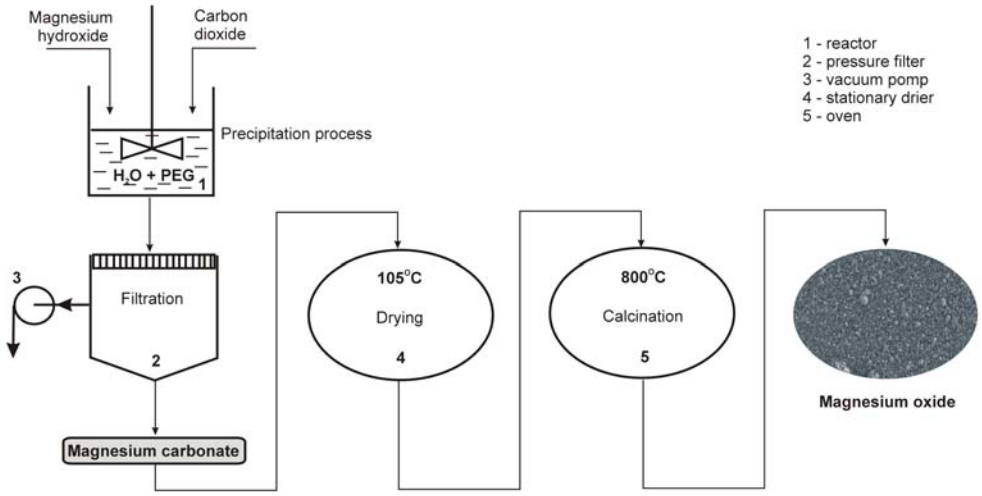

Fig. 1. A scheme of precipitation process of magnesium carbonate from a suspension of magnesium hydroxide and carbon dioxide with a modifier

The final products obtained were subjected to determination of bulk density and particle size distribution. The particle size distribution was measured by two instruments: Zetasizer Nano ZS and Mastersizer 2000 made by Malvern Instruments Ltd., allowing measurements in the range 0.6–6000 nm (NIBS method) and 0.2–2000 μm (diffraction laser scattering technique). The wettability of the final products was evaluated by using a K100 tensiometer made by Krüss. For selected MgO samples also the adsorption parameters were determined such as specific surface area (BET), total volume and mean size of pores calculated according to the BJH method. The measurements were made using an ASAP 2020 instrument made by Micromeritics Instrument Co. The crystalline structures of magnesium carbonate and magnesium oxide were characterised by the WAXS method with the use of a computer controlled horizontal diffractometer TUR M-62 with a HZG-3 type goniometer. The TG/DTA thermal analysis was made using the instrument for thermal stability measurements Jupiter STA 449 F3 made by Netzsch GmbH.

3. Results and discussion

Table 1 presents the physicochemical properties of magnesium oxide samples obtained by calcination of magnesium carbonate at 800ºC, for 1.5 hour. The process of

precipitation was performed at 40ºC by introducing carbon dioxide at the rate of 1 dm^3/min into a 10% suspension of magnesium hydroxide with a modifier. The modifiers used were solutions of poly(ethylene glycol) compounds: PEG 200, PEG 400, PEG 8000 and PEG 20000, of concentrations from the range 0.5–2%.

Table 1. Dispersive properties of magnesium oxide samples obtained from magnesium carbonate precipitated by introduction of carbon dioxide at the rate 1dm^3/min to a 10% suspension of magnesium hydroxide and a modifier, at 40°C

Sample No.	Precipitation process conditions		Dispersive properties				
	Mean molecular weight of PEG	PEG concentration (%)	PdI	Particle diameter from Zetasizer Nano ZS (nm)	Particle diameter from Mastersizer 2000 (μm)		
					d(0.1)	d(0.5)	d(0.9)
1	–	–	0.692	1990 – 5560	2.95	13.30	36.25
2	200	0.5	0.400	955 – 5560	2.54	11.85	32.88
3		1	0.351	1110 – 3580	2.26	8.22	30.01
4		2	0.247	122 – 531	1.74	5.05	17.37
5	400	0.5	0.620	1990 – 5560	2.87	11.09	35.65
6		1	0.580	1720 – 5560	2.85	9.04	33.35
7		2	0.243	38 – 79; 825 – 2300	8.98	8.98	26.67
8	8000	0.5	0.501	1480 – 5560	3.45	14.61	38.21
9		1	0.429	1480 – 5560	3.28	12.93	34.90
10		2	0.683	1480 – 5560	3.51	14.79	39.41
11	20000	0.5	0.679	38 – 51; 2670 – 5560	3.14	12.38	33.41
12		1	0.432	396 – 615; 955 – 5560	3.35	8.39	23.04
13		2	0.304	1990 – 5560	2.41	7.13	19.86

Comparative analysis of the dispersive-morphological properties of MgO samples synthesized with a PEG modifier and without a modifier (Sample 1) has shown a beneficial effect of the modifiers applied except for PEG 8000. The samples of magnesium oxide obtained with the use of a modifier (samples 2–7 and samples 11–13) show lower values of the polydispersity index indicating their more uniform character and smaller particle sizes. The results of measurements by Mastersizer 2000 (range up to 2000 μm) prove that the sizes of particles in the modified samples are much smaller than in the unmodified sample. Much smaller particle diameters and much lower polydispersity index values were recorded for magnesium oxide synthesised with a PEG modifier used at the highest concentration. These results

illustrate the benefits following from the use of modifiers and confirm their positive effect on nucleation of the crystalline phase.

The best properties were determined for the samples of magnesium oxide synthesised with the use of PEG 200 (samples 2, 3, 4). In sample 4, 10% of the particles have diameters smaller than 1.74 μm, 50% have diameters up to 8.22 μm, and 90% of the particles have diameters smaller than 17.37 μm. A relatively low value of d(0.9) informs about a restricted tendency towards formation of large secondary agglomerations. These observations are confirmed by PdI=0.247 and SEM microphotograph presented in Fig. 2b. Figure 3a presents the particle size distribution obtained on the basis of measurements by Zetasizer Nano ZS, revealing a single band covering the particle diameters range 122–531 nm.

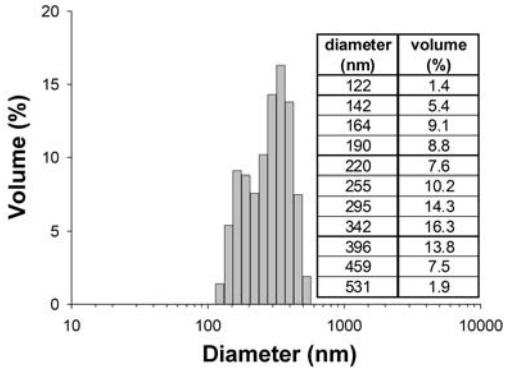

diameter (nm)	volume (%)
122	1.4
142	5.4
164	9.1
190	8.8
220	7.6
255	10.2
295	14.3
342	16.3
396	13.8
459	7.5
531	1.9

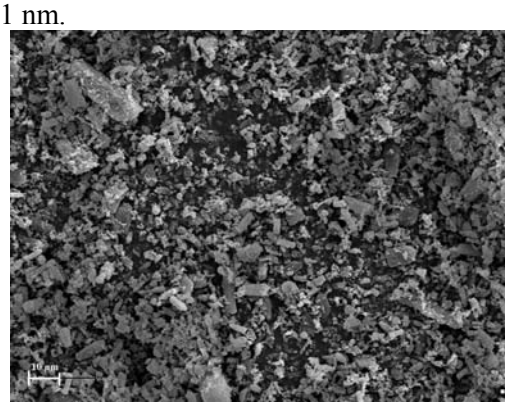

(a) (b)

Fig. 2. (a) Particle size distribution (Zetasier Nano ZS) and (b) SEM microphotograph of magnesium oxide (sample 4) obtained from magnesium carbonate precipitated by introducing carbon dioxide into the magnesium hydroxide suspension with 2% PEG 200

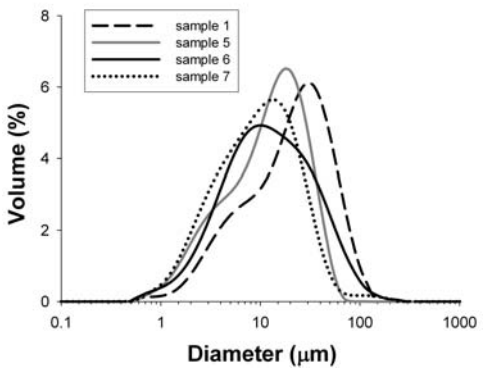

Fig. 3. Particle size distribution (Mastersizer 2000) of unmodified magnesium oxide – sample 1 and modified with PEG 400 – samples 5, 6, 7

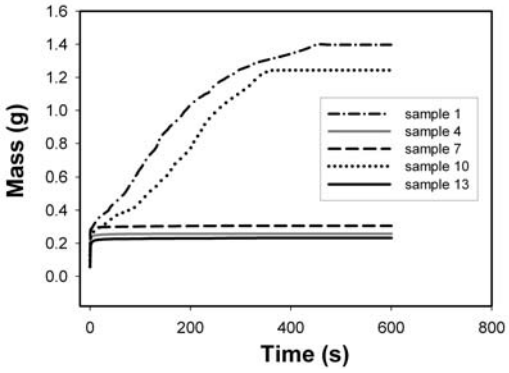

Fig. 4. Wettability profiles of unmodified magnesium oxide (sample 1) and grafted MgO (samples 4, 7, 10, 13)

The beneficial effect of the modifier on dispersive and morphological properties of MgO samples obtained by carbonatization is best manifested by a comparison of the particle size distribution curves for the unmodified sample 1 and for samples 5, 6 and 7 obtained with the use of PEG 400 of different concentrations. The shape of the band recorded for sample 1 points to polydispersity of this sample and this band is shifted towards greater diameters and dominant contribution of greater particles.

No report has been found in hitherto published literature on modification of magnesium carbonate synthesis with addition of PEG compounds. However, such a surfactant has been used in the process of precipitation of magnesium hydroxide from which magnesium oxide was obtained as a final product. Wang (2007) has provided evidence proving the influence of PEG 400 on the formation of nanosized MgO. The same author described the mechanism of PEG effect which involves adsorption of PEG on the $Mg(OH)_2$ crystal inducing changes in the surface density of Mg atoms. Generally, the face with a higher density of surface atoms is blocked by the adsorption of surfactant during the crystal growth of nanocrystals and the growth along this face is therefore considerably restricted. This mechanism can be also applied to explain the effect of PEG on magnesium carbonate.

Besides microstructural properties, another parameter determining the technological applicability of materials is their water absorption capacity. Much attention has been devoted to production of hydrophobic materials by simple and cheap methods. An exemplary modification applied to reduce water absorption is a one-step method of magnesium hydroxide precipitation with addition of octadecyl dihydrogen phosphate as a surface modifier (Dongmin 2009). This modifier has been used to control the growth of the crystal and to modify the surface properties of $Mg(OH)_2$.

Figure 4 presents the wettability profiles of magnesium oxide samples 4, 7, 10, 13 modified with PEGs 200, 400, 8000 and 20000, respectively, used in a concentration of 2% and for comparison the wettability profile of unmodified sample 1. The greatest ability to absorb water is shown by sample 1, obtained without modification and sample 10 modified by PEG 8000. Much higher hydrophobicity was shown by the samples obtained with the use of PEGs 200, 400, 20000 (0.2–0.3 g in the same time). The enhanced hydrophobic character of these samples is related to their microstructural features and partial adsorption of surfactants. An exception is the result for sample 10 obtained with the use of PEG 8000 as for this modifier no beneficial changes in the dispersive and morphological properties were noted. Most probably the relatively high ability to absorb water follows from the presence of large size agglomerates and inhomogeneous morphology of particles, similar as that observed for the unmodified sample.

At the second stage of the study magnesium carbonate was precipitated by simultaneous supply of a 5% of magnesium hydroxide and carbon dioxide (at the rate of 7 dm^3/min) into a water system without a modifier (sample 14) and with PEG modifiers of different masses and in different concentrations (samples 15–26). All

samples were synthesised at 40ºC. As at the first stage, the non-ionic compounds from the group of poly(ethylene glycols) of different molecular masses and at different concentrations were used as modifiers.

Table 2. Dispersive properties of magnesium oxide samples synthesised with the use of a 5% suspension of magnesium hydroxide with an addition of a modifier, with CO_2 supplied at the rate of 7 dm^3/min and at 40°C

Sample No.	Precipitation process conditions		Dispesive properties				
	Mean molecular weight of PEG	PEG concentration (%)	PdI	Particle diameter from Zetasizer Nano ZS (nm)	Particle diameter from Mastersizer 2000 (μm)		
					d(0.1)	d(0.5)	d(0.9)
14	–	–	0.743	1280 – 3580	3.54	17.59	45.49
15	PEG 200	0.5	0.638	1720 – 4150	3.20	9.79	30.41
16		1	0.538	1480 – 5560	3.28	9.19	27.07
17		2	0.435	1480 – 5560	2.26	5.13	12.80
18	PEG 400	0.5	0.664	21 – 43; 2670 – 5560	3.08	12.23	37.89
19		1	0.599	712 – 5560	2.70	12.86	31.53
20		2	0.480	164 – 295	1.95	5.71	23.83
21	PEG 8000	0.5	0.502	1480 – 5560	2.86	9.84	36.24
22		1	0.632	2670 – 5560	3.16	13.46	46.19
23		2	0.499	3090 – 5560	2.27	11.80	42.93
24	PEG 20000	0.5	0.303	28 – 59; 955 – 1990	1.97	6.22	21.39
25		1	0.418	68 – 220; 3580 – 5560	2.19	6.11	19.92
26		2	0.373	106 – 5560	1.77	5.19	16.57

Figure 5 confirms improvement in the dispersive and morphological properties of as a result of the use of PEG 400 as a modifier. Sample 20 obtained with addition of PEG 400 in the highest concentration has particles of much smaller size than those in the unmodified sample. The best properties from the viewpoint of future technological use are shown by the samples modified with PEG 20000. These samples have the lowest tendency towards formation of large agglomerations: d(0.9) in the range 16.57–21.39 μm. The presence of nanometric particles was proved almost in all volume of sample 24 modified with a 0.5% solution of PEG 20000, which points to high effectively of this type of modifier applied in the simultaneous mode of reagents supply. The particle size distribution presented in Fig. 4a shows two bands. One is narrow, of high intensity and covers the diameters from the range 28–59 nm, with the

maximum volume contribution of 39% is brought by particles of 38 nm in diameter. The second low intensity band testifies to the formation of secondary agglomerates. The results obtained for the samples synthesised in the mode of simultaneous supply of reagents confirmed the unfavourable influence of modification with PEG 8000. Samples 21–23 obtained with addition of PEG 8000 were found to be made of particles of sizes close to those of the unmodified sample 14.

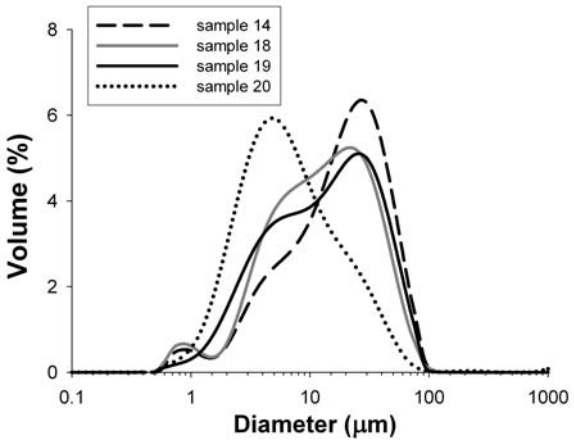

Fig. 5. Particle size distribution (Mastersizer 2000) of unmodified magnesium oxide (sample 14) obtained without a modifier and obtained with addition of PEG 400 in different concentrations (samples 18, 19, 20)

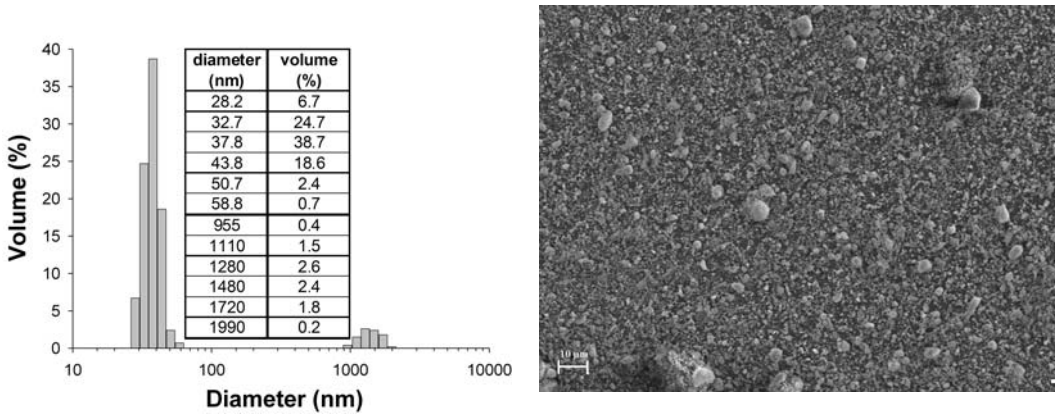

diameter (nm)	volume (%)
28.2	6.7
32.7	24.7
37.8	38.7
43.8	18.6
50.7	2.4
58.8	0.7
955	0.4
1110	1.5
1280	2.6
1480	2.4
1720	1.8
1990	0.2

(a) (b)

Fig. 6. (a) Particle size distribution (Zetasier Nano ZS) and (b) SEM microphotograph of magnesium oxide (sample 24) obtained in the mode of simultaneous supply of reagents into a water system with addition of 0.5% solution of PEG 20000

In order to evaluate the product purity and determination of the range of temperatures corresponding to significant chemical or structural transformations of magnesium carbonate, the samples were subjected to a TG/DTA study (see Fig. 6). As the results were similar for all samples, only the results obtained for the unmodified sample (sample 14) and the sample modified with 2% PEG 20000 are shown. DTA measurements permit detection of thermal effects accompanying the physical or chemical transformations. No significant changes in the courses of TG/DTA curves for the unmodified and modified samples were noted. The results obtained for modified samples revealed an exothermic effect in the range 25–370ºC related to the loss of crystallization water. The TG curve informing about the mass change upon heating shows in the corresponding point a signal indicating the mass loss of 22.47%. The second effect observed on the DTA curve was endothermic and occurred in the range 450–900°C. It was interpreted as a manifestation of decomposition of magnesium carbonate and reorganization of the $MgCO_3$ structure to the pure crystalline form of MgO, related to the loss of CO_2 recorded in the TG curve as a rapid mass loss of 43.42%.

The purposefulness of calcination of magnesium carbonate at much elevated temperatures was confirmed by the results of WAXS studies (see Fig. 7). The WAXS analysis was made for the same material but calcined at three different temperatures 300ºC, 600ºC and 800ºC. For the material calcined at 600ºC the maxima characteristic of MgO structure (cubic structure of periclase). For the material calcined at 800ºC the maxima are even more intense and have regular shapes, which proves the presence of a well-developed magnesium oxide crystals. Cloudhary (1994) has reported detection of traces of carbon in MgO samples calcined at 900ºC. He interpreted this observation by strong ability of CO_2 adsorption from the atmospheric air of MgO centres.

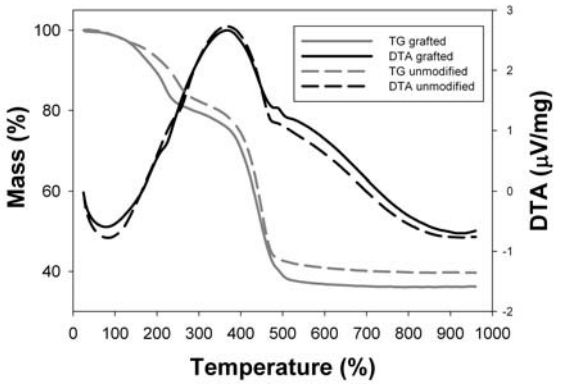

Fig. 7. TG/DTA of unmodified magnesium oxide (sample 14) and grafted MgO (sample 26)

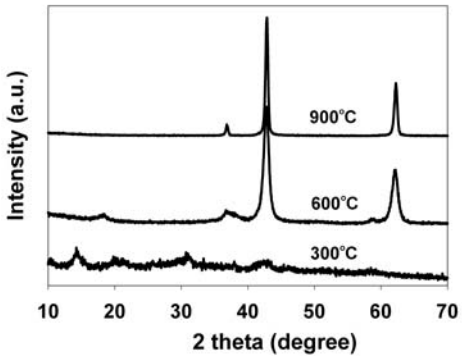

Fig. 8. X-ray diffraction patterns for a selected magnesium oxide (sample 24) for different temperatures of decomposition

Table 3 presents results of the adsorption study of some selected magnesium oxide samples unmodified (samples 1, 14) and modified obtained as a result of thermal composition of appropriate magnesium carbonates at 800ºC. The values of specific surface area were low, but a bit higher for the samples obtained with an addition of a modifier. This observation is explained, similarly as the wettability results, by a beneficial effect of PEG on surface activity of magnesium oxide.

The highest values of specific surface area were found for samples 4 and 24, which also showed the best dispersive properties (see Tables 1, 2). The samples obtained in the first mode, when CO_2 was introduced into the suspension, are definitely mesoporous as their pore diameters vary in the range 22.4–28.5 nm.

The results presented in this paper are a continuation of the previous study (Pilarska, 2011), on synthesis of magnesium carbonates and their calcinates by the method of carbonatization. The previous work concerned determination of the conditions of the process of synthesis on the basis physicochemical parameters of the final product, MgO. On the basis of the results from the previous work we could choose and apply the best parameters of the process of magnesium carbonate precipitation. The optimum reaction systems (leading to samples 1 and 14) were modified by addition of a non-ionic surfactant. The results presented in this paper prove a beneficial effect of modification with PEG compounds. Depending on the molecular mass and concentration of a modifying PEG and on the mode of reagents supply, the final materials were characterised by different dispersive-morphological and physicochemical properties.

Table 3. Adsorptive properties of selected magnesium oxide samples precipitated at different precipitation process conditions with and without a modifier

Sample No.	BET surface area (m^2/g)	Total volume of pores (cm^3/g)	Mean size of pores (nm)
1	21	0.15	28.5
4	36	0.21	22.8
7	33	0.19	22.4
14	17	0.01	2.9
20	34	0.02	2.8
24	35	0.02	2.9
26	30	0.02	2.7

4. Conclusions

As follows from the dispersive measurements, the final samples obtained with the use of a modifier contain of smaller size particles and have a more uniform morphology. In the mode of gaseous CO_2 supply to a 10% suspension of magnesium hydroxide, the sample of the most favourable properties was that obtained with the addition of PEG 200 in a concentration of 2% (particle size varied from 122 to 531

nm). In the case of simultaneous supply of the reagents into a water system, with the use of a 5% magnesium hydroxide suspension, the samples of the most attractive properties was that obtained with the addition of PEG 20 000 in a concentration of 0.5% (particles size varied from 28 to 531 nm, low tendency towards agglomerate formation). Changes in the microstructure were found to affect the sample wettability. The samples obtained with the addition of 2% PEGs 200, 400 or 20000 were almost fully hydrophobic. The MgO samples obtained with the use of a modifier show specific surface areas in the range 30–36 m^2/g, which is somewhat greater than those of the unmodified samples. All finally obtained MgO samples are characterised by a well-developed crystalline structure.

Acknowledgements

This work was supported by Poznan University of Technology research grant no. 32-125/2011-DS.

References

BANDI W.R., KRAPF G., 1976, *Effect of CO, pressure and alkali salt on the. Mechanism of decomposition of dolomite,* Thermochim. Acta, 14, 221-243.

BOTHA A., STRYDOM C.A., 2001, *Preparation of a magnesium carbonate from magnesium hydroxide*, Hydrometallurgy, 62, 175-183.

CHOUDHARY V.R., RANE V.H., GADRE R.V., 1994, *Influence of precursors used in preparation of MgO on its surface properties and catalytic activity in oxidative coupling of methane,* J. Catal., 145, 300-311.

GENNARO A.R. (Ed.), 1985, Remington's Pharmaceutical Sciences, 17 th Ed., Mack Publishing Company, Easton, 795-799.

HOLLINGBERG L.A., HULL T.R., 2010, *The thermal decomposition of hunite and hydromagnesite – a review*, Thermochim. Acta, 509, 1-11.

HONGCHANG H., SHAN H., JINGING F., HULIANG G., 2011, *Effect of stearic acid, zinc stearate coating on the properties of synthetic hydromagnesite,* Appl. Surf. Sci., 257, 2677-2682.

KHAN N., DOLLIMORE D., ALEXANDER K., WILBURN F.W., 2001, *The origin of the exothermic peak in the thermal decomposition of basic magnesium carbonate*, Thermochim. Acta, 367-368, 321-333.

MESHKANI F., REZAEI M., 2010, *Effect of process parameters on the synthesis of nanocrystalline magnesium oxide with high surface area and plate-like shape by surfactant assisted,* Powder Technol., 199, 144-148.

MOROZOW S.A., MALKOV A.A., MALYGIN A.A., 2003, *Synthesis of porous magnesium oxide by thermal decomposition of basic magnesium carbonate,* Russ. J. Gen. Chem., 73, 37-42.

PANG C.L., THORNTON G., 2009, *Manipulation of oxide surfaces,* Surf. Sci., 603, 3255-3261.

PILARSKA A., JESIONOWSKI T., 2011, *Synthesis of MgO in magnesium hydroxide carbonatisation process,* Physicochem. Probl. Miner. Process, 46, 83 –94.

WANG W., QIAO X., CHEN J., LI H., 2007, *Facile synthesis of magnesium oxide nanoplates via chemical precipitation,* Mater. Lett., 61, 3218-3220.
VAGVÖLGYI V., HALES M., FROST R.L., LOCKE A., KRISTOF J., HORVATH E., 2008, *Conventional and controlled rate thermal analysis of nesquehonite $Mg(HCO_3)(OH)\cdot 2(H_2O)$,* J. Therm. Anal. Calorim., 94, 523-528.
YILDRIM M., AKARSU H., 2010, *Preparation of magnesium oxide (MgO) from dolomite by leach – precipitation – pyrohydrolysis process,* Physicochem. Probl. Miner. Process, 44, 257-272.

Pilarska A., Paukszta D., Szwarc K., Jesionowski T., *Wpływ modyfikatorów i warunków strącania na właściwości fizykochemiczne $MgCO_3$ i jego kalcynatów*, Physicochem. Probl. Miner. Process., 47 (2011) 79-90, (w jęz. ang.)

Przedstawiono badania nad wpływem modyfikatorów i warunków procesowych na otrzymywanie tlenku magnezu metodą karbonizacji. Otrzymany z użyciem wodorotlenku magnezu i ditlenku węgla – węglan magnezu, poddano termicznemu rozkładowi w temperaturze 800ºC. Reakcję strącania przeprowadzono uwzględniając warunki eksperymentalne takie, jak: temperatura, sposób i szybkość dozowania reagentów oraz stężenie i rodzaj modyfikatora. Jako modyfikatory zastosowano związki niejonowe z grupy glikoli polietylenowych. Dla wytworzonych tlenków magnezu określono właściwości dyspersyjno–morfologiczne, profile zwilżalności oraz wyznaczono podstawowe parametry adsorpcji: powierzchnię właściwą BET, całkowitą objętość i średnią średnicę porów. Ponadto uzyskane produkty poddano identyfikacji metodą rentgenograficzną oraz analizie TG/DTA. Dowiedziono istotnego wpływu stężenia i rodzaju modyfikatorów na parametry fizykochemiczne otrzymanego MgO oraz wyłoniono produkty o najbardziej reprezentatywnych właściwościach.

słowa kluczowe: MgO, karbonizacja, modyfikacja, rozkład termiczny, wielkość cząstek, morfologia powierzchni

Physicochem. Probl. Miner. Process. 47(2011) 91-104
www.minproc.pwr.wroc.pl/journal/

Physicochemical Problems of Mineral Processing
ISSN 1643-1049

Received March 30, 2011; reviewed; accepted April 16, 7 2011

Acidic leaching of cadmium from zinc plant residue

Mahdi GHARABAGHI, Mehdi IRANNAJAD, Amir Reza AZADMEHR

Department of Mining and Metallurgical Eng., Amirkabir University of Technology, Hafez Ave., Tehran, Iran, email: iranajad@aut.ac.ir, Tel:+98-21-64542900

Abstract. In the present paper cadmium leaching from zinc plant residue by sulphuric acid leaching was examined. Zinc plant residue is a hazardous waste which is produced in hydrometallurgical zinc plant and it contains considerable amounts of metal values, such as zinc, cadmium and nickel. The effect of sulphuric acid and other important factors such as reaction time, solid/liquid ratio, particle size, stirring speed and temperature on cadmium recovery was investigated. The concentration of cadmium in solution was observed to increase with an increase of reaction time, acid concentration, stirring speed and temperature. Decreasing of solid/liquid ratio and particle size were also beneficial for cadmium recovery. The largest cadmium leaching recovery (97%) was obtained after 30 minutes of treatment at 25°C, H_2SO_4 (8% (v/v)) and with solid/liquid ratio of 0.10. XRD and SEM analyses of the residues obtained after leaching showed that the cadmium containing phase had been decomposed in the leaching residues. The results indicated that it is possible to use this waste as a secondary resource for cadmium recovery.

keywords: hazardous waste, leaching, cadmium extraction, zinc plant residue

1. Introduction

Cadmium is an important metal which is extensively used in solar batteries, electronic, electroplating, metallurgical industries, synthetic chemicals, ceramics, etc. (Arntz et al., 1999; Cheremisinoff, 1995; Reddy et al., 2005). Cadmium is relatively rare metal in the earth's crust and occurs naturally as a minor constituent of base metal ores (Habashi, 1997). Cadmium is obtained as a by-product from base metals production or recovered from other secondary resources such as Ni-Cd batteries, cadmium–tellurium solar cells, zinc sinter plant fume, cadmium-containing alloys and, etc. (Agrawal and Sahu, 2006; Butterman, 2002; Freitas and Rosalém, 2005; Huang, 2007; Reddy, 2006). Hydro and pyrometallurgical processes have employed for the recovery of metals from these resources.

In the hydrometallurgical zinc extraction, waste material containing cadmium is generated in the form of solid residue. This waste contains considerable amounts of metals values, such as zinc, cadmium and nickel. The disposal of zinc plant residue causes not only the environmental pollution but loss of resources as cadmium and its

compounds are highly toxic and carcinogenic in nature (Agrawal and Sahu, 2006; Altundoğan, 1998; Elyahyaoui and Bouhlassa, 2001; Kumar et al., 2009; Turan, 2004; Safarzadeh, 2008). Contributing to metal losses and potential environmental pollution, it is possible to manage zinc plant residue by using this waste as cadmium secondary resource. Recycling of metals will conserve the natural resources to meet the future demand of materials and also reduce the environmental pollution. The extraction of metal from hazardous wastes has coincidence with the legislations assigned to protect the environment in the world and can mitigate unfavorable environmental impacts (Chen et al., 2011).

In the recent years, a lot of research has performed for recovery of cadmium and nickel from some waste as secondary resources (Agrawal and Sahu, 2006; Alonso et al., 2006; Bernardes, 2004; Cortina, 1996; Freitas and Rosalém, 2005; Huang, 2007; Nogueira and Margarido, 2004; Reddy et al., 2005; Safarzadeh, 2007, 2009). Zinc plant residue contains high concentration of cadmium, and it can be used for cadmium extraction. In addition, this waste contains a desirable amount of nickel and other valuable metals, and it can be considered as a secondary resource for these metals. This waste composition is varied due to the origin of zinc concentrate and process conditions which have used for zinc production. The average cadmium content in these wastes which are produced in different zinc plants in the world are shown in Table 1.

Table 1. Cadmium content in zinc plant wastes

Country	Cadmium concentration (%)	Reference
Turkey	3.0	(Kumbasar, 2009)
Iran	14.5	(Safarzadeh, 2009)
Turkey	1.33	(Kul, 2008)
Yugoslavia	2-6	(Stanojevic et al., 2000)
India	6-7	(Singh, 1996)
Brazil	26	(Gouvea and Morais, 2007)

As can be seen in the table 1, there are considerable cadmium concentrations in these wastes, and they can be considered as cadmium secondary resources. Recycling of these wastes for other industries is a good approach for minimizing environmental problems. Recycling of hazardous waste becomes more important in recent years due to the shortage of high quality ore reserve.

In this study, the leaching of cadmium in aqueous sulphuric acid solution was investigated. The effects of the acid concentration, reaction time, particle size, solid/liquid, reaction temperature and stirrer speed on the dissolution rate have been

evaluated. In addition, optimum conditions which provided maximum cadmium extraction using a hydrometallurgical process were determined. The results of this study are important from the environmental point of view in the treatment and recovery of cadmium from wastes.

2. Experimental

The zinc plant residue used in the study was provided from zinc plant in Zanjan, Iran. The sample was ground and sieved by ASTM standard sieves to obtain the nominal particle size fractions of -850+425, -425+250, -250+75, -250, -75 μm in diameter. The chemical composition of the sample is given in table 2. As shown in table 2, the sample contained high amounts of cadmium and zinc. The XRD results indicated that metals were in the oxide form.

In the leaching experiments, sulphuric acid (Merck, Germany) and distilled water were used. Leaching experiments were carried out in a 500 ml Pyrex reactor equipped with a stirrer motor for mixing and reflux condenser to prevent losses by evaporation. The reactor was inserted into a temperature controlled water bath for controlling the reaction temperature. 100 milliliters of sulphuric acid at pre-determined concentrations (v/v) was transferred into the reactor, brought to the desired temperature and then 10 g of dried sample was added onto the acid solution. The leaching was continued for the pre-determined periods and the content of reactor was filtered as soon as the process finished. The cadmium concentration in solution was analyzed using an Atomic Absorption Spectrophotometer (AAS) of Perkin-Elmer.

Table 2. The chemical analysis of the sample

Component	ZnO	CdO	NiO	CuO	PbO	SO_3	CaO	Fe_2O_3	MgO	Al_2O_3	LOI*
Amount, %	38.92	16.56	4.21	1.99	1.38	12.10	2.61	0.44	0.20	0.34	20.54

Loss on ignition (LOI) is the sample weight reduction after being ignited.

3. Results and discussion

The solubilisation of metals can be predicted from Eh-pH (or Pourbaix) diagrams and also the Cd, Zn, Ni and Cu sulphates solubility products can be obtained from thermodynamic data (Nogueira and Margarido, 2004; Pourbaix, 1978). In the leaching system, the concentration of metals depend on the equilibrium pH of the solution and equilibrium solubility constant of the metals sulphate.

The Eh–pH diagram for the Cd–S–H_2O system is shown in Fig. 1, which has been drawn using a Medusa software. From the Fig. 1 it is obvious that SO_4^{-2} ion increases the solubility of Cd ion in the leaching system and the following complexation reaction occurs through sulfuric acid leaching:

$$Cd^{2+} + SO_4^{-2} = CdSO_4. \quad (1)$$

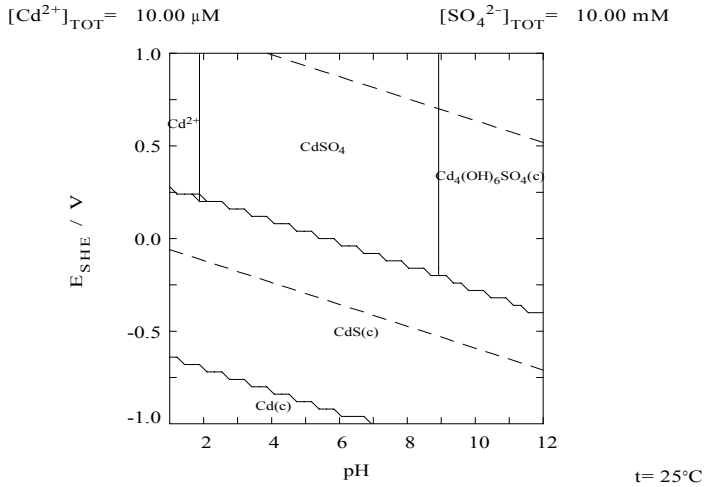

Fig. 1- Eh–pH diagrams Cd–S–H_2O system, Medusa software (Royal Institute of Technology, Sweden, http://www.kemi.kth.se/medusa)

3.1. Effects of leaching time

Using a constant sulphuric acid concentration (8% (v/v)), the effect of leaching time on the cadmium extraction was investigated at a temperature of 25 °C, a stirring speed of 500 rpm and solid/liquid ratio of 0.10. The percentage extraction of cadmium vs. time was plotted and presented in Fig. 2. The results clearly demonstrate that cadmium extraction was fast and reached equilibrium within 30 minutes. Within the first 10 minute, 78% cadmium extraction was achieved. This increased to 93% after 20 minutes dissolution. After an initial fast reaction rate, cadmium concentration in leach solution increased slowly with time. For example, after an initial increase of cadmium extraction up to 97% within 20 minutes, cadmium concentration slowly increased and reached 97% after 30 minutes. This can be attributed to the increase in solution pH with time because of the consumption of acid as the leaching proceeds.

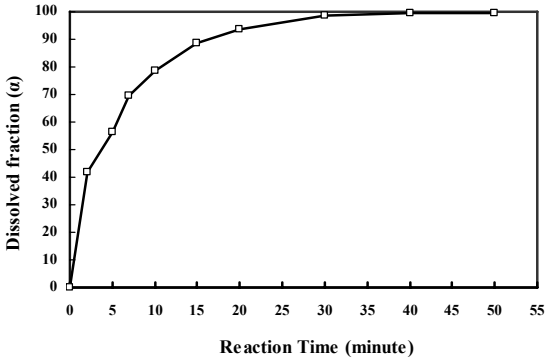

Fig. 2. The effects of reaction time on cadmium extraction (8% acid concentration (v/v), S/L=0.10, T=25° C, 500 rpm, -250 µm)

The results clearly demonstrate the effects of leaching time on the cadmium extraction. With the leaching time of 30 minutes, the leaching efficiency reached about 97% at 25 °C using solid to liquid ratio of 10%. When the leaching time was above 30 minutes, there was not any significant difference on leaching efficiencies. Therefore, 30 minutes was the optimum leaching time and extended leaching times had no significant effects on cadmium extraction.

3.2. Effects of acid concentration

The effects of sulphuric acid concentration on the dissolution of cadmium for 40 minutes of leaching time are given in Fig. 3. Experiments were performed with five different acid concentrations (v/v) at a reaction temperature of 25 °C, a stirring speed of 500 rpm, a particle size of −250 μm and solid/liquid ratio of 0.10. There was low cadmium extraction efficiency in low acid concentration, namely 2 and 5% (v/v). By increasing the acid concentration, the extraction values were greatly increased and reached to 99.0% at 15% (v/v) sulphuric acid concentration. In the 2 and 5% (v/v) acid concentration, the amount of acid was not adequate to extract all of leachable cadmium. As observed from the experimental results given in Fig. 3, using 8% (v/v) acid concentration, the cadmium contents increased and reached to its maximum by increasing the leaching time up to 30 minutes, and then remained almost constant.

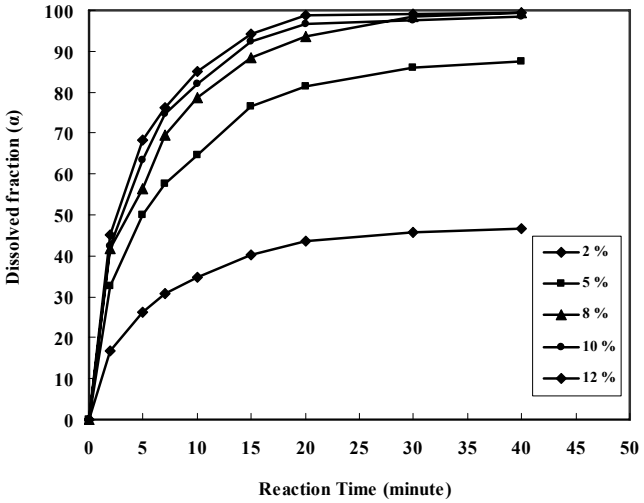

Fig. 3. Effects of acid concentration on cadmium extraction from waste (25°C; 500 rpm, S/L=1/10, particle size: -250 μm)

Increasing cadmium extraction as acid concentration increases is due to acid concentration effect on increasing the H^+ activity, that result further dissolution of cadmium containing material. Similarly, (Babu et al., 2002) also confirmed that the zinc extraction from zinc sulphide concentrate is a function of sulphuric acid

concentration. Similar results were also observed by Bodas (Bodas, 1996) and Souza et al. (Souza et al., 2007).

After 30 minutes the reaction reached equilibrium and the formation of solid products at the system prevented further leaching of the cadmium. In addition, the precipitation of gypsum or other insoluble minerals which were present in the leaching prevented further dissolution is. However, regarding to the obtained results, there were no beneficial effects of increasing acid concentration more than 8% (v/v) in 30 minutes leaching.

3.3. Effects of solid-liquid ratio

In order to evaluate the influence of solid to liquid ratio on the cadmium leaching recovery, experiments were carried out for 40 minutes at 25 ◦C and acid concentration of 8% (v/v). The results presented in Table 3 indicate that the cadmium concentration in the solution increased with decrease in solid liquid ratio. Cadmium extraction rises from 71.2 % at S/L 0.30 to 98.65% at S/L 0.05. However the cadmium recovery was 97.5% at S/L 0.05. When S/L was lower than 0.10, cadmium leaching recovery increased slowly. The improvement of leaching results in low solid percent can be attributed to the fact of the amount of reagent to each particle increases with decreasing solid amounts in the leaching process. Therefore, in the diluted pulp it was expected to achieve increasing in dissolution rate. Similar results for dissolution were found in other studies (Zhang and Nicol, 2010).

For economy and cadmium leaching recovery, lower S/L led to a dilute solution which was unfriendly to the filtration. Thus, solid to liquid 0.10 is considered the optimal.

Table 3. Effect of solid to liquid ratio on cadmium extraction (25^{o}C; 500 min^{-1}, 30 minutes; Acid concentration: 8% (v/v))

Test No.	Solid to liquid ratio	Cadmium extraction (%)
1	0.05	98.65
2	0.10	97.50
3	0.15	86.15
4	0.20	79.10
5	0.30	71.20

3.4. Effects of particle size

To investigate the effect of the particle size on the cadmium dissolution rate, experiments were carried out using five different particle sizes of the sample (-850+425, -425+250, -250+75, -250, -75 μm) at a reaction temperature of 25 °C, a stirring speed of 500 rpm and an acid concentration of 8% (v/v). As can be seen in table 4, as the particle size decreases, the cadmium dissolution rate increases. After 5

minutes leaching time, 48.2 % cadmium was extracted using sample size -850+425 micron, and it improved to 63.5% using sample size finer 75 micron. The cadmium leaching recovery kept at the level between 97% and 99% when samples size was lower than 250 μm. This situation can be attributed to the increasing contact surface of the samples as the particle size decreases. Regarding to the obtained results, we have considered -250 micron as optimum particle size.

Table 4. Variation of cadmium extraction with particle size

Fraction	Particle size (μm)	Cadmium extraction (%)
1	-850+425	89.15
2	-425+250	92.12
3	-250+75	96.52
4	-250	97.61
5	-75	99.19

3.5. Effects of stirring speed

To observe the effect of stirring speed on the dissolution rate, experiments were carried out at particle size of −250 μm, a reaction temperature of 25 °C and an acid concentration 8% (v/v). As shown in Table 5, the stirring speed had a significant influence the cadmium dissolution rate and higher extraction values were achieved at higher stirring speed. The cadmium extraction The increased more than 25% when the stirring speed increased from 100 to 400 rpm, further increase of the stirring speed had a little effect on cadmium extraction. The maximum extraction values reached at this condition was more than 97%. The experimental results showed that the dissolution rate is practically independent of the stirring speed after 500 rpm. So the stirring speed of 500 rpm was considered as optimum agitating rate.

Table 5. Effect of stirring speed on cadmium leaching, (8 %(v/v) acid, 25 °C, 500 min^{-1}, 30 min, S/L=0.10)

Test No.	Stirring speed (rpm)	Cadmium extraction (%)
1	0	32.11
2	100	74.94
3	200	85.64
4	300	93.31
5	400	96.57
6	500	97.21
7	600	98.83

3.6. Effects of temperature on the leaching

The effect of the temperature on the dissolution rate was studied using four different reaction temperatures 25 to 75°C) at a particle size of −250 μm, a stirring

speed of 500 rpm and an acid concentration of 8% (v/v). Fig. 4 shows that increasing reaction temperature increases the dissolution rate, as expected from the exponential dependence of the rate constant in the Arrhenius equation. More than 88% of the cadmium present in the sample was extracted after 15 minutes at a reaction temperature of 25 °C and it improved to 97% at 75°C. However, the obtained results show that by increasing the leaching time, the effects of temperature decreased. This behavior was observed in previous work carried out by Abdel-Aal and Rashad (2004), Mulak et al. (2005) as well as Nogueira and Margarido (2004).

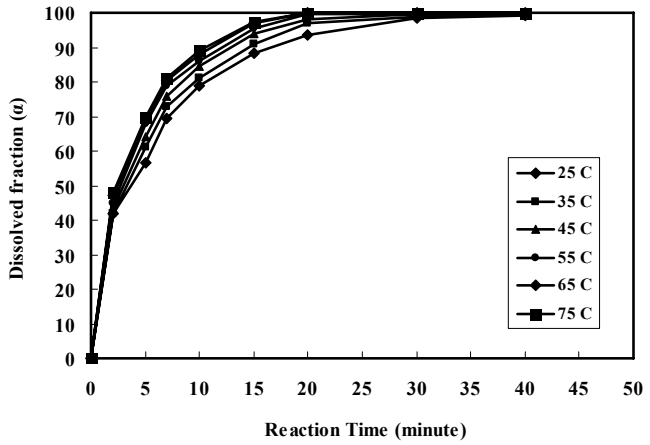

Fig. 4. Effect of reaction temperature on the cadmium extraction (8% (v/v) acid, 25°C; 500 rpm, S/L=1/10, particle size: -250 micrometer, 500 min^{-1})

4. Characterization of leaching residue

A series of analyses were performed to measure the chemical composition and to determine the mineralogy, morphology and particle size of leaching residues obtained under different leaching time. The chemical composition of the three residues obtained at an acid addition of 8% (v/v) stirring speed 500 rpm, solid to liquid ratio of 0.10, 25 °C after 5, 15 and 30 minutes leaching is shown table 6.

It can be seen that only about 0.01–0.02% of cadmium remains in the residue. As can be observed in table 6, by increasing the leaching time, the Cu, Ca and Pb amounts increased markedly while the cadmium content decreased correspondingly. In fact, the amounts of Ca and Pb remained almost the same and increasing of Cu, Ca and Pb amounts in the leach residues were due to the decreases in the Ni, Cd and Zn containing materials.

A XRD analysis of the same residues in table 6 was also performed. Gypsum, $ZnSO_3.2H_2O$, PbO were identified by XRD and cadmium compounds amounts decreased in residues by increasing leaching time. After 15 minutes leaching the gypsum, copper oxide and different lead compounds were formed. There was a little amount of cadmium in the leaching residue yet. After 30 minutes leaching, only

copper, lead, calcite compounds were identified and gypsum was the main constituent. No cadmium containing materials were detected in the residue. This gives rise to the assumption that all the cadmium had been leached by sulphuric acid.

Table 6. Cadmium amounts in residue after different leaching time

Leaching Time (min)	5	15	30
Nickel (%)	3.01	1.24	0.17
Cd (%)	9.31	3.12	1.13
Zn (%)	21.36	8.73	2.11
Cu (%)	4.12	9.14	12.61
Pb (%)	7.32	15.41	18.46
Ca (%)	12.35	27.72	37.62

The gypsum and lead oxide intensity in the sample increased markedly after leaching, and the nickel and cadmium intensity decreased extremely. It could be expected that nickel and cadmium compound dissolved in the system. Furthermore, the Fe_2O_3 intensity also increased slightly.

Figure 5 to 8 show SEM images the residues obtained at leaching condition. The particle size distributions for these residues are shown in Fig. 5. From Fig. 5, it can be seen that the particles vary in size and they showed wide particle size distribution (Fig. 5a). The sample particles have irregular shapes (Fig. 5b). The micrographs of the leaching residues show a progressive reduction in particle diameter (Fig. 6) and then an increase in roughness and porosity of the solids as shown in Fig. 7.

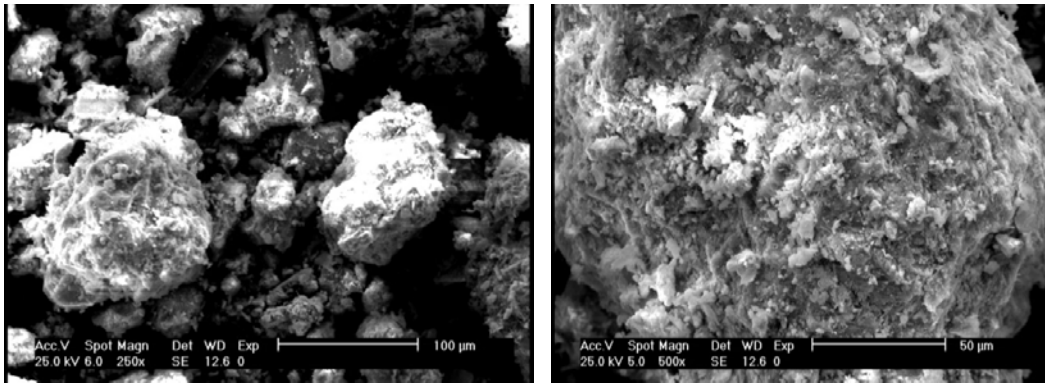

a b

Fig. 5. (a, b). Particles of the sample before leaching

There was a large area of erosion at the sample surface (Fig. 7) and the surface was very rough and loose, approaching a porous structure. The EDAX analysis showed the amount of cadmium in the leaching residue decreased and amount of calcite and gypsum increased by increasing leaching time. This situation may be

because the cadmium compounds were dissolved at the first. After 30 minutes leaching, other compounds such as calcite and gypsum were remained in the residue (Fig. 8).

The characterization study showed that the cadmium containing phases progressively disappeared as indicated by XRF results. Fewer soluble calcite and lead containing phases predominated at later stages and their grains are also observed in the leaching residue (Fig. 8).

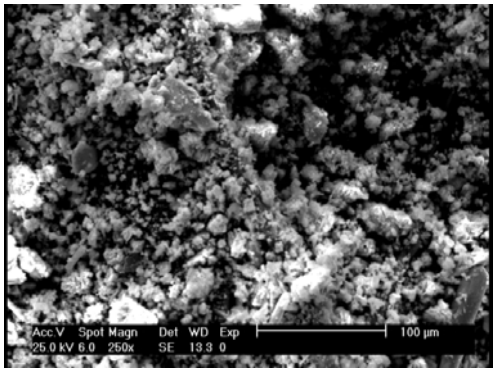

Fig. 6. Particles of the sample after 15 minutes leaching. Leaching conditions: 8% Acid concentration (v/v), 25 °C, 500 min^{-1}, 100 g/dm^3 solids

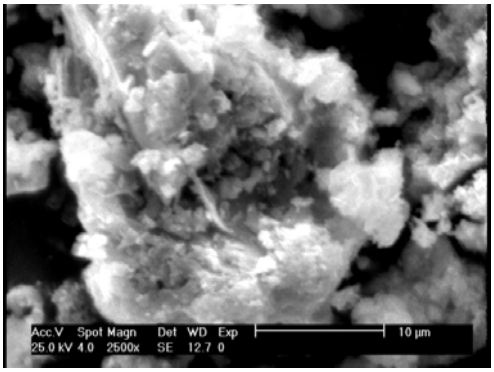

Fig. 7. Surface of particle after 20 minutes leaching. Leaching conditions: 8% Acid concentration (v/v), 25 °C, 500 min^{-1}, 100 g/dm^3 solids

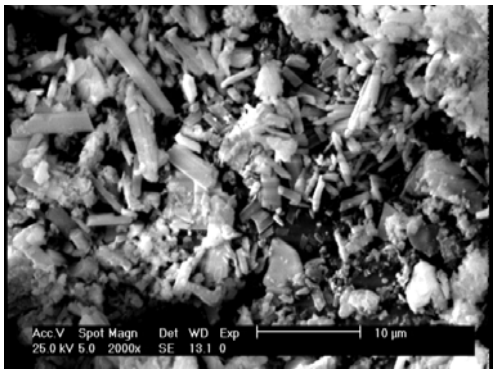

Fig. 8. Particles of the samples after 30 minutes leaching. Leaching conditions: 8% Acid concentration (v/v), 25 °C, 500 min^{-1}, 100 g/dm^3 solids

5. Final optimum experiment and process flowsheet

By optimization of the leaching variables summarised in table 7 the final test was performed. The results showed with using these optimum parameters, it was possible to extract more than 97% of cadmium in the sample. The process flowsheet for cadmium and other metals recovery from this waste is presented in Fig. 9.

Table 7. The results of leaching under optimum process conditions

Time (minute)	Acid Consumption (v/v) %	Solid/Liquid ratio (%)	Temperature (C)	Stirring Speed (min^{-1})	Ni Extraction (%)
30	8	0.10	25	500	97

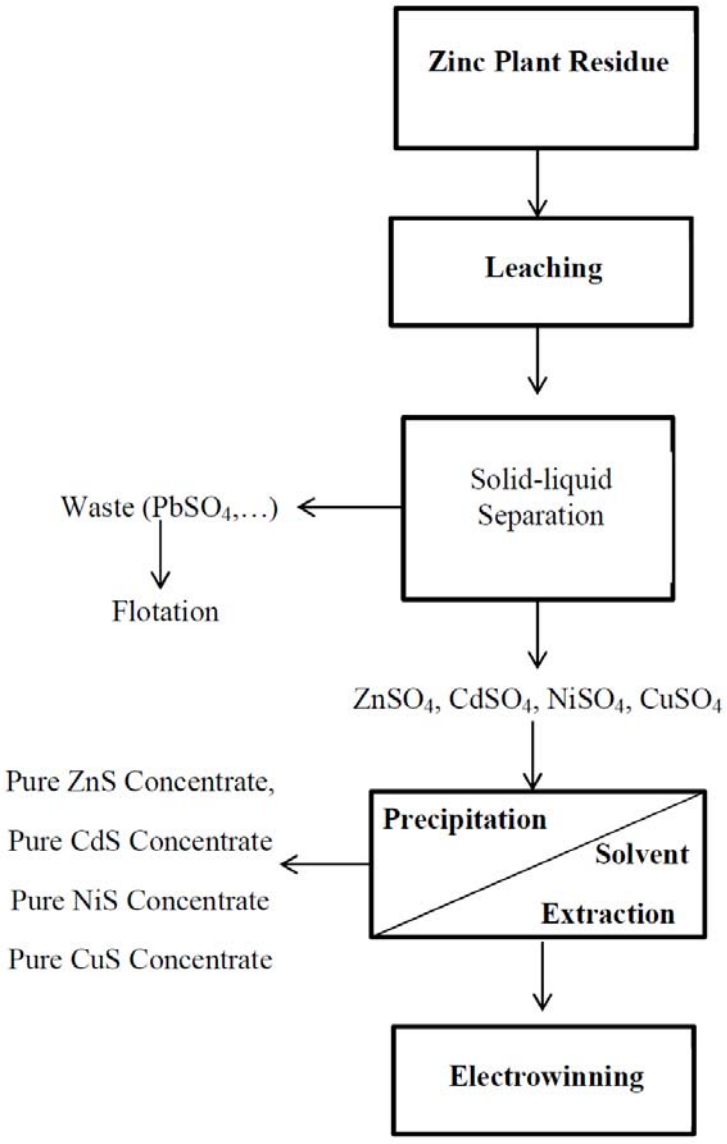

Fig. 9. Flowsheet for the metals recovery from zinc plant residues

6. Conclusions

Sulphuric acid leaching tests performed on Iranian zinc plant residue show that 98 of cadmium can be leached in 30 minutes at 25°C using 8% sulphuric acid solutions. Evaluation of the experimental data showed that cadmium extraction rate increased with increasing leaching time, acid concentration, stirring speed and decreasing solid to liquid ratio. Decreasing particle size was beneficial for leaching performance. SEM and XRD results showed that by increasing leaching time, the cadmium compounds have leached faster than other minerals in the leaching system.

The results indicated that it is possible to extract more than 97% cadmium content using these optimum parameters.

References

Abdel-Aal, E.A., Rashad, M.M., Kinetic study on the leaching of spent nickel oxide catalyst with sulfuric acid. Hydrometallurgy, 2004, 74(3-4), 189-194.

Agrawal, A., Sahu, K.K., Kinetic and isotherm studies of cadmium adsorption on manganese nodule residue. Journal of Hazardous Materials, 2006, 137(2), 915-924.

Alonso, M., López-Delgado, A., Sastre, A.M., Alguacil, F.J., Kinetic modelling of the facilitated transport of cadmium (II) using Cyanex 923 as ionophore. Chemical Engineering Journal, 2006, 118(3), 213-219.

Altundoğan, H.S., Erdem, M., Orhan, R., Özer, A., Tümen, F., Heavy Metal Pollution Potential of Zinc Leach Residues discarded in Çinkur Plant,. Turkish Journal of Engineering and Environmental Science, 1998, 22, 167-177.

Arntz, Y., Chambron, J., Dumitresco, B., Eclancher, B., Prat, V., A portable cadmium telluride multidetector probe for cardiac function monitoring. Nuclear Instruments and Methods in Physics Research Section A: Accelerators, Spectrometers, Detectors and Associated Equipment, 1999, 428(1), 150-157.

Babu, M.N., Sahu, K.K., Pandey, B.D., Zinc recovery from sphalerite concentrate by direct oxidative leaching with ammonium, sodium and potassium persulphates. Hydrometallurgy, 2002, 64(2), 119-129.

Bernardes, A.M., Espinosa, D. C. R., Tenório, J. A. S., Recycling of batteries: a review of current processes and technologies. Journal of Power Sources, 2004, 130(1-2), 291-298.

Bodas, M.G., Hydrometallurgical treatment of zinc silicate ore from Thailand. Hydrometallurgy, 1996, 40(1-2), 37-49.

Butterman, W.C., Plachy, J.,, 2002. Cadmium, mineral commodity profiles. U.S. Geological Survey.

Chen, Y., Mariba, E.R.M., Van Dyk, L., Potgieter, J.H., A review of non-conventional metals extracting technologies from ore and waste. International Journal of Mineral Processing, 2011, 98(1-2), 1-7.

Cheremisinoff, P.N., Handbook of Water and Wastewater Treatment Technology. 1995, Marcel Dekker, New York.

Cortina, J.L., Miralles, N., Aguilar, M., Sastre, A. M., Distribution studies of Zn(II), Cu(II) and Cd(II) with Levextrel resins containing di(2,4,4-trimethylpentyl)phosphonic acid (Lewatit TP807'84). Hydrometallurgy, 1996, 40(1-2), 195-206.

Elyahyaoui, A., Bouhlassa, S., Extraction of cadmium and iodocadmat species by di(2-ethylhexyl) phosphoric acid from perchloric and phosphoric media. Applied Radiation and Isotopes, 2001, 54(6), 921-926.

Freitas, M.B.J.G., Rosalém, S.F., Electrochemical recovery of cadmium from spent Ni-Cd batteries. Journal of Power Sources, 2005, 139(1-2), 366-370.

Gouvea, L.R., Morais, C.A., Recovery of zinc and cadmium from industrial waste by leaching/cementation. Minerals Engineering, 2007, 20(9), 956-958.

Habashi, F., Handbook of Extractive Metallurgy. 1997, Wiley/VCH, Weinheim

Huang, K., Ghimire, K.N., Inoue, K., Ohto, K., Kawakita, H., Harada, H., Morita, M., Leaching Kinetics of Cadmium from Scallop Waste by Dilute Sulfuric Acid Solution. JOURNAL OF CHEMICAL ENGINEERING OF JAPAN, 2007, 40(9), 786-791.

Kul, M., Topkaya, Y., Recovery of germanium and other valuable metals from zinc plant residues. Hydrometallurgy, 2008, 92(3-4), 87-94.

Kumar, V., Kumar, M., Jha, M.K., Jeong, J., Lee, J.-c., Solvent extraction of cadmium from sulfate solution with di-(2-ethylhexyl) phosphoric acid diluted in kerosene. Hydrometallurgy, 2009, 96(3), 230-234.

Kumbasar, R.A., Extraction and concentration study of cadmium from zinc plant leach solutions by emulsion liquid membrane using trioctylamine as extractant. Hydrometallurgy, 2009, 95(3-4), 290-296.

Mulak, W., Miazga, B., Szymczycha, A., Kinetics of nickel leaching from spent catalyst in sulphuric acid solution. International Journal of Mineral Processing, 2005, 77(4), 231-235.

Nogueira, C.A., Margarido, F., Leaching behaviour of electrode materials of spent nickel-cadmium batteries in sulphuric acid media. Hydrometallurgy, 2004, 72(1-2), 111-118.

Pourbaix, M., Atlas of Electrochemical Equilibria. 1978, Pergamon, New York.

Reddy, B.R., Neela Priya, D., Venkateswara Rao, S., Radhika, P., Solvent extraction and separation of Cd(II), Ni(II) and Co(II) from chloride leach liquors of spent Ni-Cd batteries using commercial organo-phosphorus extractants. Hydrometallurgy, 2005, 77(3-4), 253-261.

Reddy, B.R., Priya, D.N., Chloride leaching and solvent extraction of cadmium, cobalt and nickel from spent nickel-cadmium, batteries using Cyanex 923 and 272. Journal of Power Sources, 2006, 161(2), 1428-1434.

Safarzadeh, M.S., Moradkhani, D.,Ojaghi Ilkhchi, M. , Determination of the optimum conditions for the cementation of cadmium with zinc powder in sulfate medium. Chemical Engineering and Processing: Process Intensification, 2007, 46(12), 1332-1340.

Safarzadeh, M., Moradkhani, D., Ojaghi Ilkhchi, M., Hamedani Golshan, N., Determination of the optimum conditions for the leaching of Cd-Ni residues from electrolytic zinc plant using statistical design of experiments. Separation and Purification Technology, 2008, 58(3), 367-376.

Safarzadeh, M.S., Moradkhani, D., Ojaghi Ilkhchi, M., Kinetics of sulfuric acid leaching of cadmium from Cd-Ni zinc plant residues. Journal of Hazardous Materials, 2009, 163(2-3), 880-890.

Singh, V., Technological innovation in the zinc electrolyte purification process of a hydrometallurgical zinc plant through reduction in zinc dust consumption. Hydrometallurgy, 1996, 40(1-2), 247-262.

Souza, A.D., Pina, P.S., Leão, V.A., Silva, C.A., Siqueira, P.F., The leaching kinetics of a zinc sulphide concentrate in acid ferric sulphate. Hydrometallurgy, 2007, 89(1-2), 72-81.

Stanojevic, D., Nikolic, B., Todorovic, M., Evaluation of cobalt from cobaltic waste products from the production of electrolytic zinc and cadmium. Hydrometallurgy, 2000, 54(2-3), 151-160.

Turan, M.D., Altundogan, H.S., Tümen, F., Recovery of zinc and lead from zinc plant residue. Hydrometallurgy, 2004, 75(1-4), 169-176.

Zhang, S., Nicol, M.J., Kinetics of the dissolution of ilmenite in sulfuric acid solutions under reducing conditions. Hydrometallurgy, 2010, 103(1-4), 196-204.

Physicochem. Probl. Miner. Process. 47(2011) 105-112
www.minproc.pwr.wroc.pl/journal/

Physicochemical Problems of Mineral Processing
ISSN 1643-1049

Received January12, 2011; reviewed; accepted March 1, 2011

Hydrometallurgical recovery of molybdenum from Egyptian Qattar molybdenite concentrate

Ashraf M. AMER

Environmental Science Dept., Faculty of Science, Alexandria Univ., Egypt, ashrafamer0408@yahoo.com

Abstract. An attempt has been made in this investigation to develop a chemical method for treating molybdenite concentrate from Qattar (Eastern Desert, Egypt). The core of the process lies in replacement of pyrometallurgical processing with a hydrometallurgical method using oxygenated nitric acid leaching under atmospheric and oxygen pressure. The effects of temperature, acid concentration, partial pressure as well as the kinetics of leaching process were studied.

keywords: hydrometallurgy, flotation, leaching, molybdenum, kinetics

1. Introduction

Molybdenite deposits in Egypt are located in four main localities in the northern part of the Eastern Desert. These localities are Gebel Qattar, Abu Marwa, Abu Harba and Umm Disi. The Qattar molybdenite deposit is considered the largest (Dardir 1968; Said, 1990). At Gebel Qattar molybdenite mineralization occurs at the intersection of 27° 05' 29" N and 33° 16' 10" E. Molybdenite occurs in quartz veins as disseminations in the host granite. Total reserve of the area was estimated to be about 4.5 gigagrams (Gg) (Burgov 1983). Hydrometallurgical processing of molybdenite has received attention recently by process which involves roasting and pressure leaching with ammonium sulphate (Janngg, 1963). Oxidation and leaching of molybdenite concentrate using sodium hypochlorite (Bhappu et al. 1965; Iordanov 1962; He et al., 2007; Peng et al., 2007), acid chlorate or sulphuric acid with added managanese dioxide were also triad (Reznikov and Necheava 1962; and Zelikman and yashine et al., 1991). The use of hypochlorite or chlorine solution for leaching was abandoned due to the corrosive effects of leachants and problems associated with using highly toxic gases. Other methods were examined using sodium chromate as a leaching agent (Bartecki and Rycerz,L. 1988; Antonigeric and pacovic 1992) and bacterial leaching (Ivanov, 1962; Yashine et al., 1991). In India chlorination is used for treatment of low-grade molybdenite concentrate in fluidized bed reactor (Evans 1988; Nair et al. 1988; Johnston and Pickles 1990). In Russia, interaction of molybdenite concentrate with

nitric acid was investigated (Bjarling, G. and Kolta, G.A. 1964; Chursanov et al., 1987; Peters, 1992; Zhang (2009); Smirnov et al., 2010).

The objective of this investigation is to study nitric acid leaching of molybdenite concentrate under atmospheric and oxygen pressure as well as the kinetics of pressure leaching process.

2. Experimental

2.1. Material and Methods

Gebel Qattar molybdenite ore occurs in two forms. The fist form, crystals, are irregularly distributed in the quartz veinlets. They are well developed showing length variation between 2 to 3 cm. The second form is massive ore at wall rock confined to areas between molybdenite crystals bearing quartz veins and the granitic host rock. The chemical composition of the investigated Gebel Qattar molybdenite concentrate is given Table 1.

Table 1. Chemical analysis of the investigated Gebel Qattar molybdenite concentrate

composition	percentage (by weight)
Mo	30.2
S	24.3
Ni	0.17
Cu	0.35
Fe	1.62
Si	7.05
Total	99.5

2.2. Apparatus

The pressure leaching experiments were carried out in 2 dm^3 laboratory autoclave. The autoclave had the following features: a maximum working pressure of 20.6 MPa temperatures of 300°C and stirring speed of 1600 rpm. Description of used apparatus is given ells where (Amer, 1996)

Details on leaching experiments in open vessel and in autoclave are given elsewhere (Amer, 1996).

2.3. Analysis

Molybdenum in solution and in solid samples was analyzed spectrophotometrically. The technique follows that of Jefferry and Justschison (1981) which was modified by the Chemistry Division of the Federal Geological Survey in Germany.

3. Results and discussion

3.1. Mineralogical study

X-ray examination along with microscopic investigation of representative molybdenite sample revealed that molybdenite mineral content is about 1%. Quartz seems to be the main gangue mineral, present mainly as coarse anhedral crystals with smooth interlocking borders, constitutes about 70 % of the sample. Feldspars follows quartz in abundance. Oligoclase and orthoclase occur as fine to coarse anhedral grains, occasionally interstitial, or being enclosed in quartz. They form about 17% of the volume in the studied sample. Some micaceous minerals are present as muscovite and biotite (about 7%). Molybdenite is represented by globular forms having well developed concentric texture. Molybdenite grains show wide size variation.

3.2. Hydrometallurgical processing of molybdenite concentrate

3.2.1. Atmospheric leaching

The purpose of atmospheric acid leaching of molybdenite is to produce a very pure molybdenite oxide as the ordinary roasting process does not involve any purification and provide volatilization losses. Leaching of molybdenite with aqueous nitric acid is carried out according to the following reaction:

$$MoS_2 + 6NO^-_3 \rightarrow MoO^{2-}_4 + 2SO^{2-}_4 + 6NO \,. \quad (1)$$

Factors which influence the leaching rate of molybdenite are temperature, leaching time and nitric acid concentration. Results showing the effect of these factors on the leaching of molybdenite are illustrated in Figs 1 and 2. Molybdenum extraction has been found to increase with the increase of temperature and leaching time. Maximum molybdenum leaching recovery (96%) was reached at temperature of 100°C after 225 min of leaching a time. The effect of nitric acid concentration on molybdenum extraction is shown in Fig. 2. Generally as nitric acid concentration increases from 5 to 10 %, the molybdenum recovery increases at different leaching times. Practically, an increase of the acid concentration more than 10%, especially at long leaching time of 180-225 min had no effect on the molybdenum leaching recovery. It could be concluded that under atmospheric leaching conditions the maximum molybdenum extraction of 96% is reached under the following conditions:

temperature : 100°C
leaching time : 225 min
nitric acid concentration : 10%
pulp density : 10%.

From these conditions, it appears that the process of molybdenite leaching is slow under atmospheric conditions. For that, a series of experiments were carried out using autoclave to accelerate the rate of molybdenum recovery and to increase Mo recovery.

The temperature effect on the molybdenum leaching recovery has been studied over a temperature range from 120° to 200°C and the results are given in Fig. 3.

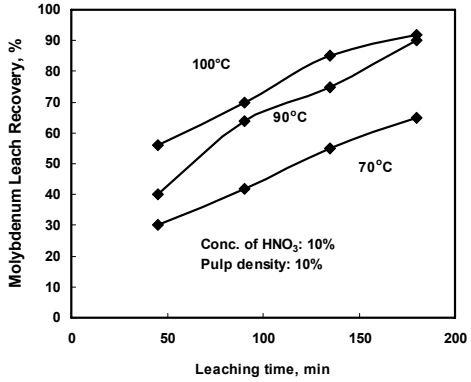

Fig. 1. Effect of leaching temperature on molybdenum extraction

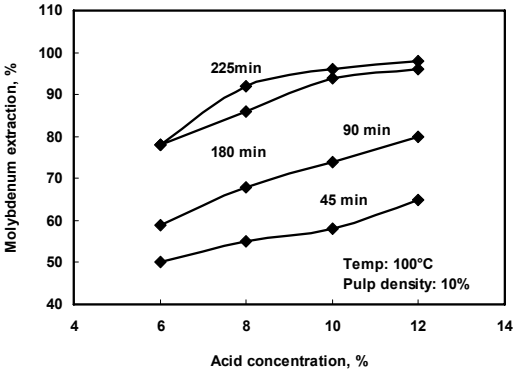

Fig. 2. Effect of acid concentration on molybdenum extraction

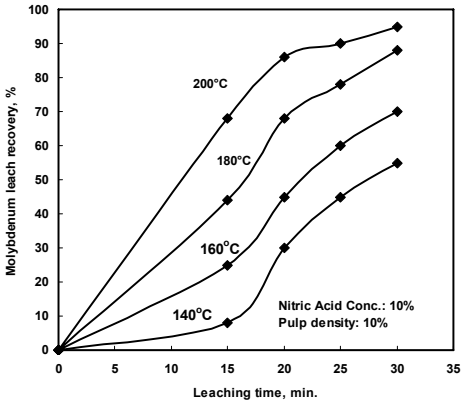

Fig. 3. Effect of leaching temperature on molybdenum extraction

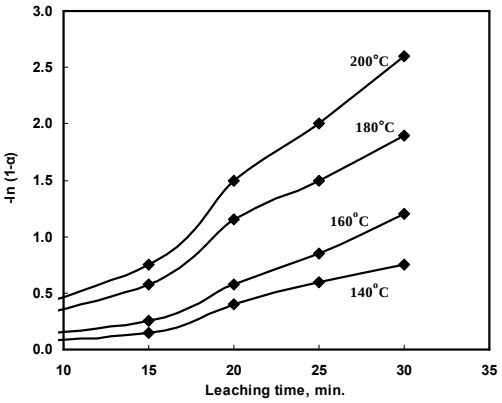

Fig. 4. Relation between ln(1-α) and time

It is obvious that the reaction rate increases with increasing temperature and reaches its maximum value at 200°C (2.9×10^3 sec^{-1}). As illustrated in Fig. 4 the plot of ln (1-α) versus t over the studied temperature range consists of a series of straight lines indicating that leaching of molybdenite fits a first order reaction, where slopes of these lines gives the rate of reaction (K).

An Arrhenius plot is constructed and shown in Fig. 5. The calculated apparent activation energy is 49 kJ/mol. This value is in a good agreement with the values reported by Kanome et al. (1987) for capper sulfide and nickel sulfide, respectively. The obtained value of activation energy (49 kJ/mol) is too high for the reaction to be controlled by mass transfer through the boundary layer but is possible for chemically controlled reactions (Wadsworth, 1972).

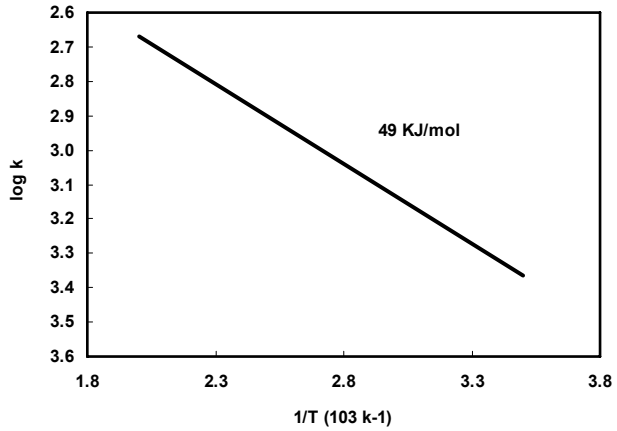

Fig. 5. The Arrhenius plot for determination of activation energy

The effect of oxygen partial pressure on molybdenum extraction is shown in Fig. 6. It is obvious that, at different leaching times of 15, 20 and 30 min, an increase of oxygen partial pressure from 0.5 up to 1.5 MPa leads to a remarkable increase in the molybdenum recovery while an increase of oxygen partial pressure to more than 1.5 MPa has practically no effect on improving molybdenum recovery.

Ninety six percent leaching recovery of molybdenum by nitric acid pressure leaching of the molybdenite concentrate seems to be an alternative applicable method of molybdenite processing.

The effect of acid concentration on the leaching recovery of molybdenum is shown in Fig. 7.

Ninety six percent leaching recovery of molybdenum is reached after 30 min of leaching time compared with 225 min in case of atmospheric leaching. A technological flow sheet of enrichment and processing of Qattar molybdenite deposits is given in Fig. 8.

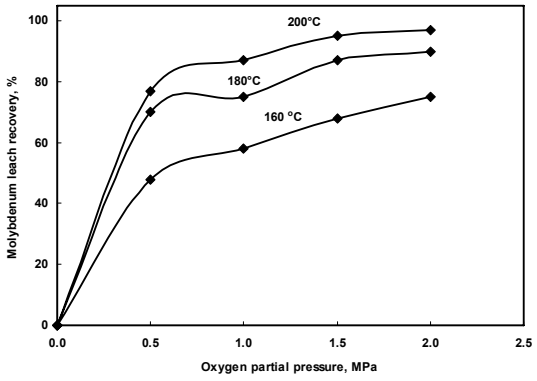

Fig. 6. Effect of oxygen partial reassure on molybdenum extraction

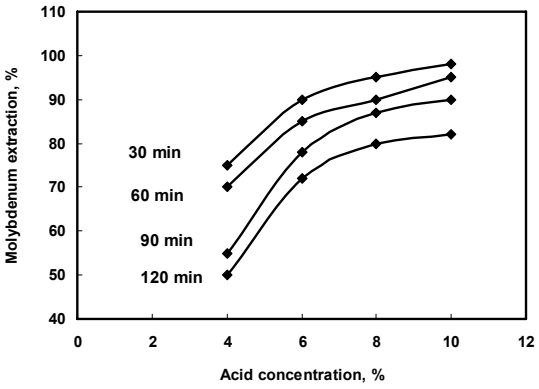

Fig. 7. Effect of acid concentration on molybdenum extraction

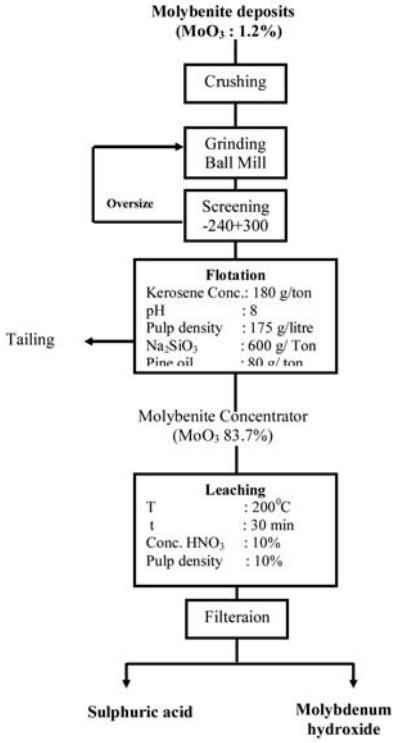

Fig. 8. Flowsheet of enrichment and processing of Qattar molybdenite deposits

4. Conclusions

Pressure leaching of molybdenite concentrates with nitric acid represents a new possible method for processing of molybdenite. The most favorable conditions for the 96% leaching recovery of molybdenum under atmospheric conditions are: temperature of 100^0 C, 225 min of leaching and nitric acid concentration equal to 10%. The most favorable conditions for pressure leaching of molybdenite to get 96% recovery are: 200˚C, 30 min of leaching, nitric acid concentration equal to 10% and oxygen partial pressure 1.5 MPa.

Refrerences

Ang, M.; Wang, X and Liu, W. (2009): A novel technology of molybdenum extraction from low Ni-Mo are, Hydrometallurgy, Vol. 97, Issues 1-2, PP. 126-130.

Amer, A.M. (1996): leaching of a low grade Egyptian chramite ore Hydrometallurgy, 43, 307-16.

Arbiter, N.; Fuju, Y,; Hansen, B. and Raja, A. (1975): Surface properties of hydrophobic solids. ALCHE Symposium series, 71 (150), 176-82.

Antonigevic, M.M. and Pacovic, N.V. (1992): Investigation of molybdenite oxidation by sodium dichromate. Miner. Eng. 5 (2), 223-33.

Bartecki, A. and Rycerz, L. (1988): Kinetics and mechanism of dissolution of synthetic molybdenum disulfide MoS2 in bromate solutions. Part I, hydrometallurgy, 20 (2), 235-48.

Burgov, V. (1983): Technical report on follow-up geochemical operations in the period 1968-1968-1972. Aswan mineral survey project, Geol. Surv. Egypt.

Bhappu, R.B.; Reynolsd, D.H. and Roman, R.J. (1965): molybdenite recovery from sulfide and oxide ores. J. Metals, 17, 1199-1205.

Bjarling, G. and Kolta, G.A. (1964): Oxidizing leach of sulfide concentrates and other materials catalyzed by nitric acid. Int. Min. process. Cong. VII.

Chander, S.; Wie, J.M. and Fuerstenau, D.W. (1975): On the native floatability and surface properties of naturally hydrophobic solids. ALCHE symp. Series, 71 (150), 183-8.

Chursanov, Yu. V.; Potashnikov, Yn. M. and Rumyantsev, V.K. (1987): Interaction of molybdenum disulfide with nitric acid. Isvetn. Met. (9), 56-7.

Dardir, A.A; and Gadalla, S.H.A. (1968): Report on expedition 7168, Eastern Desert. Geol. Surv. Egypt.

Dardir, A.A.; Abu Zeid, K.M. and Gadalla, S.H.A. (1983): molybdenite deposits of Gebel Qattar area. Annals. Geol. Surv. Egypt. XIII, 23-37.

Evans, D.F. (1980): Principles of extractive metallurgy, Gordon and Breach, New York, Vol. 2.

He, D-S.; Feng,Q.M, Zhang. L-M. and Lu,Y.P. (2007): An environmentally – friendly technology o vanadium extraction from stone coal. Miner. Eng. 20,PP. 1184-1186 .

Ivanov, V.I. (1962): Role of sulfur bacteria in the leaching of sulfide ores. Dobl. Akad. Nauk SSR, 146, 447-9.

Iodavov, K. and Zelikman, A.N. (1962): Kinetics of oxidation of molybdenite in a solution of NaOCL, Khim. Ind. (Sofia) 56, 109-26.

Jangg, G. (1963): Alkalische drucklaugung sulfidischer erze, Z. Erzbergbau metallhuttenw. 16, 508-14.

Johnston, C. and Pickles, C.A. (1990): Study of the reaction of molybdenum disulfide with lime and carbon at plasma temperature, Trans. Inst. Min. Metall., 100-4.

Jeffery, P.G. and Hutchinson, D. (1981): chemical methods of rock analysis. 3rd ed. Oxford: pergmon Press, 379 P.

Kanome, O., Abe, H.; Okuwaki, A. and Okabe, T. (1987): Sulfuric acid Oxygen-pressure leaching of Ni_3S_2 prepared by a wet Process. Hydrometallurgy, 19, 1-9.

Leja, J. (1982): Surface chemistry of frith floatation. Plenum Press, New York, 488P.,

Nair, K.U.; Sathiyamoothy, D.; Bose, D.K. and Cupta, C.K. (1988): Processing of low grade Indian molybdenite concentrate by chlorination in fluidized bed reactor. Int. J. Miner Process. 23 (3-4), 171-80.

Peng, J.R.; Yang, D.J.; Chen, J.X. and Yan, J.F.(2007): Experimental study on alkaline leaching of crude molybdenite under pressure of Oxygen.

Peters, E. (1992); Hydrometallurgical process innovation. Hydrometallurgy, Vol.29, Issue 1-3, pp. 43-55.

Papangelakis, V.G. and Demopoulos, G.P. (1991): Acid pressure oxidation of pyrite: reaction Kinetics, Hydrometallurgy, 26, 309-25.

Pesic, B. (1984): Dissolution of bornite in sulfuric acid using oxygen oxidant. Hydrometallurgy, 12, 195-215.

Reznikov, A.A and Necheava, A.A. (1962): Oxidation of molybdenite, Inform. Sb. Vses. Nauchn. Issled. Geol, Inst., 56, 109-26.

Said, R. (1990): The geology of Egypt. Balkema: Rotterdam, 525-29.

Somasundaran, P. and Anantapadmanabhan, K.P. (1979): Physico-Chemical aspects of floatation. Trans. Indian Inst. Met., 32, 177-97.

Smirnov, K.M.; Raspopov, N.A. Shneerson, Y.M., Lapin, A.Y.; Bitkov, G.A.; Menshikov, Y. A., Paskhin, P.N. and Kinehenko, v.p. (2011) Autoclave leaching of Molybdenite concentrates with catalytic attitives of nitric acid. Russian Metallurgy (Metally). Vol. 20,Issue 7,pp.58-95.

Wakamatsu, T. and Numate, Y. (1991): Floatation of graphite, Min. Eng. (4), 975-82.

Wadsworth, M.E. (1972): Rate processes in hydrometallurgy, Second Tutorial Symp. On extractive metallurgy, AIME, Salt Lake City, Utah.

Yashina, G.M.; Kostareva, M.A. and Nesterova, S.V. (1991): Leaching of Copper – molybdenum ores by chemical and biochemical methods. Fiz. Tekh. Probl. Razrab. Polezn. Iskop. (6), 93-7.

Yashina, G.M.; Kostareva, M.A. and Kameav, V.D. (1991): Prospects for leaching of molybdenum – containing ores. Tsv. Met. (16), 13-5.

Zhan. Fang Cao; Hang Zhang; Zhao-hui Oui, Guang – y Liu and Wen-xian Zhang (2009); A novel technology for Molybdenum extraction from Molybdenite concentrate. Hydrometallurgy , Vol.99, issues 1-2, pages 2-6.

Physicochem. Probl. Miner. Process. 47(2011) 113-122
www.minproc.pwr.wroc.pl/journal/

Physicochemical Problems of Mineral Processing
ISSN 1643-1049

Received January 20, 2011; reviewed; accepted April 21, 2011

Evaluation of Egyptian diatomite for filter aid applications

Suzan S. IBRAHIM *, Ali Q. SELIM **

* Central Metallurgical R&D Institute, P.O. Box 87, Helwan, Egypt, suzansibrahim@gmail.com

** Geology Dept., Faculty of Science, Beni Suif Univ., Egypt

Abstract. Diatomite is fine-grained fossil siliceous sedimentary rock. It consists of micronized amorphous silica with a special porous structure. In this study, a technological diatomite sample was subjected to characterization by XRD, XRF, SEM and TEM techniques. Results showed the high grade of the sample with silica content exceeding 90% SiO2. The main accompanying minerals were fine sands, calcite, and kaolinite. The sample was subjected to gentle size reduction to avoid ore cell destruction. The attrition +74μm fraction was rejected, where the -74μm slurry continued refining via the 7.62cm Sprout Bauer and the 5.08cm Mosley hydrocyclones. The -25μm fraction was investigated as the final refined diatomite product.

keywords: diatomaceous earth, diatomite, porous materials, surface texture, filtration, processing

1. Introduction

Diatomite ores are microscopic single-celled algae with characteristic rigid cell walls (frustules) composed of amorphous silica (Fig. 1). They consist normally of 87-91% silicon oxide (SiO_2), with significant quantities of alumina (Al_2O_3) and iron oxide (Fe_2O_3). The physical properties of natural and processed diatomite that provide unique commercial value in a broad spectrum of market end-uses include ornate fine structure, low bulk density, and high porosity and surface area. The properties of equal importance are mild abrasiveness, high absorptive capacity, insulating ability, relative inertness, and high brightness. End-use markets are diverse and range from insulating brick and absorbents through quality sensitive filter aids and premium quality functional fillers (Sterrenburg and Seckbach, 2007).

Although many thousands of species of diatoms have been classified, Figure 2, diatoms of salt water origin have been generally preferred as a source of filter aid materials because the major contaminant in saltwater diatom deposits tends to be sand or grit which is easily removed. In contrast, the major contaminant in fresh water deposits tends to be clay which has been difficult and costly to remove. In addition it

has been considered that a large variety of particle shapes of marine diatoms gives the most efficient filter medium, Figure 2. It has been discovered that many deposits of diatoms of freshwater origin are comprised substantially of the species Melosora Granulata which, when cleaned of clay impurities, provides a filter aid with superior filtration qualities (Potter, 2000; Sterrenburg and Seckbach, 2007).

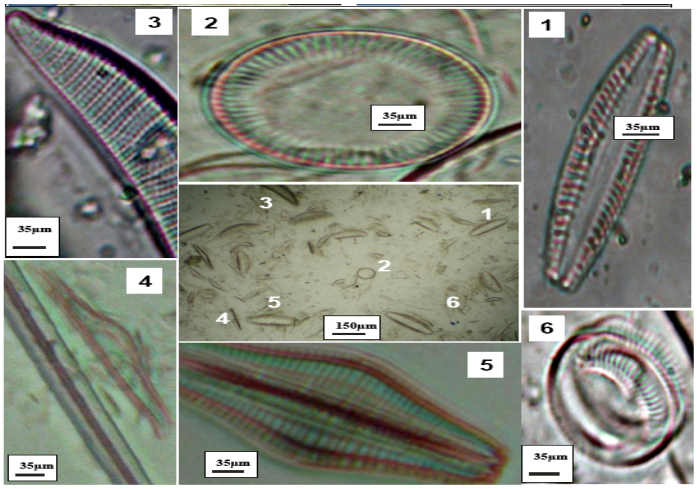

Fig. 1. Different shapes of diatomite particles

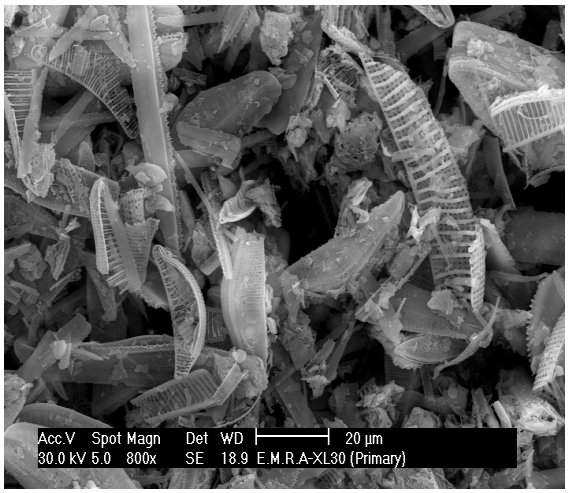

Fig. 2. Tremendous types of diatoms: recent and fossil, freshwater and marine

Diatomite is used in cleaning drinking water or industrial and sewage waste water. Sometimes it is blended with aluminium chloride or ferric chloride to enhance the filtration processes. From one to five percent, by volume, of polyacrylamide is preferably added to the mixture for use in sewage waste water treatment applications (Gordon et al., 2005).

Diatomaceous filter aids may be broadly categorized as falling into one of three grades - "natural", "calcined" and "flux-calcined" (Agdi et al., 1999; Alvarez et al., 1999; Andrews, 1991; Aytas et al., 1999; Engh, 1993; Harben, 1995; Skillen, 1995). The production of diatomaceous filter aid from diatomaceous ore is termed beneficiation. Natural diatomite is usually prepared by crushing the raw ore in a hammer mill and then drying the crushed material to remove substantially all moisture. The crushed material is then classified in air cyclones to remove the sand contamination and to effect a rough particle size separation. This initial processing causes undesirable breakage of frustules during the milling and classification steps. It was suggested that ultrasonic energy was an efficient means to induce a shear force to liberate the clayey particulates, which have particle size of -2μm, from the diatomaceous particles which were found naturally between 30-2μm, before classification through hydrocyclone classifiers (Agdi et al., 1999; Alvarez et al., 1999; Al-Wakeel, 2009; Andrews, 1991; Aytas et al., 1999; Engh, 1993; Neesse et al., 2004).

Diatomite may be used in a filtering process as a "pre-coat" or as a "body feed" depending on the nature of the material to be filtered. The shape and size of the filter aid particles is a relevant consideration for optimized performance. Particulate materials having a wide particle size distribution make efficient filter aids in terms of the clarity of filtrate, but their tendency to pack tightly results in very low filtration rates (Agdi et al., 1999; Alvarez et al., 1999; Andrews, 1991; Aytas et al., 1999; Crossley, 2000; Engh, 1993).

Coarse particles having a regular particle shape permit high filtration rates but will allow fine impurities to remain in the filtrate. Diatomaceous earths often comprise a mixture of substantially intact frustules together with a proportion of broken frustules (Christensen et al., 2001; El-Shafey et al., 2004; Lemonas, 1997; Loukina et al., 1994; Ridha et al., 1998; Shwabken and Tutinji, 2003).

Although many thousands of species of diatoms have been classified, diatoms of salt water origin have been generally preferred as a source of filter aid materials because the major contaminant in saltwater diatom deposits tends to be sand or grit which is easily removed. In contrast, the major contaminant in fresh water deposits tends to be clay which has been difficult and costly to remove. In addition it has been considered that the large variety of particle shapes of marine diatoms gives the most efficient filter medium (Breese, 1994; Carr, 1994; El-Shafey et al., 2004; Lemonas, 1997; Loukina et al., 1994; Martinovic et al., 2006; Ridha et al., 1998; Schuller, 1991; Shwabken and Tutinji, 2003).

Egypt is blessed with huge reserves of diatomite deposits, varying in grade from high, moderate to low rank (Abdel Aleem, 1958a; Abdel Aleem, 1958b; Basta et al., 1971; Basta et al., 1972; Faris and Girgis, 1969a, Faris and Girgis, 1969b, 1969; Hassan et al, 1999; Ibrahim, 2007; Said, 1962; Said, 1972; Zalat, 2002). This study focuses on the evaluation and processing of Gebel Elow El Masakheet Diatomite for filter aid applications. It is important to mention that the diatomite ore deposit; under

investigation; covers a large area in the southwest of the El- Fayoum Depression in the area between Wadi El Rayan to the south east of Gabel Elow El Masakheet locality, Figure 3. This area is located to the south west of El- Fayoum city by about 28km. Figure 4. Illustrates the Landsat of these reserves that extend for bout 10km in the ENE-WSW direction and for about 5km in the NNW-SSE direction.

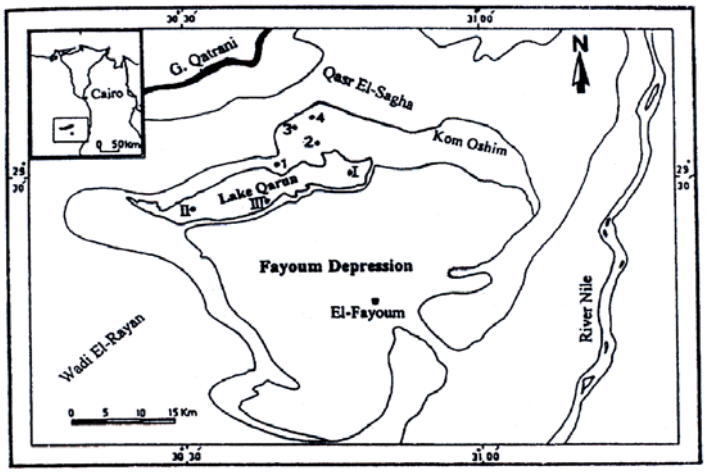

Fig. 3. Different diatomite deposits in El-Fayoum Depression, Egypt

2. Experimental

A representative sample from the well-exposed outcrop of the Gebel Elow El Masakheet diatomite was collected. The sample was gently crushed by hammers to -10cm. The primary crushed sample was left soaked in water over night and then transferred to the 40 liter capacity Denver attrition scrubber at 40-50 solid% and for 30min. The attrition process was in closed circuit with a 74μm Russell vibrating screen. The over screen product was collected as rejected fraction and subjected to evaluation and storage. The under screen slurry pulp was subjected to the 7.08cm Sprout Bauer and the 5.08 Mosley hydrocyclones after dilution to 20-25 solid %. The pressures inside the hydrocyclones were kept at maximum values reaching 345-379 kPa (50-55 psi), and 275 kPa (40 psi) for the two hydrocyclones, respectively. The products after hydrocyclone classification were evaluated with respect to diatomite wt. % and grade i.e. recovery (Schulz, 1970). The 5.08cm Mosley hydrocyclone overflow product was collected as the diatomite concentrate and directed to complete characterization. Whiteness measure of diatomite was measured (TAPPI, 1973). The concentrate product skeleton has been microscopically viewed using scanning electron microscope (SEM) of the type JEM-1230, JEOL and transmission electron microscope JSM T-20, JEOL. Evaluation of the concentrate product as filter aid was conducted via the microstructure analysis to provide reliable information about shape, structure, pore spaces and size.

3. Results and discussion

3.1. Deposit field relations and stratigraphy

It is believed that the Gebel Elow El Masakheet deposit is a depositional basin, which was filled with lacustrine facies during the Holocene, as most places of El-Fayoum Depression. These lacustrine acies were characterized by diatomite-rich horizons intercalated with calcite matrix, sand and silt. These sediments rested unconformably on the Middle Eocene rocks. Stratigraphy and structural relationships between these sediments and surrounding rocks are less complicated and were affected by varied local depositional topography (Basta, 1971).

In general, the Gebel Elow El Masakheet diatomite deposit is of white to grayish white color. Sometimes these horizons are intercalating with each other, displaying textural lamination and fissures. They range in thickness between centimeters to meters, Figures 4a and 4b. Thickness of the deposits depends mainly on the geomorphology of the basin during their deposition (Basta, 1971]) The diatomaceous earth deposits occurred as jointed layers with gradation in colour from bright white at the base to pale white in the top, Figure 4a or as successive cycles of deposition separated from each other by beds of grayish white or yellowish white friable fine sand, Figure 4b It is important to mention here that diatomite deposits of type (a) were the only type under investigation in this study.

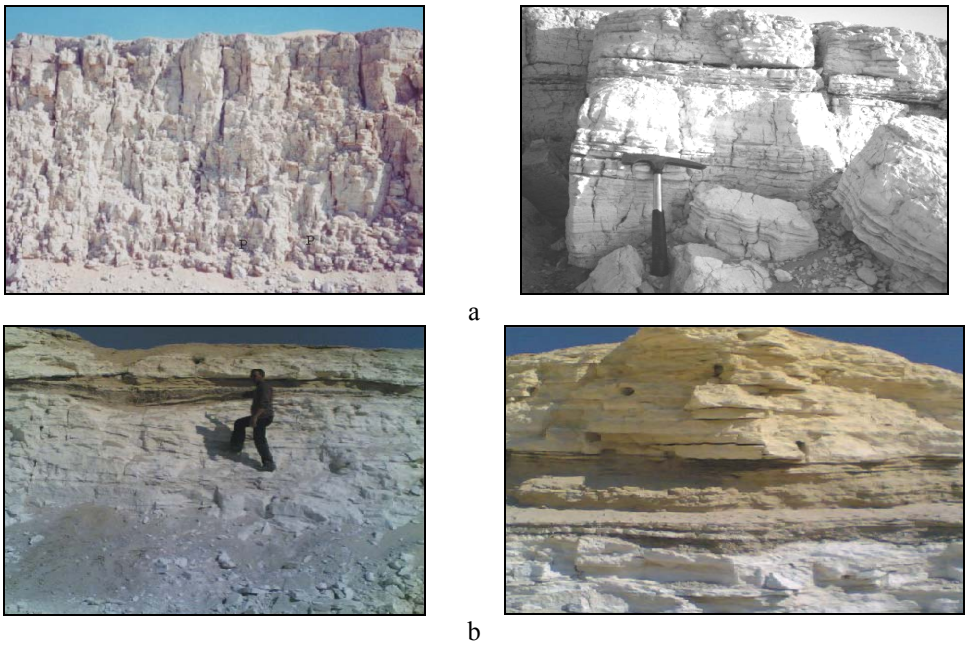

Fig. 4. a) the jointed fissile diatomite with gradation in colour from bright white at the base to off white in the top; b) white diatomite overlain by yellowish white blown sand enclosed with conglomeritic lenses of yellowish friable sand

3.2. Sample characterization

The microscopic studies and the XRD analysis of the Gebel Elow El Masakheet diatomite original sample showed that the sample was high grade diatomite composed of diatomaceous skeletons (frustules) containing minor amounts of calcite, kaolin, and crystalline silica minerals. The XRD pattern of the sample depicted clearly the highly crystalline peaks of calcite, clays, quartz, beside the amorphous peak related to the diatomite phase. On the other hand, Table 1 illustrates the chemical analysis of the original sample. The broad XRD peak between 20 9-19, as well as the high silica content of the sample showed the high grade of the diatomite sample. Table 2 depicts the density values of different minerals which constituted the diatomite ore sample under study, i.e. diatomite, silica, calcite and kaolinite.

Table 1. Chemical analysis of Gebel Elow El Masakheet diatomite original sample

Constituent	Wt.%
SiO_2	90.03
CaO	5.01
Al_2O_3	1.88
Fe_2O_3	0.08
LOI	2.20

Table 2. Specific gravity values of different minerals constituents of the diatomite ore sample

Mineral	Density, g/cm^3
diatomite	1.66
kaolinite	2.60
silica sand	2.65
calcite	2.71
iron oxide	5.10

3.3. Processing of the crushed diatomite sample

Table 3 illustrates the refining processing stages of the sample. It was obvious that the attrition scrubbing-closed circuit with 74 μm sieving of the hammer crushed sample was efficient to liberate the diatomite particles from the attached fine silica (+74 μm tailings). Different separation tests using the 7.62 cm Sprout Bauer cyclone showed that at pressure rate of 345-379 kPa (50-55 psi), a tail fraction weighing 7.40% containing most of the calcite impurities and fine silica remains was separated, Figure 5. Separation results of the 5.08cm Mosley hydrocyclone indicated that, the diatomite separation is highly sensitive to changes in hydrocyclone pressure (Neesse, et al., 2004; Schulz, 1970; Svarovsky, 2000). At relatively low pressures, there was poor separation, where the diatomite was distributed indiscriminately between the overflow and the underflow cuts. With increasing pressure, the separation was improved till reaches its maximum separation efficiency >80% with high grade product (96.03% SiO_2) at 275 kPa (40 psi). It was noticed that by increasing the

pressure sharp deterioration in separation of diatomite with respect to weight% took place. The measured mean diatomite particle diameter (d_{50}) was about 13 µm where d_{10} and d_{90} was 4µm and 26 µm, respectively (Fig. 6).

The physical characteristics of the final product are given in Table 4. From the data shown in Table 4, it could be concluded that the processed diatomite is amenable for filter aid application according to the international criteria (Carr, 1994 and Crossley, 2000). The morphology as well as the porous structure and the surface texture of the product sample are shown in Figs 9 and 10. SEM pictures show that the main diatomite structures were of types Cocconeis klamathensis and Cymbella prostrate, which related to fresh water environment, Figure 7 (Sterrenburg and Seckbach, 2007). The final product showed to have a pore diameter of about 0.25µm (Fig. 8).

Table 3. Refining results for the Gebel Elow El Masakheet diatomite original sample

Process	Wt.%	SiO_2%	Al_20_3%	CaO%	LOI%
Original sample	100.0	90.91	1.88	5.01	2.20
Attrition scrubbing:					
Over Screen, +74µm fraction	9.31	96.44	0.18	3.07	0.31
Hydrocyclone classification:					
7.62cm Hydrocyclone UF Fraction, -74+45µm	7.40	31.30	3.70	36.20	28.80
5.08cm Hydrocyclone UF Fraction, +45+25µm	3.09	54.88	27.23	7.76	10.13
5.08cm Hydrocyclone OF Product, -25µm	80.20	96.03	0.91	1.65	1.41

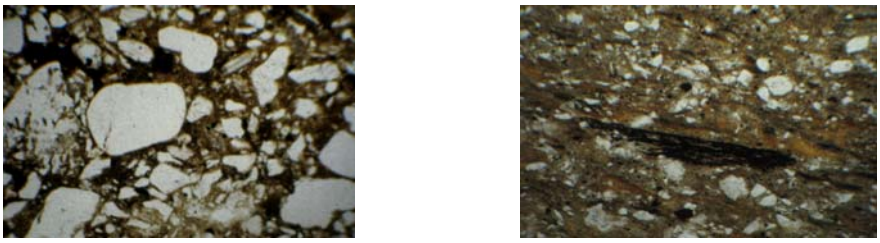

a b

Fig. 5. a) Rejected +74µm fraction (silica and fossil remains) and b) rejected +45µm fractions (muddy calcite and fine silica) after the refining process

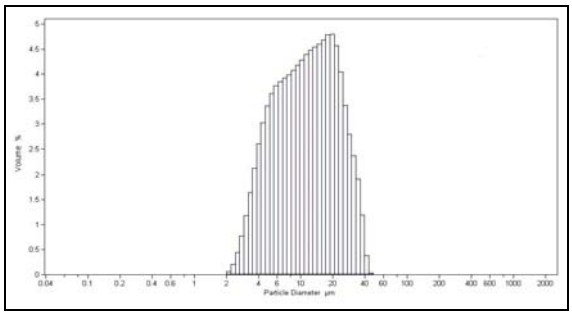

Fig. 6. Size distribution of the final diatomite concentrate

Table 4. Main physical characteristics of diatomite final product

Physical Properties	Final Product
Specific surface area, m^2 / g	195
Specific gravity, g/cm^3	1.66(crude) , 0.43 (dry base)
Water Absorption (% by weight)	262, 322.36 (After drying)
Oil Absorption (g /100 g)	139-208, 221.92(After drying)
Whiteness	97.70
% Passing 45 µm	100.00
Porosity %	51.49
Refractive index	1.462-1.558
pH	5.85

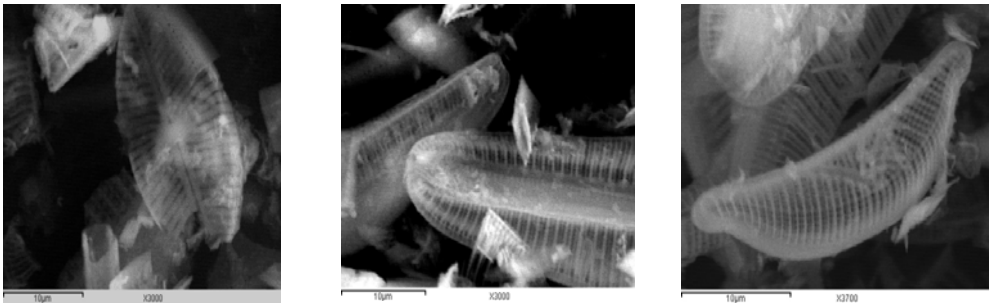

Fig. 7. SEM pictures of diatomite end-product

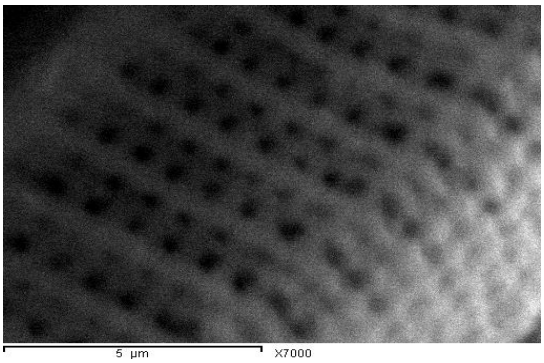

Fig. 8. The porous structure of diatomite particle end-product

4. Conclusions

In this study, a technological diatomite sample was collected from the Gabel Elow El- Masakheet locality, south west El- Fayoum Governorate, Egypt. The sample was subjected to characterization by the XRD and the XRF. The morphology as well as the porous structure and the surface texture of the product sample were observed using SEM and TEM techniques. The sample was subjected to gentle size reduction to avoid ore cell destruction. This was carried out through hammers crushing of the ore

lumps, followed by attrition scrubbing of the -10cm crushed sample. Russell 74μm vibrating screening processed the attrition slurry to reject the overscreen organic and the earthy remains fraction, where the underscreen slurry continued to the refining circuit via the 7.62cm and the 5.08cm hydrocyclone units. The -25 μm product was collected, dried, and investigated as the final purified diatomite product. The final refined product recovery was 80.20% by weight and silica assay reached 96.03%. The D_{50} and D_{90} for the product were 13μm and 26μm, respectively. The morphology as well as the porous structure and the surface texture of the product sample were observed, showing that the pore diameter averaged 250nm. The study recommends that the refined diatomite of the Gabel Elow El- Masakheet locality, south west El-Fayoum Governorate, Egypt, is suitable for filter aid applications.

References

ABDEL ALEEM A., 1958, A taxonomic and paleoecological investigation of the diatomite flora of the extinct. Fayium Lake- Upper Egypt, Faculty of Science Bulletin, Alex. Univ., Egypt, 2, 99-137.

ABDEL ALEEM A., 1958, A taxonomic and paleoecological investigation of the diatomite flora of the extinct. Fayium Lake- Upper Egypt, Faculty of Science Bulletin, Alex. Univ., Egypt, 2, 217-244.

AGADI K., BOUADI A., ESTBAN A.M., HEMANDO P.F., AZMANI A., CAMARA C., 1999, J. Environ. Monit. , 2, 420.

Al-WAKEEL M.I., 2009, Characterization and process development of the Nile diatomaceous sediment, Int. J. Miner. Processing, 92, 128–136.

ALVAREZ E., BLANCO J., AVILA P., KNAPP C., 1999, Catal. Today, 557.

ANDREWS P.R.A., 1991, Canmet, Summary Report, 15, 15-28.

AYTAS S., AKYIL S., ASLANI M. A. A., AYTEKIN U., RAIONAL J., 1999, Nucl. Chem., 240, 973.

BASTA E.Z., ABDALLAH A.M., KADI M.B., 1971a, Geology and Mineralogy of Diatomite Clay Deposits North of Fayoum, Faculty of Science Bulletin, Cairo Univ., Egypt.

BASTA E.Z., ABDALLAH A. M., El KADI M. B., 1972b, Faculty of Science Bulletin, 45, 319-329, Cairo Univ., Egypt.

BREESE O.Y., 1994, Diatomite. Industrial Minerals and Rocks, 6th Edition, 397-412.

CARR D.D., 1994, Industrial Minerals and Rocks. 6th Edition, Published by Society for Mining, Metallurgy, and Exploration, Inc. Littleton, Colorado.

CHRISTENSEN A. N., LUNDTOFT B., MADSEN L. C., 2001, American Ceramic Society. 84, 4, 878-880.

CROSSLEY P., 2000, March, Clarifying Matters, World Diatomite Reviewed. Industrial Minerals, 119-141.

ENGH K. R., 1993, Kirk-Othmer Encyclopedia of Chemical Technology. M. Howe Grant (Ed.), Fourth Edition, 8, Wiley, New York.

FARIS M.I., GIRGIS G.F., 1969, Proc.6th Arab Sci. Congress, 4b, 751-767.

FARIS M. I., GIRGIS G. F., 1969, Faculty of Science Bulletin. 14, Ain Shams Univ., Egypt.

EL-SHAFEY E.L., GAMERIO M., CORREIA P., 2004, J.de Cravalho, Sep. Sci. Tech., 39, 32-37.

ENGH K. R., 1993, in: M. Howe Grant (Ed.), Kirk-Othmer Encyclopedia of Chemical Technology, vol. 8, p 108, Fourth Edition, pp 108, Wiley, New York.

GORDON R., STERRENBURG F.A.S., SANDHAGE K., 2005, A Special Issue on Diatom Nanotechnology, Journal of Nano-science and Nanotechnology, 5(1), 1–4.

HASSAN M.S., IBRAHIM I.A., ISMAEL I.S., 1999, Sedimentology of Egypt, 7, 505-512.

HARBEN P.W., 1995, Diatomite, The Industrial Minerals Handy Book, 2nd edn., Industrial Minerals Div., 57-61, Warwick, England.

IBRAHIM S.S., 2007, Preparation of Different Diatomite Concentrates for Special Industrial Applications, The Academy of Scientific Research &Technology (Funded from NSF, USA), Egypt.

LEMONAS J.F., 1997, Am. Ceram. Soc. Bull., 76, 92.

LOUKINA S. M., EL HEFNAWI M. A., ABAY ZEED S. D., 1994, Mineralogy and Geochemistry of Diatomaceous Earth from Fayium Region, Egypt, Mineralogy Society of Egypt, 282-305.

MARTINVIC S., VLAHOVIC M., BOLJANAC T., PAVLOVIC L., 2006, Preparation of Filter Aids Based on Diatomite, Int. J. Mine. Process, 80, 255-260.

NEESSE T., DUECK J., MiNKOV L., 2004, Separation of finest particles in hydrocyclones, Minerals Engineering, 17, 689–696.

POTTER M. J., 2000, February, Diatomite, U.S Geological Survey, Mineral Commodity Summaries.

RIDHA A., ADERDOUR H., ZINEDDINE H., BENABDAALLAH M.Z., 1998, Ann. Chim. Sci. Mater., 23, 161.

SAID R., 1972, Teras, Publication, No. 4.

SAID R., 1962, The Geology of Egypt. 377, Elsevier, New York.

SHAWABKEN R. A., TUTINJI M.F., 2003, Experimental study and modeling of basic dye sorption by diatomaceous clay, Appl. Clay Sci. 24, 111.

SCHULER P.F., GHOSH M.M., GOPALAN P., 1991, Slow and diatomaceous earth filtration of cysts and other particulates, Water Res., 25, 995–1005

SCHULZ N.F., 1970, Separation efficiency, Trans. SME-AIME, 247, 56.

SKILLEN A., 1995, Diatomite, Raw Materials for Pigments, Fillers and Extender, Industrial Minerals, Second Edition, 76-78.

STERRENBURG F., SECKBACH J., 2007, algae and Cyan-bacteria in Extreme Environments, Springer, 141–172.

SVAROVSKY L., 2000, Solid-Liquid Separation, Handbook, Fourth Edition.

TAPPI (Technical Association of the Pulp and Paper Industry), 1973, International Paper Trade Journal, November, 56.

ZALAT A. A., 2002, An Assessment of Palaeoecological and Palaeoclimatological changes During the Holocene of Fayoum Depression, Egypt, based on Fossil Diatoms, Journal of Environmental Research, 4, 22-43.

Physicochem. Probl. Miner. Process. 47(2011) 123-130
www.minproc.pwr.wroc.pl/journal/

Physicochemical Problems of Mineral Processing
ISSN 1643-1049

Received February 6, 2011; reviewed; accepted April 5, 2011

Transformation of equation y=a(100-x)/(a-x) for approximation of separation results plotted as Fuerstenau's upgrading curve for application in other upgrading curves

Magdalena DUCHNOWSKA, Jan DRZYMALA

Wroclaw University of Technology, Wybrzeze Wyspianskiego 27, 50-370 Wroclaw, magdalena.duchnowska@pwr.wroc.pl

Abstract. Equation y= a(100-x)/(a-x), frequently used for approximation of separation results plotted in the Fuerstenau upgrading curve, relating recovery of a selected component of the feed in the concentrate (x = ε) with recovery of another component in the tailing (y = ε_r), can be transformed into one-fitting parameter equation suitable for other upgrading curves. The mathematical formulas for the so-called Luszczkiewicz, Mayer, Henry, Stepinski, Hall, and Halbich separation upgrading curves were derived and presented.

keywords: upgrading curve, upgrading parameter, separation, ore beneficiation

1. Introduction

Material balance, separation graphs and mathematical equations are used for analysis and evaluation of separation results. In case of the Fuerstenau plot (Fig. 1), relating recovery of a selected component of the feed in the concentrate ε with the recovery of another component in the tailing ε_r, the number of available equations is great (Drzymala and Ahmed, 2005). One of them has a form of

$$\varepsilon_r = a\frac{100-\varepsilon}{a-\varepsilon} \tag{1}$$

and is based on a single fitting parameter a. Equation (1) is very useful because it not only approximates numerous literature separation results but also can serve as a single parameter reflecting separation selectivity (efficiency), while in normal situations two upgrading parameters are needed. This is possible due to a special property of the Fuerstenau upgrading curve since its principal lines, that is no upgrading, ideal upgrading, ideal remixing do not change their location with variation of the of feed composition.

Mathematical equations used for other separation upgrading curves are usually more complex and two and more fitting parameters formulas are used. Examples are presented in Table (1).

The goal of this work is to transform Eq. (1) into forms applicable for other than Fuerstenau upgrading separation curves, that is for the Mayer, Halbich, Henry, Luszczkiewicz, Hall, and Stepinski plots (Drzymala, 2006-8).

Table 1. Mathematical equations used for approximation of different upgrading curves

Upgrading curve and parameters	Equation	Source
Halbich ε, β	$\varepsilon = a - b\beta$ a and b - fitting parameters (for high recoveries)	Dell, 1969
	$\frac{\beta_{\max}}{100-\beta} = z(100-\varepsilon)^{z-1}\frac{\alpha}{100-\alpha}$ z and β_{max} - fitting parameters	Digre, 1960
Hall ε, H	$H = A\frac{100-(100-\varepsilon)}{100+A-\varepsilon}$ (A - fitting parameter)	Hall, 1971
Henry β, γ	$\gamma = c - d\beta$ c and d - fitting parameters	Foszcz et al., 2010
Halbich (II) ε, β/α	$\varepsilon = \varepsilon_{\max} - 2\sinh(k[(\beta/\alpha)-1])$ k and ε_{max} - fitting parameters	Vera et al., 1999
Mayer III (Dell) ε, γ/α	$(a_1x + b_1y + c_1)(a_1x + b_2y + c_2) = K$ a_1, a_2, b_1, b_2, c_1, c_2, and K - fitting parameters	Jowett, 1969
Stepinski β, ϑ	$\beta = l + m\vartheta$ l and m - fitting parameters	Pudlo, 1971; Luszczkiewicz, 1975; Neethling and Cilliers, 2008;
Mayer II ε, γ	$\varepsilon = g + h\gamma$ g and h - fitting parameters	Nixon and Moir, 1956-7

γ – concentrate yield, , α – content of a considered component in feed, β – content of a considered component in concentrate, ε – recovery of a considered component in concentrate

2. Transformation

Separation results fitted with Eq. (1) in the Fuerstenau separation upgrading plot (Fig.1) form a symmetrical, in respect to the diagonal, curve. A closer literature survey indicates that Eq. 1 has many mathematical forms which depend on the definition of the fitting parameter (Table 2).

In this work we will use only Eq. (1) with a as the fitting parameter. Transformation of Eq.(1) to forms useful for other separation upgrading curves was performed manually by replacing ε and ε_r with appropriate formulas based on the original upgrading parameters, that is contents of a considered component in the feed (α), concentrate (β) and in the tailing (ϑ) (Table 3), and next rearranging the obtained

equation until a relation between the two characteristic, for a given separation curve, parameters were obtained.

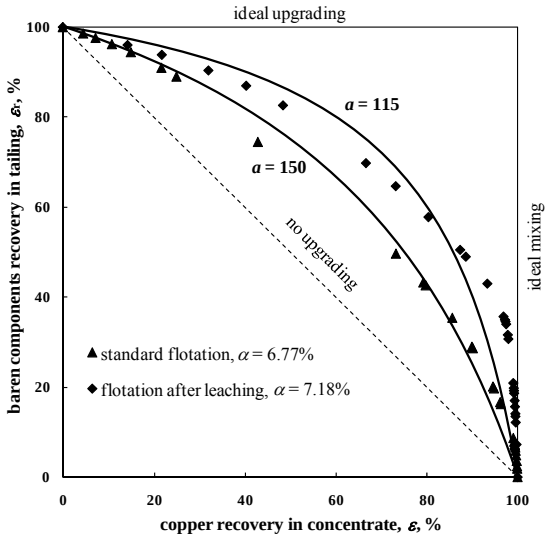

Fig. 1. The Fuerstenau separation upgrading curve showing fixed background lines and real separation data adopted from Luszczkiewicz and Chmielewski (2008)

Table 2. Mathematical forms of Eq. (1) depending on definitions of fitting parameter

Formula	Fitting parameter	Limits	Relation to *a*	Source
$\varepsilon = a\frac{100-\varepsilon_r}{a-\varepsilon_r}$	*a*	*a* = ∞ (no) *a* = 100 (ideal)	*a* = *a*	Drzymala and Ahmed, 2005
$\varepsilon_r = A\frac{100-\varepsilon}{A+\varepsilon}$	*A*	*A* = ∞ (no) *A* = -100 (ideal)	*a* = -*A*	Hall, 1971
$Z = \frac{(100-\varepsilon_r)(100-\varepsilon)}{\varepsilon\varepsilon_r}$	*Z*	*Z* = 1 (no) *Z* = 0 (ideal)	$a = \frac{1}{-0.01Z+0.01}$	Laplante, 1989
$\varepsilon = F^2\frac{100-\varepsilon_r}{(2F-100)(\frac{F^2}{2F-100}-\varepsilon_r)}$	*F*	*F* = 50 (no) *F* = 100 (ideal)	$a = \frac{F^2}{2F-100}$	this work
$y = 100\Phi(a+b\Phi^{-1}(x))$ Φ – distribution function	*a*, *b*	*a* = 0 (no) *a* = ∞ (ideal) *b* = 1 (for symmetrical curve)		Krzanowski and Hand, 2009; Wlodarski, 2009

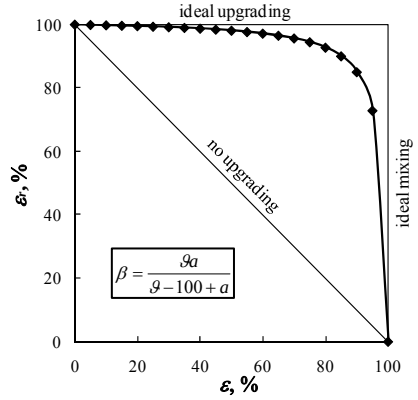

Fig. 2. Fuerstenau's curve

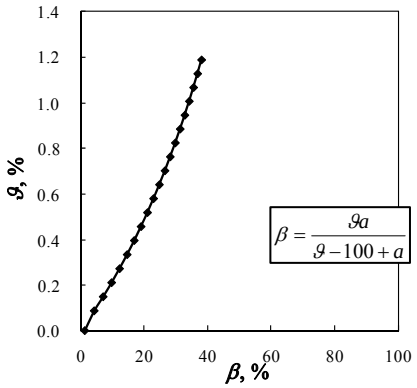

Fig. 3. Stepinski's (I) curve

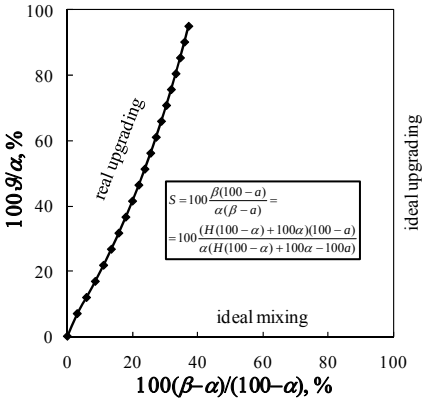

Fig. 4. Stepinski's (V) curve

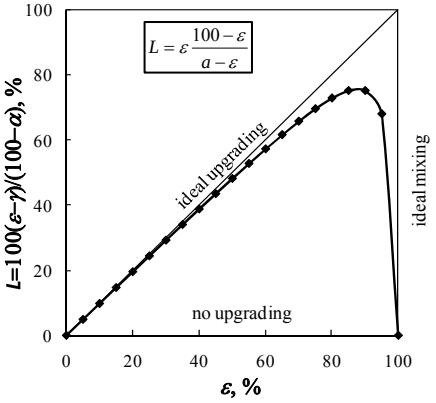

Fig. 5. Luszczkiewicz's curve

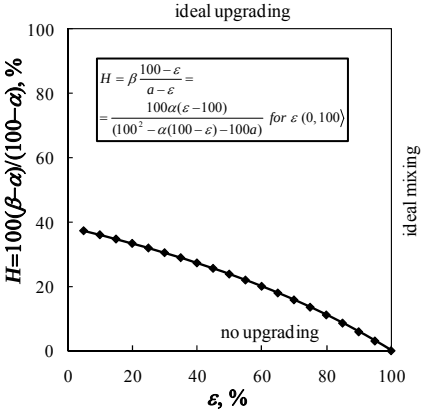

Fig. 6. Hall's curve

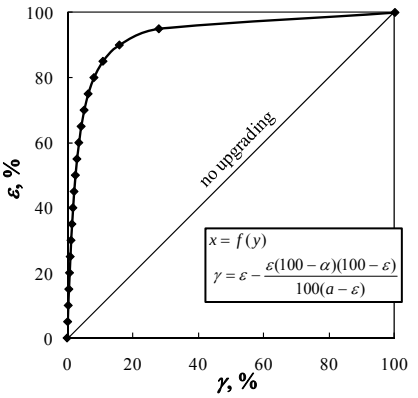

Fig. 7. Mayer's curve

Table 3. Upgrading curves, their characteristic parameters based on α, β, ϑ, and equations for approximating separation results based on fitting parameter a

Upgrading plot	Upgrading parameters	Formulas based on α, β, ϑ	Form of Eq. 1 suitable for considered upgrading plot
Fuerstenau (1988/1992)	ε, ε_r	$\varepsilon = \frac{\alpha-\vartheta}{\beta-\vartheta}\frac{\beta}{\alpha}100$ $\varepsilon_r = (100-\frac{\alpha-\vartheta}{\beta-\vartheta}100)\frac{100-\vartheta}{100-\alpha}$	$\varepsilon_r = a\frac{100-\varepsilon}{a-\varepsilon}$
Luszczkiewicz (2002)	ε, L	$\varepsilon = \frac{\alpha-\vartheta}{\beta-\vartheta}\frac{\beta}{\alpha}100$ $L = \frac{\alpha-\vartheta}{\beta-\vartheta}100(\frac{\beta}{\alpha}-\frac{(100-\beta)}{(100-\alpha)})$	$L = \varepsilon\frac{100-\varepsilon}{a-\varepsilon}$
Mayer (1950)	ε, γ	$\varepsilon = \frac{\alpha-\vartheta}{\beta-\vartheta}\frac{\beta}{\alpha}100$ $\gamma = \frac{\alpha-\vartheta}{\beta-\vartheta}100$	$\gamma = \varepsilon - \frac{\varepsilon(100-\alpha)(100-\varepsilon)}{100(a-\varepsilon)}$
Henry (1905)	β, γ	β $\gamma = \frac{\alpha-\vartheta}{\beta-\vartheta}100$	$\gamma = \frac{100(\beta(100-\alpha)-a(\beta-\alpha))}{\beta(100-\beta)}$
Stepinski V (1964, 1965); Drzymala, (2005, 2006)	ϑ/α, S	ϑ/α, $S = 100\frac{\beta(100-a)}{\alpha(\beta-a)}$	$S = 100\frac{\beta(100-a)}{\alpha(\beta-a)} =$ $= 100\frac{(H(100-\alpha)+100\alpha)(100-a)}{\alpha(H(100-\alpha)+100\alpha-100a)}$
Hall (1971)	H, β	β $H = \frac{100-\beta}{100-\alpha}100$	$H = \beta\frac{100-\varepsilon}{a-\varepsilon} =$ $\frac{100\alpha(\varepsilon-100)}{(100^2-\alpha(100-\varepsilon)-100a)}$
Halbich (1934)	β, ε	β $\varepsilon = \frac{\alpha-\vartheta}{\beta-\vartheta}\frac{\beta}{\alpha}100$	$\beta = \frac{100\alpha(\varepsilon-a)}{100^2-\alpha(100-\varepsilon)-100a}$
Stepinski I	β, ϑ	β $\vartheta = \frac{100\alpha-\gamma\beta}{100-\gamma}$	$\beta = \frac{\vartheta a}{\vartheta-100+a}$

α – content of a considered component in feed, β – content of a considered component in concentrate, ϑ – content of considered component in tailing, γ – yield, ε – recovery of the considered component in concentrate, ε_r – recovery of remaining (100% - considered component) in tailing, H – Hall parameter, L – Hancock (ε - ε_2) parameter where ε_2 denotes recovery of a second (here other than first component) in concentrate

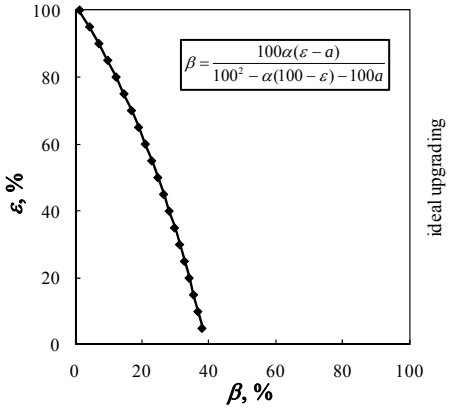

Fig. 8. Halbich's curve

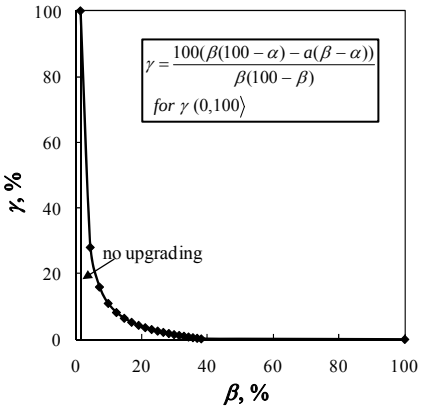

Fig. 9. Henry's curve

Arbitrary separation data with a = 102 and α =1.25% were fitted with Eq. 1 and plotted in Fig. 2 as the Fuerstenau upgrading curve. Presented in Fig. 2 data can be now re-plotted in other separation upgrading plots (Figs 3-9) and approximated with the newly derived (Table 3) equations.

3. Conclusions

The symmetrical in relation to diagonal, one-fitting parameter y = a(100 - x)/(a-x) equation used for approximation of separation results in the Fuerstenau upgrading plot can be transformed into one-fitting parameter equations consisting of a for any other separation upgrading plot. Some of them have been presented in this paper.

Acknowledgements

Financial support by the Polish Statutory Research Grant (343-165) is greatly acknowledged.

References

Dell, C.C., 1969. An expression for the degree of liberation of an ore, Trans. Inst. Min. Metal., Sec. C, Mineral Process Extr. Metal., 78, C152

Digre M., 1960. Separation factor analysis for mineral dressing processes, IMPC, Group IX, Paper 49, p.999-1113, IMM publisher, London

Drzymala J, 2005. Evaluation and comparison of separation performance for varying feed composition and scattered separation results, Int. J. Miner. Process., 75, s. 189-196.

Drzymala J. 2006-8. Atlas of upgrading curves used in separation and mineral science and technology. Physicochem. Probl. Miner. Process., Part I, 40, 19-29, 2006; Part II, 41, 27-35, 2007; Part III, 42, 75-84, 2008.

Drzymala J., Ahmed H. A. M., 2005. Mathematical equations for approximation of separation results using the Fuerstenau upgrading curves, Int. J. Miner. Process., vol. 76 (1–2), s. 55–65.

Foszcz D., Niedoba T., Tumidajski T., 2010. Analiza mozliwosci prognozowania wynikow wzbogacania polskich rud miedzi uwzgledniajacego stosowana technologie, Gornictwo i Geoinzynieria z. 4/1, s. 25–36

Fuerstenau D.W., et al., 1988-1992, Coal surface control for advanced fine coal flotation, Final Report, University of California, Berkeley, Final Report DOE/PC/88878-T13, DE92 015625 for U.S. Dept. of Energy. Prepared by Univ. California, Columbia Univ., Univ. of Utah, and Praxis Engineers Inc.

Halbich W., 1934. Über die Anwendungsmöglichkeiten einiger Netzmittel in der Flotation, Kondrad Triltsch, Würzburg

Hall W.B., 1971. The mathematical form of separation curves based on two known ore parameters and a single liberation coefficient, Trans. IMM., Sec.C, 80, C213–C222.

Henry, 1905. Le lavage des charbons, Revue Universelle, ser. 4, vol. V, p.274 (Information after H. Czeczott, Przerobka mechaniczna uzytecznych ciał kopalnych, Krakow, 1937).

Jowett A., 1969. A mathematical form of minerals separation curves, Trans. IMM, Sec. C., 78, C185.

Krzanowski W. J., Hand D. J., 2009. ROC curves for continuous data, CRC Press/Taylor & Francis Group, Boca Raton, London, New York.

Laplante A., Kaya M., Smith H. W., 1989. The Effect of Forth on Flotation Kinetics-A Mass Transfer Approach, Mineral Processing and Extractive Metallurgy Review, vol. 5, s. 147-168.

Luszczkiewicz A., 1975. Korelacje pomiedzy podstawowymi wskaznikami przemyslowego procesu flotacji miedzi w swietle laboratoryjnych charakterystyk wzbogacalnosci, Physicochem. Prob. Miner. Process., 9, 121-131

Luszczkiewicz A., 2002. Evaluation of efficiency of separation of multi-component concentrates of disseminated elements, Prace Naukowe Instytutu Politechniki Wroclawskiej, nr 101, Konference 35, s. 87-103 (in Polish).

Luszczkiewicz A., Chmielewski T., 2008. Acid treatment of copper sulfide middlings and rougher concentrates in the flotation circuit of carbonate ores, Int. J. Miner. Process., vol.88, nr 1-2, s. 45-52.

Mayer F.W., 1950. Die Mittelwertkurve, eine neue Verwacksungskurve, Glückauf, 26, 498–509.

Neethling S.J., Cilliers J.J., 2008. Predicting and correcting grade recovery curves. Theoretical aspects, Int. J. Miner. Process., 89, 17-22

Nixon J.C., and Moir D.N., 1956-7. The assessment of flotation results, Trans. IMM (Bull. IMM), 66, 453-469.

Pudło W., 1971. O pewnej metodzie aproksymacji krzywych wzbogacania, Zeszyty Problemowe Gornictwa PAN 2, 83–103.

Stepiński W., 1964, Krzywe srednich wartosci jako miernik oceny dwustadialnej flotacji, Rudy i Metale Nieżelazne R9, nr 10, 532-535

Stepiński W., 1965, Krzywe srednich wartosci dwustadialnej flotacji rudy ubogiej, Rudy i Metale Nieżelazne, R10, nr 3, 117-120

Vera M.A., Franzidis J_P., Manlapig E. V. An empirical equation for recovery - enrichment ratio curve (AREV model), Coppper 99-Cobre 99 International Environment Conference, Volume II - Mineral Processing/Environment, Health and Safety, B.A. Hancock and M.R.L. Pon Eds, The Minerals, Metals & Materials Society, 1999, 69-82

Włodarski M., 2009. Porownanie parametrycznej i nieparametrycznej metody obliczania krzywej ROC na przykladzie zbioru sygnalow elektroretinograficznych, Metody Informatyki Stosowanej, nr 2 (19), s. 177-192.

Physicochem. Probl. Miner. Process. 47(2011) 131-138
www.minproc.pwr.wroc.pl/journal/

Physicochemical Problems of Mineral Processing
ISSN 1643-1049

Received December 15, 2010; reviewed; accepted April 18, 2011

Controlled adsorption at the surface of copper sulfide minerals – a way to abate the problem of environment contamination by the copper sulfide oxidation products?

Pawel NOWAK *, Maria NASTAWNY **, Ilona KOZYRA ***

Adam WEGRZYNOWICZ *

* J. Haber Institute of Catalysis and Surface Chemistry, Polish Academy of Sciences, ul. Niezapominajek 8, 30239 Kraków, Poland, ncnowak@cyfronet.pl

** Jagiellonian University, Faculty of Chemistry, Kraków, Poland

*** Technical University of Kraków, Faculty of Chemistry

Abstract. Electrochemical impedance spectroscopy was used to study the adsorption of several surface active substances at the surface of non-stoichiometric copper(I) sulfide. Simultaneously the influence of the treatment of the copper sulfide by the solution of those surface active substances on the leaching rate of the sulfide in oxygenated sulfuric acid solution was investigated and correlated with the type of adsorptive bond formed between the sulfide surface and adsorbed molecules. Both chemisorption and surface precipitation may lead to the formation of a strongly bound product that prevents the dissolution of a mineral. Contrary, physical adsorption is too week to protect the surface from the attack of aggressive medium.

keywords: copper sulfides, adsorption on minerals, corrosion of minerals, prevention of mineral corrosion

1. Introduction

Almost all metals form metal sulfides that appear in the nature as sulfide minerals (Jellinek, 1968, Vaughan and Craig, 1978) and for almost all economically important metals (except iron and aluminum) sulfide minerals are the main ore-forming minerals. Metal sulfides form large ore bodies but they also can accompany other, non-sulfide minerals. Large quantities of pyrite (and other sulfides in much lower concentration) appear in coal (Twardowska et al, 1978). In the case of many metals mining of an ore of the metal concentration much below 1% is still profitable. So, metallurgical industry produces large quantities of wastes containing metal sulfides. For example the Polish copper industry, during fifty years of its activity, left on the depository places approximately 600 million tons of flotation wastes, occupying for that purpose 2300 hectares of ground (Łuszczkiewicz, 2000). So,

mining creates a big thread to the environment which led to the appearance of a new field of mineralogy – environmental mineralogy (Vaughan and Wogelius, 2000).

The solubility of metal sulfides is very low. However, when subjected to the attack of an oxidative agent (molecular oxygen, ferric ions) they oxidize to better soluble compounds – oxides, sulfates. So, the presence of sulfides in an ore may cause liberation of the metal ions to the environment at all stages of the ore processing. The wastes from the non-ferrous metal industry are especially dangerous (Helios-Rybicka, 1996, Jambor et al., 2000). The most abundant sulfide mineral is pyrite. Oxidation of pyrite liberates iron species and sulfuric acid, causing so-called acid mine drainage (Doyle, 1990, Evangelou, 1995). Neither sulfates nor iron species belong to important environmental contaminants, however the decrease in pH of the water flowing through the wastes and soils causes the dissolution of otherwise insoluble constituents increasing the concentration of metal ions in effluents. The other reason of the environment acidification which can also lead to the liberation of metal ions is so called acid rain caused by the emission of aggressive gases (SO_2, nitrogen oxides) to the atmosphere.

Weathering of metal sulfides may be considered as a corrosion process and, like in the case of the corrosion of metals, it may be prevented by the application of inhibitors. Many papers concerning the possible prevention of pyrite oxidation by application of inhibitors appeared in the literature. Huang and Evangelou (1994) applied soluble phosphates for that purpose, Belzile et al. (1997) showed the applicability of several natural compounds (humic acids for example) in pyrite oxidation inhibition, Jiang et al. (2000) found oleic acid to be effective as an inhibitor of pyrite oxidation whereas Zhang et al. (2003) and Kargbo et al. (2004) applied successfully lipids for that purpose. Pyrite leaching occurs usually with the active participation of bacteria. So, addition of antibacterial agents should depress the oxidation of pyrite. That problem was investigated by Sand et al. (2007) with a partial success.

It is generally believed, that inhibitors act on metals by forming protective overlayers which decreases the rate of metal dissolution as well as the reduction of oxidizing agents (Lipkowski, 1992). Inhibitors may be attached to the surface of minerals by physical adsorption, chemisorption or surface precipitation. In the present paper authors attempted to test which type of sorption would be most effective in the creation of a good protective layer at the mineral surface, preventing the mineral weathering. Synthetic non-stoichiometric copper (I) sulfide of the composition $Cu_{1.87}S$ was chosen as a model mineral. Using synthetic minerals offers the privilege that large samples of perfectly uniform composition may be prepared. Non-stoichiometric copper (I) sulfide is a very good electrical conductor – its electrical conductivity is comparable to metals (Shuey, 1975). That enabled the application of the electrochemical methods in the investigations. Measurement of the electrical double layer (EDL) capacitance is one of the main methods to study the adsorption of inhibitors at the metal surfaces. The other reason that we used non-stoichiometric

copper (I) sulfide as the model mineral is our interest in copper sulfides. Contrary to most world copper ore deposits, where the main copper mineral is chalcopyrite, in Polish copper ores the main copper-bearing constituents are copper sulfides (Large et al., 1995). The synthetic mineral we used is close in composition to the copper sulfides present in Polish copper deposits. Copper sulfides oxidize easily, comparing to other minerals, especially when they form so called galvanic local cells with pyrite (Nowak et al., 1984). So, the rate of their oxidation may be measured relatively easily. No information was found in the literature on the possibility of application of inhibitors to prevent the oxidation of copper sulfides, except the preliminary communications of the present author and coworker (Nowak and Gucwa, 2008, Nowak, 2010).

2. Experimental

Copper sulfide of the composition $Cu_{1.87}S$ was synthesized from high purity copper and sulfur. After synthesis copper sulfide was melted and cast in the form of a grand lump. According to the results of diffraction analysis that sulfide was the mixture of djurleite and low digenite. Part of it was ground and sieved into fractions, part was used to make the electrodes for electrochemical experiments. Electrodes were made from the sulfide by fixing a piece of sulfide in a glass tube with epoxy resin. Electrical contact was made with the use of conducting silver glue. Sieved fraction of the particle diameter of 10 – 15 μm was used in the leaching experiments. More details on the synthesis and the properties of the investigated sulfide as well as preparation of electrodes may be found in our previous publication (Nowak and Pomianowski, 1989). All measurements were performed at the temperature of 25 ^{o}C, More information on the details of the experiments may be found in our previous communications (Nowak and Gucwa, 2008, Nowak, 2010).

Several different possible inhibitors were tested: sodium oleate (NaOL), sodium dodecylsulfate (SDS), dodecyltrimethylammonium chloride (CTACl), N-dodecylpyridinium chloride (NDPCl), n-octanol (n-Oct), potassium ethyl xanthate (EtXK), 2-mercaptobenzothiazole (MBT), (all p.a. purity grade)). Some of them served only as model compounds (n-octanol, for example), some other might become real inhibitors with practical application.

Two types of experiments were performed

(1) Adsorption of investigated compounds at the surface of a non-stoichiometric copper (I) sulfide electrode was investigated by measuring the capacitance of the EDL at the surface of the electrode using electrochemical impedance spectroscopy (EIS) (Nowak, 2010). The surface of the electrode was polished gently on emery papers (Struers) of the grade 500, 1000, 2400 and finally 4000, then it was introduced to the measuring cell containing the solution of the base electrolyte (0.5 mol dm^{-3} Na_2SO_4) and the investigated compound of the predetermined concentration. The measured capacitance was compared to the capacitance of a freshly polished electrode in pure base electrolyte,

(2) The effectiveness of the inhibiting action of investigated compounds was tested in leaching experiments. Weighted portion of the sulfide (usually 1 g) was conditioned in the solution of the inhibitor (30 minutes if not otherwise stated), washed with water then poured to the Erlenmeyer flask containing 50 ml of 0.05 mol dm^{-3} H_2SO_4 solution and vigorously stirred in controlled manner at the free access of air. After the predetermined period of time (usually 24 hours) the solid sample was separated from the solution and the concentration of copper in the solution determined by iodometric titration. Before the conditioning in the surfactant solution the oxidation products were removed from the surface by washing with 0.05 mol dm^{-3} H_2SO_4 solution, from which oxygen was removed by bubbling with argon. The amount of copper released was compared to the amount of copper released from the not-treated sample.

3. Results and discussion

Figure 1 presents the capacitance of the non-stoichiometric copper (I) sulfide electrode in the solutions of several compounds which are known to be surface active agents. The investigated potential range covered practically full potential range of non-stoichiometric copper (I) sulfide thermodynamic stability. Outside that potential range significant currents of either cathodic or anodic dissolution flew. Note that both cationic surfactants (dodecyltrimethylammonium chloride and N-dodecylpyridinium chloride) diminish strongly the capacitance of the EDL. That decrease is due to the adsorption of their molecules at the surface of non-stoichiometric copper (I) sulfide electrode. Adsorption of organic molecules at the surface causes the replacement of water molecules with the organic molecules which leads to significant decrease of the dielectric constant of the surface layer and, consequently, to the decrease of the capacitance of the molecular condenser formed at the surface. Both anionic surfactants did not cause any change in the capacitance of the EDL (within the limit of the accuracy of the measurement).

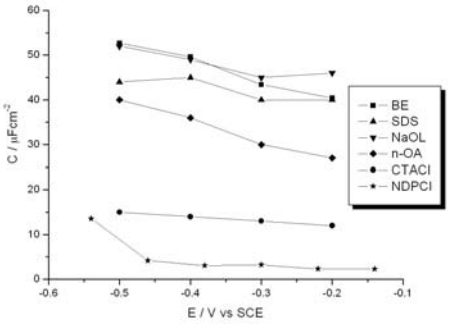

Fig. 1. The dependence of the capacitance of the EDL at the surface of non-stoichiometric copper (I) sulfide electrode in the solution of pure base electrolyte (0.5 mol dm^{-3} Na_2SO_4) (BE) and in the solutions containing, besides base electrolyte, surface active substances: sodium dodecylsulfate (SDS), sodium oleate (NaOL), n-octanol (n-OA), dodecyltrimethylammonium chloride (CTACl) or N-dodecylpyridinium chloride (NDPCl) – all at the concentration of 0.001 mol dm^{-3}

So, no adsorption of those substances at the non-stoichiometric copper (I) sulfide surface has occurred. The nonionic surfactant (n-octanol) caused limited decrease in the capacitance of the EDL and the course of the dependence of capacitance on potential suggests that higher surface coverage occurred at the anodic limit of the investigated potential range.

All those observations may be explained assuming that the potential of zero charge of the electrode lays outside the investigated potential range, on its anodic side. Surfactants molecules adsorb mainly due to the electrostatic interactions. So, cationic surfactants adsorb strongly due to the attraction between the positively charged surfactant ions and negatively charged electrode surface, anionic surfactants do not adsorb due to the repulsion of negative surfactant ions and negatively charged electrode surface and non-ionic surfactant adsorbs better in the range of potentials closer to the potential of zero charge. All above described surfactants (except sodium oleate, see later) decreased the dissolution rate of non-stoichiometric copper (I) sulfide in a very limited manner (see Table 1). Evidently, the electrostatic, physical adsorption is not strong enough to create the protective layer at the surface of the sulfide.

Very strong adsorption was observed in the case of 2-mercaptobenzthiazole (Fig. 2). Similar behavior was observed in the case of potassium ethylxanthate (Nowak, 2010). Note that both compounds form negatively charged ions (anions) in the solution. Both compounds belong to so-called sulfhydryl compounds, strongly adsorbing at the surface of metal sulfides (Woods, 1996). Such compounds form a monolayer of chemisorbed radicals at the surface of a metal sulfide which is compact and impermeable. That monolayer protects the surface against the attack of corroding species effectively. Indeed, very significant decrease of the leaching rate in the case of both compounds was observed (see Table 1). However some desorption of xanthate from the surface was observed when xanthate-covered non-stoichiometric copper (I) sulfide sample was subjected to the desorption in strongly acidic environment. Potasium ethylxanthate is used as a flotation collector. So, one can expect that metal sulfides, present in the flotation wastes, should show relatively low leachability, when xanthate is used as a flotation collector.

A special case, worth to be specially described is sodium oleate. As may be inferred from Figure 1 this compound does not adsorb at the surface of non-stoichiometric copper (I) sulfide. However, when non-stoichiometric copper (I) sulfide was conditioned in the solution of sodium oleate at the free access of air significant decrease in the leaching rate in 0.05 mol dm^{-3} sulfuric acid was observed (Table 1).

Noticeable diminishing of the leaching rate was observed after 1 hour of treatment at so low concentration of sodium oleate as 10^{-6} mol dm^{-3}. Similar decrease of the leaching rate in perchloric acid solutions after treatment in sodium oleate at different conditions was observed in our previous work (Nowak and Gucwa, 2008). It was observed that prolongation of the conditioning leads to even more significant decrease in leaching rate and that the protecting layer, formed on the surface by

conditioning in sodium oleate solutions is stable in acidic solutions. The influence of sodium oleate on the surface of non-stoichiometric copper (I) sulfide may be explained in a similar manner like in the case of phosphate influence on pyrite (Huang and Evangelou, 1994). During the oxidation of the non-stoichiometric copper (I) sulfide surface copper ions are liberated. Those ions react with oleate anions forming an overlayer of copper oleate which protects effectively the surface from the attack of the corrosive agents.

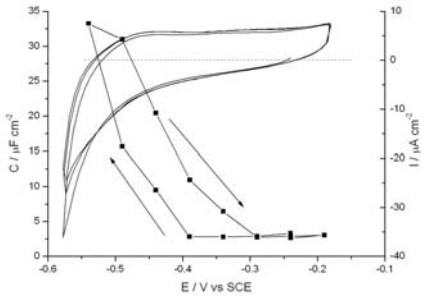

Fig. 2. Cyclic voltammogram (continuous line) of the $Cu_{1.87}S$ electrode in 0.5 mol dm^{-3} Na_2SO_4 solution containing 0.1 mmol dm^{-3} 2-mercaptobenzthiazole and capacitance of the same electrode measured consecutively at different potentials (full squares)

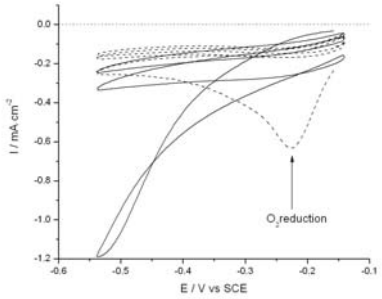

Fig. 3. Cyclic voltammograms in air-saturated 0.5 mol dm^{-3} Na_2SO_4 solution of a freshly polished $Cu_{1.87}S$ electrode (dashed line) and the electrode conditioned 24 hours in 0.001 mol dm^{-3} sodium oleate solution (solid line)

Table 1. The influence of the conditioning of non-stoichiometric copper (I) sulfide in the solutions of surfactants on the amount of copper (II) ions liberated during 24 hours of leaching in air-saturated 0.05 mol dm^{-3} H_2SO_4 solution.

Surfactant	-	SDS	NaOL	NDPCl	DTACl	MBT	EtXK
Concentration, mol sm^{-3}		0.001	0.0001	0.0001	0.0001	0.0001	0.0001
Leached copper, mmol/g	2.16	2.03	0.26	0.61	2.01	0.17	0.43

That may be inferred from Fig. 3, when the voltammogram of a $Cu_{1.87}S$ electrode, conditioned in sodium oleate solution is presented and compared to the voltammogram of a freshly polished electrode. It is to be seen that after the treatment in oleate solution the peak of oxygen reduction on sulfide electrode (marked with an arrow) disappeared, whereas strong cathodic current started to flow at the cathodic limit of the investigated potential range. That current may be ascribed to the reduction of some overlayer formed on the surface during the treatment in oleate solution at the free access of air (presumably copper II oleate). It is worthwhile to mention that similar compound, sodium stearate did not show any positive influence on the corrosion resistance of non-stoichiometric copper (I) sulfide (Nowak and Gucwa, 2008). That may be probably attributed to much lower solubility of sodium stearate in comparison to sodium oleate.

4. Conclusions

Copper sulfides differ from other minerals. Most of the copper sulfide minerals are either diamagnetics or semiconductors, with low free charge carriers concentrations and low capacitance of the space charge layer at the surface. Only very small charge may be stored on the solid side of the mineral/solution interface, so the surface charge is defined by the adsorption of ions and molecules at the surface. In the case of copper sulfides high capacitance of the space charge layer enables accumulation of charge in the surface layer on the solid side of the interface – due to this fact surface charge may be controlled by external polarization. So, the behavior of copper sulfides may be investigated by electrochemical methods. Also in natural conditions the charge of the surface of a copper sulfide mineral may by partly controlled by the charge stored in the space-charge layer formed at the solid side of the interface. That charge may originate from the redox reaction occurring between the sulfide and the oxidative/reductive agent present in the solution.

Physical, electrostatic adsorption does not protect the surface of non-stoichiometric copper (I) sulfide against corrosive attack of the oxidative environment. Either strong chemisorption, or the formation of an overlayer of precipitated salt which is resistive to the action of oxidizing agents is required to protect the surface of a sulfide mineral against oxidative dissolution. The best protective action against the , among the investigated compound, exerted sodium oleate, which does not adsorb at the surface but forms the protective layer by surface precipitation.

Acknowledgments

This work was financed by Polish Ministry of Science and Higher Education from the financial resources for the years 2009 – 2011 (grant 4513/B/T02/2009/36).

This paper is based partially on the MSc theses presented by IK (2009) and MN (2010) at the Faculty of Chemistry, Jagiellonian University, Kraków, Poland.

References

BELZILE, N., MAKI, S., CHEN, Y.-W., GOLDSACK, D., 1997. *Inhibition of pyrite oxidation by surface treatment*, Sci. Total Environ. 196, 177-186.

DOYLE F.M., 1990, *Acid mine drainage from sulfide ore deposits, in: Sulfide deposits – their origin and processing* (P.M.J. Gray, G.J. Bowyer, J.F. Castle, D.J. Vaughan and N.A. Warner, editors), The Institution of Mining and Metallurgy, London, 301-310.

EVANGELOU, V.P., 1995. *Pyrite Oxidation and its Control*, CRC Press, Boca Raton.

HELIOS-RYBICKA, E., 1996. *Impact of mining and metallurgical industries on the environment in Poland*, Appl. Geochem., 11, 3 – 9.

HUANG, X., EVANGELOU, V. P., 1994. *Suppression of pyrite oxidation rate by phosphate addition*, in : *Environmental Geochemistry of Sulfide Oxidation*, ACS Symposium Series 550, 562-573.

JAMBOR, J.L., BLOWES, D.W., PTACEK, C.J., 2000. *Mineralogy of mine wastes and strategies for remediation*, in: *Environmental Mineralogy, European Mineralogical Union Notes in Mineralogy*: (Vaughan and Wogelius, editors), Eötvös University Press, Budapest, Vol. 2, 255 – 290.

JELLINEK, F., 1968, *Sulphides*, in: *Inorganic Sulphur Chemistry* (G. Nickless - editor), Elsevier, New York, 669 – 747.

Jiang, C.L., Wang, X.H., Parekh, B.K., 2000. *Effect of sodium oleate on inhibiting pyrite oxidation*, Int. J. Miner. Process., 58, 305-318.

KARGBO, D. M., ATALLAH, G., CHATTERJEE, S., 2004. *Inhibition of Pyrite Oxidation by a Phospholipid in the Presence of Silicate*, Environ. Sci. Technol., 38, 3432-3441.

LARGE, G.J., MACQUAKER, J., VAUGHAN, D.J., SAWLOWICZ, Z., GIZE A.P., 1995. *Evidence for low-temperature alteration of sulfides in the kupferschifer copper deposits of southwestern Poland*, Econ. Geol., 90, 2143-2155.

LIPKOWSKI, J., 1992. *Ion and electron transfer across monolayers of organic surfactants*, in: *Modern Aspects of Electrochemistry*, 23, 1-99.

ŁUSZCZKIEWICZ, A., 2000,*Conception of the utilization of the flotation wastes from the copper ore processing in the Legnica-Głogów region*, Inżynieria Mineralna (Mineral Engineering), 1, 25-35 (in Polish).

NOWAK, P., 2010. *Influence of Surfactant Adsorption on the Leaching of Copper Sulfides*, in: *Electrochemistry in Mineral and Metal Processing VIII, ECS Transactions* 28(6), (F.M. Doyle, R. Woods and G.H. Kelsall - editors), The Electrochemical Society, Pennington, USA, 143 – 153.

NOWAK, P. AND GUCWA, A., 2008. *Influence of surfactant adsorption on the leaching of copper sulfides*, Acta Metallurgica Slovaca, 14, 196 – 203.

NOWAK, P., KRAUS, E., POMIANOWSKI, A., 1984. *The electrochemical characteristics of the galvanic corrosion of sulfide minerals in short-circuited model galvanic cells*", Hydrometallurgy, 12, 95-110.

NOWAK, P., POMIANOWSKI, A, 1989. *Surface properties of cuprous sulfide in aqueous solutions", Colloids and Surfaces,* 41,15-21.

SAND, W., JOZSA, P. – G., KOVACS, Z. – M., SĂSĂRAN, N., SCHIPPERS, A., 2007. *Long-term evaluation of acid rock drainage mitigation measures in large lysimeters*, Journal of Geochemical Exploration, 92, 205-211.

SHUEY R.T., 1975. *Semiconducting Ore Minerals,* Elsevier, New York

TWARDOWSKA, I., SZCZEPAŃSKA, J., WITCZAK, S., 1988. *Influence of wastes from the coal mining industry on the aqueous environment, estimation of hazard, prediction and prevention*, Prace i Studia 35, Ossolineum, Wrocław (in Polish).

VAUGHAN, D.J. AND CRAIG, J.R., 1978. *Mineral Chemistry of Metal Sulphides*, Cambridge University Press, Cambridge

VAUGHAN, D.J. AND WOGELIUS, R.A. (editors), 2000, *Environmental Mineralogy, European Mineralogical Union Notes In Mineralogy*: Vol. 2, Eötvös University Press, Budapest

WOODS, R., 1996. *Chemisorption of thiols on metals and metal sulfides*, in: *Modern Aspects of Electrochemistry* (O'M. Bockris, B. E. Conway and R. E. White, Editors), vol. 29, 401-453, Elsevier.

ZHANG, X., BORDA, M. J., SCHOONEN, M. A. A., STRONGIN, D.R., 2003. *Pyrite oxidation inhibition by a cross-linked lipid coating*, Geochem. Trans., 4, 8-11.

Physicochem. Probl. Miner. Process. 47(2011) 139-148
www.minproc.pwr.wroc.pl/journal/

Physicochemical Problems of Mineral Processing
ISSN 1643-1049

Received October 20, 2010; reviewed; accepted March 27, 2011

Leaching kinetics of ulexite in oxalic acid

Yuksel ABALI *, Salih U. BAYCA **, Elvan MISTINCIK *

* Celal Bayar University, Department of Chemistry, 45040 Manisa, Turkey

** Celal Bayar University, Soma Technical Vocational School, 45500 Soma, Manisa, Turkey, salihbayca@gmail.com, phone: +90236612 0063, fax: +902366122002

Abstract. Leaching of ulexite in oxalic acid, which is an organic acid, was studied. The parameters were solid-to-liquid ratio, acid concentration, stirring speed and temperature. The experimental data were applied to the homogeneous and heterogeneous kinetic models to determine the best one. The results showed that the leaching rate increases with increasing reaction temperature, stirring speed, acid concentration, but decreases with solid-to-liquid ratio and particle size. The leaching kinetics of ulexite was determined as the product layer model. The activation energy of the process was calculated.

keywords: concrete aggregates, shape, mechanical resistance, mobile plant, fixed plant

1. Introduction

Ulexite is a hydrated sodium–calcium borate. In Turkey commercially produced boron minerals are colemanite, ulexite, and tincal. These borate mineral are produced in large amounts in Turkey where ulexite is produced in Balikesir – Bigadic. In Bigadic, a ulexite ore is produced in open mines. Ulexite processing is carried out in ore preparation facilities near ore mines in Bigadic. Ulexite is enriched by crushing, wetting in water, washing in a tumbling mill, sieving, triage and classification, and produced in different grain sizes as well as chemical compositions as concentrated ulexite, and offered for sale. A major portion of the ulexite concentrate produced is exported (Bayca, 2009).

Pure boron element does not exist in nature. Rather it is found as boron oxides. Boron minerals, produced as compounds of boron oxide and alkaline or earth alkaline elements exist widely in nature. Although there are many varieties of boron minerals in nature, only a small amount of these varieties can be used commercially (Brotherton, 1995). Ulexite is a sodium-calcium borate mineral with a chemical composition of $NaCaB_5O_9 \cdot 8H_2O$ and contains theoretically 42.95% B_2O_3. The water in the structure of ulexite exists as 3 moles of hydroxyl groups and 5 moles of crystal water ($NaCa[B_5O_8(OH)_6] \cdot 5H_2O$). Ulexite exists as a white parallel fiber and has a

triclinic crystal structure. It has relatively low water solubility: 0.5% at 25^{o}C (Brotherton, 1995; Gerhartz, 1985).

The leaching kinetics of boron minerals in various acid solutions has been investigated. The leaching kinetics of colemanite in acetic acid (Ozmetin et al. 1996), phosphoric acid (Temur et al., 2000), citric acid (Cavus et al., 2005), oxalic acid (Alkan et al., 2004a) were studied. The dissolution kinetics of tincal in phosphoric acid (Abali et al., 2007) and oxalic acid (Abali et al., 2006) were studied. Many studies have been carried out on the dissolution kinetics of ulexite in different solutions. Kunkul et al. (2003) investigated the dissolution kinetics of ulexite in ammonium sulfate solutions. They found that the dissolution rate increased with increasing ammonium sulfate concentration, stirring speed, and reaction temperature. However, increasing the particle size and solid-to-liquid ratio decreased the dissolution rate. They determined that the heterogeneous diffusion-controlled ash or product layer may describe the dissolution rate. Demirkiran (2008) studied the dissolution of ulexite in ammonium acetate solutions. He found that the dissolution rate increased with an increase in concentration and reaction temperature, and with a decrease in particle size and solid-to-liquid ratio. No effect of stirring speed was observed on the conversion. It was determined that the dissolution rate fit the chemical reaction control model. Tunc et al. (1999) have investigated the dissolution kinetic of ulexite in aqueous acetic acid solutions. They reported that the dissolution rate increased with increasing temperature and stirring speed and decreasing solid-to-liquid ratio and particle size. Demirkiran and Kunkul (2007) have studied the dissolution kinetics of ulexite in perchloric acid solutions. They found that the dissolution rate increased with increasing concentration, stirring speed, reaction temperature and with decreasing particle size. The dissolution process was described by the Avrami model. Kunkul et al., (1997a) have studied the dissolution kinetics of ulexite in ammonia solutions saturated with CO_2. It was found that the dissolution rate of ulexite can be described by a first-order pseudo-homogenous reaction model. Alkan et al. (2004b) have conducted the dissolution kinetics of ulexite in oxalic acid solutions. They found that the dissolution rate was controlled by product layer diffusion model. Kunkul et al. (1997b) have studied the dissolution of thermally dehydrated ulexite in sulfuric acid solutions. They reported that the process fits the first-order pseudo homogeneous kinetic model.

The aim of this paper is to investigate leaching kinetics of ulexite in oxalic acid solutions. The effects of reaction temperature, solid-to-liquid ratio, stirring speed, particle size, and acid concentration on the leaching rate have been studied. The leaching kinetics of ulexite was examined according to the heterogeneous and homogenous reaction models, and the best fitted equation to the experimental data was determined. Activation energy was calculated by using the best model and Arrhenious equation.

2. Material and methods

Ulexite (3 – 125 mm) used in the present study was obtained from Eti Mine Bigadic Boron Works, Balikesir, Turkey. The sample was crushed by a jaw crusher and sieved using ASTM Standard sieves to obtain the following size fractions: 160 – 315, 315 – 500, 710 – 1000, and 1000 – 1600 μm. The X-ray diffraction analysis is given in the Fig. 1.

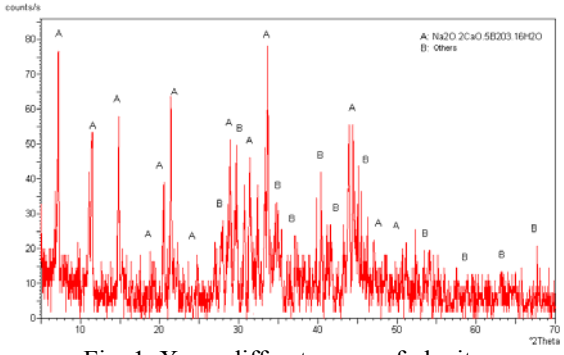

Fig. 1. X-ray diffractogram of ulexite

The chemical analysis of the studied ulexite fraction is shown in Table 1. The boron oxide chemical analysis was determined by the volumetric method (Scott, 1963) and others were determined by X-ray fluorescence (XRF). Oxalic acid and other reagents used were of analytical grade. Distilled water was used to prepare solutions.

Table 1. Chemical analysis of the studied ulexite

Oxides	Percent
B_2O_3	37.3
CaO	15.8
Na_2O	9.2
H_2O	36.4
Others	1.3

The leaching experiments were performed in a 250 dm^3 glass reactor at atmospheric pressure. A mechanical stirrer was used and a thermostat was employed to keep reaction medium at constant temperature. In the dissolution process, 100 dm^3 of oxalic acid solution was placed into the reactor. After the desired reaction temperature was reached, a given amount of ulexite was added to the solution and the stirring was started.

After a certain period of time, the solution was filtered without any change in temperature. The percent of B_2O_3 in the filtrate was determined by volumetric method and experimental parameters used in the dissolution process are given in Table 2.

Table 2. Parameters and their values

Parameters and Values	1	2	3	4
Reaction temperature, °C	13	25	35	60
Acid concentration, % w/v	1	2	5	10
Solid/liquid ratio, % w/v	0.5	1	2	5
Particle size, μm	1000 – 1600	710 – 1000	315 – 500	315 – 160
Stirring speed, rpm	250	450	750	

3. Results and discussion

3.1. Leaching reaction

The dissolution of oxalic acid is as follows:

$$C_2H_2O_{4(aq)} + 4H_2O = 2C_2O_4^{2-}{}_{(aq)} + 4H_3O^+{}_{(aq)} \quad (1)$$

while the dissolution of ulexite in oxalic acid solution proceeds as follows:

$$Na_2O{\cdot}2CaO{\cdot}5B_2O_3{\cdot}16H_2O_{(s)} + 3C_2H_2O_{4(aq)} + 2H_2O =$$
$$10H_3BO_{3(aq)} + 2Na^+{}_{(aq)} + 2CaC_2O_{4(s)} + C_2O_4^{2-}{}_{(aq)} + 6H_2O_{(l)} \quad (2)$$

The reaction between ulexite and oxalic acid leads to boric acid (H_3BO_3), sodium oxalate and calcium oxalate.

3.2. Effects of leaching parameters

The experiments were performed at different particle sizes between 13 and 60°C while other parameters were kept constant.

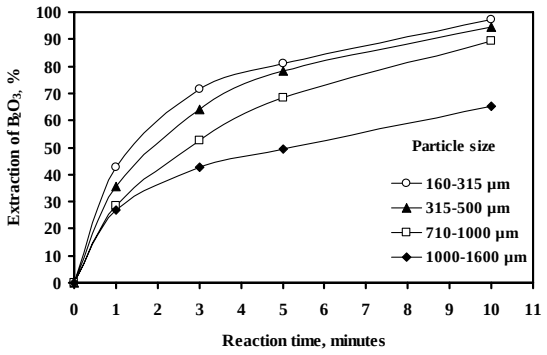

Fig. 2. Effect of time and particle size on the dissolution of ulexite (10% $C_2H_2O_4$, 1% solid, 450 rpm, 25°C)

Figure 2 indicates that the lowest dissolution rate was obtained at 1000 – 1600 μm particle size. The dissolution rate quickly increases when particle size of ulexite reaches 500 μm. Since the particle size decreases, the dissolution rate increases.

Ekmekyapar et al. (2008) reported that the dissolution rate of ulexite in acetic acid solutions increased with decreasing particle size.

Figure 3 shows the effect of time and solid-to-liquid ratio on the dissolution rate of ulexite. The dissolution rate increases from 58.4 to 98.6 % when the solid-to-liquid ratios is reduced from 0.5 to 5%. It might be explained by insufficient dissolution reagent in the medium. It was observed that the dissolution rate increases with decreasing solid-to-liquid ratio. Similar results were found for borogypsum in SO_2 saturated solutions (Demirbas, 2000) and for ulexite in ammonia solutions saturated with CO_2 (Kunkul, 1997).

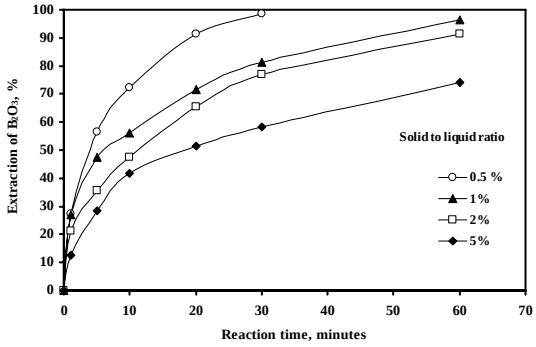

Fig. 3. Effect of time and solid to liquid ratio on the dissolution of ulexite (10% $C_2H_2O_4$, 315 – 500 μm, 450 rpm, 25°C)

It was observed (Fig. 4) that the maximum dissolution rate was 78.2% at 1% acid concentration for 60 min. The boron oxide extraction increased from 78.2 to 96.3% at 10% acid concentration for 60 min. When acid concentration increases the dissolution rate increases.

The effects of temperature on the dissolution rate of ulexite are studied at different temperatures. The results are given in Fig. 5. They show that the maximum dissolution rate was 84.4% at 13°C for 60 minutes.

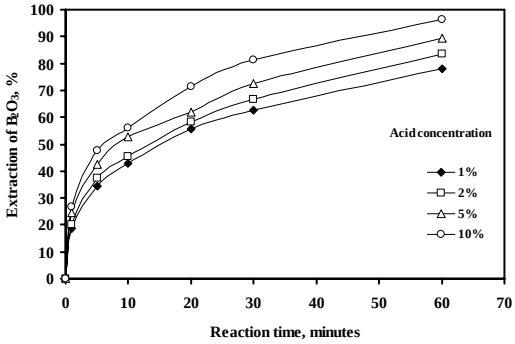

Fig. 4. Effect of time and acid concentration on the dissolution of ulexite (315 – 500 μm, 1% solid, 450 rpm, 25°C)

The extraction of boron oxide increases from 84.4 to 99.9% at 60°C for 60 minutes. The dissolution rate increases with increasing temperature. Demirkiran and Kunkul (2007) found that dissolution of ulexite in perchloric acid solutions increased with increasing temperatures.

The experiments on influence of stirring speed on the dissolution rate of ulexite were performed between 250 and 750 rpm. The results (Fig. 6) indicate that changing the stirring speed from 250 to 750 rpm improves dissolution rate from 58.4 to 73.8% for 10 minutes of stirring. The dissolution rate was increasing with increasing stirring speed.

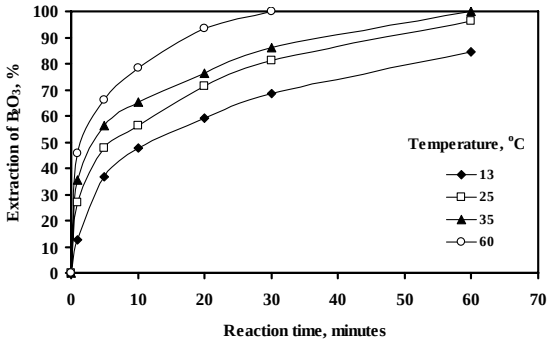

Fig. 5. Effect of time and temperature on the dissolution of ulexite (10% $C_2H_2O_4$, 1% solid, 315 – 500 μm, 450 rpm)

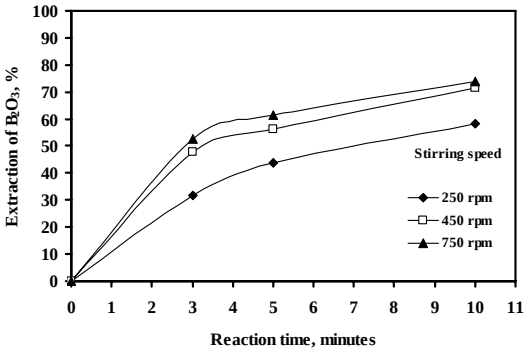

Fig. 6. Effect of time and stirring speed on the dissolution of ulexite (10% $C_2H_2O_4$, 1% solid, 315 – 500 μm, 25°C)

3.3. Kinetic analysis

The rate of reaction between the solid and fluid phases can be expressed in terms of heterogeneous reaction models. The rate may be described by film diffusion, chemical reaction, product layer diffusion models (Levenspiel, 1972). Reaction time *t* is given as a function of fractional dissolution for surface chemical reaction, diffusion through fluid film, and diffusion product layer control model cases.

The kinetics of film diffusion control model is given by:

$$X = \frac{t}{\tau} \quad , \tag{3}$$

the chemical reaction control model by:

$$1-(1-X)^{1/3} = \frac{t}{\tau}, \tag{4}$$

while the product layer diffusion control model by:

$$1-3(1-X)^{2/3}+2(1-X) = \frac{t}{\tau}. \tag{5}$$

The dissolution rates of ulexite were determined at different temperatures. The results were given in Fig. 4. The results were analyzed using Eq. 3, 4 and 5. The experimental data were analyzed using equations of the homogeneous kinetic models. The regression coefficient values R^2 found in the range of 0.9197 – 0.9958 for the first order pseudo homogeneous control model and as 0.6473 – 0.9824 for the second order pseudo homogeneous control model. It indicates that these models cannot be fitted due to nonlinear regression.

The values for calculated from Eqs. 3-5 are plotted to find regression coefficients. The correlation coefficients (R^2) and k values of heterogeneous models for each temperature were calculated using the slope of the lines. The correlation coefficients was calculated between 0.6858 and 0.7735 for the film diffusion control model, between 0.9045 and 0.9600 for the surface chemical reaction control model and between 0.9939 and 0.9976 for the product layer diffusion control model (Table 3).

Table 3. Values k_f, k_r, k_d and correlation coefficients

Models	Heterogeneous control models					
	Film diffusion		Surface chemical reaction		Product layer diffusion	
Temperature, K	k_f, min^{-1}	R^2	k_r, min^{-1}	R^2	k_d, min^{-1}	R^2
286	0.0124	0.7735	0.0071	0.9045	0.0073	0.9948
298	0.0132	0.7339	0.0100	0.9413	0.0121	0.9976
308	0.0128	0.6637	0.0132	0.9598	0.0155	0.9939
333	0.0258	0.6858	0.0263	0.9600	0.0310	0.9960

The kinetic analysis indicated that the dissolution rate of ulexite in oxalic acid does not fit the film diffusion control model and the surface chemical reaction control model due to nonlinear relationships. However, linear relationships were obtained for the product layer diffusion control model. The dissolution rate of ulexite in oxalic acid results fits the product layer diffusion control model. The dissolution rate increased

between 250 and 450 rpm stirring speed (Fig. 6). The solid product layer formed on the surface of ulexite particle is CaC_2O_4. This layer prevents diffusion of oxalic acid to the surface of the particle. The low dissolution rate was due to insufficient, 250 rpm stirring speed. The solid product layer removal from the surface of particle was sufficient at 450 rpm stirring speed (increase in extraction).

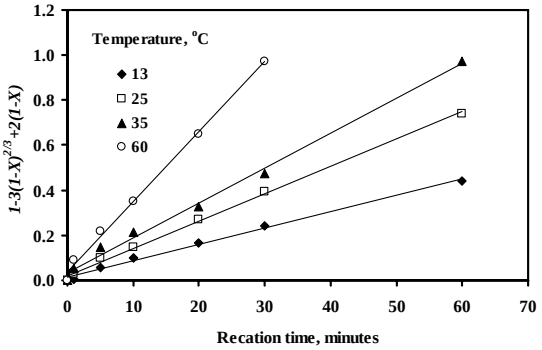

Fig. 7. The variation in $1 - 3(1 - X)^{2/3} + 2(1 - X)$ with time at different temperatures

Figure 7 shows results of leaching at different temperatures. It indicates that the dissolution rate increases with increasing stirring speed, which may be the result of film layer forming on the surface of ulexite particle. Because the stirring speed of solution increased, the film layer formed on the particle surface was probably removed. The product layer diffusion control model, which was determined for ulexite in oxalic acid solution, confirmed these results. Similar results were reported by Kunkul et al. (2003).

In our process Ca^{2+} ions and $C_2O_4^{2-}$ formed solid CaC_2O_4 while ulexite completely dissolved in oxalic acid solution. This solid formed an insoluble layer on the surface of particles. The layer causes that the kinetics of ulexite in oxalic acid solutions fits the product or ash layer diffusion control model. This kinetics model is also confirmed by the fact that the dissolution rate increases with increasing stirring speed from 250 to 450 rpm.

3.4. Activation energy

The activation energy of the leaching was calculated from the Arrhenius equation

$$k = k_o \exp(-E/RT), \tag{6}$$

because ln$k$ versus $1/T$ gives a straight line of slope $-E/R$. From the slope of the straight line in Fig. 8, the activation energy (E) of dissolution rate of ulexite in oxalic acid can be determined.

The reaction control model of ulexite in oxalic acid solution was determined as $1 - 3(1 - X)^{2/3} + 2(1 - X)$. In this study, the activation energy of dissolution rate of ulexite in oxalic acid solutions was calculated as 24 kJ/mol. Similar results were

reported by researchers who reported that the activation energies of ulexite in dissolution reagents solutions is 46.00 kJ/mol in sulfuric acid, 58.20 kJ/mol in ammonium nitrate, 55.70 kJ/mol in ammonium acetate, 83.50 kJ/mol in ammonium sulphate, 19.12 kJ/mol in perchloric acid, 30.24 kJ/mol in oxalic acid, 30.69 kJ/mol in acetic acid (Kunkul et al., 1997; Demirkiran, 2009; Demirkiran, 2008; Kunkul et al., 2003; Demirkiran et al., 2007; Alkan et al., 2004b; Tunc et al., 1999, respectively).

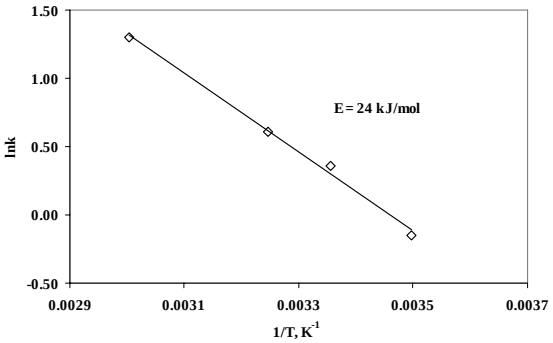

Fig. 8. Arrhenius plot for the dissolution of ulexite

4. Conclusions

The leaching kinetics of ulexite in oxalic acid solutions was investigated in a batch reactor. The results showed that the dissolution rate increases with increasing reaction temperature, acid concentration, stirring speed and decreasing with solid-to-liquid ratio and particle size. The most influential parameter on the dissolution rate was found to be temperature of ulexite while the least influential was acid concentration. Boric acid, sodium oxalate and calcium oxalate were formed in the course of dissolution of ulexite in oxalic acid. The formed boric acid and sodium oxalate which go into the filtrate. The calcium oxalate and undissolved ulexite remained as solids. Ulexite dissolution kinetics was best described by formula $1-3(1-X)^{2/3}+2(1-X)$. The activation energy of ulexite in oxalic acid solution is 24 kJ/mol.

References

ABALI, Y., BAYCA, S. U., MISTINCIK, E. (2006). Kinetics of oxalic acid leaching of tincal, *Chemical Engineering Journal*, 123, 25–30.

ABALI, Y., BAYCA, S. U., GULER, A. E. (2007). The dissolution kinetics of tincal in phosphoric acid solutions, *International Journal of Chemical Reactor Engineering*, 5, 1–10.

ALKAN, M., DOGAN, M. (2004a). Dissolution kinetics of colemanite in oxalic acid solutions, *Chemical Engineering and Processing,* 43, 867–872.

ALKAN, M, DOGAN M, NAMLI, H. (2004b). Dissolution kinetics and mechanism of ulexite in oxalic acid solutions, *Ind. Eng. Chem. Res*., 43, 1591–1598.

BAYCA, S. U. (2009). Effects of the addition of ulexite to the sintering behavior of a ceramic body, *Journal of Ceramic Processing Research*, 10, 162–166.
BROTHERTON, R. J. (1995). *Encyclopedia of Inorganic Chemistry*, Wiley, New York, USA.
CAVUS, F., KUSLU, S. (2005). Dissolution kinetics of colemanite in citric acid solutions assisted by mechanical agitation and microwaves, *Ind. Eng. Chem. Res*., 44, 8164–8170.
DEMIRBAS, A., H., YUKSEK, I., CAKMAK, M., M., KUCUK, CENGIZ M., ALKAN, M. (2000). *Resources, Conservation and Recycling*, 28, 135–146.
DEMIRKIRAN, N., KUNKUL, A., 2007, Dissolution kinetics of ulexite in perchloric acid solutions, *International Journal of Mineral Processing*, 83, 76–80.
DEMIRKIRAN, N. (2008). A study on dissolution of ulexite in ammonium acetate solutions, *Chemical Engineering Journal*, 141, 180–186.
DEMIRKIRAN, N. (2009). Dissolution kinetics of ulexite in ammonium nitrate solutions, *Hydrometallurgy*, 95, 198–202.
EKMEKYAPAR A., DEMIRKIRAN N., KUNKUL, A. (2008). *Chemical Engineering Research and Design*, 86, 1011–1016.
GERHARTZ, W. (1985). *Ullmann's Encyclopedia of Industrial Chemistry*, Wiley, Germany.
KUNKUL,A., YAPICI, S., KOCAKERIM, M., M., COPUR, M. (1997a). The dissolution kinetics of ulexite in ammonia solutions saturated with CO_2, *Hydrometallurgy*, 44, 135–145.
KUNKUL, A., TUNC, M., YAPICI, S., ERSAHAN, H., KOCAKERIM, M. M. (1997b). Dissolution of thermally dehydrated ulexite in sulphuric acid solution, *Ind. Eng. Chem. Res*., 36, 4847–4851.
KUNKUL, A., DEMIRKIRAN, N., and BAYSAR, A., 2003, Dissolution kinetics of ulexite in ammonium sulphate solutions, *Ind. Eng. Chem. Res*., 42, 982–986.
LEVENSPIEL, O. (1972). *Chemical Reaction Engineering*, 2nd edition, Wiley, New York.
OZMETIN, C., KOCAKERIM, M. M., YAPICI, S and YARTASI, A. (1996). A semi empirical kinetic model for dissolution of colemanite in aqueous acetic acid solutions, *Ind.Eng. Chem. Res.* 35, 2355–2359.
SCOTT, W. W. (1963). *Standard Methods of Chemical Analysis*, D. Van Nostrand, New York.
TEMUR, H., YARTAŞI, A., COPUR, M., KOCAKERIM, M. (2000). The kinetics of dissolution of colemanite in phosphoric acid solutions, *Ind. Eng. Chem. Res*., 39, 4114.
TUNC, M., KOCAKERIM, M. M., GUR, A., YARTASI, A. (1999). A semi empirical kinetic model for dissolution of ulexite in aqueous acetic acid solutions, *Energy, Education, Science and Technology*, 3, 1–10.

List of symbols

k	reaction rate constant (min^{-1})
t	reaction time (min),
T	temperature, K
E	activation energy, J/mol
R	universal gas constant, J/mol.K
τ	time for complete reaction of a particle (min)
X	fraction of extracted B_2O_3

Physicochem. Probl. Miner. Process. 47(2011) 149-158
www.minproc.pwr.wroc.pl/journal/

Physicochemical Problems of Mineral Processing
ISSN 1643-1049

Received January 17, 2011; reviewed; accepted April 22, 2011

Recovery of zinc from arduous wastes using solvent extraction technique Part I. Preliminary laboratory studies

Leszek GOTFRYD, Andrzej CHMIELARZ, Zbigniew SZOŁOMICKI

Institute of Non-Ferrous Metals, Sowińskiego 5; 44-100 Gliwice, Poland, leszekg@imn.gliwice.pl

Abstract. Solvent extraction technique with 40 volume percent of bis(2-ethylhexyl)phosphoric acid as an extractant was applied for recovery of zinc from technological solutions. Crude zinc oxides from Waelz processing of electric arc furnace dusts or ferrous waste of zinc hydrometallurgy were used for preparation of feed solutions by leaching them with diluted sulfuric acid and by preliminary hydrometallurgical purification. The studies were conducted step by step from elementary laboratory experiment to advanced level of pilot plant tests in a continuously operating installation consisting of a counter-current set of mixer-settler type extractors and necessary equipment. The paper describes the course and results of initial laboratory works undertaken to choose proper extractant and establish conditions for further successful zinc extraction in the pilot plant installation.

keywords: solvent extraction, zinc recovery, crude zinc oxide,electric arc furnace dust

1. Introduction

Heavily contaminated semi-products or waste (dusts, slimes, dross, slag) of troublesome and negative influence on production processes are often encountered in important sections of technological flow-sheets in many plants of non-ferrous metals industry. The main components of those “troublesome” materials are zinc and lead, and also other ingredients such as copper, manganese, iron, silica, calcium, along with their typical contaminants including As, Cd, F, Cl, Na, and K. Nowadays, the steel industry becomes the main source of secondary zinc materials and generates continuously growing volume of electric arc furnace dusts (EAFD). The dusts are further processed by pyrometallurgical methods to produce crude zinc oxides which usually contain mainly zinc, lead and iron oxides and also zinc ferrites and their characteristic contaminants (Cd, Cl, F).

1.1. Dealing with zinc-bearing secondary materials

There are many pyro- and a few hydrometallurgical processes used for a direct treatment of electric arc furnace dust, crude zinc oxides or similar oxidized zinc-

bearing materials (dusts, fumes, dross). Their wide variety, especially within area of pyrometallurgy, reflects a broad diversity and variability of the recyclable materials and also shows the difficulty of the discussed problem (Kapias et al., 1999; Frias et al., 2009; Ruetten, 2009; ZincOx website). Within the area of hydrometallurgy the most important technology seems to be extraction based Zincex Process (Technicas Reunidas, Spain) or its modified version (MZP). These methods use the solvent extraction technique with an organic solution of bis(2-ethylhexyl)phosphoric acid (DEHPA) as an extractant. The biggest and most important of the MZP-based installations is successfully operating in Namibia on the natural silicate ore (Skorpion Project) (Diaz et al., 1995; Garcia et al., 2005; Gnoinski et al., 2005).

A similar installation, in a form of an annex to the traditional RLE refinery of Dowa Metals & Mining Akita Zinc, was almost ready for commencing in Iijima, Japan. The expected capacity is 20 Gg per year of SGH zinc from zinc oxide secondaries (Frias et al., 2009). Another installation is under preparation in Italy (Portovesme).

ZincOx Resources plc, a British company, has developed an original method for treatment of oxidized secondary zinc-bearing materials (including EAFD), called LTC (Leach-to-Chemical). The technology produces high quality zinc oxide which can be used in ceramic and rubber industry as well as in farming applications (Woollett, 2006; ZincOx website)**.** In the case of the SERH and Ezinex processes, they consist of electric arc furnace dust leaching with a solution of NaOH or sodium and ammonium chloride, respectively, and then cementation of Pb (as well as Cu, Cd) with zinc dust and zinc electrolyses are conducted (Olper, 1998; Kapias et al., 1999).

In Poland zinc materials are processed in a Waelz kiln (Bolesław Recycling) for production of crude zinc oxides /CZO/. Their samples were the subject of this work. The research was mainly focused on comparison of natural zinc extraction with extraction under controlled pH conditions from solutions, prepared by leaching CZO with sulfuric acid. Preliminary laboratory works were based on elementary extractive experiments on synthetic single component solutions of metal salt.

1.2. Extraction technique as a method for cations separation - solution pretreatment

Cation exchanging solvent extraction is a good method for Zn separation from heavily contaminated solutions because this technique is naturally selective against contaminants other then cationic (i.e. neutral /SiO_2/ or anionic /Cl^-, SO_4^{2-}, PO_4^{3-}, AsO_4^{3-}/). The cationic ingredients of solutions may be assigned to groups:

- susceptible to (oxy)hydrolysis, e.g. Fe^{3+}, Al^{3+}, Ga^{3+}, In^{3+}, Tl^{3+}, Ni^{3+}, Co^{3+} (also As(III/V) and Sb(III/V) and typically extracted comparably or stronger then zinc(II); they should be mandatorily removed before extraction of zinc(II);
- susceptible for cementation on zinc and typically extracted comparably or less then zinc(II), including Cu^{2+}, Cd^{2+}, Ni^{2+}, Co^{2+}, Sn^{2+}, Pb^{2+};
- almost ignored by extractants, e.g. Mg^{2+}, Na^+, K^+, NH_4^+ and the alike;
- others, e.g. Ca^{2+}, Fe^{2+}, Mn^{2+}, Cr^{3+}.

The members of the first group must be removed before zinc(II) extraction because they can permanently poison the extractant. Lowering the concentration levels of the members of the next group also is in favor when one expects a good quality of the zinc product but is not critical. Selection of a good extractant for further extractive solution treatment to separate selectively zinc(II) from remaining contaminants was the aim of this work. Initial laboratory works, described here, were focused on observing extractants behavior versus chosen cations of metals against equilibrium pH of extraction. Next, extraction and stripping isotherms were observed and analyzed by the McCabe-Thiele method. After that quite a sophisticated experiment, simulating counter-current action, was performed to verify the theoretical assumptions for a real, continuously working, counter-current system, described in part II of this work (Gotfryd, 2011).

2. Experimental

2.1. Materials

Extractants, bis(2-ethylhexyl)phosphoric acid (DEHPA) and bis(2,4,4-trimetylpentyl) phosphinic acid (Cyanex 272), were used as received from their producers (Rhodia Ltd. and Cytec Industries, respectively) after dilution with hydrocarbon organic solvents - Exxsol D80 AZ or Escaid 110 (Exxon Chemicals/Brenntag Polska). Chemical reagents: lead(II) nitrate(V), sulfates(VI) of the other metals (Zn, Cd, Cu, Ni, Co, Mn, Fe), NaOH and sulfuric(VI) acid of p.a. purity were used to prepare single-component 0.1 mol/dm^3 solutions for preliminary extractive experiments or solutions for extractant preneutralization and stripping, respectively. They were delivered by local suppliers (POCH Gliwice, FOCH Lublin). Technical grade sulfuric acid was used in leaching and $Ca(OH)_2$ (PTH ChemLand) in water suspension was applied for treatment of raffinates.

Crude zinc oxides of industrial origin were used for both laboratory and pilot plant experiments. Their composition is presented in Table 1. Samples 1 and 2 come from treatment of EAFD in a Waelz kiln, while sample 3 from similar treatment of iron slime, generated in a classical hydrometallurgical processing of zinc calcine.

Table 1. Composition of the used in investigation samples of crude zinc oxides

No.*)	Zn	Pb	Fe	Cd	Mn	Mg	Cu	Sn	K	Na	Cl	F	As	
1	58.20	6.32	2.64	0.17	-	0.20	-	-	2.8	2.8	7.95	0.15	-	
2	54.46	5.80	5.00	0.50	0.40	0.12	0.063	0.10	3.46	2.45	7.59	0.15	0.0045	%
3	42.70	18.3	5.84	1.25	0.16	0.35	-	<0.05	0.58	0.29	1.37	0.023	0.30	

*) – samples No. 1 and 2 come from steel industry, No. 3 – from zinc hydrometallurgy

2.2. Solutions and preliminary purification

For elementary experiments, the solutions of metals(II) sulfates(VI) as well as lead(II) nitrate(V) have been prepared by simple dissolution of the crystalline salts in

proper amounts of distilled water to obtain their 0.1 mol/dm^3 concentration. 'Industrial' solutions were prepared by acidic leaching of crude zinc oxide /CZO/ samples. Treatment of CZO dust consisted of the following steps:

- preparation of aqueous pulp of the dust of predetermined solid/liquid ratio, typically 250 g/dm^3,
- careful addition of a fixed portion of concentrated 96 % sulfuric acid,
- stirring the pulp for a defined period of time, typically 1.0 hour at 80-90^{o}C,
- solid/liquid separation (sedimentation and filtration).

The solutions produced in the one-stage leaching process were subjected to further purification processes, consisting of oxy-hydrolysis and cementation on zinc powder. More details of these processes are presented within Part II of this work (Gotfryd, 2011).

2.3. Extraction

Two liquid cationic exchangers, DEHPA and Cyanex 272, were selected for examination and comparison of their basic properties in zinc extraction.

Elementary extractive experiment consisted of mechanical mixing of two reacting phases, an organic extractant (O) and an aqueous solution (A), for a chosen period of time at established O:A volumetric ratio and at a constant ambient temperature. Then, the two phases were separated and either analyzed for content of extracted species or sent for further treatment. The content of zinc (and other components) in the organic phase was determined indirectly by stripping them twice with 2 mol/dm^3 sulfuric acid at O:A ratio of 2:1 and by analysis of the merged stripped liquor.

Extraction – pH isotherms were determined by mixing (10 min at ambient temperature) of organic phase of the extractant with aqueous 0.1 mol/dm^3 Me^{2+} salt solution at the organic (O) to aqueous (A) ratio O:A = 1:1 (500 cm^3 / 500 cm^3) and gradually adding batches of 2.5 mol/dm^3 NaOH solution. All the investigated metal cations (Me^{2+} = Cu^{2+}, Cd^{2+}, Mn^{2+}, Co^{2+}, Ni^{2+}…) were used in a form of individual solutions of their sulfates(VI) (p.a. grade) – except for Pb^{2+}, which was used in a form of its nitrate(V). After each step of extraction even samples (typically 50 cm^3) of both phases was being taken to carry out necessary chemical analyses.

Classical isotherms of zinc extraction and stripping were determined by contacting reacting phases at several different levels of their volumetric proportions. In the extraction and stripping experiments the zinc sulfate or sulfuric acid solutions of predetermined concentrations were used as aqueous phase and fresh or saturated with zinc(II) organic extractant as organic phase, respectively. Extractions at established equilibrium pH were stabilized by adding portions of 2.5-5.0 mol/dm^3 NaOH solution.

Laboratory extractive tests consisted of several dozens of elementary extractive experiments in which by application of the same fixed portion of an extractant, a complete complex treatment of the feed solution was carried out. The three general stages of extraction (extraction proper, scrubbing and stripping) were performed

alternately and repeatedly in cycles. In a single cycle, a portion of the extractant is contacted in turns consequently with three different types of aqueous phases. At the beginning, in emulation of a counter-current flow, it is mixed, a few times (the number equals the number of extraction steps), one by one, with partially refined aqueous solutions (raffinates), and at the end of this stage also with the proper feed solution. Then, in a similar way, in emulation of mutual counter-current flows, it is contacted several times (the number equals the number of extraction washing steps) with scrubbing solutions in their different states, and at the end, also in a similar way, several times (the number equals the number of stripping steps) with stripping solutions, which show gradually growing acid concentration. The first cycles (three in this case, see Fig. 4 in the Result and Discussion section) are not typical, since they are not complete, starting cycles. Each of the rectangles in the diagram represents a single step in one of the conducted processes of extraction. The described experiments were performed in laboratory glassware. Contents of the beakers were stirred at ambient temperature with a mechanical mixer to maintain both reacting phases in the state of mutual dispersion for 10 minutes. The numbers (from 1 to 8) represent a sequence of consecutive steps within a particular extraction cycle (numbers 1-3 represent three stages of extraction, No. 4 - scrubbing /one step/ and 5-8 - four steps of stripping) while the letters (from A to H) identify subsequent cycles. Horizontal and vertical lines show directions of the organic phase 'movement', while the diagonals represent the same for the aqueous phases. In every extraction step (No. 1, 2 and 3) appropriate portions of 2.5 mol/dm^3 NaOH solution were added to reach equilibrium pH at arbitrarily predetermined level (2.0±0.05).

2.4. Analytical procedures

All samples and solutions were processed and analyzed by modern instrumental methods: ASA or AES-ICP (Horizon or Perkin-Elmer Optima 5300 V) for complex mixed solutions, and by more traditional titration methods for pure single components.

3. Results and discussion

3.1. Solutions for extraction

Basic laboratory experiments were performed on synthetic solutions of metals sulfates ($ZnSO_4$, $CuSO_4$, $CdSO_4$, $MnSO_4$, $CoSO_4$, $NiSO_4$, $FeSO_4$) or nitrates ($Pb(NO_3)_2$) of 0.1 mol/dm^3 concentrations.

More advanced, quite sophisticated experiments, emulating in laboratory action of counter-current system, were done using solution, obtained by acidic (H_2SO_4) leaching of crude zinc oxide and hydrometallurgical purification. It's composition was as follows (g/dm^3):

Zn 146.1, Cd 0.0087, Cu <0.0002, Fe 0.0006, Mn 0.3, Mg 0.40, Al 0.01, As <0.001, Sb <0.001, Na 10.1, K 6.81, Si <0.01, Cl 19.7, F 0.10. Before extraction it was diluted to the level of 15.0 g/dm^3 Zn(II). More details about 'industrial' solutions preparation are presented in Part II of this work (Gotfryd, 2011).

3.2. Preliminary tests of extraction

3.2.1. Extraction – pH isotherms

The data in Fig. 1 show the results of "monitoring" extraction of cations with 0.2 mol/dm^3 Cyanex 272, 0.3 mol/dm^3 and 1.15 mol/dm^3 (40 % vol.) DEHPA. Data were collected using separate 0.1 mol/dm^3 aqueous solutions of metal(II) sulfates(VI), except Pb^{2+}, which was used in a form of nitrate(V), by applying the method described in section 2.3.

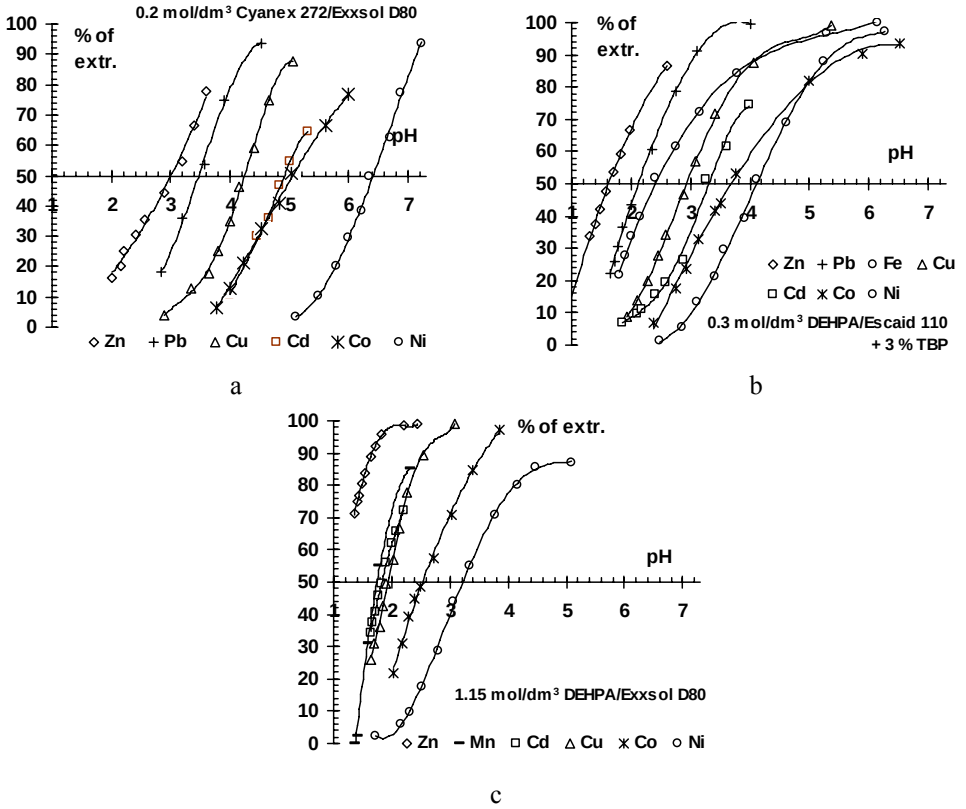

Fig. 1. Extraction of metal cations from their independent 0.1 mol/dm^3 solutions versus equilibrium pH; a) 0.2 mol/dm^3 Cyanex 272/Exxsol D80 AZ; b) 0.3 mol/dm^3 DEHPA /Escaid 110 + 3 % tributylphosphate; c) 1.15 mol/dm^3 DEHPA/Exxsol D80 AZ

The results reached with 1.15 mol/dm^3 (40 % vol.) DEHPA (Fig. 1c) are most interesting because the curves of individual ions extraction, although relatively close to each other, are the steepest. That provides possibilities for better separation of zinc from its typical contaminants (Cd, Cu, Ni, Co, even Mn and also Pb). On this basis further part of the investigations was done with organic 1.15 mol/dm^3 (= 40 % vol.) DEHPA solutions in Exxsol D80 AZ.

3.2.2. Classical isotherms of zinc(II) extraction and stripping

The shapes of extraction isotherms strongly depend on pH of extraction, which can be seen in a few examples provided in Fig. 2. Extractions were performed at predetermined levels of equilibrium pH of 2.0, 3.0 and 4.0 (all with accuracy of ± 0.05) and, for comparison, without any pH regulation (natural isotherm) with solutions of $ZnSO_4$. The feed solution contained 15.0 g/dm^3 Zn^{2+}.

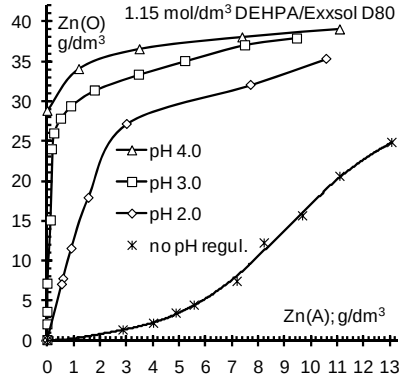

Fig. 2. Isotherms of Zn^{2+} extraction at different equilibrium pH levels; 1.15 mol/dm^3 DEHPA/Exxsol D80 AZ

Even though the isotherms, following the data shown in Fig. 2, raise favorably with the increase of pH, it is pH of 2.0 or less (i.e. extraction with no pH regulations) which provides much better conditions for higher selectivity of Zn^{2+} extraction over its contaminants than pH of 3.0 or 4.0.

Results of analogical stripping tests are shown in Fig. 3. An efficient Zn^{2+} stripping can be forced by application of strong acid solution. Two samples of acidic solutions were used as stripping agents: a) pure acid with 240 g/dm^3 H_2SO_4 and b) zinc electrolyte containing 135 g/dm^3 H_2SO_4 + 58.5 g/dm^3 Zn(II).

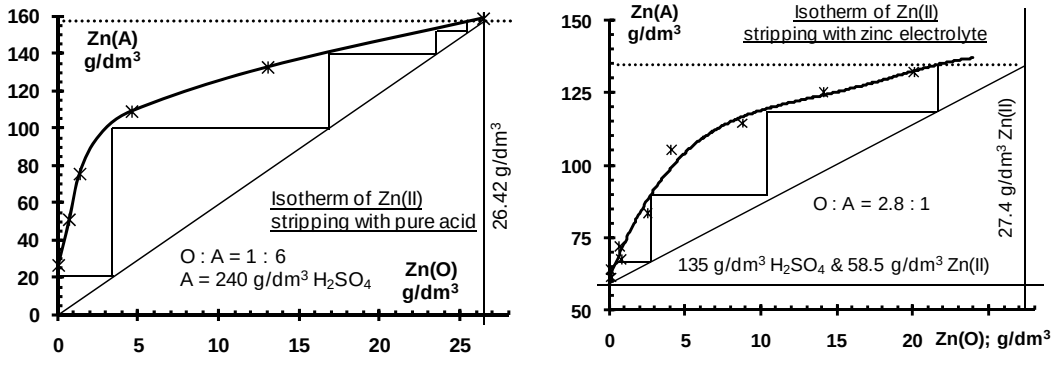

a b

Fig. 3. Isotherms of Zn^{2+} stripping: a) with pure acid [240 g/dm^3 H_2SO_4]; b) with zinc electrolyte [135 g/dm^3 H_2SO_4 and 58.5 g/dm^3 Zn(II)]; 1.15 mol/dm^3 DEHPA/Exxsol D80 AZ

McCabe-Thiele diagrams (characteristic steps) show that to reach almost full efficiency of the counter-current stripping (with almost complete acid consumption), 4-5 extraction stages are required.

3.3. Laboratory experiments simulating continuous counter–current action

The whole performed procedure is clearly presented in the extraction diagram of (0)-3-1-4 type (Fig. 4), where individual numbers represent: (0) - no extractant preneutralization; three steps of proper extraction performed in emulation of counter-current system; one step of scrubbing and four steps of stripping, respectively. Operation of the system is described in section 2.3.

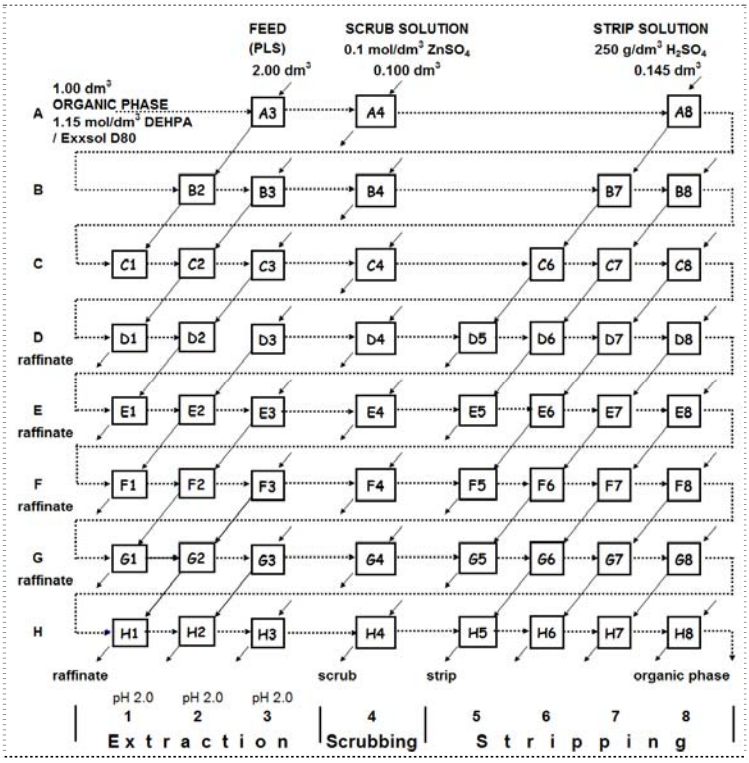

Fig. 4. Laboratory system of extraction emulating counter-current flows

In the examined case, the industrial solution of preliminary purified zinc sulfate with their characteristic contaminants (see section 3.1), after its dilution to the level of 15.0 g/dm^3 Zn^{2+}, was used as the feed for extraction. Physical result of these such laborious procedures is an averaged electrolyte (here of combined D5-H5 samples). In this case its composition was as follows (g/dm^3):

Zn	H_2SO_4	Na	K	Mg	Cu	Cd	Ni	Co	Sb	As	Cl	F
155.5	4.5	<0.005	<0.005	0.0007	<0.001	<0.0005	<0.001	<0.001	<0.005	<0.01	0.0041	0.0001

The described procedure provides possibilities to produce numerous additional information on extraction processes. Separate (step by step for all cycles) analyses of all individual aqueous phases, which form during the procedure, can be performed, i.e. covering all end products (subsequent raffinates and strip liquors /Zn electrolytes/) and all other liquors which are generated in the meantime. Results of analyzes of all available solutions, which at this stage conclude the procedure (solutions of cycle H), are shown in Table 2.

The figures represent profiles of concentrations of sulfuric acid and zinc(II) in aqueous phases as well as zinc(II) concentrations in organic phase. There are also possibilities to analyze all the other ingredients (contaminants), which are present in the produced solutions.

Table 2. Profile of Zn(II) and acid concentrations across all steps of extractive procedure (concluding cycle H)

		H1	H2	H3	H4	H5	H6	H7	H8	
		(raffinate)	(intermediates)		(scrub)	(electrolyte)	(acidic intermediates)			
(A)	Zn	4.31	11.23	12.54	3.50	156	158.8	148.3	100.3	g/L
	H_2SO_4	1.57	1.96	2.25	0.78	4.1	11.76	27.68	92.61	
(O)	Zn(O)	27.57	34.63	35.61	35.61	37.24	34.95	17.64	4.60	

(A) – aqueous, (O) – organic phase

4. Conclusions

Results and experience gained during laboratory extractive experiments, especially in form of satisfactory composition of zinc electrolyte obtained, provided a good basis for further, more advanced trials. Next stage of the research activity, described in Part II of this work, was based on pilot plant experiments, conducted in a train of mixer-settler type extractors, joined in counter-current manner. Prepared extractive system was flexible enough to be ready to work in different combinations of easily changeable number of stages for all important part of extraction processes (extractant preneutralization, extraction proper, scrubbing and stripping). A number of such combinations were examined and the results described in Part II of the paper (Gotfryd, 2011).

Acknowledgment

The study was supported within the scope of Research & Development Project of Polish Ministry of Science and Higher Education No. PBR R 07 032 02 (Contract number 0570/R/2/T02/0702).

References

Diaz G., Martin D., Lombera C., 1995. Zinc recycling through the modified Zincex process. Proc. 3-th Int. Symp. Recycling of Metals and Engineered Materials;

MM&MS, Alabama, November 12-15, 623-635
Frenay J., 1985, Leaching of Oxidized Zinc Ores in Various Media. Hydrometallurgy 15, 243-253
Frias C., Diaz G., Martin D., Sanchez F., 2009. Implementation of first ZINCEX commercial plant treating zinc oxides secondaries. Proc. EMC 2009, June 28-July 1, Innsbruck, Austria
Frias C., Frades M., Mejias A., Martin D., Diaz G., 2008. Dual plant to produce SGH zinc and pure zinc sulfate from zinc oxide secondaries by using the Zincex™ technology. REWAS 2008, Global Symp. on Recycling, Waste Treatment and Clean Technology, MM&MS
Garcia M.A., Ruiz F.S., Mejias A.B., Frades M., 2005. The Skorpion zinc plant, ZINCEX™ solvent extraction. The best expectations confirmed after commissioning. Proc. Inter. Symp. of Lead & Zinc Processing.; Kyoto. Japan, October 17-19, Vol. II, Chapter 10, 1327-1336
Gnoinski J., Bachmann T., Holtzhausen S., 2005. Skorpion zinc: defining the cutting edge of zinc refining. Proc. Inter. Symp. of Lead & Zinc Processing.; Kyoto. Japan, October 17-19, Vol. II, Chapter 10, 1315-1325
Gotfryd L., Chmielarz A., Szołomicki Z., 2011. Recovery of zinc from arduous wastes using solvent extraction technique, Part II. Pilot plant tests. Physicochemical Problems of Mineral Processing, 47, 249-258.
Kapias P., Stelmach R., Gazda J., 1999. Rozpoznanie metod odzysku cynku i olowiu z pyłów powstających w procesie przerobu zlomow stali. (Examination of the recovery of zinc and lead from the dust of working ferrous scrap); Rudy Metale R44, nr 6, 280-286 (in Polish)
(Mineweb) http://www.mineweb.net
Olper M.: 1998. The EZINTEX process - Five years of development from bench scale to a commercial plant. Zinc & Lead Processing; Dutrizac J. E. et all (Eds.); The Metallurgical Society of CIM, 545-558
Ruetten J., 2009. The Waelz Process for the Treatment of EAF Dust 2004 - 2008 – 2012. Presentation for GDMB - Zinc Experts Meeting; Kokkola, September 17, 2009; ValoRes GmbH
Woollett A., 2006. A New Business Model for the Big River Zinc Smelter. Proc. The 4-th International Conf. ZINC 2006, 83-88
(ZincOx website) http://www.zincox.com

Physicochem. Probl. Miner. Process. 47(2011) 159-168
www.minproc.pwr.wroc.pl/journal/

Physicochemical Problems of Mineral Processing
ISSN 1643-1049

Received March 16, 2011; reviewed; accepted April 25, 2011

Discrepancies in the assessment of CO_2 storage capacity and methane recovery from coal with selected equations of state

Part I. Experimental isotherm calculation

Marcin A. LUTYNSKI *, Elisa BATTISTUTTA **, Hans BRUINING **, Karl-Heinz A.A. WOLF **

* Silesian University of Technology , Gliwice, Poland. Marcin.Lutynski@polsl.pl

** Delft University of Technology (TU Delft), Department of Geotechnology, Delft, The Netherlands

Abstract. The injection of carbon dioxide into coalbeds to increase methane recovery is an emerging technology which was tested in various pilot installations. Carbon dioxide stored in coalbeds is usually in supercritical state and therefore investigation of supercritical adsorption of this gas on coal is a subject of various studies. In the paper impact of three equations of state i.e. Peng Robinson (PR), Soave-Redlich-Kwong (SRK) and the most accurate Span-Wagner, as a reference, on the calculation of sorption capacity was investigated. Langmuir parameters were calculated on the basis of experimental results of CO_2 volumetric sorption by a Selar Cornish coal sample. It is concluded that the use of cubic equation of state (PR and SRK) for the calculation of supercritical CO_2 sorption on coal gives unreliable results by lowering apparent absolute adsorption in the lower pressure range (< 9 MPa) and unrealistically increasing it at higher pressures.

keywords: enhanced coalbed methane, carbon dioxide sequestration, equation of state, sorption by coal

1. Introduction

Enhanced Coalbed Methane Recovery is a technology that was developed in order to increase extraction of methane from coal seams and at the same time mitigate carbon dioxide emissions (Reeves 2003; Pini et al. 2007; Balan and Gumrah 2009). Pilot installations with stimulation of methane recovery by CO_2 injection have been already tested all over the World e.g. Ishikari Coal Basin in Japan (Fujioka et al. 2010), RECOPOL project in Poland (Pagnier et al. 2005), Big Fenn Valley in Canada (Mavor et al. 2004), San Juan Basin in USA (Reeves 2002). An increase of methane production from coal by ECBM technologies is obtained due to a higher affinity of CO_2 to coal resulting in displacement of methane. Once CO_2 is injected, it is permanently trapped as a dense gas in coal cleats and adsorbed on and in coal matrix.

In Europe, coalbeds saturated with methane are located below 750 meters (i.e. where pressure is above 7.5 MPa) and have temperature above 40°C. Therefore, injected CO_2 is under supercritical conditions. Not only storage capacity is an important issue but in order to consider coalbed as suitable for ECBM, the following parameters have to be assessed (Katyal et al. 2007): *P*, *T* and depth of coalbed; coalbed characteristic; type, rank, thickness of coal; mineral matter; moisture content; multi-component sorption/desorption, exchange ratio; coal matrix swelling/shrinkage during adsorption/desorption; cleat permeability and porosity.

Extensive laboratory experiments and geological survey are conducted to obtain all of the above parameters. Later, reservoir simulators are used to incorporate all the abovementioned parameters in order to give an overview of anticipated gas injection/production rates with time. One of the key parameters in ECBM is CO_2 adsorption capacity which is measured in laboratory. Such analyses are performed with the use of either manometric or gravimetric setups (Gensterblum et al. 2009; Li et al. 2010; Pini et al. 2010). On the basis of lab data sorption models such as Langmuir isotherm, BET or Dubinin-Raduschkevich are fit (Ottiger et al. 2006; Sakurovs et al. 2007; Dutta et al. 2008). Accuracy of measurements can have a significant impact on derived parameters of these models. Calculated model parameters are later key input data for reservoir simulators.

In this study, we investigate the impact of equation of state (EoS) on the Langmuir parameters calculated from the same raw laboratory data.

2. Experimental approach

2.1. Sample preparation

Table 1. Properties of U.K Selar Cornish coal used for the experiments

Proximate analysis[1]				
Moisture, wt%	Volatile matter, wt%	Fixed Carbon, wt%		Ash, wt%
0.64±0.04	9.61±0.02	85.37±0.01		4.38±0.06
Ultimate analysis[1]				
Carbon, wt%	Hydrogen, wt%	Nitrogen, wt%	Sulfur, wt%	Oxygen, wt%
85.2±1.3	3.28±0.03	0.77±0.05	0.92±0.01	5.60±0.01
Microscope analysis				
R_{max}, %	Vitrinite, vol%	Liptinite, vol%	Inertinite, vol%	Minerals, vol%
2.41	73.6	24.6	0	1.8

[1] Standard deviations reflect the variability of coal from one block used for the experiments. These values are larger for the entire coal layer

Experiments were performed on a semi-anthracite coal sample from a Selar Cornish, South Wales Coalfield. Properties of the coal are presented in Table 1. Coal used for experiments was crushed and sieved to fractions between 1.5 and 2.0 mm. Batches of 50 to 70 cm^3 were sealed and stored at temperature of approximately 276 K until the start of experiments. Before the experiment, the sample is evacuated at 322 K for 24 hours in order to remove moisture content. After evacuation the sample is weighted and placed in the cell and experiments are started.

2.2. Experimental setup and procedure

For the purpose of the study highly accurate manometric apparatus was used (Van Hemert et al. 2009). The setup consists of 5 stainless steel cells: two sample cells, two reference cells and one reservoir. Simplified scheme of the setup is presented in Fig. 1. Pressures are measured using highly accurate pressure transducers PTX611 manufactured by DRUCK (+/- 0.001% F.S). In order to keep the temperature of the experiments constant the entire setup is immersed in water bath. Temperature of the experiments is monitored using a PT100 sensor manufactured by Automated System Laboratories. The pressure and temperature sensors are connected to a data acquisition system recording data every 10 seconds.

Before starting the experiment the setup leak-proof was tested by pressurizing He at approximately 20 MPa for more than 25 hours. After the leak test, void volume of the sample cell was determined by He expansion method, with the assumption that He does not adsorb on coal.

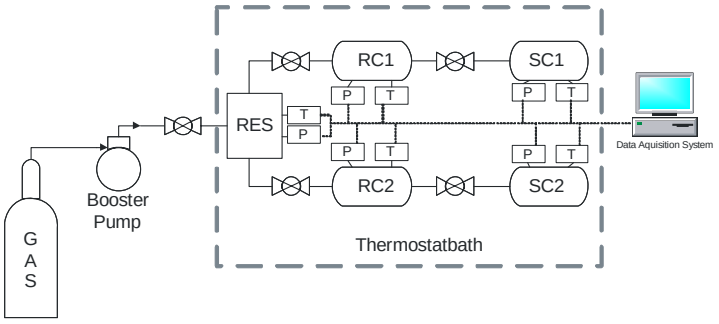

Fig. 1. Scheme of manometric sorption setup used in a study. RES is the reservoir. RC1 and RC2 are reference cells, SC1 and SC2 are sample cells, P and T are pressure transducers and thermocouples respectively

The measuring procedure consists of decompressing known volume of the gas from the reference cell (RC) to the sample cell (SC) under constant temperature. Process of physical adsorption removes adsorbate gas molecules from the free phase to adsorbed phase resulting in decrease in free gas pressure within the system. The total number of moles adsorbed during each pressure step is the difference between the total amount of gas introduced into the void volume of the sample cell and the

amount of free gas occupying the void volume. Repeating this procedure in consecutive steps enables to establish an adsorption isotherm i.e. relation between gas pressure and amount of gas adsorbed under constant temperature.

Physical adsorption of gases in coal is a relatively long lasting process and in order to establish an adsorption isotherm proper equilibration times are needed. In case of carbon dioxide each pressure step may last for up to two weeks whereas for methane up to 10 days. For technical reasons equilibration time at each step was reduced to approximately 48 hours which is in agreement with other publications (Fitzgerald et al. 2005; Prusty 2008; Majewska et al. 2009).

3. Data analysis

In order to obtain adsorption isotherm it is necessary to use equation of state (EoS) for the calculation of gas density. Void volume of the sample was calculated with the use of He EoS published by McCarty (McCarty and Arp 1990). Methane sorption values were calculated using Wagner and Span EoS (Wagner and Span 1993). Carbon dioxide densities were calculated with the use of the following equations of state:

- Peng-Robinson (PR) (Peng and Robinson 1976) and Soave Redlich Kwong (SRK) (Soave 1972) – two cubic equations of state commonly used for carbon dioxide property calculation,
- Span & Wagner (SW) – recently developed accurate equation of state which accuracy up to 523 K and pressure up to 30 MPa ranges from ±0.03% to ±0.05% in the density (Span and Wagner 1996).

Figure 2 shows the carbon dioxide density at 318.15 K computed by three equations of states used in a study. It is clear that the difference in density between reference EoS (i.e. SW) and PR and SRK is much bigger in critical region i.e. above ≈ 7.3 MPa. The relative deviations of SRK and PR from the reference EoS are presented in Fig. 3. Maximum negative deviation is almost 20% in case of SRK and 10% in the pressure region of 10.0-11.0 MPa. Positive deviations are almost 3% for PR near the critical point.

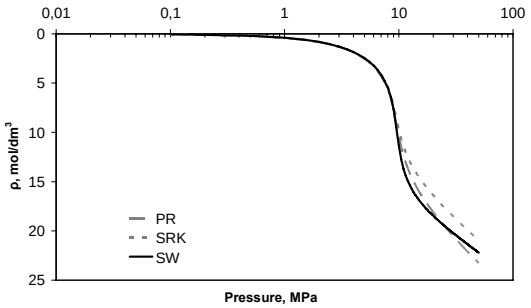

Fig. 2. Density of carbon dioxide (ρ) calculated with three equations of state used in a study (i.e. PR, SRK and SW) at 318.15 K

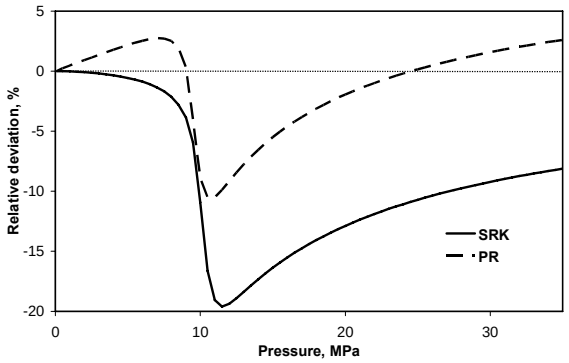

Fig. 3. Relative deviations of SRK and PR for carbon dioxide densities calculated at 318.15 K

Density of carbon dioxide ρ (in mol/m^3) is calculated as a function of P [MPa] and T [K] by EoS. The following formula was used for calculation of excess sorption m^N [mol/kg] for measurement N:

$$m^N = \frac{V_{ref}}{M}\left[\sum_{i=1}^{N}\left(\rho_{fill}^{i} - \rho_{eq}^{i}\right) - \chi\rho_{eq}^{N}\right] \tag{1}$$

where the superscript *i* indicates each sorption step and V_{ref} [cm^3] is the volume of the reference cell. M [g] is the mass of the coal sample after evacuation, χ is the volume ratio of the reference cell to the sample cell. Filling and equilibrium stage are denoted by subscripts *fill* and *eq*, respectively.

4. Results and discussion

4.1. Sorption isotherm and Langmuir model fitting

As indicated in the introduction, the purpose of the study was to assess the difference in the calculation of Langmuir parameters based on the isotherm computed with the use of different equations of state. Langmuir parameters are crucial input data in any coalbed methane reservoir simulator and have to be given for an absolute adsorption values in order to represent real gas adsorption of coal. Absolute adsorption can be calculated using the following formula:

$$m^A = m^N\left(\frac{\rho_{ads}}{\rho_{ads} - \rho_{free}}\right), \tag{2}$$

where m^A is the absolute amount of moles adsorbed, m^N is the excess sorption in moles, ρ_{free} and ρ_{ads} is the density of the gas in free and sorbed phase respectively. The density of carbon dioxide in adsorbed phase was calculated by extrapolating experimental data of excess sorption curve on coal to the point where it intersects horizontal axis (i.e. density of free phase reaches the density of sorbed phase) and was assumed to be 42.06 mol/dm^3. Such an approach and high values of CO_2 sorbed density were suggested also by other authors (Day et al. 2008; Pini et al. 2009;

Sakurovs et al. 2009), The density of CH_4 sorbed phase was assumed, after Sudibandriyo et al. 2003, to be equal to liquid density (26.41 mol/dm^3).

Gas sorption/desorption behaviour on coal is well described by the Langmuir model and indeed it is the most frequently model used in reservoir simulators. The most common form of the Langmuir equation for coalbed methane application is the following:

$$V = \frac{V_L \cdot P}{P_L + P} \tag{3}$$

where V is the volume of gas sorbed per unit mass of coal, V_L is a maximum gas content at infinite pressure (called Langmuir volume) and P_L is the pressure at which half of that gas is in coal (called Langmuir pressure). The Langmuir isotherm model was fitted to experimental data by minimizing the sum of squared residuals with the Excel solver.

In Fig. 4 isotherms calculated with PR, SRK and SW equations of state from the same set of experimental data are presented. It is clear that only in case of SW EoS plotted curve has a shape of type I isotherm (according to IUPAC classification) whereas use of other two equations of state gives erratic results, in particular at pressures above 5 MPa. The reason of these errors lies in the principle of manometric gas sorption measurements and deviations in density calculation by the cubic equations of state. Density of the gas in the Reference Cell calculated by SRK and PR at ~20 MPa is lower in comparison to reference SW EoS (see Fig. 3) but the density at pressures below critical point (i.e. in the Sample Cell) is calculated fairly well. Thus, established isotherm has an apparent lower adsorption at pressures up to critical point. When pressure in the Sample Cell increases above critical region errors in case of PR EoS cancel out to some extent. In case of SRK error at higher pressures is still significant and misrepresents results in the whole range. As it can be seen in Fig. 4 both PR and SRK unrealistically increase calculated sorption capacity above the critical point. The reason for it is again the error in calculated density in the pressure range of approximately 7 – 13 MPa where gas density is significantly lowered with respect to the pressure in the Reference Cell (~20 MPa). This apparently increases calculated adsorption capacity to unrealistic values. In fact, in earlier publications where cubic EoS were used this sudden increase of sorption at higher pressures was visible and could be attributed to the effect explained above (Hall et al. 1994). The above mentioned observations lead to the problem of Langmuir model fitting. Only in the case of SW EoS Langmuir isotherm fitting is satisfactory for the whole range of measured data points. However, gas adsorption on coal is commonly measured in setups which operate within the range of 0-10 MPa. Thus, it was decided to fit Langmuir isotherm model to experimental data of PR calculated points below 10 MPa where the curve has a shape of an isotherm. SRK EoS as far more inaccurate was rejected for further considerations. The calculated Langmuir parameters V_L and P_L for SW are 0.03648 sm^3/kg and 0.597 MPa respectively and for PR 0.03071 sm^3/kg and 0.406 MPa, respectively. As defined by the ECLIPSE software cubic meter of gas at

standard conditions, that is at 16°C and 1013.25 hPa, per unit mass of coal under *in-situ* conditions is given as sm^3/kg.

The deviation in calculated Langmuir parameters V_L and P_L with respect to reference SW EoS is -18.8% and -31.9% respectively.

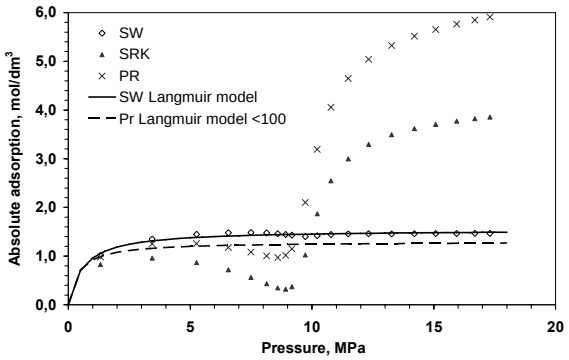

Fig. 4. Absolute adsorption calculated with three equations of state (PR, SRK and SW) and Langmuir model fitting. Note: Langmuir parameters for PR EoS were obtained by fitting experimental points up to 10 MPa

5. Conclusions

From the above study it can be concluded that the use of cubic equation of state (PR and SRK) for the calculation of supercritical CO_2 sorption on coal gives unreliable results by lowering apparent absolute adsorption in the lower pressure range (< 9 MPa) and unrealistically increasing at higher pressures. Fitting the Langmuir model into data calculated with PR is only possible for data points below ~10 MPa and lowers both Langmuir parameters (V_L and P_L). In case of data calculated with SRK EoS it is impossible to fit Langmuir model. In order to assess the impact of these deviations a sensitivity study with the use of reservoir simulator is needed and will be performed in the future.

Acknowledgments

The research was conducted under Marie Curie RTN GRASP Project (Greenhouse Gas Removal Apprenticeship and Student Program). The authors of this study would like to thank Prof. Sevket Durucan and Dr. Caglar Sinayuc from Imperial College London for their help and input to this study.

References

Balan H.O., Gumrah F. (2009). Enhanced coalbed methane recovery with respect to physical properties of coal and operational parameters. Journal of Canadian Petroleum Technology 48(8): 56-61.

Day S., Duffy G., Sakurovs R., Weir S. (2008). Effect of coal properties on CO_2 sorption capacity under supercritical conditions. International Journal of Greenhouse Gas Control 2(3): 342-352.

Dutta P., Harpalani S., Prusty B. (2008). Modeling of CO_2 sorption on coal. Fuel 87(10-11): 2023-2036.

Fitzgerald J.E., Pan Z., Sudibandriyo M., Robinson Jr R.L., Gasem K.A.M., Reeves S. (2005). Adsorption of methane, nitrogen, carbon dioxide and their mixtures on wet Tiffany coal. Fuel 84(18): 2351-2363.

Fujioka M., Yamaguchi S., Nako M. (2010). CO_2-ECBM field tests in the Ishikari Coal Basin of Japan. International Journal of Coal Geology.

Gensterblum Y., van Hemert P., Billemont P., Busch A., Charriere D., Li D., Krooss B.M., de Weireld G., Prinz D., Wolf K.H.A.A. (2009). European inter-laboratory comparison of high pressure CO_2 sorption isotherms. I: Activated carbon. Carbon 47(13): 2958-2969.

Hall F.E., Zhou C., Gasem K.A.M., Robinson Jr R.L., Yee D. (1994). Adsorption of pure methane, nitrogen, and carbon dioxide and their binary mixtures on wet fruitland coal. Proceedings - SPE Eastern Regional Conference and Exhibition.

Katyal S., Valix M., Thambimuthu K. (2007). Study of Parameters Affecting Enhanced Coal Bed Methane Recovery. Energy Sources, Part A: Recovery, Utilization, and Environmental Effects 29(3): 193 - 205.

Li D., Liu Q., Weniger P., Gensterblum Y., Busch A., Krooss B.M. (2010). High-pressure sorption isotherms and sorption kinetics of CH_4 and CO_2 on coals. Fuel 89(3): 569-580.

Majewska Z., Ceglarska-Stefańska G., Majewski S., Zietek J. (2009). Binary gas sorption/desorption experiments on a bituminous coal: Simultaneous measurements on sorption kinetics, volumetric strain and acoustic emission. International Journal of Coal Geology 77(1-2): 90-102.

Mavor M.J., Gunter W.D., Robinson J.R. (2004). Alberta multiwell micro-pilot testing for CBM properties, enhanced methane recovery and CO_2 storage potential. SPE Annual Technical Conference Proceedings.

McCarty R.D., Arp V.D. (1990). A new wide range equation of state for helium. Adv Cryog Eng 35, pp. 1465–1475.

Ottiger S., Pini R., Storti G., Mazzotti M. (2006). Experimental and modeling study of the adsorption of CO_2 on coal aimed at ECBM recovery. AIChE Annual Meeting, Conference Proceedings.

Pagnier H.J.M., Van Bergen F., Kreft E., Van Der Meer L.G.H., Simmelink H.J. (2005). Field experiment of ECBM-CO_2 in the upper Silesian Basin of Poland (RECOPOL). 67th European Association of Geoscientists and Engineers, EAGE Conference and Exhibition, incorporating SPE EUROPE2005 - Extended Abstracts.

Peng D.Y., Robinson D.B. (1976). A new two-constant equation of state. Industrial and Engineering Chemistry Fundamentals 15(1): 59-64.

Pini R., Ottiger S., Burlini L., Storti G., Mazzotti M. (2007). Fundamental mechanisms involved in enhanced coal bed methane recovery for CO_2 storage. Chemie-Ingenieur-Technik 79(9): 1318.

Pini R., Ottiger S., Burlini L., Storti G., Mazzotti M. (2009). Role of adsorption and swelling on the dynamics of gas injection in coal. Journal of Geophysical Research B: Solid Earth 114(4).

Pini R., Ottiger S., Burlini L., Storti G., Mazzotti M. (2010). Sorption of carbon dioxide, methane and nitrogen in dry coals at high pressure and moderate temperature. International Journal of Greenhouse Gas Control 4(1): 90-101.

Prusty B.K. (2008). Sorption of methane and CO_2 for enhanced coalbed methane recovery and carbon dioxide sequestration. Journal of Natural Gas Chemistry 17(1): 29-38.

Reeves S. (2002). Field studies of enhanced methane recovery and CO_2 sequestration in coal seams. World Oil 223(12): 56-60.

Reeves S.R. (2003). Enhanced CBM recovery, coalbed CO_2 sequestration assessed. Oil and Gas Journal 101(27): 49-53.

Sakurovs R., Day S., Weir S. (2009). Causes and consequences of errors in determining sorption capacity of coals for carbon dioxide at high pressure. International Journal of Coal Geology 77(1-2): 16-22.

Sakurovs R., Day S., Weir S., Duffy G. (2007). Application of a modified Dubinin - Radushkevich equation to adsorption of gases by coals under supercritical conditions. Energy and Fuels 21(2): 992-997.

Soave G. (1972). Equilibrium constants from a modified Redlich-Kwong equation of state. Chemical Engineering Science 27(6): 1197-1203.

Span R., Wagner W. (1996). A new equation of state for carbon dioxide covering the fluid region from the triple-point temperature to 1100 K at pressures up to 800 MPa. Journal of Physical and Chemical Reference Data 25(6): 1509-1596.

Sudibandriyo M., Pan Z., Fitzgerald J.E., Robinson Jr R.L., Gasem K.A.M. (2003). Adsorption of methane, nitrogen, carbon dioxide, and their binary mixtures on dry activated carbon at 318.2 K and pressures up to 13.6 MPa. Langmuir 19(13): 5323-5331.

Van Hemert P., Bruining H., Rudolph E.S.J., Wolf K.H.A.A., Maas J.G. (2009). Improved manometric setup for the accurate determination of supercritical carbon dioxide sorption. Review of Scientific Instruments 80(3).

Wagner W., Span R. (1993). Special Equations of State for Methane, Argon, and Nitrogen for the Temperature Range from 270 to 350 K at Pressures up to 30 MPa. International Journal of Thermophysics 14(4): 699-725.

Lutynski, M.A., Battistutta, E., Bruining, H., Wolf, K.A.A., Rozbieżności w ocenie ilości składowanego CO_2 i odzysku metanu z pokładu węgla jako wynik zastosowania wybranych równań stanu gazu. Część I. Wyznaczanie izotermy, Physicochem. Probl. Miner. Process., 47 (2011) 159-168, (w jęz. ang.)

Intensyfikacja wydobycia metanu z pokładu węgla za pomocą zatłaczania dwutlenku węgla jest technologią, która nie tylko przyczynia się do zwiększenia uzysku tego surowca energetycznego ale jednocześnie zmniejsza emisję CO_2. Obecnie na Świecie istnieje kilka instalacji pilotowych, w których ta technologia poddawana jest badaniom. W Europie pokłady węglowe bogate w metan występują zazwyczaj na głębokościach przekraczających 750 m i temperaturach powyżej 40°C, a więc w warunkach, w których CO_2 jest w stanie krytycznym. Adsorpcja tego gazu w stanie krytycznym na węglach jest obecnie przedmiotem intensywnych badań. Do wyznaczonych w laboratorium izoterm sorpcji dopasowywane są następnie modele sorpcyjne jak np. izoterma Langmuira, izoterma BET czy model Dubinina-Raduszkiewicza. W pracy przedstawiono wyniki badań sorpcji dwutlenku węgla na węglu antracytowym Selar Cornish z zagłębia Południowej Walii (Wielka Brytania). Do analiz wyników użyto trzech równań stanu gazu stosowanych do określenia gęstości CO_2 tj. równania Penga-Robinsowa (PR), równania Soave-Redlicha-Kwonga (SRK) oraz bardzo dokładnego równania stanu gazu dla CO_2

Spana i Wagnera (SW), jako równania referencyjnego. Do uzyskanych danych sorpcji całkowitej dopasowano model izotermy Langmuira jako powszechnie stosowany w symulatorach złożowych. Obliczone parametry izotermy Langmuira tj. VL oraz PL w przypadku równania SW wyniosły odpowiednio 0.03648 sm^3/kg oraz 0,597 MPa, natomiast dla równania PR wartości te wyniosły odpowiednio 0.03071 sm^3/kg oraz 0,406 MPa. Odchyłka w obliczonych parametrach w stosunku do równania referencyjnego dla tej samej izotermy wyniosła odpowiednio -18,8% oraz -31,9%

słowa kluczowe: intensyfikacja wydobycia metanu, sekwestracja dwutlenku węgla, równanie stanu gazu, sorpcja na węglu

Physicochem. Probl. Miner. Process. 47(2011) 169-182
www.minproc.pwr.wroc.pl/journal/

Physicochemical Problems of Mineral Processing
ISSN 1643-1049

Received March 2, 2011; reviewed; accepted April 26, 2011

When and how α-terpineol and n-octanol can inhibit the bubble attachment to hydrophobic surfaces

Dominik KOSIOR, Jan ZAWALA, Kazimierz MALYSA

Jerzy Haber Institute of Catalysis and Surface Chemistry Polish Academy of Sciences,
ul. Niezapominajek 8, 30-239 Kraków, ncmalysa@cyf-kr.edu.pl

Abstract. Kinetics of the three phase contact (TPC) formation and phenomena occurring during collision of the rising bubble with Teflon plates of different surface roughness were studied in distilled water, α-terpineol and n-octanol solutions, using a high-speed camera of frequency 1040 Hz. Influence of solution concentration and surface roughness on time of the TPC formation and the time of drainage of the film formed between the colliding bubble and Teflon surface was determined. The surface roughness of the Teflon plates was varied within range 1-100 μm. It was found that at small α-terpineol and n-octanol concentrations the time of the TPC formation was shortened in respect to distilled water. However, at their high concentrations the time of TPC formation was again longer and magnitude of this effect depended on the surface roughness. For example for Teflon surface of roughness 40-60 μm the time of TPC formation was even 20-30 ms longer. The data obtained indicate that this effect is related to presence of air at the hydrophobic solid surfaces. The mechanism of this prolongation of the time of TPC formation due to the frother overdosage is proposed.

keywords: three phase contact, hydrophobic surface, frother, bubble collision, thin liquid film, surface roughness

1. Introduction

Frothers are reagents used in flotation mainly: i) for facilitation air dispersion into fine bubbles, ii) to prevent bubbles from coalescence (Cho and Laskowski, 2002a,b), iii) to assure formation of a froth layer of a suitable stability, and iv) to facilitate the three phase contact formation (Leja and Schulman, 1954). In flotation systems the three phase contact is formed in so-called elementary flotation act, that is, formation of stable bubble-grain aggregates as a result of the bubbles and grains collisions. For flotation separation the grains having hydrophobic surface need to form the three phase (TPC) contact and stay attached to the colliding bubble. Thus, kinetics of the TPC formation is of great importance for efficiency of the bubble attachment and flotation separation. For the TPC formation the liquid film separating the colliding bubble and grain surface needs to be ruptured during the collision time. Process of

formation of the stable bubble-grain aggregate can be divided into three elementary steps: i) thinning of the liquid film formed by the colliding bubble to a critical thickness, ii) the film rupture and formation of a three-phase contact nucleus, and iii) expansion of three-phase contact line (Nguyen et al. 1997). As time of the film rupture and formation of a three-phase contact nucleus is significantly shorter than first sub-process so the process of film thinning is important to elucidate (Ralston et al., 2002) and seems to be the step determining kinetics of the three phase contact formation.

When the bubble collides with solid surface then a liquid layer (liquid film) separating the bubble and the solid surfaces starts to drain. For the TPC formation the draining film needs to reach its critical thickness of rupture. The kinetic of the liquid film drainage strongly depends on the film radius and properties of the film interfaces. Generally, the time needed to reach a definite thickness increases with the film size and depends on mobility of the film interfaces. When the mobility of the film interfaces is retarded, for example as a result of surfactant adsorption, then the time of the film thinning increases. In the case of wetting films the velocity of the thinning is, according to Scheludko equation (Scheludko, 1967), inversely proportional to the film radius and directly proportional to mobility of the film gas/solution interface, which is lowered in presence of an adsorption layer. Adsorption of surface active substances (frothers) can also significantly lower the bubble velocity (Krzan et al., 2004; Malysa et al. 2005, Kracht and Finch, 2010). Lower velocity of the rising bubble means a prolongation of the contact time during collision with particle and higher probability of the TPC formation. It is generally accepted that high hydrophobicity of solid surface is the factor ensuring the TPC formation and bubble attachment. However, it was showed recently (Malysa et al., 2005; Krasowska and Malysa, 2007) that even in the case of highly hydrophobic solid (Teflon of contact angle above 110^{o}) the rising bubble was not attached during the first collision but could bounce a few times prior to the three phase contact (TPC) formation at the smooth solid surface (roughness below 1μm). The bubble bouncing is one of important factors leading to prolongation (up to over 80ms) the time of the TPC formation at Teflon surface.

This paper presents results of studies on influence of α-terpineol and n-octanol concentration on kinetics of the TPC formation and the bubble attachment to Teflon surfaces of different roughness. It was found that at high frother (α-terpineol and n-octanol) concentration the time of the TPC formation was prolonged. Mechanism of this important finding that a frother overdosage can inhibit the bubble attachment to hydrophobic surface is proposed.

2. Experimental

Phenomena occurring during the bubble collisions with and attachment to solid hydrophobic surfaces (Teflon plates) were monitored using the experimental set-up consisting of: (i) square glass column (50x50mm) with capillary of inner diameter 0.075mm at the bottom, (ii) high speed camera (SpeedCam MacroVis, 1040 frames per second), (iii) high precision pump with gas-tight syringe (Hamilton, 5ml), and (iv)

light source (optical fiber). The Teflon plate was positioned horizontally beneath the solution surface at the distance ca. L=250mm from the capillary orifice (bubble formation point). Single bubbles were formed at the capillary orifice and the time interval between each subsequent detaching bubble was 30s. The equivalent diameter of the bubble (d_{eq}) detaching from the capillary in distilled water was 1.48±0.03 mm. To record the bubble collisions and attachment the camera was positioned slightly below the solid/liquid interface with inclination of 3-4^o in respect to the Teflon surface. The image of a nylon sphere of 3.89 mm diameter was recorded after each experiment for calculation of absolute dimensions of the bubble size. The movies recorded were analyzed either using the SigmaScan Pro Image Analyze Software and/or the WinAnalyze Motion Analyze Software. Variations of the bubble velocity during collisions with the Teflon plates were determined from measurements of subsequent positions of the bubble bottom pole. Further details of the experimental set-up and determination of the bubble velocity have been described elsewhere (Krasowska and Malysa, 2007; Malysa et al., 2005). All Teflon plates were prepared from the same piece of the commercial Teflon. Surface roughness of the Teflon plates was modified mechanically using an abrasive paper of grid numbers ranging from No. 2500 to No. 100. Figure 1 presents, as an example, the photos of the three Teflon surfaces (T2500, T1200 and T600) used in the experiments. Optical inverted microscope Nikon Epiphot 200 with magnification 20x was used to take the photos of the Teflon surfaces. Roughness of the Teflon plates was determined by measurements of the scratches sizes using SigmaScan Pro Image Analyze Software**.** Teflon 2500 was the solid with the smoothest surface (roughness 1-5μm), while Teflon100 with the roughest one (roughness 80-100μm). The roughness of T1200 and T600 surfaces was 10-20 and 40-60 μm, respectively.

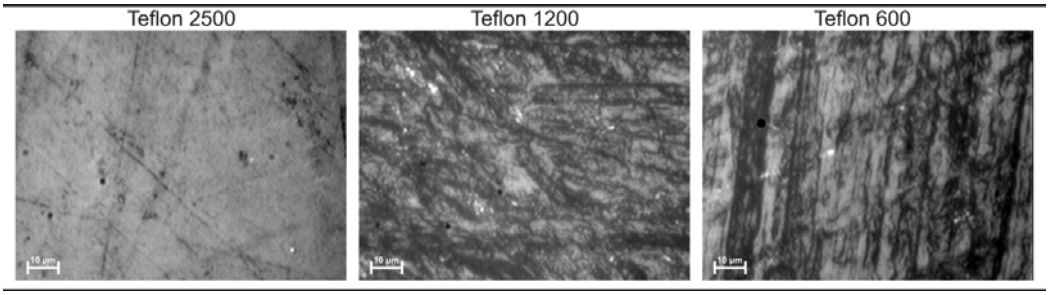

Fig.1 Photos of the Teflon surfaces of different roughness

The Teflon plates were carefully cleaned, using a chromic mixture. Next, they were washed-out with large quantity of 2-fold distilled water and then in the Milli-Q water. Next, the plates were boiled in the Milli-Q water for 1hour and stored in the Milli-Q water prior to the experiments. Measurements of the bubble collision and attachment to the Teflon surfaces of different roughness were performed in distilled water and in n-octanol (Fluka ≥99,5%) and α-terpineol (SAFC ≥96%) solutions of

various concentrations. The experiments were carried out at room temperature (20-22ºC) and the distilled (Milli-Q) water used had the surface tension 72.4 mN/m and conductivity 0.05 μS/cm.

3. Results and discussion

The sequences of photos showing phenomena occurring during the bubble collisions in distilled water with Teflon surfaces of the roughness T600 and T2500 are presented in Fig. 2. As for a sake of comparisons the moment of the first collision was arbitrary denoted as the time t=0, so the negative time values refer to the bubble motion prior to the first collision. The photos of Fig. 2 clearly illustrate that, as reported earlier (Krasowska et al., 2007), the time of the bubble attachment to Teflon surface is strongly affected by the surface roughness. As seen there was no attachment to the Teflon2500 and Teflon600 surfaces during the first collision and the bubble bounced backward. However, the outcome of the second collision the situation was completely different. In the case of surface of higher roughness (Teflon600) the intervening liquid film was ruptured and the three phase contact (TPC) was formed, while the bubble bounced backwards from much smoother surface of Teflon2500. Moreover, there were up to five bouncing-approach cycles prior to the TPC formation and the amplitude of each subsequent bubble bounce was lowered as a consequence of dissipation of the kinetic energy associated with the bubble motion (E_k). The TPC was formed at Teflon2500 surface only after practically complete dissipation of the kinetic energy. The variations of the bubble velocity during collisions with the Telfon2500 and Teflon600 surface (see Fig. 2) are presented in Fig. 3. There are also defined two important parameters, the time of TPC formation (t_{TPC}) and the time of liquid film drainage (t_D) used for characterizing the kinetics of the three phase contact formation and the bubble attachment. As can be seen the t_{TPC} is the time interval from the moment of the bubble first collision till the moment of the TPC formation at the solid surface. It needs to be stressed here and remembered that as the t_{TPC} values cover also the bouncing periods of the colliding bubble so their magnitude can be affected by the bubble impact velocity – higher impact velocity leads to prolonged bouncing (Zawala and Malysa, 2011). The drainage time marked (t_D) is the time interval from the moment when the bubble stayed captured (practically "motionless") beneath the solid surface till the moment of the TPC formation. Thus, the t_D values depend only on stability of the thin liquid films formed by the colliding bubble. Determination of the starting point for the t_D measurements is a bit arbitrary because determination of the moment when the bubble stays "motionless" beneath the Teflon surface can be quite difficult. Therefore, the measurements were always repeated 20-40 times for each Teflon plate and the t_D values reported below are the mean values with different scatter – the scatter diminished with the surface roughness increase.

As described above and can be observed in Fig. 3 there was no attachment of the colliding bubble to either Teflon2500 or Teflon600 surface during the first collision. The bubble bounced backward (negative velocity values) and velocity of

each subsequent bubble approach to the plates was decreasing. In the case of Teflon2500, when the kinetic energy associated with the bubble motion was dissipated, the bubble stayed practically motionless till the moment of the TPC formation, which was easily detected due to rapid motion of the bubble bottom pole. In the case of the Teflon600 surface the TPC was formed during the second collision. Note please that the impact velocity of the bubble first collisions was the same in both cases. Despite this fact the significant difference in the t_{TPC} and t_D values for Teflon surfaces of different roughness are easily noticeable. In the case of Teflon2500 surface the t_{TPC} and t_D was 105±4 and 22±4ms, while for T600 the t_{TPC} and t_D was lowered to 37±2 ms and ca. 2ms, respectively.

Figure 4 presents the sequences of photos showing the bubble collisions with Teflon600 plate in $1 \cdot 10^{-5}$ and $1 \cdot 10^{-3}$ M α-terpineol solutions. It can be seen in Fig. 4 that α-terpineol presence, that is, the presence of a classical flotation frother (Gaudin, 1957; Leja, 1982; Laskowski, 1998), influenced the time of the bubble attachmet to the Teflon surface. At low α-terpineol concentration ($1 \cdot 10^{-5}$ M) the TPC was formed during the first collision and the t_{TPC} was ca. 2ms, i.e. was ca. 20 times shorter than in distilled water (see Figs 2 and 3).

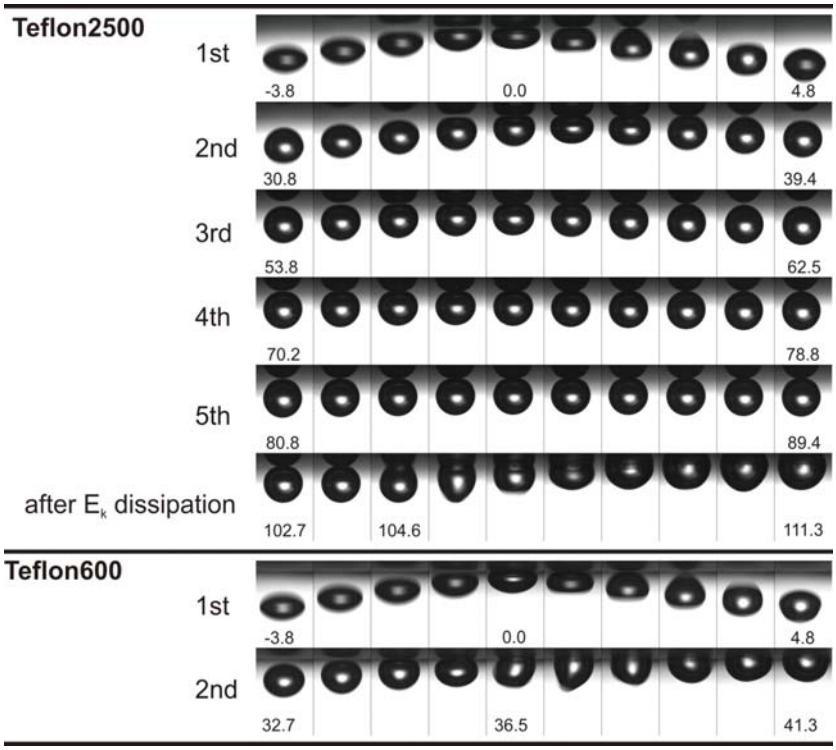

Fig. 2. Sequences of photos of the bubble colliding in distilled water with Teflon2500 and Teflon600 surfaces. 0.96 ms is the time interval between subsequent photos of the sequence

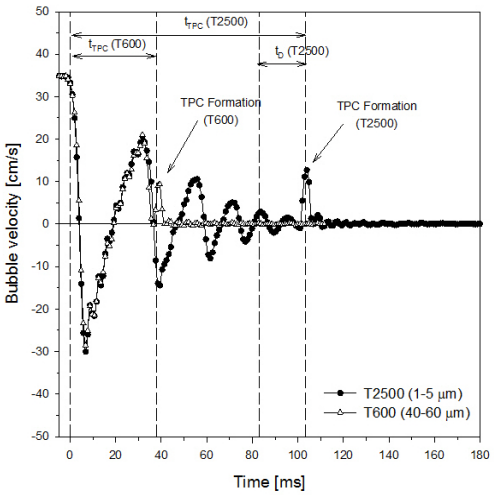

Fig. 3. Variations of the bubble velocity during collisions with Teflon2500 (black circles) and Teflon600 (white triangles) surfaces in distilled water

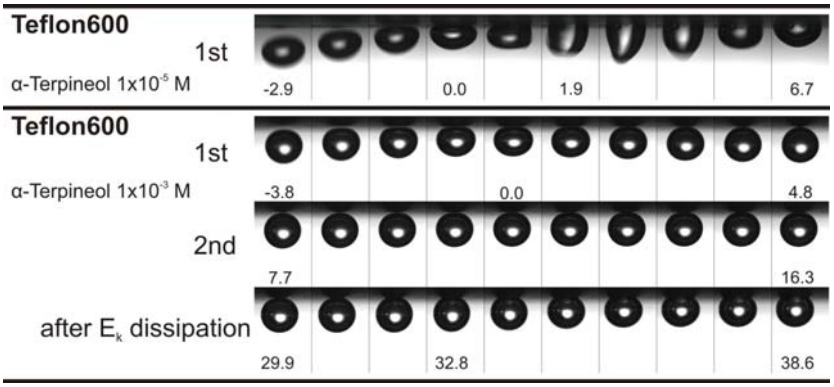

Fig. 4. Sequences of photos of the bubble colliding with Teflon600 surface in of $1 \cdot 10^{-5}$ M and $1 \cdot 10^{-3}$ M α-terpineol solutions

Surprisingly however, the increased α-terpineol concentration ($1 \cdot 10^{-3}$ M) caused prolongation of the t_{TPC} from ca. 2 to 33±6 ms. Similar effect was observed also for high concentrations of n-octanol solutions. Figure 5 presents the comparisons of the velocity variations during collisions with Teflon600 surface in α-terpineol and n-octanol solutions of low and high concentrations. The effect of the t_{TPC} prolongation at high concentrations of α-terpineol and n-octanol solutions is clearly seen in Fig. 5. At low concentration of these two frothers the TPC was formed during the first collision (t_{TPC} ca. 2ms) and the t_{TPC} were significantly longer (33 and 22 ms for α-terpineol and n-octanol, respectively) at their much higher (two orders of magnitude) concentrations. Note also please that at high α-terpineol and n-octanol concentrations the bubble impact velocity (velocity of the first collision) was smaller but still the t_{TPC}

were longer despite diminished tendency for the bubble bouncing (Zawala et al., 2007).

Figures 6 and 7 present the dependences of the t_{TPC} and t_D values on concentrations α-terpineol (Fig. 6) and n-octanol (Fig. 7) for the Teflon surfaces of different roughness. Note please that only values of the time of liquid film drainage (t_D) (Figs 6A and 7A) are not affected by the bubble impact velocity and therefore they refer straightforward to stability of the liquid films formed by the colliding bubble. It is seen there that indeed, at high α-terpineol and n-octanol concentration the time of the liquid film drainage (Fig. 6B and 7B) were significantly prolonged and also values of the time of the TPC formation (Figs 6A nad7A) were higher, but not in every case. For the Teflon surface roughness within the range 1-60μm (Teflon2500 - Teflon600) the t_{TPC} values were significantly shorter in α-terpineol solutions of concentration $1 \cdot 10^{-5}$ M and $6 \cdot 10^{-5}$ M as well as n-octanol solutions of concentrations $6 \cdot 10^{-6}$ and $3 \cdot 10^{-5}$ M than those in distilled water. Further increase in concentration of both frothers, to $3 \cdot 10^{-4}$M for α-terpineol and $6 \cdot 10^{-4}$M for n-octanol, caused prolongation of the t_{TPC}, despite the fact that the bubble impact velocity was identical as in solutions of smaller ($6 \cdot 10^{-5}$ and $3 \cdot 10^{-5}$ M for α-terpineol and n-octanol, respectively) concentrations. Thus, in these cases the t_{TPC} values were not affected by differences in the bubble impact velocity. In the case of the roughest surface (Teflon100) the t_{TPC} values were very short, ca. 1-3ms in distilled water, and practically did not change with α-terpineol and n-octanol concentration. Prolongation of the time of the film drainage, t_D, at high α-terpineol and n-octanol is clearly seen in Figs 6B and 7B. For the Teflon surface roughness within the range of 1-60μm (Teflon2500 – Teflon600) the t_D were the longest at $1 \cdot 10^{-3}$M α-terpineol and $6 \cdot 10^{-4}$ M n-octanol concentration. There was practically no effect of α-terpineol and n-octanol concentration on the t_D values in the case of the roughest Teflon surface (Teflon100).

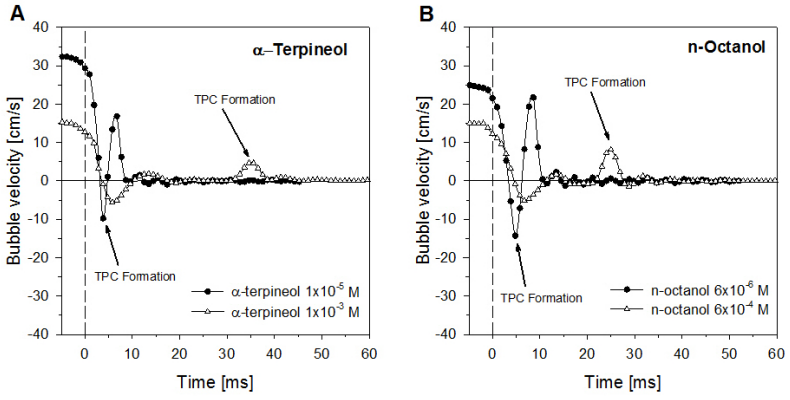

Fig. 5. Velocity variations during the bubble collision with Teflon600 surface in solutions of: (A) α-terpineol - concentration $1 \cdot 10^{-5}$ and $1 \cdot 10^{-3}$ M, and (B) n-octanol - concentration $6 \cdot 10^{-6}$ and $6 \cdot 10^{-4}$ M

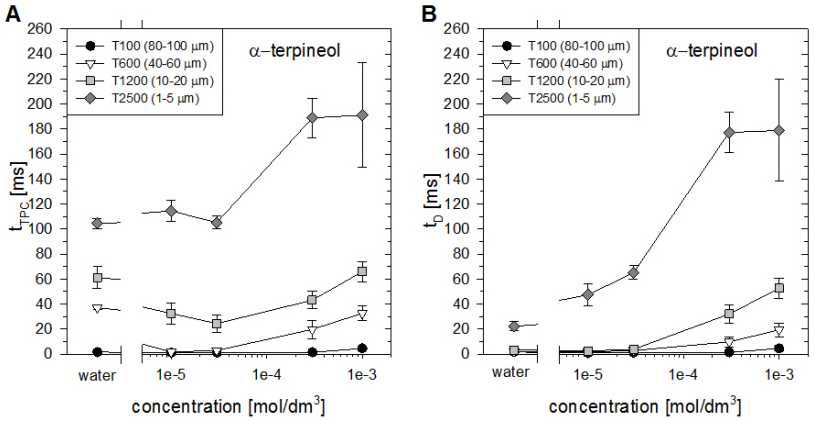

Fig. 6. Values of (A) t_{TPC} and (B) t_D as a function of α-terpineol concentration for Teflon of different surface roughness

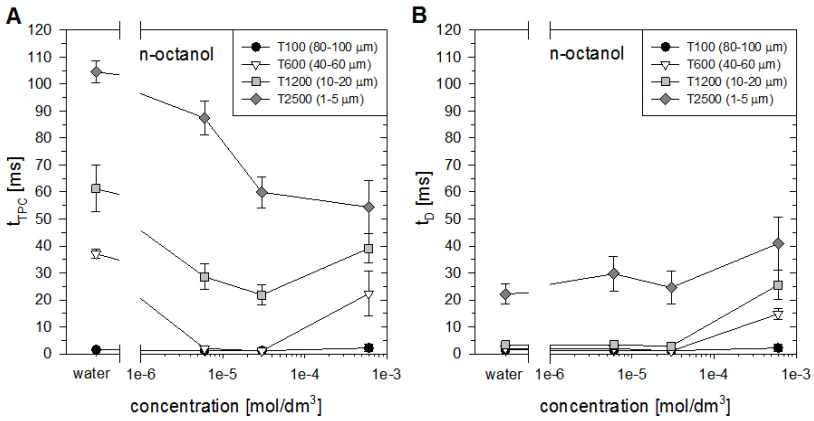

Fig. 7. Values of (A) t_{TPC} and (B) t_D as a function of n-octanol concentration for Teflon of different surface roughness

What is the mechanism responsible for prolongation of the time of the bubble attachment to hydrophobic surfaces at high α-terpineol and n-octanol concentrations? To explain it we need to consider in more details the phenomena occurring during the bubble collisions and immersion a hydrophobic surface into aqueous phase. Generally, the bubble colliding with any interface can either bounce or rupture (free surface) or form the three phase contact (hydrophobic surface) or stay captured (hydrophilic solid surface). The bubble bouncing is a consequence of competition between two simultaneous processes (Chester and Hofman 1982, Zawala et al. 2007): (1) thinning of the intervening liquid film; and (2) the increase of the free energy of the system resulting from the surface area increase due to the deformation of liquid/gas interface. During the collision of the rising bubble a dissipation of energy associated with the bubble motion takes place what causes decrease in the bubble shape pulsations and the

amplitude of each subsequent approach-bounce cycle. This effect is more pronounced in distilled water (see Fig. 2) due to highest impact velocity of the colliding bubble. The bubble bouncing is the reason that for the Teflon plates of the smallest roughness the time of the TPC formation ($t_{TPC,}$) was significantly longer than the time of the liquid film drainage (t_D). For the roughest Teflon surfaces the t_{TPC} and t_D values were practically identical because the drainage and rupture of the intervening liquid film occurred during the first collision - there was no bouncing of the bubble.

In our previous papers (Malysa et al. 2005, Krasowska and Malysa 2007, Krasowska et al. 2007) two possible mechanisms, explaining the influence of roughness on kinetics of the TPC formation and the bubble attachment to hydrophobic solid surface in distilled water, were proposed. The crucial role of roughness of the hydrophobic solid surface, affecting time scale of TPC formation and bubble attachment, was attributed to: (i) local differences in radius of the liquid film formed at irregularities and pillars of rough solid surface, and (ii) presence of air entrapped in surface scratches and irregularities of the hydrophobic surface. The first mechanism takes into account fact that kinetics of the liquid film drainage is strongly affected by the film lateral dimensions – smaller film radius means that time needed for the film to reach a definite thickness is shorter. At rough hydrophobic surface the TPC can be formed due to rupture of various local wetting films formed at pillars of the rough surface. As lateral dimensions of such local wetting films are much smaller than radius of the entire liquid film formed by the colliding bubble so these films need shorter time to drain to a critical thickness of their rupture. This mechanism seems to be most probable for surfaces of highest roughness, i.e. in the case of Teflon100 plates. The second mechanism postulated takes into account influence of air presence at hydrophobic surface on kinetics of the TPC formation by the colliding bubble. It is worthy to add here that in studies on long range attractive interactions between hydrophobic bodies immersed into solution it was showed in 2000 (Ishida et al. 2000), using the TM AFM, that nanobubbles were attached to the hydrophobic surfaces immersed into aqueous solution. A number of papers documenting existence of nanobubbles at hydrophobic surfaces is increasing rapidly (Ishida et al., 2000; Tyrrel and Attard, 2002; Attard, 2003; Steitz et al., 2003; Nguyen et al., 2003; Yang et al., 2003; Zhang et al., 2006,). As high affinity to air is a typical feature of hydrophobic surfaces so air can be entrapped in scratches of hydrophobic surface during its immersion into aqueous phase. The mechanism of air entrapment during immersion of the Teflon plate into water (see Fig. 8) was described in details elsewhere (Krasowska et al., 2007; Krasowska et al., 2009) and it was showed that the amount of air entrapped was increasing with roughness of the hydrophobic surface. Thus, diminishing the t_{TPC} values with surface roughness can be a consequence of coalescence of the colliding bubble with nano and/or microbubbles present at larger amounts at rougher hydrophobic surface. In the case of smooth hydrophobic surface the amounts of entrapped air is lower and therefore the t_{TPC} values are higher. The results presented above strongly support the hypothesis put forward in our previous

papers (Krasowska and Malysa, 2007; Krasowska et al., 2007; Krasowska et al., 2009) that air is entrapped at hydrophobic surfaces and its presence can significantly affect kinetics of the TPC formation. As can be observed in Figs 6 and 7 in distilled water, devoid of any surface active substances, the t_{TPC} values were monotonically decreasing with increasing roughness of the Teflon plates. This effect can be attributed to increase in amount of air entrapped into the solid surface irregularities. As more air can be captured at rougher surface so the probability is higher that the bubble hit the area where air (in form of nano- and miro-bubbles) is present.

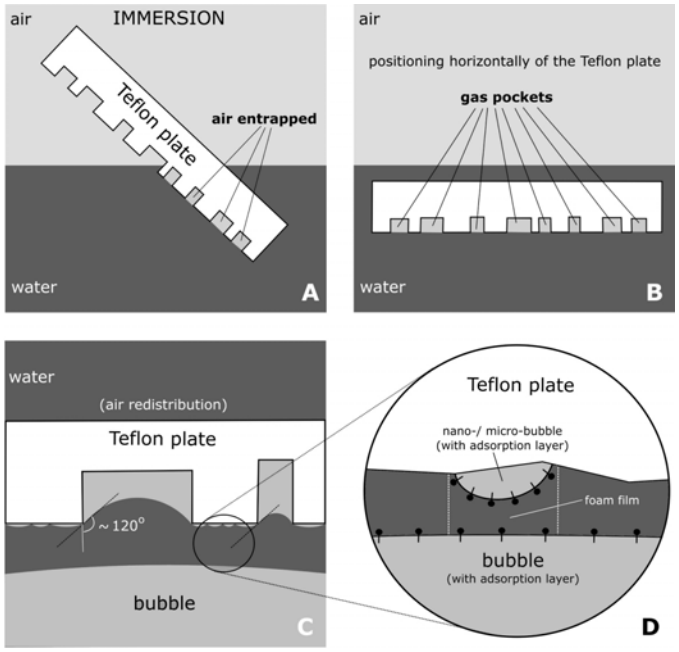

Fig.8. Schematic illustration of the liquid (foam) film formed in a frother solution between the colliding bubble and air micro- and/or nano-bubbles present at Teflon surface

The mechanism of inhibition of the bubble attachment at high α-terpineol and n-octanol concentrations, due to air presence at hydrophobic surface, is depicted schematically in Fig. 8. When air is present at hydrophobic surface then the colliding bubble hits micro- and/or nano-bubbles present and already having locally formed three phase contact of very small perimeter. In solutions of any surface active substance (each flotation frother) an adsorption layer is formed at solution/gas interface, that is, at the colliding bubble surface and at surfaces of the micro- and/or nano-bubbles attached to Teflon surface. Thus, instead of a wetting film formed between solid surface and the colliding bubble surface there are formed locally the symmetric (foam) films between the colliding macro-bubble and the micro- and/or nano-bubbles attached to the Teflon surface. It also means that rupture of the film and the TPC formation is occurring as a result of bridging (coalescence) of the colliding

bubble and nano- or sub-microscopic bubbles already attached to the Teflon surface. As it is well known that stability of symmetric foam films increases with surfactant concentration (Exerowa and Kruglyakow, 1998) so the prolongation of the time of the TPC formation and the time of the film drainage in α-terpineol and n-octanol of high concentration is a strong evidence that there were locally the foam films formed, that is, there were air micro-bubbles attached to the Teflon surfaces. In distilled water and low concentrations of α-terpineol and n-octanol solutions the stability of those foam films formed locally was low because either there was no adsorption layer (distilled water) or the adsorption coverage's were too low to assure a sufficient stability of these local foam films. Moreover, velocity of the film drainage decreases with surfactant concentrations (adsorption coverage) due to immobilization of the solution/air interfaces (Exerowa et al., 2003). Results of studies on critical coalescence concentration (CCC) (Cho and Laskowski, 2002a,b), which show that the bubble coalescence is stopped above the CCC value (Cho and Laskowski, 2002a,b; Grau et al, 2005; Szyszka et al, 2006; Grau and Laskowski, 2006), indicate also that increased frother concentration leads to increased stability of the thin liquid films. Lack of the bubble coalescence means that stability of the liquid film formed between colliding bubbles is increased and therefore there is no bubble coalescence.

4. Concluding remarks

It was found that the time of the three phase contact formation at hydrophobic surface (Teflon) by colliding bubble is strongly affected by frother (α-terpineol, n-octanol) presence in the system. Low concentrations of α-terpineol and n-octanol caused that the time of the TPC formation and the time of drainage of the liquid film separating the colliding bubble from Teflon surface were shortened. This effect was also dependent on the solid surface roughness. At high solutions concentration the opposite effect was observed, that is the t_{TPC} and t_D values were higher. This is rather surprising but important finding because it straightforwardly shows that overdosage of a frother can be disadvantageous for flotation efficiency. The mechanism of prolongation of the time of the bubble attachment to hydrophobic surfaces at high frother concentrations is described in details. This effect is attributed to a presence of air at the hydrophobic surfaces in a form of micro- and/or nano-bubbles. When air is entrapped in cavities of hydrophobic surface then foam films are formed locally between the micro- and/or nano-bubbles and the colliding bubble. Stability of these foam films is increased at high α-terpineol, n-octanol concentrations and therefore the time of the bubble attachment was prolonged.

Acknowledgements

This work was supported by the "Krakow Interdisciplinary Ph.D. Project in Nanoscience and Advanced Nanostructures" operated within the Foundation for Polish Science MPD Programme co-financed by the EU European Regional Development Fund and MNiSW grant No. NN204 133640.

References

ATTARD P., 2003. *Nanobubbles and the hydrophobic attraction,* Adv. Colloid Interface Sci., 104, 75-91.

CHESTER A. K., HOFMAN G., 1982. *Bubble Coalescence in Pure Liquids*, Appl. Sci. Research, 38, 353-361.

CHO Y.S., LASKOWSKI J.S., 2002a. *Effect of flotation frothers on bubble size and foam stability*, Int. J. Miner. Process., 64, 69– 80.

CHO, Y.S., LASKOWSKI, J. S., 2002b, *Bubble Coalescence and Its Effect on Bubble Size and Foam Stability*, Canadian J. Chem. Eng. 80, 299-305.

EXEROWA D., KRUGLYAKOV P.M., 1998. *Foam and Foam Films – Theory, Experiments, Application*, Elsevier, Amsterdam.

EXEROWA D., CHURAEV N.V., KOLAROVA T., ESIPOVA N.E., PANCHEV N., ZORIN Z.M., 2003. *Foam and wetting films: electrostatic and steric stabilization*, Adv. Colloid Interface Sci., 104, 1–24.

GAUDIN A.M., 1957. *Flotation*, McGraw-Hill, New-York.

GRAU R.A., LASKOWSKI J.S., HEISKANEN K., 2005. *Effect of frothers on bubble size,* Int. J. Miner. Process., 76 (4), 225-233.

GRAU R.A., LASKOWSKI J.S., 2006. *Role of frothers in bubble generation and coalescence in a mechanical flotation cell*, Canadian J. Chem. Eng. 84 (2), 170-182.

KRASOWSKA M., MALYSA K., 2007. *Wetting films in attachment of the colliding bubble*, Adv. Colloid Interface Sci., 134–135, 138–150.

ISHIDA N., INOUE T., MIYAHARA M., HIGASHITANI K., 2000. *Nano Bubbles on a Hydrophobic Surface in Water Observed by Tapping-Mode Atomic Force Microscopy,* Langmuir, 16, 6377-6380

KRASOWSKA M., KRASTEV R., ROGALSKI M., MALYSA K., 2007. *Air-Facilitated Three-Phase Contact Formation at Hydrophobic Solid Surfaces under Dynamic Conditions*, Langumir, 23, 549-557.

KRASOWSKA M., ZAWALA J., MALYSA K., 2009. *Air at hydrophobic surfaces and kinetics of three phase contact formation*, Adv. Colloid Interface Sci., 147–148, 155–169.

KRZAN M., LUNKENHEIMER K., MALYSA K., 2004. *On the influence of the surfactant's polar group on the local and terminal velocities of bubbles*, Colloids Surfaces A, 250, 431-441.

KRACHT W., FINCH J.A., 2010. *Effect of frother on initial bubble shape and velocity*, J. Miner. Process., 94, 115–120.

LEJA J., SCHULMAN J.H., 1954. *Flotation Theory: Molecular Interactions between Frothers and Collectors at Solid-Liquid-Air Interfaces*, Trans. AIME, 199, 221-228.

MALYSA K., KRASOWSKA M., KRZAN M., 2005. *Influence of surface active substances on bubble motion and collision with various interfaces*, Adv. Colloid Interface Sci., 114-115, 205-225

NGUYEN A.V., SCHULZE H.J., RALSTON J., 1997. *Elementary steps in particle-bubble attachment*, Int. J. Miner. Process., 51, 183-195.

NGUYEN A.V., NALASKOWSKI J., MILLER J. D., BUTT H-J., 2003. *Attraction between hydrophobic surfaces by atomic force microscopy*, Int. J. Miner. Process., 72, 215–225.

RALSTON J., DUKHIN S.S., MISHCHUK N.A., 2002. *Wetting film stability and flotation kinetics*, Adv. Colloid Interface Sci., 95, 145-236.

SCHELUDKO A., 1967. *Wetting film stability and flotation kinetics*, Adv. Colloid Interface Sci., 1, 391-464.

STEITZ R., GUTBERLET T., HAUSS T., KLÖSGEN B., KRASTEV R., SCHEMMEL S., SIMONSEN A.C., FINDENEGG G. H., 2003. *Nanobubbles and their precursor layer at the interface of water against a hydrophobic substrate*, Langmuir, 19, 2409–2418.

SZYSZKA D., DRZYMAŁA J., ŁUCZYŃSKI J., WILK K.A., PATKOWSKI J., 2006. *Concentration of α-terpineol and (2-dodecanoyloxyethyl)trimethyl ammonium bromide required for prevention of air bubble coalescence in aqueous solutions***,** Physicochemical Problems of Mineral Process., 40, 53-59

TYRREL J.W.G., ATTARD P., 2002. *Atomic Force Microscope Images of Nanobubbles on a Hydrophobic Surface and Corresponding Force-Separation Data,* Langmuir, 18, 160-167.

YANG J., DUAN J., FORNASIERO D., RALSTON J., 2003. *Very small bubble formation at the solid–water interface*, J. Phys. Chem. B, 107, 6139–6147.

ZAWALA J., KRASOWSKA M., DABROS T., MALYSA K., 2007. *Influence of Bubble Kinetic Energy on its Bouncing During Collisions with Various Interfaces*, Can. J. Chem. Eng., 85, 669–678.

ZAWALA J., MALYSA K., 2011. *Influence of the Impact Velocity and Size of the Film Formed on Bubble Coalescence Time at Water Surface,* Langmuir, 27 (6), 2250-2257.

ZHANG H. X., MAEDA N., CRAIG V. S. J., 2006. *Physical Properties of Nanobubbles on Hydrophobic Surfaces in Water and Aqueous Solutions,* Langmuir, 22, 5025-5035.

Kosior, D., Zawala, J., Malysa, K., Kiedy i w jaki sposób α-terpineol and n-octanol mogą opóźniać (hamować) przyczepienie pęcherzyka do hydrofobowych powierzchni, Physicochem. Probl. Miner. Process., 47 (2011) 169-182, (w jęz. ang.)

Badano kinetykę powstawania kontaktu trójfazowego podczas kolizji pęcherzyka w wodzie i w roztworach α-terpineolu i n-oktanolu z płytkami Teflonowymi o różnej szorstkości powierzchniowej, przy użyciu szybkiej kamery o częstotliwości 1040Hz. Określono wpływ stężenia substancji powierzchniowo aktywnych i szorstkości powierzchniowej na czas powstawania kontaktu trójfazowego i czas wyciekania cienkiego filmu ciekłego powstającego pomiędzy pęcherzykiem i powierzchnią Teflonu. Szorstkość powierzchniowa Teflonu była modyfikowana w zakresie 1-100 μm. Wykazano, że w roztworach o małych stężeniach α-terpineolu i n-oktanolu czas powstawania kontaktu trójfazowego uległ

skróceniu w porównaniu do wartości zmierzonych w czystej wodzie. Jednakże, przy wysokich stężeniach badanych spieniaczy następowało znowu wydłużenie czasu powstawania kontaktu trójfazowego, a wielkość tego efektu była uzależniona od szorstkości powierzchni płytki teflonowej. Przykładowo dla płytki teflonowej o szorstkości powierzchniowej 40-60 μm czas powstawania kontaktu trójfazowego uległ wydłużeniu nawet o 20-30 ms. Wyniki uzyskane wskazują, że efekt ten jest związany z obecnością powietrza na hydrofobowej powierzchni ciała stałego. W pracy przedstawiono mechanizm wydłużenia czasu powstawania kontaktu trójfazowego przy nadmiernej dawce spieniacza.

Physicochem. Probl. Miner. Process. 47(2011) 183-192
www.minproc.pwr.wroc.pl/journal/

Physicochemical Problems of Mineral Processing
ISSN 1643-1049

Received March 15, 2011; reviewed; accepted May 21, 2011

Determination of grindability characteristics of zeolite

Halil IPEK *, Ferihan GOKTEPE **

* Department of Mining Engineering, Osmangazi University, 26480, Eskisehir, Turkey, hipek@ogu.edu.tr

** Balikesir Technical College, Balikesir University, Balıkesir,Turkey, fgoktepe@balikesir.edu.tr

Abstract. In this study grindability of zeolite was studied. The work index of zeolite was determined for three different test sieves. In terms of work indexes, there was insignificant difference between the test sieves. Additionally, the breakage rate and distribution parameters were also determined. The fastest breakage rate was obtained for -1700+1180 μm feed sizes and found breakage distributions functions were non-normalisable.

keywords: Bond work index, zeolite, breakage rate function, breakage distribution function, ball milling

1. Introduction

Zeolites are crystalline aluminosilicates of the alkaline and alkaline earth minerals. Zeolites are widely used in mineral industries such as animal nutrition, detergent, pozzolanic cement and agricultural products (Englert and Rubio, 2005). They posses many desirable properties (ion exchange, molecular sieving, catalytic etc.) which make them valuable mineral commodities (Clifton, 1987). In recent years, natural zeolites, especially clinoptilotile (CLN), are gaining growing interest in environmental application such as ammonium and heavy metal removal from wastewater. They are readily available from several producers, less expensive then synthetic counter parts and have advantages of high selectivity towards the ammonium ions removal from wastewater.

Grinding is an important industrial operation that is used for size reduction of materials, production of large surface area and liberation of valuable minerals from their matrices. As it is known, a significant amount of energy, which is used in grinding, turns into heat energy and cannot be used in grinding effectively. However, it is possible to obtain a more effective grinding by setting up more effective grinding systems which consume less energy (Ipek et.al, 2004). Increased rates and efficiencies of milling have been sought through the optimization of milling by providing favorable physical and operational conditions for the mills used (Ozkan et.al, 2009).

Therefore, the design and scale-up of ball mills are important issues in size reduction processes.

The objective of this study is to determine the grindability characteristics of zeolite and to investigate the effect of feed particle size upon grinding.

2. Theoretical background

The Bond ball mill grindability test gives the Bond ball mill work index. This index expresses the resistance of a material to ball milling since the higher the value of the Bond ball mill work index, the more difficult it is to grind the material using a ball mill. This index is widely used in the mineral industry for comparing the resistance of difference material to ball milling, estimating the energy required for ball milling and scaling-up ball mill (Man, 2002). Test results were converted to a work index (in kWh/Mg) by the following empirical equation:

$$W_i - \frac{48.95}{P_t^{0.23}\, G^{0.82} \left[10/P_{80}^{0.5} - 10/F_{80}^{0.5} \right]}, \text{kWh/Mg} \tag{1}$$

where: P_t is selected test size (μm); G is net mass (grams) of undersize product per unit revolution of the mill, in g/rev; P_{80} is the 80% passing product particle size (μm); F_{80} the 80% passing feed particle size (μm).

The value of W_i obtained by above equation is representative of the required energy to tumble the charge of a 30.5 cm interior diameter overflow ball mill dry grinding in a closed circuit. Estimation of W_i is realized only after attainment of steady-state conditions for a locked-cycle batch grinding test. A grinding cycle consists of the following two parts:

- dry grinding of 700 cm^3 bulk volume of material prepared to -3350 micrometers in a 30.5 by 30.5 cm ball mill rotating at 70 rpm and charged with 22,648 grams of grinding balls. Balls plus ore charge is ground for desired revolutions which is usually 50 or 100 revolutions,
- removal by sieving the portion of the product which was ground finer than a pre-selected test size, P_t. In preparation for the next cycle, the undersize portion is replaced by an equivalent amount of fresh feed in order to maintain constant charge.

The duration of grinding is establish as the time required to produce, for the next cycle, a simulated 250% re-circulating load of particles coarser than the selected test size. An estimate of the grinding time is obtained using the grindability, G, of the previous cycle. G is defined as the grams of particles finer than test size produced per mill revolution. An initial value of G is obtained by waiving the 250% re-circulating load requirement for the first cycle and replacing it with a grind period of 100 mill revolutions. When G reverses its direction and remains constant from cycle to cycle, steady-state grinding conditions are said to prevail. The average value of G for the final three cycles is taken as G, the steady, state grindability (McIntyre and Plitt, 1980, Deister, 1987).

Selection of the test size, P_t, is usually based on the fineness of grind desired in the milling operation. Typical choices for P_t are 106, 75 and 53 micrometers. Care must be taken to minimize the possibility of sieve blinding. Blinding will cause underestimation of G, with direct consequences on the calculate value of W_i. (Bond, 1961)

In the analysis of the breakage materials, it is useful to make the initial assumption that the breakage of each size fraction is first order in nature. The rate of disappearance of size 1 due to breakage is proportional to the amount of size 1 material in the mill holdup (Yan and Eaton, 1994):

$$-\frac{d[w_1(t)W]}{dt} \propto w_1(t)W \tag{2}$$

Since the mill hold up, W, is constant, this becomes:

$$dw_i(t)/dt = -S_1\, w_1(t) \tag{3}$$

where S_1 is a proportionality constant and it is called the specific rate of breakage, with units of time^{-1}. If S_1 does not vary with time (Austin at.al, 1984)

$$w_1(t) = w_1(\mathbf{0})\exp(-S_1 t) \tag{4}$$

that is,

$$\log[w_1(t)] = \log[w_1(0)] - S_1 t/2.3 \tag{5}$$

where $w_1(t)$ is the weight fraction of mill hold up that is of size 1 at time t (Austin and Bagga, 1981). The formula proposed by Austin et al. (1984) for the variation of the specific rate of breakage S_i with particle size is

$$S_i = a_T \left(x_i / x_0 \right)^{\alpha} Q_i \tag{6}$$

where x_i is the upper limits of the size interval indexed by i, x_0 is 1 mm, a_T and α are model parameters that depend on the properties of the material and the grinding conditions. Q_i is a correction factor which is 1 for smaller sizes (normal breakage) and less than 1 (abnormal breakage) for particles too large to be nipped and fractured properly by the ball size in the mill. In abnormal breakage region, each size behaves as if it has some fraction of weak material and the remaining fraction of stronger material. Using a mean value for S_i in this region, values of Q_i are empirically described by

$$Q_i = \frac{1}{1+(x_i/\mu)^{\Lambda}}, \Lambda \geq 0 \tag{7}$$

where μ is the particle size at which correction factor is 0.5 and Λ a positive number which an index of how rapidly the rates of breakage fall as size increases that is the higher the value of Λ, the more rapidly the values decrease.

The Cumulative Breakage Distribution, $B_{i,j}$, is defined as "the weight fraction of material broken from size j which falls less than the upper size of size interval i" is commonly used to characterize the size distribution resulting from breakage of

material from a particular size interval to a smaller size (Austin at.al, 1984,Austin and Luckie, 1971/72).

The values of the primary breakage distribution function are deduced from the size distributions at short grinding times where there is mainly size 1 material breaking and only a small amount of smaller sizes to rebreak (Austin at.al, 1984). *B* values can be calculated by using BII method which is described following formula:

$$B_{i,j} = \frac{\log\left[\left(1 - P_i(0)\right)\right] / \log\left[\left(1 - P_i(t)\right)\right]}{\log\left[\left(1 - P_{j+1}(0)\right)\right] / \log\left[\left(1 - P_{j+1}(t)\right)\right]} \quad , \tag{8}$$

where j is the top size of the charge, $P_i(t)$ is the cumulative percent undersize of size interval i at the short grinding time which gives no more than about 30% broken out of the top size interval. Cumulative primary breakage distribution function $B_{i,j}$ is also defined in an empirical form by

$$B_{i,j} = \phi_j \left(\frac{x_{i-1}}{x_j} \right)^{\gamma} + \left(1 - \phi_j\right) \left(\frac{x_{i-1}}{x_j} \right)^{\beta} \quad , \tag{9}$$

where x_i is the top size and $B_{i,j}$ is the weight fraction of primary breakage products. The parameters Φ, γ and β define the size distribution of the material being ground. On plotting size versus $B_{i,j}$ on the log scale, the slope of the lower portion of the curve gives the value of γ while the slope of the upper portion of the curve gives the value of β, and Φ is the intercept as shown in Fig. 1.

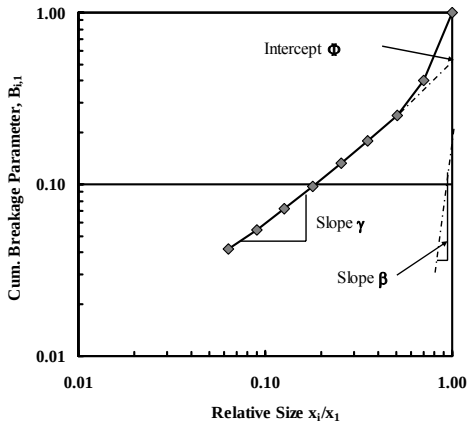

Fig. 1. Obtaining primary breakage distribution function parameters for any single size fraction feed ground in the mill

The primary characteristic of the B_{ij} curves is the final slope of each plot γ. The smaller the curve of γ, the higher the relative amounts of progeny fines that are produced from breakage. Conversely, materials having a large γ value give less relative amounts of fines and can therefore be expected to produce steeper size distributions when ground in a given machine. The β, and Φ values show how rapidly

fractions close to feed size are reduced to a lower size. The $B_{i,j}$ values are said to be normalisable if the fraction which appears at sizes less than the starting size is indepented of the starting size. In terms of plots, the curves should be super-imposed on each other if the $B_{i,j}$ values are normalisable. If the values of breakage distribution are dependent on starting feed size, that is, if they are normalisable, the $B_{i,j}$ values are represented by the following equation (Austin at.al, 1984, Austin and Bagga, 1981, Austin and Luckie, 1971/72):

$$B_{i,j} = \Phi_j \left(\frac{x_{i,1}}{x_1} \right)^{\gamma} + \left(1 - \Phi_j\right) \left(\frac{x_{i-1}}{x_1} \right)^{\beta}, \qquad 0 \le \Phi_j \le 1 \tag{10}$$

$$\Phi_j = \Phi_1 \left[\frac{x_j}{x_1} \right]^{-\delta} \tag{11}$$

for normalized B values δ=0.

3. Materials and experimental methods

3.1. Material

The zeolite sample was taken from Bigadic Boron Works, Balikesir/Turkey. The sample contains zeolite group minerals (heulandite-clinoptilolite) and amorphous materials (www.etimaden.gov.tr). The chemical analysis of sample is given in Table 1.

The sample was crushed to -3350 μm by a laboratory jaw crusher for Bond test. In order to determine the breakage parameters, crushed material of -3350 μm was classified in to seven mono size fractions which were -3350+2360, -2360+1700, -1700+1180,-1180+850, -850+600, -600+425, -425+300 μm, where for example -3350+2360 μm denotes that 100 % of the particles are passing by weight at 3350 μm size and 100 % of particles are remaining at 2360 μm. The density of zeolite sample which was determined by a pycnometer and it was averaged 2.07 g/cm^3 over thirteen measurements. Mohr's hardness of sample was measured by hardness pens and it was found to be 3.5-4.

Table 1. Chemical composition of materials

SiO_2 (%)	Al_2O_3 (%)	Fe_2O_3 (%)	TiO_2 (%)	CaO (%)	MgO (%)	Na_2O (ppm)	K_2O (%)	L O I (%)	B in acid (ppm)	B in water (ppm)
70.14	11.46	0.85	0.097	2.98	1.46	354	4.37	9.50	131.13	8.00

3.2. Experimental

The stainless steel Bond mill used in the experiments was 30.5 cm in diameter and 30.5 cm in length. The mill was loaded with 22,648 g of 38.1, 31.75, 25.40, 19.05 and 12.70 mm diameters of stainless steel balls which correspond to 22% of the struck

volume of the mill and mill was operated at 70 rpm which was 86% of its critical speed.

In Bond test experiment, the mill was loaded to 32.6% of the interstitial void volume of the ball charge and was filled with the -3350 microns of sample. Test was done in the three different test sieves.

In the kinetic tests, the mill was loaded to 100% of the interstitial void volume of the ball charge, *U*. The breakage parameters were determined experimentally using one size fraction technique (Austin and Bagga, 1981). Tests were carried out for 7 different mono size fractions which were mentioned above. In order to obtain the breakage parameters, the mono size fractions were ground dry for 0.5, 1.0, 2.0, 4.0, 8.0 minutes separately. At the end of the each run, the ground product was weighed and the loss was no more than 0.15% of the total charge. Due to grinding, sampling, sieving and regrinding the same sample for several times, some weight losses are expected. The loss in this study was less than 1 % which is acceptable.

The characteristics of the Bond mill used in grinding tests and test conditions are outlined in Table 2.

Table 2. Bond mill characteristic and test conditions for grinding of zeolite

Mill	Diameter, *D*, cm	30.5				
	Length, *L*, cm	30.5				
	Volume, *V*, cm^3	22,272				
	Speed, rpm	70				
	Critical speed, N_c[a]	86.55				
Mill charge	Diameter, *d*, mm	38.10	31.75	25.40	19.05	12.70
	Number	43	67	10	71	94
	Total mass, *g*	22,648				
	Specific gravity g/cm^3	7.79				
	Fractional ball filling, J[b]	0.22				
Media charge	Sample	Zeolite				
	Specific gravity g/cm^3	2.07				
	Powder weight, *g*	2489.56				
	Fractional. Powder filling, f_c[c]	0.09				
	Powder-ball loading ratio, U[d]	1.00				

[a] $N_c = \frac{42.3}{\sqrt{D-d}}$,

[b] $J = \left(\frac{mass\ of\ balls / ball\ density}{mill\ volume} \right) x \frac{1.0}{0.6}$,

[c] $f_c = \left(\frac{mass\ of\ powder / powder\ density}{mill\ volume} \right) x \frac{1.0}{0.6}$

[d] $U = \frac{f_c}{0.4\,J}$.

4. Results and Discussion

4.1. Bond Work Index

Bond work tests were done in three different test sieves which were 300, 212 and 150 micrometers. The average size distribution of feed and products were given in Fig 2. Bond work indexes were 10.55, 10.71, 10.18 kWh/t respectively for this zeolite sample. Fig 3 shows the test sieve sizes versus work index values. These results are very close to each other which is unusual situation. Generally, it is expected that, the less the test sieve sizes, the higher the work index. Therefore, all tests were repeated 3 times and the difference was not more than 2%. In literature, similar results were observed for galena by Smith and Lee in 1968 (Smith and Lee, 1968).

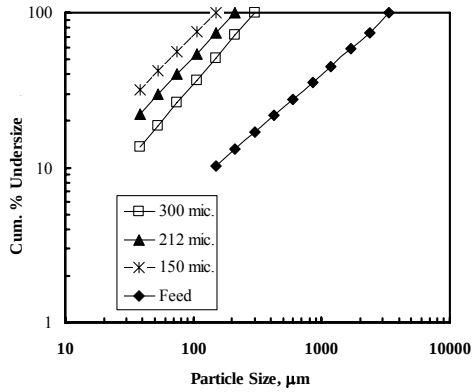

Fig. 2. Size distribution of feed and products of zeolite

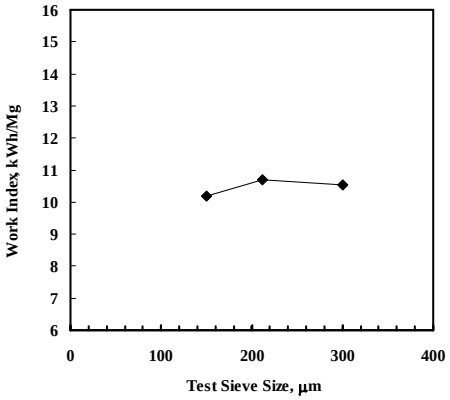

Fig. 3. Test sieve sizes versus work index values

4.2. Determination of the breakage rate function

Figure 4 shows the initial grinding results of sample plotted in first-order form for varying feed size fractions. Samples were ground individually as batch-wise for 0.5, 1.0, 2.0, 4.0, and 8.0 minutes to obtain both the breakage parameters and particle size distributions. It can be seen that, all feed size fractions match first-order rate kinetics. Coefficients of correlation are between 0.9989 to 0.9863.

Variation of the specific rates of breakage (S_i) with particle size of the sample is shown in Fig. 5. It is clearly seen that S_i values increase up to a maximum particle size then started to decrease at 1700 µm. This was due to the inefficiency of the largest feed sizes that were not nipped properly in the mill.

The initial grinding results obey the first-order breakage form as in Eq. (6). When the values of S_i are fitted to the expression (6), the a_T value is obtained by inserting α, x_i and x_0. Using Eq.(6), S_i, a_T, α, μ and λ parameters were obtained and outlined in Table 3 as the breakage parameters that were utilized in the simulations.

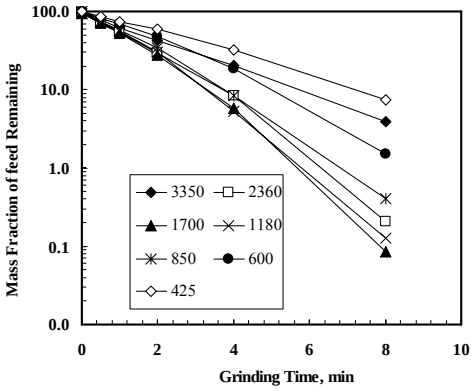

Fig. 4. First order plots for dry grinding of different feed sizes of zeolite

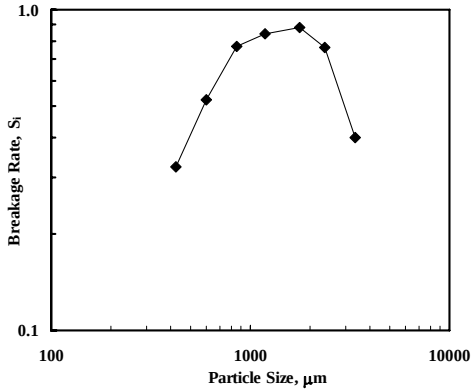

Fig. 5. Variation of the S_i values zeolite with particle size

Table 3. The overall breakage parameters for zeolite sample

a_T	α	μ	Λ	Φ	γ	β	δ
0.98	1.23	1.65	3.10	0.44	1.09	2.52	0.16

4.3. Determination of the primary breakage distribution function

The values of $B_{i,j}$ were determined from the size distributions at short grinding times using the BII method (Eq. 8). The primary breakage distribution function variations at different particle feed sizes are shown in Fig 6. The primary breakage distribution parameters were determined as indicated in Fig. 1 and results are listed in Table 4.

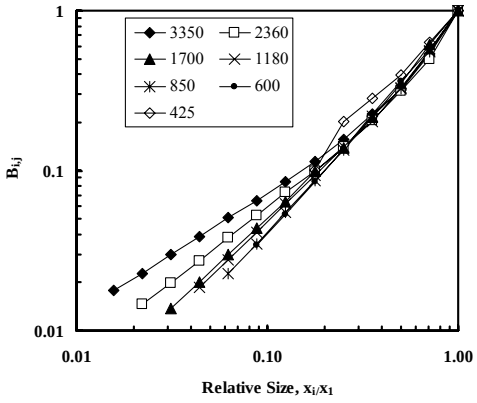

Fig. 6. Primary breakage distribution functions of zeolite

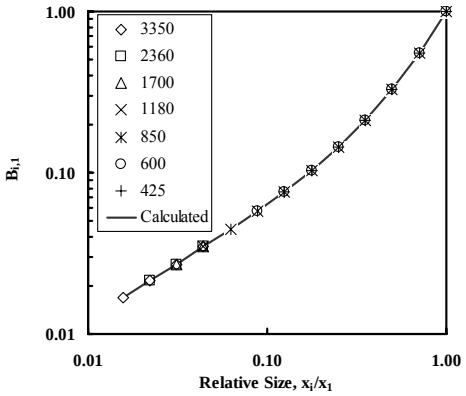

Fig. 7. Normalized primary breakage distribution functions of zeolite

Figure 6 and Table 4 show that, the primary breakage distribution functions were dependent on feed size. In order to normalize breakage distribution parameters, nonlinear regression technique was used to obtain the sum of the square of differences between the measured and calculated breakage distribution values. In this calculation, Eq. 11 was used instead of ϕ in Eq. 10. These parameters ($\phi, \gamma, \beta, \delta$) are listed in Table 3 and normalized breakage distribution functions are shown in Fig.7. This figure shows that calculated and experimental data were in good agreements.

Table 4. The primary breakage distribution parameters obtained from short grinding times

Particle Size (μm)	Φ	γ	β
-3350+2360	0.47	0.80	2.71
-2360+1700	0.53	0.95	3.10
-1700+1180	0.68	1.13	2.27
-1180+850	0.69	1.16	2.95
-850+600	0.80	1.29	3.69
-600+425	0.92	1.37	7.73
-425+300	0.94	1.36	2.29

5. Conclusion

No significant differences in the Bond work index test were found for three different test sieves. That means that the work index values of zeolite was independent of test sieve sizes. The grinding of zeolite obeys the first order breakage kinetics in the case of all feed sizes. Faster breakage (represented by α parameters) from higher values to lower values were at –1700+1180 micrometers fraction. Different $B_{i,j}$ values (ϕ, β and γ) were obtained for each feed size fractions. It was seen that the breakage distributions obtained by the BII method were dependent on all starting feed sizes and this could not be normalized. When all model parameters were used, it was determined that all sizes were in conformity with all laboratory grinding data. The breakage parameters, obtained from the laboratory size mill, could be used for scaling up the industrial mills. This is performed by choosing the scale-up option in the simulation program for the mineral studied.

References

Austin, L.G., Bagga, P., 1981, An analysis of fine dry grinding in ball mills, Powder Tech, 28, 836-90

Austin, L.G., Klimpel, P.T., Luckie, P.T., 1984, The Process Engineering of Size Reduction, SME-AIME, New York, p. 561

Austin, L.G., Luckie, P.T., 1971/1972, Methods for determination of breakage distribution parameters, Powder Tech, 5, 215-221

Bond, F.C., 1961, Crushing and grinding calculations. Part I, British Chemical Eng. 6, 378-385

Clifton, R.A., 1987, Natural and Synthetic Zeolites, US Bureau of Mines Inf. Cir., IC 9140,1987.

Deister, R.J., 1987. How to determine the Bond work index using lab ball mill grindability tets, Engineering and Mining Journal, 188 (2), 42-45

Englert, A. H., Rubio, J., 2005, Characterization and environmental application of a Chilien natural zeolite. Int. J. Miner. Process. 75, 21-29.

Ipek, H., Ucbas, Y., Hosten, C., Determination of the grindability characteristics of ceramic raw materials, 10th Int. Mineral Processing Symposium, 5-7 October, Cesme, Turkey, 113-117, 2004.

Man., Y.T., 2002, Why is the Bond Ball Mill Grindability Test done the way it is done? The European Journal of Mineral Processing and Environmental Protection, 2, 34-39.

McIntyre, A., Plitt, L.R., 1980, The interrelationship between Bond and Hardgrove grindabilities, Canadian Institute of Mining, Metallurgy and Petroleum Bulletin, June, 149-155

Ozkan, A., Yekeler, M., Calkaya, M., 2009, Kinetics of fine wet grinding of zeolite in a steel ball mill in comparison to dry grinding. Int. J. Miner. Process. 90, 67-73.

Smith, R.W., Lee, K. H., 1968, A comparison of data from Bont type simulated closed-circuit and batch type grindability tests, AIME, Transactions, 241, 91-101.

www.etimaden.gov.tr-Etimaden, Bigadic Bor Works report.

Yan, D., Eaton, R., 1994, Breakage properties of ore blends, Minerals Eng. 7, 1485-199

Physicochem. Probl. Miner. Process. 47(2011) 193-206
www.minproc.pwr.wroc.pl/journal/

Physicochemical Problems of Mineral Processing
ISSN 1643-1049

Received April 1, 2011; reviewed; accepted May 4, 2011

Atmospheric leaching of copper flotation concentrate with oxygenated sulphuric acid solutions

Tomasz CHMIELEWSKI, Kamil BOROWSKI, Krzysztof GIBAS, Katarzyna OCHROMOWICZ, Barbara WOZNIAK

Wroclaw University of Technology, Faculty of Chemistry, Division of Chemical Metallurgy, Wybrzeze Wyspianskiego 27, 50-370 Wroclaw, tomasz.chmielewski@pwr.wroc.pl

Abstract. Results of atmospheric leaching of copper sulphide concentrate from Lubin Concentrator (ZWR Lubin) with oxygenated aqueous H_2SO_4 and in the presence of Fe(III) have been presented. It was found that oxidative atmospheric leaching performed in acidified and oxygenated iron(III) solutions has to be preceded by a controlled, non-oxidative decomposition of acid-consuming carbonate components in order to further liberate finely disseminated metal-bearing minerals. Atmospheric leaching appeared to be a very efficient process for recovering Cu, Zn, Co and Ni from the Lubin concentrate due to favorable mineralogical composition and fine size of leached particles. A maximum recovery of Cu (95%), Zn (90%), Ni (40%) and Co (50%) was observed after 5-7 hours of leaching at 90°C in the oxygenated solutions containing 20-30 g/dm^3 of Fe(III). The solid residue after atmospheric leaching will be further processed by flotation or chloride leaching to recover Ag, Pb and precious metals.

keywords: leaching, copper, sulphuric acid, industrial concentrate, galvanic interactions

1. Introduction

The application of modern hydrometallurgy, well known and already approved in the world for copper recovering, becomes an urgent necessity in Polish copper industry to reverse unfavorable trends in flotation results (decreasing concentrate grade and metals recovery), particularly at Lubin Concentrator (Grotowski, 2007). The application of atmospheric leaching can be considered as a complimentary process for processing of copper flotation concentrate in order to elevate the recovery of copper and to recover metals, which are being lost in the current technologies (Zn, Co, Mo, V).

The standard treatment of copper flotation sulphide concentrates by smelting, converting and electrorefining has dominated the World copper industry.

Pyrometallurgy is undoubtedly more feasible for high capacity processing and became not acceptable for small scale operations for economical reason. Research and development for hydrometallurgical alternatives to traditional pyrometallurgical processes has remarkably intensified in the recent years. A wide range of chemical and biological processes for copper recovery from concentrates have emerged (Dreisinger 2006, Gupta 1990, Habashi 1999, 2005, 2007, Jansen and Taylor 2000, Marsden 2007a, b, c, d, e, Peacey et al. 2003, Ramahadran et al. 2007, Letowski 1975). These processes are all successful in leaching of copper and accompanying metals from polymineral and chalcopyrite concentrates, purifying the leach solutions (PLS) using modern separation processes, mainly solvent extraction (SX), and recovering a high value, high purity copper metal product.

It is well known that the Polish copper deposits (LGOM - Lubin-Glogow Copper Basin, SW Poland) exhibit unique, sedimentary nature (Rydzewski 1996, Konstantynowicz 1990). They consist of three lithological fractions: dolomitic, sandstone, and shale. From those three ore fractions the shale fraction reveals two exceptional and opposite properties. It contains the highest concentrations of copper and accompanying metals (Ag, Ni, Co, Zn, Pb, V, Mo and others) and simultaneously is the most troublesome in the flotation circuits (Tomaszewski 1995, Konieczny and Kasińska 2009). In the case of the shale fraction, dissemination of fine metal sulfides in the carbonate matter and black shale-clay rocks that form the majority of the gangue is observed. Such fine dissemination of copper sulfides in the carbonate-organic matrix considerably reduces the susceptibility of the ore to both effective liberation and flotation. A relative increase of quantity of the shale-clay and carbonate fractions in flotation feeds, which are known as mostly hard-to-treat in flotation circuits, is currently observed. According to the latest data (Kubacz and Skorupska 2007) content of the shale fraction in the Lubin deposit can even occasionally exceed 25% and is expected to be at high levels in coming years.

A complex and unique mineralogical structure as well as chemical composition of the Polish copper ores mined from sedimentary deposits is the principal reasons for copper, silver and other metals losses to flotation tailings (Łuszczkiewicz 2000, 2004). The presence of shale creates additional technical, economical and ecological issues. Selective liberation of the fine metals-bearing sulphide particles from the carbonate host matrix would be the only way to enhance metals recovery. However, it appears to be ineffective in the existing milling circuits. Consequently, the hydrophilic gangue-sulphide intergrowths seriously reduce both the flotation selectivity and the metal grade in the concentrate (Luszczkiewicz et al. 2006). Therefore, it can be concluded that the existing beneficiation technologies currently applied to Polish copper ores have reached the limit of their technological efficiency (Chmielewski and Charewicz 2006, Łuszczkiewicz and Chmielewski 2008, Chmielewski et al. 2007a).

The hydrometallurgical processes can be divided into predominantly sulphate, mixed sulphate/chloride, and chloride types (Ramahadran et al. 2007). Within the sulphate grouping, processes can be sub-grouped as either atmospheric or super-

atmospheric in pressure, and chemical or biological in the leaching process. There are fewer chloride processes but advances in chemistry, equipment, and process development have vaulted the chloride systems back into the competition. The sulphate atmospheric leaching has been previously investigated as an alternative for processing of flotation middlings (shale enriched feed) from the technological circuit at Lubin Concentrator (Chmielewski 2007).

This paper presents the results of initial investigations on atmospheric leaching of the Lubin flotation concentrate in oxygenated aqueous sulphuric acid in the presence of iron(III) ions.

2. Material and experimental procedure

A commercial flotation concentrate from flotation circuit at Lubin Concentrator (ZWR Lubin) was used as leaching feed. The output of the concentrate at the Lubin plant is almost 0.5 Tg (teragrams)/year and corresponds to the copper production of 65 Gg/year. The feed for leaching had been collected in the form of water slurry for about two weeks to provide a representative leaching feed. The slurry of the industrial sample was then vigorously stirred and split on 1-2 dm^3 laboratory samples, which were kept in sealed containers isolated from the effect of air.

The feed material applied for the laboratory experiments of non-oxidative leaching followed by atmospheric leaching in oxygenated sulphuric acid was subjected to various analyses including chemical assay, granulometric composition, demand for sulphuric acid for total decompostion of carbonates ($z^{max}_{H_2SO_4}$), mineralogical composition, organic and total carbon as well as total sulphur content. The results of analyses are given in Tables 1 and 2 and in Fig.1. The content of organic carbon was observed to be very high (about 8.1 %) and is not acceptable for flash smelting.

Table 1. Chemical compositions of copper flotation concentrate from Lubin Concentrator

Cu, %	Ag, g/Mg	Pb, %	Ni, g/Mg	Co, g/Mg	Zn,%	As, %	Mo, g/Mg	V, g/Mg	C_{org}, %
15.4%	870	2.67	475	1 160	0.95	0.29	290	650	8.1

The content of carbonates in two concentrate samples corresponds to the utilization of 220-260 g H_2SO_4/kg of dry solid for total decomposition of carbonates. Therefore, the application of atmospheric leaching, taking place in acidic conditions, required previous non-oxidative leaching with acid in order to decompose totally the acid consuming components, mainly calcium and magnesium carbonates (Luszczkiewicz and Chmielewski 2006) Chmielewski et al. 2007a, b).

Non-oxidative leaching was always performed before each atmospheric leaching experiment. The particle size composition of the leaching feed was in reported examinations the same as in flotation (D_{80} = 110-120 μm, Fig.1). The feed was not subjected to additional particle size reduction.

The flotation concentrate from Lubin Concentrator (Table 1) exhibits considerably lower content of copper (15.5% Cu) with regard to Rudna and Polkowice, but the content of silver (870 g/Mg) and other base metals, particularly zinc (0.95%) and cobalt (1 160 g/Mg), which are present as sulphides, was remarkably higher with regard to other concentrates produced at KGHM. Unfortunately, the high value of accompanying metals is currently underestimated, taking into account their market value. The content of molybdenum (290 g/Mg) and vanadium (650 g/Mg) is also evidently elevated. Zinc, cobalt, vanadium and molybdenum are not recovered in currently applied technologies. Moreover, extremely high content of organic carbon (Table 1) makes the Lubin concentrate not suitable for flash smelter.

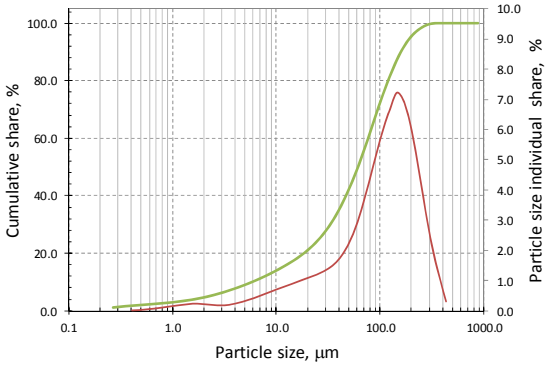

Fig. 1. Granulometric analysis of copper concentrate from Lubin Concentrator

Table 2. Maximum demand for sulphuric acid, organic and total carbon content and total sulphur content in two samples of Lubin flotation concentrate

	Concentrate sample	Maksimum demand for H_2SO_4, $Z^{max}_{H_2SO_4}$	Organic carbon	Total carbon	Total sulphur	Particle size, D_{80}
		g H_2SO_4/kg	%	%	%	µm
1.	KLA	220	8.1	10.20	12.41	110-120
2.	KLB	260	8.1	10.19	12.40	110-120

Effective leaching of copper and accompanying metals from their sulphidic minerals is only possible when an oxidation agent is present in the leaching system. Gaseous oxygen and iron(III) ions were selected for this purpopose, taking into account technical, economical and ecological aspects. Laboratory tests were performed at various temperatures (50, 70, and 90^{o}C), various iron(III) concentration (0, 10, 20, 30 g/dm^3) and constant concentration of sulphuric acid (50 g/dm^3). The concentration – leaching time relationship for Cu, Zn, Fe, Ni, Co, and As, concentration of sulphuric acid and redox potential of the slurry during leaching was examined. The solid residue was examined for metals content and mineralogical SEM

observation were conducted to asses liberation of the remaining metals (mainly Ag and Pb) for further recovery.

Table 3. Mineralogical composition of copper ores - feed for flotation at KGHM „Polska Miedź" SA Concentrators (Luszczkiewicz and Drzymala, 2009)

Mean data 2007-2008	Bornite Cu_5FeS_4	Chalcocite digenite $Cu_2S/Cu_{1.8}S$	Chalko-pyrite $CuFeS_2$	Pyrite Markasite FeS_2	Covellite CuS	Sphalerite ZnS	Tennantite $Cu_{12}As_4S_{13}$	Galena PbS
Lubin	33.1	14.5	26.1	17.4	3.5	1.8	2.0	1.9
Polkowice	13.6	55.5	12.0	10.9	3.7	1.2	1.5	1.6
Rudna	24.8	40.4	7.2	15.0	5.8	3.1	1.5	2.3

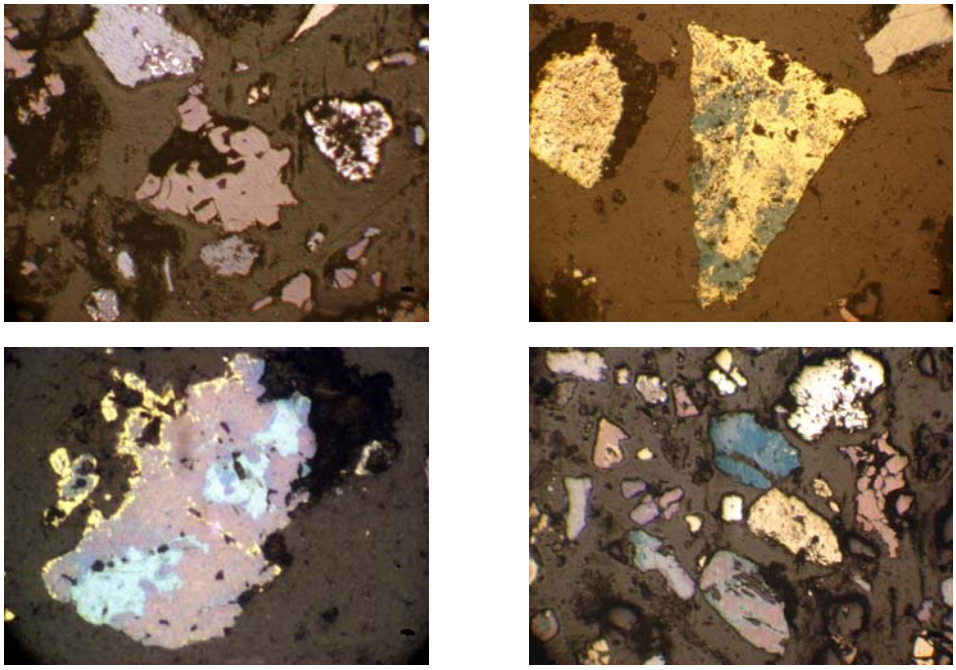

Multimineral intergrowths of sulphide minerals in flotation concentrate from Lubin. Reflected light, original magnification about 120x

The Polish copper ores mined from the Lubin, Polkowice-Sieroszowice and Rudna deposits, in contrast to majority of world copper chalcopyrite (primary deposits), are of sedimentary origin and exhibit very favorable mineralogical composition with regard to hydrometallurgical processing. Chalcocite (Cu_2S) and bornite (Cu_5FeS_4) are the dominating, while chalcopyrite ($CeFeS_2$) and covellite (CuS) minor copper minerals (Table 3). Moreover, the presence of pyrite and marcasite, particularly in the Lubin ore, is expected to be beneficial for oxidative leaching, due to

the presence of galvanic contacts between copper mineral and pyrite – marcasite grains (Chmielewski and Kaleta 2010).

Detailed mineralogical analysis of the flotation feed for Lubin, Polkowice and Rudna Concentrators are given in Table 3. Photographs on page 201 exhibits examples of galvanic intergrowths existing in the examined concentrate. Consequently, one can expect rather high leaching recovery of copper and other base metals from by-products or concentrates even under mild conditions of atmospheric leaching. The presence of finely dispersed grains of copper sulphide in the shale-dolomitic gangue and sulphide-sulphide intergrowths is an additional beneficial factor, particularly after their chemical liberation by non-oxidative leaching.

Separation of the Lubin concentrate exhibiting a very high content of organic carbon (Table 1 and 2) for alternative processing has an additional beneficial effect leading to reduction of organic carbon in the flash smelter feed, what is particularly significant for the Glogow II metallurgical plant. Presently, the observed elevated content of organic carbon in the concentrates already exceeds 8 % and is the main reason for undesirable, significant decrease in the smelter throughput (Kubacz and Skorupska 2007).

The leaching experiment were performed in a thermostatic, stirred 1 dm^3 glass reactor with an oxygen sparger. The effect of temperature, Fe(III) concentration, and s/l ratio on the recovery of Cu, Zn, Ni and Co was examined. The samples of leaching slurry were taken during leaching, filtered and subjected to chemical analyses. Additionally, a potential of Pt electrode was monitored to evaluate leaching conditions.

3. Results and discussion

The leaching experiments of the Lubin concentrate under atmospheric conditions evidently showed that two parameters are most essential for the process kinetics and copper leaching efficiency: temperature (Fig. 2) and iron(III) concentration (Fig. 3). The results of experiments confirmed earlier expectations that due to the beneficial mineralogical composition of the concentrate (Table 3), copper can be relatively easily subjected to leaching. It is seen, that even in the solution without addition of iron(III) (Figs. 2 and 3) the process is quite fast and leads to the final concentration of Cu in the solution about 20 g/dm^3.

The presence of iron(III) ions remarkably improves leaching conditions and process rates. The leaching process becomes much faster and the maximum concentration of copper can reach 25 g/dm^3. According to experimental data shown in Fig.3, the initial concentration of 20 g/dm^3 of Fe(III) in leaching solution is high enough for effective leaching of copper. The following chemical reactions can be attributed to the leaching of copper sulphides from Lubin concentrate:

$$Cu_2S + 2Fe_2(SO_4)_3 \rightarrow 2CuSO_4 + 4FeSO_4 + S^o \quad (1)$$

$$CuS + Fe_2(SO_4)_3 \rightarrow CuSO_4 + 2\,FeSO_4 + S^o \quad (2)$$

$$Cu_5FeS_4 + 6Fe_2(SO_4)_3 \rightarrow 5CuSO_4 + 13FeSO_4 + 4S^o \quad (3)$$

$$CuFeS_2 + 2Fe_2(SO_4)_3 \rightarrow CuSO_4 + 5FeSO_4 + 2S^o. \quad (4)$$

Elemental sulphur is a dominating product of oxidation of sulphidic sulphur. To maintain the effective leaching conditions iron(II) sulphate has to be continuously regenerated to iron(III) sulphate by gaseous oxygen in the following reaction:

$$4FeSO_4 + O_2 + 2H_2SO_4 \rightarrow 2Fe_2(SO_4)_3 + 2H_2O. \quad (5)$$

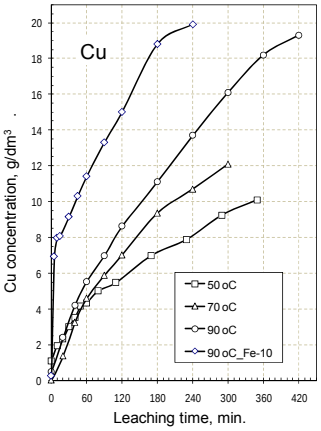

Fig. 2. Effect of temperature (50, 70 and 90°C) and presence of Fe(III) ions (10 g/dm^3) on the Cu leaching rate from Lubin concentrate in oxygenated sulphuric acid (50 g/dm^3). Solid/liquid = 1:8. Initial H_2SO_4 concentration – 50 g/dm^3, oxygen flow rate – 30 dm^3/h

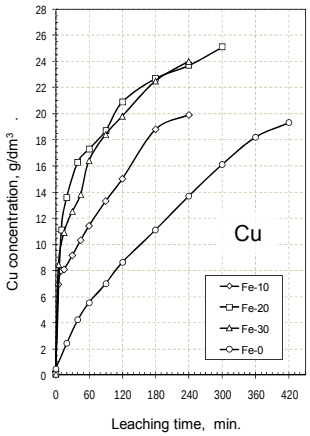

Fig. 3. Effect of concentration of Fe(III) ions on the Cu leaching rate from Lubin concentrate in oxygenated sulphuric acid (50 g/dm^3) at 90°C. Solid/liquid = 1:8. Fe(III) conc. – 0, 10, 20 and 30 g/dm^3). Initial H_2SO_4 concentration – 50 g/dm^3, oxygen flow rate – 30 dm^3/h

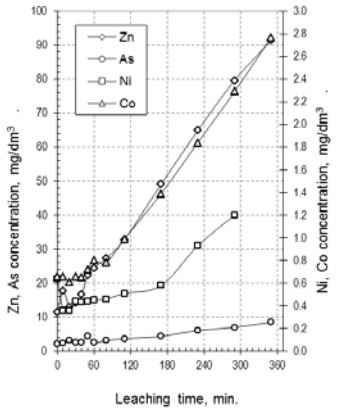

Fig. 4. Concentration – leaching time plots for Zn, As, Ni and Co during copper concentrate leaching in oxygenated solphuric acid (50 g/dm^3) at 90°C. Initial H_2SO_4 concentration – 50 g/dm^3, s/l = 1:8, no Fe(III) added, oxygen flow rate – 30 dm^3/h

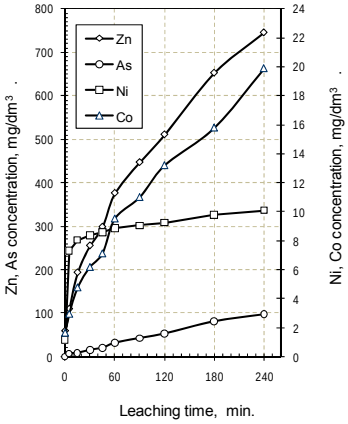

Fig. 5. Concentration – leaching time plots for Zn, As, Ni and Co during copper concentrate leaching in oxygenated solphuric acid (50 g/dm^3) at 90°C and presence of Fe(III) ions (30 g/dm^3). Initial H_2SO_4 concentration – 50 g/dm^3, s/l = 1:8, oxygen flow rate – 30 dm^3/h

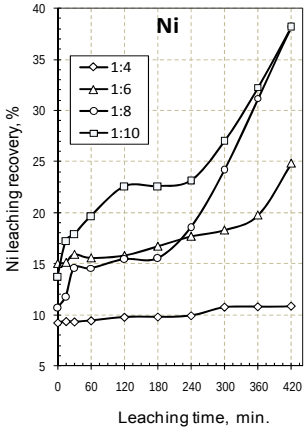

Fig. 6. Effect of solid/liquid ratio on the leaching recovery for nickel during copper concentrate leaching in oxygenated solphuric acid (50 g/dm^3) at 90^{o}C. Initial H_2SO_4 concentration – 50 g/dm^3, temperature 90^{o}C, Fe(III) conc - 30 g/dm^3, oxygen flow rate – 30 dm^3/h

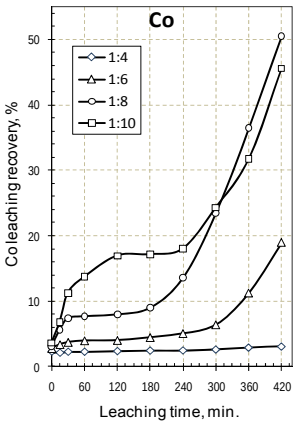

Fig. 7. Effect of solid/liquid ratio on the leaching recovery for cobalt during copper concentrate leaching in oxygenated solphuric acid (50 g/dm^3) at 90^{o}C. Initial H_2SO_4 concentration – 50 g/dm^3, temperature 90^{o}C, Fe(III) conc - 30 g/dm^3, oxygen flow rate – 30 dm^3/h

According to leaching and regeneration reactions taking place during concentrate atmospheric leaching, one can evaluate that the need for oxygen and acid depends remarkably on the mineralogical composition of the leached feed and has to be determined by laboratory examinations.

Zinc, nickel, cobalt and arsenic were also leached from the copper concentrate. The effect of oxygen and Fe(III) on leaching rate of Zn, As, Ni and Co (Figs. 4 and 5) was similar to that observed for leaching of copper (Figs. 1 and 2). The leaching rate and concentration of metals remarkably increased in the presence of iron(III) ions (Fig. 5). From the shape of concentration–time plots for nickel and cobalt, we could preliminarily assume that both metals are entrapped or disseminated in particles of copper or iron sulphides. The leaching rate of Ni and Co increases with increasing recovery of copper.

The effect of solid/liquid ratio was examined on the recovery of nickel and cobalt during atmospheric leaching (Figs. 6 and 7). The results confirmed the previous assumption that the observed, after about 4 hours of leaching, acceleration of Ni and Co leaching can be attributed to dissemination of nickel and cobalt sulphides in the copper sulphide matrix. The observed recovery of nickel (about 40%) and recovery of cobalt (50%) are somewhat low and a further increase of this parameter will require a reduction of the particles size and further optimization of the leaching parameters. It can also be concluded that the s/l ratio is an essential leaching parameter and the process has to be conducted at s/l above 1:6. When the s/l ratio was 1:4, the observed recovery of Ni and Co was very low (Figs.. 6 and 7).

Zinc, which according to the mineralogical examinations, was in the Lubin concentrate in the form of liberated particles of sphalerite, was found to be

surprisingly very easily leachable under atmospheric conditions (Figs.. 8 and 9). It may suggest an important effect of a direct chemical reaction between sphalerite and sulphuric acid. Detailed examination of the effect of temperature and concentration of iron(III) on leaching of zinc exhibited that temperature of 90°C is recommended for zinc leaching. The optimum initial concentration of Fe(III) was found to in the range of 20–30 g/dm^3.

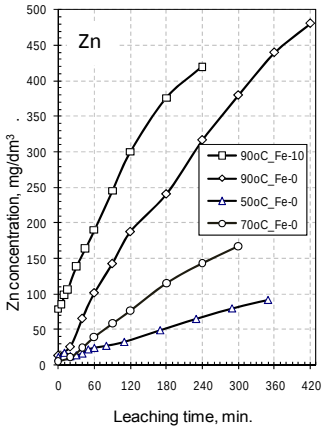

Fig. 8. Effect of temperature (50, 70 and 90°C) and presence of Fe(III) ions (10 g/dm^3) on the Zn leaching rate from Lubin concentrate in oxygenated sulphuric acid (50 g/dm^3). Solid/liquid = 1:8

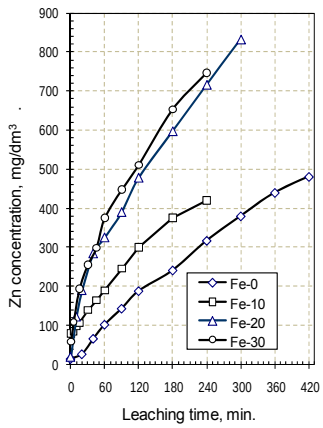

Fig. 9. Effect of concentration of Fe(III) ions on the Cu leaching rate from Lubin concentrate in oxygenated sulphuric acid (50 g/dm^3) at 90°C. Solid/liquid = 1:8. Fe(III) conc. – 0, 10, 20 and 30 g/dm^3)

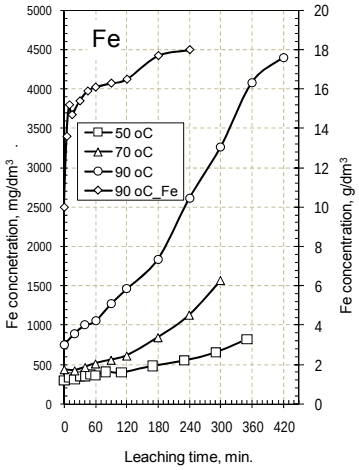

Fig. 10. Effect of temperature (50, 70 and 90°C) and presence of Fe(III) ions (10 g/dm^3) on the Fe leaching rate from Lubin concentrate in oxygenated sulphuric acid (50 g/dm^3). Solid/liquid = 1:8

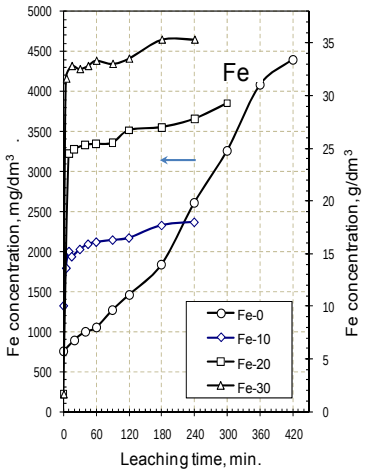

Fig. 11. Effect of concentration of Fe(III) ions on the Cu leaching rate from Lubin concentrate in oxygenated sulphuric acid (50 g/dm^3) at 90°C. Solid/liquid = 1:8. Fe(III) conc. – 0, 10, 20 and 30 g/dm^3)

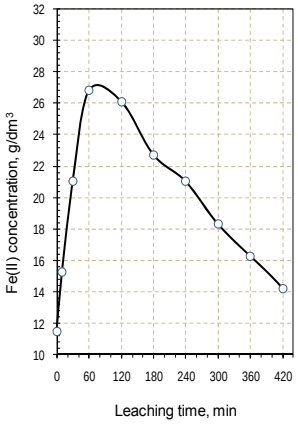

Fig. 12. Fe(II) concentration – leaching time during atmospheric leaching of Lubin concentrate in oxygenated sulphuric acid (50 g/dm^3). Solid/liquid = 1:8, Fe(III) conc. - 30g/dm^3, temperature 90^{o}C, oxygen flow rate – 30 dm^3/h

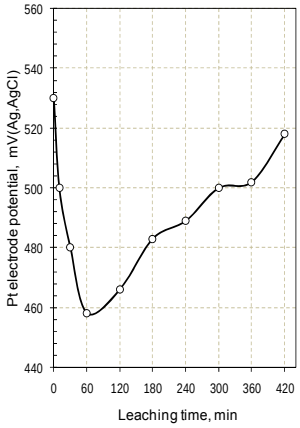

Fig. 13. Potential of Pt electrode – leaching time during atmospheric leaching of Lubin concentrate in oxygenated sulphuric acid (50 g/dm^3). Solid/liquid = 1:8, Fe(III) conc. - 30g/dm^3, temperature 90^{o}C, oxygen flow rate – 30 dm^3/h

The presence of bornite, chalcopyrite and pyrite–marcasite results in leaching of iron to the solution. Even if iron(III) were initially not introduced to the solution, its concentration after 7 hours of atmospheric leaching at 90^{o}C reached about 4.5 g/dm^3 (Fig. 10). When leaching process was performed in the iron(III) solution with initial concentration of 10 g/dm^3 the observed increase of Fe concentration was 8 g/dm^3 (Fig. 10). A similar increase of Fe(III) was observed during leaching at higher initial concentration of Fe(III) (Fig 11). The increase of concentration of iron(III) in leaching solution is undoubtedly beneficial for the copper leaching rate but the excess of Fe has to be reduced to an optimum level in downstream separation processes.

Two reactions take place during the examined process using iron(III) as a leaching medium. First is the leaching of copper or copper and iron with simultaneous formation of elemental sulphur and iron(II) ions (reactions 1–5). Second is the regeneration of Fe(II) to Fe(III) with gaseous oxygen (reaction 5). The rates of these processes are changing in the course of leaching and the momentary concentration of Fe(II) reflects their mutual relation (Fig. 12). In the first hour of the process leaching reaction rates are remarkably higher than regeneration of Fe(II) to Fe(III) and the concentration of Fe(II) increases rapidly. Subsequently, the leaching became slower than regeneration and Fe(II) concentration decreases with increasing concentration of Fe(III). Then, a favorable improvement of leaching conditions is observed.

The conditions of leaching can also be monitored by means of electrochemical measurements of potential of a Pt electrode immersed in the leaching slurry (Fig. 13). At the starting point of leaching the potential was 520 mV(Ag, AgCl). In parallel to the increase of Fe(II) (Fig. 12) a decrease of Pt electrode potential was recorded down to nearly 430 mV. After about 1-2 hours, when regeneration rate was higher that leaching rate, the potential of Pt electrode was found to increase.

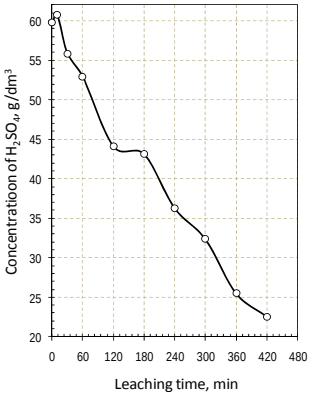

Fig. 14. Concentration of sulphuric acid during atmospheric leaching of copper concentrate at 90°C , initial concentration of Fe(III) – 30 g/dm^3, oxygen flow rate – 30 dm^3/h, and s/l - 1:4

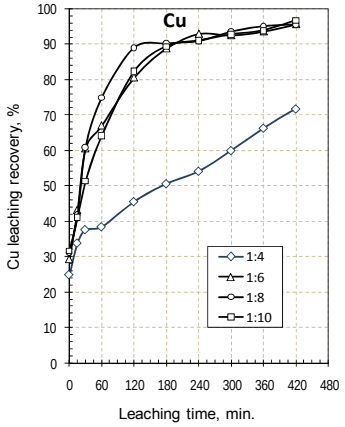

Fig. 15. Effect of s/l ratio on the recovery of copper during atmospheric leaching of Lubin concentrate in oxygenated sulphuric acid (50 g/dm^3), Fe(III) conc. - 30g/dm^3, temperature 90 °C, oxygen flow rate – 30 dm^3/h

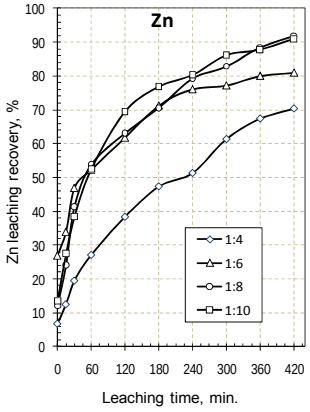

Fig. 16. Effect of s/l ratio on the recovery of zinc during atmospheric leaching of Lubin concentrate in oxygenated sulphuric acid (50 g/dm^3), Fe(III) conc. - 30 g/dm^3, temperature 90 °C, oxygen flow rate – 30 dm^3/h

Sulphuric acid concentration is a parameter which has also to be monitored in atmospheric leaching. In numerous literature data the initial concentration of H_2SO_4 is recommended at the level of 50 g/dm^3, as it was applied in this work. From the leaching reactions 1–4 we may assume that concentration of acid is expected to be constant. However, in the course of Fe(III) regeneration reaction (5), sulphuric acid is consumed. According to chemical analyses of acid concentration during leaching (Fig. 14), a decrease in the concentration by about 40 g/dm^3 was observed. The magnitude of the decrease can vary with leaching parameters.

The results of atmospheric leaching were summarized for the best leachable metals - copper and zinc in the form of leaching recovery–time relationships (Figs. 15 and 16). It is well seen that copper recovery exceeds 90% after about 180 minutes of leaching at 90°C and at 30 g/dm^3 of initial Fe(III). When the leaching time is 420

minutes the copper recovery reaches 95%. Zinc recovery was also surprisingly very high and reached 90% after 420 minutes of leaching. For both copper and zinc the s/l ratio from 1:6 to 1:10 is recommended. When s/l was 1:4 the efficiency of the process was to low to be acceptable.

4. Conclusions

Hydrometallurgy appears to be the only real chance for more rational utilization of the copper flotation concentrate of Lubin Concentrator. Hydrometallurgy, being more suitable for low grade feeds, can remarkably elevate copper recovery at ZWR Lubin and simultaneously produce metals, which are being have been lost for many years (Zn, Co, Mo, V). The advantageous chemical and mineralogical composition of the Lubin concentrate and easy access to sulphuric acid demonstrate the need for systematic and comprehensive research work on atmospheric and pressure leaching commenced at Wroclaw University of Technology in HYDRO Project.

Leaching time, temperature, iron(III) concentration and solid/liquid ration are key parameters for atmospheric leaching of Cu, Zn, Ni and Co from the copper flotation concentrate from Lubin Concentrator. When the leaching process is conducted for about 7 hours at 90^{o}C in oxygenated sulphuric acid acidic solution of Fe(III) at concentration of 20–30 g/dm^3 and at s/l from 1:6 to 1:10 it is possible to recover above 95% of copper and 90% of zinc even without additional grinding of the feed.

The leaching recovery of Ni and Co from under the same conditions appeared to be much lower (from 40 to 50%) due to dissemination of nickel and cobalt sulphides in the copper sulphides matrix. Elevation of Ni and Co recovery is possible by additional grinding of the leaching feed and optimization of leaching parameters.

Atmospheric leaching conditions can be monitored by means of analysis of Fe(II) concentration as well as by measurement of the Pt electrode potential in leaching slurry.

Acknowledgements

This work was carried out in the frame of HYDRO project (Polish NCBiR project contract ZBP/56/66309/IT2/10). Authors acknowledges the financial support given to this project by the NCBiR (National Center for Research and Development) under the IniTech Enterprise. We also wish to thank our various partners of the project for their contributions to the work reported in this paper.

References

Chmielewski T., Atmospheric leaching of shale by-product from Lubin concentrator, Physicochemical Problems of Mineral Processing, 41 (2007) 337-348.

Chmielewski T., Charewicz W., 2006, Hydrometallurgical processing of shale by-products from beneficiation circuits of Lubin Concentrator, In: Perspectives for applying boleaching Technology to process shale-bearing copper ores, BIOPROCOP'06, Lubin 2006, KGHM Cuprum, Wrocław 2006, 125-145.

Chmielewski T., Łuszczkiewicz A., Konieczny A., Kowalska M., Non-oxidative acidic treatment of copper sulfide concentrates in the flotation circuit, Proceedings of the 6th International Copper-Cobre Conference, Toronto, Canada 27-29 August 2007, Vol. II (del Villar R., Nesset J.E., Gomez C.O., and Stradling A.W. – Eds.), Can. Inst. Min. Metal. Petrol., 2007a, 53-62.

Chmielewski T., Łuszczkiewicz A., Konopacka Ż., 2007b, Separation and concept of processing of black shale copper ore from Lubin Mine, 7th International Conference on Non-ferrous Ore Processing, May 21-23,Wojcieszyce, Poland, KGHM Cuprum, Wrocław 2007, 171-184.

Chmielewski T.,2009, „Ługowanie atmosferyczne frakcji łupkowej jako alternatywa zmian technologicznych w ZWR Lubin", Materiały XII Seminarium Lubin 17 Lutego 2009 (str. 37).

Chmielewski T., Kaleta R., Galvanic interactions of sulphide minerals in leaching of flotation concentrate from Lubin Concentrator, Physicochemical Problems of Mineral Processing. 46 (2011) 21-34.

Dreisinger D., 2006, Copper leaching from primary sulphides: Options for biological and chemical extraction of copper, Hydrometallurgy, 83, 10-20.

Grotowski A., 2007, Possibilies and perspectives for implementation of hydrometallurgical methods in KGHM Polska Miedz S.A., Proc. VIII International Conference on Non-ferrous Ore Processing, Wojcieszyce (Poland), May 21-23, KGHM Cuprum Wroclaw 2007, 29-46.

Gupta C.K., Mukherjee T.K., 1990, Hydrometallurgy in extraction processes, Vol.. I and II, CRC Press.

Habashi F., 1999, Textbook of hydrometallurgy, Metall. Extract. Quebec.

Habashi F., 2005, Recent Advances in the Hydrometallurgy of Copper, Proc.Int. Copper Hydrometallurgy Workshop "Hydrocoper 2005" (Menacho J.M., Casas de Prada J.M., Eds.), Santiago, Chile, pp. 43-55.

Habashi F., 2007, Abandoned but not forgotten – the recent history of copper hydrometallurgy, The John Dutrizac Symposium on Copper Hydrometallurgy, Proceedings 6th International Copper-Cobre International Conference, August 3-20, 2007, Toronto, Canada, vol. IV, Met. Soc.

Jansen M., Taylor A., 2000, Key elements in the selection of sulphide leach processes for copper concentrate leaching, Alta Cu 2000, August 2000, Int. Proj. Dev. Serv. Pty Ltd.,

Konieczny A., Kasinska , 2009, Problemy Technologiczne I Techniczne Procesów Przeróbki Mechanicznej Rud Miedzi w Świetle Działalności i Roli Oddziału Zakładu Wzbogacania Rud KGHM, IX Międzynarodowa Konferencja Przeróbki Rud Metali Nieżelaznych, ICNOP Lądek Zdrój, 18 – 20 maj 2009.

Konstantynowicz-Zielinska J. 1990, Petrology and genesis of the copper shale of the Foresudetic Monocline. Rudy i Metale Niezelazne. Vol. 35, No. 5-6, 128-133 (in Polish).

Kubacz N., Skorupska B. 2007. Estimation of influence of organic carbon on concentration and smelting processes. Conf. Proc. VIII International Conference On Non-ferrous Ore Processing, ICNOP'07, 21-23 May, Wojcieszyce, Poland, KGHM, IMN, 157-166 (in Polish).

Luszczkiewicz A. 2004, Evaluation of upgradeability of the ore with elevated content of black shale Report of Investigation, Archive of Laboratory of Mineral Processing, Wroclaw University of Technology, Wroclaw, (in Polish).

Luszczkiewicz A., 2000, Utilisation of black copper shale ores from Lubin-Glogow region. in: Recent problems on copper ores processing in Poland, November 16, 2000., Conference Proceedings, Mining Committee of Polish Academy of Sciences and KGHM "Polish Copper", 137-156 (in Polish).

Luszczkiewicz A., Chmielewski T., 2008, Acid treatment of copper sulfide middlings and rougher concentrates in the flotation circuit of carbonate ores, Int.J.Min.Process 88, 45-52.

Luszczkiewicz A., Konopacka Z., Drzymala J., 2006, Flotation of black shale of Polish copper ore from Lubin. Proceedings: Perspectives for applying bioleaching technology to process shale-bearing copper ores, BIOPPROCOP '06, Lubin, June 19, 2006, Publ. KGHM Cuprum Sp. z O.O., Wroclaw 2006, 29-47, in Polish.

Łuszczkiewicz A., Drzymała J., 2009. Possibility of reduction of lead, arsenic and organic carbon content in copper concentrates. Physicochem. Prob. Min. Process., 44th Seminar, Niepołomice, Plenary Lecture (in Polish).

Łętowski F., 1975, Podstawy hydrometalurgii, WNT, Warszawa.

Marsden J.O., 2007e, Sulphate-based flowsheet options for hydrometallurgical treatment of copper sulphide concentrates, The John Dutrizac Symposium on Copper Hydrometallurgy, Proceedings 6th International Copper-Cobre Conference, August 25-30, 2007, Toronto, Canada, vol. IV, Met. Soc., pp.77-100.

Marsden J.O., Wilmot J.C., 2007a, Medium-temperature pressure leaching of copper concentrates – Part I: Chemistry and initial process development, Min. Metall. Processing, 24(4) 193-204,

Marsden J.O., Wilmot J.C., 2007b, Medium-temperature pressure leaching of copper concentrates – Part II: Development of direct electrowinning and acid-autogenous process, Min. Metall. Processing, 24(4) 205-217.

Marsden J.O., Wilmot J.C., 2007c, Medium-temperature pressure leaching of copper concentrates – Part III: Commercial demonstration at Bagdad, Arizona, Min. Metall. Processing, 24(4) 218-225.

Marsden J.O., Wilmot J.C., 2007d, Medium-temperature pressure leaching of copper concentrates – Part IV: Application at Morenci, Arizona, Min. Metall. Processing, 24(4) 226-236.,

Marsden, J., Brewer, B. and Hazen, N., 2003, Copper Concentrate Leaching Developments by Phelps Dodge Corporation, Hydro 2003, TMS Warrendale, 1429-1446.

Peacey J.I., Guo X.J., Robles E., 2003, Copper Hydrometallurgy – Current Status, Preliminary economics, Future Direction and Positioning versus Smelting, Copper 2003 - Cobre 2003, vol.VI, (Book 1) Santiago – Chile (Riveros P.A., Dixon D., Dreisinger D., Eds.), pp. 205-222.

Ramachadran V., Laksmanan V.I., Kondos P.D., 2007, Hydrometallurgy of copper sulphide concentrate, The John Dutrizac Symposium on Copper Hydrometallurgy, Proceedings 6th International Copper-Cobre Conference, August 25-30, 2007, Toronto, Canada, vol. IV, Met. Soc., pp.101-128.

Rydzewski A., 1996, Lithology of the deposit rocks. In: A. Piestrzynski (Ed.) Monography of KGHM Polska Miedź S.A., CPBM Cuprum Sp. z o.o. Publisher, Lubin, 137-141 (in Polish).

Tomaszewski J., 1985, The problems of the efficient utilization of copper- polymetalic ores in the Foresudetic Monocline. Physicochemical Problems of Mineral Processing, Vol. 17, 131-141 (in Polish)

Physicochem. Probl. Miner. Process. 47(2011) 207-212
www.minproc.pwr.wroc.pl/journal/

Physicochemical Problems of Mineral Processing
ISSN 1643-1049

Received March 16, 2011; reviewed; accepted April 27, 2011

Discrepancies in the assessment of CO_2 storage capacity and methane recovery from coal with selected equations of state

Part II. Reservoir simulation

Marcin A. LUTYNSKI **, Elisa BATTISTUTTA **, Hans BRUINING **, Karl-Heinz A.A. WOLF **

[*] Silesian University of Technology , Gliwice, Poland. Marcin.Lutynski@polsl.pl

[**] Delft University of Technology (TU Delft), Department of Geotechnology, Delft, The Netherlands

Abstract. Enhanced Coalbed Methane is a technology that helps mitigate CO2 emissions and at the same time recover methane from coal seams. Usually CO2 in coalbeds is stored under supercritical conditions and adsorption, as a crucial parameter, is responsible for the capacity of coalbed to store CO2. In the first part of this study three equations of state with the same set of experimental data were tested. In this study Langmuir parameters serve as an input data for the reservoir simulator. A sensitivity study for the two sets of Langmuir parameters and two permeability values was performed. Although differences in the results of simulation with Langmuir parameters calculated with PR and SW seem to be insignificant, on a larger field scale these discrepancies can be noteworthy. Improper calculation of sorption data may lead into a significant mismatch with field production.

keywords: enhanced coalbed methane, carbon dioxide sequestration, equation of state, sorption in coal

1. Introduction

Enhanced Coalbed Methane is a technology that helps mitigate CO_2 emissions and at the same time recover methane from coal seams. One of the crucial parameters of ECBM is CO_2 adsorption capacity which is measured in laboratory during sorption tests. Calculated model parameters from experimental sorption isotherms are later key input data for reservoir simulators. There are many commercially available simulators which are specifically design to model the CBM/ECBM problems (Law et al. 2002; Hower 2003; Jessen et al. 2007; Wei et al. 2007).

In part I of this study (Lutyński et al. 2011) sorption isotherm calculation with three equations of state as well as Langmuir model fitting was presented. The calculated Langmuir parameters V_L and P_L for Span and Wagner EoS were 0.03648 sm^3/kg and 0.597 MPa, respectively and for Peng Robinson EoS 0.03071 sm^3/kg and

0.406 MPa, respectively. As defined by the ECLIPSE software, cubic meter of gas at standard conditions, that is at 16°C and 1013.25 hPa, per unit mass of coal under *in-situ* conditions is given as sm^3/kg. Soave-Redlich Kwong EoS did not give satisfactory fitting and was rejected for further considerations.

In this study, we investigate the influence of Langmuir parameters calculated in the previous study from raw laboratory data on the results of reservoir simulations.

In order to assess the impact of the calculated parameters on the results of reservoir simulation sensitivity, study with the use of ECLIPSE 300 simulator was performed. The software selected for the study is a three dimensional compositional simulator with a Coalbed Methane option. Basic features of this software are as follows: darcy flow of gas and water in the natural fracture system, adsorption/diffusion of two different gas components at the coal surface, diffusive flow between matrix and natural fracture system, and shrinkage/swelling of coal matrix due to desorption/adsorption of gases.

2. Simulation input data

Simulation grid (Fig. 1) and some of the parameters (e.g. relative permeability) were same as problem set 2 considered by Law et al. (2002). Other input data (depth, permeability, etc.) were typical for the coal basins in Europe. Swelling coefficient and methane sorption capacity were experimentally measured in a laboratory for the same Selar Cornish coal and compared with Durucan et al. 2009.

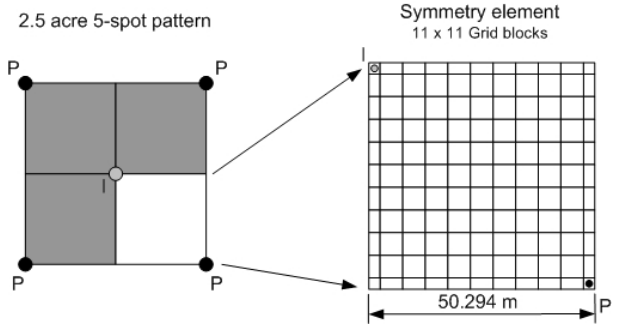

Fig. 1. Schematic diagram of grid system used in simulations

Major input parameters and coalbed characteristics are presented in table 1. The simulation were run for two values of permeability 1.5 md (milidarcy) and 20 md representing tight European coals and permeable US coalbasins respectively.

First case with fracture permeability of 1.5 md considers continuous CO_2 injection and CH_4 production for the period of 730 days whereas the second case (20 md) for the period of 365 days.

Injection rate (full well) was set as 36 000 sm^3/d for the first case (1.5 md) and 120 000 sm^3/d for the second case (20 md). Maximum bottomhole pressure of 15.0

MPa and maximum gas production rate of 20 000 sm^3/day (1.5 md case) and 100 000 sm^3/day (20 md case) were constraints.

In Figures 2 and 4 the results of gas production simulation are presented for both study cases (i.e. 1.5 md and 20 md). In case of low permeability case initial gas production rate calculated with PR is slightly higher than obtained with SW. The difference is insignificant (below 3%) although by the time when CO_2 concentration in the production well is higher than CH_4 the difference is increasing to 13%. These discrepancies are different in case of high permeability case. At the initial stage total gas production is higher in case of SW Langmuir parameters whereas after CO_2 breakthrough the total gas production rate is higher in case of parameters calculated with PR EoS. Figures 3 and 5 present mole fractions of gases in production wells. In either case CO_2 breakthrough time is shorter for the parameters calculated with SW EoS – for the high permeability case the difference is 6 days whereas for the low permeability case this difference is 46 days.

Table 1. Reservoir parameters and mechanical properties of coal used in the sensitivity study simulation

Parameter	Value	Unit
Reservoir properties and initial conditions		
Coal seam depth	1000	m
Coal seam thickness	9	m
Fracture porosity	0.01	-
Temperature	45 (318.15)	°C (K)
Pressure	9.0	MPa
Gas saturation/Water saturation	0.6/0.4	-
V_L (CH_4)	0.024457	sm^3/kg
P_L (CH_4)	0.72	MPa
Mechanical properties of coal		
Young's modulus (E)	2.165	GPa
CO_2 swelling coefficient	1.02	kg/m^3
CH_4 swelling coefficient	0.47	kg/m^3
Mechanical compliance	$40.10 \cdot 10^{-6}$	MPa^{-1}

Higher production rates obtained with SW EoS in the 20 md case at the initial stage can be explained by higher value of calculated V_L parameter. The influence of coal swelling during CO_2 is not that significant in case of high permeability. Therefore, CO_2 injection notably boosts methane production rates. For low permeability coal seams coal matrix swelling plays an important role and inhibits CO_2 migration within the coal. In such case the higher adsorption the bigger swelling and

permeability decrease. This effect was observed for laboratory experiments with the same Selar Cornish coal (Mazumder and Wolf 2008). Accuracy of calculated Langmuir parameters has in this case a major impact on the coal matrix swelling as the Palmer-Mansoori compositional model accounts for this effect (Palmer and Mansoori 1998).

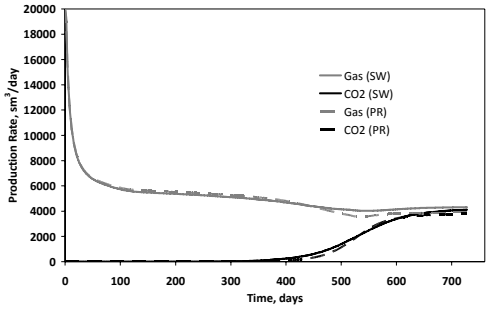

Fig. 2. CO_2 and total gas production rate for 1.5 md permeability case

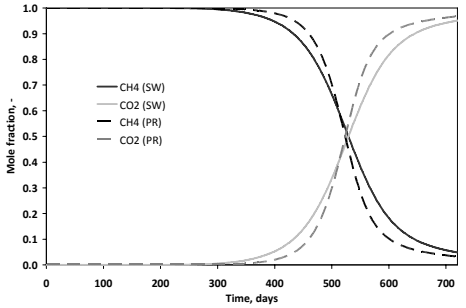

Fig. 3. Production gas composition for 1.5 md permeability case

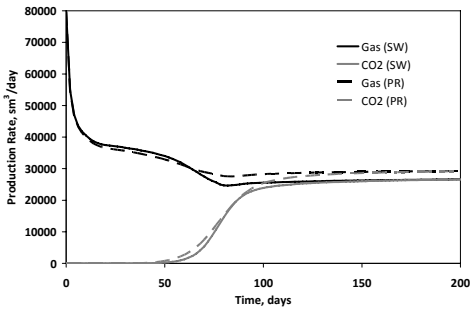

Fig. 4. CO_2 and total gas production rate for 20 md permeability case

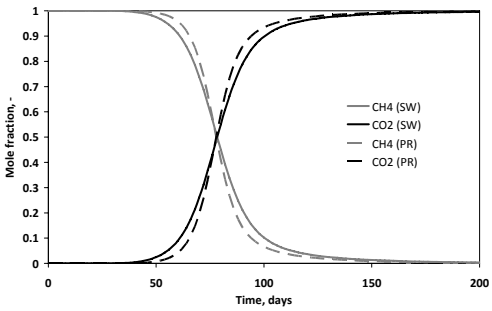

Fig. 5. Production gas composition for 20 md permeability case

3. Conclusions

From the above study it can be concluded that although differences in the results of simulation with Langmuir parameters calculated with Peng-Robinson and Span and Wagner seem to be negligible, on a larger field scale these discrepancies can be significant. More accurate calculation of gas sorption on coal can gives a better fit for history matching. The results of simulation show that selection of representative coal sample for the sorption experiments might be a crucial issue as slight differences in Langmuir parameters are reflected in production rates even for a small area.

Acknowledgments

The research was conducted under Marie Curie RTN GRASP Project (Greenhouse gas Removal Apprenticeship and Student Program). The authors of this

study would like to thank Prof. Sevket Durucan and Dr. Caglar Sinayuc from Imperial College London for their help and input to this study.

References

Durucan S., Ahsanb M. and Shia J.Q. (2009). Matrix shrinkage and swelling characteristics of European coals. Energy Procedia Vol. 1, Issue. 1. p. 3055-3062.

Hower T.L. (2003). Coalbed Methane Reservoir Simulation: An Evolving Science. SPE Annual Technical Conference and Exhibition. Denver, Colorado, Society of Petroleum Engineers.

Jessen K., Lin W. and Kovscek A.R. (2007). Multicomponent sorption modeling in ECBM displacement calculations. SPE-110258. Proceedings - SPE Annual Technical Conference and Exhibition, Anaheim, CA, November 11 - 14, 2007

Law D.H.-S., Meer L.G.H.v.d. and Gunter W.D. (2002). Numerical Simulator Comparison Study for Enhanced Coalbed Methane Recovery Processes, Part I: Pure Carbon Dioxide Injection. SPE Gas Technology Symposium. Calgary, Alberta, Canada, Copyright 2002, Society of Petroleum Engineers Inc.

Lutyński M., Battistutta E., Bruining H., Wolf K-H.A.A. (2011). Discrepancies in the assessment of CO2 storage capacity and methane recovery from coal with selected Equations of State. Part I - Experimental isotherm calculation. Physicochemical Problems of Mineral Processing 47, 159-168.

Mazumder S. and Wolf K.H. (2008). Differential swelling and permeability change of coal in response to CO_2 injection for ECBM. SPE Asia Pacific Oil and Gas Conference and Exhibition 2008 - "Gas Now: Delivering on Expectations".

Palmer I. and Mansoori J. (1998). How Permeability Depends on Stress and Pore Pressure in Coalbeds: A New Model. SPE Reservoir Engineering (Society of Petroleum Engineers) 1(6): 539-543.

Wei X.R., Wang G.X., Massarotto P., Golding S.D. and Rudolph V. (2007). A Review on Recent Advances in the Numerical Simulation for Coalbed-Methane-Recovery Process. SPE Reservoir Evaluation & Engineering 10(6): pp. 657-666.

Lutynski, M.A., Battistutta, E., Bruining, H., Wolf, K.A.A., Rozbieżności w ocenie ilości składowanego CO2 i odzysku metanu z pokładu węgla jako wynik zastosowania wybranych równań stanu gazu. Część II . Symulacje złożowe, Physicochem. Probl. Miner. Process., 47 (2011) 207-212, (w jęz. ang.)

Intensyfikacja wydobycia metanu z pokładu węgla za pomocą zatłaczania dwutlenku węgla jest technologią, która nie tylko przyczynia się do zwiększenia uzysku tego surowca energetycznego ale jednocześnie zmniejsza emisję CO_2. Pojemność pokładu węglowego jako zbiornika CO_2 wyznacza się na podstawie badań sorpcji w laboratorium. Zaadsorbowany w matrycy węglowej CO_2 znajduje się w stanie krytycznym i pomiar jego sorpcyjności jest istotnym czynnikiem, który determinuje wykorzystanie danego pokładu węgla jako zbiornika tego gazu. W pierwszej części studium dokonano analizy wpływu zastosowanego trzech równań stanu gazu tj. równania Penga-Robinsona (PR), równania Soave-Redlicha-Kwonga (SRK) oraz bardzo dokładnego równania stanu gazu dla CO_2 Spana i Wagnera (SW), jako

równania referencyjnego na obliczenie pojemności sorpcyjnej tego gazu na węglu na podstawie tych samych danych eksperymentalnych. Wyznaczone parametry Langmuira posłużyły jako dane wejściowe do symulatora złożowego. W celu określenia wpływu obliczonych parametrów Langmuira na uzysk metanu wykorzystano symulator złożowy ECLIPSE 300 z opcją Coalbed Methane. Symulacje przeprowadzono dla dwóch wartości przepuszczalności pokładu węgla: 1.5 md reprezentującej niskoprzepuszczalne węgle europejskie oraz 20 md reprezentującej wysokoprzepuszczlane węgle północnoamerykańskie. Z przeprowadzonych analiz wynika, że wyznaczenie parametrów izotermy Langmuira dla danych obliczonych za pomocą równania stanu gazu PR zawyża dzienny uzysk gazu w początkowym okresie produkcji w przypadku pokładu o przepuszczalności 1.5 md, natomiast w przypadku pokładu o przepuszczalności 20 md produkcja w początkowym okresie jest zaniżona. Pomimo, że różnice w uzysku gazu dla parametrów Langmuira obliczonych z równania PR i SW wydają się być niewielkie w przypadku większej skali rozpatrywanego problemu różnica ta może być znacząca.

słowa kluczowe: intensyfikacja wydobycia metanu, sekwestracja dwutlenku węgla, równanie stanu gazu, sorpcja na węglu

Physicochem. Probl. Miner. Process. 47(2011) 213-228
www.minproc.pwr.wroc.pl/journal/

Physicochemical Problems of Mineral Processing
ISSN 1643-1049

Received April 4, 2011; reviewed; accepted April 26, 2011

Dry magnetic separation of olivine sand

Rolf Arne KLEIV, Maria THORNHILL

Dept. of Geology and Min. Resources Eng., Norwegian University of Science and Technology, N-7491 Trondheim, Norway. maria.thornhill@ntnu.no

Abstract. This paper investigates the potential for using dry magnetic separation to reduce the chromium content of a dried high quality olivine sand product in order to meet with anticipated future quality demands. The original feed contained 0.28-0.29% Cr_2O_3 of which approximately one third occurred as chromite and two thirds as chlorite. Two stage Permroll separation (at 0.50 T (max) and 0.92 T (max)) produced a concentrated product containing 0.13% Cr_2O_3 at a product recovery of 85.28%, thus reducing the chromium content by 55%. Some 80% of this reduction was achieved as a result of the first separation stage where chromite reported to the magnetic tailings at a recovery close to 100%. The chromium remaining in the concentrated product must be attributed to chlorite. Leachates obtained from leaching tests performed on the feed and the products were characterised by very low chromium concentrations, and the results suggest that chromium is more easily released from chlorite than chromite. This study shows that dry magnetic separation could be considered when a reduction of the chromium content of dried high quality olivine sand products is required.

keywords: magnetic separation, Permroll, olivine, chromium, chromite, chlorite

1. Introduction

Due to its many favourable properties, olivine ($(Mg,Fe)_2SiO_4$) is a versatile industrial mineral which has found a number of uses. However, when excluding the domestic Japanese use of olivine for civil engineering purposes, the majority of the world's olivine production is consumed as slag conditioner by the metallurgical industry where the mineral is exploited for its high magnesium content (Skillen, 1995; Harben, 1999; Rudi, 2001, Roberts, 2008). Slag conditioner is a low-cost bulk commodity subject to relatively tolerant product specifications, and volume rather than grade has been seen as the key to success. Hence, the production lines comprise comminution and sizing, but little or no beneficiation. However, increasing competition, relatively low olivine prices and strong dependence on the fortunes of a single market have been an incentive for producers to diversify their product range. Entering into novel markets, producers are now facing a new set of specifications

reflecting stricter demands on quality. As a consequence, mineral separation could to a greater extent become part of the production process.

Commercially, the term olivine could represent a range of different rock types including dunites, peridotites, serpentinites and sometimes even calcined products. Applying a mineralogical definition, olivine usually designates members of the continuous magnesium-iron solid solution series bound by the end-members *forsterite* (Mg_2SiO_4) and *fayalite* (Fe_2SiO_4) (Bowen and Schairer, 1935). The composition of olivines is frequently expressed in terms of the relative molar content (%) of forsterite (Fo_x) or fayalite (Fa_{100-x}). Forsterite (i.e. Fo_{90} to Fo_{100}) accounts for approximately 85% of commercial olivine (Harben, 1995; Roberts, 2008) and is predominantly produced from dunite, a rock defined as containing more than 90% olivine. In addition, dunites usually contain a range of accessory minerals such as enstatite, augite, anthophyllite, clinoamphiboles, talc, serpentine, phlogophite, chlorite and chromite. As a result, the overall chemical composition of the material could comprise heavy metals and other trace elements not found in the olivine lattice itself. This is the case for chromium, which is commonly present as chromite ($(Mg,Fe)Cr_2O_4$), in chlorite ($(Mg,Al,Fe,Cr)_{12}[(Si,Al)_8O_{20}](OH)_{16}$) or in even smaller amounts as a substitution element in the structures of amphiboles or phlogophites.

As explained in the first paragraph, olivine ores are subject to little or no beneficiation. However, some attempts have been made to reduce the Loss On Ignition (LOI) value of the product to improve the thermal stability of olivine sand used for foundry purposed. The LOI value (i.e. the relative weight loss when the sample is kept at 900°C for 30 min) can be attributed to the presence of minor amounts of chlorite and serpentine. Due to the flaky nature of the chlorite, dust removal by air classification (e.g. simple zig-zag sieves or classifiers) can produce a significant reduction of LOI value of sieved olivine sand products, typically from a value of 2% to 0.5% for a high quality olivine ore (Kleiv, 2001). At Åheim, the world's largest commercially exploited olivine deposit, some 5-10% of the feed to the sieving plant is removed as fines by air sweeping during sieving (Kleiv, 2001). Chmelar et al. (2003) used a SINTEF forced vortex Air Classifier to retrieve the olivine fraction from the fines, and demonstrated that the technology can be used to produce a fine sand product low in chlorite. The LOI value is closely correlated with content of aluminium, calcium and alkali oxides which are also unwanted in metallurgical applications. A successful alternative to air classification in order to lower the content of the latter constituents have been reported by Grishin et al. (2000) who used dry magnetic separation to produce a concentrated olivine middlings product. As for attempts to lower the chromium content of the olivine sands, little is reported in literature. As chromium frequently occur in olivine sands in both chromite and chlorite, air classification and magnetic separation could be considered.

During the last two decades, a number of new olivine applications have been developed based on the mineral's potential environmental benefits. This includes olivine for water treatment as an adsorbent for heavy metals (El Aamrani et al., 2002;

Kleiv and Sandvik 2002; Kleiv and Thornhill 2004, Bhakhar, 2006), dissolved natural organic matter (NOM) and microbial pathogens (McMeen and Benjamin, 1997), as well as olivine for the neutralisation of acid mine drainage (Morales and Herbert 2001; Kleiv and Thornhill, 2004, 2008) or waste acids (Schuiling, 1986; Herk et al., 1989; Jonckbloedt, 1998). Research is also being conducted on the use of olivine as a catalyst for the breakdown of tars in fluidised bed combustion reactors (Devi et al., 2005) and as an agent for carbon dioxide sequestration (Haug, 2010, and references within).

Some of these applications represent low cost bulk products, but others have the potential of becoming highly priced commodities that could easily defend the costs of additional beneficiation in order to meet with more stringent quality demands. This is particularly the case for the adsorbents and the catalysts, i.e. applications basing their value on the surface properties of the mineral rather than those of its bulk. Heavy metal adsorbents based on pellets, granulates or size fraction combining high reactivity with the necessary permeability could obtain prices up to several hundred USD per tonne. These environmental applications, including the somewhat lower priced olivine sand and olivine fines used for capping of polluted sediments as well as passive treatment of acid mine drainage and industrial seepage, represent a growing sector and are the focus point of this study.

Products used in water treatment or for environmental applications must in themselves be very low in heavy metals and other detrimental substances in order for their use to be approved by the relevant governmental regulatory bodies. Recently there has been growing concern with respect to the chromium content of olivine commodities and several new products are likely to face stricter compliance limits in the future. For both precautionary and practical reasons, regulatory limits are often based on the total contents of the substance in question and take little or no account of its state of occurrence or real potential for harm. Hence, even producers facing limitations on truly harmless products could, when possible, find it easier to perform the necessary separation rather than to fully verify their innocuous nature. As an example, the Norwegian Waste Directive (NME 2004) uses an elemental concentration limit (hereby referred to as the NWD-limit) of 0.1% for selected metals (corresponding to 0.146% Cr_2O_3) to determine whether a waste product should be classified as hazardous or not. Prior to depositing (or recycling) spent olivine based adsorbents and saturated filter media will probably have to comply with these limits as they no longer can be classified as production waste form mining, but will be subject to new classification and evaluation. Hence, in lack of concrete application specific limits for the new line of products, the NWD-limits could be used as a reference point and a preliminary target for the chromium concentration of olivine sand for environmental purposes.

To facilitate the strategy outlined in the previous paragraph, this paper investigates the potential for using dry magnetic separation to lower the chromium content in a high quality olivine sand product. The olivine sand in question is a dried

and sieved standard product with a size distribution that is directly applicable for a several new high price applications. This would represent a typical situation for a number of producers working to expand their product portfolio. Consequently, a dry beneficiation method is preferred where the separation is performed on the material 'as is' without any preceding comminution.

Traditionally, the development of olivine applications has been spurred by the olivine producers (Kleiv, 2001), and it is here the results presented in this paper could be utilised. However, due to the interdisciplinary nature of the new environmental products and applications (spanning from mineralogy, surface science and geochemistry to toxicology and civil engineering), cooperation with research institutions, universities and consultancy firms will usually be required to achieve results. Such cooperation is also necessary to get access to the new markets as these can be very divers and governed by different mechanism than the traditional olivine markets. As an example, target customers for olivine based adsorbents would include both industry and public authorities with markets ranging from municipal water treatment plants, treatment of acid mine drainage problems from disused mines, run off from shooting ranges, metallurgical industry, sand blasting facilities, garages and tool shops, as well as remediation of polluted soil and sediments.

2. Materials and methods

2.1. Chemical and mineralogical analysis

The chemical composition of solid samples was determined by x-ray fluorescence (XRF) analysis using a Bruker AXS S8 Tiger wavelength dispersive spectrometer. Main element and trace element analysis were obtained using pressed powder disks and glass disks, respectively. All analyses were calibrated against dunite standards. Analytical detection (i.e. qualitative analysis) of specific mineralogical phases was obtained through X-ray powder diffraction analysis (XRD), using a Bruker D8 Advance diffractometer with a Krystalloflex K780 generator, scanning from 2° to 70° (2θ) with monochromatised CuK_{α} radiation. The pulverised material required for the XRF and XRD analysis was produced by 30 s milling in a Siebtechnik agate disk mill. Great care was taken to minimise the risk of cross-contamination between samples.

The chemical composition of filtrates from the leaching test were analysed by inductively coupled plasma mass spectrometry analysis (ICP-MS) using a PerkinElmer DRCII ICP-MS equipped with a dynamic reaction cell.

2.2. The original olivine sand sample

The olivine sand used in this study was kindly supplied by the Norwegian mining company *A/S Olivin* and originates from the production plant at Åheim in western Norway. The material is a standard foundry sand produced by crushing, drying and sieving the dunite ore. Prior to sieving, are removed by air sweeping, thus

leaving a purified product containing almost 95% forsterite olivine. The particular foundry sand used in this study consists of well sized material ranging from d_5 = 150 µm to d_{95} = 390 µm. The original sample was delivered as a single 25 kg bag. All subsamples used for characterisation or separation experiments were carefully split out from this batch.

Table 1. Feed assay obtained from XRF analysis

Constituent	Assay, %
MgO	49.7
SiO_2	41.5
Fe_2O_3	7.23
Al_2O_3	0.72
NiO	0.33
Cr_2O_3	0.29
CaO	0.26
MnO	0.09
K_2O	0.03
Na_2O	0.01
LOI	0.29
Sum	100.45

The geology, mineralogy and mineral chemistry of the Almklovdalen ultramafic massif from which the olivine sand originates has been described in detail by Osland (1998). The 8 km^2 ring-shaped exposure of the massif displays a continuous layering of dunite, chlorite-bearing and chlorite dunite, blastogranular dunite and Fe-rich eclogites. Whereas the composition of the olivine exhibits a slight variation through the different layers with MgO contents ranging from 48% to 51% in the dunites, its average composition can be represented by $Mg_{1.86}Fe_{0.14}SiO_4$ (i.e. Fo_{93}). In addition to the olivine, the dunites also contain minor quantities of accessory minerals such as chlorite, enstatite, calcic amphiboles, serpentine, talc, and chromite. Table 1 shows the chemical composition of the original olivine sand sample as obtained from XRF analysis.

Based on these results, employing the mineralogical data and the principles and assumptions described in section 2.6, the respective content of chlorite and chromite in the original olivine sand sample was found to be approximately 5.3-5.6% and 0.1-0.2%. This suggests that approximately one third of the total chromium content can be attributed to chromite.

2.3. Frantz separation

To provide an initial assessment of the relative magnetic susceptibility distribution of the original olivine sand sample a standard Frantz LB-1 isodynamic laboratory magnetic separator was used to produce a total of nine successively less

magnetic fractions from a feed sample of 988 g. Each successive magnetic fraction was obtained from a single pass. The nine fractions were all subjected to XRF analysis. The separator was operated with a side slope of 7° and a forward tilt of 10°.

2.4. Permroll separation

A 6555 g subsample of the original olivine sand sample was subjected to dry magnetic separation in two stages using two laboratory Permroll separators with different effective field strengths. The diameter and width of the rolls were 90 mm diameter and 130 mm, respectively. Based on the results from the Frantz separation (see section 3.1), the separation flowsheet (Fig. 1) was designed to produce a cutpoint at either end of the susceptibility range, thus producing a concentrated olivine product.

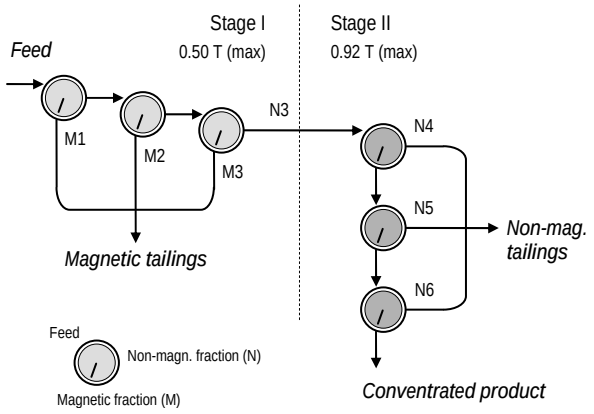

Fig. 1. Flowsheet for Permroll separation

The effective field strengths of the separators were estimated using a Hirst GM05 Gaussmeter equipped with a transverse P3110 Hall effect probe. The respective maximum flux densities of the stage I and stage II separators, as measured on the belt, were found to be approximately 0.50 T and 0.92 T.

The first separation stage, removing the magnetic tailings, consisted of three consecutive runs where the nonmagnetic fraction (i.e. as defined by the separation) from the first became the feed to the next. The mass of the magnetic fraction from each run (M1 to M3) was determined before the subsamples were split out for XRF-analysis. The remaining mass was mixed in the correct proportions to achieve a combined magnetic tailings product that could be submitted to the leaching test. The remaining nonmagnetic fraction (N3) reported to the second separation stage where the separation was conducted according to the same pattern, but with the removal of the consecutive nonmagnetic (N4 to N6) rather than magnetic fractions. As with the first separation stage, the mass of these outputs was determined and analytical samples were obtained before the material was recombined.

Prior to each of the two stages the position of the separating knife and the speed of the separator were adjusted until a clear cut was produced at the desired cut point. During the first stage the separator was operated at a speed of 120 rpm, whereas a speed of 190 rpm was used during the second stage. The feed rate was kept constant at 120 kg/h per metre roller width during both stages.

2.5. Leaching tests

In order to determine the effect of the magnetic separation on the leaching potential of the concentrated product as well as to assess the relative mobility of chromium in the different separation products, the original feed, the concentrated product and the two combined tailings materials were all subjected to a leaching test according to the procedure given in EN-12457-2 (CEN, 2002). This is a compliance test that was originally developed for the testing of waste materials. Due to its simplicity, variations of the test have later been used for range of purposes.

The leaching tests were performed using clean HDPE bottles as reactors by mixing 90 g of dry solid sample with 900 cm^3 of distilled water, thus establishing a liquid to solid ratio of 10:1. The resulting suspensions were agitated at room temperature for 24 hours using an end-over-end sample agitator. On completion of the agitation period, the pH of the suspensions was determined using a Metrohm 713 pH Meter equipped with an Aquatrode Plus combined glass electrode (spherical bulb). A 10 cm^3 sample of each suspension was then retrieved by syringe and filtered using serially connected disposable 0.45 μm and 0.20 μm syringe filters. The filtrates were collected in glass vials and acidified by adding 20 μl of 65% suprapure nitric acid. Finally, the filtrates were analysed using the ICP-MS technique as described in section 2.1. Great care was taken to minimise the risk of contamination throughout the test and during the subsequent handling of the filtrates.

2.6. Estimating mineralogical composition

To aid in the interpretation of the separation results, the content of chlorite and chromite in each sample was estimated based on its chemical assay and the average chemical composition of each mineral. These calculations were based on the simplifying assumption that chlorite and chromite were the only minerals present that contribute significantly to the total amount of aluminium and chromium that can be found in a sample. As shown by Osland (1998), this is truly the case for chromium, whereas aluminium could also occur in minor amounts in calcic amphiboles or in phlogophite. The contribution from the latter could be ignored as significant amounts of this mineral would produce elevated potassium assays, a feature not encountered in any of the samples. A small amount of calcic amphibole was probably present as indicated by the 0.26% CaO found in the feed. However, as the amphibole most likely would report to the non-magnetic tailings due to its low iron content (approximately

2% FeO_{tot}), the simplifying assumption was expected to be reasonable when applied to the feed or to fractions where chromite is present.

Based on microprobe analysis, Osland (1998) found that the Cr_2O_3 content in the chromite varied from 51% to 62% with 58% as an estimate of the average. The analysis also showed 26-31% FeO_{tot} and 6-9% MgO, whereas the average chromite contained approximately 3.7% Al_2O_3 (varying from 2.4% to 4.2%). The chlorite contained on average 3.6% Cr_2O_3, with values ranging from 3.1% to 4.3%, whereas the estimated average Al_2O_3 content was found to be 13.6% (varying from 12% to 15%). The chlorite also contained some 2-3% FeO_{tot} and 33-34% MgO.

The relative error between the true assay a_i of a sample (i.e. the assay value for oxide i obtained from XRF analysis) and the assay value that can be calculated by assigning values to the samples content of chlorite and chlorite can be defined as:

$$\varepsilon_i = \frac{a_i - \sum_j g_{ij} x_j}{a_i} \quad , \tag{1}$$

where x_j is the relative amount of mineral j in the sample and g_{ij} is the assumed average concentration of oxide i in mineral j. The best estimates for $x_{chlorite}$ and $x_{chromite}$ where found by minimising the sum of $(\varepsilon_i)^2$ for the two oxides Al_2O_3 and Cr_2O_3. Note that estimates are given to two decimal places simply in order to facilitate internal comparison, and that his does not in any way reflect their level of accuracy. The reported values must only be seen as semi-quantitative estimates.

3. Results and discussion

3.1. The magnetic properties of the feed

Table 2 presents the complete data from the Frantz separation, including the current applied during separation, the assays of each successive fraction and the estimated mineralogy derived from the latter. Note that the estimates for the contents of chlorite and chromite are calculated directly from the assays of each respective fraction, and that no attempt has been made to achieve a normalised mineralogical mass balance. From the data displayed in Table 2 it is clear that chromium is enriched in the fractions at either end of the magnetic susceptibility range, with some 30% of the total content found in the most magnetic fraction representing only 5% of the total mass. This feature is illustrated in Fig. 2 where the cumulative chromium distribution is shown. Note the logarithmic scale of the ordinate axis.

The estimated mineralogy suggests that chromium reports to the most magnetic fractions and that the least magnetic third of the material is virtually chromite free. Chlorite shows the opposite trend, although some chlorite appears to occur in every fraction. The relative estimation error ε_i is very low for the six first fractions, i.e. as long as chromite is present. Beyond this point, the estimated mineralogy will underestimate the aluminium content of the material. Here, as expected, the

assumption that chlorite represents the only significant aluminium-bearing mineral is no longer valid.

A simple qualitative XRD analysis was performed on the original olivine sand sample (i.e. the feed) and the F1, F5 and F9 fractions. The results supported the picture displayed by the estimated mineralogy as it was impossible to detect chromite in the F9 fraction, whereas chlorite could be detected in all the analysed samples. Chromite was clearly enriched in the F1 fraction and marginally present in F5 and the feed. The many overlapping diffraction peaks of forsterite and the fact that both chlorite and chromite only occur as trace minerals made it impossible to use XRD as a tool to quantify mineralogy. Hence, in spite of its obvious flaws, the model described in section 2.6 provides a better initial estimate.

Table 2. Results from Frantz separation. The chemical composition is obtained from XRF analysis

Fraction	Current[a] [A]	Mass distr. [Cum.%]	Cr distr. [Cum.%]	Chemical composition [%Al_2O_3]	[%Cr_2O_3]	Estimated mineralogy [%chlorite]	[%chromite]	Relative error ε_i [%] in Al_2O_3	in Cr_2O_3	% Cr as chromite
F1	0.230	0.50	12.3	2.03	7.39	11.40	12.96	0.0	0.0	94.8
F2	0.293	4.35	28.9	0.39	1.30	2.30	2.10	0.1	0.1	93.6
F3	0.311	10.38	37.4	0.33	0.42	2.27	0.58	0.1	-0.4	80.5
F4	0.318	23.79	46.8	0.54	0.21	3.93	0.12	-0.2	0.5	33.0
F5	0.339	47.33	63.4	0.51	0.21	3.72	0.13	0.1	-0.3	36.0
F6	0.358	71.95	80.1	0.74	0.20	5.42	0.01	-0.3	0.5	2.9
F7	0.381	93.64	94.9	0.98	0.20	6.17	0	-14.4	11.1	0
F8	0.400	96.50	97.0	1.34	0.23	7.41	0	-24.8	16.0	0
F9	0.410	100	100	1.89	0.26	8.64	0	-37.8	19.6	0

[a] Applied current during separation

The bipolar chromium distribution must be attributed to the differences in specific magnetic susceptibility between the two chromium-bearing minerals and the olivine itself. The mass magnetic susceptibility of olivine is known to be a function of the mineral's iron content, with the fayalite (Fe_2SiO_4) end-member being the most magnetic. Hopstock (1985) gives a range of $0.11–1.26\cdot10^{-6}$ m^3/kg, whereas Grishin et al. (2000) reports a value of $0.226\cdot10^{-6}$ m^3/kg for Fo_{92}. In a more recent study, Belley et al. (2009) found that the pure forsterite (Mg_2SiO_4) end-member is diamagnetic and suggests a range from $-6.8\cdot10^{-10}$ m^3/kg to $1.10\cdot10^{-6}$ m^3/kg. However, as shown by Belley et al. (2009), the susceptibility does not vary linearly with iron content and the interpolated approximate value of $0.15\cdot10^{-6}$ m^3/kg for Fo_{93} is in agreement with the data presented by Hopstock (1985) and Grishin et al. (2000). Turning to chromite, the reported values for mass magnetic susceptibility shows a much wider range, clearly reflecting the compositional variation that can be found within the spinel structure. As pointed out by Svoboda (1987), the existence of contradictory reports prevents a

simple correlation with the mineral's magnetite content (i.e. the content of ferric iron). Whereas Hopstock (1985) reports a very narrow range of $0.32\text{-}0.38 \cdot 10^{-6}$ m^3/kg, Svoboda (1987) presents a range of values starting at $0.5 \cdot 10^{-6}$ m^3/kg spanning four orders of magnitude. Mass magnetic susceptibility values for chlorite proved difficult to obtain. Grishin et al. (2000) does not give direct information, but provides values for phlogophite and muscovite (i.e. other sheet silicates) that are 55-85% lower than that of Fo_{92}. In their study on magnetic separation of olivines form the Kola peninsula, Grishin et al. (2000) found that all the accessory minerals apart from magnetite where less magnetic than the forsterite olivine.

Based on the results from the Frantz separation, the separation results reported by Grishin et al. (2000) as well as the susceptibility data reported in literature, it was reasonable to assume that magnetic separation could be employed to produce a concentrated Fo_{92} olivine middlings product with chromite reporting to the magnetic tailings. The results of Table 2 suggest a considerable overlap in magnetic susceptibility between the olivine and the chromium-bearing minerals, particularly in the case of chlorite, but it must be kept in mind that the successive fractions are obtained from a single pass at each step in the current applied to the separator. An even more polarised distribution was expected from the Permroll separation where three successive runs would be conducted at each cut point.

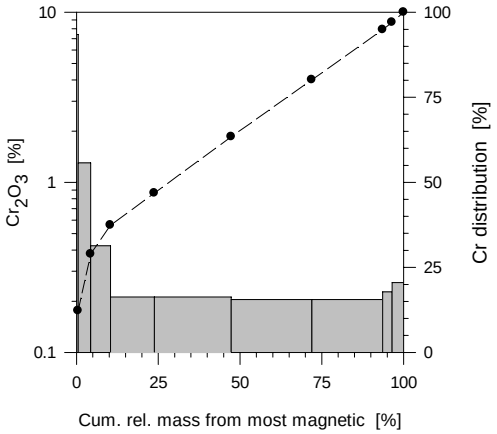

Fig. 2. Chromium distribution obtained from Frantz separation

3.2. The effect of Permroll separation

The results from the Permroll separation are shown in Table 3. Here, the chemical composition of the feed and the two (combined) tailings products is calculated based on the analysis of the recovered product and the yields and assays of the respective fractions from each individual run (i.e. M1 to M3 and N4 to N6). As shown in Table 3, the data set displays a fair agreement between the calculated and analysed feed composition. The total loss of material during separation was found to

be 0.23%. As with the results from the Frantz separation, no attempt has been made to achieved a normalised mineralogical mass balance.

Table 3. Results from Permroll separation. The chemical composition is obtained from XRF analysis unless otherwise indicated.

Process stream	Mass distr.[a] [%]	Cr distr.[a] [%]	Chemical composition [% Al_2O_3]	[% Cr_2O_3]	Estimated mineralogy [% chlorite]	[% chromite]	Relative error ε_i [%] in Al_2O_3	in Cr_2O_3	% Cr as chromite
Feed (analysed)	-	-	0.72	0.29	5.27	0.17	0.4	-0.6	34.2
M1	3.29	41.0	0.83	3.43	4.57	5.63	0.0	0.0	95.2
M2	1.13	3.9	0.42	0.96	2.68	1.49	-0.1	0.1	90.0
M3	0.43	0.6	0.26	0.38	1.76	0.55	-0.1	0.6	83.4
N3 (stage II feed)	(95.14)	(54.5)	0.75	0.17	5.06	0	-8.2	7.2	0
N4	3.27	4.9	2.32	0.41	13.14	0	-23.0	15.4	0
N5	3.33	5.1	2.19	0.42	13.19	0	-18.1	13.1	0
N6	3.25	4.3	1.96	0.37	11.67	0	-19.0	13.5	0
Feed (calculated)	100	100	0.77[b]	0.28[b]	5.59	0.13	-0.1	0.2	27.3
Magnetic tailings	4.86	45.5	0.68[b]	2.58[b]	3.85	4.21	-0.1	0.0	94.6
Nonmag. tailings	9.86	14.3	2.16[b]	0.40[b]	12.68	0	-20.2	14.1	0
Conc. product	85.28	40.2	0.61	0.13	3.95	0	-11.9	9.4	0

[a] Based on recovered mass, ignoring loss

[b] Calculated from mass balance

The concentrated olivine product from the Permroll separation contained 0.13% Cr_2O_3 at a recovery of 85.28%, which corresponds to a 54-55% reduction in the chromium content depending on the chosen value for the feed composition (i.e. the analysed value of 0.29% Cr_2O_3 or the 0.276% Cr_2O_3 derived from the calculated mass balance for chromium). This brings the concentrated product in compliance with the NWD-limit for classification as non-hazardous waste (i.e. less than 0.146% Cr_2O_3).When analysing the data given in Table 3, it is clear that some 80% of this reduction can be attributed to the first separation stage. Fig. 3 shows the relationship between the cumulative product recovery and the resulting product quality for the successive removal of the individual fractions M1 to M3 and N4 to N6.

The tailings from the Permroll separation consists mainly of olivine and their comparatively small volumes could therefore easily be mixed with the much larger volumes of slag conditioner and sold as such. At A/S Olivin's deposit at Åheim, approximately 85% of the roughly 2 million tonnes of broken olivine ore is sold as

slag conditioner. Slag conditioner is a low cost product that allows little beneficiation, but the product's tolerant specifications and large production volumes offer olivine producers a very favourable opportunity to turn the much smaller volumes of off-spec olivine, fines and alternative process tailings in to sellable products (Kleiv, 2001). Hence, as long as the concentrated olivine product from the Permroll separation can justify the separation costs, the corresponding tailings will only add positively to the economic balance.

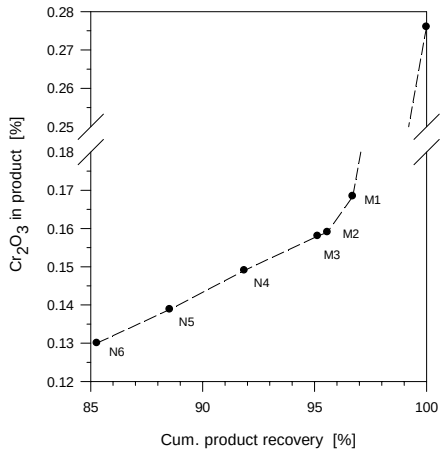

Fig. 3. Product quality as a function of cumulative recovery

As suggested by the estimated mineralogy as well as the rapid decrease in both the yield and chromium assays of the successive magnetic fractions from the first separation stage, the chromite is easily removed, thus leaving a virtually chromite free product. This conclusion is supported by the fact that the simple qualitative XRD analysis was unable to detect chromite in the concentrated product. As expected, the three successive runs performed during the first separation stage resulted in a much better concentration of chromium than was achieved during the Frantz separation. If only a single run had been conducted, an additional 4.5% of the total chromium present in the feed would have ended in the concentrated product.

Less efficient separation was achieved with respect to chlorite, as evident from the near constant yields and assays of the N4, N5 and N6 fractions. In spite of a significant enrichment in the non-magnetic tailings, chlorite appears to occur in all fractions. The possible compositional variations aside, chlorite is inherently a more problematic mineral to reject due to its flaky particle shape. This feature promotes pinning to the separator belt due to adhesive forces, as well as entrapment caused by more magnetic particles. Hence, a further reduction in the chromium content of the concentrated product would probably result in a significantly reduced recovery. The recovery of chlorite in the non-magnetic tailings was probably between 20% and 30%.

The total dissolved chromium concentrations in the filtered leachates from the leaching test are presented in Table 4. The values are very low and in the

concentration range usually regarded as the geochemical background of natural waters. In comparison, the current US-EPA maximum contaminant level goal (MCLG) for chromium in drinking water is 0.1 mg/L. Being almost three orders of magnitude lower than the theoretical solubility of chromium hydroxide (Stumm and Morgan, 1996) the concentrations are probably controlled by kinetic factors and the availability of easily leachable surface sites. At first sight the values appear to show little variation, and it is evident that the 34% reduction in the leachate concentration achieved by Permroll separation is smaller than the corresponding reduction in the solid assays. However, the results clearly indicate the difference in relative leachability of the chlorite and the chromite. The concentration obtained for the 'chromite concentrate' is not much higher than that of the non-magnetic tailings even though the former contains 6.45 times more chromium than the latter. The higher leachability of the chlorite is also evident from the results obtained for the feed to the second separating stage (i.e. the N3 fraction). After the first separation stage has lowered the chromium concentration by more than 40%, the material still produces a leachate concentration only 17% lower than that obtained for the feed.

Table 4. Chromium concentration (C_{cr}) and pH in the leachates

Process stream	Assay [%Cr_2O_3]	pH	C_{Cr} [µg/L]
Feed	0.28[a]	9.23	0.86
N3 (stage II feed)	0.16[a]	9.42	0.71
Magnetic tailings	2.58[a]	9.05	1.14
Non-mag. tailings	0.40[a]	9.34	0.97
Concentrated product	0.13	9.49	0.57

[a] Calculated from mass balance

As shown by this study, a single separation stage, removing the chromite, goes a long way with respect to reducing the chromium content of the original olivine sand as it is responsible for some 80% of the total reduction achieved by the separation circuit. In applications were the foundry sand is used as an additive or a reactive agent in mixtures or composites and where its relative concentration in the receipt is limited by restrictions on the chromium content, the removal of chromite could allow the use of an additional 80-85% product mass. This could be of great practical importance for applications such as adsorbents and catalysts where the effect is strongly related to the concentration of the active phase or reagent. When facing restrictions with respect to the total chromium content even a small reduction could be of vital importance if it brings the product within the limits of tolerance. Hence, even the much less efficient second stage should be considered if the additional reduction is needed.

The second separation stage of the proposed flowsheet becomes more important if compliance with restrictions placed on aqueous concentrations is an issue, as approximately half the reduction in the leachate concentration can be attributed to the removal of chlorite. It is beyond the scope of this paper to assess the relative mobility

of chromium as a function of its mineralogical occurrence or the pH and composition of the leachant to which the materials are exposed. However, as one would expect based on their different structures, the study indicates that the two chromium-bearing minerals could possess quite different leaching characteristics. Consequently, in spite of and as a contrast to the general and often indiscriminate nature of compliance limits, a more comprehensive approach is needed to optimise the beneficiation of the initial olivine sand products.

4. Conclusions

The following conclusions were reached based on the results from the Frantz and Permroll separation performed on the original olivine sand sample and the subsequent EN-12457-2 leaching test performed on the feed, product and tailings.

— The original olivine sand sample contained 0.28-0.29% Cr_2O_3 of which approximately one third occurred as chromite and two thirds as chlorite. These two minerals were enriched at either end of the sample's magnetic susceptibility range, thus enabling the production of concentrated olivine middlings.

— The two stage Permroll separation produced a concentrated product containing 0.13% Cr_2O_3 at a product recovery of 85.28%, thus reducing the chromium content by 55% and bringing the product in compliance with the NWD-limit for classification as non-hazardous waste (i.e. less than 0.146% Cr_2O_3). Some 80% of this reduction was achieved as a result of the first separation stage where chromite reported to the magnetic tailings at a recovery close to 100%. Hence, the chromium remaining in the concentrated product must be attributed to chlorite. The recovery of chlorite in the non-magnetic tailings was probably between 20% and 30%.

— The leachates were characterised by very low chromium concentrations. The concentrated product produced a value of 0.57 µg/L as opposed to the 0.86 µg/L produced by the feed. The results suggest that chromium is more easily released from chlorite than chromite. Hence, if a lower leachate concentration will be required, more chlorite will have to be removed from the concentrate. As the results indicate, this will be difficult to achieve with magnetic separation without sacrificing recovery.

— The study shows that dry magnetic separation should be considered when a reduction of the chromium content of dried high quality olivine sand products is required even though the potential enhancement is limited by the overlapping magnetic susceptibilities of olivine and chlorite.

References

BELLEY, F., FERRÉ, E.C., MARTÍN-HERNÁNDES, F., JACKSON, M.J., DYAR, M.D., CATLOS, E.J., 2009. The magnetic properties of natural and syntetic olivines. Earth and Planetary Science Letters 284, 516-526.

BHAKHAR, N., 2006. Antimony removal by iron-oxide coated olivine and water treatment residual. Master thesis, Royal Institute of Technology – KTH, Stockholm, Sweden, ISSN 1651-064X

BOWEN, N.L., SCHAIRER, J.F., 1935. The system, MgO-FeO-SiO_2. American Journal of Science 29, 151-217.

CEN, 2002. EN-12457-2:2002E - Compliance test for leaching of granular waste material and sludges - Part 2: One stage batch test at a liquid to solid ratio of 10 l/kg for materials with particle size below 4mm (with or without size reduction)., European Committee for Standardization (CEN)

CHMELAR, J., KLEIV, R.A., REKKEDAL, J., SLAGNES, S., 2003. Enhancing the value of olivine process dust by air classification. In: Proc. of Conference of Mineral Processing, Luleå, pp. 42-51

DEVI, L., PTASINSKI, K.J., JANSSEN, F.J.J.G., VAN PAASEN, S.V.B., BERGMAN, P.C.A., KIEL, J.H.A., 2005. Catalytic decomposition of biomass tars: use of dolomite and untreated olivine. Renewable Energy 30 (4), 565-587.

EL AAMRANI, F.Z., DURO, L., DE PABLO, J., BRUNO, J., 2002. Experimental study and modeling of the sorption of uranium(VI) onto olivine-rock. Applied Geochemistry 17, 399-408.

GRISHIN, N.N., RAKAEV, A.I., KALINNIKOV, V.T., 2000. Olivines of the Kola peninsula. II. Magnetic concentration of olivinites. Refractories and Industrial Ceramics 41 (11-12), 444-449.

HARBEN, P.W., 1999. The Industrial Minerals Handbook, 3rd edition. Industrial Minerals Information Ltd, London, 242-245.

HAUG, T.A., 2010. Dissolution and carbonation of mechanically activated olivine – Investigating CO_2 sequestration possibilities. Doctoral thesis, Norwegian University of Science and Technology, Trondheim, Norway, ISSN 1503-8181.

HERK, J.VAN, PIETERSEN, H.S., SCHUILING, R.D., 1989. Neutralization of industrial waste acids with olivine - The dissolution of forsteritic olivine at 40 degrees-C - 70degrees C. Chemical Geology 76, 341-352.

HOPSTOCK, D.M., 1985. Magnetic properties of minerals. In: Weiss, N.L. (ed.), SME Mineral processing handbook, Section 6, Chapter 6

JONCKBLOEDT, R.C.L., 1998. Olivine dissolution in sulphuric acid at elevated temperatures: Implications for the Olivine process, an alternative waste acid neutralizing process. Journal of Geochemical Exploration 62, 337-346.

KLEIV, R.A., 2001. Heavy metal adsorption on silicate tailings – A study of nepheline syenite and olivine process dusts. Doctoral thesis, Norwegian University of Science and Technology, Trondheim, Norway, ISBN 82-471-5332-7.

KLEIV, R.A., SANDVIK, K.L., 2002. Modelling copper adsorption on olivine process dust using a simple linear multivariable regression model. Minerals Engineering 15 (10), 737-744.

KLEIV, R.A., THORNHILL, M., 2004. Adsorptive retention of copper from acidic mine water at the disused sulphide mine at Løkken, central Norway - Initial experiments using olivine. Minerals Engineering 17, 195-203.

KLEIV, R.A., THORNHILL, M., 2008. Predicting the neutralisation of acid mine drainage in anoxic olivine drains. Minerals Engineering 21 (4), 279-287.

MCMEEN, C.R., BENJAMIN, M.M., 1997. NOM removal by slow sand filtration through iron oxide-coated olivine: A 16-month study indicates slow sand filtration through iron oxide-coated olivine significantly improves NOM removal. Jornal of the American Water Works Association 89 (2), 57-71.

MORALES, T.A., HERBERT, R.B., 2001. Sulphur and iron chemistry in a barrier system for the remediation of groundwater contaminated by AMD; Kristineberg mine site, Nothern Sweden. In: Securing the Future - International Conference on Mining and the Environment – Proceedings, 1st Volume. The Swedish Mining Association, Skellefteå, Sweden, pp. 546-555.

NME, 2004. The Norwegian Waste Directive (FOR 2004-06-01 nr 930). Chapter 11. The Norwegian Minestry of the Environment

OSLAND, R., 1998. Modelling of variations in Norwegian olivine deposits – Causes of variations and estimation of key quality factors. Doctoral thesis, Norwegian University of Science and Technology, Trondheim, Norway, ISSN 0802-3271.

ROBERTS, J., 2008. Olivine's future in flux. Industrial Minerals, November 2008, 40-49.

RUDI, F., 2001. Olivine – A Norwegian forte. Industrial Minerals, November 2001, 45-49.

SCHUILING, R.D., 1986. A method for neutralizing waste sulfuric acid by adding a silicate. European Patent Application No. 8590353.5, Utrecht University, Netherlands, 1986.

SKILLEN, A., 1995. Olivine - Long live the evolution. Industrial Minerals no 329, 23-31.

STUMM, W., MORGAN, J.J., 1996. Aquatic chemistry - Chemical equilibria and rates in natural waters, 3rd edition. John Wiley & Sons, Inc., New York

SVOBODA, J., 1987. Magnetic methods for the treatment of minerals. Developments in mineral processing 8, Elsevier, pp. 692.

Physicochem. Probl. Miner. Process. 47(2011) 229–236
www.minproc.pwr.wroc.pl/journal/

Physicochemical Problems of Mineral Processing
ISSN 1643–1049

Received March 2, 2011; reviewed; accepted May 14, 2011

Flotation of components of Polish copper ores using n–dodecane as a collector

Alicja BAKALARZ

Faculty of Geoengineering, Mining and Geology, Wroclaw University of Technology, Wybrzeze Wyspianskiego 27, 50–370 Wroclaw, alicja.bakalarz@pwr.wroc.pl

Abstract. Investigations on influence of aqueous emulsion of n–dodecane on flotation of sulfides and organic–carbon–containing shale from Legnica–Glogow Copper Basin (LGOM, Poland) are presented in the paper. Seven flotation experiments were conducted. Each flotation feed consisted of dolomite, quartz and one of following components: chalcopyrite, chalcocite, bornite, covellite, galena and shale containing organic carbon. The results indicate that chalcopyrite, bornite, covellite and shale float well in the presence of 200 g/Mg of n–dodecane and in a short period of time. Chalcocite and galena do not float with n–dodecane, even when the dose of the nonpolar collector for chalcocite flotation is increased. The studies explain a selective influence of the nonpolar collector on flotation of the copper sulfides ore from LGOM.

keywords: flotation, nonpolar collectors, sulfides, shale, chalcopyrite, chalcocite, bornite, covellite, galena

1. Introduction

Various sulfides are present in copper ores occurring in the Fore–Sudetic Monocline of SW Poland. According to Piestrzynski (2007) and Kucha (2007) the main copper sulfides are chalcocite, bornite, digenite, chalcopyrite, djurleite, covellite, spioncopite, geerite, yarrowite, tennantite and anilite. They are the source of copper produced from the concentrates of the flotation process. The collectorless and standard collector flotation of copper minerals originated from the Fore–Sudetic Monocline have been investigated by many investigators including Drzymala et al. (1993), Drzymala and Bigosinski (1995), and Lekki (1996, 1997, 2006). Typical collectors used for sulfide minerals flotation are xanthates (dithiocarbonates) and aerofloats (ditiophosphates) because they provide good separation (Gaudin, 1963; Bulatovic, 2007; Fuerstenau, 2007). However, the use of nonpolar reagents (oils) for copper sulfides flotation has not been investigated extensively.

Nonpolar reagents can be used in flotation of naturally hydrophobic minerals such as coal, graphite, sulfur, molybdenum, talc and mica (Seitz and Kawatra, 1986;

Vidlář and Pasiowiec, 2009). Literature on sulfides flotation indicates that complex hydrocarbons mixtures, like kerosene, fuel, engine, and plant oils (Nowakowska and Janicka, 1975; Seitz and Kawatra, 1986; Bos and Quast, 2000; Kondraty'ev and Izotov, 2000; Krausz et al., 2005; Rubio et al., 2007; Drzymala et al., 2008) can be used for flotation. This group of reagents plays many roles in flotation. These roles include (Seitz and Kawatra, 1986; Rubio et al., 2007; Drzymala et al., 2008) improving or inducing hydrophobicity of particles, reducing overall reagent costs by replacing part of the standard collector addition (nonpolar oils are less expensive reagents), improving selectivity of process, and increasing recovery of coarse and fine particles without reducing selectivity.

The nonpolar reagents are not soluble in water. It results in different mode of interaction with sulfides than that of soluble reagents. Oils must be emulsified before their application in separation processes. The emulsification of oils is important also in other ores beneficiation methods including selective agglomeration, solvent extraction and waste water treatment (Finkelstein, 1979).

Introduction of nonpolar reagents to flotation circuits changes the mechanism of air bubble–particle aggregate formation. Oils, due to their insolubility and high hydrophobicity, affect the air bubble–particle–water system differently than water soluble flotation collectors. The main difference is related to the physical adhesion of nonpolar reagent to the particle surface (Laskowski, 1992) by the van der Waals forces. The mechanism by which the oil acts is based on coating either a weakly or strongly hydrophobic particle leading to an improved adhesion of the air bubble to the particle (Seitz and Kawatra, 1986). Kondraty'ev and Izotov (2000) showed that an addition of oil to flotation systems increases hydrophobicity of particles and reduces the time of interruption of the aqueous layer between the liquid and air bubble.

Nonpolar reagents such as hydrocarbons and their derivatives are used in flotation as collectors which the main function is selective hydrophobization of the surface of particle. Usually complex mixture of hydrocarbons (Nowakowska and Janicka, 1975; Seitz and Kawatra, 1986; Bos and Quast, 2000; Krausz et al., 2005; Luszczkiewicz et al., 2006; Rubio et al., 2007; Drzymala et al., 2002, 2008) as used as a collector for copper sulfide ore flotation. In most papers, when the complex nonpolar reagent including kerosene, fuel, plant oils was used, the results of upgrading were worse than those with standard copper ore flotation such as xanthates (Drzymala et al., 2002, 2008; Luszczkiewicz et al., 2006; Bakalarz, 2011). The authors of these studies suggested that probably only selected sulfides float in the presence of the nonpolar collectors. The remaining sulfides float only with xanthates. So far, it has not been determined which sulfides float well with the nonpolar collectors. The investigation on this aspect of sulfide flotation should explain the process of sulfide ore flotation in the presence of nonpolar collectors.

2. Experimental

2.1. Materials

Seven model ores were prepared. Each consisted of dolomite (47.5%, from Dolomite Mine in Libiaz, Poland), quartz (47.5%, from Osiecznica, Poland) and 5.0% of a given component (either chalcocite, bornite, chalcopyrite, covellite, galena or organic–carbon–containing shale from Polkowice–Sieroszowice or Rudna Mines, KGHM Polska Miedz S.A., Poland). Dolomite was wet ground in a laboratory ball mill (Alvarez Redondo) and next wet screened to get narrow size fractions of 40–71 micrometer used for the model feed. Quartz was only wet screened to get proper size fractions. Last component added to the model feed were prepared fresh daily by crushing manually in an agate mortar and dry screening to get the 40–71 micrometer size fraction. This procedure was dictated by the fact that microscopic analysis is accurate only for narrow size fractions of particles.

2.2. Reagents

n–dodecane (DD, 99%, Alfa Aestor) was used as a model nonpolar collector in all experiments. It was emulsified in distilled water directly before experiments in a laboratory whipper (POL–EKO Aparatura) for 8 minutes applying 18 000 rpm. The concentration of emulsion was 5 g/dm^3. Methyl dipropylene glycol ether (C_1P_2, 97%, Aldrich) was used as a frother. The solution containing 3 g/dm^3 of C_1P_2 was prepared in distilled water. In each experiment the dose of frother was 200 g/Mg.

2.3. Methods

Seven flotation experiments were conducted. In six flotation tests with either chalcocite, bornite, chalcopyrite, covellite, galena or shale the aqueous emulsion of n–dodecane (DD) was used as the collector in the amount of 200 g/Mg. Additionally, one more experiment with chalcocite was conducted in the presence of 400 g/Mg of n–dodecane. The flotation tests were conducted in a Mechanobr laboratory flotation machine (IMN Gliwice) equipped with 250 cm^3 flotation cell, which was made from stainless steel. The mass of each feed was 70 g. The speed of stirrer was 760 min^{-1} (rpm) and the flow of air 30 dm^3/h.

Each feed sample was stirred with distilled water for 3 minutes. Next, the collector was added and the suspension was agitated for further 5 minutes. After that, frother was added and the suspension stirred for 1 minute. Next, the air valve was opened and the flotation initiated. The flotation concentrates were collected for about 10 minutes. All the flotation products were dried in a laboratory drier at 80°C and next weighted.

The samples for microscopic analysis were prepared using Canadian balm. A monolayer of particles in the balm was analyzed with a microscopic digital color camera (Nikon DS–Fi1–U2) and the Nikon NIS Elements BR software. The assay of

sulfide/shale was estimated in all flotations products by measurement the surface area of all particles.

The results of the experiments are presented as kinetic and upgrading separation curves known as the Halbich, Luszczkiewicz and Fuerstenau plots, which were described in details by Drzymala (2006–8).

3. Results and discussion

The results of investigations are presented in Figs. 1–4. The solid lines in Fig. 1 indicate kinetics (recovery of material vs. flotation time) of all flotation experiments. Around the first five minutes of flotation, a high recovery of the four materials was observed with the exception of galena and chalcocite, despite the fact that dose of n–dodecane for chalcocite flotation was increased. It can be also seen that chalcopyrite was the fastest floating component.

Flotation upgrading curves are presented in Figs. 2–4. It is assumed that chalcopyrite flotation is the most efficient since its upgrading curve lies very close to the ideal upgrading line shown in Fig. 2. Worse results were obtained for bornite, covellite and shale. It can be also seen that galena and chalcocite do not float when aqueous emulsion of n–dodecane is used as the collector, even if the dose of n–dodecane was increased from 200 to 400 g/Mg for chalcocite flotation. Three upgrading curves, both for chalcocite and one for shale lie almost on the "no upgrading" line. The next figure (Fig. 3), known as the Luszczkiewicz upgrading curve, shows similar situation. The closest curve to the ideal separation lines was obtained for chalcopyrite.

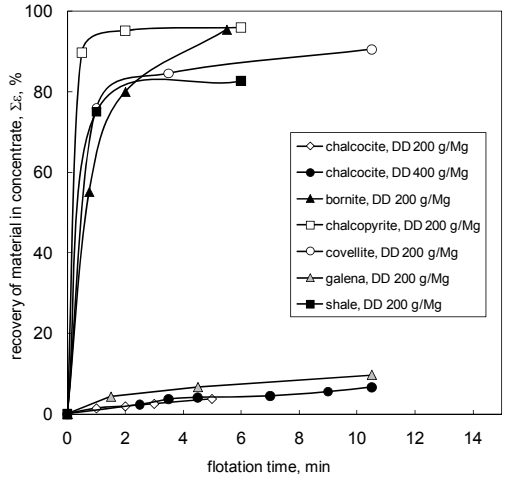

Fig. 1. Comparison of kinetic curves for all flotation experiments

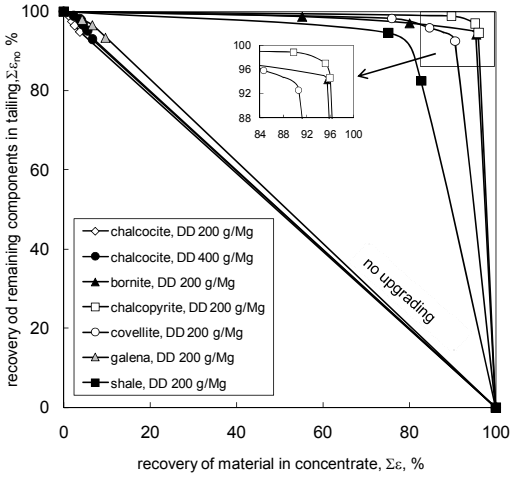

Fig. 2. Upgrading Fuerstenau's curves as recovery of remaining components in tailing vs. recovery of considered component in concentrate for all flotation experiments

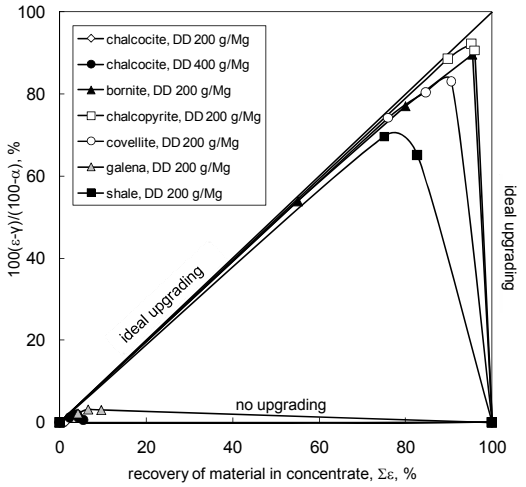

Fig. 3. Upgrading Luszczkiewicz's curves as a relationship between $100(\varepsilon-\gamma)/(100-\alpha)$ reflecting a component content in concentrate and recovery of the considered component in concentrate for all flotation experiments (γ, concentrate yield; ε, recovery in concentrate; α, content in feed)

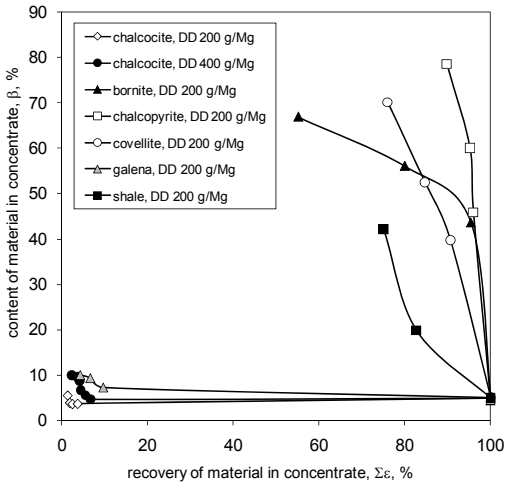

Fig. 4. Upgrading Halbich's curves as a relationship between component content in concentrate and recovery of the considered component in concentrate for all flotation experiments

Figure 4 shows, that the richest first concentrate was obtained during chalcopyrite flotation. The content of copper sulfide was around 80% at the recovery of about 90%. According to Figs. 2–4, not all covellite and organic–carbon–containing shale are recovered during flotation with n–dodecane. Probably, to float the rest of covellite an addition of a standard collector, such as xanthate to the flotation suspension would be necessary.

4. Conclusions

The effect of nonpolar collector on flotation of the main sulfides minerals and organic–carbon–containing shale from Legnica–Glogow Copper Basin has been investigated in the paper. The flotation of five minerals (chalcocite, bornite, chalcopyrite, covellite and galena) and organic–carbon–containing shale in the presence of n–dodecane has been studied. Results of the work indicate that chalcopyrite, bornite, covellite and shale float in the presence of n–dodecane as a collector. The time of their flotation was short, equal to about 2–10 minutes. The best results were obtained for chalcopyrite flotation. Chalcocite and galena do not float with n–dodecane and to float all covellite particles, probably an addition of one of the standard sulfide minerals collectors (xanthates or aerofloats) is necessary.

The obtained results explain the process of Polish copper sulfide ore flotation with nonpolar reagents. Presumably, the main reason of worse results of copper upgrading is that chalcocite or other copper sulfides which have not been examined in

the paper, do not float in the presence of oils. High recovery of the rest of examined copper minerals points to positive effect of the nonpolar collector. Good floatability of organic–carbon–containing shale in the flotation using n–dodecane explains high recovery of organic carbon in copper sulfide ore flotation. All the results suggest that the nonpolar collector can be used as an effective collector of sulfide minerals from LGOM, if combined with one of the standard collectors of sulfides, for instance xanthates. Additional detailed investigations on the natural copper ore, coupled with mineralogical characterization, should confirm selectivity of flotation using nonpolar reagents. This subject should be further investigated.

Acknowledgements

Financial support by Polish Research Grant (N N524 370037) and a fellowship co–financed by the European Union within the European Social Fund are greatly acknowledged.

References

BAKALARZ, A., 2011. *Flotacja rudy miedzi z rejonu Rudnej przy użyciu n–heptanu jako odczynnika zbierającego*. Gospodarka Surowcami Mineralnymi, Vol. 27(1), 69–83.

BOS, J.L., QUAST, K.B., 2000. *Technical note effects of oils and lubricants on the flotation of copper sulphide minerals*. Miner. Eng., 13/14–15, 1623–1627.

BULATOVIC, S.M., 2007. *Handbook of Flotation reagents: chemistry, theory and practice. Flotation of sulfide ores*. Elsevier, Netherlands.

DRZYMALA, J., SZULMANOWICZ, A., LUSZCZKIEWICZ, A., CHMIELEWSKI, T., 1993. *Bezkolektorowa flotowalność siarczków z Lubińsko–Głogowskiego Zagłębia Miedziowego. Problemy technologiczne, projektowe, ekonomiczne i organizacyjne w przeróbce surowców mineralnych*. XXV Krakowska Konferencja Naukowo–Techniczna Przeróbki Kopalin, Szczawnica, 8–10 września 1993, Oficyna Wyd. Jaxa, Kraków, 133–142.

DRZYMALA, J., BIGOSINSKI, J., 1995. *Collectorless flotation of sulfides occurring in the Fore–Sudetic copper minerals deposit of SW Poland.* Mineralogia Polonica, Vol. 26, No. 1, 63–73.

DRZYMALA, J., KUCAL, J., KOZLOWSKI, A., 2002. *Flotacja rudy miedzi z Lubina za pomocą kolektorów stosowanych jako promotory flotacji węgla*. Prace Naukowe Instytutu Górnictwa Politechniki Wrocławskiej, Studia i Materiały, Nr 29, 102, 45–53.

DRZYMALA, J., GRODZKA, J., POMIANOWSKI, A., 2008. *Rapeseed oil as a collector in flotation of sulphide copper ore*. Oils and fuels for sustainable development. Gdansk University of Technology, 201–204.

DRZYMALA, J., 2006–8. *Atlas of upgrading curves used in separation and mineral science and technology*. Physicochem. Probl. Miner. Process., part I, 40, 2006, 19–29; part II, 41, 2007, 27–35; part III, 42, 2008, 75–84.

FINKELSTEIN, N.P., 1979. *Beneficiation of mineral fines*. P. Somasundaran, N. Arbiter (Eds), AIME, 331–340.

FUERSTENAU, D.W., 2007. *A century of developments in the chemistry of flotation processing. In: Froth flotation. A century of innovation*. M.C. Fuerstenau, G. James, R.–H. Yoon (Eds.), Society for Mining, Metallurgy and Exploration, Inc. (SME).

GAUDIN, A. M., 1963. *Flotacja*. Translation from 2nd ed. by J. Olszewski and T. Piaseczny. Wyd. "Slask", Katowice.

KONDRATY'EV, S.A., IZOTOV, A.S., 2000. *Effect of apolar reagents and surfactants on the stability of a flotation complex*. J. Min. Sci., Vol. 36, No. 4, 399–407.

KRAUSZ, S., MĂRĂCINEANU, G., CIOCANI, V., 2005. *The flotation of Rosia Poieni copper ore in column machine, with non–polar oils addition*. Acta Montanistica Slovaca, 10, No. 1, 39–44.

KUCHA, H., 2007. *Mineralogia kruszcowa i geochemia ciała rudnego złoża Lubin–Sieroszowice*. Biuletyn Państwowego Instytutu Geologicznego, 423, 77–94.

LEKKI, J., 1996. *Termodynamiczna interpretacja bezkolektorowej oraz ksantogenianowej flotacji rudy miedzi w kontrolowanych warunkach potencjału redoks*. Górnictwo. Zeszyty Naukowe Politechniki Śląskiej, Gliwice, No. 1349 (231), 315–331.

LEKKI, J., 1997. *Flotometryczna ocena flotowalności naturalnej, bezkolektorowej oraz ksantogenianowej minerałów siarczkowych*. Physicochem. Probl. Miner. Process, 31, 175–196.

LEKKI, J., 2006. *Ksantogenianowa hydrofobizacja siarczków lubińskich złóż miedziowych*. Cuprum Czasopismo Naukowo–Techniczne Górnictwa Rud, Wrocław, 2 (39).

LUSZCZKIEWICZ, A., KONOPACKA, Z., DRZYMALA, J., 2006. *Flotacja czarnych łupków z lubińskich rud miedzi*. Materiały konferencji BIOPROCOP'06, "Perspektywy zastosowania technologii bioługowania do przerobu rud miedzi zawierających łupki", Lubin, 29–47.

NOWAKOWSKA, B., JANICKA, E., 1975. *Zastosowanie olejów apolarnych do flotacji siarczkowych rud miedzi*. Rudy i Metale Nieżelazne, 20/8, 402–405.

PIESTRZYNSKI, A., 2007. *Okruszcowanie. In: Monografia KGHM Polska Miedź S.A.*, A. Piestrzynski, A. Banaszak and M. Zaleska–Kuczmierczyk (Eds), Lubin, 167–196.

RUBIO, J., CAPPONI, F., RODRIGUES, R.T., MATIOLO, E., 2007. *Enhanced flotation of sulfide fines using the emulsified oil extender technique*. Int. J. Miner. Process., Vol. 84, No. 1–4, 41–50.

SEITZ, R.A., KAWATRA, S.K., 1986. *The role of nonpolar oils as flotation reagents. Chapter 19 in: Chemical Reagents in the Mineral Processing Industry*. D. Malhotra and W.F. Riggs (Eds), SME/AIME, 171–180.

SONG, S., LOPEZ–VALDIVIESO, A., REYES–BAHENA, J.L., LARA–VALENZUELA, C., 2001. *Floc flotation of galena and sphalerite fines*. Miner. Eng., vol. 14, No 1, 87–98.

VIDLÁŘ, J., PASIOWIEC, P., 2009. *New directions in the research and development of reagents for flotation of coal and non–polar minerals*. Inżynieria Mineralna, Vol. 10, No. 2, 1–7.

Bakalarz, A., *Flotacja składników polskich rud miedzi przy użyciu n–dodekanu jako odczynnika zbierającego*, Physicochem. Probl. Miner. Process., 47 (2011) 229–236, (w jęz. ang.)

W pracy przedstawiono wyniki flotacji głównych minerałów siarczkowych oraz łupka pochodzących z rejonu Legnicko–Głogowskiego Okręgu Miedziowego w obecności apolarnego odczynnika zbierającego. Zbadano wpływ wodnej emulsji n–dodekanu na flotowalność kolejno: chalkozynu, chalkopirytu, covellinu, bornitu, galeny oraz łupka w mieszaninie z dolomitem oraz kwarcem. Badania przeprowadzono dla wąskiej klasy ziarnowej 40–71 μm, a zawartość poszczególnych minerałów w produktach flotacji oznaczano mikroskopowo przy użyciu specjalistycznego oprogramowania. W obecności n–dodekanu w ilości 200 g/Mg zaobserwowano flotację chalkopirytu, bornitu, covellinu oraz łupka. Galena oraz chalkozyn nie uległy procesowi flotacji. Według dotychczas opublikowanych wyników badań flotacji siarczkowych rud miedzi, stwierdzono, że tylko część nośników miedzi wykazuje flotowalność w obecności olejów. Prawdopodobnie, stwierdzony brak flotowalności chalkozynu, a być może także innych siarczków miedzi nieanalizowanych w pracy, jest przyczyną gorszych wskaźników wzbogacalności procesów flotacji rud miedzi w obecności olejów. Dobra flotowalność łupka, który jest nośnikiem węgla organicznego, potwierdza wysokie uzyski tego składnika w procesach flotacji krajowej rudy miedzi w obecności odczynnika apolarnego. Zagadnienie wymaga dalszych szczegółowych badań

słowa kluczowe: flotacja, apolarne odczynniki zbierające, siarczki, łupek, chalkopiryt, chalkozyn, covellin, bornit, galena

Physicochem. Probl. Miner. Process. 46(2011) 237-248
www.minproc.pwr.wroc.pl/journal/

Physicochemical Problems of Mineral Processing
ISSN 1643-1049

Received March 15, 2011; reviewed; accepted May 5, 2011

Influence of adsorption of n-alkyltrimethylammonium bromides (C_8, C_{12}, C_{16}) and bubble motion on kinetics of bubble attachment to mica surface

Anna NIECIKOWSKA, Jan ZAWALA, Kazimierz MALYSA

[a] Jerzy Haber Institute of Catalysis and Surface Chemistry Polish Academy of Sciences, Niezapominajek 8, 30-239 Krakow, ncmalysa@cyf-kr.edu.pl

Abstract. Influence of adsorption of n-alkyltrimethylammonium bromides (C_8, C_{12}, C_{16}) and formation of motion induced dynamic architecture of adsorption layer (DAL) over surface of the colliding bubble on kinetics of three-phase contact (TPC) formation at mica surface was studied. The dynamic phenomena occurring during the bubble collisions were monitored using a high-speed camera of frequency 1040 Hz. The effect of solution concentration and the DAL formation, due to the bubble motion, was determined. It was showed that stability of the wetting film formed between the colliding bubble and mica surface was governed by the electrostatic interactions between the film interfaces. It was found that when the distance covered by the bubble (i.e. the distance between the capillary and the mica surface) was L=3 mm (location "close") then the time of the three phase contact formation (t_{TPC}), was significantly shorter than for the L=100 mm (location "far"). The differences between the t_{TPC} for the locations "close" and "far" were the largest at lowest concentration. The mechanism responsible for significant differences in the t_{TPC} values for the location "close" and "far" is described..

keywords: three phase contact, cationic surfactant, bubble collision, thin liquid film, electrostatic interactions, charge reversal

1. Introduction

Flotation separation is a dynamic process, where motion and collisions of bubbles and grains leading to formation of stable bubble-grain aggregates are of crucial importance. The collision time of the gas bubble and grain is rather short (milliseconds) and the three phase contact (TPC) and formation of needs to occur during the collision. For facilitation the TPC and stable bubble-gas aggregates various flotation reagents are used. The flotation reagents (surface active substances) are added mainly to modify properties of the gas/liquid and liquid/solid interfaces. The addition of these substances can change the hydrophobic/hydrophilic properties of solid/liquid interface and/or electrostatic properties of both solid/liquid and gas/liquid interfaces and facilitates the TPC formation (Zawala et al., 2008). For the TPC formation a liquid film separating the colliding bubble and grain needs to be ruptured.

Stability of the liquid films is determined, according to the DLVO theory, by interrelation between electrostatic interactions of the electrical double layers of two interfaces (long-range, 1-100 nm), and the van der Waals interactions (short, 1-10 nm) (Scheludko, 1967). Thus, when a wetting film is formed during the bubble collision with solid surface then the electrostatic interactions start to operate when the draining film reaches locally a thickness ca. 100nm. When the film interfaces are similarly charged, the repulsive interactions between the surfaces stabilize the film. Otherwise, that is, when the film interfaces are oppositely charged, the attractive electrostatic forces act as a destabilizing factor leading to the film rupture. Thus, a preferential adsorption of ionic surfactant on one of the film interfaces can cause a reversal of the surface electrical charge. As a result the electrical interactions can be changed from repulsive to attractive, leading to the film rupture and the TPC formation.

Adsorption of surface active substances (SAS) can also affect strongly the bubble motion (Levich, 1962, Dukhin et al., 1959, 1995, Malysa et al., 2005, Zhang et al., 2001, Krzan et al., 2007). Velocity of the bubble can be strongly lowered in solutions of surface active substances (SAS) and as a result the time of contact between the colliding bubble and grain is prolonged. When the bubble formed in SAS solution is motionless then adsorption coverage over its surface is uniform. As a consequence of viscous drag exerted by continuous medium on the rising bubble interface the uneven distribution of adsorption coverage, due to surface advection flow from the bubble top to the bottom stagnation point, is induced (Frumkin, 1947, Levich, 1962). This non-uniform bubble adsorption coverage leads to inducement of surface tension gradient and causes a tangential ‘Marangoni’ stress opposing the flow shear stress. The uneven distribution of the surfactant molecules over the bubble surface, with practically no adsorption coverage at the top bubble pole, is called dynamic adsorption layer (DAL). As a consequence of the DAL formation the bubble interface mobility is retarded and its velocity can be lowered even by over 50% (Malysa et al., 2005; Krzan, et al., 2007).

The paper presents results of experiments on kinetics of the TPC formation by the bubble colliding with mica surface in solutions of three n-alkyltrimethylammonium bromides, having 8, 12 and 16 carbon atoms in alkyl chain (OTAB, DDTAB and CTAB, respectively). The effect of (i) preferential adsorption of SAS at the gas/liquid interface, and (ii) the DAL formation at the bubble surface was investigated. It is showed that stability of the wetting film (time of the TPC formation) vary with the n-alkyltrimethylammonium bromides concentration and depends on the molecule chain-length. The TPC formation at mica surface is governed by the attractive electrostatic interactions and the time of the TPC formation is affected by the DAL formation induced by the bubble motion - wetting film ruptures when the adsorption coverage at the bubble surface is high enough to change the sign of the bubble surface from negative to positive.

2. Experimental

Experiments were carried out using experimental set-up presented schematically in Fig. 1. It consisted of: (i) a square glass column (cross section 50x50mm), (ii) glass capillary of inner diameter 0.075 at the bottom, (iii) syringe pump with gas tight high precision glass syringes (Hamillton), enabling well-controlled air supply, (iv) high-speed camera (SpeedCam MacroVis), (v) PC with image analysis software. Collisions of the single bubbles with mica plates were recorded at the camera frequency 1040 Hz and analyzed using the WinAnalyze 3D software. The movies were also transformed into BMP pictures and analyzed using the SigmaScan Pro 5.0 Image Analysis Software. The bubble velocity variations were determined from measurements of the bubble bottom pole positions on subsequent frames of the camera recording.

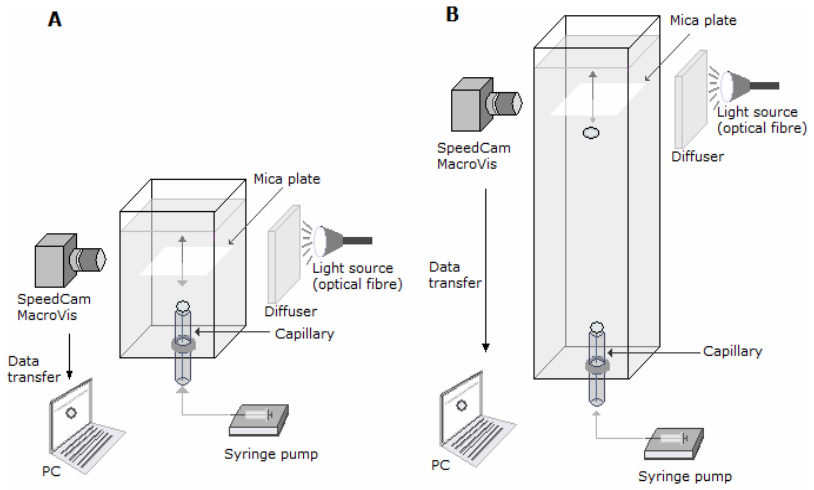

Fig. 1. Schematic of the experimental set-up - A) mica plate at location "close" (L=3mm), B) mica plate at location "far" (L=100mm)

Prior to each experiment the gas flow was adjusted carefully to get the time interval of ca. 30 s between two subsequent bubbles detaching from the capillary. The mica plates, freshly cleaved from sheets of layered mica sample, were positioned horizontally inside the column, just below the solution surface. Two series of experiments were carried out in the solutions studied to find if and how the motion induced dynamic (non-equilibrium) architecture of adsorption layer (DAL) affects an outcome of the collisions and time of the bubble attachment to mica surface. In the first series the distance between the bubble formation point and the surface of mica plate (L) was ca. 3 mm (see Fig. 1A). This location of mica plate will be further called the location "close" to underline the fact that the bubble collided with mica plate immediately after detachment from the capillary and therefore the adsorption coverage over its surface was uniform. In the second series (see Fig. 1B) the mica plated was

fixed at the distance L=100 mm (location “far) and at this distance, as showed previously (Krzan et al., 2007), the DAL was formed over the bubble. To get reliable data the experiments were repeated 20-30 times for each solution concentration and the mica plate location.

All experiments were carried out at room temperature. N-octyltrimethylammonium (OTABr), n-dodecytrimethylammonium (DDTABr) and n-hexadecyltrimethylammonium (CTABr) bromides were commercial reagents (Fluka) of high purity (≥99%). High purity distilled water was used in the experiments.

3. Results and discussion

3.1. Uniform adsorption coverage over surface of the colliding bubble

Adsorption coverage of surface active molecules over surface of the motionless bubble, i.e. when the bubble is growing at the capillary orifice, is uniform. Thus, when the mica plate is located in close vicinity of the capillary then the adsorption coverage over the colliding bubble is still almost uniform. Figure 2 presents the series of photos illustrating the bubble collision with mica plate at the location”close” (L=3mm) in distilled water and OTABr and CTABr solutions of concentration $1 \cdot 10^{-2}$ and $5 \cdot 10^{-6}$ M, respectively. For the sake of convenience the moment of the bubble first collision was denoted as t=0. It is seen in Fig. 2 that in all cases the bubble bounced from the mica surface after the first collision and the amplitude of the bounce was the largest one in distilled water. In the OTABr and DDTABr solutions the bouncing distance was shorter due to smaller impact velocity of the colliding bubble resulting from presence of adsorption layer over the bubble surface. Note please, in the last sequence of each of the photo series (Fig. 2), that the TPC was not formed at mica surface in distilled water but was formed in the OTABr and CTABr solutions. After a complete dissipation of the kinetic energy, that is, when the bubble was almost motionless, the bubble stayed captured beneath the mica plate without the TPC formation in distilled water. As there was no TPC formation even after long time (bubble was monitored for 15min) so it means that the wetting film formed was stable and did not rupture. Otherwise occurred in OTABr and CTABr solutions - the wetting film was unstable and the TPC was formed on mica surface after the film rupture (see the marked photos in Fig. 2). The time of TPC formation (t_{TPC}), determined as the time interval between the bubble first collisions till the moment of bubble attachment, was 55±19 and 138±23 ms for these OTABr and CTABr solutions, respectively.

Figure 3 presents a comparison of the velocity variations during the bubble collisions in distilled water, $1 \cdot 10^{-2}$ M OTABr and in $5 \cdot 10^{-6}$ M CTABr solutions with the mica plates at location “close”. The bubble velocity variations are presented as a function of time and there are also marked moments of the bubble attachment (TPC formation) to the mica surface. It is clearly seen in Fig. 3 that at location “close” the

bubbles were at the acceleration stage of their motion and the impact velocity of the bubble collision was the highest (ca. 27cm/s) in distilled water. In the OTABr and CTABr solutions the bubble impact velocity was lower - ca. 14.5 cm/s and 13 cm/s, respectively. It needs to be added here that the velocity was determined in respect to the bubble bottom pole. Thus, moment of the TPC formation means a rapid jump in position of the bubble bottom pole and therefore is clearly noticeable when the bubble stays motionless. after dissipation of the kinetic energy associated with its motion (see Figs. 3 and 4).

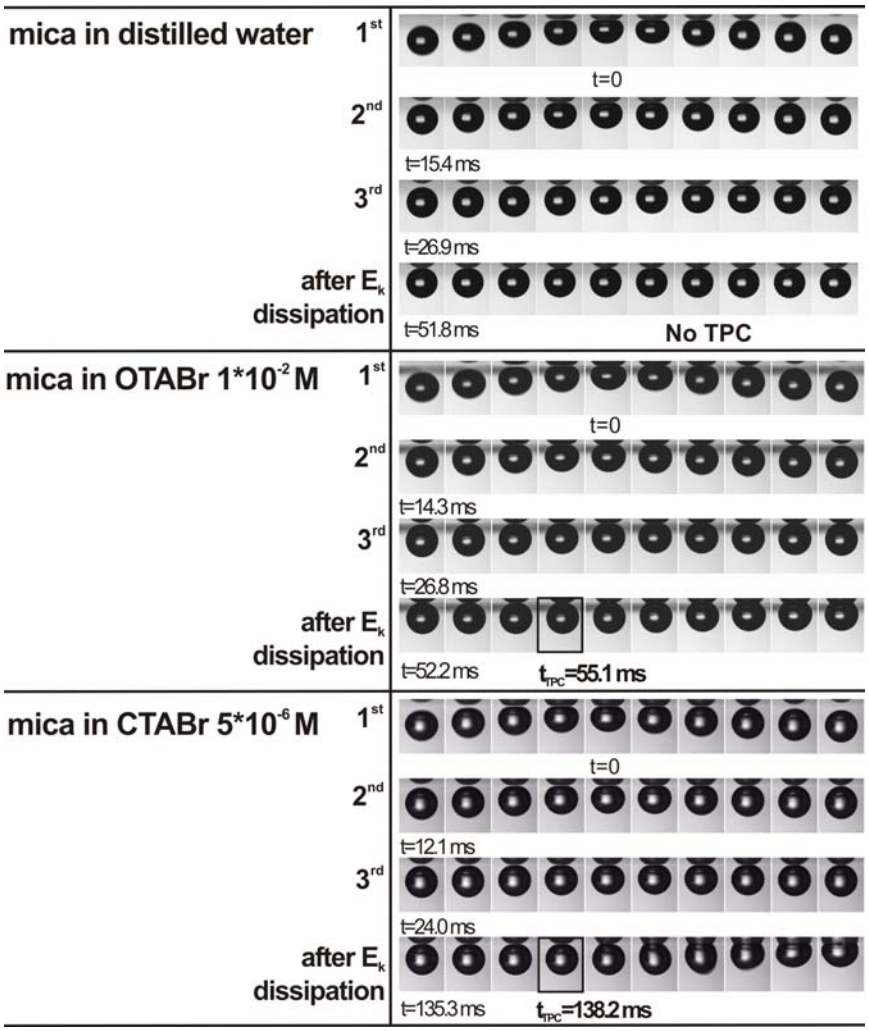

Fig. 2. Sequences of photos illustrating the bubble collision with mica plate (location "close") in distilled water and OTABr and CTABr solutions of concentration $1 \cdot 10^{-2}$ and $5 \cdot 10^{-6}$ M, respectively. Time interval between subsequent photos Δt=0.96ms - when not marked

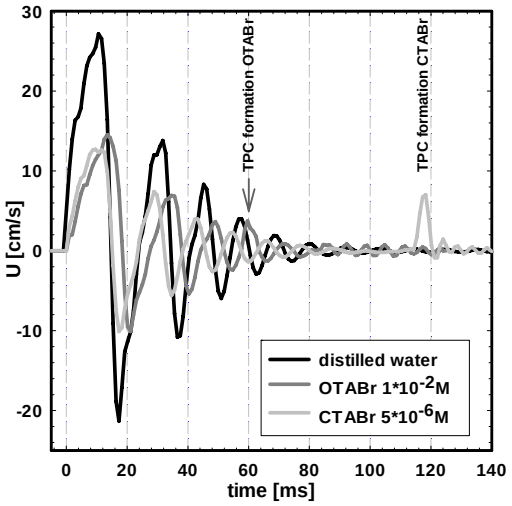

Fig. 3. Velocity variations during the bubble collisions in distilled water $1 \cdot 10^{-2}$ M OTABr and $5 \cdot 10^{-6}$ M CTABr solutions with mica plate located at the distance L=3 mm from the capillary orifice

Let us discuss reasons of differences in stability of the wetting films formed at mica surface in distilled water and solutions of the n-alkylthrimethylammonium bromides studied. Mica is a model hydrophilic surface with water contact angle equal zero. As was demonstrated (see Figs 2-3) there was no the TPC formation and the bubble attachment when the rising bubble collided with mica surface in water because the water wetting film formed at mica surface was stable. Mica surface immersed in distilled water is negatively charged and its zeta potential value is reported to be in the range between -80 and -120 mV (Scales et al., 1992, Debacher and Ottewill, 1992; Zembala et al., 2001, 2003; Zembala and Adamczyk, 2000). In distilled water the bubble surface is also negatively charged and zeta potential values reported in literature varied from -35 mV (Stockelhuber, 2003) to -65mV (Graciaa et al., 1995; Lee and Li, 2006). Thus, in distilled water both the air/water and water/mica interfaces of the wetting films, formed by the colliding bubble, are negatively charged. These repulsive electrostatic interactions assure stability of the wetting film and prevent formation of the TPC in distilled water. In the case of n-alkylthimethylammonium bromides (cationic surfactants) solutions the situation was different – the film was unstable and TPC formation was observed. It was due to the fact that the cationic surfactant molecules were preferentially adsorbed and caused a reversal of the bubble surface electrostatic charge from negative to positive. As a consequence of the charge reversal there were attractions interactions between oppositely charged interfaces of the wetting film formed in solutions of n-alkylthrimethylammonium bromides studied.

3.2. Non-uniform adsorption coverage over the bubbles – DAL is formed

Motion leads, as described above, to formation a dynamic architecture of the adsorption layer with significantly diminished adsorption coverage at the bubble top

pole. The bubble velocity variations during its collisions with mica plate located at L="close" and "far" in $1 \cdot 10^{-6}$ M DDTABr solution are presented in Fig. 4. It is seen that due to different distances covered by the bubble before the collision, the bubble impact velocity was different for these two interface locations. In the case of L=100 mm the bubble impact velocity was 34 cm/s, while for L=3 mm it was 12.8 cm/s, only. This difference in the impact velocity is the reason that longer time was needed for dissipation of the bubble kinetic energy when the mica plate was at location "far", but this time difference was ca. 40 ms, only. For the both mica plate locations the TPC was formed in 1·10-6 M DDTABr solution, after the kinetic energy dissipation, i.e. when the bubble was motionless beneath the mica surface. Note please that the time of the TPC formation was much longer when the mica was located at the distance L=100 mm. In the case of L=3 mm the t_{TPC}=542±79 ms while for L=100 mm was elongated to 1837±440 ms.

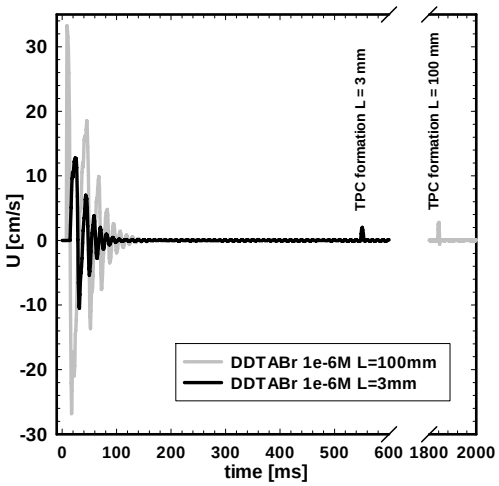

Fig. 4. Variation of the bubble local velocity during collisions with mica plate located "close" (L=3mm) and "far" (L= 100 mm) in $1 \cdot 10^{-6}$M DDTABr

Figure 5 presents the t_{TPC} values as a function of the OTABr, DDTABr and CTABr concentration. As there are given the t_{TPC} values for the mica plate locations "close" and "far" so a few important features can be noticed there: i) the differences in the time of the TPC formation are the largest at lowest concentrations, ii) differences in the t_{TPC} values between both mica locations depend on the surfactant type, iii) these differences are tending to zero at high concentrations, and iv) regions of the t_{TPC} variations are shifted towards higher concentrations with decreasing n-alkylthrimethylammonium bromide surface activity, that is, when the hydrocarbon chain is shorter. As described above the TPC formation at mica in OTABr, DDTABr and CTABr solutions is due, in our opinion, to a charge reversal of the bubble surface charge, from positive to negative, resulting from a preferential adsorption of these cationic surfactant molecules at solution/gas interface. However, possibility of the mica surface charge reversal and/or hydrophobization due to adsorption of cationic

surfactant on negatively charged surface needs to be taken also into considerations and its potential importance should be evaluated. Influence of n-alkyltrimethylammonium bromides on the mica zeta potential was studied by Debacher and Ottewill (1992) and Fa et al. (2005).

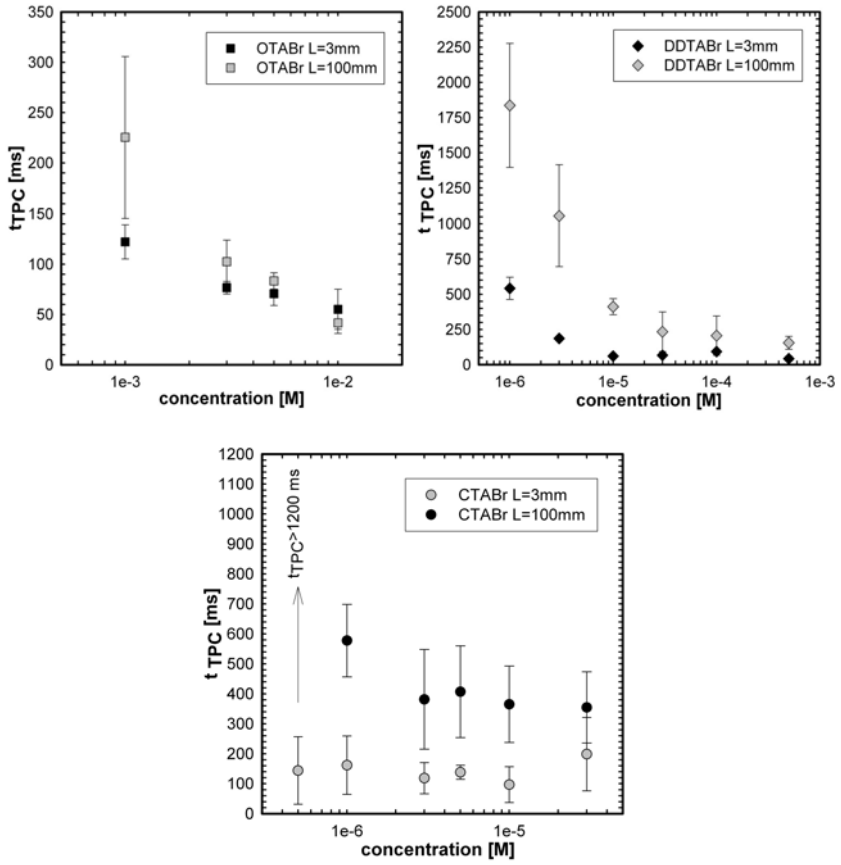

Fig. 5 Time of the TPC formation as a function of OTABr, DDTABr and CTABr concentration for the mica plate location "close" and "far"

Debacher and Ottewill (1992) reported that mica surface charge was reversed at CTABr, DDTABr and OTABr concentrations higher than ca. $6 \cdot 10^{-6}$, $6 \cdot 10^{-4}$ and $8 \cdot 10^{-2}$ M, respectively. Fa et al. (2005), who determined so called "point of zeta reversal" (PZR) reported that the PZR values were $2 \cdot 10^{-5}$ M for CTABr and $1 \cdot 10^{-3}$ M for DDTABr solutions, i.e. the similar but not identical to values found by Debacher and Ottewill (1992). Despite some discrepancy regarding exact values of the n-alkylammonium bromides concentrations causing the mica surface charge reversal these literature data indicate that in our experiments there was no charge reversal of the mica plates because the upper limits of the concentrations used (see Fig. 5) were

smaller or similar as the PZR values. This comparison indicates that the TPC formation in our experiments was indeed due to the charge reversal at the bubble surface. This conclusion is supported also by the experiments (Zawala et al., 2008) in which the mica plate was immersed in OTABr solution ($1 \cdot 10^{-3}$ M) for 30 minutes prior to measurements of the TPC formation by the colliding bubble in distilled water. As there was TPC formation so it confirms that adsorption of OTABr molecules at mica surface did not cause either electrical charge reversal or the mica surface hydrophobization, high enough to cause instability of the wetting film formed by the colliding bubble.

The results presented in Fig. 5 show clearly that the t_{TPC} values were dependent, especially at lowest solution concentrations, on location of the mica plate. Let us discuss and explain the reasons of the differences between the times of TPC formation at mica surface located "close" and "far". Locations "close" and "far" mean that the bubble covered different distances prior to the collision with mica surface and, as a consequence, the state of the adsorption layer at the bubble surface at the moment of collision was also different – this is presented schematically in Fig. 6. When the bubble was formed at the capillary orifice in surfactants solution studied there was adsorption layer formation at the growing gas/liquid interface. At the moment of the bubble detachment the adsorption coverage was uniform. As described above (Introduction) the bubble motion induces non-uniform distribution of the surfactant molecules over surface of the rising bubble and there is needed some distance for establishment of the DAL (Krzan et al., 2007). Therefore, the adsorption coverage over top poles of the bubble colliding with mica plate located "close" and "far" was different (see Fig. 6). At the location "close" the adsorption coverage was still uniform and at the moment of collision the bottom interface of the wetting film formed was positively charged. The attractive interactions between negatively charged mica surface and positively charged bubble top pole caused rupture of the wetting film formed and the TPC formation. When the mica was at the location "far" the distance covered by the bubble was long enough for the DAL formation. As a consequence, when the wetting film was formed, the bubble top pole was practically devoid of surface active molecules (see Fig. 6) Thus, at the very beginning of the film existence, the electrical charge of the bubble top pole was still negative - there were electrostatic repulsions between interfaces and the film was stabilized. When the bubble stayed motionless beneath the mica plate then the diffusion processes tended to re-establish uniform and equilibrium adsorption coverage of the cationic surfactant over entire bubble surface. The longer time of TPC formation in the case of the location "far" was caused by the fact that an additional time was needed to restore such adsorption coverage, over top pole of the bubble forming the bottom interface of the wetting film, which ensures the charge reversal from negative to positive. As diffusion kinetics depends strongly on surfactant concentration so the differences between the t_{TPC} values were the largest ones at lowest concentrations of CTABr, DDTABr OTABr solutions.

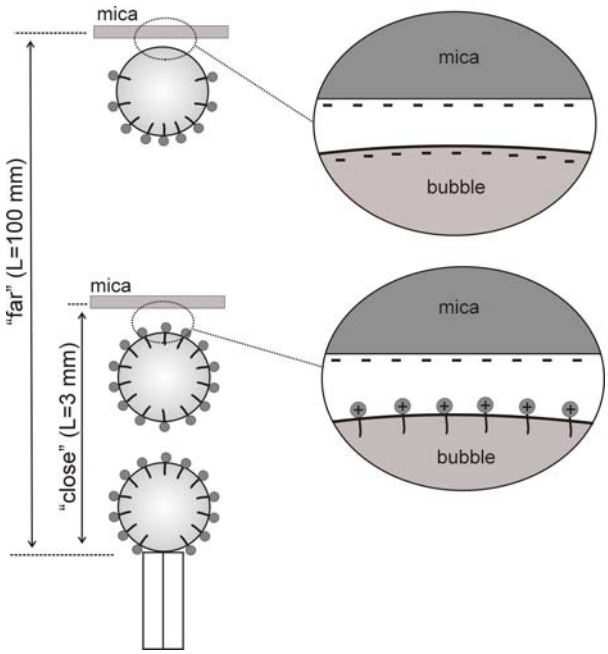

Fig. 6. Schematic presentation of the DAL formation and state of adsorption layer at solution/air interface of wetting film formed by the bubble colliding with mica plate located "close" and "far"

4. Concluding remarks

It was showed that stability of the wetting film, formed at mica surface by the colliding bubble, is governed by the electrostatic interactions between the film interfaces. Both bubble and mica surface are negatively charged in distilled water. In solutions of the cationic surfactants studied (OTABr, DDTABr and CTABr) a preferential adsorption at solution/gas interface caused reversal of the bubble electrical charge from negative to positive and the wetting film formed was destabilized. It was found that time of the three-phase contact formation (t_{TPC}) at mica surface in cationic surfactants solutions strongly depends on: (i) solution concentration and (ii) state of the adsorption layer at the bubble surface. When the distance from the capillary orifice (bubble formation point) to the mica plate was L= 3mm (location "close") then the time of the three phase contact formation (t_{TPC}) was significantly shorter than for the location "far" (L=100mm). The differences between the t_{TPC} for the locations "close" and "far" were the largest at lowest concentration. Significant difference in t_{TPC} for location "close" and "far" was caused by formation of the dynamic adsorption layer (DAL) at the bubble surface. For location "far", where the adsorption coverage at the top pole of the colliding bubble was almost zero an additional time was needed to restore such adsorption coverage which caused the charge reversal from negative to positive and the film destabilization.

Acknowledgements

Financial support of MNiSW (grant N N204 1794/B/H03/2010/39 and Iuventus Plus 0490/H03/2010/70) is acknowledged with gratitude.

References

DAI, Z., FORNASIERO, D., RALSTON, J., 2000. *Particle–bubble collision models — a review,* Adv. Coll. Interface Sci., 85, 231-256.

DEBACHER, N., OTTEWILL, R.H., 1992. *An electrokinetic examination of mica surfaces in aqueous media*, Colloids and Surfaces, 65, 51-59.

DIAKOVA, B., FILIATRE, C., PLATIKANOV, D., FOISSY, A. KAISHEVA, M., 2002. *Thin wetting films from aqueous electrolyte solutions on SiC/Si wafer*, Adv. Coll. Interface Sci., 96, 193-211.

Dukhin, S.S., Deryaguin, B.V., Lisichenko, V.A., 1959. *Kinetika prilipania mineralnykh czastic k puzyrkam pri flotacii*, Zh. Fiz. Khim., 33, 2280-2287.

DUKHIN, S.S., KRETZSCHMAR, G., MILLER, R., 1995. *Dynamics of adsorption at liquid interfaces. Theory, Experiments, Application*, Elsevier.

FA, K., PARUCHURI, K.V., BROWN, S.C., MOUDGIL, B.M., MILLER, J.D., 2005. *The significance of electrokinetic characterization for interpreting interfacial phenomena at planar, macroscopic interfaces*, Phys . Chem. Chem. Phys., 7, 678-684.

FRUMKIN, A.N., LEVICH, V.G., 1947 . *Effect of surface-active substances on movements at the boundaries of liquid phases*, Zh. Phys. Chim., 21, 1183-1204

GU, G., XU, Z., NADAKUMAR, K., MASLIYAH, J., 2003. *Effects of physical environment on induction time of air–bitumen attachment*, Int. J. Miner. Process., 69, 235-250.

GRACIAA, A., MOREL, G., SAULNE,R P., LACHAISE, J., SCHECHTER, R.S., 1995. *The ζ-Potential of Gas Bubbles*, J. Coll. Interface Sci., 172, 131-136.

ISRAELACHVILI, J.N., 1994. *Intermolecular and Surface Forces*, Academic Press, London.

KRZAN, M., ZAWALA, J., MALYSA, K., 2007. *Development of steady state adsorption distribution over interface of a bubble rising in solutions of n-alkanols (C_5, C_8) and n-alkyltrimethylammonium bromides (C_8, C_{12}, C_{16})*, Coll. and Surface A., 298, 42-51.

LEE, J.S.H., LI, D., 2006. *Electroosmotic Flow at a Liquid-Air Interface,* Microfluid Nanofluid, 2, 361-365.

LEVICH, V.G., 1962. *Physicochemical Hydrodynamics*, Prentice-Hall, Englewood Clifts.

MALYSA, K., KRASOWSKA, M., KRZAN, M., 2005. *Influence of Surface Active Substances on Bubble Motion and Collision with Various Interfaces*, Adv. Colloid Interf. Sci., 205, 114-115.

NGUYEN, A.V., SCHULZE, H.J., 2003. *Colloidal Science of Flotation*, Surfactant Science Series, Marcel Dekker.

RALSTON, J., DUKHIN, S.S., 1999. *The interaction between particles and bubbles*, Colloids and Surfaces A., 151, 3-14.

SCALES, P. J., GRIESER, F., HEALY, T.W., 1992. *Electrokinetics of the silica-solution interface: a flat plate streaming potential study,* Langmuir, 8, 965-974.

SCHELUDKO, A., 1967. *Thin liquid films*, Adv. Coll. Interface Sci., 1, 391-464.

STECHEMESSER, H. J., NGUYEN, A. V., 1999. *Time of gas–solid–liquid three-phase contact expansion in flotation*, Int. J. Miner. Process., 56, 117-132.

STOCKELHUBER, K.W., 2004. *Stability and rupture of aqueous wetting films*, Eur. Phys. J. E., 12, 431-434.

ZEMBALA, M., ADAMCZYK, Z., 2000. *Measurements of Streaming Potential for Mica Covered by Colloid Particles*, Langmuir, 16, 1593-1601.

ZEMBALA, M., ADAMCZYK, Z., WARSZYŃSKI, P., 2001. *Influence of adsorbed particles on streaming potential of mica*, Colloids and Surfaces A., 195, 3-15.

ZEMBALA, M., ADAMCZYK, Z., WARSZYŃSKI, P., 2003. *Streaming potential of mica covered by latex particles*, Colloids and Surfaces A., 222, 329-339.

ZAWALA, J., DRZYMALA, J., MALYSA, K., 2008. *An investigation into the mechanism of the three-phase contact formation at fluorite surface by colliding bubble*, Int. J. Miner. Process, 88, 72-79.

ZHANG, Y., MCLAUGHLIN, J.B., FINCH, J.A., 2001. *Bubble velocity profile and model of surfactant mass transfer to bubble surface*, Chem. Eng. Sci., 56, 6605–6616.

A. Niecikowska, J. Zawala, K. Malysa, *Wpływ adsorpcji bromków n-alkilotrimetyloamoniowych (C_8, C_{12}, C_{16}) i ruchu pęcherzyka na kinetykę przyczepienia pęcherzyka do powierzchni miki*, Physicochem. Probl. Miner. Process., 47 (2011) 237-248, (w jęz. ang.)

Badano wpływ adsorpcji n-alkilotrimetyloamoniowych bromków (C_8, C_{12}, C_{16}) oraz utworzenia na powierzchni pęcherzyka, ruchem indukowanej dynamicznej architektury warstwy adsorpcyjnej (DAL), na kinetykę powstawania kontaktu trójfazowego (TPC) na powierzchni miki. Zjawiska zachodzące podczas kolizji pęcherzyka były rejestrowane przy użyciu szybkiej kamery o częstotliwości 1040 Hz. Określono wpływ stężenia roztworów i utworzenia DAL na kinetykę powstawania TPC. Wykazano, że stabilność ciekłego filmu, powstającego w trakcie kolizji pomiędzy pęcherzykiem a powierzchnią miki, jest determinowana przez siły elektrostatyczne pomiędzy granicami faz, które tworzą ciekły film. Kiedy pęcherzyk pokonywał odległość (od kapilary do powierzchni miki) L=3 mm (lokalizacja „blisko") czas powstawania kontaktu trójfazowego był znacznie krótszy, w porównaniu z odległością L=100 mm („daleko"). Różnice obserwowane dla L=3 mm i L=100 mm wzrastały wraz ze zmniejszeniem stężenia. Przedstawiono mechanizm wyjaśniający znaczące różnice w czasie powstawania kontaktu trójfazowego dla położenia „blisko" i „daleko".

słowa kluczowe: kontakt trójfazowy, kationowy surfaktant, zderzenia pęcherzyka, ciekły film, oddziaływania elektrostatyczne, zmiana ładunku

Physicochem. Probl. Miner. Process. 47(2011) 249-258
www.minproc.pwr.wroc.pl/journal/

Physicochemical Problems of Mineral Processing
ISSN 1643-1049

Received January 17, 2011; reviewed; accepted April 22, 2011

Recovery of zinc from arduous wastes using solvent extraction technique Part II. Pilot plant tests

Leszek GOTFRYD, Andrzej CHMIELARZ, Zbigniew SZOŁOMICKI

Institute of Non-Ferrous Metals, Sowińskiego 5; 44-100 Gliwice, Poland, leszekg@imn.gliwice.pl

Abstract. Solvent extraction technique using 40 vol. % bis(2-ethylhexyl)phosphoric acid as an extractant was applied for recovery of zinc from technological solutions. Crude zinc oxides from Waelz processing of electric arc furnace dusts or ferrous waste of zinc hydrometallurgy were used for preparation of feed solutions by leaching them with diluted sulfuric acid and by pre-liminary hydrometallurgical purification. The studies were conducted step by step from labor-atory to advanced pilot plant tests in continuously operating installation. Part II describes preparations and results of pilot plant counter-current experiments performed using laboratory extractive system, built from a train of mixer-settler type extractors, set in changeable counter-current manner, necessary pumps and automation systems, coupling pH measurements with neutralization agent supply. Excellent results in a form of very pure zinc sulfate solutions were obtained. $ZnSO_4$ concentrations are appropriate and the purity of the strip solutions very good. Comparison of natural and accelerated method of zinc extraction is done.

keywords: solvent extraction, zinc recovery, crude zinc oxide, electric arc furnace dust

1. Introduction

Background of the presented issue and a short literature survey has been presented in Part I of this paper (Gotfryd, 2011). The results of the preliminary and laboratory studies have also been presented there. These works were necessary to chose the best extractant and to establish conditions for further activities, which are described here. Part II presents the results of the pilot plant experiments of zinc recovery from preliminary purified zinc bearing technical solutions, especially prepared by leaching of industrial crude zinc oxides. Experiments, performed on pilot plant apparatus, used different solutions, prepared for this purpose from industrial crude zinc oxides by their leaching in sulfuric acid solutions. They covered also a number of extractors configurations and conditions, applied for particular series of the trials.

2. Experimental

2.1. Preparatory procedures

2.1.1. Leaching – solutions preparation

Treatment of crude zinc oxide dust consisted of the following steps:
- preparation of aqueous pulp of CZO of predetermined solid/liquid ratio, typically 250 g/dm^3,
- careful addition of a fixed portion of concentrated 96 % sulfuric acid,
- stirring the reacting pulp for a defined period of time, typically 1.0 hour, at 80-90 ^{o}C,
- solid/liquid separation (sedimentation and filtration).

2.1.2. Oxy-hydrolysis and cementation – preliminary solution purification

The solutions produced in the one-stage leaching process contain mainly zinc sulfate(VI) and also its typical contaminants: cations of non-ferrous (cadmium, copper, manganese, aluminum) and alkali/alkali earth (sodium, potassium, magnesium, calcium) metals, small amounts of iron and others anionic or neutral ingredients (As, Sb, chlorides, fluorides, SiO_2). Application of oxidative conditions (a batch of H_2O_2 and/or stirring with typical flotation aerator), combined with partial neutralization of the reaction environment (with milk of lime) to the level of pH ≥ 3.5-4.0, resulted in oxy-hydrolysis of unnecessary elements. After that operation iron was practically not observed in the solution (< 0.001 g/dm^3).

Absence of arsenic in the solution after this process provided grounds for starting further activities, i.e. precipitation of such elements as Cu, Cd, Sn, Pb, (Ni, Co) by addition of zinc powder (102 % of stoichiometry). Fifteen minutes of stirring turned out to be the proper period for carrying out the process.

2.2. Continuous counter-current experiments (pilot plant test)

Experiments on that scale were performed in an installation composed of a set of extractors of mixer-settler type (each of 0.5/1.5 dm^3 capacity), arranged in a counter-current systems with cooperation of necessary equipment and instrumentation: membrane pumps, pH-meters, automatic systems for pH controlling, based on feedback signals to pumps providing NaOH solution and submersible ceramic heaters, coupled with automatic temperature controllers.

Media were pumped by membrane pumps at the following rates:
- organic phase: 2.75-3.00 dm^3/h,
- feed solution: 9.0-10.0 dm^3/h,
- acid for stripping: 0.45-0.50 dm^3/h,
- scrubbing solution - diluted 0.05 M $ZnSO_4$: 0.40-0.60 dm^3/h.

These parameters were adjusted within given ranges according to the current needs. A more comprehensive description of the system is included in the Results and Discussion section.

A general idea of the pilot tests is depicted in Fig. 1, while the photograph in Fig. 2 presents the installation.

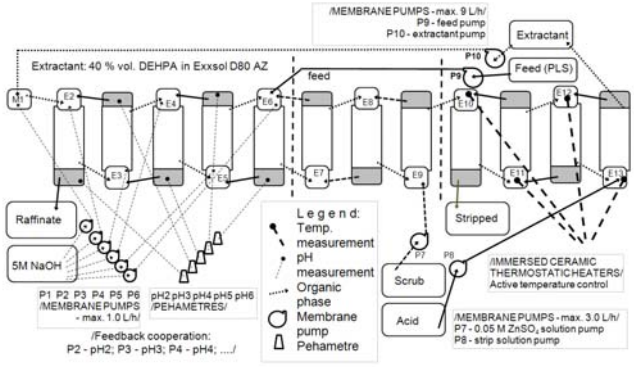

Fig. 1. Diagram of extraction, scrubbing and stripping system applied for recovery of zinc from preliminary prepared post-leaching solutions

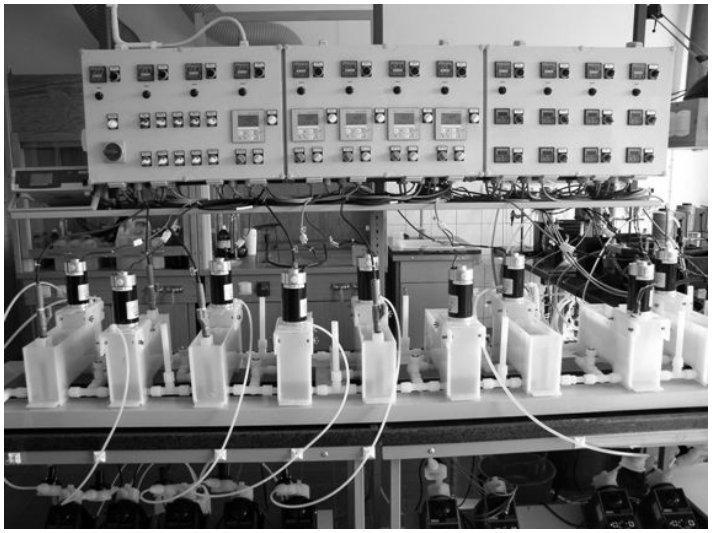

Fig. 2. Laboratory equipment, consisting of a set of mixer-settlers with systems of their feeding and control

3. Results and discussion

3.1. Leaching and solution purification

Composition of all solution used for extractive experiments are shown in Table 1. After applying the described leaching conditions, then the two steps of solution purification (oxyhydrolysis and Zn powder cementation), the solutions ‘b’ are ready

for further extractive treatment, even though the levels of some contaminants (e.g. Cd, Cu) are different.

The origin of the solutions was diversified as indicated below Table 1. Almost all of the solutions before extraction were routinely diluted with water or recycled from previous extraction experiments raffinates /RR/ to the values of 15-20 g Zn/dm^3, to adjust zinc(II) concentration to the level optimal for extraction.

Table 1. Composition of the solutions prepared for extractive zinc purification

*)	Sol. No.	Zn	Cd	Cu	Fe	Mn	Mg	Al	As	Sb	Na	K	Si	Cl	F	
1	1a	145.8	0.48	0.082	0.018	-	0.40	-	<0.001	<0.001	10.1	6.81	0,20	19.7	0.10	g/dm^3
	1b	146.1	0.0087	<0.0002	0.0006	-	0.40	-	<0.001	<0.001	10.1	6.81	<0.01	19.7	0.10	
2	2a	123.5	2.93	<0.001	0.36	-	0.53	-	0.028	0.005	0.91	1.62	-	3.64	0.006	
	2b	125.2	0.034	<0.001	0.0001	0.35	0.53	-	<0.001	<0.001	1.60	1.62	-	3.64	0.006	
	3a	113.3	2.90	<0.001	0.36	-	0.60	-	<0.005	0.005	0.80	1.40	-	3.50	0.02	
	3b	115.0	0.064	<0.001	0.0001	0.32	0.58	-	<0.001	<0.001	1.38	1.41	-	3.45	0.018	
	4b	107.0	0.010	0.010	<0.001	0.30	0.50	<0.01	<0.001	<0.001	0.20	1.10	<0.01	2.40	0.13	
	5b	116.6	0.013	<0.0005	<0.001	-	-	0.014	<0.001	<0.001	0.20	1.13	0.045	2.60	-	
1	6a	53.5	0.47	0.058	0.042	-	-	0.035	-	-	-	-	0.27	7.80	0.13	
	7b	88.6	0.027	<0.05	<0.001	-	-	0.11	<0.001	<0.001	-	5.39	0.028	2.50	-	
3	8a	51.0	1.12	0.051	0.0019	-	-	-	0.83	-	5.7	3.10	-	26.2	-	
	In fully purified solutions 'b': Ni and Co < 0.001 g/L															

*) - origin of leached crude zinc oxides: 1 – steel industry; 2 - classical zinc hydrometallurgy (Waelz processing of RLE process residues); 3 - copper pyrometallurgy (dusts).
Solutions: 'a' - as produced by leaching; 'b' - after additional preliminary hydrometallurgical purification (oxyhydrolysis + Zn powder cementation).

3.2. Pilot plant extraction

The range of extraction schemes which were applied for zinc purification in their fully developed form covered different counter-current systems, from set of extractors of (0)-4-1-4 type, through (1)-5-3-4 (see Fig. 1) to (1)-3-3-6 type, where the figures (p)-x-y-z denote a number of reactors assigned for extractant preneutralization (p), extraction proper (x), scrubbing (y) and stripping (z), respectively. All the tested systems and their characteristics are listed in Table 2.

Experiments lasted several weeks and covered not only different extraction systems but also various feed solutions (see Table 1 and 2). At the beginning and at the end of this period crude, unpurified solutions (No. 1a and 8a) were used. A few experiments (No. 1-5) were performed at ambient temperature – close to 22-25 ^{o}C. In the experiments No. 6 through 11 the temperature of the stripping area was elevated to 45-50 ^{o}C.

Each experiment was conducted for at least 4-6 days and then collected stripped

solutions were separated and analyzed for their purity (concentrations of 18 elements). The results of the analyses are shown in Table 3.

Table 2. Characteristics of tested extractive systems

No. of exp.	System of counter-current zinc extraction				Feed solution				Temp.
	Mixer-settlers config.*)	Solvent pretreat-ment	Autom. pH adjust.	Extractive process	No.	Predilution		Zn	
					**)		agent	g/L	°C
1	(0)-4-1-4	no	no	natural	1a	yes	water	15.60	ambient
2	(0)-3-3-3	no	no	natural	1b	yes	water	14.62	
3	(0)-5-3-3	no	no	natural	1b	yes	water	14.62	
4					2b	yes	water	12.35	
5	(0)-3-3-5	no	no	natural	3b	no	RR***)	115***)	
6	(0)-5-3-4	no	no	natural	5b	yes	water	14.6	45-50 (strip)
7					6a	no	none	53.5	
8					5b	yes	neutr. RR	20.3-22.5	
9	(1)-5-3-4	yes	yes	active: steady pH ≥2.0	7b	yes	RR	15.0-15.7	
10					7b	yes	water	15.0	
11	(1)-3-3-6	yes	yes		8a	yes	RR	13.8-15.0	

*) - figures (p)-x-y-z denote the number of reactors in the counter-current set of devices assigned for extractant preneutralization (p), extraction proper (x), scrubbing (y) and stripping (z), respectively,

**) – the number of mother feed solution as per Table 1; before extraction they were prepared (diluted) with water or recycled raffinate /RR/ to appropriate concentration,

***) - mother solution systematically diluted with raffinate recycled internally, i.e. directly in mixer of the extractor, which receives feed solution, with aqueous phase, taken straight from its own settler.

The results are discussed in details in the Conclusion section. Almost all experiments gave positive results in a form of satisfactory pure zinc electrolytes. Only one of them (No. 7 in Table 2), in which solution 6a was used, resulted in a complete failure. Because of high silica content in the solution used as a feed material, after several hours of reaction all the organic solutions turned into extremely viscous, very slowly flowing liquid, completely unfit for further operation. Mixing and/or pumping was still possible but further separation and transportation by gravity failed. The experiment ended with organics overflowed and spilled on the table under the extractors.

During the experiments temperature and pH in all settlers of extraction section were continuously measured and registered. The most interesting part of the pH measurements is shown in Fig. 3, where behavior of extraction system in the moment of the change from natural type extraction system No. 8 (no pH control) to the active pH control system No. 9 /see Table 2/ is presented.

The period from 0 to 130 minutes presents situation in five consecutive extractors, accomplishing experiment No. 8, where, without any external intervention,

pH within the settlers of extractors No. 1 to 5 has stabilized on the levels of about 1.0, 1.2, 1.3, 1.7, 2.0, respectively. Then (in 130 minute on the graph) electronic automation systems, coupling pumps of NaOH solution with pH-meters, adjusted with intention to sustain pH at the levels within the range of 2.0-2.2, were switched on. The full effect of that operation was observed not earlier then after 770 minute, which means that there was over ten hour period needed for the system to adapt to the new circumstances. After that period, even though the situation in the extractor No. 2 still isn't fully stable, the other ones (including the most important No. 5) operated quite correctly, according to the new conditions, i.e. sustaining pH values nearby expected point ≥ 2.

Figures 4 and 5 present cross-sections of all extractors with the registered concentrations of zinc(II) and sulfuric acid in the state of equilibrium of the extractive system as reached after several days of operation.

Table 3. Composition of zinc electrolytes produced with different schemes of extraction

	*)	1	2	3	4	5	6	8**)	9	10	11	***)
Zn	g/dm^3	126.5	140.8	155.0	147.4	162.1	165.9	169.0	170.0	158.8	158.4	164.8
Ca	g/dm^3		-	-	-	-	0.011	0.028	0.022	0.024	0.004	0.235
K	g/dm^3	-	0.0006	0.0003	0.004	< 0.6	0.029	0.003	0.063	0.047	0.015	0.999
Na	g/dm^3	-	0.0001	0.0008	0.006	0.0025	0.095	0.0075	0.325	0.251	0.116	3.04
Cl	g/dm^3	0.001	0.001	0.0018	0.096	0.010	0.021	0.041	0.017	0.11	0.0002	< 0.3
Mg	mg/dm^3	20	20	30	2	1	13	1	8	6	1	7290
Mn	mg/dm^3	-	-	-	-	-	23	0.4	0.9	1.1	0.6	6410
Cd	mg/dm^3	7.7	< 0.1	< 0.1	< 0.1	1.12	0.15	0.12	0.13	0.11	0.78	0.52
Ni	mg/dm^3	3.4	< 0.2	< 0.2	< 0.2	< 0.2	0.040	0.075	0.27	0.33	0.11	0.025
Co	mg/dm^3	1.1	< 0.2	< 0.2	< 0.2	< 0.2	0.18	0.14	0.14	0.12	0.16	0.36
As	mg/dm^3	0.057	< 0.1	0.025	0.05	0.05	0.1	0.1	0.1	0.1	8.7	< 0.1
Ge	mg/dm^3	-	-	-	-	-	0.01	0.01	0.01	0.01	0.22	0.02
Sb	mg/dm^3	0.077	< 0.1	<0.06	<0.06	<0.06	0.04	0.02	0.02	0.01	0.13	0.24
Fe	mg/dm^3	-	-	-	-	-	0.52	0.68	0.48	0.56	0.30	0.34
Sn	mg/dm^3	-	-	-	-	-	< 0.1	< 0.1	0.1	< 0.1	< 0.1	< 0.1
Pb	mg/dm^3	-	-	-	-	-	0.62	0.78	0.60	0.74	0.78	0.96
Cu	mg/dm^3	10	< 0.2	< 0.2	< 0.2	< 1.0	< 0.1	< 0.1	< 0.1	< 0.1	< 0.1	< 0.1
F	mg/dm^3	< 0.6	0.09	0.22	0.18	0.15	2.2	0.6	2.8	1.6	3.4	3.6

*) - the number of the extraction system as in Table 2

**) - experiment No. 7 failed because of silica excess in feed solution

***) - composition of the sample of industrial zinc electrolyte

The graphs provide possibilities to compare two typical situations, which were observed during the testing with the counter-current sets of extractors. They evidently show difference between the two main systems of extraction – the natural one, without any pH regulations, and automatically controlled.

The natural extraction (Fig. 4) shows almost linear progress and a

moderate slope of zinc(II) concentration along the row of five counter-currently configured extractors.

The extractions conducted with the extractant promoted with NaOH solution, which was added at the beginning to organic phase of the extractant in a separate mixer (partial 60-70 % preneutralization) and then continuously supplied to the mixer-settlers, can be seen as more progressive (Fig. 5). Therefore, the number of reactors could be limited here from five to three or even two units of mixer-settler type. But in a continuously operating system even that type of extraction does not provide possibilities for easy and complete removal of zinc from raffinates.

Figures 4 and 5 provide additionally the possibilities to observe how long it lasts in these both particular cases to attain extraction equilibrium. In the pictures there are inserted concentrations profiles after 4-5 consecutive days of action of each of them.

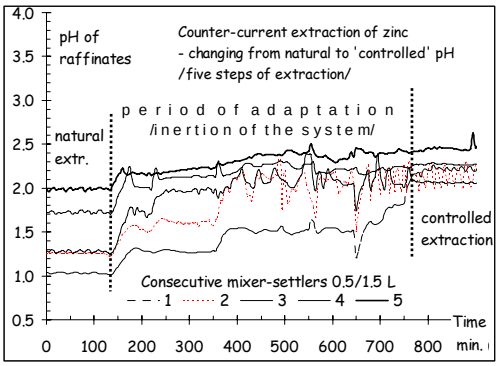

Fig. 3. pH variations in the period after switching from natural to automatically controlled pH of extraction

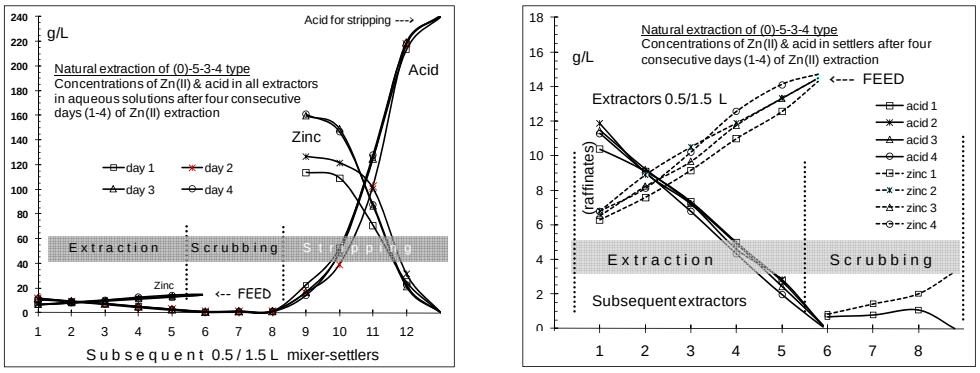

a b

Fig. 4. Acid and Zn^{2+} concentration in consecutive extractors after over 50 hours of operation ((0)-5-3-4 system of counter-current zinc extraction): a) full range, b) extraction and stripping

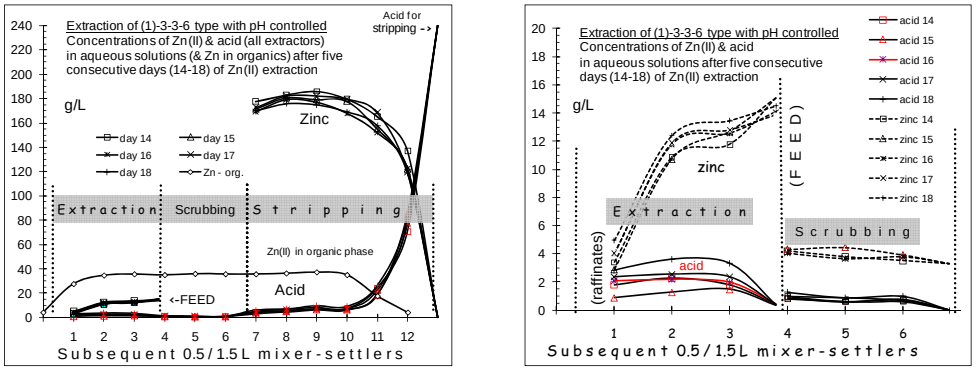

Fig. 5. Acid and Zn^{2+} concentration in consecutive extractors after over 50 hours of operation ((1)-3-3-6 system of counter-current zinc extraction): a) full range, b) extraction and stripping

4. Conclusions

The evaluation of technical results of the experiments, especially with regards to the composition of the produced zinc electrolytes (stripped solutions - Table 3), shows very low level of all technologically important contaminants. Only few of the samples can be qualified as solutions in which concentration of some, i.e. one or two, elements (Cu, Cd, Ni or As) very slightly exceeds the expected value. This especially applies to the solution No. 1 ('dirty' feed solution and too short scrubbing system), and to a lesser extent to solutions No. 5 and 11. The other are almost ready to be used as electrolytes in zinc electrolysis. To be fully accepted they should be only additionally treated for final removal of organic phase (e.g. by filtration through a layer of active carbon).

It is absolutely impossible to use the feed solution which contains colloidal SiO_2 (e.g. solution 6a in Table 1). This can lead to disastrous increase of organic phase viscosity. In such a situation the mixer-settlers and pumps are unable to operate properly.

Systems of zinc(II) extraction, promoted with current addition of alkali solution into each extractor, can be applied in very short (2-3 counter-current steps) extraction circuits, however they can be economically viable when using not expensive waste $NaOH/Na_2CO_3$ solutions only (even if contaminated, e.g. with NaCl). During such processes raffinates can be generated which contain mainly highly concentrated Na_2SO_4. They can be used (in about 90 %) cyclically for dilution of next batches of rich in zinc mother liquor, especially prepared in a reasonably concentrated form (e.g. containing 120-150 g/dm^3 Zn^{2+}) by leaching zinc-bearing materials at high solid-to-liquid ratio. The rest of the raffinate, some 10 % of the bleeding, which still contain small amounts of zinc, must be treated for further zinc recovery, e.g. by carbonate precipitation, before sending it to an effluent treatment plant or rather for Na_2SO_4 recovery in crystalline form.

Schematic flow sheet of proposed course of extractive technology based on such sort of extractive processes is depicted in Fig. 6.

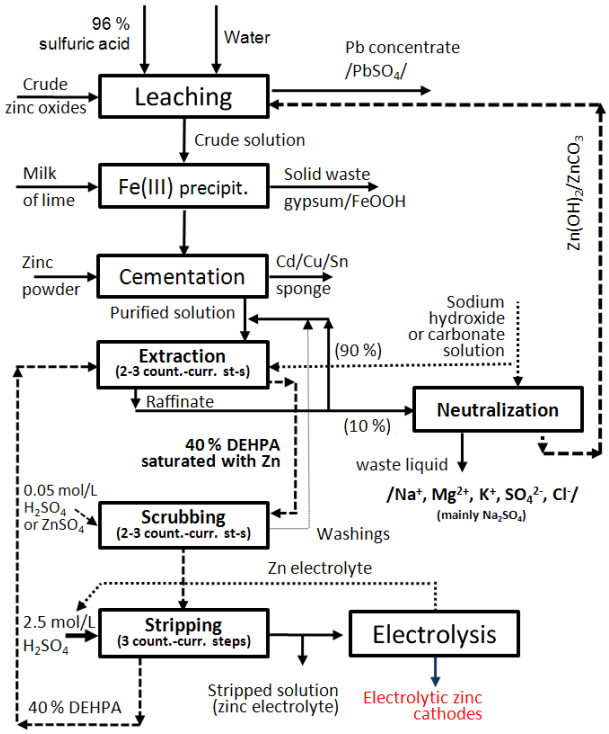

Fig. 6. Flow sheet of the proposed process for crude zinc oxide hydrometallurgical treatment based on promoted extraction of zinc(II)

The natural extraction is not as efficient as the promoted one, but it is performed without any additional reagents added currently to extraction, and these conditions (pH as low as naturally possible, even $\leq$ 1.0) favor higher zinc(II) extraction selectivity. Extractions can be organized and performed depending on Zn(II) concentration in PLS, i.e. the obtained acidic raffinates can be used again, in some 90 %, alternatively:

- recycled as acidic lixiviants for leaching of next batches of raw material (Alternative I for diluted PLS),
- recycled, but after their neutralization with lime stone powder, for PLS dilution, thus preparing it to be ready for direct zinc extraction (Alternative II for concentrated PLS).

Of course, in both cases, there is a need to bleed and treat a small fraction of the post-extraction solution (raffinate I) to recover the remainder of zinc(II) and other components (Cu, Cd), if they were not removed previously. Excessive acid can be earlier eliminated in a form of gypsum.

Both alternative raffinates I (i.e. their about 10% bleed) can be treated again by further additional extraction, however a significantly higher organic-to-aqueous ratio should be applied to reach higher efficiency of total zinc(II) extraction. The produced secondary raffinates II should be treated with limestone and/or milk of lime to separate zinc-containing and recyclable to the leaching stage sediments, and then disposed of to an effluent plant. A flow sheet of the proposed process for crude zinc oxide treatment with natural extraction involved, is shown in Fig. 7.

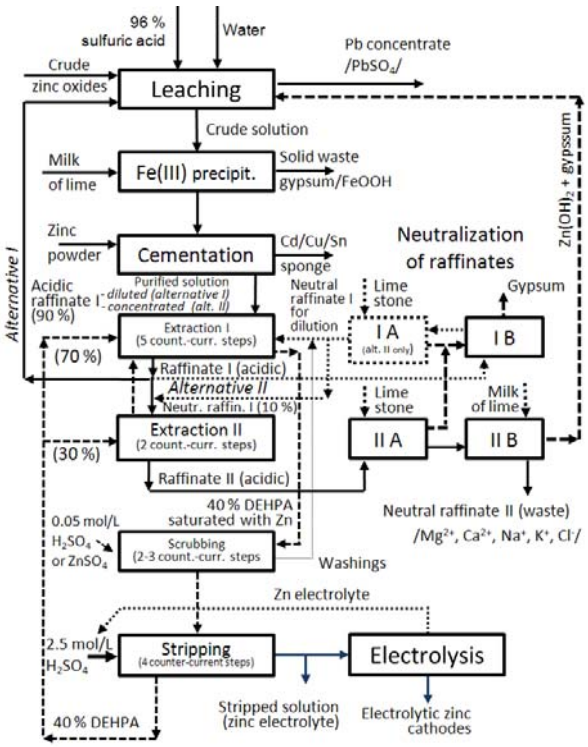

Fig. 7. Flow sheet of the proposed process for crude zinc oxide hydrometallurgical treatment based on natural extraction of zinc(II)

Acknowledgment

The study was supported within the scope of Research & Development Project of Polish Ministry of Science and Higher Education No. PBR R 07 032 02 (Contract number 0570/R/2/T02/0702).

References

Gotfryd, L., Chmielarz, A., Szołomicki, Z., 2011, Recovery of zinc from arduous wastes using solvent extraction technique, Part I. Preliminary laboratory studies, Physicochem. Probl. Miner. Process. 47, 149-158.

Physicochem. Probl. Miner. Process. 47(2011) 259-266
www.minproc.pwr.wroc.pl/journal/

Physicochemical Problems of Mineral Processing
ISSN 1643-1049

Received February 9, 2011; reviewed; accepted March 22, 2011

Aggregates from tunnel muck treatments. Properties and uses

Rossana BELLOPEDE, Paola MARINI

Land, Environment and Geo-Engineering Department, Politecnico di Torino, Corso Duca degli Abruzzi, 24, 10129, Torino, Italy, rossana.bellopede@polito.it

Abstract. Tunnel muck should be considered as a valuable resource: if it is managed and treated correctly, it can be used for different purposes. This would lead not only to environmental benefits but also those of an economic nature.

This work is part of the REMUCK project and it has the purpose of evaluating the effects of different treatments on different types of excavated rock. Five case studies have been selected and, of these, two were excavated with TBM (the Torrent-La Thuile tunnel and the Brennero tunnel), one with EPB (the Turin underground railway) and two using traditional excavation methods (Turin underground railway station and the Omegna tunnel).

Tests have been carried out in the laboratory on both the muck in its natural state and on muck treated in two different plants (a mobile plant and a fixed plant) in order to characterise the aggregates from the shape and mechanical resistance points of view (according to EN 933-3 and EN 1097-2, respectively). The results of these tests have been compared with the threshold values foreseen in a muck management plan for a tunnel in Switzerland in order to verify the quality of the treatments the recycled aggregates were subjected to. This has made it possible to evaluate the suitability of the treatments, on the basis of the foreseen types of use, and to propose alternative working schemes for the nonconforming cases.

keywords: concrete aggregates, shape, mechanical resistance, mobile plant, fixed plant

1. Introduction

Each production process is obliged to respect sustainability principles, which means complying with the economic soundness, quality of the product, safety of the workers and environmental safety requirements. This involves paying special attention to the environment and major efforts are required even by companies in the infrastructures sector.

In this context, and in particular in the “sustainable mobility” sector, REMUCK project (Innovative methods for the eco-compatible and sustainable recycling of muck from tunnel excavation, also considering the potential content of noxious minerals – Regione Piemonte – CIPE 2006 call-to-tender) has been financed with the aim of developing and turning innovative methods to face the problems posed by waste muck

disposal and of optimising the management of waste recycling, in order to take economic advantage from the reuse of excavated waste materials.

The current survey and the potential increase in underground constructions (and tunnels in particular) foreseen for the future to answer the increasing demand for infrastructures, will involve a huge amount of tunnel muck , which, if not re-used, has to be dumped , with high costs concerning both the impact on the territory and the project itself. In tunnelling excavation, two very important aspects have to be taken into account: the dumping of the excavated material and the opening of new quarries to supply raw materials.

A solution that could be proposed to minimize these relevant environmental problems is the recycling, or reusing, of the muck from tunnel excavations which can be employed as aggregates for concrete, for bituminous conglomerates, for road construction, or for raw materials for industry. Tunnel muck can be used: in its natural form, as obtained from the excavation, treated in plants, treated or in its natural form with addition of other materials or as raw material for industrial products (not very common use).

Tunnel muck is more frequently used as:

- refilling material
- material for reliefs
- road construction
- concrete
- raw material for industrial production.

The properties considered to determine the final use vary according to its final use and refer, as far as the physical aspect is concerned, to the size distribution, the maximum dimension, the shape and the density, whereas from the chemical point of view, they concern the presence of some reactive minerals.

Before muck can be used as concrete aggregates, it must have suitable properties: as far as the petrographic properties are concerned, the presence of a significant quantity of brittle minerals (clay, gypsum, talc), of very hard minerals (garnet) and of foliated and fibrous minerals (mica, graphite, asbestos), should be avoided, whereas, as far as the chemical properties are concerned, high solubility (chloride, sulphate, gypsum), low resistance to decay (anhydrite, pyrite) and alkali reactivity have a negative affect.

No notable publication concerning the reuse of tunnel muck, with treatment processes has been published since 1999. In that year the CIRIA project which was carried out in Great Britain (Kwan and Jardine, 1999), analysed 32 underground excavation cases and their related waste management systems. Some general guidelines have emerged from the CIRIA project concerning the planning, designing and building of underground construction. Moreover, the CIRIA project, took into account the different possible uses of the tunnel muck, even though in general terms. With the new large roadworks (St. Gothard, Loetschberg, Turin-Lyon, Brennero), this matter has been dealt with in different papers, on the basis of studies and investigations executed at the same time as the works are underway (Darmendrail et al., 2003; Lombardi et al., 2008;

Thalmann et al., 2005). The importance of a suitable tunnel muck classification emerges from the literature pertaining to its recovery but, above all, to the necessity of correlating the kind of rock, the excavation technique, the treatment method and the possible uses; this is the aim the REMUCK project has set itself.

2. Materials and methods

Five case studies have been selected in the REMUCK project: two cases of the Torino underground railway and the Omegna tunnel –regional road 229 in Piedmont (Italy), the Torrent – La Thuile tunnel for a hydroelectric power station in Aosta Valley (Italy) and the Brennero tunnel which connects Innsbruck (Austria) to Fortezza (Trentino Alto Adige – Italy). The studied cases, the kind of muck analysed and the excavation techniques are reported in Table 1.

Table 1. The studied cases in the REMUCK project with the analyzed muck and the excavation methods

tunnel	Torino - Corso Dante	Torino - Largo Marconi	Omegna	Torrent - La Thuille	Brennero (Aica)
muck	alluvial rocks: quartz, green rocks, cemented rocks	alluvial rock: quartz, green rocks, cemented rocks	granite	calcareous schist	granite
excavation method	cut&cover	earth pressure balance	drilling&blasting	tunnel boring machine	tunnel boring machine

A sample of muck has been taken from each tunnel and analysed in the Politecnico di Torino laboratories, in order to verify the suitability of the muck for re-use either in its natural state or after treatment. As far as the treatments concerned, the tunnel muck taken from the excavation yards has been treated in two different plants of two companies involved in the REMUCK project: one mobile and the other fixed.

The mobile plant (Figure 1) has an output of 280 t/h and a maximum input dimension of 600 mm. It is essentially made up of a vibrating screen above a primary jaw crusher and a magnetic separator above a conveyor belt, before the point where the treated material exits. The procedure produces only one kind of output.

The fixed plant (Figure 2) has an output of 250 t/h and a maximum input dimension of 300 mm. It is made up of two compartments: the one of the aggregates in their natural state with only a screen and washing process and that of the crushed aggregates. Water is used in the treatment plant. Two hammer crushers and a jaw crusher (secondary crushing) are placed in sequence in the crushing compartments and these are followed by vibrating screens.

From an accurate analysis of the EN standards concerning the different test methods foreseen for the different aggregate uses (which are the same Standards for

the EC marking of aggregates), the following characterization tests have been selected and carried on the tunnel muck materials:

- petrographic description (see Table 1);
- grain size distribution;
- shape of coarse aggregates (flakiness index and shape index);
- resistance to fragmentation of the course aggregates.

The evaluation of the finest content has been performed on the Torino underground railway muck, because of its high content of fine grained material.

Fig. 1. The mobile plant

Fig. 2. The fixed plant

3. Comparison with the requirements foreseen for the aggregate control plan of a Swiss tunnel

In the planning of an underground construction, the management of the excavation materials should be an integral part of the project which should also

contain a control plan. This plan should include tests that have to be executed on tunnel muck to verify the suitability for different uses.

The control plan of a Swiss tunnel has been taken into account due to the extensive experience of this country in the reuse of tunnel muck. This plan foresees five different uses, according to the quality of muck: concrete with high – medium compression resistance, second quality aggregates, third quality aggregates for relief and refilling, non compactable and silty, polluted materials. It should be pointed out that all the tunnel muck that has been analysed shows good petrographic properties, according to UNI 8981-8, EN 12620 and EN 932-3. The following tests are included in the control plan for the first three kinds of use: the flakiness index (according to EN 933-3: 2003) and resistance to fragmentation (according to EN 1097-2: 2008 - Los Angeles test).

The threshold values required by the Swiss control plan are reported in Table 2, together with the laboratory test results.

Table 2. The studied cases in the REMUCK project: variation of shape and flakiness index and mechanical resistance after the two different treatment plant
(N: not treated; M: mobile plant; F: fixed plant)

		Torino-Corso Dante	Torino - Largo Marconi	Omegna	Torrent - La Thuile	Brennero (Aica)	Threshold values from Swiss control plan		
							Concrete	Aggregates 2nd quality	Aggregates 3rd quality
Shape/Flakiness index	N	21/36	14/13	14/15	53/44	36/22	flakiness 20	flakiness 35	flakiness 50
	M	19/16	4/10	7/10	29/40	-			
	F	-	-	7/2	17/21	6/10			
Mechanical resistance (Los Angeles /Micro Deval)	N	28/19	22/11	-	-	24/9	30	40	not required
	M	29/18	24/12	31/23	27/-	-			
	F	-	-	38/11,5	22/-	23/-			

4. Results and discussion

The two different treatment technologies have led to different effects on the size distribution of the studied tunnel muck. Fundamentally, the treatment in the mobile plant does not furnish a suitable size distribution for the treated tunnel muck to be used as concrete aggregates. An example of this is the granulometric distribution of the Omegna tunnel muck after the treatment in the mobile plant, that has been compared, in figure 3 with Fuller and Bolomey curves referring to ideal concrete aggregate distributions (Collepardi, 1991). The fixed plant offers a suitable product for concrete, if the different size fractions obtained in the plant are mixed appropriately.

The shape and flakiness of the tunnel muck condition the suitability of use as concrete aggregates to a great extent. Very flat particles are not suitable for use as concrete aggregates. The jaw crusher in the mobile plant causes a slight decrease in the shape and flakiness index but, the jaw crusher is not suitable for schistose rocks, like that of Torrent-La Thuile tunnel (excavated by means of TBM). As far as the

Torrent – La Thuile muck is concerned, after the crushing in the mobile plant, the flakiness index decreased from 44 to 40 (and the shape index from 53 to 29); this value is however still too high. The results pertaining to the muck shape, after the treatment in the fixed plant, are undoubtedly better: this treatment causes a decrease in the flakiness index of 50%. The mechanical resistance values, instead, are not affected by the different treatment processes (Table 2).

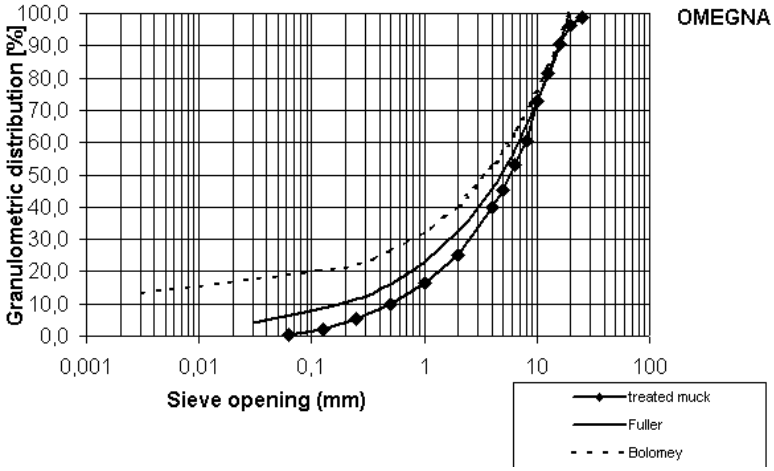

Fig. 3: Granulometric distribution of the Omegna muck after treatment in the mobile plant, compared with the Fuller and Bolomey curves for concrete

If a comparison is made of the test results, on the different tunnel mucks, with the threshold values of the Swiss tunnel control plan (Table 2), it is possible to note that among the studied tunnels, the Torino underground railway (Largo Marconi) muck is the only one that is suitable for use as it is for concrete (taking into account only the shape and mechanical resistance). The Omegna tunnel muck complies with the shape requirements but, being a weakly jointed rock, does not have a satisfactory mechanical resistance. The rocks excavated by TBMs (Torrent and Brennero) are suitable for use as concrete aggregates but only after treatment in the fixed plant.

5. Conclusions

The flaky shaped particles of tunnel muck excavated by TBMs have proved to be unsuitable for reuse as concrete aggregates since, during the concrete mixture, the particles tend to deposit according to horizontal levels, trapping water in the mixture which consequently causes a decay in the structure. The surface roughness and the presence of sharp corners make the bond between the aggregates and cement better, but at the same time reduce the workability, as the muck requires a higher amounts of water and cement which , therefore, leads to an increase in costs. Only the treatment in the fixed plant (with two hammer crusher and a secondary jaw crusher) makes the

aggregates rounder and isodiametrical and reduces the flakiness index therefore making it comply with the requirement for concrete.

As the outputs of the two treatment plants are different, especially concerning the shape of the treated muck, it is possible to assert that the action of the hammer crusher is important. A mobile plant with a primary "hammer" or "impact" crusher could result in products that are more suitable for use in concrete and which could answer to versatility requirement that is often required in this kind of yards

The use of tunnel muck in concrete, roads, refilling and relief is not the only possible final utilization. Some kinds of rocks such as the granite (found in the Omegna and Brennero tunnels) can also be further valorised and some of their minerals such as quartz and feldspars can be recuperated and employed in the glass or ceramic sector.

Aknowledgements

This research has been possible thanks to the collaboration of: BBT, ARES PIEMONTE, AK Ingegneria Geotecnica S.r.l and GTT which offered the material used to conduct the tests and RADIS Spa and CO.GE. FA. Spa (partners in the REMUCK project) which are involved in the transport and treatment of tunnel muck.

References

COLLEPARDI M., 1991, *Scienza e Tecnologia del Calcestruzzo*, Terza Edizione, Hoepli, Milano, Italy, pp. 541.

KWAN J.C.T. AND JARDINE F.M., 1999, *Ground engineering spoil: practices of disposal and reuse*. In Engineering Geology n. 53, pp. 161–166

DARMENDRAIL X., BURDIN J., RIMEY J. AND BRINO L., 2003. *Nouvelle liaison ferroviaire Lyon – Turin Une approche d'étude originale pour la valorisation des déblais des tunnels* . In Tunnels et ouvrages souterrains, n. 176, pp. 55-61

EN 12620: 2008 Aggregates for concrete CEN Brussels 53p

EN 932-3: 2004 Tests for general properties of aggregates - Procedure and terminology for simplified petrographic description. 16p

EN 933- 3: 2003 Tests for geometrical properties of aggregates - Determination of particle shape - Flakiness index. CEN Brussels 7p.

EN 993-4: 2008 Tests for geometrical properties of aggregates - Determination of particle shape - Shape index. CEN Brussels 11p

EN 1097-1: 2004 Tests for mechanical and physical properties of aggregates - Determination of the resistance to wear (micro-Deval) 16p.

EN 1097-2: 2008 Tests for mechanical and physical properties of aggregates - Part 2: Methods for the determination of resistance to fragmentation. CEN Brussels 24p.

LOMBARDI A., FRANZÈ F., FUOCO S., PASQUALI F., RAUSA L. AND PIZZAROTTI E.M., 2008, *Il cunicolo di Aica: il primo passo verso Monaco*.In Strade & Autostrade, vol. 1, pp.106-116

UNI 8981-8: 1999 Durabilità delle opere e degli elementi prefabbricati di calcestruzzo - Istruzioni per prevenire la reazione alcali-silice. 20p.

THALMANN C., CARRON C., BRINO L. AND BURDIN J., 2005, *Gestion et Valorisation des Matériaux d'Excavation de Tunnels Analyse comparative de 3 grands projets St. GOTHARD, LOETSCHBERG, MAURIENNE-AMBIN*. Communication Chambery 2005

Physicochem. Probl. Miner. Process. 47(2011) 267-274
www.minproc.pwr.wroc.pl/journal/

Physicochemical Problems of Mineral Processing
ISSN 1643-1049

Received April 5, 2011; reviewed; accepted May 5, 2011

Screens for segregation of mineral waste

Remigiusz MODRZEWSKI, Piotr WODZINSKI

Łódź University of Technology, ul. Wólczańska 175, 90-942 Łódź, Poland, wodzinsk@wipos.p.lodz.pl

Abstract. The paper presents the results of investigations on classification of different mineral waste on screens with flat screens and rectangular riddles. We developed three different constructions of such screening and subjected them to tests and process examinations aimed to determine their efficiency and productivity on the semi-technical scale. Basing on the presented studies we developed the design assumptions and the industrial screen was constructed for industrial processing of mineral waste.

keywords: screening, screen, sub-sieve, grained material, grain classes

1. Introduction

Processing of mineral waste is of great importance in the economy, first and foremost due to the large amount of waste, as well as their diversity. Mineral wastes are present in many branches of industry, particularly in the mining of coal and rock materials and energy and metallurgy. The vast majority of waste is indeed of a high usable value and the possibility of their use is very broad. Hence, often, instead of "waste" it is reported that there occur raw materials accompanying the extraction of the main mine raw material.

One of the most important unit operations in processing of mineral waste is a screening process (Rogers, 1982; Schmidt, 1984). The most appropriate machines for the implementation of the process are, according to the authors, modern screens of flat screens and rectangular riddles and with a linear flow of the feed. Those machines have been constructed in recent years and examined at the Technical University of Lodz to apply, inter alia, for the treatment of mineral waste.

2. Mineral waste

The area of industrial activity in which the mineral wastes pose the greatest problems is undoubtedly opencast mining. Lignite mining is always the appearance of large quantities of associated minerals, having the nature of mineral waste generated as a result of mining activity. Those minerals constitute a major problem throughout the mining industry, not only in the opencast mining of brown coal, though they occur

there the most numerously. Raw materials accompanying lignite mines are applied to various branches of industry. Under conditions of mass occurrence of minerals it is possible to exploit the most valuable varieties being in demand, or there is a chance for their protection by the formation of secondary deposits. Opencast lignite exploitation is associated with handling very large quantities of overburden - sediments lying above the coal bed. Simultaneously, the slopes of the pit mine and in the under-lignite zone rocks and sediments are uncovered – so far inaccessible from the surface. A large amount of sediments and rocks is a commodity of high relevance. The recovery of even 1% of outlay as accompanying minerals is crucial for resource economy of the country, and especially of the central region, where the availability of mineral resources is extremely limited.

Based on several years of research and experience with the screening of various mineral waste, the authors of the present paper believe that the freely vibrating screens with flat screens are most appropriate machinery to perform those processes. There were selected three modern structures such screens, which were tested for their suitability for the segregation of different mineral waste.

3. Screens for classification of mineral waste

The first of the tested machines was a circling and revolving screen - (Fig. 1) being a construction of spatial screen movement of the sieve. It consists of a riddle with 4 screens spread inside, suspended on an elastic spring suspension 5. A feature of the screen is the location of extreme vibrators 2 and 3 being synchronized concurrently or counter-currently cause the movement of the riddle in the plane screens.

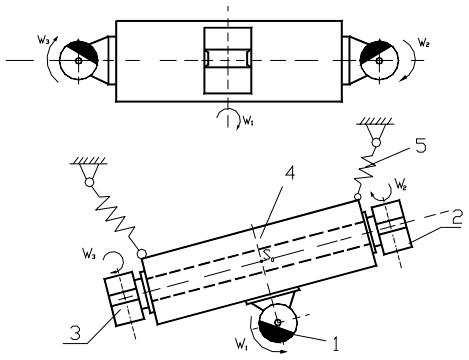

Fig. 1. Circling-and-revolving screen

This movement is applied to the circulating movement caused by a middle vibrator 1 positioned under or the rectangular sieve. This results in a complex spatial movement of the sieve (Fig. 2). Figure 3 shows selected example courses of efficiency curves of circling-and-revolving screen for different drive variants during segregation of typical mineral waste.

Another one-plane screener being characterized by high development potential is the linear-elliptical screen (Fig. 4). It has many elements in common with the other machines discussed here. A characteristic feature of the screen is its drive, made of two rotary vibrators 4 and 5.

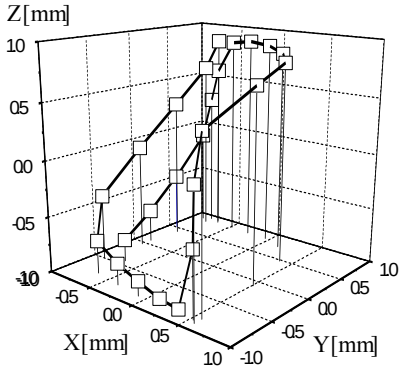

Fig. 2. Example trajectory of circling-and-revolving screen

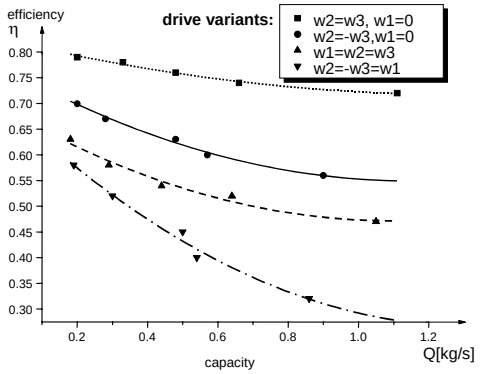

Fig. 3. Efficiency and capacity of circling-and-revolving screen

Vibrators may have identical or different static moments. If those moments are different, it is preferred that the drive shaft with a higher static movement was under the sieve (as low as possible) as shown in Figure 4.

A linear - elliptical screen can be horizontal or slope in the direction of intended movement of the particulate material movement. With the deployment of both vibrators both locations of vibrators ensure the transport of the granular layer along the screen.

Figure 5 shows comparison of theoretical and experimental trajectory of linear-elliptic screen.

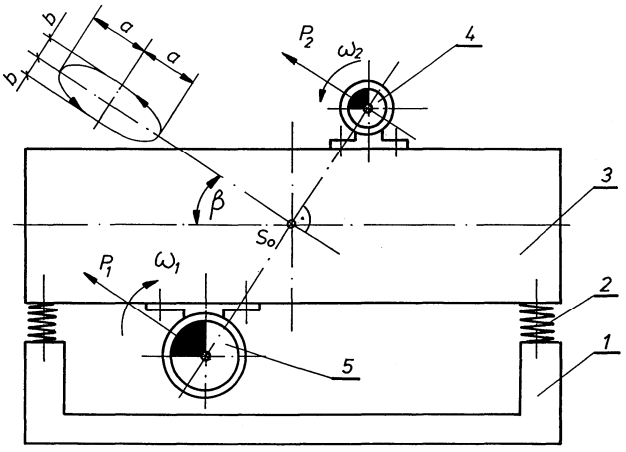

Fig. 4. Linear-elliptic screen

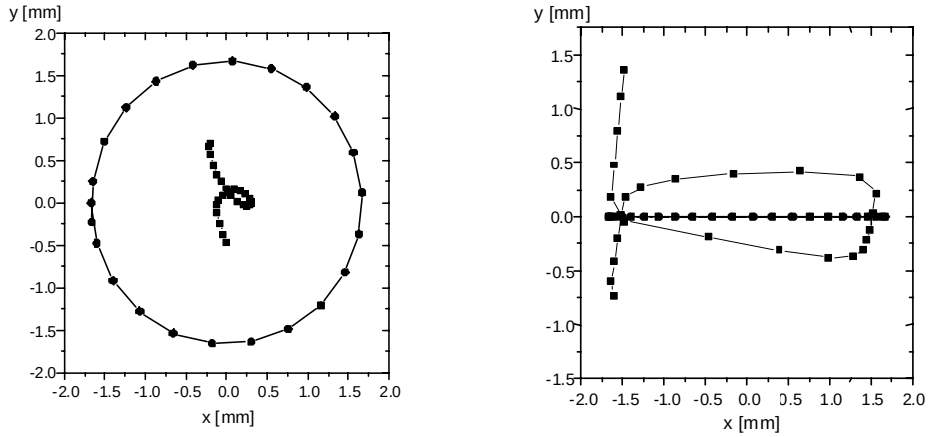

Fig. 5. Comparison of theoretical and experimental trajectory

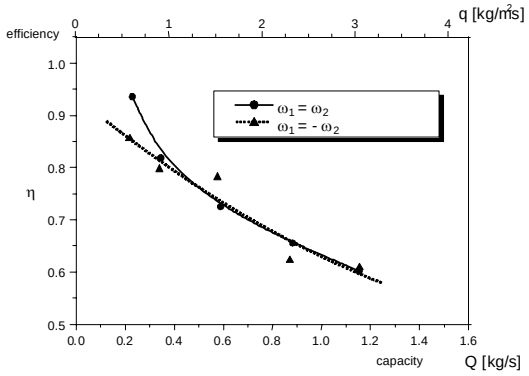

Fig 6. Efficiency curves for different drive vibrators synchronization

Efficiency curves for different drive vibrators synchronization of linear-elliptic screen, during segregation of mineral waste are shown in figure 6.

The last of the tested machines was a two-frequency screen. This machine is schematically shown in Figure 7 with a horizontal variant being presented in Figure 7, however, this machine can also be tilted at an angle α, at $15 – 20^0$. To drive this screen one may apply two rotary vibrators of equal or unequal static moments. The machine can have positioned a differently kinematic axis (eg OK_1 or OK_2 in Figure 7), it depends on the deployment of propulsion vibrators on a riddle. An extremely important parameter characterizing the work of a two-frequency screen is the coefficient of a speed transmission ratio defined as

$$\xi = \frac{\omega_1}{\omega_2} = \frac{n_1}{n_2}. \tag{1}$$

This quantity tells us if they differ from each angular velocity (or rotational) of two rotary vibrators. Depending on the applied speed gear ratio and direction of rotation (in line and in the opposite line), one can attain different paths of a vibrating motion for example shown in Figure 8.

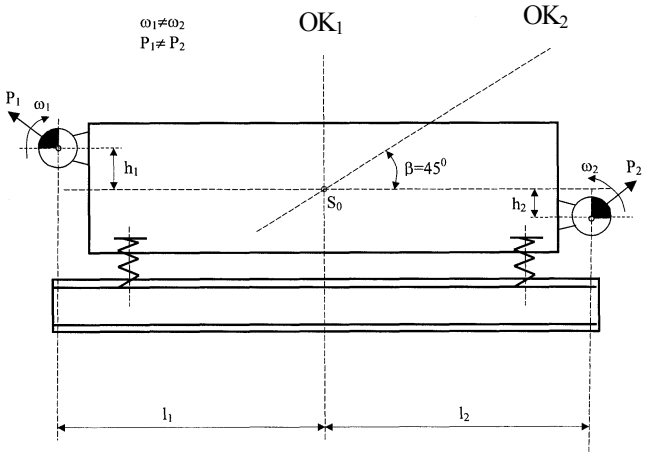

Fig. 7. Double-frequency screen

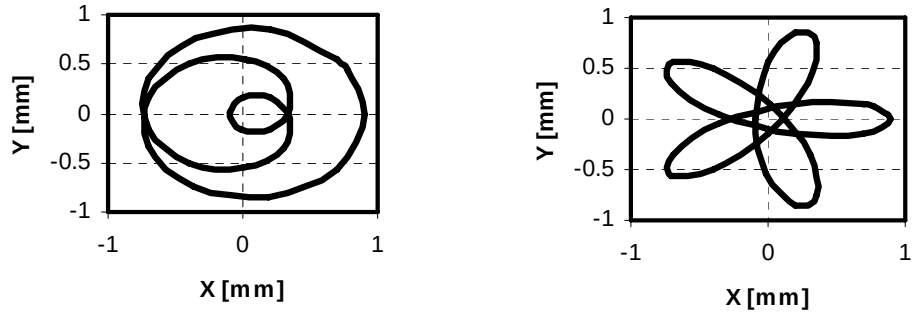

Fig. 8. Example trajectory ($\xi = \frac{1}{3}$ and $\xi = -\frac{1}{3}$)

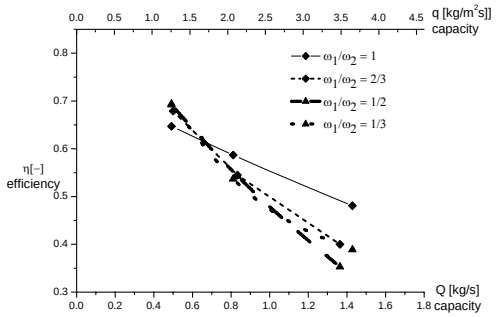

Fig. 9. Efficiency curves for different drive variants

Efficiency and capacity for different drive vibrators variants of double-frequency screen for mineral waste segregation presented figure 9.

Works performed so far were aimed at kinematical and process examinations of screens described above in terms of their suitability for the segregation of different types of mineral waste.

4. Conclusions

As a criterion of assessing the quality of the work mentioned above the screening efficiency and mass efficiency, parameters being crucial for the economy of the process. The research process constitute the only way to achieve the objective that is the optimization of the propulsion system as even the correct operation of mechanical systems does not yet provide a sufficiently good conditions for screening (Fischer, 1982).

Figure 10 shows selected example courses of efficiency curves of screens discussed previously. The presented examples concern screening of all kinds of mineral waste. Due to the multiplicity of construction and driving variants of those screens, the total number of such plots attained during the years of research is enormous. The conclusions concerning individual screens, presented in isolation, have been presented in numerous publications (Modrzewski and Wodziński, 2010; Modrzewski and Wodziński, 2011).

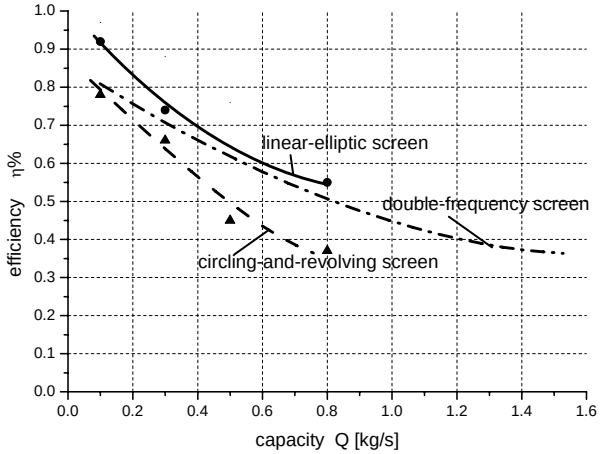

Fig. 10. Comparison of efficiency and capacity of described screens

Based on the investigations one may state that the majority of presented types of screens may find an application to screening both rock aggregates and application to both rock aggregates and mineral waste.

However, in situations where one deals with fine grained materials that are known to impede screening, the most advisable would be a double-frequency screen. Particularly, in situations where the process requires a high efficiency of mass, and as often happens when the processing of waste, a double-frequency screen due to its ability to intense segregation of a layer on the wire ensures a satisfactory performance.

This also happens while screening of relatively thick layers with which typical screens do not succeed. The situation resembles the one which occurs in the case of wet materials. Moisture content significantly hinders the process of screening, yet the majority of minerals and mineral waste is not a dry material . Screening resistance occurring at the time are mainly associated with the resistance of the granular layer

and not the passage of grain through a sieve. The resistance of such superbly two-frequency screen due to its distinctive dynamics of the movement of the sieve.

In situations being less cumbersome and thus, for example, when screening of dry materials of larger grains or more oval beans, the best screen is, according to the authors, the linear-elyptical screen. His ability to segregate is slightly smaller than the double-frequency screen but the same design is a bit simpler - especially in the field of electrical control (no alternating current power inverters). This has a positive economic impact, both at the stage of investment and later - operational (lower power consumption).

As for the construction of the spatial motion filters whose representative is the circling and revolving screen it is the least useful for the classification of mineral waste from those screens, at least at the present stage of development of this construction. The reason is too low stiffness of the riddle causing difficulties in ensuring proper motion granular layer on the sieve, and this in turn adversely affects the efficiency and productivity of the process. These machines require the riddles of high stiffness in three mutually perpendicular directions. It is possible to achieve but requires an entirely new design of the riddle and the resignation from its current simple design. A double-frequency screen was constructed in the industrial version. It works in the mining industry and is used for sifting of fine and very fine-grain mineral waste in the mine. The screen is equipped with a three-stage sieve and the vibrating mass is 4500 kg. Schematically, this machine is shown in Figure 11.

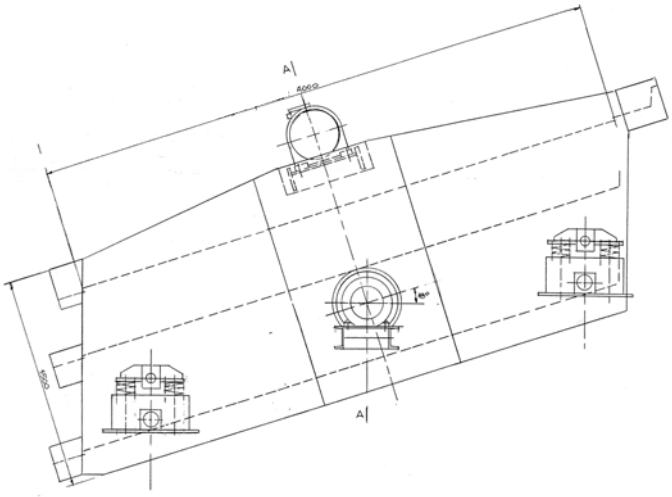

Fig. 11. Industrial double-frequency screen

Acknowledgments

This study was performed as a part of chartered assignment W-10/12/2011/Dz.St.

References

FISCHER M., 1982. *Doppel-Frequenz-Siebmaschinen in der Bewahrung*, Aufbereitungs Technik., 12, 687-693

MODRZEWSKI R., WODZIŃSKI P., 2010. *The results of process investigations of a double-frequency screen*, Physicochem. Probl. Miner. Process., 44, 169-178

MODRZEWSKI R., WODZIŃSKI P., 2011. *Grained material classification on a double-frequency screen,* Physicochem. Probl. Miner. Process., 46, 5-12

ROGERS R.S.C., 1982. *A classification function for vibrating screens*, Powder Technology, 1, 135-137

SCHMIDT P., 1984. *Das Siebklassieren*, Chem. Ing. Techn., 56, nr 12.

Physicochem. Probl. Miner. Process. 47(2011) 275-284
www.minproc.pwr.wroc.pl/journal/

Physicochemical Problems of Mineral Processing
ISSN 1643-1049

Received March 25, 2011; reviewed; accepted May 8, 2011

Research on adsorptive and electrokinetic properties of SiO_2 in the presence of polyethylene oxide of different purities

Jacek PATKOWSKI, Stanislaw CHIBOWSKI

Department of Radiochemistry and Chemistry of Colloids, Faculty of Chemistry, UMCS, pl. Marii Curie-Skłodowskiej 3, 20-031 Lublin, Poland, jpatkows@hermes.umcs.lublin.pl

Abstract. The influence of impurities present in polymer solutions on adsorptive and electrokinetic properties of PEO 100 000 with commercial silica was analysed. Adsorption was measured with a spectrophotometric method and zeta potential with a zetasizer. A XRF method was used to estimate the quality and quantity of impurities in polyethylene oxide solutions. Impurities left after the polymerisation process, present in polymer solutions can adsorb competitively with macromolecules of the polymer. As a result of that, they block active centres on the surface of the adsorbent thus leaving less surface available for polymer molecules. Purification process is conducted in order to improve the quality of analysed polymer material. Polyethylene oxides used in the presented research were purified by filtration process and fractionation on chromatographic column. Overall, three different samples of PEO were used: commercial of high quality, filtrated and fractionated. Results show that adsorption of polyethylene oxide of high purity is independent on pH of the solution. Adsorption isotherms of fractionated and analytical-grade polymer are sharp, which indicates their low polydispersity ratio. An adsorption amount of analysed polymers is dependent only on the amount of impurities present in polymer material. Zeta potential measurements show, that polyethylene oxide always increases zeta potential of silica.

keywords: polyethylene oxide, polymer adsorption, silica, zeta potential

1. Introduction

Adsorption of macromolecules onto oxides is a very complicated process and it varies s ignificantly from the adsorption of small molecules and ions (i.e. inorganic ions). There are m any applications for adsorption of macromolecules including food, cosmetic, dyer industries and many technological processes used in environmental protection (Fleer et al., 1993; Fleer et al., 1993; Markovic,1996; Zhonghua et al. 2001). One very important field at which adsorption of polymers is of great value is mineral processing. An addition of high-molecular weight substances may change a stability of mineral suspensions. This is very often used in separation of various

minerals or ores of metals in process of flocculation (Ansari et al., 2007a, b; Xiaodong et al., 2007).

Studies on adsorption of polymers are very important from both scientific and practical point of view (Wind, 1998). Results of such data show relationship between changing factors (pH, molecular weight of polymer, ionic strength, purity of used materials, type of surface used and many more) and results of adsorption experiments. These can be next used for practical applications as ones mentioned above. One of the ways to study an adsorption process is to measure adsorption amount and zeta potential of the system. Both of these parameters give a good approximation what processes are really occurring on the surface, while a polymer is being adsorbed.

Commercial polymers, available to purchase, have a fairly high degree of polydispersity as well a content of inorganic impurities, which are left after the polymerisation process. Those substances cannot be used for a model research on polymer's adsorption onto metal oxides with application of various adsorption theories (e.g. Scheutjens's – Fleer theory). In order to improve their quality a filtration process (purification and initial fractionation) as well as fractionation on chromatographic column can be used.

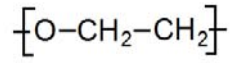

Fig. 1. Example of PEO monomer

Polyethylene oxide was used as a polymer in the presented research. It is a non-ionic, hydrophilic polymer with a very simple structure (Fig. 1). It has many interesting applications including paper industry (sheet formation aid, paper and paper board filler retention aid), glass fibre sizing, construction industry (slurry transport, board extrusion, polymer cement, painting), binder for ceramics, pickup and ending adhesive for paper rolls, mining industry (removal of silica clays, flocculation of phosphatic slimes), suspension polymerization, cosmetics industry (hair care products, skin care products, toothpaste), electronics industry (binder for battery, fluorescent lamp), pharmaceutical industry (controlled-release preparations) (www.sumito-moseika. co.jp/peo/).

The aim of the presented research was to determine the amount of adsorption of polyethylene oxide on silica, define the influence of impurities present in polymer material on the process of adsorption on silica, obtain the zeta potential of polyethylene oxide on silica, and define the influence of impurities present in polymer material on the zeta potential on silica. The presented research is a second part of extensive measurements on influence of PEO of various degrees of purity on stability of silica (Chibowski et al., 2007).

2. Experimental

SiO_2, used as an adsorbent was obtained from Aldrich. Silica was washed with doubly distilled water until conductivity of supernatant decreased down to 2 μS/cm.

Specific surface of SiO_2 measured by a BET method was 261.7 m^2/g. Average size of silica molecules was 157 nm with polydispersity ratio 0.252, which was estimated using Zetasizer 3000 by Malvern Instruments. Similar results for the radius of silica particles were obtained using electron microscopy.

Applied commercial polymers PEO 100 000 and PEO 108 000 were produced by Aldrich and Fluka respectively. Commercial as well as filtrated and fractionated polymers were used. The aim of a filtration process was to remove both inorganic impurities and macromolecules which molecular weights were much lower than those of the examined polymers. The process was carried out in an ultrafiltrating cell TCF-10 by Amicon. A XM-30 membrane (blocking macromolecules of molecular weight greater than 30 000) was applied for a PEO 100 000. Apart from purification an initial fractionation was also a result of this process because of separation of macromolecules of masses lower than 30 000 from the final solution. A fractionation of the polymers was carried out on a chromatographic column filled with Sephacryl S-300 HR gel by Amersham Biosciences.

A background electrolyte 10^{-2} $mol \cdot dm^{-3}$ NaCl was used. Absorbance was measured with a Specord M42 by Carl Zeiss using a wavelength of 500 nm. pH of the measured samples was 3, 6 or 9 and the amount of an added oxide equalled a surface of 10.5 m^2. All measurements were carried out in a constant temperature of 25°C.

2.1. Measurements of adsorption of PEO onto SiO_2

In order to measure adsorption amount of polyethylene oxide, 15 portions of commercial SiO_2 of 0.04 g each, was carefully measured. The amounts of SiO_2 were chosen, taking into account a surface area of the adsorbent. Next, they were placed in 15 Erlenmeyer flasks of 25ml volume, containing 2.5ml of 10^{-1}M NaCl each. PEO was added to Erlenmeyer flasks in sufficient amounts, so that final concentrations were as follows: 10, 50, 100, 150, 200 (ppm). Adsorption process was carried out in pH 3, 6, and 9, set by addition of small amounts of HCl and NaOH. The value of pH was set initially and controlled throughout the entire adsorption process. Flasks were shaken for 24 hours on mechanical shaker in temperature 25°C. After that time, solutions were centrifuged and 2 ml of supernatant was taken from each sample and transferred to 15 test-tubes. Next 8 ml of tannic acid was added to each test tube and left for 60 minutes in dark place. After that time an absorbance measurement was conducted on a UV-VIS spectrophotometer.

With a help of a calibration curve, values of unknown concentration of PEO were obtained from measured absorbance values. By simple subtracting of equilibrium from initial concentration of PEO, it was possible to calculate a concentration of adsorbed PEO. From this value, an amount of adsorbed PEO was calculated.

2.2. Zeta potential measurements

A 500 cm^3 sample of 10^{-2}M NaCl along with a polymer of a certain concentration (10, 50, 100 ppm) was transferred to a beaker. 0.05g of SiO_2 was added

to prepared solution. A resulting suspension was ultrasonificated for 3 minutes. Such a solution was introduced into five 100ml Erlenmeyer flasks, where a constant value of pH was set (3, 5, 7, 9, 11). Prior to the measurement, a measuring system was flushed with measured solution. Next, 10 ml of a solution was introduced into zetasizer to measure zeta potential. Measurements were taken in 25°C. From obtained data a dependence of ζ=f(pH) was created.

3. Results and discussion

3.1. Adsorption measurements

Figures 2, 3 and 4 present adsorption isotherms of filtrated, fractionated PEO of molecular weight 100 000 and high-analytical grade (Fluka) PEO of molecular weight 108 000 onto SiO_2, with background electrolyte NaCl 10^{-2}M, respectively. Presented experimental data indicate, that pH of the solution does not influence the adsorption amount of PEO onto SiO_2. The cause for such a behaviour is a character of adsorbing polymer. PEO, by nature, is a non-ionic polymer, which does not possess functional groups in its chain that are dissociable. Thus, their character does not change upon changes of pH and its properties are not pH-dependent. In such a way, the only possible explanation of adsorption of PEO onto SiO_2 is a hydrogen bonding between hydrogen atom in –OH groups in silica and highly electronegative oxygen atom in PEO chain (Bjelopavlic et al. 2000).

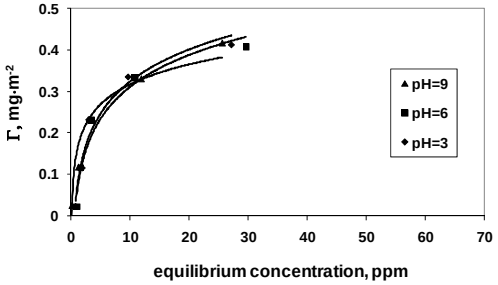

Fig. 2. Adsorption isotherms of filtrated PEO 100 000 onto SiO_2

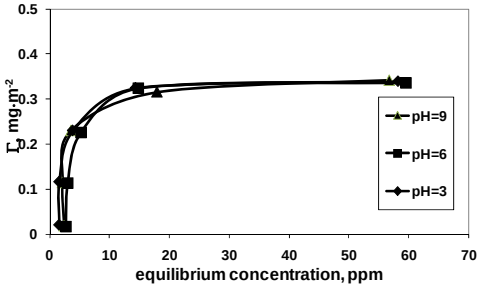

Fig. 3. Adsorption isotherms of fractionated PEO 100 000 onto SiO_2

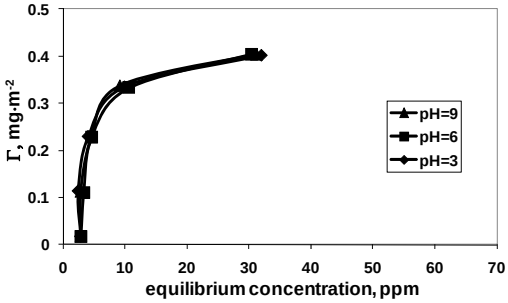

Fig. 4. Adsorption isotherms of analytical-grade PEO 108 000 onto SiO_2

Comparison of experimental data brings the result that adsorption amount for fractionated PEO is the lowest compared to the other two. Maximum surface coverage in this case is 0.33 $mg \cdot m^{-2}$, while for filtrated polymer is gives a value of 0.4 $mg \cdot m^{-2}$ and analytical grade PEO 0.41 $mg \cdot m^{-2}$. Such a result can be easily explained by presence of impurities in analysed samples (Table 1 and Table 2).

Table 1. Measured conductivities ($\mu S \cdot cm^{-1}$) of water solutions of PEO 100 000, concentration of polymer 100 ppm

degree of purification	conductivity ($\mu S \cdot cm^{-1}$)
filtrated	1.45
fractionated	2.09
analytical-grade	1.53

Table 2. Amount of impurities (wt percentage) in analysed samples

degree of purification	amount of impurities (wt %) in PEO 100 000
commercial (non-purified)	Si 0.9, Ca 0.3, Cu, Zn on ppm level
filtrated	Si 0.2, Cu, Zn on ppm level
fractionated	Cl, K, Cr, Fe, Zn on ppm level

The diversity and type of ions being impurities in fractionated sample is higher compared to the commercial non-purified one. This is probably a result of elution of inorganic ions from the material of chromatographic column, that the process of fractionation was carried out on. Presence of inorganic ions in solutions of polyelectrolytes can cause distinct changes in adsorption amount of a polymer on the surface of a solid. These additional ions can cause either an increase or a decrease of adsorption amount. This is dependent on type of inorganic ions, nature of polymer and a type of surface groups. For instance, when an inorganic ion is bonded more strongly to the surface than a polymer segment, a competitive adsorption between the two will result in greater adsorption of an inorganic ion. Thus it will decrease an adsorption of the polymer. On the other hand, when an ion is less strongly adsorbed to the surface of the solid than a polymer, it will not significantly influence the adsorption amount of the polymer. It might, though, influence a time required to reach equilibrium between polymer in the solution and polymer adsorbed on the surface, due to interference between inorganic ions and polymer segments.

In the analysed case specifically adsorbed inorganic ions cause a blockage of active sites on the surface of an oxide. While a competitive adsorption between polymer segments and inorganic ions take place, this limits a number of active sites available to polymer molecules which results in a decrease of adsorption amount.

An analysis of a shape of adsorption isotherm can help to estimate the degree of polydispersity of adsorbed polymer. More rounded isotherms are a result of an adsorption of a more polydisperse macromolecular substance. So, the system where adsorption of filtrated polymer is analysed (Fig. 2) is characterized with a significant rounding of adsorption isotherm and a lack of *plateau*. Rounding of an isotherm is caused by a gradual increase of the amount of adsorbed polymer with its increasing concentration. It is caused by a fact that smaller molecules are adsorbed in the first place (because of their faster movements). After that they are being gradually desorbed from the surface by high-molecular weight molecules, which are adsorbed more strongly by a surface (but move slower due to their size). The amount of molecules of high molecular weight increases with increasing concentration of a solution. Therefore, the greater a polydispersity of a polymer, the greater a rounding of an isotherm is.

So-called 'sharp' isotherms with a distinct *plateau*, are a result of an adsorption process of low polydispersed polymers. In such a case, a surface of oxide is very quickly coated with molecules of similar of even identical molecular weight. A desorption process does not take place or its significance is negligible. Such a shape is observed for fractionated PEO (Fig. 3) and analytical-grade PEO (Fig. 4). From these data comes a conclusion that a fractionation process helps to gain substances with a very low polydispersity, or low spread of molecular weights.

Results obtained with fractionated polymer can be used for a quantitative research on the process of adsorption and can be compared with theoretical results, that comply with present theories which concern adsorption in polymer systems.

3.2. Zeta potential measurements

Figures 5, 6 and 7 present a dependence of zeta potential on pH for filtrated, fractionated PEO 100 000 and analytical-grade PEO 108 000, concentrations 10, 50 and 100ppm onto SiO_2, background electrolyte $NaCl \cdot 10^{-2}M$, respectively. It can be stated that for all presented systems, zeta potential does not change for pure silica and silica with polymer in pH range from 3 to 5. One can also state, that above pH 5 an addition of polymer always causes an increase of zeta potential of silica in all presented systems compared to silica without a polymer. A value of zeta potential is always negative and because of that fact, the pH_{IEP} is never observed in analysed pH range. When individual systems are more closely analysed, some differences start to appear though.

In a case of filtered PEO (Fig. 5) an increasing concentration of polymer increases a zeta potential of a system. The greater the concentration of PEO, the less negative the value of zeta potential is. A change of zeta potential by adsorbing polymer can be explained with three phenomena: 1) an introduction of ionised functional groups into electrical double layer, 2) a desorption of counterions from compact layer of electrical double layer by adsorbing polymer chains, 3) a shift of slipping plane of electrical double layer. In presented systems, the first phenomenon

cannot take place, due to a lack of functional groups in polymer chain that are capable of dissociation. As the shift of slipping plane moves it away from the surface of a solid, therefore always decreases an absolute value of a zeta potential of a system. In presented results an addition of polymer always increases zeta potential, but since all values are negative, this means an decrease of an absolute value of a zeta potential. Therefore, desorption of counterions and a shift of slipping plane are two phenomena responsible for observed changes.

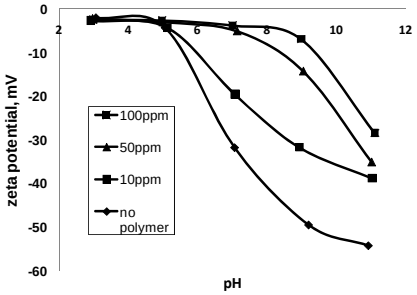

Fig. 5. Zeta potential of PEO 100 000 filtrated onto SiO_2

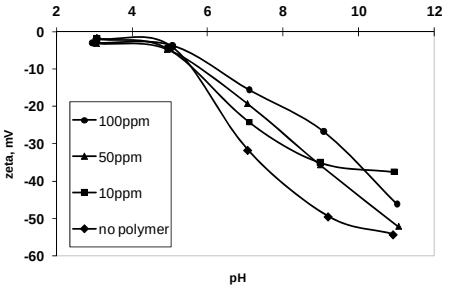

Fig. 6. Zeta potential of PEO 100 000 fractionated onto SiO_2

In a presented system, negatively charged surface of silica, attracts positively charged cations form a solution. In this specific case, cations being $Na^{+}_{(aq)}$ ions, which come from dissociation of a background electrolyte – NaCl and $Cu^{2+}_{(aq)}$, $Zn^{2+}_{(aq)}$ present as impurities. Competitive adsorption between previously mentioned cations and polymer molecules of the smallest concentration (10 ppm) results in desorption of cations by the latter. It seems that a hydrogen bond interaction between a surface groups and functional groups of PEO are stronger that electrostatic attraction between negatively charged silica and positively charged sodium ions. In such a case positively charged counterions move outward the surface into a solution and are placed near a slipping plane of electrical double layer. This is observed as an increase of a zeta potential of analysed system. Now, with increasing concentration of polyethylene oxide (50 and 100 ppm), more polymer molecules are adsorbed on a surface of silica. This only approves a proposed mechanism of changes, since increasing number of polymer segments account for greater overall strength of hydrogen bond compared to electrostatic attraction between surface and counterions. As a result of that, more counterions are desorbed from the surface. The zeta potential therefore, increases gradually with increasing concentration of polymer, what can be clearly observed in Fig. 5.

Additionally, adsorbing polymer shifts a slipping plane away from the surface, thus it decreases an absolute value of a zeta potential. For low concentrations of a polymer conformations that lie flat on the surface are preferred (e.g trains). This does not shift a slipping plane significantly, and does not influence a zeta potential. With increasing concentration of a polymer, more spatial conformations are preferred (e.g loops and tails). Those type of conformations affect a shift of slipping plane in greater

degree. This is observed for polymer concentrations of 50 and 100ppm. The greatest differences can be seen at pH=9. If conformations are more spatial, it means that slipping plane will be further shifted. This of course accounts for the greatest decrease in the absolute value of zeta potential.

To sum up, both phenomena affect a change of zeta potential. But for small polymer concentrations (10 ppm) a change of position of counterions is the most significant and for higher concentrations of polymer (50 and 100 ppm) both a change of position of counterions and a shift of slipping plane affect observed changes.

A system with fractionated PEO 100 000 adsorbing on silica is presented in Fig. 6. For pH range 3-5, the changes in zeta potential are negligible, so it can be clearly stated that in this pH range, a polymer does not influence zeta potential of this system. For pH range 5-11, for all used concentrations, an increase of value of zeta potential is observed. Once again, similarly to a system presented on Fig. 5, the two mechanisms responsible for observed changes are a change of position of positively charged counterions in electrical double layer and a shift of slipping plane away from the surface. Adsorbing polymer molecules desorb previously adsorbed positive cations from the surface, which are then shifted to diffuse part of edl. Those adsorbing polymer molecules also slightly shift a slipping plane towards bulk solution. These two facts add together and are observed as an increase of a zeta potential of a system.

What is interesting though, is a comparison of plots in Figs 5 and 6. For a system with filtrated PEO (Fig. 5), changes of zeta potential with increasing concentration of polymer are much greater, compared to a system with a fractionated polymer (Fig. 6). This might indicate that a fractionated polymer is being adsorbed with much flatter conformation (mostly conformations where polymer segments are directly bonded to the surface). Such a conformation does not provide an additional factor that shifts a slipping plane away from the surface of silica and does not decrease an absolute value of a zeta potential. In spite of data from purification of presented polymers (Table 1, Table 2), where there are more impurities present in fractionated polymer compared to filtrated, those additional impurities does not seem to interfere with adsorbing polymer molecules. PEO segments have a greater tendency for adsorption to the surface than those inorganic ions and thus create a more flat conformation on the surface of silica. This accounts for smaller increase of zeta potential for a fractionated polymer compared with filtrated.

The last of the analysed systems – PEO 108 000 (analytical grade) on silica is presented in Fig. 7. Once again, for all measured concentrations, zeta potential is almost the same for pH range 3-5, so it can be stated that a polymer does not influence zeta potential for this specific pH range. For pH range 5-11, it is always increased by adsorbing polymer compared to pure silica, no matter which concentration was used. As in previous cases, the reason for such behaviour is a change of position of counterions in compact part of electrical double layer and a shift of slipping plane. Polymer molecules are more preferentially adsorbed by the surface that cations,

therefore the latter is desorbed from the surface. This results in increase of zeta potential of the analysed system.

The difference compared to filtrated PEO (Fig. 5) and fractionated PEO (Fig. 6) is that observed increase is almost independent of concentration of polymer used. This might suggest that it does not matter which concentration of the polymer is used (10, 50 or 100ppm) – the amount of counterions that is removed from the compact layer of edl is almost the same. Indeed this is no surprise for an adsorption of polymer of such a high quality like analytical grade PEO. Used polymer sample has a very low polydispersity ratio, which means that this sample contains mostly molecules of almost the same mass. As a result of that, those molecules immediately adsorb on the surface with maximum possible amount, even when relatively small concentration of polymer is used (Fig. 4). Surface of the solid becomes saturated with polymer segments and increasing concentration does not significantly change the amount of segments directly bonded to the surface of silica. As a result of that number of counterions that are removed almost does not change and minute changes of zeta potential are observed.

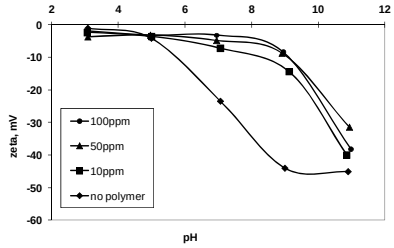

Fig. 7. Zeta potential of PEO 108 000 onto SiO_2

What is more, conformations created by PEO in all used concentrations are very similar. Analysed sample of PEO, having mostly molecules of the same molecular weight, create similar conformations, regardless of concentration. This shifts a slipping plane in every analysed concentration almost the same and that is why no significant differences between zeta potential of polymer with various concentrations are observed.

Thus, one can safely state that zeta potential in presented system almost does not change with changing concentration of polyethylene oxide.

4. Conclusions

1. Adsorption of polyethylene oxide of high purity (PEO 100 000 filtrated and fractionated as well as analytical-grade PEO 108 000) is independent on pH of the solution. It is a result of a lack of dissociable groups in its chain.
2. Adsorption isotherms of fractionated and analytical-grade polymer are sharp, which indicates their low polydispersity ratio.
3. Adsorption amount is dependent on the amount of impurities present in polymer material. The lower the amount of impurities, the higher the

adsorption is (greater number of accessible active sites for polymer molecules on surface of an oxide).

4. Polyethylene oxide always increases zeta potential of silica. For analytical-grade polymers this increase is independent on the concentration of the polymer used. For polymers, where some amount of impurities is present, the increase depends on the concentration of the polymer.

References

ANSARI A., PAWLIK M., 2007a, *Floatability of chalcopyrite and molybdenite in the presence of lignosulfonates. Part I. Adsorption studies*, Minerals Engineering 20, 600-608.

ANSARI A., PAWLIK M., 2007b, *Floatability of chalcopyrite and molybdenite in the presence of lignosulfonates. Part II. Hallimond tube flotation*, Minerals Engineering 20, 609-616.

BJELOPAVLIC M., SINGH P.K., EL-SHALL H., MOUDGIL B.M., 2000, *Role of Surface Molecular Architecture and Energetics of Hydrogen Bonding Sites in Adsorption of Polymers and Surfactants*, J Coll. Int. Sci. 226, 159-165.

CHIBOWSKI S., PATKOWSKI J., 2007, *A research on stability of SiO_2 in the presence of polyethylene oxide of different purities,* Physicochemical Problems of Mineral Processing, 41, 177-184.

FLEER G.J., COHEN STUART M.A., SCHEUTJENS J.M.H.M., COSGROVE T., VINCENT B., 1993, Polymers at Interfaces, Chapman & Hall, London.

FLEER G.J., SCHEUTJENS J.M.H.M.,1993, in: B. Dobias (Ed.), Coagulation and Flocculation; Theory and Applications, Chapter 5, Marcel Dekker, New York.

MARKOVIC B., 1996, Adsorption of Polyacrilic Acid on Alumina and Silicon Carbide, Doctoral Thesis, University of Zagreb, Croatia.

WIND B., KILLMANN E., 1998, *Adsorption of polyethylene oxide on surface modified silica – stability of bare and covered particles in suspension,* Colloid Polym Sci 276, 903-912.

XIAODONG M., PAWLIK M., 2007, *The effect of lignosulfonates on the floatability of talc,* Int. J. Miner. Process. 83, 19–27.

ZHONGHUA P., CAMPBELL A., SOMASUNDARAN P., 2001, *Polyacrylic acid adsorption and conformation in concentrated alumina suspension,* Colloids and Surfaces A: Physicochemical and Engineering Aspects, 191, 71 – 78.

http://www.sumitomoseika.co.jp/peo/

Patkowski, J., Chibowski, S., *Badania adsorpcyjnych i elektrokinetycznych właściwości SiO_2 w obecności tlenku polietylenu o różnej czystości*, Physicochem. Probl. Miner. Process., 47 (2011) 275-284, (w jęz. ang.)

Zbadano wpływ zanieczyszczeń obecnych w materiale polimeru na adsorpcyjne i elektrokinetyczne właściwości PEO 100 000 na komercyjnej krzemionce. Adsorpcję badano przy pomocy metody spektrofotometrycznej, potencjał zeta przy pomocy zetasizera. Metodą XRF ustalono stężenie oraz jakość zanieczyszczeń w badanych roztworach polimerów.Przeprowadzone badania wskazują, że adsorpcja tlenku polietylenu o wysokiej czystości jest niezależna od pH roztworu. Izotermy adsorpcji PEO frakcjonowanego oraz o wysokiej czystości są ostre, co wskazuje na ich niski stopień polidyspersyjności. Ilość zaadsorbowanego polimeru jest zależna tylko od ilości zanieczyszczeń obecnych w materiale polimeru. Pomiary potencjału zeta wskazują, że obecność tlenku polietylenu zawsze zwiększa potencjał zeta krzemionki.

słowa kluczowe: tlenek polietylenu, adsorpcja polimerów, krzemionka, potencjał dzeta

Prof. Dr. Eng. Wiesław S. Blaschke

a tribute on his 70th birthday

Wiesław Stanislaw Blaschke was born on 10 June 1941 in Krakow. Parents: Franciszka née Czechowska and Stanisław - author of books in the field of mineral processing, an employee of the hard coal mining industry, a lecturer at the University of Mining and Metallurgy (AGH) and the Silesian University of Technology. His grandfather was Ignacy Engelbert, a sculptor in Vienna, Lvov and Krakow, who graduated from the Academy of Fine Arts in Krakow and in 1918 was awarded a Lwow Defense Cross. Wiesław Blaschke attended primary school in Radlin, and then in Sosnowiec, where he received a certificate of secondary education completion at St. Staszic Secondary Comprehensive School. In 1963 he graduated with an M.Sc. Engineer degree in mechanical processing from the Academy of Mining and Metallurgy in Krakow, Department of Mining. In 1971 he received the title of doctor of technical sciences after defending his thesis entitled "A method for determining the optimal parameters of steam coal beneficiation". He received the scientific degree of *doctor habilitatus* in the technical sciences in the field of mineral processing in 1983 after submitting a habilitation thesis entitled "A method for predicting the economic effects of the gravitational beneficiation of coking coal". In the same year he completed the Managerial Staff Development Study at the Academy of Economics in

Krakow in the specialty of economics and organization of company management. The President of Poland conferred on him the title of professor of engineering sciences in 2000.

Professor W. Blaschke specializes in the gravitational beneficiation of the fine grains of minerals: he conducts research into the separation of particles of coal, galena and nickel-iron "luppen" in fan-shaped trough separators and developed the fluidization hypothesis of these processes. He deals with the issues of mineral resources management and works on the construction of models of resource management, evaluation of fuel-energy base in Poland, prognoses for the development of solid mineral mining, establishing combined mining and preparation plants, the profitability of coal exports, the organization of coal trading, and coal washing services. He is involved in work in the field of economics of the operation of coal mining by introducing a new pricing system for coal, known as the coal pricing formulae, approved by the Ministry of Industry and Finance; he has created the concepts of coal price level and structure, developed a method for calculating coal import parity prices, a method for determining the profitability of mines, and the calculation of the cost of obtaining commercial products; he is a co-creator of the first concept of the adaptation of coal mining to the conditions of the market economy; he analyzes the problems of the adaptation of the Polish mining industry to the principles of the European Union.

He specializes in the economics of the beneficiation of mineral resources, continuing the work of his mentor Professor Włodzimierz Stępiński. He has developed a method for determining the cost-effectiveness of beneficiation and introduced the concepts of the economic efficiency of beneficiation, the value of coal production, calorific value curves for coal; he has proposed the construction of diagrams of coal preparation plant economics, and works on the technological and economic optimization of the beneficiation of steam and coking coals in the manufacturers-users system. In recent years, he has been working on the use of coal slurry deposits, and technologies to use waste products from the coal mining industry. He also popularizes issues of clean coal technologies involving the 1st stage, i.e. preparation of coal for combustion.

The results of his own research and that of co-operating teams have been published in national (160 publications) and foreign (7) journals, at internal conferences in Poland (97), at foreign conferences (46) and international ones organized in Poland (13). He is the author (co-author) of 4 books, 44 chapters in collective books, 12 monographs and 7 chapters in collective monographs, 3 course books for students and also co-author entries in 7 encyclopaedias; he is also the author of five patents.

For scientific activity he has received the Officer's and Knight's Crosses of the Polonia Restituta Order, the Gold and Silver Crosses of Merit, five awards from the Minister of Science and Higher Education and the Minister of National Education, 17 awards of the Rector of AGH and the Prof. W. Budryk award.

Professor W. Blaschke is a member of the scientific committees of the Polish Academy of Sciences (PAN), dealing with Mining; the Sustainable Management of Mineral Resources; Energy Problems; Mineralogical Sciences (until 1988), the Mining Commission of the Katowice Division of PAN and the Interfaculty Commission of Engineering Sciences of the Polish Academy of Sciences. He is a member of the editorial boards of the Physicochemical Problems of Mineral Processing, Przegląd Górniczy (Mining Review) (editor in chief), Management of Mineral Resources, Mineral Engineering (until 2011), Czasopismo Techniczne KTT (Engineering Journal) (editor in chief), Górnictwo i Geologia (Mining and Geology Journal of the Silesian University of Technology), and the Mining Bulletin of the Mining Chamber of Industry and Commerce. He is also a journalist of the Polish-Canadian Independent Courier in Toronto (has written more than 80 articles).

W. Blaschke cooperates with foreign scientific centres. He has been invited to participate in the organizing committees of international conferences and congresses: Brisbane (Australia), Johannesburg (South Africa), Beijing (China), Lexington (USA), Sarajevo (Bosnia-Herzegovina), Kosice (Slovakia), Ostrava (Czech Republic), Demänovská Dolina (Slovakia), Ha Long (Vietnam). Prof. Blaschke is a member of the Coal Preparation Society of America. He has had short-term internships and study visits to Australia, Bulgaria, China, Czech Republic, Finland, France, Yugoslavia, Germany, Peru, Russia, South Africa, Slovakia, Sweden, Ukraine, USA, Hungary, Vietnam and the United Kingdom.

Prof. W. Blaschke has prepared more than 150 research papers for the industry in which he works. He has reviewed doctoral and postdoctoral dissertations and reviewed applications for the position and title of professor. Professor Blaschke has reviewed more than 100 scientific papers submitted to professional journals, books and monographs in addition to 126 research projects, 19 development projects, 12 targeted projects and 16 final projects.

Between 1963-2011 Prof. W. Blaschke worked (in some cases simultaneously) in the Ziemowit coal mine, at the University of Mining and Metallurgy, the Institute of Fundamental Technological Research of PAN, the Mineral and Energy Economy Research Institute of PAN, Węglozbyt Coal Trading Company, the National Agency for the Restructuring of Mining, the Silesian University of Technology, the Institute of Mechanized Construction and Rock Mining and the Institute for the Chemical Processing of Coal.

He acted as the Deputy Scientific Director of the AGH Institute for the Use of Mineral Resources and Deputy Scientific Director for the centre of the Fundamental Issues of Raw Materials and Energy Management (now IGSMiE PAN). He was the head of the laboratories for Design, Economics and Organization, the Industrial Evaluation of Energy Resources, the Extraction and Processing of Fuel Resources. Professor Blaschke also managed the research units for Energy Resource Management, the Fundamentals of Mineral Resources Management, the Use of Mineral Resources, Mineral Preparation and Processing, and Fuel and Energy Market

Economics and Market Research. He was a deputy director of the Department of Mineral Processing and Waste Utilization. He was a member of the Ministerial Working Groups and Experts in the Ministry of Environment, Ministry of Industry and Trade, and Ministry of Economy.

He was a Supervisory Board member of the National Coal Agency, the Polish Energy Industry Foundation, Eco-Carbon, Węglozbyt Coal Trading Company S.A., Węglokoks S.A. He has been a member (and is some cases still is) of the scientific boards of the Scientific Board of the Department of Geology and Environmental Protection of AGH, the Mineral and Energy Economy Research Institute of PAN, Division of Mining and Geology of the Silesian University of Technology and the Institute of Building Mechanization and Rock Mining.

Prof. W. Blaschke is a member of the Association of Mining Engineers and Technicians (Chairman), the AGH Alumni Association, the Polish Association of Mineral Processing (Chairman for 11 years), the Polish Committee of the World Energy Council, the Polish Committee of World Mining Congress, the Society of the Upper Silesian Miners' Guild, the International Organizing Committee for the Coal Preparation Congress (Poland's representative), Lions Clubs International - LC Krakow Old Town (former Governor of District 121 Poland).

For his community work Professor Blaschke has received dozens of awards, medals and distinctions in Poland and abroad, including Slovakia (Banicka Spoločnosť) and USA (Lions Clubs International). He has received the Honorary Miner's Sword and the Miner's Dagger – the most prestigious awards in mining. He holds the title of General Director of Mining of the first class.

LIST OF PUBLICATION

W. Blaschke: Metody określania optymalnego ciężaru właściwego rozdziału i wychodu produktów wzbogacania węgla energetycznego. Inf. Techn. Ekon. JMZPW Mysłowice. 1964. Z. 3. ss. 48–74.

W. Blaschke: Określenie optymalnych parametrów jakościowych wzbogacania węgli energetycznych. Inf. Techn. Ekon. JMZPW Mysłowice. 1964. Z. 5. ss. 65–78.

Z. Blaschke, W. Blaschke: Graficzna metoda określania wielkości odjemników przy przeliczaniu ciepła spalania na wartość opałową. Inf. Techn. Ekon. JMZPW Mysłowice. 1966. Z. 2. ss. 31–37.

W. Blaschke: Graficzna metoda ekonomicznej analizy wzbogacalności węgla energetycznego. Przegląd Górniczy. 1967. Nr 11. ss. 542–545.

W. Blaschke, Z. Blaschke: Niektóre ekonomiczne zagadnienia wzbogacania węgla dla potrzeb energetyki. VII Krakowska Konferencja Przeróbki Mechanicznej Kopalin. Wyd. Inf. Techn. Ekon. JMZPW Mysłowice. 1968. Z. 5. ss. 112–127.

W. Blaschke: Ekonomiczna sprawność wzbogacania węgla energetycznego. Przegląd Górniczy. 1970. Nr 7–8. ss. 346–351.

W. Blaschke: Analiza technologiczno-ekonomiczna trójproduktowego sposobu wzbogacania węgla energetycznego. Przegląd Górniczy. 1970. Nr 10. ss. 468–474.

W. Blaschke: Krzywe charakterystyki cieplnej węgla energetycznego. Biuletyn Zagadnień Przeróbki Mechanicznej Węgla SEPARATOR. 1970. Nr 3. ss. 1–9.

T. Tumidajski, W. Blaschke: Metoda wyznaczania parametrów równania krzywej wzbogacalności. Przegląd Górniczy. 1971. Nr 2. ss. 78–81.

Z. Blaschke, W. Blaschke: Wzbogacalniki strumieniowo-wachlarzowe. Rudy Żelaza. 1971. Nr 7–8. ss. 8–15.

W. Blaschke: Wyznaczanie przedziałów opłacalności wzbogacania węgla energetycznego przy pomocy krzywej opłacalności produkcji. Biuletyn Zagadnień Przeróbki Mechanicznej Węgla SEPARATOR. 1971. Nr 1. ss. 20–25.

K. Sztaba, W. Blaschke: Koncepcje układów technologicznych wydzielania koncentratów pirytowych z odpadów węgli energetycznych. Materiały Zjazdowe XXI Sesji Naukowej AGH. Tom 1. Referat XXV. Kraków. AGH. 1971.
W. Blaschke: Obliczanie zysku i rentowności wzbogacania węgla energetycznego w zależności od przyjętej zawartości popiołu w koncentracie. Przegląd Górniczy. 1972. Nr 1. ss. 21–25. (Errata – Przegląd Górniczy. 1972. Nr 3. s.120).
W. Blaschke, T. Tumidajski: Aproksymacja krzywych wzbogacalności koncentratów węgla energetycznego za pomocą rozkładu Weibulla. Zeszyty Naukowe AGH. Nr 318. Górnictwo 35. 1972. ss. 7–11.
W. Pilch, K. Sztaba, W. Blaschke, E. Kucowicz, T. Łapeta, C. Chmura: Możliwości otrzymania koncentratów pirytowych z miału węgla energetycznego kopalni Jaworzno. Zeszyty Naukowe AGH. Nr 318. Górnictwo 35. 1972. ss. 57–66.
W. Blaschke: Metoda wyznaczania ekonomicznie optymalnych parametrów wzbogacania węgla energetycznego. XXIII Sesja Naukowa AGH. 1972. Zeszyty Naukowe AGH. Nr 373. Zeszyt Specjalny 35. ss. 99–121.
W. Blaschke: Analiza metod określania optymalnych parametrów wzbogacania węgla. XXIII Sesja Naukowa AGH. 1972. Zeszyty Naukowe AGH. Nr 373. Zeszyt Specjalny 35. ss. 123–142.
W. Blaschke, E. Mokrzycki: Kształtowanie się kosztów wzbogacania oddzielnych klas ziarnowych węgla. XXIII Sesja Naukowa AGH. 1972. Zeszyty Naukowe AGH. Nr 381. Zeszyt Specjalny 39. ss. 195–203.
W. Blaschke, W. Pudło: Ocena ekonomiczna procesu ręcznego wzbogacania węgla energetycznego. XXIII Sesja Naukowa AGH. 1972. Zeszyty Naukowe AGH. Nr 381. Zeszyt Specjalny 39. ss. 205–218.
Z. Blaschke, W. Blaschke: Wstępne badania nad sedymentacją brunkitu z kopalni Olkusz. Mat. VIII Krakowskiej Konf. Przeróbki Mechanicznej Kopalin. Wyd. AGH. Kraków. 1972. ss. 179–193.
K. Sztaba, W. Blaschke, W. Pudło, W. Pilch: Possible separation of pyrites concentrate from Polish power coal discards. VI International Coal Preparation Congress. Paper 25. Paryż. 1973.
W. Blaschke, W. Pilch, S. Sanak: Próba zastosowania separacji elektrostatycznej do odsiarczania węgli kamiennych. Zbiór referatów Sesji Naukowej nt. Odsiarczanie węgla i spalin. Zeszyt 1. Katowice – Ustroń. 1973. ss. 55–67.
A. Karcz, W. Blaschke, T. Kapała: Zastosowanie węgli o zróżnicowanej zawartości popiołu jako kierunek racjonalnego wykorzystania bazy surowcowej koksownictwa. Koks, Smoła, Gaz. 1974. Nr 9. ss. 232–236.
W. Blaschke, K. Sztaba: Wydzielanie koncentratów galenowych we wzbogacalnikach strumieniowo-wachlarzowych. Rudy i Metale Nieżelazne. 1974. Nr 9. ss. 482–488.
W. Blaschke, B. Mika, W. Kisielewski: Analiza pracy węzła mielenia i klasyfikacji zakładu wzbogacania siarki. XXIX Sesja Naukowa AGH. 1974. Zeszyty Naukowe AGH. Nr 462. Górnictwo 63. ss. 31–43.
K. Sztaba, W. Blaschke, E. Małysa, C. Kotowski: Wstępne badania nad otrzymaniem kolektywnych koncentratów Zn-Pb we wzbogacalnikach strumieniowo-wachlarzowych. Zeszyty Naukowe AGH. Nr 473. Górnictwo 66. 1975. ss. 7–18.
W. Blaschke: Metoda obliczania kosztów wzbogacania oraz ocena efektów ekonomicznych pracy zakładów przeróbki mechanicznej węgla. Mat. Międzynarodowego Symp. nt. Projektowanie, budowa i eksploatacja zakładów przeróbki węgla. Referat 28. Wyd. SEPARATOR. Katowice. 1975.
W. Blaschke, T. Kapała, A. Karcz: Wpływ stopnia metamorfizmu węgli stosowanych w koksownictwie na przyszłościowe rozwiązania zakładów przeróbki mechanicznej węgla. Mat. Inf. Międzynarodowego Symp. nt. Projektowanie budowa i eksploatacja zakładów przeróbki mechanicznej węgla. Wyd. SEPARATOR. Katowice. 1975. ss. 139–148.
W. Blaschke, E. Małysa: Opłacalność trójproduktowego wzbogacania węgla koksowego. XXXI Sesja Naukowa AGH. 1975. Zeszyty Naukowe AGH. Nr 523. Górnictwo 77. ss. 101–115.
W. Blaschke, Z. Blaschke: Beryl. Przeróbka mechaniczna.. W: Surowce Mineralne Świata. Tom Al-Be-Li-Mg. Pod red. A. Bolewskiego. Wydawnictwo Geologiczne. Warszawa. 1976. s. 200–205.
W. Blaschke, Z. Blaschke: Lit. Przeróbka mechaniczna. W: Surowce Mineralne Świata. Tom Al-Be-Li-Mg. Pod red. A. Bolewskiego. Wydawnictwo Geologiczne. Warszawa. 1976. s. 252–261.
W. Blaschke: Wzbogacanie we wzbogacalnikach strumieniowych. Poradnik Górnika. Tom V. Wyd. Śląsk. Katowice. 1976. ss. 433–465.
W. Blaschke: Wzbogacanie powietrzne. Poradnik Górnika. Tom V. Wyd. Śląsk. Katowice. 1976. ss. 556–563.
W. Blaschke: Ekonomika wzbogacania węgla. Poradnik Górnika. Tom V. Wyd. Śląsk. Katowice. 1976. ss. 940–968.
W. Blaschke, A. Siwiec: Wzbogacalniki strumieniowe. Poradnik Górnika. Tom V. Wyd. Śląsk. Katowice. 1976. ss. 1171–1205.
M. Baran, W. Blaschke i inni: Wykorzystanie węgla w krajach uprzemysłowionych. Raport dla ONZ. Wyd. – Główny Instytut Górnictwa. Katowice. 1976. (wersja polska) Wyd. – Natural Resources Energy and Transport. Nowy York. 1976. (wersja angielska).
K. Sztaba, W. Blaschke: Grawitacyjne wzbogacanie najdrobniejszych klas ziarnowych rud Zn-Pb. Mat. IV Krajowego Zjazdu Górnictwa Rud. Olkusz. 1976. ss. 303–311.
W. Blaschke, Z. Blaschke: Cyna. Przeróbka mechaniczna. W: Surowce Mineralne Świata. Tom Sn. Pod red. A. Bolewskiego. Wydawnictwo Geologiczne. Warszawa. 1977. s. 102–117.

W. Blaschke, Z. Blaschke, W. Mączka: Miedź. Przeróbka mechaniczna. W: Surowce Mineralne Świata. Tom Cu. Pod red. A. Bolewskiego. Wydawnictwo Geologiczne. Warszawa. 1977. s. 176–206.
W. Blaschke: Metoda określania najkorzystniejszych ekonomicznie zawartości popiołu w koncentratach węgli koksowych. Zeszyty Naukowe AGH. nr 551. Górnictwo 83. 1977. ss. 29–42.
W. Blaschke, W. Pilch, W. Pudło, K. Sztaba: Badania nad utylizacją pirytonośnych produktów odpadowych kopalin węgla kamiennego. Zeszyty Naukowe AGH. Nr 551. Górnictwo 83. 1977. ss. 57–72.
W. Blaschke: Przewidywanie rezultatów wzbogacania węgla. Zeszyty Naukowe AGH. Nr 551. Górnictwo 83. 1977. ss. 145–159.
W. Blaschke: Nomogramy do wyznaczania rzeczywistych parametrów jakościowych wzbogacania węgla. Zeszyty Naukowe AGH. Nr 551. Górnictwo 83. 1977. ss. 161–174.
W. Blaschke, W. Sikora: Perspektywy dostaw i jakości węgla dla energetyki w latach 2005 – 2010. Mat. Semin. Nowe technologie wytwarzania energii elektrycznej z paliw konwencjonalnych. Komitet Problemów Energetyki PAN. Instytut Elektroenergetyki Politechniki Poznańskiej. Poznań. 1977. ss. 7–17.
W. Blaschke, Z. Blaschke: Cynk – ołów. Przeróbka mechaniczna. W: Surowce Mineralne Świata. Tom Zn-Pb. Pod red. A. Bolewskiego. Wydawnictwo Geologiczne. Warszawa. 1978. s. 258–274.
W. Blaschke, Z. Blaschke, A. Siwiec: Żelazo. Przeróbka mechaniczna. W: Surowce Mineralne Świata. Tom Fe. Pod red. A. Bolewskiego. Wydawnictwo Geologiczne. Warszawa. 1978. s. 306–322.
W. Blaschke, Z. Blaschke: Bar. Przeróbka mechaniczna. W: Surowce Mineralne Świata. Tom Ba-B-F-Sr. Pod red. A. Bolewskiego. Wydawnictwo Geologiczne. Warszawa. 1978. s. 84–88.
W. Blaschke, Z. Blaschke: Bor. Przeróbka mechaniczna. W: Surowce Mineralne Świata. Tom Ba-B-F-Sr. Pod red. A. Bolewskiego. Wydawnictwo Geologiczne. Warszawa. 1978. s. 181–183.
W. Blaschke, Z. Blaschke: Przeróbka mechaniczna kopalin fluorytowych. W: Surowce Mineralne Świata. Tom Ba-B-F-Sr. Pod red. A. Bolewskiego. Wydawnictwo Geologiczne. Warszawa. 1978. s. 284–290.
W. Blaschke: Propozycja podziału zakładów przeróbki mechanicznej węgla na stanowiska powstawania kosztów. Zeszyty Naukowe AGH. Nr 589. Górnictwo 90. 1978. ss. 87–108.
W. Blaschke: Modelowanie kosztów własnych przeróbki oddzielnych klas ziarnowych węgla kamiennego. Mat. XII Krakowskiej Konf. Przeróbki Kopalin. Wyd. AGH. Kraków. 1978. ss.232–239.
W. Blaschke, W. Suwała: Modelowanie oddzielnych węzłów technologicznych zakładu przeróbczego. Mat. XII Krakowskiej Konf. Przeróbki Kopalin. Wyd. AGH. Kraków. 1978. ss. 240–252.
S. Blaschke, W. Blaschke: Technika wzbogacania węgla. Cz. I. Skrypt AGH. nr 658. Kraków. 1979. ss. 1–349.
S. Blaschke, W. Blaschke: Technika wzbogacania węgla. Cz. II. Skrypt AGH. nr 736. Kraków. 1979. ss. 1–346.
W. Blaschke: Określenie parametrów jakościowych koncentratów węglowych możliwych do osiągnięcia w warunkach przemysłowych. Prace Komisji Górniczo-Geologicznej PAN. Górnictwo. 19. Ossolineum. 1979. ss. 69–86.
W. Blaschke, A. Siwiec: Grawitacyjne wzbogacanie najdrobniejszych ziaren. Zeszyty Naukowe AGH. Nr 547. Górnictwo 82. 1979. ss. 53–69.
W. Blaschke, J.Migda, E. Mokrzycki: Model rachunku kosztów własnych pozyskania i przeróbki węgla kamiennego. Mat. Konf. nt. Zagadnienia surowców energetycznych w gospodarce krajowej. Kraków. 1979. Wyd. AGH. ss. 147–161.
W. Blaschke, E. Mokrzycki: Koszty wzbogacania węgla kamiennego w wybranych zakładach górniczych. Mat. Konf. nt. Zagadnienia surowców energetycznych w gospodarce krajowej. Wyd. AGH. Kraków. 1979. ss. 175–191.
W. Blaschke, Z. Blaschke: Niektóre problemy przeróbki mechanicznej węgla brunatnego. Mat. Konf. nt. Zagadnienia surowców energetycznych w gospodarce krajowej. Wyd. AGH. Kraków. 1979. ss. 335–354.
K. Sztaba, J. Nawrocki, W. Blaschke: Stan i perspektywy rozwojowe badań w zakresie przeróbki kopalin w Polsce. Mat. Semin. nt. Stan przeróbki kopalin w Polsce. SITG. Katowice. 1979. s.15.
W. Blaschke, Z. Blaschke: Torf. Przeróbka mechaniczna. W: Surowce Mineralne Świata. Tom Torf. Pod red. A. Bolewskiego. Wydawnictwo Geologiczne. Warszawa. 1980. s. 170–173.
W. Blaschke, E. Małysa: Gravitational beneficiation of ultrafine grains of Zinc-Lead ores from Olkusz Region. Proceedings of the International Symposium on Fine Particles. Published by AIMM & PE, Inc. New York. Las Vegas. Nevada. USA. 1980. Volume 2. Chapter 70. pp. 1376–1389.
W. Blaschke, L. Górska, E. Mokrzycki: Kierunki wykorzystania odpadów powęglowych. Mat. XIV Krakowskiej Konf. Przeróbki Kopalin. Wyd. AGH. 1980. ss. 255–262.
L. Górska, E. Mokrzycki, W. Blaschke: Kierunki utylizacji węgla kamiennego. Mat. Symp. nt. Przeróbka i wykorzystanie stałych surowców energetycznych. PAN – SITG. Zagadnienia Postępu Technicznego i Ekonomiki Górnictwa. Wyd. SITG. 1980. ss. 63–88.
W. Blaschke, A. Jaworski: Aspekty ekonomiczne wzbogacania węgli kamiennych w Polsce. Mat. Symp. nt. Przeróbka i wykorzystanie stałych surowców energetycznych. PAN – SITG. Zagadnienia Postępu Technicznego i Ekonomiki Górnictwa. Wyd. SITG. 1980. ss. 193–208.

W. Blaschke, E. Mokrzycki, M. Morawska-Horawska, M. Rysz, T.Tumidajski: Problem doboru węgla zużywanego w aglomeracji krakowskiej w aspekcie ochrony środowiska. Mat. XIV Krakowskiej Konf. Przeróbki Kopalin. Wyd. AGH. 1980. ss. 123–134.
W. Blaschke, Z. Blaschke: Węgiel brunatny. Przeróbka mechaniczna. W: Surowce Mineralne Świata. Tom Węgiel brunatny. Pod red. A. Bolewskiego. Wydwanictwo Geologiczne. Warszawa 1981. s. 119–130.
W. Blaschke, Z. Blaschke: Mangan. Przeróbka mechaniczna. W: Surowce Mineralne Świata. Tom Mn-Cr. Pod red. A. Bolewskiego. Wydawnictwo Geologiczne. Warszawa 1981. s. 93–106.
W. Blaschke, Z. Blaschke: Chrom. Przeróbka mechaniczna. W: Surowce Mineralne Świata. Tom Mn-Cr. Pod red. A. Bolewskiego. Wydawnictwo Geologiczne. Warszawa 1981. s. 218–227.
W. Blaschke, E. Małysa: Badania nad zachowaniem się różnej wielkości ziarn rud cynkowo-ołowiowych w procesie rozdziału we wzbogacalnikach strumieniowo-wachlarzowych. Prace Komisji Górniczo-Geodezyjnej PAN. Górnictwo 21. Ossolineum. 1981. ss. 67–74.
W. Blaschke: Metoda prognozowania ekonomicznych efektów grawitacyjnego wzbogacania węgli koksowych. Zeszyty Naukowe AGH. Nr 778. Górnictwo 106. 1981. ss. 1–112.
W. Blaschke, L. Górska, E. Mokrzycki: Wykorzystanie odpadów powęglowych. Aura. 1981. Nr 3. ss. 14–15.
W. Blaschke, E. Mokrzycki, S. Blaschke, W. Suwała: Zagadnienia wzbogacania węgli kamiennych energetycznych w Polsce. PAN–IPPT–ZPE. Wyd. Warszawska Drukarnia Narodowa. Warszawa. 1981. ss. 1–76.
W. Blaschke, L. Górska, E. Mokrzycki, W. Suwała: Rol obogatitielnych zawodow w modeli bałansirowanija kamiennougolnego chozjajstwa. Sbornik dokładow. Nauczna Konferencija Techniczeskijat progres w minnoto i geołogo-prouczwatielnoto dieło. Warna. Tom 4. Wyd. WMGI. Rocznik XXVII. Sofia. 1981. pp. 173–187.
W. Blaschke, L. Górska, E. Mokrzycki, W. Suwała: Propozycja podziału węgli kamiennych na rodzaje paliw dla potrzeb modelu bilansu gospodarki węglem. Mat. II Konf. nt. Zagadnienia surowców energetycznych w gospodarce krajowej. PAN – AGH – SITG. Wyd. AGH. Kraków. 1981. ss. 431–453.
W. Blaschke, E. Mokrzycki, W. Pudło: Analiza wpływu zmian zawartości popiołu na cenę i koszt mieszanek koksowniczych. Mat. Symp. nt. Wybrane zagadnienia ekonomiczne procesów pozyskania i przetwarzania węgla. PAN – SITG. Zagadnienia Postępu Technicznego i Ekonomiki Górnictwa. Wyd. ZG SITG. 1981. ss. 135–147.
W. Blaschke, L. Górska, E. Mokrzycki, W. Suwała: Koncepcja budowy modelu bilansowania produkcji i zapotrzebowania węgla kamiennego. Mat. Symp. nt. Wybrane zagadnienia ekonomiki procesów pozyskania i przetwarzania węgla. PAN – SITG. Zagadnienia Postępu Technicznego i Ekonomiki Górnictwa. Wyd. ZG SITG. 1981. ss. 156–166.
W. Blaschke, L. Górska, E. Mokrzycki, W. Suwała: Rola zakładów przeróbczych w modelu bilansowania gospodarki węglem kamiennym. Mat. XV Krakowskiej Konf. Przeróbki Kopalin. Zbiór referatów. AGH – SITG. Wyd. GBSiPW SEPARATOR. Kraków. 1981. ss. 42–55.
W. Blaschke: Koncepcje poprawy efektywności wzbogacania węgli krajowych. Materiały na naradę środowiskową przeróbki węgla kamiennego przed VI Krajowym Zjazdem Górniczym. Katowice. 1982. ss. 15–29.
W. Blaschke, Z. Blaschke: Wanad. Przeróbka mechaniczna. W: Surowce Mineralne Świata. Tom V-Ti-Zr-Hf. Pod red. A. Bolewskiego. Wydawnictwo Geologiczne. Warszawa 1982. s. 76–80.
W. Blaschke, Z. Blaschke: Tytan. Przeróbka mechaniczna. W: Surowce Mineralne Świata. Tom V-Ti-Zr-Hf. Pod red. A. Bolewskiego. Wydawnictwo Geologiczne. Warszawa 1982. s. 229–244.
W. Blaschke, Z. Blaschke: Cyrkon. Przeróbka mechaniczna. W: Surowce Mineralne Świata. Tom V-Ti-Zr-Hf. Pod red. A. Bolewskiego. Wydawnictwo Geologiczne. Warszawa 1982. s. 348–357.
W. Blaschke, E. Mokrzycki, W. Pudło: Analiza wpływu zmian zawartości popiołu na cenę i koszt mieszanek koksowniczych. Archiwum Górnictwa. Tom 27. z. 3. 1982.
J. Blaschke, W. Blaschke: Równania ceny zbytu węgla koksowego. Budownictwo Węglowe. Projekty – Problemy. Śląsk. Katowice. 1982. Nr 1 (295). ss. 31–36.
W. Blaschke, L. Górska, E. Mokrzycki, W. Suwała: The possibilities of pyrites concentrates production at hard coal preparation plants. International Symposium on Recent Advances. In Particulate science and technology. Paper 54. Madras. India. 1982. pp. 583–590.
W. Blaschke, L. Górska, E. Mokrzycki, W. Suwała: Kierunki wykorzystania węgli brunatnych z lokalnych złóż w oparciu o ich parametry jakościowe. Mat. XI Sesji Naukowej AGH i XIV Zjazdu SW AGH. Kraków. 1982. ss. 75–91.
W. Blaschke, Z. Blaschke: Nikiel. Przeróbka mechaniczna. W: Surowce Mineralne Świata. Tom Ni-Co. Pod red. A. Bolewskiego. Wydawnictwa Geologiczne. Warszawa. 1984. s. 152–165.
W. Blaschke, Z. Blaschke: Kobalt. Przeróbka mechaniczna. W: Surowce Mineralne Świata. Tom Ni-Co. Pod red. A. Bolewskiego. Wydawnictwa Geologiczne. Warszawa. 1984. s. 253–263.
W. Blaschke, L. Górska, E. Mokrzycki, W. Suwała: Technologiczne możliwości uzyskiwania koncentratów pirytowych z odpadów niektórych kopalń węgla kamiennego. Przegląd Górniczy. 1984. Nr 12. ss. 433–437.

W. Blaschke, K. Adamczyk, E. Mokrzycki, I. Soliński, W. Suwała: Koszty pozyskania paliw węglowych i węglowodorowych w warunkach krajowych. Mat. Konf.. PAN. Energetyka czynnikiem wzrostu. Komitet Problemów Energetyki. Warszawa – Jabłonna. 1984. ss. 23–30.
W. Blaschke, L. Górska, E. Mokrzycki, W. Suwała: Parametry jakościowe oraz kierunki wykorzystania węgli kamiennych. Mat. Ogólnokrajowej Konf. Problemy badań węgla w pracach geologiczno-złożowych w aspekcie nowych technologii jego utylizacji. Bielsko-Jaworze. 1984. ss. 23–37.
W. Blaschke, L. Górska, E. Mokrzycki, W. Suwała: Parametry jakościowe oraz możliwości zagospodarowania krajowych węgli brunatnych. Mat. Ogólnokrajowej Konf. Problemy badań węgla w pracach geologiczno-złożowych w aspekcie nowych technologii jego utylizacji. Bielsko-Jaworze. 1984. ss. 62–66.
W. Blaschke, Z. Blaschke: Molibden. Przeróbka mechaniczna. W: Surowce Mineralne Świata. Tom Mo-W-Re-Sc. Pod red. A. Bolewskiego. Wydawnictwa Geologiczne. Warszawa 1985. s. 104–114.
W. Blaschke, Z. Blaschke: Wolfram. Przeróbka mechaniczna. W: Surowce Mineralne Świata. Tom Mo-W-Re-Sc. Pod red. A. Bolewskiego. Wydawnictwa Geologiczne. Warszawa 1985. s. 264–294.
W. Blaschke, Z. Blaschke: Piryt. Przeróbka mechaniczna. W: Surowce Mineralne Świata. Tom Siarka. Pod red. A. Bolewskiego. Wydawnictwa Geologiczne. Warszawa 1985. s. 310–327.
W. Blaschke, Z. Blaschke: Przeróbka kopalin apatytu. W: Surowce Mineralne Świata. Tom Fosfor. Pod red. A. Bolewskiego. Wydawnictwa Geologiczne. Warszawa 1985. s. 192–201.
W. Blaschke, Z. Blaschke: Przeróbka fosforytów. W: Surowce Mineralne Świata. Tom Fosfor. Pod red. A. Bolewskiego. Wydawnictwa Geologiczne. Warszawa 1985. s. 201–215.
W. Blaschke, H. Gruszczyk: Jakość koncentratów molibdenowych. W: Surowce Mineralne Świata. Tom Mo-W-Re-Sc. Pod red. A. Bolewskiego. Wydawnictwa Geologiczne. Warszawa. 1985. ss. 114–115.
W. Blaschke: Efektywność wzbogacania węgli kamiennych. Gospodarka Surowcami Mineralnymi. Kwartalnik PAN. 1985. Zeszyt 1. ss. 161–187.
W. Blaschke, L. Górska, E. Mokrzycki, I. Soliński, W. Suwała: Koszty pozyskiwania podstawowych nośników energii w warunkach Polski. Gospodarka Surowcami Mineralnymi. Kwartalnik PAN. 1985. Zeszyt 2. ss. 339–351.
W. Blaschke, E. Mokrzycki, W. Suwała: Wyznaczanie i porównanie kosztów rozwiązań modelowych zakładów przeróbczych w Polsce i w USA. Gospodarka Surowcami Mineralnymi. Kwartalnik PAN. 1985. Zeszyt 2. ss. 363–377.
W. Blaschke, L. Górska, E. Mokrzycki, W. Suwała: Technological method of modelling the costs of kaolin cleaning. Proceedings of World Congress on Non Metallic Minerals. Belgrad. Jugosławia. 1985.
S. Blaschke, W. Blaschke: Technika wzbogacania węgla. Wyd. II. Skrypt AGH Nr 1048. Kraków. 1986. ss. 1–649.
W. Blaschke: Ocena bazy paliwowo-energetycznej kraju. Gospodarka Surowcami Mineralnymi. Kwartalnik PAN. 1986. Zeszyt 1. ss. 63–81.
R. Ney, W. Blaschke, A. Jankowska-Kłapkowska i inni: Aktualne i przyszłe możliwości rozbudowy Lubelskiego Zagłębia Węglowego. Ekspertyza PAN. Wyd. Komitetu Gospodarki Surowcami Mineralnymi. Kraków. 1986. ss. 1–68.
W. Blaschke, Z. Blaschke: Organizacja, zaplecze naukowe, zaplecze projektowo-badawcze oraz szkolenie kadr dla zakładów przeróbki mechanicznej kopalin. Mat. XIII Jugosłowiańsko-polskiego Symp. Górniczego. Opatija – Jugosławia. 1986. Wydawnictwo ZG SITG. ss. 74–78.
S. Blaschke, W. Blaschke: Technika wzbogacania węgla. Wyd. III. Skrypt AGH Nr 1112. Kraków. 1987. ss. 1–649.
W. Blaschke, L. Górska, E. Mokrzycki, W. Suwała: Parametry jakościowe węgli brunatnych występujących w złożach polskich. Gospodarka Surowcami Mineralnymi. Kwartalnik PAN. 1987. Zeszyt 2. ss. 245–256.
R. Ney, W. Blaschke, K. Matl, E. Mokrzycki, W. Suwała: Możliwości pokrycia zapotrzebowania na pierwotne nośniki energii w przemyśle cementowo-wapienniczym. Cement–Wapno–Gips. 1987. Zeszyt 4–5. ss. 77–81.
W. Blaschke. L. Górska, E. Mokrzycki, W. Suwała: Użytkowanie węgla brunatnego. W: Problematyka wykorzystania małych powierzchniowych złóż węgla brunatnego dla potrzeb gospodarki lokalnej. (pod red. K. Matla). Wyd. AGH. Kraków. 1988. ss. 123–132.
W. Blaschke, L. Pluta: Prognoza rozwoju górnictwa kopalin stałych do 1995 roku. Gospodarka Surowcami Mineralnymi. Kwartalnik PAN. 1988. Zeszyt 2. ss. 189–212.
W. Blaschke, A. Jaworski: Produkcja maszyn oraz elementów automatyki dla przeróbki mechanicznej kopalin w Polsce. Mat. II Polsko-jugosłowiańskiego Symp. Przeróbki Mechanicznej Kopalin. Katowice. 1988. ss. 131–137.
S. Blaschke, W. Blaschke: Maszyny i urządzenia do przeróbki kopalin. Sita. Skrypt AGH. Nr 1145. Kraków. 1989. ss. 1–292.
A. Ofanowska, W. Blaschke, E. Mokrzycki, Z. Grudziński: Analiza kosztów przeróbki krajowych siarczkowych rud cynkowo-ołowiowych. Gospodarka Surowcami Mineralnymi. Kwartalnik PAN. 1989. Zeszyt 4. ss. 1091–1118.

W. Blaschke, E. Mokrzycki, A. Jaworski, S. A. Blaschke, Z. Grudziński: Prognozowana wartość produkcji węgla handlowego w kraju (dla zróżnicowanych przedziałów jakości) z uwzględnieniem tzw. gospodarki wolnorynkowej, w odniesieniu do krajowych i zagranicznych odbiorców. W: Analiza stanu oraz koncepcja zmian systemowych i organizacyjnych w górnictwie węgla kamiennego. Wyd. GIG. 1989. ss. 35–40.

A. Jaworski, W. Blaschke: Analiza i wybór formuł ustalania cen krajowego węgla z uwzględnieniem jego zróżnicowanej jakości. W: Analiza stanu oraz koncepcja zmian systemowych i organizacyjnych w górnictwie węgla kamiennego. Wyd. GIG. 1989. ss. 41–44.

Z. Szarafiński, W. Blaschke, A. Jaworski, W. Drogoń, J. Średniawa, A. Prynda: Zadania w zakresie przeróbki mechanicznej węgla do roku 2010/40. W: Analiza stanu oraz koncepcja zmian systemowych i organizacyjnych w górnictwie węgla kamiennego. Wyd. GIG. 1989. ss. 119–122.

W. Kociela, J. Zabierowski, W. Blaschke i inni: Doskonalenie rozwiązań struktur organizacyjnych w górnictwie węgla kamiennego. W: Analiza stanu oraz koncepcja zmian systemowych i organizacyjnych w górnictwie węgla kamiennego. Wyd. GIG. 1989. ss. 123–126.

W. Blaschke, E. Mokrzycki, S. A. Blaschke, Z. Grudziński, A. Jaworski: Prognozowana wartość produkcji węgla handlowego w kopalniach węgla kamiennego. Mat. Symp. Koncepcje racjonalnych zmian systemowych i organizacyjnych w górnictwie węgla kamiennego. Wyd. GIG. Katowice. 1989. ss. 77–93.

Z. Szarafiński, W. Blaschke, A. Jaworski: Zadania w zakresie przeróbki mechanicznej węgla. Mat. Symp. Koncepcje racjonalnych zmian systemowych i organizacyjnych w górnictwie węgla kamiennego. Wyd. GIG. Katowice. 1989. ss. 157–165.

W. Blaschke, A. Kapłanek, E. Woźnica, T. Zygadłowicz: Kierunki racjonalnych zmian w zakresie rozwiązań i struktur organizacyjnych w górnictwie węgla kamiennego. Mat. Symp. Koncepcje racjonalnych zmian systemowych i organizacyjnych w górnictwie węgla kamiennego. Wyd. GIG. Katowice. 1989. ss. 201–213.

T. Napieracz, K. Bem, A. Zając, W. Blaschke: Propozycje zmian struktury zarządzania i systemu ekonomiczno-finansowego wynikające z analizy funkcjonowania górnictwa węgla kamiennego w RFN i W. Brytanii. Mat. Symp. Koncepcje racjonalnych zmian systemowych i organizacyjnych w górnictwie węgla kamiennego. Wyd. GIG. Katowice. 1989. ss. 267–279.

S. Blaschke, W. Blaschke: Maszyny i urządzenia do przeróbki kopalin. Flotowniki. Skrypt AGH Nr 1132. Kraków. 1990. ss. 1–477.

A. Ofanowska, W. Blaschke, E. Mokrzycki, E. Prorok: Analiza kosztów przeróbki rud miedzi w zakładach KGHM Lublin. Gospodarka Surowcami Mineralnymi. Kwartalnik PAN. 1990. Zeszyt 4. ss. 741–758.

R. Ney, K. Wanielista, W. Blaschke, J. Kicki: Indices of Reserves Utilization for Assessing Mineral Resources Conservation. Proceedings of 14th World Mining Congress Beijing. Wyd. Pergamon Press. Pekin. Chiny. 1990. Volume 2. pp. 681–683.

W. Blaschke, S. A. Blaschke, A. Jaworski, E. Mokrzycki: Analysis of Dependence between Complexity of Coal Preparation Schemes and their Costs. Proceedings of 11th International Coal Preparation Congress. Tokio. Japonia. 1990. pp. 85–90.

A. Bolewski, W. Blaschke, i inni: Encyklopedia Surowców Mineralnych A–G. Wyd. Gospodarka Surowcami Mineralnymi. 1991. Zeszyt 5 specjalny.

R. Ney, W. Blaschke, J. Dziewański i inni: Zwiększenie efektywności pozyskiwania i wykorzystania surowców mineralnych. Synteza CPBR 1.7. Studia i Rozprawy. Wyd. Centrum PPGSMiE PAN. Kraków. 1991. Zeszyt 12. ss. 1–147.

W. Blaschke, E. Mokrzycki, S. A. Blaschke, U. Ozga-Blaschke i inni: Metodyka optymalizacji wykorzystania surowców mineralnych w procesach przeróbki i przetwórstwa. Studia i Rozprawy. Wyd. Centrum PPGSMiE PAN. Kraków. 1991. Zeszyt 14. ss. 1–79.

W. Blaschke, Z. Blaschke, S. A. Blaschke: Wpływ parametrów jakościowych węgla energetycznego na efektywność jego użytkowania. Przegląd Górniczy. 1991. Nr 8. ss. 1–6.

W. Blaschke, E. Mokrzycki, S. A. Blaschke, Z. Grudziński: Ceny węgla kamiennego w handlu międzynarodowym. Przegląd Górniczy. 1991. Nr 2. ss. 12–15.

W. Blaschke, E. Mokrzycki, S. A. Blaschke, Z. Grudziński: Rola formuł sprzedażnych węgla kamiennego (cenników) w warunkach wolnych cen na węgiel. Przegląd Górniczy. 1991. Nr 2. ss. 15–18.

W. Blaschke, E. Mokrzycki, S. A. Blaschke, Z. Grudziński, A. Karcz, Z. Blaschke, A. Jaworski: System cen na węgiel kamienny. Przegląd Górniczy. 1991. Nr 2. ss. 18–26.

W. Blaschke, E. Mokrzycki, S. A. Blaschke, Z. Grudziński: Wpływ decyzji o dopuszczalnym poziomie cen na prognozowaną akumulację kopalń węgla kamiennego. Przegląd Górmiczy. 1991. Nr 2. ss. 29–35.

W. Blaschke, E. Mokrzycki, S. A. Blaschke, Z. Grudziński, E. Prorok: A Final Products Cost Calculation Methodology for Lead and Zinc Preparation Plants. Proceedings of XIII Oktobarsko Savetovanje Rudara, Metalurga i Technologa. Jugosławia. Bor. 1991.

W. Blaschke, L. Gawlik, W. Suwała: Evolution in Production and Use of Coal in Poland. Seminar on Energy Policy France, Hungary, Poland, Czechoslovakia. Budapest 1991. Ed. CIFOPE. Paris. France. pp. 316–329.
W. Blaschke: Wybrane elementy rachunku ekonomicznego górnictwa węgla kamiennego w świetle jego restrukturyzacji. Mat. Konf. Gospodarka surowcami energetycznymi w warunkach przejścia do gospodarki rynkowej. Wyd. Centrum PPGSMiE PAN. Osieczany. 1991. ss. 177–187.
W. Blaschke: Rozważania o koncepcji systemu i struktury cen węgla kamiennego w warunkach gospodarki rynkowej w Polsce. Mat. Symp. Kierunki modernizacji górnictwa. Wyd. Centrum PPGSMiE PAN. Kraków. 1991. Zeszyt III. ss. 77–84.
W. Blaschke, E. Mokrzycki, S. A. Blaschke, Z. Grudziński: Kształtowanie się kosztów pozyskania tony węgla wskaźnikowego w krajowych kopalniach węgla kamiennego. Mat. Symp. Kierunki modernizacji górnictwa. Wyd. Centrum PPGSMiE PAN. Kraków. 1991. Zeszyt III. ss. 119–133.
W. Blaschke: Technologie czystego węgla. Przygotowanie czystego węgla do spalania. Mat. Symp. Kierunki modernizacji górnictwa. Wyd. Centrum PPGSMiE PAN. Kraków. 1991. Zeszyt IV. ss. 143–150.
W. Blaschke, E. Mokrzycki: Wartość produkcji węgla kamiennego w świetle cen importowanych. Mat. Symp. Kierunki modernizacji górnictwa. Wyd. Centrum PPGSMiE PAN. Kraków. 1991. Zeszyt IV. ss. 151–163.
W. Blaschke, E. Mokrzycki, S. A. Blaschke, Z. Grudziński, Z. Blaschke: Opłacalność wzbogacania węgla energetycznego w nowym systemie cen na węgiel. Mat. XXIII Krakowskiej Konf. Przeróbki Kopalin. Bukowina Tatrzańska. 1991. Wyd. AGH Kraków. ss. 89–108.
W. Blaschke, E. Mokrzycki, S. A. Blaschke, Z. Grudziński: Koncepcja systemu rozdziału dotacji do kopalń węgla kamiennego w zależności od jakości węgla handlowego. Mat. XXIII Krakowskiej Konf. Przeróbki Kopalin. Bukowina Tatrzańska. 1991. Wyd. AGH Kraków. ss. 109–126.
A. Bolewski (red.), W. Blaschke i inni: Encyklopedia Surowców Mineralnych. Tom H–O. Wyd. CPPGSMiE PAN. Kraków, 1992.
W. Blaschke, L. Gawlik, J. Kicki, W. Suwała: Resources of Hard Coal in Poland, Germany and United Kingdom. [in]: Coal Mining Economy and Policy in Poland and its Prospects in the Light of Overall Economic Reforms and the Experience of Coal Industry in Germany and Great Britain. Commission of the European Communities. Bruxells. (pod red. A. Danielewskiego) Wyd. JAXA Publishing. Ltd. Cracow. 1992. pp. 55–73.
W. Blaschke, L. Gawlik, J. Kicki, W. Suwała: Hard Coal Mining Technology in Poland, Germany and Great Britain. [in]: Coal Mining Economy and Policy in Poland and its Prospects in the Light of Overall Economic Reforms and the Experience of Coal Industry in Germany and Great Britain. Commission of the European Communities. Bruxells. (pod red. A. Danielewskiego) Wyd. JAXA Publishing. Ltd. Cracow. 1992. pp. 75–112.
W. Blaschke: Technologie czystego węgla. Energetyka. 1992. Nr 2.
W. Blaschke: Konstrukcja cen węgla kamiennego (energetycznego) w warunkach gospodarki okresu przejściowego. Wiadomości Górnicze. 1992. Z. 8. ss. 202–205.
W. Blaschke: Poziom cen węgla kamiennego (energetycznego) w warunkach gospodarki okresu przejściowego. Wiadomości Górnicze. 1992. Z. 10. ss. 230–232.
W. Blaschke, E. Mokrzycki, S. A. Blaschke: Propozycja rachunku kosztów wydobycia i przeróbki węgla kamiennego. Przegląd Górniczy. 1992. Nr 11. ss. 1–6.
W. Blaschke, E. Mokrzycki, S. A. Blaschke: Koncepcja podziału zakładu przeróbczego na stanowiska powstawania kosztów. Przegląd Górniczy. 1992. Nr 11. ss. 7–15.
W. Blaschke, E. Mokrzycki, S. A. Blaschke, Z. Grudziński: Propozycja metody obliczania kosztów pozyskania produktów handlowych zakładu przeróbczego. Przegląd Górniczy. 1992. Nr 11. ss. 16–21.
W. Blaschke, E. Mokrzycki, S. A. Blaschke, Z. Grudziński, U. Lorenz: Analiza kosztów wzbogacania węgla kamiennego w zależności od stopnia złożoności układu technologicznego. Przegląd Górniczy. 1992. Nr 11. ss. 21–35.
W. Blaschke: Zasady kształtowania cen węgla kamiennego. Problemy Projektowe Przemysłu i Budownictwa. 1992. Nr 2. ss. 30–34.
W. Blaschke, E. Mokrzycki i inni: System cen ekonomicznym stymulatorem poprawy jakości węgla kamiennego. Problemy Projektowe Przemysłu i Budownictwa. 1992. Nr 4. ss. 107–111.
W. Blaschke, E. Mokrzycki, Z. Grudziński, S. A. Blaschke, L. Gawlik: Costs of Lead and Zinc Sulphide Ore Preparation. Proceedings of I International Conference on Modern Process Mineralogy and Mineral Processing. Chiny. Beijing. 1992. International Academic Publisher. pp. 745–750.
W. Blaschke, W. Suwała: Problémy reštrukturalizácie polského uholného banictva. Mat. Konf. Privatizácia a podnikanie v Banictve. Slovenska Banicka Spolocnost. Banská Bystrica. 1992. pp. 48–57.
W. Blaschke: Zasady kształtowania cen węgla kamiennego. Mat. Szkoły Eksploatacji Podziemnej. Wisła-Jawornik. Sympozja i Konferencje. Zeszyt 1. Wyd. Centrum PPGSMiE PAN. 1992. ss. 9–21.

W. Blaschke: Nowe spojrzenie na wartość węgla kamiennego w złożu. Mat. Konf. Efektywność pozyskiwania, wykorzystania i ochrony zasobów złóż kopalin użytecznych w warunkach wdrażania zasad gospodarki rynkowej. Zakopane. Sympozja i Konferencje. Zeszyt 2. Wyd. Centrum PPGSMiE PAN. 1992. ss. 15–25.
J. Zabierowski, E. Mokrzycki, W. Blaschke: Prognoza wartości produkcji krajowego węgla kamiennego do roku 2010. Mat. Konf. Efektywność pozyskiwania, wykorzystania i ochrony zasobów złóż kopalin użytecznych w warunkach wdrażania zasad gospodarki rynkowej. Zakopane. Sympozja i Konferencje. Zeszyt 2. Wyd. Centrum PPGSMiE PAN. 1992. ss. 313–341.
W. Blaschke, E. Mokrzycki i inni: System cen ekonomicznym stymulatorem poprawy jakości węgla kamiennego. Mat. Konf. nt. Działalność górnictwa węgla kamiennego w warunkach gospodarki rynkowej i ograniczeń ekologicznych. Gliwice. 1992.
A. Bolewski (red.), W. Blaschke i inni: Encyklopedia Surowców Mineralnych. Tom P–S. Wyd. CPPGSMiE PAN. Kraków. 1993.
W. Blaschke, S. A. Blaschke, Z. Grudziński, U. Lorenz, E. Mokrzycki: Koncepcja systemu cen na węgiel kamienny w warunkach przejściowych do gospodarki rynkowej. Studia i Rozprawy Nr 31. Wyd. Centrum PPGSMiE PAN. Kraków. 1993. ss. 1–115.
W. Blaschke, E. Mokrzycki, K. Wróbel: Economics of Coal Preparation in Relation to Process Technologies. Mineral Economy. Kraków. 1993. GSM z. 4. ss. 669–680.
W. Blaschke, E. Mokrzycki, S. A. Blaschke, L. Gawlik, Z. Grudziński: The Final Products Costs Calculation Methodology for Lead and Zinc Preparation Plants. Mineral Economy. Kraków. 1993. GSM z. 4. ss. 681–685.
W. Blaschke, E. Mokrzycki: Banictvo v ekonomike Polska. Mat. Konf. Banictvo v ekonomike Slovenska a Štatov Strednej Europy. Bratislava. 1993. pp. 32–42.
W. Blaschke, E. Mokrzycki, K. Wróbel: Economics of Coal Preparation in Relation to Process Technologies. Mat. United Nation Interregional Symposium on Coal Preparation and Benefication. (publikowane w języku chińskim). 1993. Yanzhan. China. pp. 128–140.
W. Blaschke, E. Mokrzycki, S. A. Blaschke, Z. Grudziński, U. Lorenz: Clean Coal Technology in Poland – Problem of Pre-combustion Coal Beneficiation. Proceedings. 5th International Energy Conference. 1993. Energex'93. Seoul. Korea. Ed. Korea Institute of Energy Research. Volume IV. Fossil Fuels and Clean Fuel Technologies. pp. 10–18.
W. Blaschke: Problem cen w systemie ekonomiczno – finansowym grup kopalń węgla kamiennego. Mat. Szkoły Eksploatacji Podziemnej. Ustroń 1993. Tom 1. Sympozja i Konferencje. Nr 6. Wyd. Centrum PPGSMiE PAN. Kraków. 1993. ss. 27–35.
W. Blaschke: Wybrane problemy polskiego górnictwa węgla kamiennego. Mat. Semin. Polskie górnictwo węglowe na tle globalnych problemów rozwoju. Akademia Ekonomiczna. Katowice. 1993. ss. 51–59.
W. Blaschke, J. Froch: Energochłonność górnictwa węgla kamiennego – zarys problemu. Mat. Konf. Racjonalizacja użytkowania energii i środowiska. Porąbka-Kozubnik. 1993. Wyd. ODKT RS NOT. Warszawa. ss. 93–96.
W. Blaschke, S. A. Blaschke, T. Olkuski, J. Rżany, Z. Blaschke: Rozkład zawartości siarki w węglach energetycznych a opłacalność ich odsiarczania. Mat. XXV Krakowskiej Konf. Przeróbki Kopalin. Szczawnica. 1993. Sympozja i Konferencje Nr 8. Wyd. Centrum PPGSMiE PAN. Kraków. ss. 93–109.
W. Blaschke, Z. Grudziński, U. Lorenz, E. Mokrzycki: Zawartość siarki a struktura cen węgla energetycznego. Mat. XXV Krakowskiej Konf. Przeróbki Kopalin. Szczawnica. 1993. Sympozja i Konferencje Nr 8. Wyd. Centrum PPGSMiE PAN. Kraków. ss. 111–126.
W. Blaschke, E. Mokrzycki: Problem określenia poziomu cen węgla kamiennego energetycznego na podstawie wartości węgla w świetle cen importowych. Mat. III Konf. Aktualia i perspektywy gospodarki surowcami mineralnymi. Zakopane. 1993. Sympozja i Konferencje Nr 9. Wyd. Centrum PPGSMiE PAN. Kraków. ss. 27.1–27.17.
W. Blaschke, Z. Blaschke: Krakowskie Konferencje Przeróbki Kopalin. Mat. XXV Krakowskiej Konf. Przeróbki Kopalin. Szczawnica. 1993. Sympozja i Konferencje Nr 8. Wyd. CPPGSMiE PAN. Kraków. ss. 5–29.
A. Bolewski (red.), W. Blaschke i inni: Encyklopedia Surowców Mineralnych. Tom Ś–Ż. Wyd. CPPGSMiE PAN. Kraków. 1994. s. 415.
E. Mokrzycki (red), W. Blaschke, S. A. Blaschke, U. Ozga-Blaschke i inni: Technologie czystego węgla na etapie przeróbki i przygotowania węgla do procesu użytkowania. Studia i Rozprawy Nr 35. Wyd. Centrum PPGSMiE PAN. Kraków 1994. ss. 1–100.
W. Blaschke: Calorific Value Curves for Steam Coal. Mineral Economy. Kraków. 1994. GSM z. 2. ss. 263–274.
W. Blaschke, T. Tumidajski: Approximation of Steam Coal Concentrate Washability Curves Using Weibull's Distribution. Mineral Economy. Kraków. 1994. GSM z. 2. ss. 285–290.
W. Blaschke, E. Mokrzycki, S.A. Blaschke, Z. Grudziński, L. Gawlik, U. Lorenz: Coal Prices Versus Coal Quality in Polish Conditions of the Transition to the Market Economy. Proceedings of 16th World Mining Congress. Sofia. Bulgaria. 1994. Vol. 3. paper G-9. pp. 199–208.
W. Blaschke, E. Mokrzycki, Z. Shan: Coal Preparation Economics. Preprint of the 12th International Coal Preparation Congress. Cracow. 1994. Volume 2. pp. 1357–1374.

E. Mokrzycki, W. Blaschke, Z. Shan: Waste Treatment versus Ecology. Preprint of the 12th International Coal Preparation Congress. Cracow. 1994. Volume 2. pp. 1375–1388.
W. Blaschke, E. Mokrzycki, Z. Shan: Ekonomika przeróbki węgla kamiennego. Mat. XII MKPW. Sympozja i Konferencje. Wyd. Centrum PPGSMiE PAN. 1994. Z. 11. Tom 5. ss. 101–121.
E. Mokrzycki, W. Blaschke, Z. Shan: Przeróbka węgla kamiennego a ochrona środowiska przyrodniczego. Mat. XII MKPW. Sympozja i Konferencje. Wyd. Centrum PPGSMiE PAN. 1994. Z. 11. Tom 5. ss. 123–139.
W. Blaschke, E. Mokrzycki: Cena jako główny stymulator rynku węglowego – możliwe rozwiązania. Mat. Konf. Społeczno-gospodarcze problemy wynikające z sezonowości rynku węglowego w Polsce w aspekcie dystrybucji grubych sortymentów węgla oraz tworzenia zapasów węgla energetycznego. Promnice. Wyd. Wenta Alfa. Katowice. 1994.
W. Blaschke: Budowa zakładów wzbogacania miałów energetycznych a modernizacja elektrowni w aspekcie procesów restrukturyzacji górnictwa węglowego. Mat. Szkoły Eksploatacji Podziemnej '94. Jastrzębie-Zdrój. Sympozja i Konferencje Nr 10. Wyd. Centrum PPGSMiE PAN. Kraków. 1994. Tom 1. ss. 243–253.
W. Blaschke, S.A. Blaschke, L. Gawlik, Z. Grudziński, E. Mokrzycki: Ceny koncernowe a ceny wewnątrzkoncernowe węgla kamiennego – zarys problemu. Mat. XXVI Krakowskiej Konf. Przeróbki Kopalin. Ustroń. Sympozja i Konferencje nr. 13. Wyd. Centrum PPGSMiE PAN. Kraków. 1994. ss. 285–290.
W. Blaschke, Z. Grudziński, J. Kapinos, E. Mokrzycki, U. Ozga: Koncepcja struktur cen koncernowych węgla energetycznego w oparciu o system cennika z 1990 r. Mat. XXVI Krakowskiej Konf. Przeróbki Kopalin. Ustroń. Sympozja i Konferencje nr. 13. Wyd. Centrum PPGSMiE PAN. Kraków 1994. ss. 291–301.
W. Blaschke, Z. Grudziński, U. Lorenz, E. Mokrzycki, T. Olkuski, U. Ozga, J. Rżany: Nowa, koncernowa formuła sprzedażna dla węgla kamiennego energetycznego. Mat. XXVI Krakowskiej Konf. Przeróbki Kopalin. Ustroń. Sympozja i Konferencje nr. 13. Wyd. Centrum PPGSMiE PAN. Kraków. 1994. ss. 303–312.
W. Blaschke, Z. Grudziński: Jakość węgla kamiennego energetycznego a jego cena. Mat. VII Konf. Zagadn. Sur. Energ. w Gosp. Kraj. Sympozja i Konferencje nr. 15. 1994. Wyd. Centrum PPGSMiE PAN. Kraków. ss. 95–108.
W. Blaschke, E. Mokrzycki, S.A. Blaschke, U. Ozga-Blaschke i inni: Węgiel koksowy na rynkach światowym i krajowym. Studia–Rozprawy–Monografie. Nr. 37. Wyd. Centrum PPGSMiE PAN. Kraków. 1995. ss. 1–129.
J.J. Hycnar, W. Blaschke, E. Mokrzycki i inni: Technologie czystego węgla – odsiarczanie i demineralizacja za pomocą silnych zasad. Studia, Rozprawy, Monografie. nr 40. Wyd. Centrum PPGSMiE PAN. Kraków. 1995. ss. 1–70.
W. Blaschke, E. Mokrzycki, W. Suwała: Comparison of Costs for Different Levels of Coal Cleaning for Coal Preparation Plants in Poland. Coal Preparation. A Multinational Journal. 1995. Vol. 16. pp.103–114. Gordon and Breach Science Publishers SA. USA.
W. Blaschke, A. Karbownik: Politika vlády a reštrukturalizácia po'lského kamennouhol'ného banictwa. Slovenská Banicka Spoločnost. Prezidium Spoločnosti. Bulletin no 5. Banská Bystrica. 1995. pp. 3–15.
T. Tumidajski, W. Blaschke: Determining the Dependence Between the Yields of Enrichments Products and the Contents of a Selected Component According to the Equation of Balance. Archiwum Górnictwa nr 2. 1995. ss. 237–246.
W. Blaschke, E. Mokrzycki, Z. Grudziński, U. Lorenz: Steam coal fines quality-pre-combustion coal beneficiation. Mineral Economy. Kraków 1995. GSM z.4. ss. 569–578.
W. Blaschke, U. Lorenz, Z. Grudziński: Przeróbka mechaniczna węgla a ekologia. Wiadomości Górnicze nr 5. 1995. ss. 199–204.
W. Blaschke, E. Mokrzycki i inni: Rynek światowy węgla koksowego. Karbo. 1995. nr 12. ss. 312–327.
W. Blaschke, L. Gawlik: Import węgla kamiennego – zagrożenie czy blef? Biuletyn Górniczy. GIPH. Nr 5. 1995. ss. 8–11.
W. Blaschke, A. Karbownik: Polityka vlády a reštrukturalizácia pol'ského kamenouhol'ného banictva. Mat. Międzyn. Konf. Surovinová politika štátu. Bańska Bystrzyca. 1995. Wyd. Biuletyn SBS. Nr 5. 1995. pp. 3–15.
W. Blaschke, Z. Grudziński i inni: Określenie ceny parytetu importowego węgla energetycznego. Mat. I Międz. Konf. Przer. Kopalin. Zakopane. 1995. Sympozja i Konferencje nr 19. Wyd. Centrum PPGSMiE PAN. ss. 421–430.
W. Blaschke, S.A. Blaschke i inni: Określenie ceny parytetu importowego węgla koksowego. Mat. I Międz. Konf. Przer. Kopalin. Zakopane. 1995. Sympozja i Konferencje nr 19. Wyd. Centrum PPGSMiE PAN. ss. 409–420.
W. Blaschke: Czy górnictwo węglowe musi płacić tak wysokie opłaty eksploatacyjne. Mat. Szkoły Eksploatacji Podziemnej 1995. Szczyrk. Sympozja i Konferencje nr 16. Wyd. Centrum PPGSMiE PAN. Kraków 1995. ss. 205–222.
W. Blaschke: Zasady kształtowania polityki cenowej węgla kamiennego. Mat. Ogólnopolskiej Konf. Węgiel i Energetyka. Bielsko-Biała. 1995. ss. 1–15.
I. Tomkowska, W. Blaschke: Problem budowy zakładów wzbogacania węgla w świetle modernizacji elektrowni i elektrociepłowni. Mat. IX Konf. Zagadnienia surowców energetycznych w gospodarce krajowej. Zakopane. październik 1995. Sympozja i Konferencje. Nr 17. Wyd. Centrum PPGSMiE PAN. ss. 223–231.

W. Blaschke, E. Mokrzycki, Z. Shan: Coal Preparation Economics. Recent Adwances in Coal Processing (Ed. J. Laskowski). Vol. 1. New Trends in Coal Preparation Technologies and Equipment (Ed. W.S. Blaschke). Gordon and Breach Science Publishers. USA. 1996. pp. 867–878.
E. Mokrzycki, W. Blaschke, Z. Shan: Waste Treatment Versus Ecology. Recent Adwances in Coal Processing (Ed. J. Laskowski). Vol. 1. New Trends in Coal Preparation Technologies and Equipment (Ed. W.S. Blaschke). Gordon and Breach Science Publishers. USA. 1996. pp. 879–888.
W. Blaschke, E. Mokrzycki, U. Ozga-Blaschke: Przeróbka i przetwórstwo węgla kamiennego. W: Surowce Mineralne Polski. (pod red. R. Neya). Tom Surowce Energetyczne. Węgiel kamienny. Węgiel brunatny. Wyd. Centrum PPGSMiE PAN. Kraków. 1996. ss. 123–176.
W. Blaschke, Z. Grudziński i inni: Aktualna i prognozowana podaż miałów węgla energetycznego w Polsce. Przegląd Górniczy nr 1. 1996. ss. 9–15.
W. Blaschke, Z. Grudziński: Węgiel kamienny energetyczny. Cz. I. Ceny światowe – wartość węgla. Wiadomości Górnicze. nr 9, 1996. ss. 403–411.
W. Blaschke, Z. Grudziński: Węgiel kamienny energetyczny. Cz. II. Ceny światowe – parytet importowy. Wiadomości Górnicze. nr 9, 1996. ss. 412–419.
W. Blaschke: Budowa zakładów wzbogacania miałów energetycznych a modernizacja elektrowni. Czasopismo Techniczne. KTT. Kraków. nr 9–10. 1996. ss. 19–25.
W. Blaschke, S.A. Blaschke i inni: Zawartość siarki w węglach energetycznych a opłacalność ich odsiarczania. Czasopismo Techniczne. KTT. Kraków. nr 9–10. 1996. ss. 26–29.
W. Blaschke: Szanse polskiego górnictwa. Biuletyn Górniczy. GIPH. nr 7. 1996. ss. 12–13.
W. Blaschke: Ceny węgla kamiennego dla energetyki zawodowej. Przyczyny kryzysów cenowych w układzie producenci – odbiorcy. Biuletyn Górniczy. GIPH. nr 8/9. 1996. ss. 4–6.
W. Blaschke: Chances of Polish Coal Mining. Szanse polskiego górnictwa węgla kamiennego. Polish Mining Review'96. Przegląd górnictwa polskiego. GIPH. 1996. ss. 3–6.
W. Blaschke: Ceny węgla kamiennego dla energetyki zawodowej. cz. II. Ustalenia poziomu cen węgla – teoria i praktyka. Biuletyn Górniczy. GIPH. 1996. nr 10. ss. 8–9.
W. Blaschke: Ceny węgla kamiennego dla energetyki zawodowej. cz.III. Kryzys cenowy – i co dalej? Biuletyn Górniczy. GIPPH. 1996. nr 11. ss. 8–9.
W. Blaschke, S.A. Blaschke, E. Mokrzycki: Identyfikacja kosztów w zakładach przeróbki mechanicznej węgla. Prace Centralnego Ośrodka Informatyki Górnictwa SA. Zeszyt nr 36. grudzień 1996.
W. Blaschke, L. Gawlik: The Future of the Polish Coal Mining Industry in the View of Energy Forecasts. Proceedings of the 6th International Energy Conference. Energex'96. 1996. Beijing. China. pp. 752–755.
W. Blaschke, L. Gawlik, L. Noras: Coal Mining in Poland in the Aspect of Present and Future Environmental Regulations. Proceedings of the Fourth International Conference on Environmental Issues and Waste Management in Energy and Mineral Production – SWEMP'96, Cagliari, Italy. 1996. pp. 69–74.
W. Blaschke, L. Gawlik: Przyszłość górnictwa węglowego w Polsce w świetle prognoz energetycznych. Mat. Szkoły Eksploatacji Podziemnej '96. Szczyrk. Sympozja i Konferencje nr 20. Suplement. Wyd. Centrum PPGSMiE PAN. 1996. ss. 1–8.
W. Blaschke, Z. Grudziński: Konkurencyjność polskiego węgla energetycznego na rynku krajowym i w eksporcie. Prace GIG. Seria Konferencje nr 12. Mat. Konf. Poprawa jakości węgla w programie dostosowania górnictwa węglowego do warunków gospodarki rynkowej. Szczyrk – Katowice 1996. ss. 153–161.
W. Blaschke: O możliwości kosztowego kształtowania cen węgla kamiennego energetycznego. Mat. X Konf. Zagadnienia surowców energetycznych w gospodarce krajowej. Sympozja i Konferencje. nr 23. Wyd. Centrum PPGSMiE PAN. Kraków. 1996. ss. 301–310.
W. Blaschke, S.A. Blaschke, E. Mokrzycki: Identyfikacja kosztów w zakładach przeróbki mechanicznej węgla. Mat. Symp. Problemy identyfikacji elementarnych zaszłości gospodarczych w górnictwie w aspekcie proefektywnościowych wymagań gospodarki rynkowej. Komitet Górnictwa PAN. Katowice. 1996. Wyd. COIG SA. ss. 119–131.
W. Blaschke, S.A. Blaschke, Z. Grudziński: System cen energetycznego węgla kamiennego a opłacalność jego wzbogacania. Przegląd Górniczy. nr 1, 1997. ss. 21–33.
W. Blaschke, L. Gawlik: Metodyka wyznaczania parytetu importowego węgla energetycznego. Biuletyn PARG WK SA. Katowice. nr 2(30)/1997. ss. 1–6.
W. Blaschke, L. Gawlik, J. Karaszewski: Problem cen węgla dla energetyki zawodowej. Biuletyn PARG WK SA. Katowice. nr 8(36) 1997. ss.18–24.
W. Blaschke, L. Gawlik: Koncepcja rozwiązań sposobów rozliczeń cen węgla energetycznego w układzie górnictwo – energetyka zawodowa. Mat. Szkoły Eksploatacji Podziemnej. Szczyrk 1997. Sympozja i Konferencje nr 25. Wyd. Centrum PPGSMiE PAN. Kraków 1997. ss. 13–23.

W. Blaschke: Budowa zakładów wzbogacania miałów energetycznych a modernizacja elektrowni. Mat. III Konf. Kompleksowe i szczegółowe problemy inżynierii środowiska. Wyd. Politechnika Koszalińska. Koszalin – Ustronie Morskie. 1997. ss. 49–63.
W. Blaschke, U. Lorenz: Koncepcja parytetu importowego węgla energetycznego. Mat. XI Konf. z cyklu: Zagadnienia surowców energetycznych w gospodarce krajowej. Sympozja i Konferencje nr 28. Wyd. Centrum PPGSMiE PAN. Kraków 1997. ss. 225–263.
W. Blaschke: Perspektywy rozwoju górnictwa – górnictwo węgla kamiennego. W: Ochrona środowiska na terenach górniczych. (pod red. J. Ostrowskiego). Biblioteka Szkoły Eksploatacji Podziemnej. Seria z Perlikiem nr 1. Kraków. 1998. ss. 11–14.
W. Blaschke: Perspektywy rozwoju górnictwa – górnictwo węgla brunatnego. W: Ochrona środowiska na terenach górniczych. (pod red. J. Ostrowskiego). Biblioteka Szkoły Eksploatacji Podziemnej. Seria z Perlikiem nr 1. Kraków. 1998. ss. 14–16.
W. Blaschke, R. Ney, S.A. Blaschke, U. Ozga-Blaschke i inni: Formuły cenowe węgla kamiennego zmodyfikowane do wymogów sprawozdawczości Unii Europejskiej. Studia, rozprawy, monografie. nr 57. Wyd. Instytut GSMiE PAN. Kraków 1998. ss. 1–102.
W. Blaschke: Problemy cen, kosztów pozyskania i jakości węgla kamiennego w okresie restrukturyzacji górnictwa. Przegląd Górniczy. 1998. nr 9. ss. 11–17.
W. Blaschke: Sytuacja górnictwa węgla kamiennego w świetle wygaśnięcia umów wieloletnich na dostawy węgla do energetyki zawodowej. Biuletyn PARG WK SA. Katowice, nr 1(41) 1998. ss. 3–8.
W. Blaschke, L. Gawlik: Przyszłość górnictwa węglowego w Polsce w świetle prognoz energetycznych. Czasopismo Techniczne. KTT. Kraków. 1998. nr 31–32, ss. 1–12.
W. Blaschke, Z. Grudziński: Opłacalność eksportu węgla kamiennego. Czasopismo Techniczne. KTT. Kraków. 1998, nr 31–32, ss. 13–18.
W. Blaschke: Problem urealnienia cen węgla i cen energii. Czasopismo Techniczne. KTT. Kraków. 1998, nr 31–32, ss. 19–25.
W. Blaschke: W opinii eksperta – To nie jest zmowa cenowa. Biuletyn Górniczy GIPH. 1998. nr 3(33), ss. 14–15.
W. Blaschke: Nie było praktyk monopolistycznych górnictwa przy ustalaniu cen węgla i warunków umów dla energetyki zawodowej. Biuletyn PARG WK SA, Katowice. nr 6(46), 1998, ss. 1–6.
W. Blaschke: Uporządkowanie relacji cenowych węgla kamiennego warunkiem prawidłowego rozwoju krajowej elektroenergetyki. Rynki Energii. 1998. nr 5(18), ss. 4–10.
W. Blaschke, Z. Grudziński: Parytet importowy węgla w świetle doświadczeń cenotwórstwa w Polsce i w Unii Europejskiej. Czasopismo Techniczne. KTT. Kraków, nr 40–41. 1998. ss. 1–6.
W. Blaschke, L. Gawlik, R. Nycz, Z. Starzak, L. Tażbirek: Problems of coal desulphurisation in Poland in processes of coal. Proceedings of the Fifth International Symposium on Environmental Issues and Waste Management in Energy and Mineral Produktion – SWEMP'98, Ankara – Turcja, 1998, pp. 623–631.
J. Blaschke, W. Blaschke: The Industrial us of Tangential Air-Blow for Cake Removal in Continuous Vacuum Filters. Proceedings of the XIII International Coal Preparation Congress – ICPC'98, Brisbane – Australia, 1998, Vol. II. Publ. by the Australian Coal Preparation Society. pp. 501–510.
W. Blaschke, E. Mokrzycki: Wybrane problemy gospodarki podstawowymi surowcami mineralnymi na etapie przeróbki mechanicznej. Mat. Międz. Konf. – Maszyny i urządzenia do przeróbki surowców mineralnych. Szczyrk, 1998. Wyd. KOMAG ss. 1–7.
W. Blaschke: Problem cen, kosztów pozyskania i jakości węgla kamiennego w okresie restrukturyzacji górnictwa. Forum dyskusyjne nt. Rekonstrukcja górnictwa węgla kamiennego. Szczyrk. Szkoła Eksploatacji Podziemnej '98, seria Wykłady nr 17, ss. 13–27.
R. Ney, E. Mokrzycki, W. Blaschke: Systemowe rozwiązanie problemów kosztów i cen szansą powodzenia reformy górnictwa węgla kamiennego energetycznego. Mat. Konf. Reforma polskiego górnictwa węgla kamiennego – szanse i zagrożenia. Ustroń. 1998, tom Suplement, ss. 11–35.
W. Blaschke: Uporządkowanie relacji cenowych węgla kamiennego warunkim prawidłowego rozwoju krajowej elektroenergetyki. Mat. XII Konf. z cyklu: Zagadnienia surowców energetycznych w gospodarce krajowej. Sympozja i Konferencje nr 34. Wyd. Instytutu GSMiE PAN. Kraków 1998. ss. 191–200.
W. Blaschke: Technika wzbogacania grawitacyjnego – wzbogacanie strumieniowe. Wydawnictwo Naukowe Śląsk. Katowice. 1999. ss.1–131.
W. Blaschke, S. Blaschke: Technika wzbogacania grawitacyjnego – wzbogacalniki strumieniowe. Wyd. Instytutu GSMiE PAN. Kraków. 1999. ss. 1–239
W. Blaschke, L. Gawlik: Coal mining industry restructuring in Poland: implications for the domestic and international coal market. Applied Energy. Vol. 64 No.1–4 Elsevier Science Ltd. 1999. pp. 453–456.
W. Blaschke, L. Gawlik: Hard Coal and Brown Coal in Poland's Energy Policy. Mineral Economy. Kraków. 1999. GSM z. 4. ss. 37–45.

W. Blaschke: Cenotwórstwo węgla kamiennego cz.1 – Funkcja i sposoby kształtowania cen węgla kamiennego. Wiadomości Górnicze. 1999. nr 4. ss. 186–191.
W. Blaschke: Cenotwórstwo węgla kamiennego cz. 2 – Założenia systemu cen węgla kamiennego energetycznego. Wiadomości Górnicze. 1999. nr 5. ss. 242–246
W. Blaschke: Cenotwórstwo węgla kamiennego cz. 3 – Założenia systemu cen węgla kamiennego koksowego. Wiadomości Górnicze. 1999. nr 6. ss. 286–291.
W. Blaschke: Cenotwórstwo węgla kamiennego cz. 4 – Krajowe formuły sprzedażne węgla kamiennego dostosowane do kontraktów na dostawy węgla produkowanego w Unii Europejskiej. Wiadomości Górnicze. 1999. nr 9. ss. 381–384.
W. Blaschke: Cenotwórstwo węgla kamiennego cz. 5 – Alternatywne rozwiązania formuł sprzedażnych węgla koksowego. Wiadomości Górnicze. 1999. nr 10. ss. 443–446.
W. Blaschke: Cenotwórstwo węgla kamiennego cz. 6 – Rozwiązania zagranicznych formuł sprzedażnych węgla energetycznego. Wiadomości Górnicze. 1999. nr 11. ss. 484–487.
W. Blaschke: Cenotwórstwo węgla kamiennego cz. 7 – Projekt nowej formuły sprzedażnej energetycznego węgla kamiennego (PAN–2000). Wiadomości Górnicze. 1999. nr 12. ss.529–534.
W. Blaschke: Węgiel kamienny w Polsce na tle górnictwa w świecie. Gospodarka Surowcami Mineralnymi. Kwartalnik PAN. 1999. zeszyt 3. ss. 5–28
W. Blaschke: Ceny minimalne węgla energetycznego na rynku krajowym. Biuletyn PARGWK SA. Katowice. nr 11. 1999. ss. 1–5.
W. Blaschke: Problem krajowych cen węgla kamiennego w świetle (hipotetycznego) importu węgla do Polski. Czasopismo Techniczne. KTT. Kraków. nr 51–52. 1999. ss. 1–5.
W. Blaschke, L. Gawlik: Hard coal and brown coal in Poland's Energy Policy. Conference Proceedings. Mineral and Power Policy of Slovak Republic. Demanovska Dolina – Slovakia. 1999. Publ. by the Slovakian Mining Society. pp. 40–47.
W. Blaschke: Zarys problemu kontowania kosztów w przemyśle węglowym w świetle dyrektyw Unii Europejskiej. Mat. Szkoły Eksploatacji Podziemnej. Sympozja i Konferencje nr 36. Wyd. IGSMiE PAN. Kraków. 1999. ss. 131–140.
W. Blaschke, U. Lorenz, U. Ozga-Blaschke: Światowy rynek węgla kamiennego. Mat. Konf. Reforma polskiego górnictwa – monitorowanie realizacji. Ustroń, 1999. ss. 163–184.
W.Blaschke: Uporządkowanie relacji cen do kosztów pozyskania węgla warunkiem prawidłowego funkcjonowania krajowego górnictwa. Mat. XIII Konf. Zagadnienia surowców energetycznych w gospodarce krajowej. Sympozja i Konferencje nr 39. Wyd. IGSMiE PAN. Kraków 1999. ss. 309–316.
W. Blaschke: System cen energetycznego węgla kamiennego. Studia, Rozprawy, Monografie nr 77. Wyd. Instytut GSMiE PAN. Kraków 2000. ss. 1–183.
W. Blaschke: Cenotwórstwo węgla kamiennego cz.8 – Alternatywne rozwiązania formuł sprzedażnych węgla energetycznego. Wiadomości Górnicze. 2000. nr 1. ss. 35–41.
W. Blaschke: Cenotwórstwo węgla kamiennego cz.9 – Sposoby ustalania poziomu cen w formułach sprzedażnych węgla kamiennego. Wiadomości Górnicze. 2000. nr 2. ss. 83–89.
W. Blaschke: Cenotwórstwo węgla kamiennego cz. 10 – Wyznaczanie poziomu cen węgla kamiennego w oparciu o parytet importowy. Wiadomości Górnicze. 2000. nr 4. ss. 185–193.
W. Blaschke: Cenotwórstwo węgla kamiennego cz. 11 – Jakość węgla kamiennego a struktura cen w formułach sprzedażnych. Wiadomości Górnicze. 2000. nr 5. ss. 248–255.
W. Blaschke, U. Ozga-Blaschke: Funkcjonowanie kompleksu górniczo – koksowniczego w świetle przystąpienia do Unii Europejskiej i cen hipotetycznego importu węgla koksowego do Polski. Karbo nr 7. 2000. ss. 223–227.
W. Blaschke: Cenotwórstwo węgla kamiennego cz. 12 – System cen a opłacalność wydobywania i wzbogacania węgla kamiennego. Wiadomości Górnicze nr 7–8. 2000. ss. 353–360.
W. Blaschke, L. Gawlik, U. Lorenz, E. Mokrzycki: Environment protection in the program of Polish Coal Mining Industry Reform. Sbornik referatu. 10 mezinarodni konference Hornicka Ostrawa 2000. Tom II. pp. 253–256.
W. Blaschke, U. Lorenz, E. Mokrzycki: Environmental problems of hard coal industry in Poland. Proceedings of the 5th Conference on Environment and Mineral Processing VŠB-TU Ostrawa. Czech Republik. 2000. pp. 11–18.
W. Blaschke, Gawlik: Long-term energy policy in Poland. Proceedings of the 8th International Energy Forum – Energex 2000. Las Vegas. USA. Baloban Publishers. 2000. pp. 1132–1137.
Z. Blaschke, W. Blaschke: Evaluation of the efficiency for coal slime benefication and desulfurisation in spirals. Zbornik prednasok I Medzinárodná Konferencia Mineralurgia a enviromentalne technologie. BERG TU Kosice. Herlany 2000. pp. 4–9.
W. Blaschke, L. Gawlik: Energy supply policies in Poland: Present and future. Proceedings of the American – Polish Mining Symposium Mining in the Millenium – Challenges and Opportunities. Las Vegas. Nevada. USA. Edited by T. S. Golosinski. Balkema. Rotterdam. Brookfield. 2000. pp. 225–229.

W. Blaschke: Rola i zadania zakładów przeróbki węgla w aktualnych uwarunkowaniach rynkowych. Międzynarodowa Konf. nt. Produkcja surowców mineralnych z uwzględnieniem problemów ochrony środowiska – KOMEKO 2000. Szczyrk, Wyd. Centrum Mechanizacji Górnictwa KOMAG.
W. Blaschke: Ceny węgla kamiennego – rynek polski i miedzynarodowy. Mat. Szkoły Eksploatacji Podziemnej. Sympozja i Konferencje nr 41. Wyd. Instytut GSMiE PAN. Kraków. 2000. ss. 5–23.
W. Blaschke: Problem cen węgla kamiennego w aktualnej sytuacji gospodarczej kraju. Semin. Wybrane problemy przeróbki węgla kamiennego. Prace Naukowe GIG. Seria Konferencje. nr 34. 2000. ss. 61–65.
W. Blaschke: Dostosowanie formuł sprzedażnych węgla kamiennego energetycznego do wymogów sprawozdawczości Unii Europejskiej . XIV Konf. Zagadnienia surowców energetycznych w gospodarce krajowej. Zakopane. Sympozja i Konferencje nr 46. Wyd. Instytut GSMiE PAN Kraków. 2000. ss. 115–121.
W. Blaschke, Z. Zabawa: Usługi wzbogacania węgla – przyszłościową formą działalności zakładów przeróbczych. XIV Konf. Zagadnienia surowców energetycznych w gospodarce krajowej. Zakopane. Sympozja i Konferencje nr 46. Wyd. Instytut GSMiE PAN Kraków. 2000. ss. 337–343.
W. Blaschke: Problem cen i kosztów węgla kamiennego w świetle wymogów sprawozdawczości Unii Europejskiej. X Międz. Konf. Aktualia i perspektywy gospodarki surowcami mineralnymi. Mąchocice – Ameliówka. Sympozja i Konferencje nr 47. Wyd. Instytut GSMiE PAN. Kraków 2000. ss. 17–24.
W. Blaschke, S. Blaschke: Technika wzbogacania grawitacyjnego. Stoły koncentracyjne. Wyd. Instytutu GSMiE PAN. Kraków 2001.
W. Blaschke, R. Nycz: Clean coal preparation barriers in Poland. International Workshop on Clean Coal Use – a reliable option for sustainable energy, 24–26 May 2001, Szczyrk. Wyd. Główny Instytut Górnictwa, Katowice 2001. ss.95–101.
W. Blaschke, L. Gawlik: Coal preparation in Poland in the view of economic reform. Gospodarka Surowcami Mineralnymi tom 17, z. 4. Wyd. Instytutu GSMiE PAN. Kraków 2001. ss. 63–71.
W. Blaschke: Zadania zakładów przeróbki węgla w warunkach gospodarki rynkowej. Przegląd Górniczy. 2001. Nr 10. Wyd. ZG SITG. Katowice 2001. ss. 41–47.
W. Blaschke: Rozwiązanie problemu poziomu cen węgla warunkiem harmonijnego rozwoju kompleksu paliwowo-energetycznego. Studia, Rozprawy, Monografie nr 91. Wyd. Instytutu GSMiE PAN. Kraków 2001. ss. 67–76.
W. Blaschke: Influence of economic reforms in Poland on the role of coal preparation. Colloquium International coal preparation practice. Witbank Civic Centre. 2001. Public. by the South African Institute of Mining Metallurgy, South African Coal Preparation Society.
W. Blaschke, J. Kulczycka: Structural and Ownership Changes in Polish Base Metals Industry. 25th Peruvian Mining Engineering Convention. Peru, Arequipa 2001.
W. Blaschke: Budowa nowych zakładów przeróbczych czy zlecanie usług wzbogacania – zarys problemu. Mat. Szkoły Eksploatacji Podziemnej. Szczyrk, Sympozja i Konferencje nr 48. Wyd. IGSMiE PAN. Kraków. 2001. ss. 385–397.
W. Blaschke: Uwarunkowania i sposoby ustalania poziomu cen węgla kamiennego u progu wejścia Polski do Unii Europejskiej. IV seminarium systemu Zbytu Węgla. Wyd. Węglozbyt. Ustroń 2001.
W. Blaschke: Rola węgla w polityce energetycznej państwa. Konf. nt.: Reforma Polskiego Górnictwa Węgla Kamiennego – Zarządzanie Innowacjami, Wyd. Politechnika Śląska 2001.
W. Blaschke: Wybrane zagadnienia krajowego systemu elektroenergetycznego. Konf. nt. Paliwa i energia dziś i jutro. Kraków, Wyd. Instytut GSMiE PAN 2001. ss. 129–135.
U. Lorenz., W. Blaschke, Z. Grudziński: Propozycja nowej formuły sprzedażnej węgla energetycznego przeznaczonego dla energetyki zawodowej. Studia, Rozprawy, Monografie nr 112. Wyd. Instytutu GSMiE PAN. Kraków 2002. ss. 1–78.
W. Blaschke: Polityka cenowa a rentowność górnictwa węgla kamiennego – pseudorynek. Biuletyn Górniczy nr 3–4 2002. Wyd. GIPH, Katowice, ss. 8–10.
W. Blaschke: Problematyka cen węgla kamiennego w polskim kompleksie paliwowo–energetycznym. Przegląd Górniczy nr 6. Wyd. ZG SITG Katowice 2002. ss. 1–5.
J. Hycnar, W. Blaschke: Ekologiczne, ekonomiczne i techniczne czynniki decydujące o roli węgla w bilansach paliwowo-energetycznych. Polityka Energetyczna tom 5, z. 1. Wyd. Instytutu GSMiE PAN. Kraków 2002. ss. 5–41.
W. Blaschke, S.A. Blaschke, Z. Grudziński, E. Mokrzycki, T. Olkuski, J. Rżany: Opłacalność wzbogacania wynikająca ze struktur cenowych formuł sprzedażnych i właściwości technologicznych energetycznego węgla kamiennego. Inżynieria Mineralna nr S.2 (8) 2002. Wyd. Polskie Towarzystwo Przeróbki Kopalin. Kraków, ss. 27–40.
W. Blaschke, J. Hycnar: The necessity of hard coal production adjustments to the future needs of its users. International Conference Mineral Resources of the Slovak Republic, Demanowska Dolina, 2002. Wyd. Slovenska Banicka Spolocnost, pp. 29–37.

Z. Blaschke, W. Blaschke: Sposób określania energetycznie optymalnych parametrów jakościowych węgla na przykładzie zakładu wzbogacania PPMW Biskupice. XVI Konf. Zagadnienia surowców energetycznych i energii w gospodarce krajowej. Zakopane, 2002. Sympozja i Konferencje nr 57. Wyd. Instytutu GSMiE PAN. Kraków, s. 589–599.

W. Blaschke, Z. Borkowski: Górnictwo węgla kamiennego w Polsce w świetle nowej regulacji Rady Unii Europejskiej dotyczącej pomocy państwa dla przemysłu węglowego po wygaśnięciu traktatu ustanawiającego Europejską Wspólnotę Węgla i Stali. XVI Konf. Zagadnienia surowców energetycznych i energii w gospodarce krajowej. Zakopane, 2002. Sympozja i Konferencje nr 57. Wyd. Instytutu GSMiE PAN. Kraków, s. 71–83.

W. Blaschke: Przepisy pomocowe dla górnictwa w Unii Europejskiej a reforma górnictwa węgla kamiennego. Konferencja Naukowa Górnictwo 2002. Kraków 2002. Wyd. Instytutu GSMiE PAN. Kraków, ss. 21–34.

W. Blaschke: Problemy dostosowania polskiego górnictwa węgla kamiennego do zasad regulacji Rady Unii Europejskiej. Mat. na V Górnicze Forum Dyskusyjne nt. Problemy krajowej gospodarki paliwowo-energetycznej. Katowice 2002. Wyd. Przegląd Górniczy oraz Zarząd Główny SITG. Katowice, s. 35–57.

W. Blaschke: Przystąpienie Polski do Unii Europejskiej – szanse i zagrożenia dla kopalni Bogdanka. Mat. Konf. nt. XX lat wydobycia węgla kamiennego w kopalni Bogdanka. Nałęczów 2002. Wyd. Lubelski Węgiel Bogdanka SA, s. 25–32.

W. Blaschke: Rentowne kopalnie?. Biuletyn Górniczy. Wyd. GIPH. nr 7–8. Katowice 2002. s. 23.

Z. Blaschke, W. Blaschke: Ocena celowości wzbogacania węgla na potrzeby energetyki w samodzielnych zakładach przeróbczych. Studia, Rozprawy, Monografie nr 116. Wyd. Instytutu GSMiE PAN. Kraków 2003. ss. 1–70.

S.A. Blaschke, W. Blaschke, L. Gawlik, Z. Grudziński, U. Lorenz, E. Mokrzycki, T. Olkuski, U. Ozga-Blaschke: Funkcjonowanie górnictwa węgla kamiennego na podstawie uregulowań prawnych Unii Europejskiej w latach 1993–2002. Studia, Rozprawy, Monografie nr 122. Wyd. Instytutu GSMiE PAN. Kraków 2003. ss. 1–75.

W. Blaschke, R. Nycz: Clean coal – preparation barriers in Poland. Applied Energy vol. 74. Wyd. Elsevier Science Ltd. 2003. pp. 343–348.

W. Blaschke, J. Hycnar: Conditions strenthening the role of coal in fuel-energy balance. Polityka Energetyczna tom 6, Zeszyt Specjalny. Wyd. Instytutu GSMiE PAN. Kraków 2003. ss. 7–13.

W. Blaschke, L. Gawlik: Analiza problemów związanych z rachunkiem opłacalności eksportu węgla kamiennego. Przegląd Górniczy nr 2. Wyd. ZG SITG Katowice 2003. ss. 1–7.

W. Blaschke, Z. Grudziński, U. Lorenz: Koncepcja formuły sprzedażnej węgla kamiennego energetycznego przeznaczonego dla energetyki zawodowej. Inżynieria Mineralna nr S.3 (10), Wyd. Polskie Towarzystwo Przeróbki Kopalin, Kraków 2003. ss. 185–193.

W. Blaschke: Ocena Programu Restrukturyzacji Górnictwa Węgla Kamiennego w Polsce w latach 2003–2006 pod kątem przepisów pomocowych Unii Europejskiej. Polityka Energetyczna tom 6, z. specjalny. Wyd. Instytutu GSMiE PAN, Kraków 2003. ss. 23–35.

W. Blaschke: Problem rentowności krajowych kopalń węgla kamiennego w świetle zasad stanowienia cen i liczenia kosztów w Unii Europejskiej. Polityka Energetyczna tom 6, z. specjalny. Wyd. Instytutu GSMiE PAN, Kraków 2003. ss. 37–47.

W. Blaschke, R. Nycz: Problemy produkcji czystych energetycznych węgli kamiennych. Zeszyty Naukowe Wydziału Budownictwa i Inżynierii Środowiska Politechniki Koszalińskiej. Zeszyt Nr 21, Seria: Inżynieria Środowiska. Wydawnictwo Uczelniane Politechniki Koszalińskiej. Koszalin 2003. ss. 755–766.

W. Blaschke: Górnictwo węgla kamiennego w Polsce w świetle przystąpienia do Unii Europejskiej. XIII Konf. Aktualia i perspektywy gospodarki surowcami mineralnymi, Zakopane, Sympozja i Konferencje nr 60. Wyd. Instytutu GSMiE PAN. Kraków 2003. ss. 13–18.

W. Blaschke: Wybrane problemy funkcjonowania krajowego górnictwa węgla kamiennego wymagające rozwiązania w związku z przystąpieniem Polski do Unii Europejskiej. Biblioteka Szkoły Eksploatacji Podziemnej. Seria wykłady nr 26. Seminarium nt. Górnictwo wobec wyzwań Unii Europejskiej. Wyd. Instytut GSMiE PAN. Kraków 2003. ss. 43–53.

W. Blaschke, Z. Borkowski: Pomoc państwa dla przemysłu węglowego w Unii Europejskiej po wygaśnięciu Traktatu Europejskiej Wspólnoty Węgla i Stali. Biblioteka Szkoły Eksploatacji Podziemnej. Seria wykłady nr 26. Seminarium nt. Górnictwo wobec wyzwań Unii Europejskiej. Wyd. Instytut GSMiE PAN. Kraków 2003. ss. 63–72.

W. Blaschke: Problem stanowienia cen węgla kamiennego w Polsce w perspektywie przystąpienia do Unii Europejskiej w świetle przepisów Rozporządzenia Rady (UE). Biblioteka Szkoły Eksploatacji Podziemnej. Seria wykłady nr 26. Seminarium nt. Górnictwo wobec wyzwań Unii Europejskiej. Wyd. Instytut GSMiE PAN. Kraków 2003. ss. 165–174.

R. Ney., W. Blaschke, S.A. Blaschke, L. Gawlik, Z. Grudziński, U. Lorenz, U. Ozga-Blaschke: Prognoza kształtowania się cen węgla. W: Model Ekologicznego i ekonomicznego prognozowania wydobycia i użytkowania czystego węgla. Tom 1 – Bazy i prognozy gospodarki surowcami energetycznymi oraz strategie i kierunki rozwoju sektora paliwowo-energetycznego. Wyd. GIG, Katowice, 2004. ss. 56–65.

R. Ney, W. Blaschke, E. Mokrzycki, U. Lorenz, Z. Grudziński – Węgiel w światowej energetyce. W: Model Ekologicznego i ekonomicznego prognozowania wydobycia i użytkowania czystego węgla. Tom 1 – Bazy i prognozy gospodarki surowcami energetycznymi oraz strategie i kierunki rozwoju sektora paliwowo-energetycznego. Wyd. GIG, Katowice, 2004. ss. 101–123.

S.A. Blaschke, W. Blaschke, L. Gawlik, Z. Grudziński, U. Lorenz, E. Mokrzycki, T. Olkuski, U. Ozga-Blaschke: Możliwość funkcjonowania kopalń węgla kamiennego w Polsce w świetle przepisów UE dotyczących zasad świadczenia pomocy państwa dla górnictwa w latach 2002–2010. Studia, Rozprawy, Monografie nr 123. Wyd. Instytutu GSMiE PAN. Kraków 2004. ss. 1–107.

W. Blaschke, U. Lorenz, Z. Grudziński: Pricing formula for hard coal sold to power plants and CHP plants in Poland. Gospodarka Surowcami Mineralnymi tom 20, z. 4. Wyd. Instytutu GSMiE PAN. Kraków 2004. ss. 115–125.

W. Blaschke: Szanse i zagrożenia – górnictwo po wejściu do UE. Biuletyn Górniczy nr 1–2. Wyd. GIPH, Katowice 2004. ss. 10–11.

W. Blaschke: Rachunek jednostkowych kosztów pozyskania węgla kamiennego kluczem do funkcjonowania kopalń po akcesji Polski do Unii Europejskiej. Biuletyn Górniczy nr 1–2. Wyd. GIPH, Katowice 2004. ss. 10–12.

W. Blaschke, S. A. Blaschke: Metodyka wyznaczania ceny mułów pochodzących z osadników kopalń węgla kamiennego. Czasopismo Techniczne KTT. Rok 124. Nr 102–107. Kraków 2004.

R. Ney, W. Blaschke, U. Lorenz, L. Gawlik: Hard Coal as a Source of Clean Energy in Poland. 19th Word Energy Congress and Exhibition. World Energy Council. Sydney 2004. Australia.

W. Blaschke, U. Lorenz, Z. Grudziński: Pricing Formula for Hard Coal Sold to Power Plants and CHP Plant in Poland. 21th Annual Pittsburg CoalConference. Osaka 2004. Japonia.

W. Blaschke, Z. Blaschke, S. Blaschke: The Method of Determination of the Most Favourable parameters of Coal Concentrates Regarding Maximum Electricity Production. Energex 2004 – 10th International Energy Forum. Wyd. Universidade Nova de Lisboa, Portugal 2004. pp. 181–186.

W. Blaschke, L. Gawlik: Current Status and Future Direction of the United States Coal Preparation Industry. International Seminar oc Coal Preparation Technology. Beijing 2004. Jiunhua Spa and Resort, China. Wyd. China National Coal Association (CNCA).

W. Blaschke, U. Lorenz: Restructuring of Polish Hard Coal Industry in the Last Decade and Perspectives for the Next Decade. Book of Plenary Papers European Conference on Raw Building and Coal: New Perspectives. Wyd IP Svjetlost, d.d., Sarajevo 2004. pp. 121–131.

Z. Blaschke, W. Blaschke, S. Blaschke: Determination of the most favourable parameters of coal concentrates allowing optimal utilisation of chemical energy of coal. 8 Coference on environment and mineral Processing. Wyd VSB-Technical University of Ostrava 2004, Part II pp. 327–332.

W. Blaschke, L. Gawlik: Coal preparation in Poland – current situation and development prospects. 8 Coference on environment and mineral Processing. Wyd VSB-Technical University of Ostrava 2004. Part II pp. 305–312.

W. Blaschke, L. Gawlik, U. Lorenz: Experience from Polish Hard Coal Industry Restructuring and Perspectives for the Nearest Future. International Conference Mining and Geology After Joining the European Union. Wyd Slovakian Mining Society. Demianowska Dolina 2004. pp. 51–62.

W. Blaschke: Problemy produkcji czystych węgli jako źródła wytwarzania czystej energii – Problems of clean coals production as a source of clean energy generetaion. Międzynarodowa Konf. Przyszłość węgla w gospodarce świata i Polski. Wyd. GIPH, Katowice 2004. ss. 170–177.

R. Ney, W. Blaschke, U. Lorenz, L. Gawlik: Węgiel kamienny jako źródło czystej energii w Polsce – Hard coal as a source clean energy in Poland. Międzynarodowa Konf. Przyszłość węgla w gospodarce świata i Polski. Wyd. GIPH, Katowice 2004. ss. 224–240.

W. Blaschke, L. Gawlik, U. Lorenz: Perspektywy górnictwa węgla kamiennego po przystąpieniu Polski do Unii Europejskiej w świetle realizowanych programów restrukturyzacyjnych. XIV Konf. Aktualia i perspektywy gospodarki surowcami mineralnymi, Zakopane, Sympozja i Konferencje nr 63. Wyd. Instytutu GSMiE PAN. Kraków 2004. ss. 15–27.

W. Blaschke, Z. Blaschke: Preparation of coal slurries deposited in ground settling ponds. Acta Montanistica Slovaca. Vol. 10 special issue 1. Košice. 2005. s. 17–21.

W. Blaschke: Perspektywy węgla w gospodarce świata i Polski – szanse polskiego węgla w Unii Europejskiej. Polityka Energetyczna tom 8, z. specjalny. Wyd. Instytutu GSMiE PAN, Kraków 2005. ss. 13–34.

W. Blaschke: Węgiel kamienny energetyczny – jego przyszłość w kraju i na świecie. Gospodarka Surowcami Mineralnymi tom 21, z. specjalny nr 1. Wydawnictwo Instytutu GSMiE PAN, Kraków 2005. ss. 71–82.

W. Blaschke: Przyszłość węgla kamiennego przeznaczonego dla użytkowania w energetyce. Zeszyty Naukowe Wydziału Budownictwa i Inżynierii Środowiska Politechniki Koszalińskiej. Zeszyt Nr 22, Seria: Inżynieria Środowiska. Wydawnictwo Uczelniane Politechniki Koszalińskiej. Koszalin 2005. ss. 35–53.
W. Blaschke: Określenie wartości mułów węglowych zdeponowanych w osadnikach ziemnych. Zeszyty Naukowe Wydziału Budownictwa i Inżynierii Środowiska Politechniki Koszalińskiej. Zeszyt nr 22, seria: Inżynieria Środowiska. Wydawnictwo Uczelniane Politechniki Koszalińskiej. Koszalin 2005. ss.345–358.
W. Blaschke, L. Gawlik, U. Lorenz: Węgiel kamienny energetyczny – ekonomia i ekologia. Zeszyty Naukowe Wydziału Budownictwa i Inżynierii Środowiska Politechniki Koszalińskiej. Zeszyt Nr 22, Seria: Inżynieria Środowiska. Wydawnictwo Uczelniane Politechniki Koszalińskiej. Koszalin 2005. ss. 359–376.
W. Blaschke, Z. Blaschke: Future of Hard Coal Designed for Utilisation in Power Industry. Konference: Současnost a perspektivy úpravy nerostných surovin. Wyd. VŠB–TU. Ostrava 2005. pp. 19–35.
W. Blaschke: Major Issues Connecetd with Functiong of Polish Hard Coal Industry after Accession to The European Union. International Conference Mining, Geology and Environment in the European Union. Wyd. Slovakian Mining Society. Demianowska Dolina 2005. pp. 48–58.
W. Blaschke, L. Gawlik, T. Olkuski: Koszty pozyskania węgla kamiennego w rozumieniu standardów Unii Europejskiej. W: Badania kosztów pozyskania węgla kamiennego i brunatnego w celu określenia optymalnej struktury paliwowej produkcji energii elektrycznej (Praca zbiorowa pod redakcją L. Gawlik). Wyd. Instytutu GSMiE PAN, s. 342, Kraków 2006.
W. Blaschke, L. Gawlik: Current Situation and Development Prospects of Coal Preparation in Poland. [W:] CPSA Journal. The Magazine by the Preparation Society of America. Summer 2006. Vol. 5, No 2. pp. 11–16.
W. Blaschke, L. Gawlik, S.A. Blaschke: Coal preparation technology in Poland. Gospodarka Surowcami Mineralnymi, tom 22, zeszyt 4. Wyd. Instytutu GSMiE PAN. Kraków. 2006. s. 5–12.
S. A. Blaschke, W. Blaschke, L. Gawlik, Z. Grudziński, U. Lorenz, U. Ozga-Blaschke: Problemy budowy struktur cen węgla kamiennego. Przegląd Górniczy nr 4. Wyd. ZG SITG Katowice 2006. ss. 60–65.
S.Blaschke, Z. Blaschke, W. Blaschke, J. Blaschke, S.A. Blaschke: Mała Encyklopedia Inżynierii Mineralnej. Inżynieria Mineralna. t. 7. z. S4 (17). Wyd. PTPK, Kraków. 2006. ss. 3–163.
W. Blaschke, U. Lorenz: Coal and Ores Preparation in Poland as a Source of Construction Materials. [W:] Proceedings 5th Pan-European Conferece on Planing for Minerals and Transport Infrastructure: The way for ward. Sarajewo 2006. Bośnia i Hercegowina: MAUNA – Fe. pp. 589–595.
W. Bartoniek, W. Blaschke, S. Głowiak, Z. Śmiejek: Polish Jig – Technological Potentiality. Proceedengs of XV International Coal Preparation Congress. Pekin 2006. Tom 1. pp. 321–331.
W. Blaschke: Uwagi do strategii działalności górnictwa węgla kamiennego. XVI Konf. Aktualia i perspektywy gospodarki surowcami mineralnymi. Sympozja i Konferencje nr 68. Wyd. Instytutu GSMiE PAN, Kraków 2006. ss. 69–78.
W. Blaschke, K. Tarnawska: Wpływ dokładności wzbogacania w zakładach przeróbczych na wyniki ekonomiczne kopalń węgla kamiennego. Polityka Energetyczna tom 10, z. specjalny 2. Wyd. Instytutu GSMiE PAN. Kraków. 2007. s. 623–632.
W. Blaschke, R. Nycz: Przeróbka mechaniczna pierwszym etapem technologii czystego węgla. Inżynieria Mineralna Nr 1(19) 2007. Wyd. Polskie Towarzystwo Przeróbki Kopalin. Kraków. 2007. ss. 29–36.
W Blaschke., B. Mazelanik, St. Blaschke: Analiza kosztów przeróbki węgla energetycznego. Monografia: Innowacyjne i przyjazne dla środowiska systemy przeróbcze surowców mineralnych. Komeko 2008, Centrum Mechanizacji Górnictwa KOMAG, Gliwice 2008. ss. 7–16.
W. Blaschke, A. Wawrzyczek, St. Blaschke: Budowa schematu ekonomicznego przeróbki węgla koksowego. Monografia: Innowacyjne i przyjazne dla środowiska systemy przeróbcze surowców mineralnych. Komeko 2008. Centrum Mechanizacji Górnictwa KOMAG. Gliwice. 2008. s. 17–28.
W. Blaschke, S. Blaschke, H. Aleksa, K. Wierzchowski: Analiza wpływu dokładności wzbogacania (imperfekcja) na wartość produkcji węgla energetycznego. Polityka Energetyczna tom 11, z. 1. Wyd. Instytutu GSMiE PAN. Kraków. 2008. ss. 89–99.
W. Blaschke: Technologie Czystego Węgla rozpoczynają się od jego wzbogacania. Polityka Energetyczna tom 11, z. 2. Wyd. Instytutu GSMiE PAN. Kraków. 2008. ss. 7–13.
Z. Blaschke, W. Blaschke: Mała Encyklopedia Technologii Przeróbki Kopalin. Inżynieria Mineralna. t. 8 i 9. z. 2(20) – 2(22) 2007–2008. Wyd. PTPK. Kraków 2011. s. 2–158.
W. Blaschke, S. Góralczyk: Czyste technologie węglowe – problem odpadów. Ekologia przemysłowa. Wydawnictwo ELAMED, nr 3/2008. s. 52–53,
W. Blaschke: Budżet państwa a inwestycje początkowe w górnictwie węgla kamiennego. Wspólne Sprawy. Biuletyn Zarządu Głównego SITG, nr 10(186), 2008 r. ss. 6–8.
W. Blaschke: Ile jest rynku w rynku węgla. SKIP Magazyn gospodarczy przemysłu surowcowego. Wydawnictwo Górnicze, Katowice, nr 2, 2008 r. s. 50–54.

W. Blaschke: Przeszłość czy przyszłość górnictwa węgla kamiennego. Cz. I. Wspólne Sprawy. Biuletyn Zarządu Głównego SITG, nr 4(180) 2008 r. s. 4–7.
W. Blaschke: Przeszłość czy przyszłość górnictwa węgla kamiennego. Cz. II. Wspólne Sprawy. Biuletyn Zarządu Głównego SITG, nr 5–6 (181–182) 2008 r. s. 8–9.
W. Blaschke: Rachunek rentowności. Wspólne Sprawy. Biuletyn Zarządu Głównego SITG, nr 8(184) 2008 r. s. 6–7.
W. Blaschke: Rentowne czy nierentowne kopalnie węgla kamiennego?. Wspólne Sprawy. Biuletyn Zarządu Głównego SITG, nr 7(183) 2008 r. str. 6–7.
W. Blaschke: Przeszłość czy przyszłość górnictwa węgla kamiennego. Mat. Konf. Górnictwo wczoraj i dziś – Stowarzyszenie Inżynierów i Techników Górnictwa, Mysłowice 2008. ss. 7–16.
W. Blaschke: Technologie Czystego Węgla rozpoczynają się od jego wzbogacania. Mat. Konf. Czysta Energia – czyste środowisko. Kraków. Wyd. Małopolsko-Podkarpacki Klaster Czystej Energii. 2008. ss. 27–32.
W. Blaschke: O górnictwie węgla kamiennego w Polsce. W: Zarządzanie: doświadczenia i problemy. Red. W. Sitko: Wyd. System-Graf Drukarnia, Agencja Reklamowo-Wydawnicza Lublin. 2009. s. 47–65,
W. Blaschke: Przeróbka węgla kamiennego – wzbogacanie grawitacyjne. Wyd. Instytutu GSMiE PAN. Kraków. 2009. s. 217.
A. Lutyński, W. Blaschke: Aktualne kierunki zagospodarowania odpadów przeróbczych węgla kamiennego. Przegląd Górniczy nr 10. (1043). Wyd. ZG SITG. Katowice. 2009. ss. 33–35.
W. Blaschke, Nguyen Thi Thuy Linh, G. Czarny: Ekonomiczne kryterium wyboru sposobu wzbogacania miałów węgla koksowego. Polityka Energetyczna tom 12, z. 2/2. Wyd. Instytutu GSMiE PAN. Kraków. 2009. ss. 29–42.
W. Blaschke, U. Lorenz, U. Ozga-Blaschke: Krajowa baza surowcowa dla przemysłu energochemicznego przetwórstwa węgla. Karbo nr 4/2009. Wyd. Górnicze. Katowice. 2009. ss. 190–196.
W. Blaschke: Czyste technologie węglowe: nowe podejście do problemu. Przegląd Górniczy Nr 10 (1043). Wyd. ZG SITG Katowice. 2009. ss. 23–27.
W. Blaschke, Z. Grudziński, U Lorenz., U. Ozga-Blaschke, T. Olkuski, K. Stala-Szlugaj: Wpływ zawartości związków alkalicznych w węglu kamiennym na procesy jego użytkowania. Zeszyty Naukowe nr 75. Wyd. Instytutu GSMiE PAN. Kraków. 2009. ss. 35–46,
W. Blaschke: Oczyszczanie węgla przed spalaniem pierwszym etapem Programu Technologii Czystego Węgla. Szkoła Eksploatacji Podziemnej 2009, Mat. Konf. Sympozja i Konferencje nr 74. Wyd. Instytutu GSMiE PAN. Kraków. 2009. ss. 31–39.
W. Blaschke: Węgiel w projekcie polityki energetycznej. XI Konf. Górnictwo wczoraj i dziś. Wyd. SITG. Katowice. 2009. ss. 15–20.
W. Blaschke: Wytwarzanie energii – z czystego czy brudnego węgla. W: Czynnik ENERGIA w praktyce gospodarczej. Red. J. Tarajkowski. Wydawnictwo Poznańskiego Towarzystwa Przyjaciół Nauk. Poznań 2010. ss. 69–80.
W. Blaschke: Energy Production – from "Clean or "Dirty Coal. W: Energy factor in Economic Policy. Publishing House of the Poznań Society for the Advancement of the Art and Sciences. Poznań 2010. pp. 81–91.
W. Blaschke, St. Ziomber, G. Czarny: Wpływ dokładności wzbogacania węgla koksowego na wychód koncentratu. Monografia: Paliwa – Bezpieczeństwo – Środowisko. Innowacyjne Techniki i Technologie. Instytut Techniki Górniczej, KOMAG. Gliwice. 2010. ss. 103–109.
I. Baic, W. Blaschke: Identyfikacja depozytów mułowych i strategia rozwoju technologicznego w zakresie ich gospodarczego wykorzystania. Monografia: Paliwa – Bezpieczeństwo – Środowisko. Innowacyjne Techniki i Technologie. Instytut Techniki Górniczej, KOMAG. Gliwice. 2010. ss. 111–123.
W. Blaschke, L. Gawlik, S.A. Blaschke: Coal Preparation Technologies in Poland. CPSA Journal, Spring 2010/Volume 9, No.1, ss. 28–32. The Magazine by the Coal Preparation Society of America. 2010.
I. Baic, W. Blaschke, J. Szafarczyk: Depozyty mułów węglowych źródłem paliwa energetycznego. Przegląd Górniczy nr 1–2 (1046–1047). Wyd. ZG SITG Katowice. 2010. ss. 73–77.
W. Blaschke, I. Baic, J. Szafarczyk: Prognozowanie parametrów jakościowych odpadów powstających podczas grawitacyjnego wzbogacania węgli kamiennych. Zeszyty Naukowe Nr 78. Wyd. Instytutu GSMiE PAN. Kraków. 2010. ss. 27–36.
W. Blaschke, Z. Grudziński, U. Lorenz, U. Ozga-Blaschke, T. Olkuski, K. Stala-Szlugaj: Geneza, formy występowania i zawartość chloru w węglu kamiennym. Zeszyty Naukowe nr 77. Wyd. Instytutu GSMiE PAN. Kraków. 2010. ss. 23–33.
W. Blaschke: Korzystajmy z czystego węgla. Polska Energia Nr 3/2010. Wyd. Tauron Polska Energia S.A. 2010.
I. Baic, W. Blaschke, J. Szafarczyk: Analiza możliwości wykorzystania depozytów mułów węglowych jako pełnowartościowego paliwa energetycznego. Workshop – Vyzkum v oblasti odpadu jako narady primarnich surovinovych zdroju. Ostrava. 2010. Czech Republic. s. 215–218.

I. Baic, W. Blaschke, W. Sobko: Identification of Coal Sludge Deposits and Technological Development of Strategy in the Field of Their Economic Usage. 14th Conference on Environment and Mineral Processing. Part II. s. 101–106. 2010. Czech Republic.

W. Blaschke, St. Ziomber: The effect of the accuracy of coking coal cleaning on the yield of cleaned coal. 14th Conference on Environment and Mineral Processing. Part II. S. 39–42. 3–5.06.20101 Ostrava, Czech Republic. 2010.

W. Blaschke. Nguyen Thi Thuy Linh: Effect of the Accuracy of Coking Coal Separation on the Washed Coal. Proceedings of the International Mining Conference – Advanced mining for sustainable development. Ha Long. Wietnam. 2010. ss. 673–678.

I.Baic, B. Witkowska-Kita, A. Lutyński, W. Blaschke, W. Kozioł, Z. Piotrowski: FORESIGHT OGWK – Analiza innowacyjności technologii zagospodarowania odpadów pochodzących z górnictwa węgla kamiennego z zastosowaniem metody Delphi. Monografia: Bezpieczeństwo – Jakość – Efektywność. Innowacyjne i przyjazne dla środowiska techniki i technologie przeróbki surowców mineralnych. Instytut Techniki Górniczej KOMAG. Gliwice 2011. ss. 7–14.

I. Baic, B. Witkowska-Kita, A. Lutyński, W. Blaschke, W. Kozioł, Z. Piotrowski: Metoda analizy krzyżowej w ocenie wpływu wybranych czynników na rozwój innowacyjnych technologii zagospodarowania odpadów pochodzących z górnictwa węgla kamiennego. Monografia: Bezpieczeństwo – Jakość – Efektywność. Innowacyjne i przyjazne dla środowiska techniki i technologie przeróbki surowców mineralnych. Instytut Techniki Górniczej KOMAG. Gliwice 2011. ss. 15–29.

W. Kozioł, Z. Piotrowski, R. Pomykała, Ł. Machniak, I.Baic, B. Witkowska-Kita, A. Lutyński, W. Blaschke: Metoda AHP jako sposób oceny innowacyjności technologii zagospodarowania odpadów z górnictwa węgla kamiennego. Monografia: Bezpieczeństwo – Jakość – Efektywność. Innowacyjne i przyjazne dla środowiska techniki i technologie przeróbki surowców mineralnych. Instytut Techniki Górniczej KOMAG. Gliwice 2011. ss. 31–40.

W. Blaschke, J. Szafarczyk, I. Baic: Prognozowanie parametrów jakościowych odpadówpowstających podczas grawitacyjnego wzbogacania węgli kamiennych. Przegląd Górniczy nr 5. 2011.

W. Blaschke, L.Róg, A.Ostatkiewicz: Jakość produktów odpadowych wydzielanych w procesach wzbogacania energetycznego węgla kamiennego. Przegląd Górniczy nr 5. 2011.

I. Baic, W. Blascke, Z. Grudziński: Wstępne badania nad możliwością przewidywania parametrów jakościowych odpadów wbogacania węgli kamiennych. Przegląd Górniczy nr 5. 2011.

I. Baic, B. Witkowska-Kita, W. Blaschke, A. Lutyński, W. Kozioł, Z. Piotrowski: Wpływ wybranych czynników na rorwój innowacyjnych technologii zagospodarowywania odpadów pochodzących z górnictwa węgla kamiennego określony metodą krzyżowej analizy wpływów. Rocznik Ochrona Środowiska, t.13. Wyd. Środkowo-Pomorskie Towarzystwo Naukowe Ochrony Środowiska. Koszalin 2011.

W. Kozioł, Z. Piotrowski, R. Pomykała, Ł. Machniak, I. Baic, B. Witkowska-Kita, A. Lutyński, W. Blaschke: Zastosowanie analitycznego procesu hierarchicznego (AHP) do wielokryterialnej oceny innowacyjności technologii zagospodarowania odpadów z górnictwa kamiennego. Rocznik Ochrona Środowiska, t.13. Wyd. Środkowo-Pomorskie Towarzystwo Naukowe Ochrony Środowiska. Koszalin 2011.

W. Sobko, I. Baic, W. Blaschke: Depozyt mułów węglowych – inwentaryzacja i identyfikacja ilościowa. Rocznik Ochrona Środowiska, t.13. Wyd. Środkowo-Pomorskie Towarzystwo Naukowe Ochrony Środowiska. Koszalin 2011.

XXVI International Mineral Processing Congress 2012
New Delhi, India
September 24-28, 2012

XXVI IMPC 2012 New Delhi, India
Innovative Processing for Sustainable Growth

Invitation

It is a great honour for the mineral engineering fraternity in India to host the XXVI International Mineral Processing Congress (IMPC) in New Delhi from September 24-28, 2012. It is indeed a privilege for us in India to invite you to come and celebrate sixty years of IMPC in New Delhi in September 2012. The Indian Institute of Mineral Engineers (IIME) and The Indian Institute of Metals (IIM) will be organising the XXVI IMPC in collaboration with and support from other professional organisations and industry.

India is known for its ancient heritage in minerals and metals. The non-corroding Delhi Iron Pillar (more than 1600 years old), the legendary Wootz steel from which famous Damascus swords were made, the ruins of ancient retorts that were used to produce thousands of tons of zinc in Rajasthan, the exquisitely crafted bronze icons from south India made by the "lost wax" process – are all testimony to the level of technological excellence achieved by the Indian sub-continent. The mining, minerals and metals industry continues to be of great importance to India and it is going through resurgence in recent times. Impressive growth projections in the production of minerals during the next decade promise huge investments in the industry.

The mining, minerals and metals industry globally and particularly in India is confronted with new challenges of reducing its environmental footprint. Land, energy and water are extremely scarce resources in India. Our theme for IMPC 2012 is therefore titled "**Innovative Processing for Sustainable Growth**". IMPC has been an excellent forum for the best professionals from the industry, academia and the research institutions to meet and deliberate on the challenges and the opportunities in the field. We shall strive to make IMPC 2012 a professionally rewarding and socially enjoyable experience.

We cordially invite you to join us in New Delhi in September 2012. Please do write to us and visit our website for more details. We look forward to meeting you in New Delhi.

Pradip
President

B. K. Mishra
Chairman (Organising Committee)

Call for Papers

We request you to submit abstracts of your papers for presentation during IMPC 2012. The theme of the Congress is **"Innovative Processing for Sustainable Growth"** and will cover broadly the following areas in mineral processing:

- **Basic Scientific Developments** (Process mineralogy, characterisation and liberation; Comminution; Gravity separation; Magnetic and electrostatic separation; Flotation; Processing of Fines and Slimes; Pelletisation, Agglomeration and Sintering; Solid-liquid separation; Bio-beneficiation; Hydrometallurgy, extraction of metals and bio-hydrometallurgy; Process modeling, simulation and optimisation; Process instrumentation and advanced model-predictive control)
- **Technological Advancements related to Specific Industrial Segments** (Minerals for Iron and Steel Industry; Minerals for Aluminium Industry; Complex Copper-Lead-Zinc-Nickel-Cobalt ores; Platinum group minerals; Industrial Minerals like Phosphate, Chromite, Wollastonite and Clays; Beach Sand Minerals; Energy Minerals such as Coal and Lignite, Uranium and Silica)
- **Special Theme Symposia** (Role of information technology in mineral processing industry; Eco-friendly technologies for waste recycling; Science and technology of reagent design, development and commercialisation; Sustainability issues in mining and mineral processing; Development of human resources for the mineral industry)

Abstract Submission Deadlines

Authors are requested to submit abstracts latest by **July 15, 2011**. The abstract, prepared as per the guidelines provided on the website, can be submitted online at **www.impc2012.org** and/or as an electronic attachment through E-mail to **contact@impc2012.org**

Sponsorship

We solicit sponsors for the Congress as well as for various events planned during IMPC 2012. Please contact us for sponsorship opportunities, for example, patrons, platinum/gold/silver sponsorship, sponsoring a theme symposium and/or a session, conference dinner, lunch, refreshments and other sponsorship options.

IMPC 2012 Technical Exhibition

We invite industries, equipment suppliers, research institutions, consulting companies and other organisations both in India and abroad for showcasing their processes, products, instruments, equipment, expertise and achievements during IMPC 2012. The technical exhibition will be organised in the Front Lawns of Hotel Ashok.

Please visit the conference website **www.impc2012.org** or send an E-mail to **contact@impc2012.org** for more details

Organised by

Indian Institute of Mineral Engineers

The Indian Institute of Metals

Supported by

सत्यमेव जयते
Ministry of Steel
Government of India

सत्यमेव जयते
Ministry of Mines
Government of India

सत्यमेव जयते
Department of Science and Technology
Government of India

Council of Scientific and Industrial Research

Our books are available in Tech bookstore
plac Grunwaldzki 13
50-377 Wrocław, D-1 PWr., tel. (071) 320 32 52
Orders can also be sent by post

ISSN 1643-1049
Physicochemical Problems of Mineral Processing, 47 (2011)